Gold-Catalyzed Synthesis of 5 and 6-Membered Rings for the Construction of Molecular Diversity

Pilar Calleja Ramos

UNIVERSITAT ROVIRA i VIRGILI

Gold-Catalyzed Synthesis of 5 and 6-Membered Rings for the Construction of Molecular Diversity

Pilar Calleja Ramos

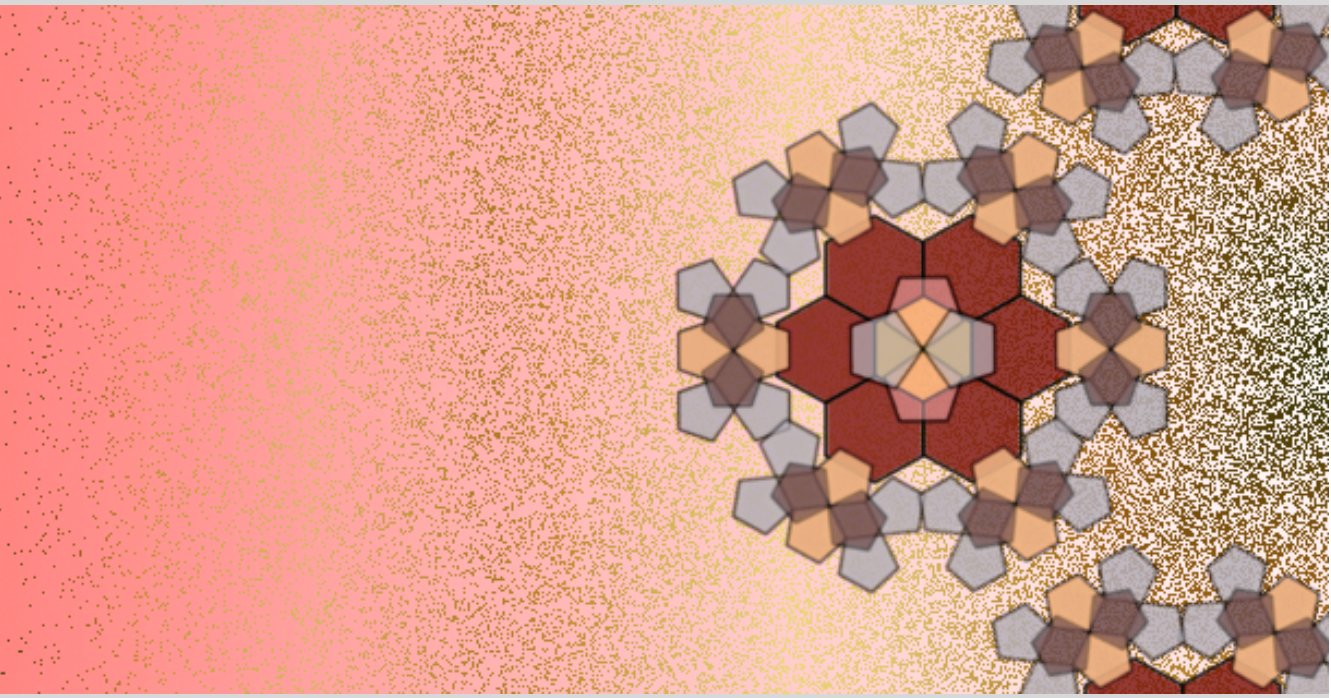

DOCTORAL THESIS
2017

Pilar Calleja Ramos

Gold-Catalyzed Synthesis of 5 and 6-Membered Rings for the Construction of Molecular Diversity

DOCTORAL THESIS

Supervised by Prof. Antonio M. Echavarren

Institut Català d'Investigació Química (ICIQ)

UNIVERSITAT ROVIRA i VIRGILI

Tarragona 2017

UNIVERSITAT ROVIRA i VIRGILI

ICIQ
Institut Català d'Investigació Química

I STATE that the present study, entitled 'Gold-Catalyzed Synthesis of 5 and 6-Membered Rings for the Construction of Molecular Diversity', presented by Pilar Calleja Ramos to receive the degree of Doctor, has been carried out under my supervision at the Institut Català d'Investigació Química (ICIQ).

Tarragona, April 28th, 2017

Doctoral Thesis Supervisor

Prof. Antonio M. Echavarren Pablos

Als meus pares

"If you hear a voice within you say "you cannot paint", then by all means paint, and that voice will be silenced"

Vincent van Gogh

Acknowledgements

Aquesta tesi doctoral s'ha dut a terme a l'Institut Català d'Investigació Química i ha estat supervisada pel Prof. Antonio M. Echavarren, a qui agraeixo l'oportunitat de formar-me en el seu grup, tant a nivell científic com a nivell personal. Le agradezco todos los recursos y las ideas que me ha proporcionado, así como sus pequeñas lecciones de cultura universal. Pero por encima de todo esto, le agradezco la gran calidad humana que siempre me ha demostrado, su preocupación por mi persona y su paciencia.

Agraeixo la Fundació ICIQ, l'AGAUR i els projectes europeus ERC i ATMOL haver-me finançat durant tot aquest temps, així com al "Ministerio de Educación, Cultura y Deporte" per la beca FPU.

I would like to thank Prof. M. Christina White (*University of Illinois Urbana-Champaign*, USA), who welcomed in her group for a short stay (April – June 2015). Thanks for making me feel a member of the group since the day I arrived as well as for the absolute trust in me. I would also like to thank all the members of the group for his help, specially: Tommy, Joe, Chris, Siraj, Connor, Takeshi, Wei, Anasheh and Jenny.

Vull agrair molt especialment a Sònia Gavaldà i Imma Escofet tota l'ajuda rebuda durant tots aquests anys. Moltes gràcies per cada estoneta que m'heu dedicat i moltes més gràcies per haver-ho fet sempre amb el millor dels somriures. També a Vanessa Martínez, li agraeixo el seu ajut durant els primers mesos que vaig passar al grup.

Agrair també a la unitat tècnica de l'ICIQ, espectrometria de masses, ressonància magnètica nuclear, unitat de difracció de Raigs X i l'unitat d'HTE.

Vull donar les gràcies a tots els membres (presents i passats) del grup Echavarren amb els que he tingut el plaer de coincidir durant aquests anys. En particular, vull agrair l'ajut rebut per part d'aquells amb els qui he pogut col·laborar: Dr. Tania Jiménez, Dr. Michael E. Muratore, Jordan R. Boothe i Ruth Dorel. També a tots aquells amb els qui he pogut compartir grans estones al laboratori 2.3: Dr. Paul McGonigal (for his huge help in my beginnig), Dr. Maria Moreno, Claudia Solís de León, Anthony Pitaval, Yahui Wang, Carla Obradors, Katia Smirnova (mi rusa favorita), Alice Johnson, Elena de Orbe (muchos ánimos, que todo sale! Muchas gracias por ayudarme cuando me peleaba con mis DFT y por acogerme unos meses en tu pisito), Sofia Ferrer (q fa no res eres màster i ja casi ets tota una doctora!), Zhouting Rong, Alejandro Bermejo (por

nuestras conversaciones de balanza a vitrina), Eric Tan, Jordan R. Boothe (for his patience and his sense of humor), Jin-Ming Yang, Otilia Stoica (mi Hotty), Joan G. Mayans (see below) y a las "más mejores" compis de pasillo que uno podría imaginar: Cristina García y Ruth Dorel (integrantes del también conocido como pasillo hostil).

A més, m'agradaria donar les gràcies a totes les persones que m'han acompanyat d'una manera més o menys efímera durant aquests anys. A l'Anna Homs (the most beautiful catalan flower ever), la Carla Obradors (una vegada més) i la Núria Huguet, per ser uns grans models a seguir. Al Dr. Óscar Pablo, por todos los buenos momentos que hemos pasado, por sus consejos, su ayuda, su música y su personalidad. Por todos esos cafés y grandes consejos, muchas gracias Ana (Bahamonde)!!! Por supuesto, no podía olvidarme de mis Summerfellows/Másters favoritos: Albano y Álvaro (porque sin vosotros todo habría sido infinitamente más duro y aburrido). Al Dr. Javier Carreras, quien además se ha convertido en un gran amigo, con el que espero tener el placer de volver a coincidir en algun lugar del mundo (y si no, ya nos buscaremos la manera de hacernos coincidir). *Last but not least*, quisiera agradecer a mi Dorel todos estos años! MUCHÍSIMAS GRACIAS por haber estado siempre a mi lado durante este largo camino, desde el momento en que como Summerfellow tuve la gran suerte de coincidir contigo. Sabes que aquí tienes una amiga para lo que necesites y con la que espero poder compartir mil historias y aventuras más.

También quisiera agradecer a los integrantes (presentes y pasados) del "piso patera": Ángel, Cris, Sofi, Ale y Ana (Pereira) todos los momentazos que compartimos en ese piso! Pero en especial, me gustaría agradecer a Ángel y Cris (mi familía onubense), cada rato que he compartido con ellos: coloreando, cocinando, limpiando, hablando, cantando, bailando... Muchísimas gracias por haberme cuidado y mimado cuando estaba lisiada! Y muchísimas gracias por haberme apoyado en los días más duros, porque la recta final ha sido muchísimo más llevadera gracias a vosotros! Espero que sepáis lo mucho que os quiere esta catalana!

Als meus tres tresors Sandra, Núria i Cris (UK), sense les quals no puc ni vull concebre la meva vida. Mil gràcies Dr. Sandra Torres, per ser sempre allà des que som ben menudes, pels grans moments viscuts i per tots els que vindran. A tú Núria, per les teves visites exprés que sempre m'omplen d'alegria i il·lusió. I a tú Cris (UK), per ser un tros de dona que triomfa allà on va i que sempre t'he temps per dedicar-me i parlar una estoneta amb mi!

También quisiera darle las gracias a Elvira (Gómez Valentín) por todos los ratos, paseos y cafés que hemos compartido en Barcelona (FYI, en Heidelberg también hay muchas cafeterías…).

A tú Celsa, per creure sempre en mi i fer-me veure que per aconseguir tot allò que vull només em cal confiar en mi mateixa. I a tú Andreu, per tantes coses…T'agraeixo la paciència, els ànims i cadascún dels somriures que em vas saber arrencar en els moments més durs. Per ser al meu costat (tot i ser a kilòmetres de distància), per tot el que vam compartir i construir; i per deixar-me anar.

Molt especialment, gràcies a tú Joan perqué des del moment en que vas aparèixer en el meu món, no he volgut res més que viure. Gràcies per fer-me gaudir de la música, de la natura, de la nit i del dia. Gràcies per fer-me tan feliç!

Por último quiero darle las gracias a mis padres, porque sin vosotros yo no sería ni una pequeña parte de lo que soy hoy. A ti papá, por darme siempre esas dosis de realismo combinadas con tu apoyo incondicional; y a ti mamá, por ser para mí el mejor ejemplo de mujer fuerte e inteligente al que parecerse. Muchísimas gracias por haberme dado siempre todo lo mejor, por cuidarme, por quererme tanto.

This work was carried out with the support of the Spanish Ministry of Economy and Competitiveness (MINECO, projects CTQ2010-16088/BQU and CTQ2013-42106-P, FPU grant to P.C., and Severo Ochoa Excellence Accreditation 2014-2018 (SEV-2013-0319)), the European Research Council (Advanced Grant No. 321066), the Agency of Management of University and Research Grants (AGAUR, 2009 SGR 47 and 2014 SGR 818), the Atomic Scale and Single Molecule Logic Gate Technologies (ATMOL, European Integrated Research Project, contract No. FP7-270028) and the Institute of Chemical Research of Catalonia (ICIQ Foundation).

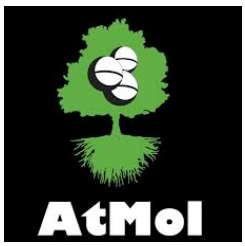

At the time of writing this manuscript, the results obtained during my PhD have given rise to the following publications:

α,β-Unsaturated Gold(I) Carbenes by Tandem Cyclization and 1,5-Alkoxy Migration of 1,6-Enynes: Mechanisms and Applications
Calleja, P.; Pablo, O.; Ranieri, B.; Gaydou, M.; Pitaval, A.; Moreno, M.; Raducan, M.; Echavarren, A. M. *Chem.–Eur. J.* **2016**, *22*, 13613–13618.

Diastereoselective Gold(I)-Catalyzed [2+2+2] Cycloaddition of Oxo-1,5-enynes
Calleja, P.; Muratore, M. E.; Jiménez, T.; Echavarren, A. M. *Synthesis* **2016**, *48*, 3183–3198. (Invited paper in memory of Professor Jean Normant)

Synthesis of a Crushed Fullerene $C_{60}H_{24}$ through Sixfold Palladium-Catalyzed Arylation
Dorel, R.; de Mendoza, P.; Calleja, P.; Pascual, S.; González-Cantalapiedra, E.; Cabello, N.; Echavarren, A. M. *Eur. J. Org. Chem*. **2016**, 3171–3176.

Catalytic Oxidations in Organic Synthesis: Oxidations of Alkynes
Calleja, P.; Dorel, R.; Echavarren, A. M. *Science of Synthesis*, In press.

In addition, the work carried out during my stay in the laboratory of Prof. M. Christina White (University of Urbana-Champaign, 2015) was published in:

Aerobic Linear Allylic C-H Amination: Overcoming Benzoquinone Inhibition
Pattillo, C. C.; Strambeanu, I. I.; Calleja, P.; Vermeulen, N. A.; Mizuno, T.; White, M. C. *J. Am. Chem. Soc.* **2016**, *138*, 1265–1272.

Table of Contents

Prologue

This Thesis manuscript has been divided into five main parts: a general introduction on gold(I) catalysis and four research chapters. Each chapter contains five sections including a specific introduction on the research topic, the objectives, the discussion of the results, which lead to the corresponding conclusions and the experimental part. The references and numbering are organized by chapters.

The **General Introduction** provides an overview of the basic principles of homogeneous gold(I) catalysis comprising the activation of alkynes, the cycloisomerization of enynes as well as the oxidative gold(I) catalyzed cyclizations.

Chapter 1 discloses the development of a method for the selective preparation of 2,3,5,6,8,9-hexahydro-1*H*-cyclopenta[*e*]-*as*-indacene-1,4,7-trione through a triple gold(I)-catalyzed oxidative cyclization. This C_{3h} C_{15} synthon was used as a platform for the preparation of 1,4,7-trifunctionalized C_{3h}-symmetric trindene derivatives, including a new trindane-based crushed C60. This work was based on the research developed by C. Rogelio Solorio-Alvarado as part of his PhD Thesis (2011) and thus, for coherence some of his results have been included. During my stay in the laboratory of Prof. M. C. White (USA), Ruth Dorel joined me in the project. This work is still unpublished.

Chapter 2 presents the development of the diastereoselective gold(I)-catalyzed [2+2+2] cycloaddition of *O*-protected homopropargylic and allylic oxo-1,5-enynes. This work was performed initially in collaboration of Dr. Tania Jiménez and later with Dr. Michael E. Muratore. The results were published in *Synthesis* **2016**, *48*, 3183–3198.

Chapter 3 collects all the results obtained towards the synthesis of two families of natural products: the pycnanthuquinones and the carexanes. The key step for the synthesis of pycnanthuquinone C features a gold(I)-catalyzed [4+2] cycloaddition reaction. This work was based on the preliminary results obtained by Núria Huguet as part of her PhD Thesis (2013), Dr. Paul McGonigal and Dr. Ricarda Miller. On the other hand, the construction of the bicyclic scaffold of carexanes involves the development of an enantioselective gold(I)-catalyzed 6-*endo*-*dig* cyclization. Jordan R. Boothe, visiting student from the University of Michigan, joined me in the project working on the development of the asymmetric version of the gold cyclization. These

two projects are currently continued by Joan G. Mayans. These results are still unpublished.

Chapter 4 gathers a detailed computational study of the gold(I)-catalyzed 1,5-migration reaction of 1,6-enynes bearing different substituents at the propargylic position and at the alkene. I thank Elena de Orbe and Dr. Óscar Pablo for fruitful discussions. The results were published in *Chem.–Eur. J.* **2016**, *22*, 13613–13618.

Abbreviations and Acronyms

In this manuscript, the abbreviations and acronyms most commonly used in organic and organometallic chemistry have been used following the recommendations of "Guidelines for authors" of *Journal of Organic Chemistry*.

Additional abbreviations and acronyms used in this manuscript are referenced in the list below:

APCI	atmospheric pressure chemical ionization
app	apparent
$BAr4^{F-}$	tetrakis [3,5-bis(trifluoromethyl)phenylborate]
CAPY	caprolactam
dppf	1,1'-bis(diphenylphosphino)ferrocene
dtbpy	4,4'-di-*tert*-butyl-2,2'-dipyridyl
ee	enantiomeric excess
JohnPhos	(2-biphenyl)di-*tert*-butylphosphine
IMD	imidazole
IPr	1,3-bis(2,4,6-trimethylphenyl)imidazole-2-ylidene
L	ligand
LDI	laser desorption ionization
MS	mass spectrometry/molecular sieves
MSA	methane sulfonic acid
MW	microwave irradiation
NTf_2^-	bis(trifluoromethyl)imidate
ODCB	orthodichlorobenzene
OTf^-	triflate
ORTEP	oak ridge thermal ellipsoid plot
ov	overlaped
Oxone ®	potassium peroxymonosulfate
PDP	(2-({(*S*)-2-[(*S*)-1-(pyridin-2-ylmethyl)pyrrolidin-2-yl]pyrrolidin-1-yl}methyl)pyridine
PTSA	*para*-toluene sulfonic acid
SPhos	2-dicyclohexylphosphino-2′,6′-dimethoxybiphenyl
*t*BuXPhos	2-(di-*tert*-butylphosphino)-2',4',6'-triisopropyl-1,1'-biphenyl
tht	tetrahydrothiophene
tmbn	trimethoxybenzonitrile

All the complexes used in this thesis are listed bellow:

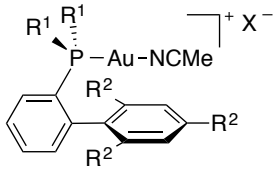

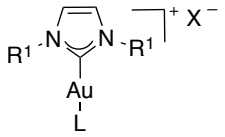

A: R^1 = *t*Bu, R^2 = H, X = SbF_6
B: R^1 = *t*Bu, R^2 = *i*Pr, X = SbF_6
C: R^1 = *t*Bu, R^2 = *i*Pr, X = BAr_4^F
D: R^1 = Cy, R^2 = H, X = SbF_6

E: R^1 = Mes, L = tmbn, X = SbF_6
F: R^1 = 2,6-(*i*Pr)$_2$C$_6$H$_3$, L = tmbn, X = SbF_6
G: R^1 = 2,6-(*i*Pr)$_2$C$_6$H$_3$, L = PhCN, X = SbF_6
H: R^1 = 2,6-(*i*Pr)$_2$C$_6$H$_3$, L = PhCN, X = BAr_4^F

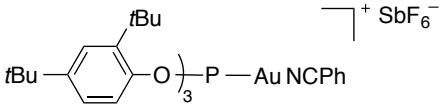

I

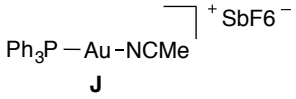

J

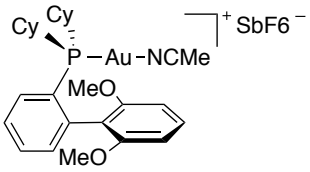

L

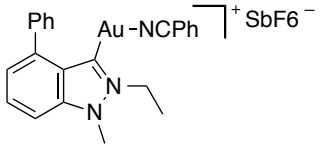

K

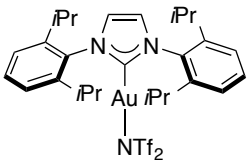

M

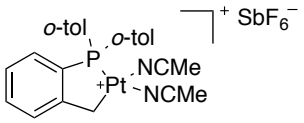

P

Abstract

Over the last years our research group has been focused on the design of new gold(I) complexes, their application to the development of new synthetic methods and the study of the intriguing mechanisms of these transformations. Besides, much effort has been devoted on the development of new strategies for the synthesis of biologically active molecules featuring complex architectures as well as large polyarenes with potential applications in material science. In this context, the main goal of this Doctoral Thesis was the development of new synthetic strategies for the preparation of polyaromatic compounds and for the synthesis of natural product-based polycyclic architectures.

A novel approach for the synthesis of a new trindane-based crushed fullerene C60 has been developed by a threefold palladium-catalyzed cross-coupling of four suitably functionalized C_{15} trindene fragments. The trindane C_{15} skeleton of the central motif has been constructed through a triple gold(I)-catalyzed oxidative cyclization, which has also enabled the preparation of a series of trindene-based C_{3h}-symmetric polyarenes.

In order to access naturally occurring compounds featuring octahydro-1*H*-indene motifs, the scope of the intramolecular gold(I)-catalyzed formal [2+2+2] cycloaddition reaction has been extended to *O*-protected homopropargylic and allylic oxo-1,5-enynes. Under the optimized reaction conditions, the cyclization of (*Z*)- and (*E*)- isomers takes place with moderate to excellent yield (38-90%) and increased selectivity in most of the cases. DFT calculations suggest that after the formation of the cyclopropyl gold(I)-carbene, two competitive pathways arising from the preferred face for the nucleophilic attack of the carbonyl group are involved in this transformation and can explain the observed lack of complete stereoselectivity.

As part of our investigations on the application of gold catalysis in the synthesis of natural products, we turned our attention to the synthesis of two families of natural products: the pycnanthuquinones and the carexanes. Pycnanthuquinone C is the simplest of the pycnanthuquinones, which was isolated from the brown alga *Cystophora harveyi*. Despite the singularity of its linear fused 5,6,6-ring core, only a biomimetic synthesis of its enantiomer has been reported in the literature. Thus, we considered the use of an intramolecular gold(I)-catalyzed [4+2] cycloaddition reaction for the synthesis of pycnanthuquinone C. Remarkably, the main tricyclic core of this molecule could be

prepared in good yield, although the late stage functionalization of the molecule proved to be more challenging than expected. On the other hand, the carexanes are a series of secondary metabolites present in the leaves of *Carex distachya*, an herbaceous Mediterranean plant. We envisioned to develop the first synthesis of these compounds by an enantioselective gold(I)-catalyzed alkoxycyclization of 1,6-enynes as the key step for the ready access to the common bicyclic core of carexanes via a 6-*endo*-*dig* process. Using the High Throughput Experimentation facility at ICIQ, a wide range of chiral gold(I) complexes were evaluated, leading to the preparation of a key enantioenriched dihydronaphthalene intermediate with promising enantioselectivities.

Finally, we have performed a detailed examination of gold(I) catalyzed skeletal rearrangements of different model 1,6-enynes bearing OR groups at the propargyl position, which are prone to undergo intramolecular 1,5-migration in the absence of external nucleophiles for a deeper understanding of these transformations. DFT calculations suggest that after the initial cyclization, the 1,5-OR migration proceeds stepwise through a cyclic intermediate, although the final cleavage occurs through a very low barrier. The nature of the propargylic alkoxy group and the substitution pattern in the alkene moiety play a crucial role for the formation of 1,5-migration products *vs.* the single-cleavage rearrangement derivatives.

General Objectives

The main general objective of this Doctoral Thesis was the development of new synthetic strategies for the construction of molecular complexity by employing homogeneous gold catalysis. Specifically, our studies focused on the following objectives:

– The development of an efficient method for the synthesis of C_{3h} star-shaped polyarenes and its application to the synthesis of a new crushed C60 fullerene.
– The extension of the scope of the intramolecular gold(I)-catalyzed [2+2+2] cycloaddition reaction to various oxo-1,5-enynes.
– The development and application of gold(I)-catalyzed cyclizations for the synthesis of different families of natural products.
– The detailed examination of the mechanism of the gold(I)-catalyzed 1,5-alkoxy migration for a depper understanding of this transformation.

Each chapter of this PhD Thesis manuscript contains a more detailed description of the objectives of the corresponding research project.

General Introduction

Gold, chemical symbol Au (from the Latin *aurum* meaning "shining dawn") and atomic number 79, is a precious metal that has fascinated humans for millennia. Due to the unreactive and durable nature of metallic gold, it became a symbol of immortality and power in many ancient cultures and it has been widely used in the production of jewelry, coinage, ornaments, dentistry, and electronics (Figure 1).

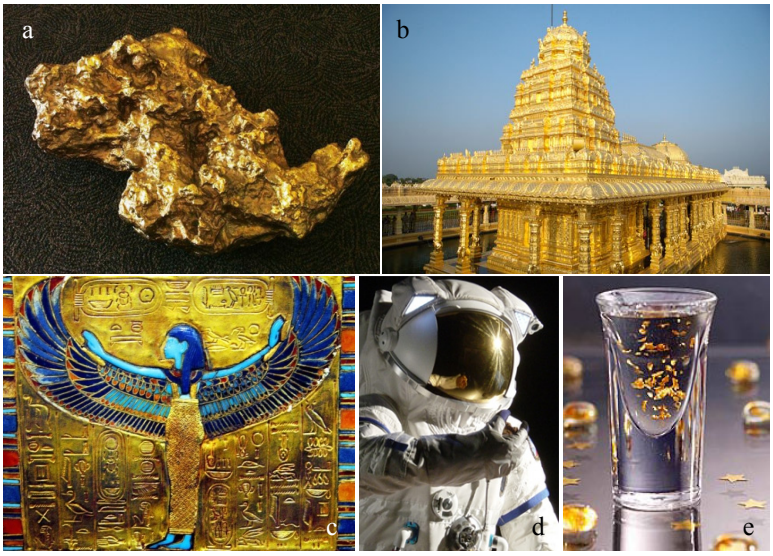

Figure 1. (a) "Welcome Stranger", the largest gold nugget ever found (72kg). (b) Sripuram temple in India. (c) goddess Nut. (d) astronaut's helmet. (e) goldschläger.

Paradoxically its perceived inertness and high price have led to neglect the use of gold in homogeneous catalysis for years. It was not until 1986 that Ito and Hayashi described the first application of gold(I) in homogeneous conditions for the asymmetric aldol reaction of aldehydes with isocyanides.[1] More than one decade later, Teles[2] and Tanaka[3] disclosed the first examples of gold(I) activation of alkynes (Scheme 1).[4]

1 Ito, Y.; Sawamura, M.; Hayashi, T. *J. Am. Chem. Soc.* **1986**, *108*, 6405−6406.

2 Teles, J. H.; Brode, S.; Chabanas, M. *Angew. Chem. Int. Ed.* **1998**, *37*, 1415−1418.

3 Mizushima, E.; Sato, K.; Hayashi, T.; Tanaka, M. *Angew. Chem. Int. Ed.* **2002**, *41*, 4563−4565.

4 For other precedents see: (a) Norman, R. O. C.; Parr, W. J. E.; Thomas, C. B. *J. Chem. Soc., Perkin Trans. 1* **1976**, 1983–1987. (b) Haruta, M.; Kobayashi, T.; Sano, H.; Yamada, N. *Chem. Lett.* **1987**, *16*, 405–408. (c) Fukuda, Y.; Utimoto, K. *J. Org. Chem.* **1991**, *56*, 3729–3731.

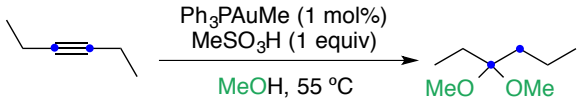

Scheme 1. Addition of alcohols to alkynes catalyzed by a gold(I) complex

Since then, gold salts and complexes have emerged as a powerful tool for the electrophilic activation of alkynes toward a variety of nucleophiles and have been employed in a plethora of organic transformations.[5,6]

Relativistic Effects

The ability of cationic gold complexes to selectively activate π-bonds can be attributed to the so-called relativistic effects, which are particularly significant for metals that have their 4*f* and 5*d* orbitals filled and reach a maximum in the periodic table with gold.[7]

Relativistic effects correspond to the acceleration of the electrons as they orbit closer to a heavy nucleus. As a result, the mass of the electron increases while the *s,* and to a lesser extend, the *p* orbitals are contracted. This entails that the electrons occupying the *d* and *f* orbitals exhibit a weaker nuclear attraction. Thus, the contraction of the gold 6*s* orbital causes the expansion of the 5*d* orbital, minimizing its electron-electron repulsion and becoming a remarkable soft Lewis acid.

The small differences in energy among the *s*, *p*, or *d* states lead to the efficient hybridization of *s*/*d* or *s*/*p* orbitals,[8] which explains the preference of gold(I) to form

5 (a) Hashmi, A. S. K. *Chem. Rev.* **2007**, *107*, 3180–3211. (b) Fürstner, A.; Davies, P. W.; *Angew. Chem. Int. Ed.* **2007**, *46*, 3410–3449. (c) Jiménez-Núñez, E.; Echavarren, A. M. *Chem. Rev.* **2008**, *108*, 3326–3350. (d) Gorin, D. J.; Sherry, B. D.; Toste, F. D. *Chem. Rev.* **2008**, *108*, 3351–3378. (e) Patil, N. T.; Yamamoto, Y. *Chem. Rev.* **2008**, *108*, 3395–3442. (f) Fürstner, A. *Chem. Soc. Rev.* **2009**, *38*, 3208–3221. (g) Shapiro, N. D.; Toste, F. D. *Synlett* **2010**, 675–691. (h) Obradors, C.; Echavarren, A. M. *Acc. Chem. Res.* **2014**, *47*, 902–912. (i) Dorel, R.; Echavarren, A. M. *Chem. Rev.* **2015**, *115*, 9028–9072.

6 Gorin, D. J.; Toste, F. D. *Nature* **2007**, *446*, 395–403.

7 (a) Pyykkö, P. *Angew. Chem. Int. Ed.* **2002**, *41*, 3573–3578. (b) Schwarz, H. *Angew. Chem. Int. Ed.* **2003**, *42*, 4442–4445. (c) Pyykkö, P. *Angew. Chem. Int. Ed.* **2004**, *43*, 4412–4456.

8 Gimeno, M. C.; Laguna, A. *Chem. Rev.* **1997**, *97*, 511–522.

linear two-coordinate complexes. Although less common, higher coordination numbers (3 or 4) are also possible. Importantly, gold(I) complexes do not easily undergo oxidative addition or β-hydride elimination.[9]

Another structural feature of gold is its *aurophilicity*[10] or tendency of the low-coordinate compounds of gold(I) to associate into dimers, oligomers or even polymers *via* direct Au–Au interaction.[11]

Gold Complexes

Despite simple gold salts such as $NaAuCl_4$ or AuCl are active enough to catalyze many transformations,[12] neutral gold complexes [LAuCl] as well as cationic gold complexes [AuLL']X have found broader applicability.[13] The nature of the complex can be easily modulated by the steric and electronic properties of the ligand used (as a result of the Au–L bond contraction). Thus, complexes containing more donating N-heterocyclic carbenes are less electrophilic than those with phosphine ligands, whereas complexes

9 (a) Nakanishi, W.; Yamanaka, M.; Nakamura, E. *J. Am. Chem. Soc.* **2005**, *127*, 1446–1453. (b) Lauterbach, T.; Livendahl, M.; Rosellón, A.; Espinet, P.; Echavarren, A. M. *Org. Lett.* **2010**, *12*, 3006–3009. (c) Livendahl, M.; Goehry, C.; Maseras, F.; Echavarren, A. M. *Chem. Commun.* **2014**, *50*, 1533–1536. For oxidative addition of Au(I) complexes, the use of a special system or ligand is required: (d) Guenther, J.; Mallet-Ladeira, S.; Estevez, L.; Miqueu, K.; Amgoune, A.; Bourissou, D. *J. Am. Chem. Soc.* **2014**, *136*, 1778–1781. (e) Joost, M.; Zeineddine, A.; Estévez, L.; Mallet−Ladeira, S.; Miqueu, K.; Amgoune, A.; Bourissou, D. *J. Am. Chem. Soc.* **2014**, *134*, 14654–14657.

10 Scherbaum, F.; Grohmann, A.; Huber, B.; Krüger, C.; Schmidbaur, H. *Angew. Chem. Int. Ed.* **1988**, *27*, 1544–1546.

11 Schmidbaur, H. *Gold Bull*. **2000**, *33*, 3–10.

12 (a) Brand, J. P.; Chevalley, C.; Waser, J. *Beilstein J. Org. Chem.* **2011**, *7*, 565–569. (b) Karmalar, S.; Kim, A.; Oh, C. H. *Synthesis* **2009**, *2*, 194-198.

13 (a) Pérez-Galán, P.; Delpont, N.; Herrero-Gómez, E.; Maseras, F.; Echavarren, A. M. *Chem.–Eur. J.* **2010**, *16*, 5324−5332. (b) Partyka, D. V.; Robilotto, T. J.; Zeller, M.; Hunter, A. D.; Gray, T. G. *Organometallics* **2008**, *27*, 28−32. (c) Hashmi, A. S. K.; Hengst, T.; Lothschütz, C.; Rominger, F. *Adv. Synth. Catal.* **2010**, *352*, 1315− 1337. (d) Fortman, G. C.; Nolan, S. P. *Organometallics* **2010**, *29*, 4579−4583. (e) Fortman, G. C.; Nolan, S. P. *Chem. Soc. Rev.* **2011**, *40*, 5151−5169.

with less donating phosphite ligands and similar species are the most electrophilic catalysts (Figure 2).[5c]

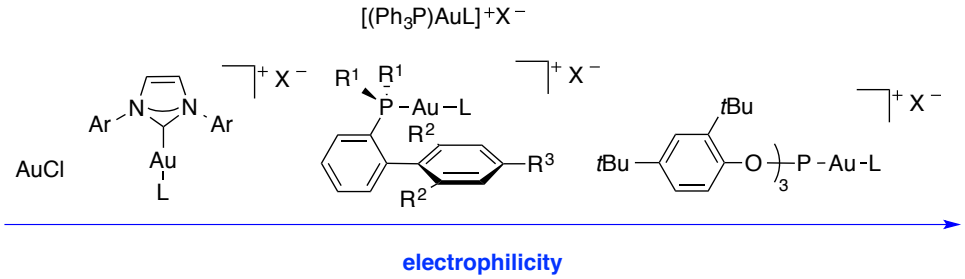

Figure 2. Increase in electrophilicity with decreased donating ligand ability in gold(I) complexes

More recently, chiral ligands have been used to induce enantioselectivity in gold(I)-catalyzed reactions.[14] However, these transformations are still particularly challenging due to the coordination mode of gold(I) complexes, which places the chiral information carried by the ligand very far from the reacting center.

Commonly, gold(I) complexes bearing labile sulfur ligands, such as (tht)AuCl have been used for the preparation of soluble gold(I) chloride precatalysts, starting from inexpensive gold(III)-chloride salts (Scheme 2).[15]

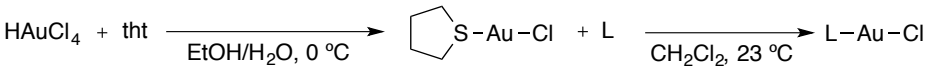

Scheme 2. General synthesis of [LAuCl] precatalysts

14 For selected reviews see: (a) Widenhoefer, R. A. *Chem.–Eur. J.* **2008**, *14*, 5382–5391. (b) Marinetti, A.; Jullien, H.; Voituriez, A. *Chem. Soc. Rev.* **2012**, *41*, 4884−4908. (c) López, F.; Mascareñas, J. L. *Beilstein J. Org. Chem.* **2013**, *9*, 2250−2264. (d) Shinde, V. S.; Mane, M. V.; Vanka, K.; Mallick, A.; Patil, N. T. *Chem.–Eur. J.* **2015**, *21*, 975–979. (e) Zi, W.; Toste, F. D. *Chem. Soc. Rev.* **2016**, *45*, 4567–4589 and references therein. (f) Huguet, N.; Echavarren, A. M. *Asymmetric Synthesis II*, Christman, M.; Bräse, S. Eds. Chapter 26, **2012**, 135–152. Wiley-VCH Verlag GmbH & Co. (g) De Mendoza, P.; Echavarren, A. M. *Modern Gold Catalyzed Synthesis*, Hashmi, A. S. K.; Toste, F. D. Eds. Chapter 5, **2012**, 205–212. Wiley-VCH Verlag GmbH & Co.

15 Al-Sa'Ady, A. K.; McAuliffe, C. A.; Parish, R. V.; Sandeank, J. A. *Inorg. Synth.* **1985**, 191−194.

In order to be catalytically active, gold(I) complexes should be coordinated with one labile ligand, which is replaced by the substrate through an associative mechanism.[16] Usually, active gold(I) species are generated *in situ* by chloride abstraction from gold chloride complexes upon treatment with a silver salt bearing a weakly coordinating anion.[13] In the absence of a coordinating substrate, much less reactive chloride-bridged dinuclear species [LAuClAuL]X are readily formed (Scheme 3).[17] The formation of these species is responsible for the so-called "silver effects",[18] which have been recently investigated in detail.[17b,19]

Alternative silver-free activation protocols include the use of copper salts as chloride scavengers,[20] or the cationization of alkylgold[21] and gold hydroxide[22] precursors via protonolysis with Brønsted acids.

---

16 (a) Dickson, P. N.; Wehrli, A.; Geier, G. *Inor. Chem.* **1988**, *27*, 2921–2925. (b) Nieto-Oberhuber, C.; López, S.; Muñoz, M. P.; Cárdenas, D. J.; Buñuel, E.; Nevado, C.; Echavarren, A. M. *Angew. Chem. Int. Ed.* **2005**, *44*, 6146−6148. (c) Brown, T. J.; Dickens, M. G.; Widenhoefer, R. A. *Chem. Commun.* **2009**, 6451−6453. (d) Schmidbaur, H.; Schier, A. Organometallics **2010**, *29*, 2–23. (e) Xi, Y.; Wang, Q.; Su, Y.; Li, M.; Shi, X. *Chem. Commun.* **2014**, *50*, 2158−2160. (f) Pacheco, E. A.; Tiekink, E. R. T; Whitehouse, M. W. *Gold Chemistry: Applications and Future Directions in the Life Sciences*, Mohr, F. Ed. Chapter 6, **2009**, 283–287. Willey-VCH Verlag, GmbH & Co.

17 Zhu, Y.; Day, C. S.; Zhang, L.; Hauser, K. J.; Jones, A. C. *Chem.–Eur. J.* **2013**, *19*, 12264−12271. (b) Homs, A.; Escofet, I.; Echavarren, A. M. *Org. Lett.* **2013**, *15*, 5782−5785.

18 Wang, D.; Cai, R.; Sharma, S.; Jirak, J.; Thummanapelli, S. K.; Akhmedov, N. G.; Zhang, H.; Liu, X.; Petersen, J. L.; Shi, X. *J. Am. Chem. Soc.* **2012**, *134*, 9012−9019.

19 Ranieri, B.; Escofet, I.; Echavarren, A. M. *Org. Biomol. Chem.* **2015**, *13*, 7103–7118.

20 Guérinot, A.; Fang, W.; Sircoglou, M.; Bour, C.; Bezzenine-Lafollée, S.; Gandon, V. *Angew. Chem. Int. Ed.* **2013**, *52*, 5848–5852.

21 Nieto-Oberhuber, C.; Muñoz, M. P.; Buñuel, E.; Nevado, C.; Cárdenas, D. J.; Echavarren, A. E. *Angew. Chem. Int. Ed.* **2004**, *43*, 2402−2406.

22 For selected examples see: (a) Gaillard, S.; Slawin, A. M. Z.; Nolan, S. P. *Chem. Commun.* **2010**, *46*, 2742−2744. (b) Gaillard, C.; Bosson, J.; Ramón, R. S.; Nun, P.; Slawin, A. M. Z.; Nolan, S. P. *Chem.–Eur. J.* **2010**, *16*, 13729−13740.

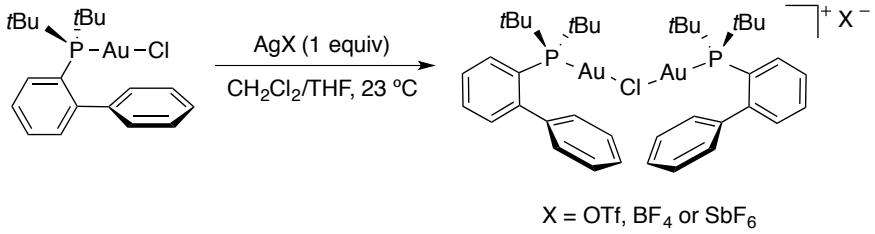

Scheme 3. Formation of bridged dinuclear gold(I) complexes [((JohnPhos)Au)$_2$Cl]X

Our group pioneered the design and synthesis of air-stable cationic gold(I) catalysts, which can be isolated as crystalline solids by reacting different [LAuCl] complexes with silver salts featuring non-coordinating anions in the presence of labile ligands, such as nitriles.[23] The most common ones are represented in Figure 3. Related complexes with 1,2,3-triazole as the ligand[16e,24] and neutral gold(I) catalysts [LAuNTf$_2$] based on the use of the bis(trifluoromethanesulfonyl)imidate ligand were also reported.[25]

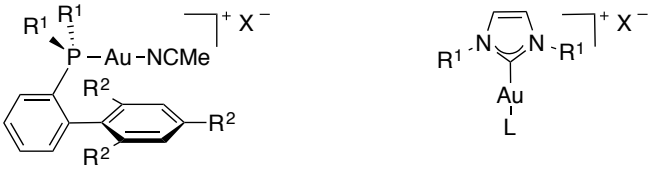

A: R^1 = *t*Bu, R^2 = H, X = SbF$_6$
B: R^1 = *t*Bu, R^2 = *i*Pr, X = SbF$_6$
C: R^1 = *t*Bu, R^2 = *i*Pr, X = BAr$_4^F$
D: R^1 = Cy, R^2 = H, X = SbF$_6$
E: R^1 = Mes, L = tmbn, X = SbF$_6$
F: R^1 = 2,6-(*i*Pr)$_2$C$_6$H$_3$, L = tmbn, X = SbF$_6$
G: R^1 = 2,6-(*i*Pr)$_2$C$_6$H$_3$, L = PhCN, X = SbF$_6$
H: R^1 = 2,6-(*i*Pr)$_2$C$_6$H$_3$, L = PhCN, X = BAr$_4^F$

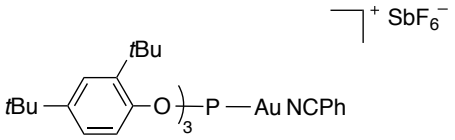

I

Figure 3. Representative cationic gold(I) complexes

23 (a) Herrero-Gómez, E.; Nieto-Oberhuber, C.; López, S.; Benet-Buchholz, J.; Echavarren, A. M. *Angew. Chem. Int. Ed.* **2006**, *45*, 5455–5459. (b) Amijs, C. H. M.; López-Carrillo, V.; Raducan, M.; Pérez-Galán, P.; Ferrer, C.; Echavarren, A. M. *J. Org. Chem.* **2008**, *73*, 7721–7730.

24 (a) Duan, H.; Sengupta, S.; Petersen, J. L.; Akhmedov, N. G.; Shi, X. *J. Am. Chem. Soc.* **2009**, *131*, 12100−12102. (b) Chen, Y.; Yan, W.; Akhmedov, N.; Shi, X. *Org. Lett*. **2010**, *12*, 344−347. (c) Wang, D.; Ye, X.; Shi, X. *Org. Lett.* **2010**, *12*, 2088−2091. (d) Hashmi, A. S. K.; Lothschütz, C. *ChemCatChem* **2010**, *2*, 133−134.

25 (a) Mézailles, N.; Ricard, L.; Gagosz, F. *Org. Lett.* **2005**, *7*, 4133–4136. (b) Ricard, L.; Gagosz, F. *Organometallics* **2007**, *26*, 4704–4707.

Homoleptic complexes such as $[Au(tmbn)_2]SbF_6$ (tmbn = trimethoxybenzonitrile) can also be used for the *in situ* preparation of a variety of chiral and achiral cationic complexes $[LAu(tmbn)]SbF_6$ by ligand exchange (Scheme 4).[26]

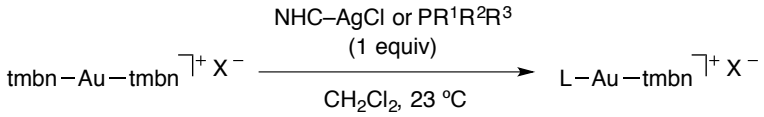

Scheme 4. Synthesis of cationic $[LAu(tmbn)]SbF_6$ starting from $[Au(tmbn)_2]SbF_6$

Gold(III) salts and complexes also present catalytic activity.[27] In some cases, switching from gold(I) to gold(III) could have a significant effect, even leading to divergent reaction pathways.[19b 28] Structurally, gold(III) complexes present a square planar geometry. Anionic, chelating ligands capable of stabilize the highly oxidizing metal are typically employed.[29]

The metal counterions proved of pivotal importance in impacting both kinetics and selectivity of gold-assisted transformations.[30,31] An important example of the anion effect was reported for intermolecular reactions of alkynes with alkenes.[32] In this case, the formation of unproductive σ,π–digold(I) alkyne complexes was minimized by using

26 Raducan, M; Rodríguez-Escrich, C; Cambeiro, X. C.; Escudero-Adán, E. C.; Pericàs, M. A.; Echavarren, A. M. *Chem. Commun.* **2011**, *47*, 4893–4895.

27 For selected examples see: (a) Hashmi, A. S. K.; Weyrauch, J. P.; Rudolph, M.; Kurpejovi, E. *Angew. Chem. Int. Ed.* **2004**, *43*, 6545–6547. (b) Corma, A., González-Arellano, C., Iglesias, M.; Sánchez, F. *Angew. Chem. Int. Ed.* **2007**, *46*, 7820–7822. (c) Kung, K. K.-Y.; Lo, V. K.-Y.; Ko, H.-M.; Li, G.-L.; Chan, P.-Y.; Leung, K.-C.; Zhou, Z.; Wang, M.-Z.; Che, C.-M.; Wong, M.-K. *Adv. Synth. Catal.* **2013**, *355*, 2055–2070. (d) Yang, Y.; Hu, W.; Ye, X.; Wang, D.; Shi, X. *Adv. Synth. Catal.* **2016**, *358*, 2583–2588.

28 (a) Ferrer, C.; Echavarren, A. M. *Angew. Chem. Int. Ed.* **2006**, *45*, 1105–1110; (b) Ung, G.; Soleilhavoup, M.; Bertrand, G. *Angew. Chem. Int. Ed.* **2013**, *52*, 758–761.

29 Lloyd-Jones, G. C. *Org. Biomol. Chem.* **2003**, *1*, 215–236.

30 Bandini, M., Bottoni, A., Chiarucci, M., Cera, G., Miscione, G. P. *J. Am. Chem. Soc.* **2012**, *134, 2*0690–20700.

31 A review on counterion effects in homogeneous gold catalysis: Jia, M.; Bandini, M. *ACS Catal.* **2015**, *5*, 1638–1652.

32 Homs, A.; Obradors, C.; Leboeuf, D.; Echavarren, A. M. *Adv. Synth. Catal.* **2014**, *356*, 221−228.

the bulky and noncoordinating anion BAr_4^{F-}. Furthermore, important counterion effects were observed in the enantioselectivity of several gold-catalyzed reactions.[31,33]

Activation of π–bonds with Gold(I) Complexes

The interaction of gold(I) with alkynes can be rationalized by the Dewar-Chatt-Duncanson model.[34] Hence, the metal-acetylene bonding is described as a combination of a σ-interaction (interaction of the π-bond of the alkyne with the empty orbital on the metal) and a backbonding π-interaction (donation of the metal to the π* orbitals to the alkyne, Figure 4). In the case of gold(I), the 5*d* electrons are too low in energy for a significant backbonding to anti-bonding orbitals but not to empty non-bonding orbitals.[6] Furthermore, alkynes are strong two-electron σ-donors but fairly weak π-acceptors towards gold(I).[35]

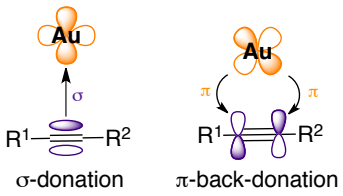

Figure 4. Dewar-Chatt-Duncanson model

Several mononuclear two-coordinate π-complexes with alkynes have been reported,[36] as well as with alkenes,[16c,37] 1,3-dienes[38] and allenes.[39]

---

33 For selected examples see: (a) Hamilton, G. L.; Kang, E. J.; Mba, M.; Toste, F. D. *Science*, **2007**, *317*, 496–499. (b) LaLonde, R. L.; Sherry, B. D.; Kang, E. J.; Toste, F. D. *J. Am. Chem. Soc.* **2007**, *129*, 2452–2453. (c) Cala, L.; Mendoza, A.; Fañanás, F. J.; Rodríguez, F. *Chem. Commun.* **2013**, *49*, 2715−2717. (d) Handa, S.; Lippincott, D. J.; Aue, D. H.; Lipshutz, B. H. *Angew. Chem. Int. Ed.* **2014**, *53*, 10658−10662.

34 (a) Dewar, M. J. S. *Bull. Soc. Chim. Fr.* **1951**, *18*, C71–C79. (b) Chatt, J.; Duncanson, L. A. *J. Chem. Soc.* **1953**, 2939–2947.

35 For selected examples see: (a) Hertwig, R. A.; Koch, W.; Schröder, D.; Schwarz, H.; Hrusak, J.; Schwerdtfeger, P. *J. Phys. Chem.* **1996**, *100*, 12253–12260. (b) Nechaev, M. S.; Rayón, V. M.; Frenking, G. *J. Phys. Chem. A* **2004**, *108*, 3134–3142.

36 For selected examples see: (a) Flügge, S.; Anoop, A.; Goddard, R.; Thiel, W.; Fürstner, A. *Chem.–Eur. J.* **2009**, *15*, 8558–8565. (b) Hooper, T. N.; Green, M.; Russell, C. A. *Chem. Commun.* **2010**, *46*, 2313–2315. (c) Brown, T. J.; Widenhoefer, R. A. *J. Organomet. Chem.* **2011**, *696*, 1216–1220.

Despite the observed selective activation of the alkyne moiety, gold(I) complexes do not coordinate selectively to alkynes over alkenes.[35b,40] Thus, it is the nucleophile present in the reaction media that shows a preference for attack at gold(I)-alkynyl species, which present a lower LUMO than their alkene analogues.[41]

Nucleophilic Attack

Typically, after coordination of the metal to the alkyne, subsequent nucleophilic attack onto η^2-alkyne Au(I) complexes gives *trans*-alkenyl species (Scheme 5).[5] On the other hand, the mechanistically very different insertion of alkynes and allenes into Au–Si bonds proceeds in a *syn* manner.[42]

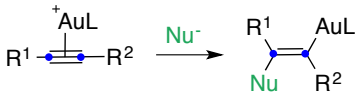

Scheme 5. Markovnikov nucleophilic attack to η^2-alkyne Au(I) complexes

Different carbon and heteroatom-containing molecules such as alkenes,[5] arenes,[43] heteroarenes,[28a,44] alcohols,[3,45] amines,[46] imines,[47] sulfoxides,[48] *N*-oxides[49] and thiols[50]

---

37 For selected examples see: (a) Brown, T. J.; Dickens, M. G.; Widenhoefer, R. A. *J. Am. Chem. Soc.* **2009**, *131*, 6350–6351. (b) Broomer, R. E. M.; Widenhoefer, R. A. *Organometallics* **2012**, *31*, 768–771. (c) Brooner, R. E. M.; Brown, T. J.; Widenhoefer, R. A. *Chem.–Eur. J.* **2013**, *19*, 8276–8284.

38 (a) Sanguramath, R. A.; Hooper, T. N.; Butts, C. P.; Green, M.; McGrady, J. E.; Russell, C. A. *Angew. Chem. Int. Ed.* **2011**, *50*, 7592− 7595. (b) Brooner, R. E. M.; Widenhoefer, R. A. *Organometallics* **2011**, *30*, 3182−3193. (c) Krossing, I. *Angew. Chem. Int. Ed.* **2011**, *50*, 11576−11578.

39 (a) Brown, T. J.; Sugie, A.; Dickens, M. G.; Widenhoefer, R. A. *Organometallics* **2010**, *29*, 4207−4209. (b) Brown, T. J.; Sugie, A.; Leed, M. G. D.; Widenhoefer, R. A. *Chem.–Eur. J.* **2012**, *18*, 6959−6971. (c) Johnson, A.; Laguna, A.; Gimeno, M. C. *J. Am. Chem. Soc.* **2014**, *136*, 12812−12815.

40 García-Mota, M.; Cabello, N.; Maseras, F.; Echavarren, A. M.; Pérez-Ramírez, J.; López, N. *ChemPhysChem* **2008**, *9*, 1624–1629.

41 Fleming, I. Frontier Orbitals and Organic Chemical Reactions **1976** (Wiley, Chichester).

42 Joost, M.; Gualco, P.; Mallet-Ladeira, S.; Amgoune, A.; Bourissou, D. *Angew. Chem. Int. Ed.* **2013**, *52*, 7160–7163.

43 (a) Reetz, M. T.; Sommer, K. *Eur. J. Org. Chem.* **2003**, 3485–3496. (b) Nevado, C.; Echavarren, A. M. *Synthesis* **2005**, *2*, 167–182.

have been used as nucleophiles in either intra- or intermolecular gold(I)-catalyzed transformations.

Nature and Evolution of Gold(I) Intermediates

Although gold carbenes have commonly been proposed as key intermediates in many gold catalyzed reactions, there is some controversy surrounding the carbenic or cationic character of these organogold species.[51] Unfortunately, most of gold intermediates are too highly reactive to be readily isolated.[52]

In 2009, Toste and Goddart proposed a fundamental description of the bonding mode of gold carbenes. Accordingly, the ligand L and the carbene both donate their paired electrons to gold, forming a 3 center – 4 electron σ-hyperbond. The gold center can also form two π-bonds by backdonation of its electrons from two filled *d*-orbitals to empty π-acceptors on the ligand and carbene (Figure 5). Therefore, the ligand and the substituents will have a significant influence on the bonding and reactivity of a given

---

44 Hashmi, A. S. K; Haufe, P.; Schmid, C.; Rivas Nass, A.; Frey, W. *Chem.–Eur. J.* **2006**, *12*, 5376–5382.

45 Krauter, C. M.; Hashmi A. S. K.; Pernpointner, M. *ChemCatChem* **2010**, *2*, 1226–1230.

46 (a) Istrate, F. M.; Gagosz, F. *Org. Lett.* **2007**, *9*, 3181–3184. (b) Qian, J.; Liu, Y.; Cui, J.; Xu, Z. *J. Org. Chem.* **2012**, *77*, 4484–4490.

47 (a) Kusama, H.; Miyashita, Y.; Takay, J.; Iwasawa, N. *Org. Lett.* **2006**, *8*, 289–292. (b) Benedetti, E.; Lemière, G.; Chapellet, L. L.; Penoni, A.; Palmisano, G.; Malacria, M.; Goddard, J. P.; Fensterbank, L. *Org. Lett.* **2010**, *12*, 4396–4399.

48 (a) Shapiro, N. D.; Toste, F. D. *J. Am. Chem. Soc.* **2007**, *129*, 4160–4161. (b) Davies, P. W.; Albrecht, S. J. C. *Angew. Chem. Int. Ed.* **2009**, *48*, 8372–8375. (c) Shi, S.; Wang, T.; Yang, W.; Rudolph, M.; Hashmi, A. S. K. *Chem.–Eur. J.* **2013**, *19*, 6576–6580.

49 Ye, L.; Cui, L.; Zhang, G.; Zhang, L. *J. Am. Chem. Soc.* **2010**, *132*, 3258–3259.

50 (a) Nakamura, I.; Sato, T.; Yamamoto, Y. *Angew. Chem. Int. Ed*. **2006**, *45*, 4473–4475. (b) Nakamura, I.; Sato, T.; Terada, M.; Yamamoto, Y. *Org. Lett.* **2007**, *9*, 4081–4083.

51 Benitez, D.; N. D. Shapiro, N. D.; Tkatchouk, E.; Wang, Y.; Goddard, W. A.; Toste, F. D. *Nat. Chem.* **2009**, *1*, 482–486.

52 For selected examples in the observation of key species see: (a) Hashmi, A. S. K. *Angew. Chem. Int. Ed.* **2010**, *49*, 5232–5241. (b) Liu, L. P.; Hammond, G. B. *Chem. Soc. Rev.* **2012**, *41*, 3129–3139.

gold carbene.[53] Several illustrative examples that highlight the effect of the ligand on the character of the intermediate gold(I) species can be found in the literature.[23b,54]

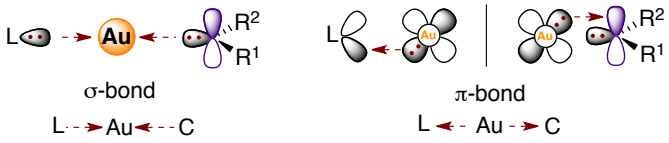

Figure 5. Schematic representation of the bonding of gold carbenes

In the case of reactions between alkynes and alkenes, the reaction takes place through proposed cyclopropyl gold(I) carbene species, which are highly distorted structures and can be represented as cyclopropyl gold(I) stabilized homoallylic carbocations (Figure 6). The nature of these species is determined by both the ligand used and the substitution pattern of the substrate.

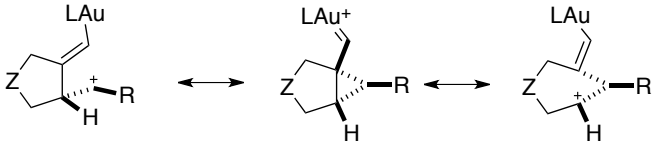

Figure 6. Structure of proposed cyclopropyl gold(I) carbene intermediates

Once the alkenyl gold(I) intermediates are formed, they can evolve through various pathways leading to a wide range of complex polycyclic structures. Although most of these transformations relied on intramolecular processes, a number of analogous intermolecular reactions have been developed in the last few years.[53]

Cycloisomerization of 1,n-Enynes

Cycloisomerizations of 1,6-enynes are one of the most extensively studied transformations in which an alkene acts as the nucleophile towards a gold(I) activated alkyne forming the proposed intermediates **II** and **VII** via *anti-5-exo-dig* or *6-endo-dig* pathway (Scheme 6).[21,55]

---

53 Wang, Y.; Muratore, M. E.; Echavarren, A. M. *Chem.–Eur. J.* **2015**, *21*, 7332–7339.

54 For selected examples see: (a) López, S.; Herrero-Gómez, E.; Pérez-Galán, P.; Nieto-Oberhuber, C.; Echavarren, A. M. *Angew. Chem. Int. Ed.* **2006**, *45*, 6029–6032. (b) Amijs, C. H. M.; Ferrer, C.; Echavarren, A. M. *Chem. Commun*. **2007**, 698–700.

55 (a) Ferrer, C.; Raducan, M.; Nevado, C.; Claverie, C. K.; Echavarren, A. M. *Tetrahedron* **2007**, *63*, 6306–6316. (b) Soriano, E.; Marco-Contelles, J. *Acc. Chem. Res.* **2009**, *42*, 1026–1036. (c) Escribano-Cuesta, A.; Perez-Galan, P.; Herrero-Gomez, E.; Sekine, M.;

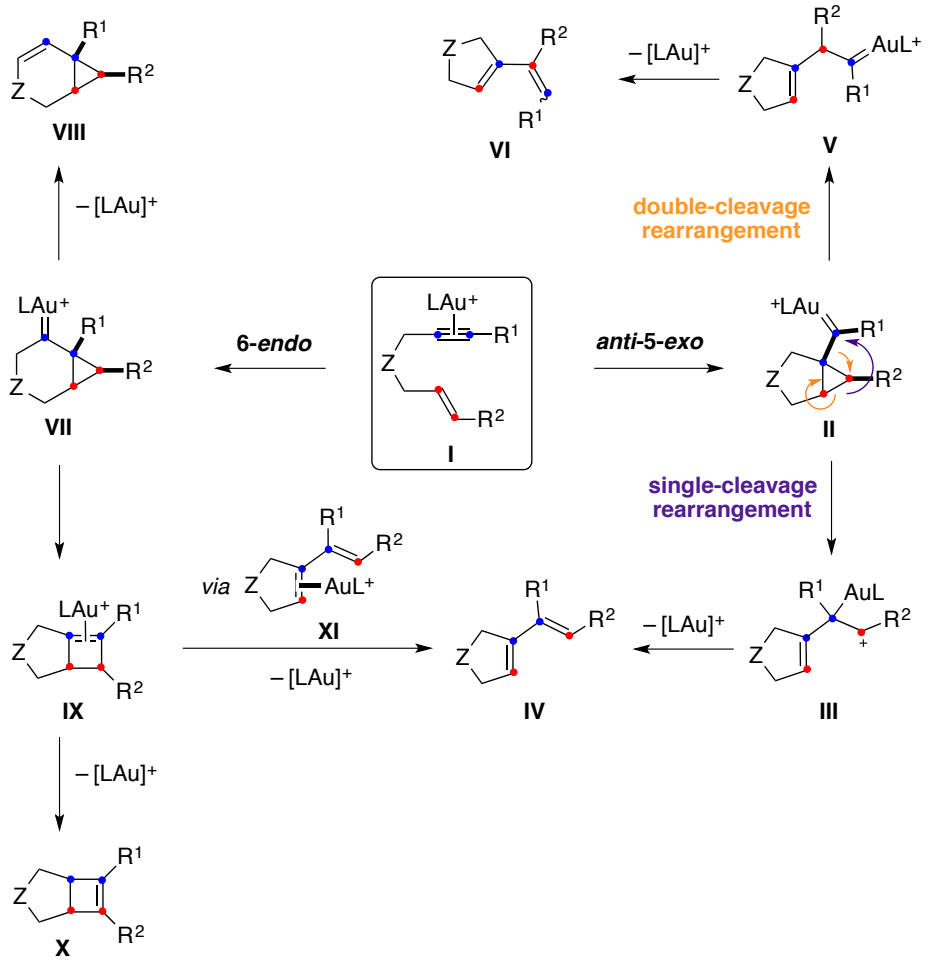

Scheme 6. General pathways for the gold(I)-catalyzed cycloisomerization of 1,6-enynes

In the absence of external or internal nucleophiles, cyclopropyl gold(I) carbene intermediates **II** (exo) can rearrange forming 1,3-dienes **IV** via a single-cleavage skeletal rearrangement. In this process, a formal 1,3-migration of the terminal carbon of the alkene towards the terminal carbon of the alkyne takes place. However, intermediates **II** can evolve to generate new rearranged carbenes **V** by the formal insertion of the terminal alkene carbon into the alkyne. A final α-proton elimination of these new carbenes gives rise to 1,3-dienes **VI**, the products of a double-cleavage rearrangement.

Braga, A. A. C.; Maseras, F.; Echavarren, A. M. *Org. Biomol. Chem.* **2012**, *10*, 6105–6111.

On the other hand, intermediates **VII** of *6-endo-dig* cyclization can lead to **VIII** by α-proton elimination and subsequent protodeauration.[56] Alternatively, **VII** can also rearrange to **IX**, which upon protodemetallation give highly strained bicyclo[3.2.0]hept-5-enes.[16b,55a, 57] Intermediates **IX** can also undergo isomerization to afford bicyclo[3.2.0]hept-2-enes derivatives **X**.[56a] Interestingly, the ring opening of **IX** give rise to gold(I) complexes **XI**, precursors of single-cleavage 1,3-dienes **IV**.

Similar mechanistic pathways are observed for 1,5-enynes[58] and 1,7-enynes.[59] However, the formation of strained bicyclic scaffolds is more common in the cyclization of higher 1,n-enynes ($7 \leq n \leq 16$)[16b,57b,60] as well as in the intermolecular reaction between alkynes and alkenes.[61]

56 (a) Nieto-Oberhuber, C.; López, S.; Echavarren, A. M. *J. Am. Chem. Soc.* **2005**, *127*, 6178–6179. (b) Nieto-Oberhuber, C.; Muñoz, M. P.; López, S.; Jiménez-Núñez, E.; Nevado, C.; Herrero-Gómez, E.; Raducan, M.; Echavarren, A. M. *Chem.–Eur. J.* **2006**, *12*, 1677–1693. (c) Nieto-Oberhuber, C.; Pérez-Galán, P.; Herrero-Gómez, E.; Lauterbach, T.; Rodríguez, C.; López, S.; Bour, C.; Rosellón, A.; Cárdenas, D. J.; Echavarren, A. M. *J. Am. Chem. Soc.* **2008**, *130*, 269–279. (d) Lee, Y. T.; Kang, Y. K.; Chung, Y. K. *J. Org. Chem.* **2009**, *74*, 7922–7934.

57 (a) Lee, S. I.; Kim, S. M.; Choi, M. R.; Kim, S. Y.; Chung, Y. K. *J. Org. Chem.* **2006**, *71*, 9366–9372. (b) Brooner, R. E. M.; Brown, T. J.; Widenhoefer, R. A. *Angew. Chem. Int. Ed.* **2013**, *52*, 6259–6261.

58 (a) Zhang, L.; Kozmin, S. *J. Am. Chem. Soc.* **2004**, *126*, 11806–11807. (b) Sun, J.; Conley, M.; Zhang, L.; Kozmin, S. *J. Am. Chem. Soc.* **2006**, *128*, 9705–9710. (c) López-Carrillo, V.; Huguet, N.; Mosquera, Á.; Echavarren, A. M. *Chem.–Eur. J.* **2011**, *17*, 10972–10978.

59 Cabello, N.; Rodríguez, C.; Echavarren, A. M. *Synlett* **2007**, 1753–1758.

60 (a) Odabachian, Y.; Gagosz, F. *Adv. Synth. Catal.* **2009**, *351*, 379–386. (b) Obradors, C.; Leboeuf, D.; Aydin, J.; Echavarren, A. M. *Org. Lett.* **2013**, *15*, 1576–1579.

61 López-Carrillo, V.; Echavarren, A. M. *J. Am. Chem. Soc.* **2010**, *132*, 9292–9294.

Nucleophilic Additions to 1,n-Enynes

Additions of oxygen, nitrogen or carbon nucleophiles to 1,n-enynes can also be carried out in the presence of gold(I) leading to products of hetero- or carbocyclization.[56b,62] As illustrated in Scheme 7, the nucleophilic attack to the cyclopropyl gold(I) carbene is regioselective and stereospecific.[21,63] Thus, the overall process is an *anti*-addition of the alkyne–gold(I) complex and the heteronucleophile to an alkene following the Markovnikov regiochemistry.

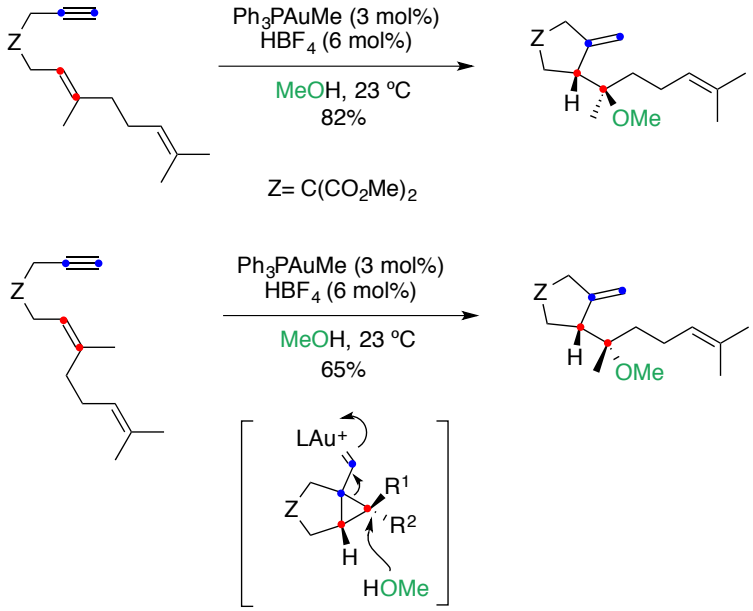

Scheme 7. *Anti*-addition of heteronucleophiles to 1,6-enynes

The intra- and intermolecular reactions of enynes with carbonyl compounds in the presence of gold(I) catalysts lead to a variety of products depending on the substitution pattern of the alkene as well as the nature of the carbonyl compound.[63] Thus, for example, oxo-1,n-enynes (n = 5, 6) are prone to undergo a formal [2+2+2] alkyne/alkene/carbonyl cycloaddition to afford oxatricyclic compounds, in which two

62 For some examples in gold(I)-catalyzed intramolecular reactions: (a) Fürstner, A.; Morency, L. *Angew. Chem. Int. Ed.* **2008**, *47*, 5030–5033. (b) Zhang, L.; Kozmin, S. A. *J. Am. Chem. Soc.* **2005**, *127*, 6962–6963. For some examples in gold(I)-catalyzed intermolecular reactions: (c) Chao, C.-M.; Toullec, P. Y.; Michelet, V. *Tetrahedron Lett.* **2009**, *50*, 3719–3722. (d) Buzas, A. K.; Istrate, F. M.; Gagosz, F. *Angew. Chem. Int. Ed.* **2007**, *46*, 1141–1144.

63 Dorel, R.; Echavarren, A. M. *J. Org. Chem.* **2015**, *80*, 7321−7332.

C–C and one C–O bonds are formed (see **Chapter 2**).[64,65] Following an analogous mechanism, 1,6-enynes **1** react with aromatic aldehydes to give oxabicyclic adducts of type **2** together with dienes **3**,[66] whilst spirocyclic cyclopentenones **4** can be obtained when cyclopropenones are used (Scheme 8).[67]

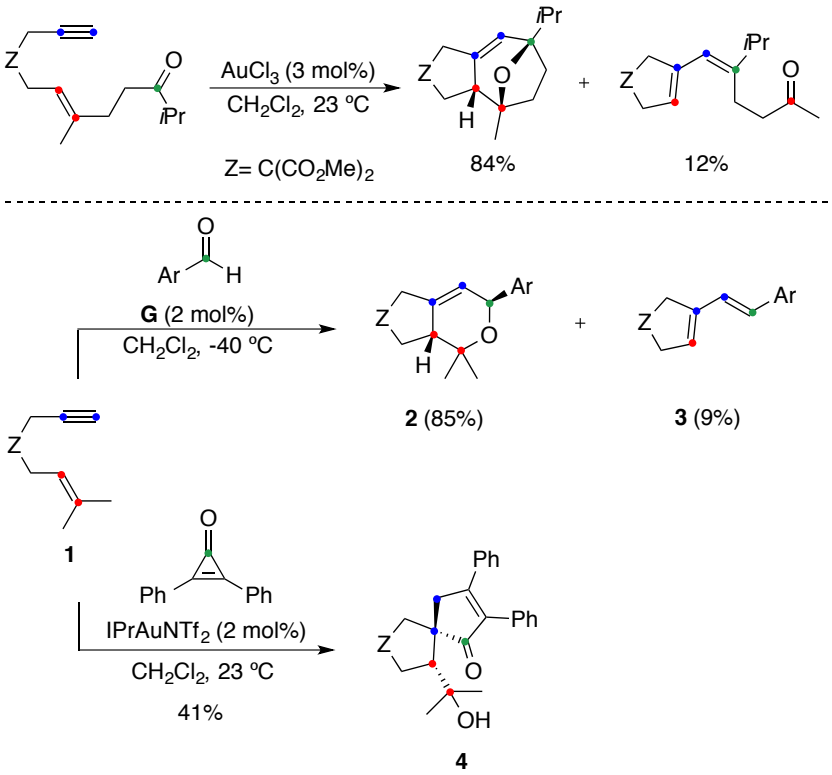

Scheme 8. Intra- and intermolecular cycloadditions of 1,6-enynes and carbonyl compounds

Electron-rich arenes and heteroarenes can also act as nucleophiles reacting with 1,n-enynes. A particular case is the cyclization of aryl-substituted enynes **5** (see **Chapter 3**), which lead stereospecifically to tricyclic products **6** through a formal [4+2] cycloaddition process (Scheme 9).[56a]

64 Jiménez-Núñez, E.; Claverie, C. K.; Nieto-Oberhuber, C.; Echavarren, A. M. *Angew. Chem. Int. Ed.* **2006**, *45*, 5452−5455.

65 For oxo-1,5-enynes see: (a) Huguet, N.; Echavarren, A. M. *Synlett* **2012**, *23*, 49−53. (b) Calleja, P.; Muratore, M. E.; Jiménez, T.; Echavarren, A. M. *Synthesis* **2016**, *48*, 3183–3198.

66 Escribano-Cuesta, A.; López-Carrillo, V.; Janssen, D.; Echavarren, A. M. *Chem.–Eur. J.* **2009**, *15*, 5646–5650.

67 Matsuda, T.; Sakurai, Y. *J. Org. Chem.* **2014**, *79*, 2739−2745.

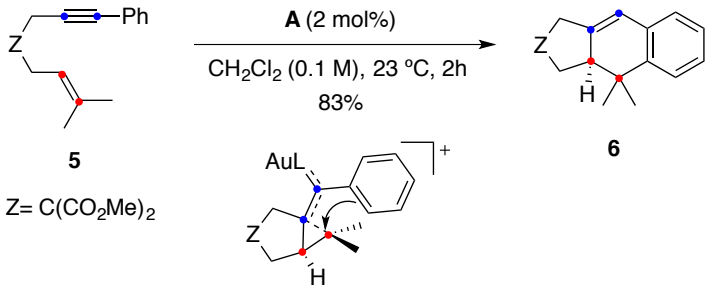

Scheme 9. [4+2] Cyclization of aryl-substituted 1,6-enyne **5**

Cyclopropanation of Enynes

Gold(I) carbene-like intermediates can also be trapped by alkenes via intra-[21,68] or intermolecular[54b,69] pathways leading to cyclopropane rings. Dienynes **7** bearing an alkoxy group at the propargylic position led to tricyclic compounds **8** through a tandem cyclization/1,5-OR migration/intramolecular cyclopropanation process (Scheme 10).[70] In the presence of an external nucleophile, intermediate **10** could also be trapped intermolecularly prior to the cyclopropanation with the pending alkene to generate **9**. Analogous 1,6-enynes react smoothly with 1,3-diketones and β-ketoesters leading to products of α-alkylation through related transformations (see **Chapter 4**).[71]

68 (a) Nieto-Oberhuber, C.; López, S.; Muñoz, M. P.; Jiménez-Núñez, E.; Buñuel, E.; Cárdenas, D. J.; Echavarren, A. M. *Chem.–Eur. J.* **2006**, *12*, 1694–1702. (b) Kim, S. M.; Park, J. H.; Choi, S. Y.; Chung, Y. K. *Angew. Chem. Int. Ed.* **2007**, *46*, 6172–6175.

69 Pérez-Galán, P.; Herrero-Gómez, E.; Hog, D. T.; Martin, N. J. A.; Maseras, F.; Echavarren, A. M. *Chem. Sci.* **2011**, *2*, 141–149.

70 Jiménez-Núñez, E.; Raducan, M.; Lauterbach, T.; Molawi, K.; Solorio, C. R.; Echavarren, A. M. *Angew. Chem. Int. Ed.* **2009**, *48*, 6152–6155.

71 Calleja, P.; Pablo, Ó.; Ranieri, B.; Gaydou, M.; Pitaval, A.; Moreno, M.; Raducan, M.; Echavarren, A. M. *Chem.–Eur. J.* **2016**, *22*, 13613–13618.

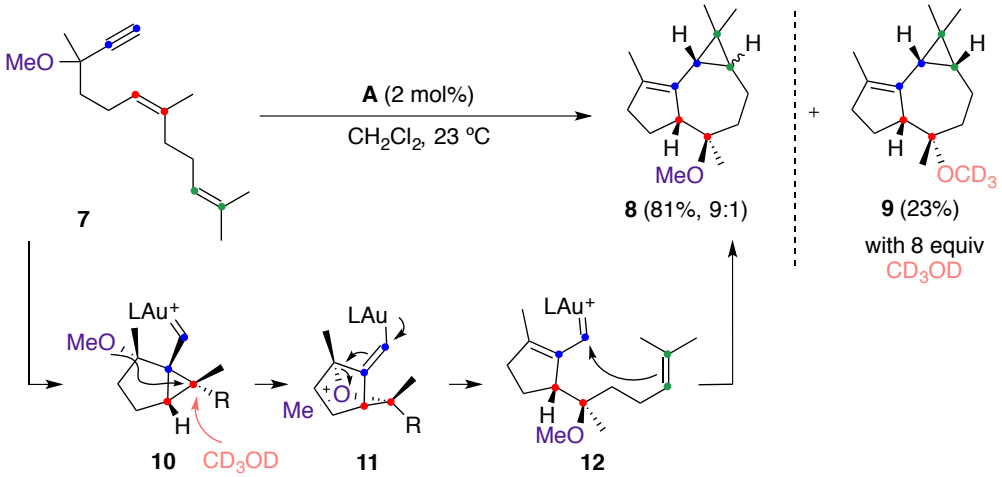

Scheme 10. Tandem cyclization/1,5-OR migration/cyclopropanation of dienyne **7**

Oxidative Gold(I)-Catalyzed Reactions

Generation of α-oxo gold(I) carbenes/carbenoids has been recently described via intra- and intermolecular gold(I)-catalyzed oxidation of alkynes (Scheme 11).[72] So far, sulfoxides,[48a,73] pyridine *N*-oxides,[74] nitrones,[75] nitroso- and nitrobenzenes,[76] as well as epoxides,[77] have been used as oxidizing agents. Remarkably, this strategy circumvents the use of hazardous diazo compounds for the generation of these reactive species.

---

72 For important reviews see: (a) Zhang, L. *Acc. Chem. Res.* **2014**, *47*, 877–888. (b) Zheng, Z.; Wang, Z.; Wang, Y. Zhang, L. *Chem. Soc. Rev*. **2016**, *45*, 4448–4458.

73 Li, G.; Zhang, L. *Angew. Chem. Int. Ed.* **2007**, *46*, 5156− 5159.

74 For selected examples see: (a) Cui, L.; Peng, Y.; Zhang, L. *J. Am. Chem. Soc.* **2009**, *131*, 8394−8395. (b) Qian, D.; Zhang, J. *Chem. Commun.* **2011**, *47*, 11152−11154. (c) Davies, P. W.; Cremonesi, A.; Martin, N. *Chem. Commun.* **2011**, *47*, 379−381. (d) Wang, T.; Huang, L.; Shi, S.; Rudolph, M.; Hashmi, A. S. K. *Chem.–Eur. J.* **2014**, *20*, 14868−14871.

75 (a) Yeom, H. S.; Lee, J. E.; Shin, S. *Angew. Chem. Int. Ed.* **2008**, *47*, 7040−7043. (b) Yeom, H. S.; Lee, Y.; Jeong, J.; So, E.; Hwang, S.; Lee, J. E.; Lee, S. S.; Shin, S. *Angew. Chem. Int. Ed.* **2010**, *49*, 1611− 1614. (c) Mukherjee, A.; Dateer, R. B.; Chaudhuri, R.; Bhunia, S.; Karad, S. N.; Liu, R.-S. *J. Am. Chem. Soc.* **2011**, *133*, 15372−15375.

76 (a) Jadhav, A. M.; Bhunia, S.; Liao, H.-Y.; Liu, R.-S. *J. Am. Chem. Soc.* **2011**, *133*, 1769−1771. (b) Kumar, C. V. S.; Ramana, C. V. *Org. Lett.* **2014**, *16*, 4766−4769. (c) Singh, R. R.; Liu, R.-S. *Chem. Commun.* **2014**, *50*, 15864−15866.

77 Hashmi, A. S. K.; Bührle, M.; Salathé, R.; Bats, J. *Adv. Synth. Catal.* **2008**, *350*, 2059−2064.

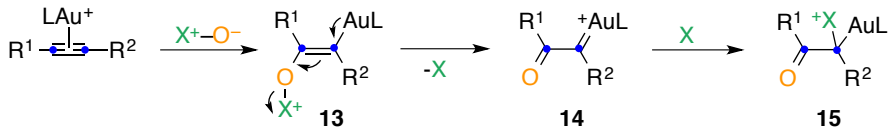

Scheme 11. Generation of α-oxo gold(I) carbenes/carbenoids by alkyne oxidation

Some controversy surrounds the involvement of α-oxo gold(I) carbenes **14** since the formation of gold(I) carbenoids **15** by attack of the nucleophile to the highly electrophilic gold(I) carbene is more likely.[78] In other related cases, β-alkoxy alkenylgold(I) intermediates **13** rather than **14** have also been proposed.[79]

The gold carbene moiety is invariably positioned at the terminus upon oxidation of terminal alkynes whilst internal alkynes show little selectivity.[72a] Nonetheless, α,β-unsaturated ketones could be obtained via highly regioselective oxidation of internal alkynes using 8-alkylquinoline *N*-oxides as oxidants and in the absence of acid additives.[80]

The initially formed α-oxo gold(I) carbenes could then be trapped intramolecularly by a nucleophile present in the starting alkyne,[81] or intermolecularly by external nucleophiles.[82] Thus, for example, chroman-3-ones **18** can be obtained from propargyl aryl ethers **16** by intramolecular Friedel-Crafts-type trapping of **17**,[81a] while

78 Schulz, J.; Jašíková , L.; Škríba, A.; Roithová, J. *J. Am. Chem. Soc.* **2014**, *136*, 11513−11523.

79 For selected examples see: (a) Henrion, G.; Chavas, T. E. J.; Le Goff, X.; Gagosz, F. *Angew. Chem. Int. Ed.* **2013**, *52*, 6277−6282. (b) Noey, E. L.; Luo, Y.; Zhang, L.; Houk, K. N. *J. Am. Chem. Soc.* **2012**, *134*, 1078−1084.

80 Lu, B.; Li, C.; Zhang, L. *J. Am. Chem. Soc.* **2010**, *132*, 14070−14072.

81 For selected examples see: (a) Wang, Y.; Ji, K.; Lan, S.; Zhang, L. *Angew. Chem. Int. Ed.* **2012**, *51*, 1915−1918. (b) Ji, K.; Zhao, Y.; Zhang, L. *Angew. Chem. Int. Ed.* **2013**, *52*, 6508−6512. (c) Shu, C.; Li, L.; Xiao, X. Y.; Yu, Y. F.; Ping, Y. F.; Zhou, J. M.; Ye, L. W. *Chem. Commun.* **2014**, *50*, 8689−8692.

82 For selected examples see: (a) Shen, C. H.; Li, L.; Zhang, W.; Liu, S.; Shu, C.; Xie, Y. E.; Yu, Y. F.; Ye, L. W. *J. Org. Chem.* **2014**, *79*, 9313−9318. (b) Nösel, P.; Moghimi, S.; Hendrich, C.; Haupt, M.; Rudolph, M.; Rominger, F.; Hashmi, A. S. K. *Adv. Synth. Catal.* **2014**, *356*, 3755−3760.

functionalized indoles **19** can be accessed from o-alkynyl anilines and ynamides through a gold(I)-catalyzed tandem cycloisomerization/intermolecular trapping of the *in situ* generated α-oxo carbene (Scheme 12).[82a]

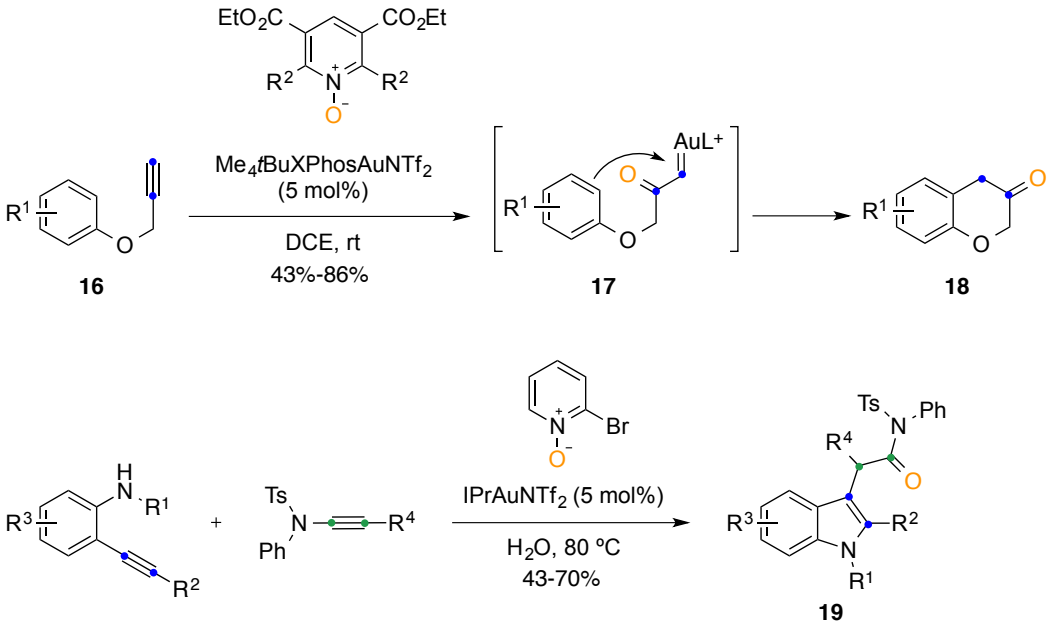

Scheme 12. Intra- *vs*. intermolecular trapping of α-oxo gold(I) carbene intermediates

The oxidative cyclization of 1,n-enynes in the presence of gold(I) has also been explored. The first example was reported for the gold(I)-catalyzed oxidative cyclization of 1,6-enynes using Ph_2SO as stoichiometric oxidant to give bicyclic products **20** with a pendant aldehyde (Scheme 13).[83]

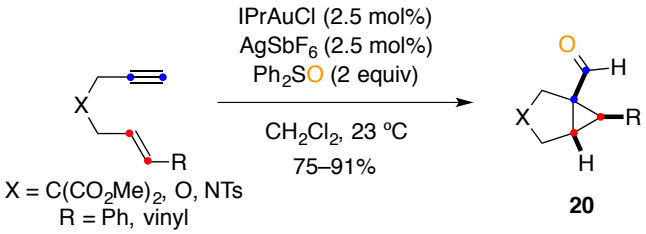

Scheme 13. First gold(I)-catalyzed oxidative rearrangement of 1,6-enynes

Similarly, bicyclo[n.1.0]alkanes **21** have been obtained by an intramolecular oxidative-cyclopropanation one-pot sequence from 1,6- and 1,7-enynes using pyridine *N*-oxides as additives (Scheme 14).[74b] Moreover, the enantioselective version of this transformation has been reported using cationic chiral phosphoramidite gold(I)

83 Witham, C. A.; Mauleón, P.; Shapiro, N. D.; Sherry, B. D.; Toste, F. D. *J. Am. Chem. Soc.* **2007**, *129*, 5838–5839.

complexes.[84] Similarly, an asymmetric intramolecular cyclopropanation of 1,5-enynes in the presence of gold(I) complexes bearing a novel P,N-bidentate ligand provides access to bicyclic products.[85]

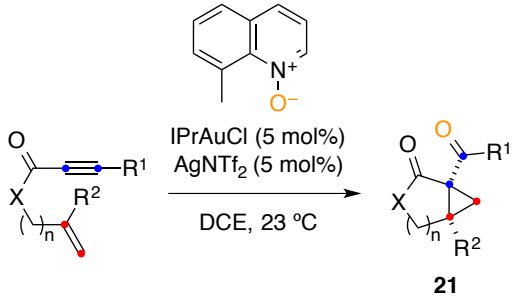

Scheme 14. Synthesis of [n.1.0]bicyclicalkanes **21** from 1,6- and 1,7-enynes

The gold(I)-catalyzed oxidative cyclization of 1,5-enynes proved to be highly dependent on the particular oxidant used and the substitution pattern of the starting substrate. As an illustrative example, the reaction of 3,5-dien-1-ynes with distinct pyridine *N*-oxides could lead to cyclopropa[*a*]inden-6(1*H*)-ones **22**[86] or cyclopentadienyl aldehydes **23** (Scheme 15).[87] Also noteworthy is the synthesis of various indanone and cyclopentenone derivatives starting from *cis*-substituted 3-en-1-ynes (see **Chapter 1**).[88] Finally, a remarkable number of reports on somewhat related transformations have been published over the last decade.[89,90,91]

---

84 Qian, D.; Hu, H.; Liu, F.; Tang, B.; Ye, W.; Wang, Y.; Zhang, J. *Angew. Chem. Int. Ed.* **2014**, *53*, 13751–13755.

85 Ji, K.; Zheng, Z.; Wang, Z.; Zhang, L. *Angew. Chem. Int. Ed.* **2015**, *54*, 1245–1249.

86 Vasu, D.; Hung, H.-H.; Bhunia, S.; Gawade, S. A.; Das, A.; Liu, R.-S. *Angew. Chem. Int. Ed.* **2011**, *50*, 6911–6914.

87 Hung, H.-H.; Liao, Y.-C.; Liu, R.-S. *J. Org. Chem.* **2013**, *78*, 7970−7976.

88 Bhunia, S.; Ghorpade, S.; Huple, D. B.; Liu, R.-S. *Angew. Chem. Int. Ed.* **2012**, *51*, 2939–2942.

89 For selected publications on related transformations see: (a) Wang, K.-B.; Ran, R.-Q.; Xiu, S.-D.; Li, C.-Y. *Org. Lett.* **2013**, *15*, 2374–2377. (b) Huple, D. B.; Ghorpade, S.; Liu, R.-S. *Chem.–Eur. J.* **2013**, *19*, 12965–12929. (c) Uetake, Y.; Niwa, T.; Nakada, M. *Tetrahedron Lett.* **2014**, *55*, 6847–6850.

90 For intramolecular additions of azides to alkynes see: (a) Yan, Z.-Y.; Xiao, Y.; Zhang, L. *Angew. Chem. Int. Ed.* **2012**, *51*, 8624–8627. (b) Tokimizu, Y.; Oishi, S.; Fujii, N.; Ohno, H. *Org. Lett.* **2014**, *16*, 3138–3141.

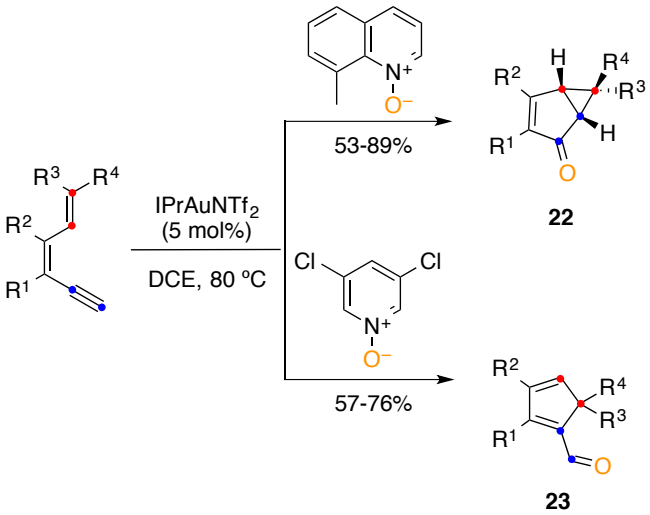

Scheme 15. Gold(I)-catalyzed oxidative cyclization of 3,5-dien-1-ynes

91 For oxidative cyclizations on 1,4-enynes see: Ghorpade, S.; Su, M.-D.; Liu, R.-S. *Angew. Chem. Int. Ed.* **2013**, *52*, 4229–4234.

Chapter I:

Gold(I)-Catalyzed Synthesis of Trindene C_{15} Cores for the Assembly of C_{3h} Star-Shaped Polyarenes and a New Crushed C60:

Introduction

Since the discovery[1] and isolation[2] of fullerene C_{60}, the development of a general and effective route for the preparation of C_{60} and other geodesic polyarenes has been an appealing challenge in organic synthesis.[3] The unusual curved networks of trigonal carbon atoms of fullerene-based materials, as well as their unique photophysical,[4] electronic,[5] and charge transfer properties[6] have stimulated significant interest in the preparation of π-conjugated systems featuring defined fragments of the skeleton of C_{60}. Indeed, much effort has been devoted to the use of simple hydrocarbons representing sizable parts of the C_{60} and, thus, with the appropriate C–C connectivity to allow the direct generation of the sphere.

In this context, trindane (tris(cyclopenteno)benzene) (**1**) features one-fourth of the carbon skeleton of C_{60}, and therefore could be an interesting building block for the synthesis of fullerene derivatives. Nevertheless, progress on the use of this C_{15} scaffold as a building block for the synthesis of polyarenes has been slow.[7,8,9]

---

1 Kroto, H. W.; Heath, J. R.; O'Brien, S. C.; Curl, R. F.; Smalley, R. E. *Nature* **1985**, *318*, 162–163.

2 (a) Krätschmer, W.; Fostiropoulos, K.; Huffman, D. R. *Nature* **1990**, *347*, 354–358. (b) Taylor, R.; Hare, J. P.; Lamb, L. D.; Abdul-Sada, A. K.; Kroto, H. W. *J. Chem. Soc., Chem. Commun.* **1990**, 1423–1425.

3 Scott, L. T. *Angew. Chem. Int. Ed*. **2004**, *43*, 4994–5007.

4 Schuster, D. I.; Cheng, P.; Jarowski, P. D.; Guldi, D. M.; Luo, C.; Echegoyen, L.; Pyo, S.; Holzwarth, A. R.; Braslavsky, S. E.; Williams, R. M.; Klihm, G. *J. Am. Chem. Soc.* **2004**, *126*, 7257–7270.

5 Arena, F.; Bullo, F.; Conti, F.; Corvaja, C.; Maggini, M.; Prato, M.; Scorrano, G. *J. Am. Chem. Soc.* **1997**, *119*, 789–795.

6 Guldi, D. M.; Feng, L.; Radhakrishnan, S. G.; Nikawa, H.; Yamada, M.; Mizorogi, N.; Tsuchiya, T.; Akasaka, T.; Nagase, S.; Herranz, M. Á.; Martín, N. *J. Am. Chem. Soc.* **2010**, *132*, 9078–9086.

7 Fabre, C.; Rassat, A. C. R. *Acad. Sci., Ser. 2* **1989**, *308*, 1223–1227.

8 Ferrier, R. J.; Holden, S. G.; Gladkikh, O. *J. Chem. Soc., Perkin Trans. 1* **2000**, 3505–3512.

9 Gupta, H. K.; Lock, P. E.; McGlinchey, M. J. *Organometallics* **1997**, *16*, 3628–3634.

Synthesis of Trindane and Trindene

Trindane (**1**) was reported for the first time in 1897 as a minor product by the action of HCl on cyclopentanone.[10] More than one hundred years later, appeared in the literature the first standard protocol for its synthesis.[11] Accordingly, treatment of cyclopentanone with sulfuric acid in dry ethanol under refluxing conditions leads to the formation of **1** in 33% yield (Scheme 1). Other reagents, such as $TiCl_4$,[12] $SiCl_4$[13] or $SOCl_2$,[14] catalyze this transformation using milder reaction conditions.[15,16]

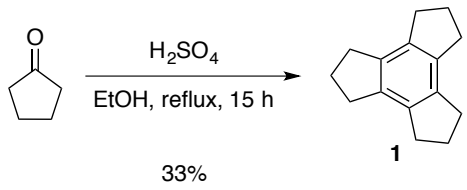

Scheme 1. Trimerization of cyclopentanone

As illustrated in Scheme 2, other synthetic alternatives have been developed. Thus, the azine of cyclopentanone (**2**) led to **1** after treatment with hydrogen chloride in tetrahydronaphtalene.[17] On the other hand, treatment of dodecachlorodihydrotrindene (**4**) with an excess of lithium and *tert*-butanol in THF afforded **1** in 50% yield.[18] Alternatively, the Diels-Alder reaction of cyclopentene-1,2-dicarboxylic anhydride (**5**)

10 Wallach, O. *Chem. Ber.* **1897**, *30*, 1094–1096.

11 Ranganathan, S.; Muraleedharan, K. M.; Bharadwaj, P.; Madhusudanan, K. P. *Chem. Commun.* **1998**, 2239–2240.

12 Li, Z.; Sun, W-H; Jin, X.; Shao, C. *Synlett* **2001**, 1947–1949.

13 (a) Elmorsey, S. S.; Pelter, A.; Smith, K. *Tetrahedron Lett.* **1991**, *32*, 4175–4176. (b) Shirai, H.; Amano, N.; Hashimoto, Y.; Fukui, E.; Ishii, Y.; Ogawa, M. *J. Org. Chem.* **1991**, *56*, 2253–2256.

14 Hu, Z.; Dong, Z.; Liu, J.; Liu, W.; Zhu, X. *J. Chem. Res.* **2005**, 603–604.

15 For alternative catalytic systems based on the trimerization of cyclopentanone see: (a) Kotsuki, H.; Mehta, B. K.; Yanagisawa, K. *Synlett* **2001**, *8*, 1323–1325. (b) Mahmoodi, N. O.; Harjati, N. *J. Chin. Chem. Soc-Taip*. **2002**, *49*, 91–94. (c) Jing, X.; Xu, F.; Zhu, Q.; Ren, X.; Li, D.; Yan, C.; Shi, Y. *J. Indian Chem. B* **2006***, 45*, 2781–2783.

16 For the synthesis of trindane using zeolites see: (a) Huang, J.; Long, W.; Agrawal, P. K.; Jones, C. W. *J. Phys. Chem. C* **2009**, *113*, 16702–16710. (b) Xu, T.; Munson, E. J.; Haw, J. F. *J. Am. Chem. Soc.* **1994**, *116*, 1962–1972.

17 Perkin, W. H.; Plant, S. G. P. *J. Chem. Soc., Trans.* **1925**, *127*, 1138–1141.

18 McBee, E. T.; Dilling, W. L.; Braendlin, H. P. *J. Org. Chem.* **1963**, *28*, 2255–2257.

with diene **6** gave 1,2,3,4-tetrahydrotricyclotrimethylenebenzene-2,3-dicarboxylic anhydride (**7**), which upon decarboxylation and dehydration led to trindane (**1**).[19,20]

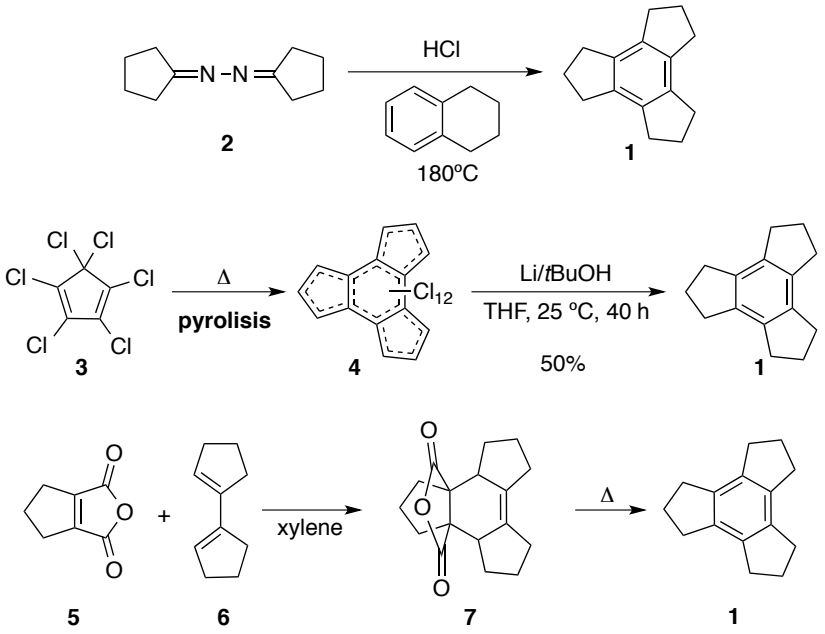

Scheme 2. Alternative synthetic routes to prepare trindane (**1**)

Another common approach for the synthesis of trisannulated benzenes is based on the trimerization of cycloalkynes.[21] Although uncatalyzed cyclotrimerization of highly strained cycloalkynes has been reported,[22] the addition of transition metal complexes as catalysts has been found determinant for the product formation in several cases.[23] With arynes, better results were achieved when palladium(0) or platinum(0) catalysts were added to the reaction mixture. Unfortunately, attempts to trimerize cyclopentyne by

19 Gupta, S. C.; Bhattacharjee, A. *J. Ind. Chem. Soc.* **1954**, *31,* 897–903.

20 Skvarehenko, V. R.; Chervoneva, L. A.; Pastukhova, I. S.; Levina, R. Y. *Zh. Obshch. Khim,* **1959**, *29,* 2174–2178**.**

21 Heilbronner, E.; Kovac, B.; Nutakul, W.; Taggart, A. D.; Thummel, R. P. *J. Org. Chem.* **1981**, *46*, 5279–5284.

22 (a) Hoffman, R. W. *Dehydrobenzene and Cycloalkynes*; Academic Press: New York, **1967**. (b) Wittig, G.; Mayer, U. *Chem. Ber.* **1963**, *96*, 329–341. (c) Wittig, G.; Mayer, U. *Chem. Ber.* **1963**, 96, 342–348. (d) Pericás, M. A.; Riera, A.; Rossell, O.; Serratosa, F.; Seco, M. *J. Chem. Soc., Chem. Commun.* **1988**, 942–943.

23 (a) Gassman, P. G.; Valcho, J. J. *J. Am. Chem. Soc.* **1975**, *97*, 4768–4770. (b) Gassman, P. G.; Gennick, I. *J. Am. Chem. Soc.* **1980***, 102,* 6863–6864. (c) Komatsu, K.; Akamatsu, H.; Okamoto, K. *J. Am. Chem. Soc.* **1988**, *110*, 633–634.

treatment of **8** with CsF in the presence of $Pd(PPh_3)_4$ failed, most probably due to the slow generation of the aryne **9** as well as its very short life (Scheme 3).[24] Nevertheless, this procedure was successfully applied to the synthesis of dodecahydrotriphenylene (**12**) and decacyclene (**15**) via trimerization of cyclohexyne (**11**) and acenaphthyne (**14**), respectively.[24] Although other aryne sources such as 1,2-dibromocyclopentene could also be used for the cyclopentyne generation,[25] trindane could only be isolated as a minor product from complex mixtures of other hydrocarbons.

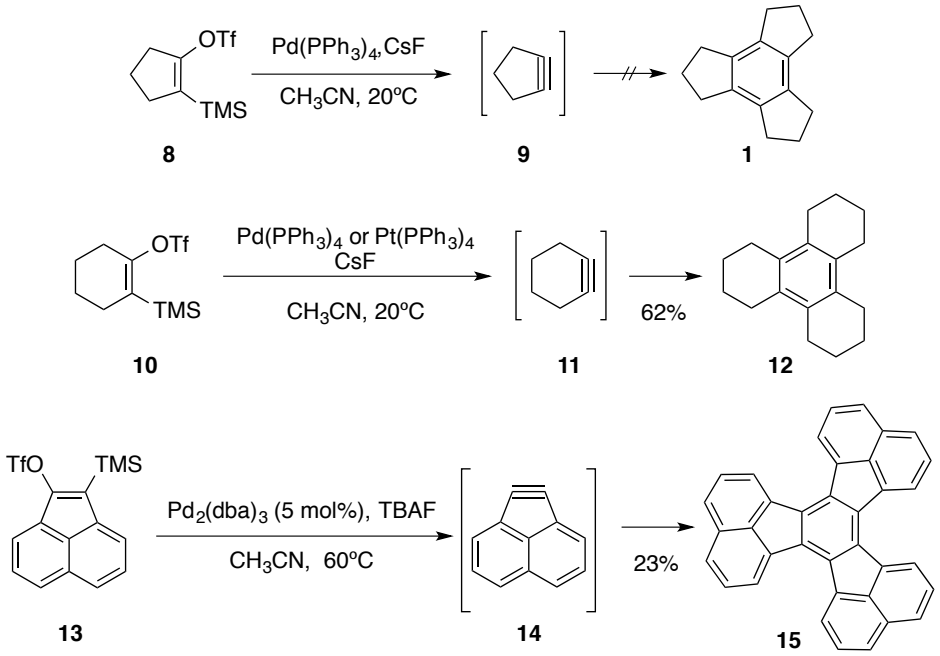

Scheme 3. Trimerization of cycloalkynes

To date, only one method has been described to synthesize dihydro-1*H*-trindenes. Reported by Katz and Slusarek in 1980,[26] these trindane derivatives were conceived as intermediates to obtain the trindene trianion **18** (Scheme 4). Initial hexabromination of trindane (**1**) was carried out with bromine in CCl_4 under light irradiation to furnish **16**. Subsequent treatment with activated zinc dust in DMF afforded debrominated products **17a** and **17b** as an inseparable 1:3 mixture of regioisomers. Finally, trindene trianion **18** could be prepared by the addition of *n*-butyllithium in THF.

24 Iglesias, B; Pena, D.; Perez, D.; Guitian, E.; Castedo, L. *Synlett* **2002**, 486–488.

25 For alternative sources of cyclopentyne generation see: (a) Favorskii, A. E. *Zh. Obshch. Khim.* **1936**, *6*, 720–731. (b) Wittig, G.; Weinlich, J.; Wilson E. R. *Chem. Ber*. **1965**, *98*, 458–470. (c) Wittig, G.; Heyn, J. *Liebigs Ann.* **1969**, *726*, 57–68.

26 Katz, T. J.; Slusarek, W. *J. Am. Chem. Soc.* **1980**, *102*, 1058–1063.

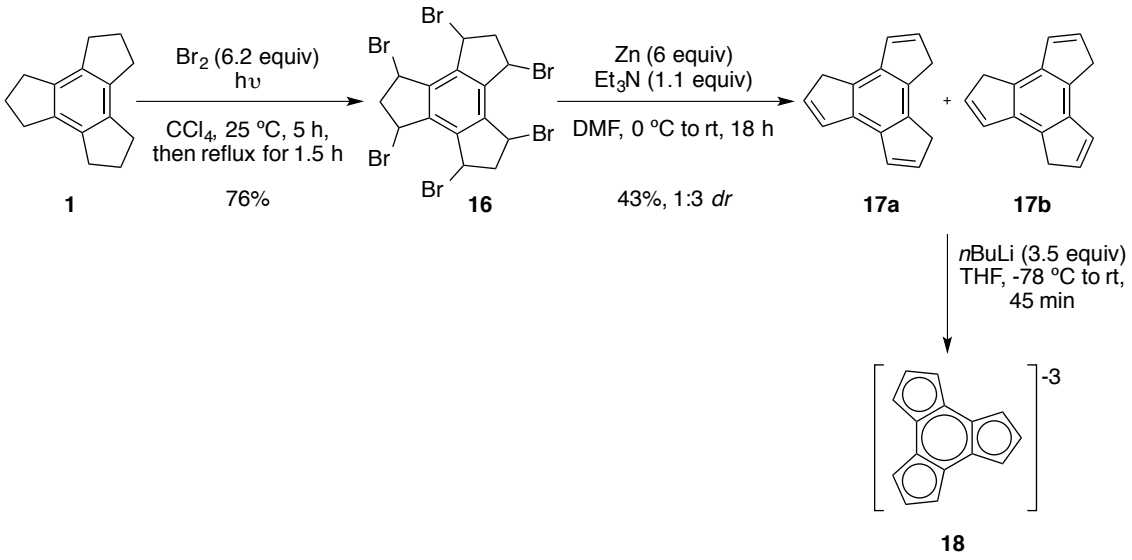

Scheme 4. Synthesis of trindenes (**17a**, **17b**) and trindene trianion (**18**)

Organometallic Derivatives

Trindane Metal Complexes

Despite the large number of studies of other arenes such as trindene or truxene,[27] very little research has focused on the development of organometallic fragments complexed with trindane.

The first example of a trindane organometallic derivative appeared in 1991, included in a study of different cationic complexes of the type $^{99m}Tc(arene)_2^+$, although no analytical or spectroscopic data were reported for $[^{99m}Tc(trindane)_2]^+BF_6^-$.[28] It was not until 1997, when Gupta *et al.* reported the synthesis and characterization of complexes of the type (η^6-trindane)ML_n (Figure 1).[9] Accordingly, trindane reacted with $Cr(CO)_6$ and $Mo(CO)_6$ under standard conditions to give (η^6-trindane)$Cr(CO)_3$ (**19**) and (η^6-trindane)$Mo(CO)_3$ (**20**), respectively. X-ray crystallographic analysis of chromium complex **19** showed that the five-membered ring envelopes were folded toward the metal and the three carbonyl ligands were staggered with respect to the cyclopentenyl

27 (a) Seka, R.; Kellerman, W. *Chem. Ber.* **1942**, *75*, 1730–1738. b) Drake, J. A. G.; Jones, D. W. *Org. Magn. Reson.* **1980**, *14*, 272–277. (c) Tisch, T. L.; Lynch, T. J.; Dominguez, R. *J. Organomet. Chem.* **1989**, *377*, 265–273.

28 Wester, D. W.; Coveney, J. R.; Nosco, D. L.; Robbins, M. S.; Dean, R. T. *J. Med. Chem.* **1991**, *34*, 3284–3290.

rings. Additionally, other monocationic complexes $[(\eta^6\text{-trindane})ML_n]^+[BF_4]^-$ have been prepared bearing iron, manganese, or rhenium as the metal center.[9]

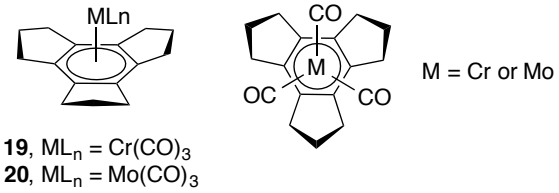

19, $ML_n = Cr(CO)_3$
20, $ML_n = Mo(CO)_3$

Figure 1. Structure models of $(\eta^6\text{-trindane})ML_n$ complexes

In contrast with the previous examples, bis(arene)-ruthenium dications (**23**) were prepared starting from the corresponding dimer $[(arene)RuCl_2]_2$ (**21**) via arene exchange and subsequent treatment with $AgBF_4$ (Scheme 5).[29] An unusual aspect of dimeric complex **22a** is the high degree of molecular crowding, which induces an *endo:endo:exo* conformation of the cyclopentane rings in each trindane moiety. Nevertheless, this double-bridged molecule appears in equilibrium with the dechlorinated species $[\{(trindane)Ru\}_2(\mu\text{-}Cl)_3]^+Cl^-$ (**22b**), which reduces the steric interaction generated by the non-bridging chlorine atoms and allows to recover the initial *endo:endo:endo* trindane conformation.

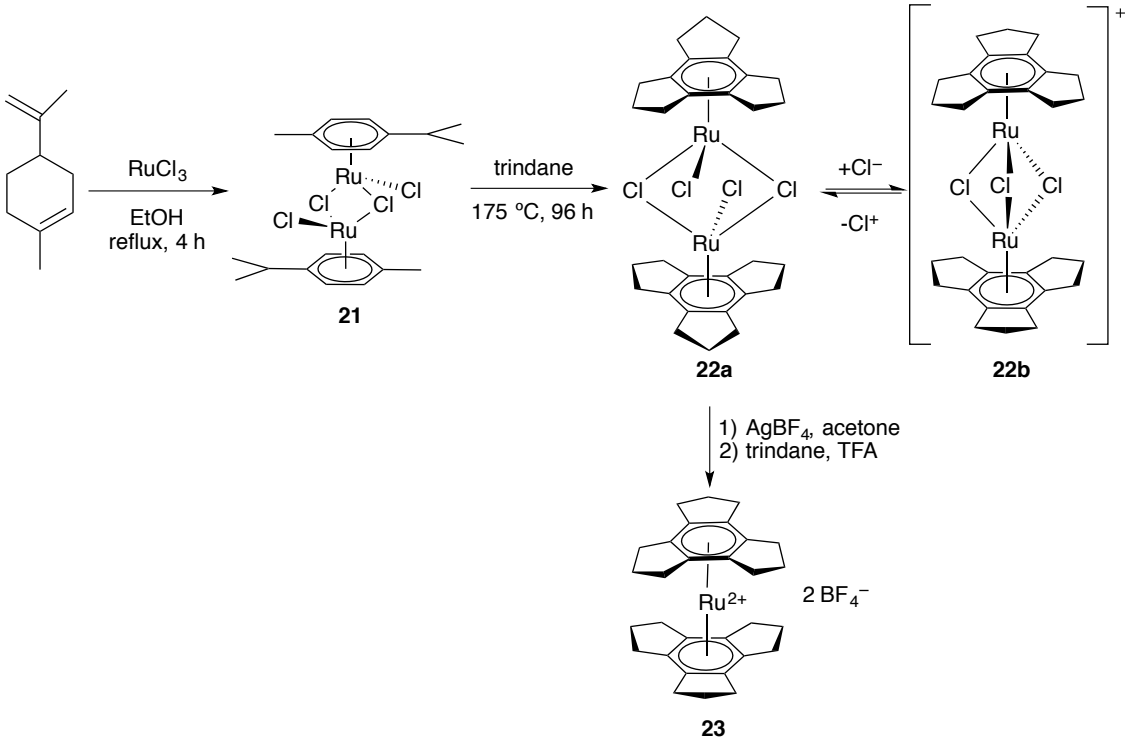

Scheme 5. Synthesis of bis(trindene)-ruthenium complexes

29 Gupta, H. K.; Lock. P. E.; Hughes, D. W.; McGlinchey, M. J. *Organometallics* **1997**, *16,* 4355–4361.

Trindenyl Metal Complexes

The first example of a trindenyl metal complex was reported by Katz and Slusarek.[26] The regioisomeric sandwich bis(trindene)diiron complexes **25a**-**b** were isolated in 53% yield when trindene dianion (**24**) was mixed with ferrous chloride (Figure 2)**.**

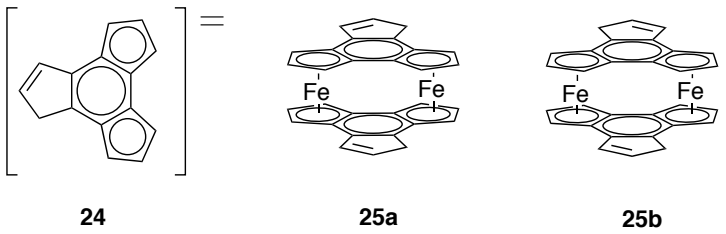

24 **25a** **25b**

Figure 2. Trindene dianion (**24**) and bis(trindene)diiron complexes **25a** and **25b**

Later, various *trans*-trimetallic[30] and -diheterotrimetallic[31] trindene complexes could also be prepared from a mixture of dihydro-1*H*-trindenes **17a** and **17b** (Figure 3).

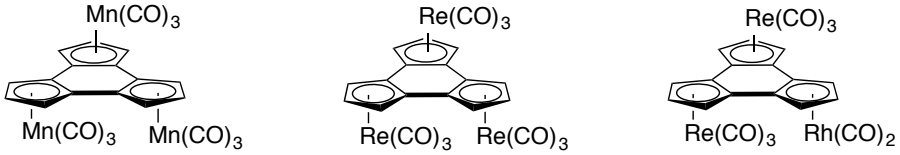

Figure 3. Examples of *trans*-trimetallic and -diheterotrimetallic trindene complexes

A cyclic metallocene triad was also prepared as a 3:1 mixture of isomers, namely *syn,syn,anti*-[(FeCp)$_3$Td] (**26a**) and *syn,syn,syn*-[(FeCp)$_3$Td] (**26b**), by an exchange reaction between K_3Td and [FeCp(η^6-fluorenyl)] (Figure 4).[32] A significant distortion from the predicted planarity in the five-membered rings of trindene was observed.

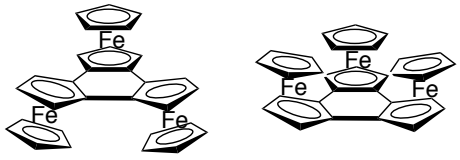

26a **26b**

Figure 4. The *syn,syn,anti*-[(FeCp)$_3$Td] (**26a**) and *syn,syn,syn*-[(FeCp)$_3$Td] (**26b**) isomers

30 Lynch, T. J.; Carroll, J. M.; Helvenston, M. C.; Tisch, T. L.; Rheingold, A. L.; Staley, D. L.; Mahmoudkhani, A. *Organometallics* **2012**, *31*, 3300–3307.

31 Lynch, T. J.; Helvenston, M. C.; Rheingold, A. L.; Staley, D. L. *Organometallics* **1989**, *8*, 1959–1963.

32 Santi, S.; Orian, L.; Donoli, A.; Bisello, A.; Scapinello, M.; Benetollo, F.; Ganis, P.; Ceccon, A. *Angew. Chem. Int. Ed.* **2008**, *47*, 5331–5334.

Finally, a new family of multi(ferrocenyl)trindenes was synthesized via Negishi coupling of tribromo-1*H*-trindene derivatives **27a** and **27b** and ferrocenylzinc chloride in the presence of a palladium catalyst (Scheme 6).[33] It is important to note that all these compounds are mixtures of isomers differing in the position of the double bond.

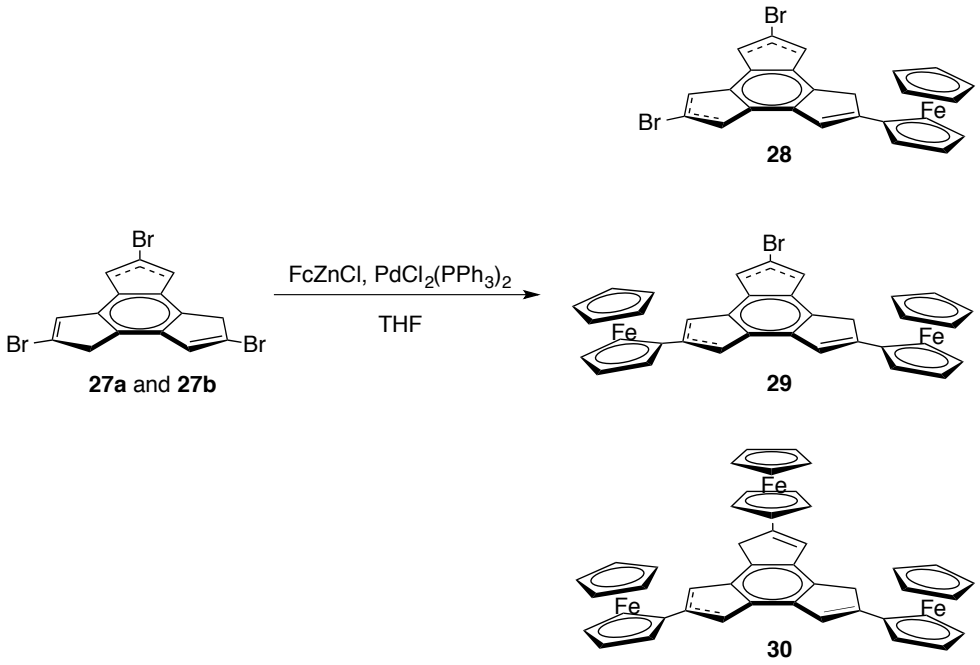

Scheme 6. Synthesis of mono- (**28**) and multi- (**29** and **30**) (ferrocenyl)trindenes

Furthermore, trindane and trindene scaffolds have found applications as ligands in multinuclear organometallic complexes,[30b,31–33] as well as in molecular recognition of small molecules and anions (Figure 5).[34,35]

33 Donoli, A.; Bisello, A.; Cardena, R.; Prinzivalli, C.; Santi, S. *Organometallics* **2013**, *32*, 1029–1036.

34 (a) Choi, H-J.; Park, Y. S.; Yun, S. H.; Kim, H-S.; Cho, C. S.; Ko, K.; Ahn, K. H. *Org. Lett.* **2002**, *4*, 795–798. (b) Choi, H-J.; Song, J.; An, C. Y.; Nguyen, Q-T.; Kim, H-S. *Synthesis* **2007**, 3290–3294. (c) Kim, W.; Sahoo, S. K.; Kim, G.-D.; Choi, H.-J. *Tetrahedron* **2015**, *71*, 8111–8116.

35 For the application of trindane on the synthesis of high-symmetric chiral molecules see: (a) Borsato, G.; Crisma, M.; De Lucchi, O.; Lucchini, V.; Zambon, A. *Angew. Chem. Int. Ed.* **2005**, *44*, 7435–7439. (b) Fabris, F.; Zonta, C.; Borsato, G.; De Lucchi, O. *Acc. Chem. Res.* **2011**, *44*, 416–423.

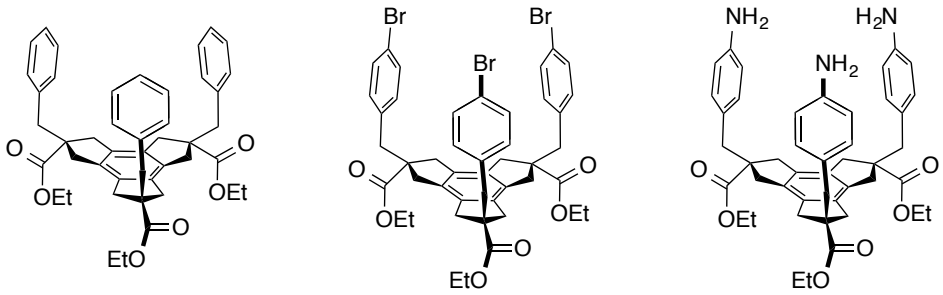

Figure 5. Examples of trindane-based scaffolds used in molecular recognition

Application on the Synthesis of Higher Polyarenes

Despite several theoretical and experimental studies have been performed in order to understand the mechanism of formation of fullerenes from small carbon species, this is still an unsolved riddle (Scheme 7).[36]

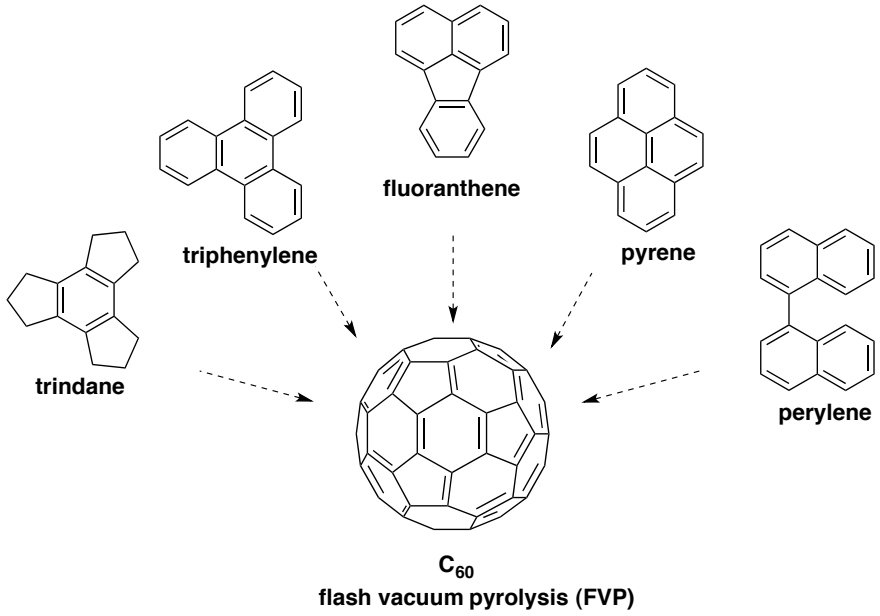

Scheme 7. Construction of buckminsterfullerene C_{60} by FVP

To date, all the rational synthetic approaches towards fullerene are based on ring-closure of adequate functionalized hydrocarbon skeletons.[2a,37] Indeed, much effort has

36 (a) Osterodt, J.; Zett, A.; Voegtle, F. *Tetrahedron* **1996**, *52*, 4949–4962. (b) Zhu, W-L.; Puah, C. M.; Ng, K. C.; Jiang, H-L.; Tan, X-J.; Chen, K-X. *J. Chem. Soc. Perkin Trans. 2* **2001**, 233–237.

37 (a) Kroto, H. W.; Allaf, A. W.; Balm, S . P. *Chem. Rev.* **1991**, *91*, 1213–1235; (b) Special issue on buckminsterfullerenes *Acc. Chem. Res.* **1992**, 25, 97–175. (c) Diederich, F.; Rubin, Y. *Angew. Chem. Int. Ed.* **1992**, *31*, 1101–1123. (d) Taylor, R.; Walton, D. R. M.

been devoted to the synthesis of π-bowls based on the structures of coranulene[38] and sumanene.[39] Significant attention has also been given to the study of the mechanism of formation of the curved surface of these[40,41] and larger compounds.[42]

On the other hand, the cyclodehydrogenation of C_{3h}-symmetric crushed fullerenes based on truxene constitutes the most extended strategy to zip-up the C_{60} cage, which has been accomplished from $C_{60}H_{30}$ precursors and other related functionalized derivatives

---

Nature **1993**, *363*, 685–693. (e) Narahari, G. H.; Jemmis, E. D.; Mehta, G.; Shah, S. R. *J. Chem. Soc. Perkin Trans.* 2 **1993,** 1867–1871. (f) Faust, R. *Angew. Chem. Int. Ed.* **1995**, *34*, 1429–1432. (g) Rabideau, P. W.; Sygula, A. *Acc. Chem. Res.* **1996**, *29*, 235–242. (h) Scott, L. T. *Pure Appl. Chem.* **1996**, *68*, 291–300. (i) Mehta, G.; Rao, H. S. P. *Tetrahedron* **1998**, *54*, 13325–13370. (j) Scott, L. T.; Bronstein, H. E.; Preda, D. V.; Ansems, R. B. M.; Bratcher, M. S.; Hagen, S. *Pure Appl. Chem.* **1999**, *71*, 209–219. (k) Gómez-Lor, B.; de Frutos, O.; Echavarren, A. M. *Chem. Commun.* **1999**, 2431–2432. (l) Boorum, M. M.; Vasil'ev, Y. V.; Drewello, T.; Scott, L. T. *Science* **2001**, *294,* 828–831.

38 (a) Barth, W. E.; Lawton, R. G. *J. Am. Chem. Soc.* **1966**, *88*, 380–381. (b) Lawton, R. G.; Barth, W. E. *J. Am. Chem. Soc.* **1971**, *93*, 1730–1745. (c) Seiders, T. J.; Baldridge, K. K.; Grube, G. H.; Siegel, J. S. *J. Am. Chem. Soc.* **2001**, *123*, 517–525. (d) Reisch, H. A.; Bratcher, M. S.; Scott, L. T. *Org. Lett.* **2000**, *2*, 1427–1430. (e) Wu, Y.-T.; Maag, R.; Linden, A.; Baldridge, K. K.; Siegel, J. S. *J. Am. Chem. Soc.* **2008**, *130*, 10729–10739. (f) Rajeshkumar, V.; Lee, Y. T.; Stuparu, M. C. *Eur. J. Org. Chem.* **2016**, 36–40.

39 (a) Scott, L. T.; Hashemi, M. M.; Meyer, D. T.; Warren, H. B. *J. Am. Chem. Soc*. **1991**, *113*, 7082–7084. (b) Scott, L. T.; Bratcher, M. S.; Hagen, S. *J. Am. Chem. Soc*. **1996**, *118*, 8743–8744. (c) Sakurai, H.; Daiko, T.; Hirao, T. *Science* **2003**, *301*, 1878; (d) Amaya, T.; Ito, T.; Hirao, T. *Angew. Chem. Int. Ed.* **2015**, *54*, 5483–5487. (e) Amaya, T.; Hirao, T. *Chem. Rec.* **2015**, *15*, 310–321.

40 Wu, X.-Z.; Yao, Y.-R.; Chen, M.-M.; Tian, H.-R.; Xiao, J.; Xu, Y.-Y.; Lin, M.-S.; Abella, L.; Tian, C.-B.; Gao, C.-L.; Zhang, Q.; Xie, S.-Y.; Huang, R.-B.; Zheng, L.-S. *J. Am. Chem. Soc.* **2016**, *138*, 9629–9633.

41 Greisch, J.-F.; Amsharov, K. Y.; Weippert, J.; Weis, P.; Böttcher, A.; Kappes, M. M. *J. Am. Chem. Soc* . **2016**, *138*, 11254–11263.

42 (a) Mueller, A.; Amsharov, K. Y. *Eur. J. Org. Chem.* **2012**, 6155–6161. (b) Sanchez-Valencia, J. R.; Dienel, T.; Gröning, O.; Shorubalko, I.; Mueller, A.; Jansen, M.; Amsharov, K.; Ruffieux, P.; Fasel, R. *Nature* **2014**, *512*, 61–64.

through laser irradiation[37f,43] and flash-vacuum pyrolysis,[44] as well as by means of surface-assisted cyclodehydrogenation.[45]

As mentioned previously, the use of the trindane scaffold as a synthetic precursor of these higher polyarenes has been less explored. Indeed, until now only two synthetic strategies based on the structure of trindane towards the synthesis of fullerene C_{60} have been reported. Those strategies were originally inspired on the "Coupe du Roi" approach outlined by Fabre and Rassat[7,46] and further developed by Ferrier *et al.*[8] Scheme 8 shows the "tennis ball" strategy, in which the T-shaped $C_{60}H_{58}O$ ketone **35** would lead to C_{60} after step-by-step dehydration-dehydrogenation.

43 (a) Gómez-Lor, B.; Koper, C.; Fokkens, R. H.; Vlietstra, E. J.; Cleij, T. J.; Jenneskens, L. W.; Nibbering, N. M. M.; Echavarren, A. M. *Chem. Commun.* **2002**, 370–371. (b) Kabdulov, M.; Jansen, M.; Amsharov, K. Y. *Chem.–Eur. J.* **2013**, *19*, 17262–17266. (c) Mueller, A.; Amsharov, K. Y. *Eur. J. Org. Chem.* **2015**, 3053–3056. (d) Dorel, R.; de Mendoza, P; Calleja, P.; Pascual, S.; González-Cantalapiedra, E.; Cabello, N.; Echavarren, A. M. *Eur. J. Org. Chem.* **2016**, 3171–3176.

44 Scott, L. T.; Boorum, M. M.; McMahon, B. J.; Hagen, S.; Mack, J.; Blank, J.; Wegner, H.; de Meijere, A. *Science* **2002**, *295*, 1500–1503.

45 (a) Otero, G.; Biddau, G.; Sánchez-Sánchez, C.; Caillard, R.; López, M. F.; Rogero, C.; Palomares, F. J.; Cabello, N.; Basanta, M. A.; Ortega, J.; Méndez, J.; Echavarren, A. M.; Pérez, R.; Gómez-Lor, B.; Martín-Gago, J. A. *Nature* **2008**, *454*, 865–868. (b) Amsharov, K.; Abdurakhmanova, N.; Stepanow, S.; Rauschenbach, S.; Jansen, M.; Kern, K. *Angew. Chem. Int. Ed.* **2010**, *49*, 9392–9396.

46 For a general discussion on other "Coupe du Roi" approaches to the synthesis of C60: Geneste, F.; Moradpour, A.; Dive, G.; Peeters, D.; Malthête, J.; Sadoc, J.-F. *J. Org. Chem.* **2002**, *67*, 605–607.

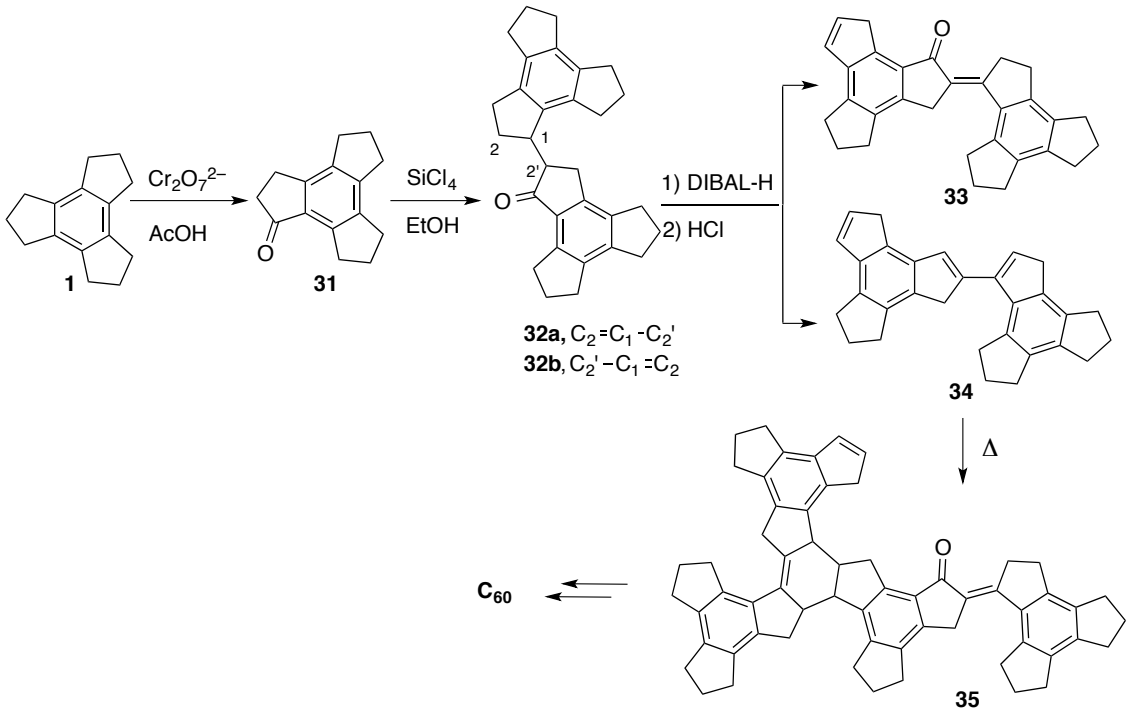

Scheme 8. "Tennis ball" approach for the synthesis of fullerene C_{60}

The other approach is based on the synthesis of C_{45} bowl-like trindane trimer **39**, which could be capped with a C_{15} lid and subsequently, dehydrogenated to form C_{60} (Scheme 9).

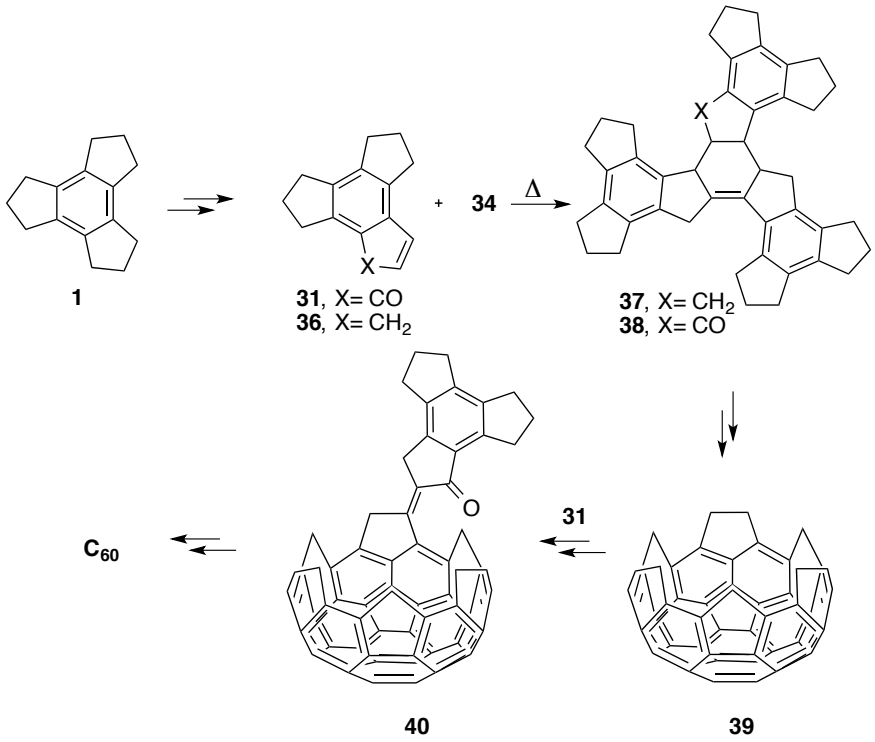

Scheme 9. "Basket- and -lid" approach for the synthesis of fullerene C_{60}

On the other hand, metal complexes of trindane have been envisioned as possible precursors of sumanene, in an alternative synthetic route in which the final flash-vacuum pyrolysis (FVP) step would not be required (Scheme 10).[47]

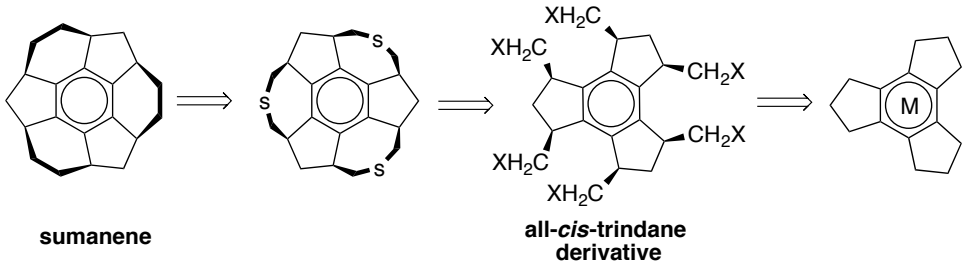

Scheme 10. Proposed retrosynthetic analysis for the synthesis of sumanene

47 (a) Priyakumar, U. D.; Sastry, G. N. *J. Org. Chem.* **2001**, *66*, 6523–6530. (b) Priyakumar, U. D.; Sastry, G. N. *Tetrahedron Lett.* **2001**, *42*, 1379–1381. (c) Immamura, K.; Takimiya, K.; Aso, Y.; Otsubo, T. *Chem. Commun*. **1999**, 1859–1860. (d) Metha, G.; Shah, S. R.; Ravikumar, K. *J. Chem. Soc. Chem. Commun*. **1993**, 1006–1008.

Objectives

In spite of its appealing architecture, progress on the use of trindene scaffold as a C_{15} building block for the synthesis of polyarenes has been scarce.[7–9] To date, the synthesis of trindene derivatives typically relies on the functionalization of trindane (**1**) via hexabromination and subsequent dehydrobromination with Zn.[26] However, this two-step protocol leads to an inseparable 1:3 mixture of symmetrical (4,7-dihydro-1*H*-trindene) and non-symmetrical (4,9-dihydro-1*H*-trindene) isomers. Thus, strategies for the preparation of isomerically pure trindenes still remain unexplored.

In this context, we focused our investigations towards the development of a method for the selective preparation of 1,4,7-trisketone **41**, which could be used as a platform for the preparation of 1,4,7-trifunctionalized C_{3h}-symmetric trindene derivatives **42** (Scheme 11). Given that initial attempts to prepare **41** through a triple benzylic oxidation of trindane (**1**) in reasonable yields proved to be more challenging than expected,[48] several strategies were envisioned to circumvent this problem.

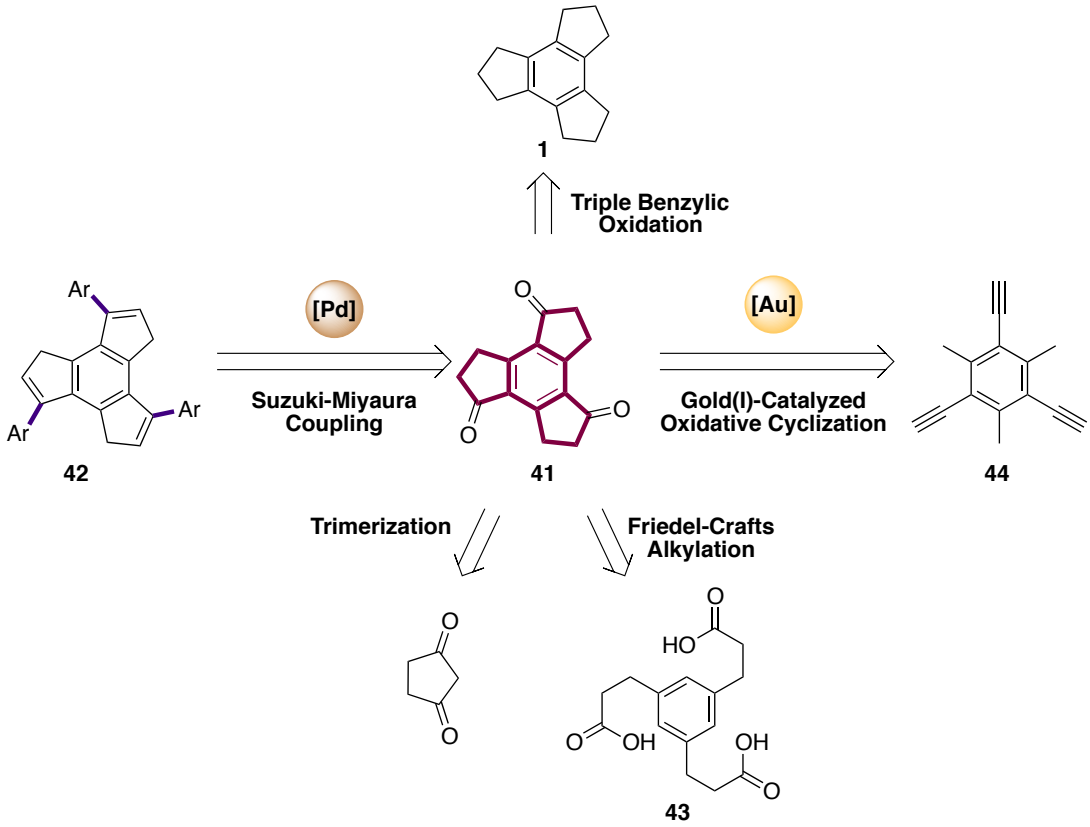

Scheme 11. Proposed synthesis of 1,4,7-trifunctionalized C_{3h}-symmetric trindene derivatives

48 Initial studies were developed by C. Rogelio Solorio Alvarado, PhD Thesis 2011.

Furthermore, the preparation of a new polyarene that features the topology of C60 fullerene could be conceived through the palladium-catalyzed coupling of four suitably functionalized C_{15} trindene fragments (Figure 6).

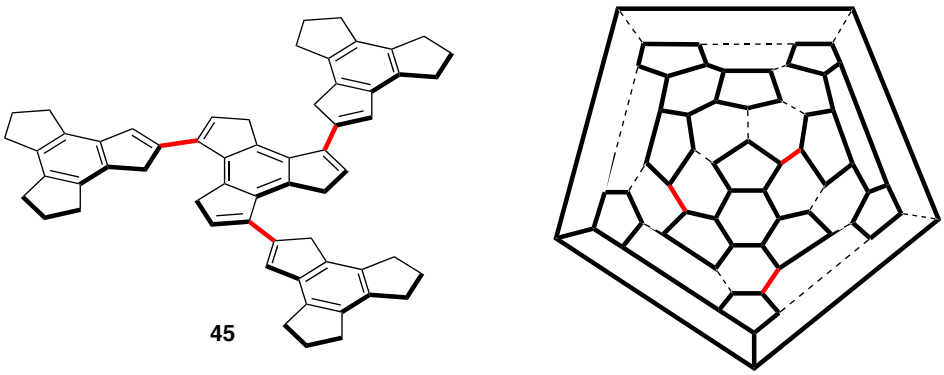

Figure 6. C_{3h}-symmetric crushed C60 fullerene **45** and its Schlegel projection

Results and Discussion

Synthesis of Trindene C_{15} Cores

Triple Benzylic Oxidation of Trindane

As mentioned in the introduction of this chapter, trindane (**1**) is readily available by the acid-catalyzed trimerization of cyclopentanone.[8] Therefore, we began our investigations by attempting the synthesis of the properly functionalized C_{15} trindene core by selective functionalization of this scaffold. While the oxidation of **1** with $Na_2Cr_2O_7$ in HOAc for 30 min furnishes 1-trindanone **31** in 47% yield,[8] 1,4-trindandione **46** can be obtained after longer reaction times,[7] albeit in low yield (Scheme 12). Unfortunately, larger amounts of oxidant, higher temperatures or prolonged reaction times did not lead to the formation of the required symmetric 1,4,7-trindantrione (**41**) by triple benzylic oxidation. Indeed, it has been reported that **1** forms the natural product-like compound **47** by exhaustive oxidation in the presence of RuO_4 through cleavage of the hexasubstituted benzene ring,[11] which is also observed when ozone is used as the oxidant.[49] Conversion of **1** into trisketone **41** required extensive optimization, and could only be achieved in a reproducible manner although in a low yield under very specific conditions using TBHP and CrO_3.[48]

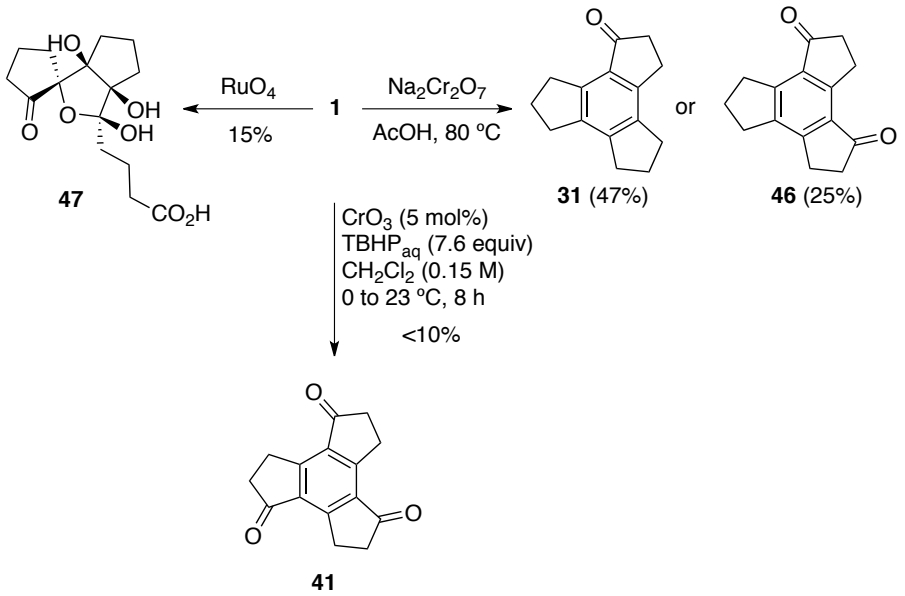

Scheme 12. Benzylic oxidations of **1** for the synthesis of mono- (**31**), di- (**46**), and triketone (**41**)

49 Ranganathan, S.; Muraleedharan, K. M.; Rao, C. C.; Vairamani, M.; Karle, I. L. *Org. Lett.* **2001**, *3*, 2447–2449.

Furthermore, we also investigated the triple oxidation of trindane (**1**) following a stepwise protocol (Scheme 13). Thus, trindane (**1**) was converted into 1-trindanone **31** in moderate yield, which was further oxidized into the corresponding 1,4-trindandione (**46**) in 31% yield. Finally, treatment of isolated **46** with CrO_3 and TBHP in CH_2Cl_2 afforded **41** in only 6% yield. Thus, even if the first and second oxidation steps proceed reproducibly in moderate yields, the oxidation on the third benzylic position is very unfavorable.

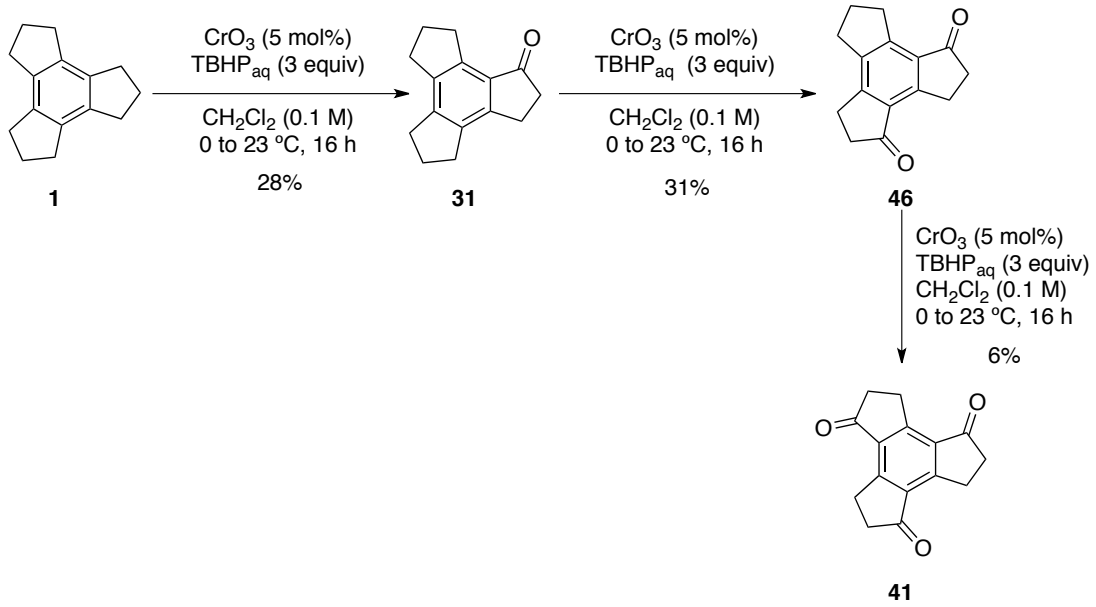

Scheme 13. Stepwise oxidation of trindane (**1**) to 1,4,7-trindantrione (**41**)

We also attempted this triple benzylic oxidation using other catalytic systems based on the combination of a transition-metal complex with an excess of peroxide. Unfortunately, White's catalyst (Fe(*S,S*-PDP), [50] a bismuth(0)-based reagent, [51] dirhodium complex $Rh_2(CAPY)_4$ [52] or NaClO/TEMPO/$Cu(OAc)_2$ [53] failed to give 1,4,7-trindantrione **41**. A metal-free method based on C–H bond abstraction using alkali metal bromides (OXONE®/KBr) [54] was also tested, although product formation was not observed. Remarkably, treatment of trindane (**1**) with $RuCl_3 \cdot xH_2O$ (1.4 equiv), TBHP

50 Chen, M. S.; White, M. C. *Science* **2010,** *327*, 566–571.

51 Bonvin, Y.; Callens, E.; Larrosa, I.; Henderson, D. A.; Oldham, J.; Burton, A. J.; Barrett, A. G. M. *Org. Lett.* **2005**, *7,* 4549–4552.

52 Wusiman, A.; Tusun, X; Lu, C-D. *Eur. J. Org. Chem*. **2012**, 3088–3092.

53 Jin, C.; Zhang, L.; Su, W. *Synlett* **2011**, *10*, 1435–1438.

54 Moriyama, K.; Takemura, M.; Togo, H. *Org. Lett.* **2012**, *14*, 2414–2417.

(19 equiv) and pyridine (2 mL) in CH_2Cl_2 at 40 ºC for 65 h afforded **41** in 31% yield (Scheme 14).[55] However, attempts to perform the reaction at larger scale resulted in significant lower yields.

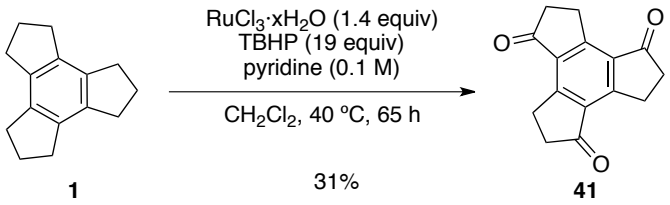

Scheme 14. Alternative benzylic oxidation method for the synthesis of **41**

Trimerization Approach

The triple self-condensation of cyclic ketones is a well-established method for the synthesis of aromatic compounds.[56] For example, trindane (**1**) can be prepared in good yield by acid-catalyzed trimerization of cyclopentanone (Scheme 15). Analogously, truxene (**48**) and truxentrione (**49**) can also be synthesized in excellent yields from 1-indanone or 1,3-indandione, respectively.

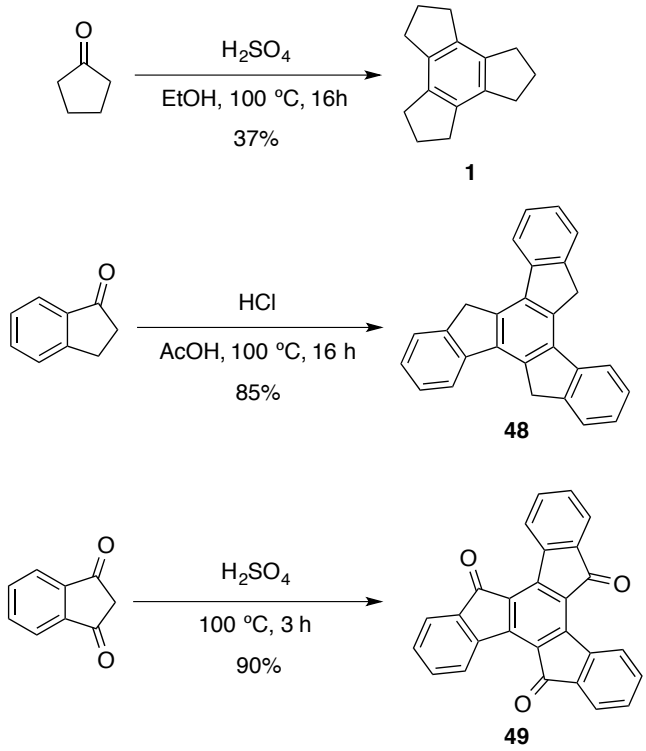

Scheme 15. Examples of triple self-condensation of cyclic ketones

55 Amaya,T.; Hifumi, M.; Okada, M.; Shimizu, Y.; Moriuchi, T.; Segawa, K.; Ando, Y.; Hirao, T. *J. Org. Chem.* **2011**, *76*, 8049–8052.

56 Dehmlow, E. V.; Kelle, T. *Synth. Commun*. **1997**, *27*, 2021–2031.

Therefore, we decided to investigate the trimerization of 1,3-cyclopentadienone in order to access to 1,4,7-trindantrione. However, as illustrated in Table 1, under a variety of acidic conditions, the cyclization failed to give the desired compound.

Table 1. Trimerization of 1,3-cyclopentadienone[a]

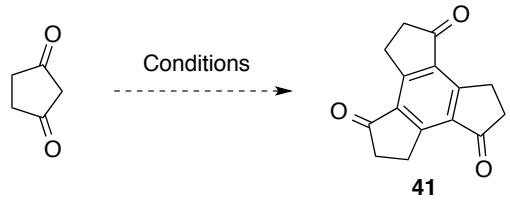

41

Entry	Acid (equiv)	Solvent (M)	T (ºC)	Time (h)	Yield (%)
1	H_2SO_4 (1.8)	EtOH (0.2)	100	16	–[b]
2	H_2SO_4 (0.9)	EtOH (0.5)	100	16	–[b]
3	H_2SO_4 (27.5)	–	100	5	–[c]
4	HCl (9.5)	AcOH (1.7)	100	16	–[c]
5	PPA (44.2)	–	120	16	–[c]
6	PTSA (0.1)	Toluene (0.2)	120	15	–[b]
7	PTSA (0.1)	Mesitylene (0.2)	160	7	–[b]
8	MSA	–	120	15	–[b]
9	$TiCl_4$ (2.4)	1,2-DCE (0.2)	100	2	–[b]

[a] All the reactions were carried out using 1 mmol of 1,3-cyclopentandione. [b] Decomposition. [c] Starting material was recovered.

Subsequently, the triple self-condensation of 1,3-cyclopentanedione was reinvestigated under basic conditions (Table 2).[57] Unfortunately, neither pyridine (Table 2, entries 1-2) nor triethylamine (Table 2, entries 3-7) led to the desired trisketone **41**. Despite the use of catalytic amounts of triethylamine and lithium perchlorate proved to be beneficial for the self-condensation of other carbonyl compounds,[58] we could only observe decomposition of the starting material. Contrary to the case of 1,3-indanone, which has only one acidic methylene group, 1,3-cyclopentadione has three different ones. Therefore, a wide range of condensation products could be formed and subsequently, the control of the trimerization process resulted more difficult.

57 Jacob, K.; Sigalov, M.; Becker, J. Y.; Ellern, A.; Khodorkovsky, V. *Eur. J. Org. Chem*. **2000**, 2047–2055.

58 Sharma, L. K.; Kim, K. B.; Elliott, G. I. *Green Chem.* **2011**, *13*, 1546–1549.

Table 2. Trimerization of 1,3-cyclopentadienone under basic conditions[a]

Entry	Base (equiv)	Additives (equiv)	Solvent (M)	T (ºC)	Time (h)	Yield (%)
1	py (6)	–	–	120	0.6	–[c]
2	py (6)	–	–	130	3	–[c]
3	Et_3N (0.4)	$LiClO_4$ (0.4)	–	120	7	–[b]
4	Et_3N (0.4)	$LiClO_4$ (0.4)	toluene (0.1)	120	15	–[b]
5	Et_3N (2.5)	$LiClO_4$ (1)	–	120 (MW)	0.3	–[b]
6	Et_3N (2.5)	$LiClO_4$ (1)	–	120	4	–[b]
7	Et_3N (2.5)	$LiClO_4$ (1)	–	120	15	–[b]

[a] All the reactions were carried out using 1 mmol of 1,3-cyclopentandione. [b] Decomposition. [c] Starting material was recovered.

Triple Friedel-Crafts Approach

We considered an alternative approach based on the preparation of 1,4,7-trindantrione (**41**) through a triple Friedel-Crafts alkylation of **43** (Scheme 16).

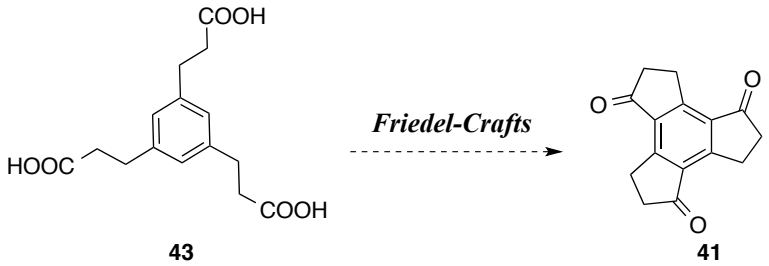

43 **41**

Scheme 16. Proposed alternative synthesis of **41**

The synthesis of required precursor was achieved following a two-step procedure from commercial available benzene-1,3,5-tricarbaldehyde (Scheme 17). Thus, treatment of benzene-1,3,5-tricarbaldehyde with piperidine and an excess of malonic acid in pyridine led to the corresponding condensation product, which upon decarboxylation afforded **50** in excellent yield.[59] Subsequent triple hydrogenation with 10% Pd/C gave **43** in good yield.[60]

59 Effenberger, K.; Kurt, W. *Chem. Ber.* **1973**, *106*, 511–524.

60 Majchrzak, M. W.; Zobel, J. N.; Obradovich, D. J.; Peterson, G. A. *OPPI* **2009**, *29*, 361–364.

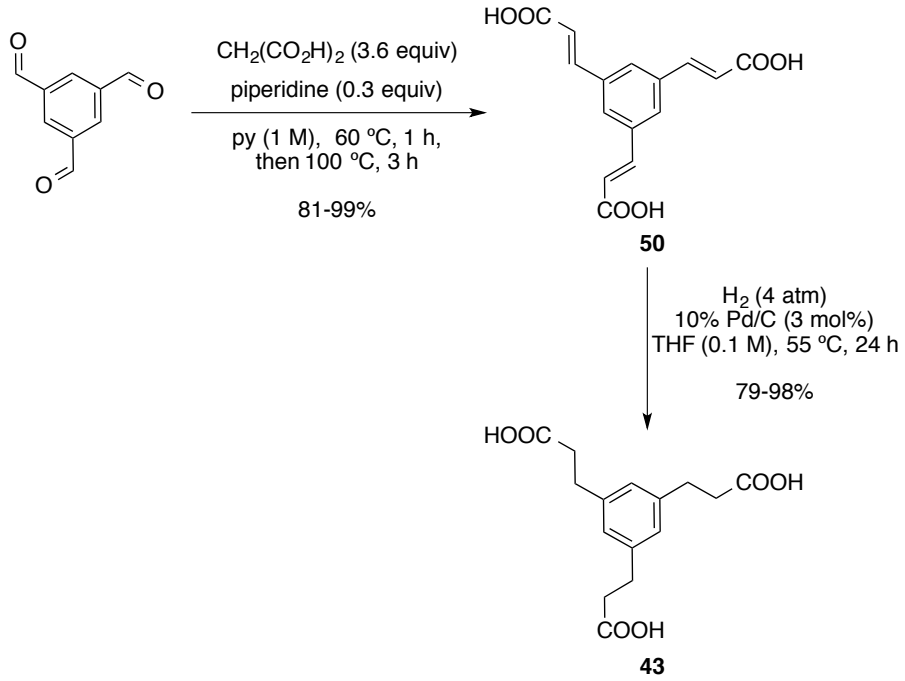

Scheme 17. Synthesis of **43** from benzene-1,3,5-tricarbaldehyde.

Several reaction conditions were tested in order to promote the threefold Friedel-Craft alkylation of **43**. While TfOH or H_2SO_4 failed to give any traces of product (Table 3, entries 1-3), when the reaction was performed with polyphosphoric acid (PPA) at 120 ºC for 90 min (Table 3, entry 5), 1,4,7-trindantrione was obtained in 11–28% yield. Unfortunately, lower temperatures (Table 3, entry 4) or larger reaction times (Table 3, entries 6-10) had a detrimental effect on this transformation. Likewise, **41** was never observed when the reaction was carried out at 150 ºC (Table 3, entry 10) or in the presence of other solvents (Table 3, entries 11-13).

Table 3. Synthesis of 1,4,7-trindantrione via triple Friedel-Crafts alkylation[a]

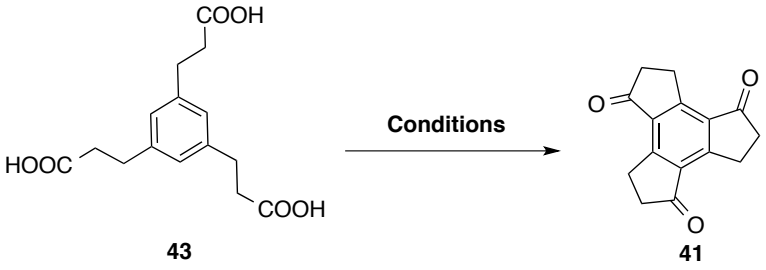

Entry	Acid (equiv)	Solvent (M)	T (ºC)	Time (h)	Yield (%)
1	TfOH (12)	–	25	16	–
2	TfOH (18)	–	120	16	–
3	H_2SO_4	–	100	2.5	–
4	PPA (91)	–	100	1.5	–

5	PPA (91)	–	120	1.5	11-28
6	PPA (91)	–	120	2.5	10
7	PPA (91)	–	120	3.5	<5
8	PPA (91)	–	120	5.5	–
9	PPA (91)	–	120	21	–
10	PPA (91)	–	150	1	–
11	PPA (12)	Xylene (0.07)	120	2	–
12	PPA (17)	Toluene (0.07)	120	2	–
13	PPA (17)	ODCB (0.07)	120	2	–

[a]All the reactions were carried out using 0.1 mmol of **43**.

However, when the reaction was performed under exact same conditions at 1 mmol scale, the isolated yields were poorly reproducible, ranging from 10 to 18%. For this reason, this three-steps procedure for the synthesis of **41** was finally abandoned.

Triple Gold(I)-catalyzed Oxidative Cyclization

We decided to attempt a different approach using the gold(I)-catalyzed oxidative cyclization previously developed by the group of Liu for the synthesis of indanones.[61] Thus, we expected that 1,4,7-trindantrione (**41**) could be obtained through a triple gold(I)-catalyzed oxidative cyclization of 1,3,5-triethynyl-2,4,6-trimethylbenzene (**44**), a trialkyne readily available in three steps from mesitylene in 59% overall yield[62] (Table 4). We first investigated this transformation using similar reaction conditions to those originally reported for the synthesis of simple indanones (Table 4, entry 1),[61] which enabled complete consumption of the starting substrate to give **41** in a remarkable 63% yield (86% average yield for each C-C bond formation). Attempts to reduce the amount of oxidant resulted in notably lower yields (Table 4, entries 2-3). Moreover, various external oxidants (Table 4, entries 4-8) and gold catalysts (Table 4, entries 9-12) were also evaluated, albeit without observing any improvement of our initial results. Nonetheless, the use of catalyst **C** turned out to be important in order to obtain **41** without significant loss of yield when the reaction was performed at larger scale (Table

61 Bhunia, S.; Ghorpade, S.; Huple, D. B.; Liu, R.-S. *Angew. Chem. Int. Ed.* **2012**, *51*, 2939–2942.

62 Ohshiro, N.; Takei, F.; Onitsuka, K.; Takahashi, S. *J. Organomet. Chem.* **1998**, *569*, 195–202.

4, entries 13 and 14). The catalyst loading was also found essential for the reaction to proceed in good yield (Table 4, entries 15 and 16).

Table 4. Initial optimization of the gold(I)-catalyzed oxidative cyclization[a]

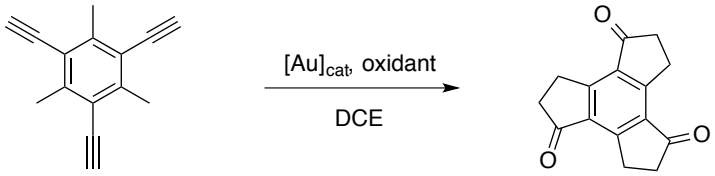

44 **41**

Entry	$[Au]_{cat}$ (mol%)	Oxidant (equiv)	Time (h)	Scale (mmol)	Yield (%)[b]
1	**M** (15)	Ox1 (6)	3.5	0.1	63
2	**M** (15)	Ox1 (4.5)	3.5	0.1	21
3	**M** (15)	Ox1 (3.3)	8	0.1	12
4	**M** (15)	Ox2 (6)	5.5	0.1	14
5	**M** (15)	Ox3 (6)	5.5	0.1	14
6	**M** (15)	Ox4 (6)	5.5	0.1	4
7	**M** (15)	Ox5 (6)	21	0.1	6
8	**M** (15)	Ox6 (6)	21	0.1	0
9	**G** (15)	Ox1 (6)	6	0.1	29
10	**A** (15)	Ox1 (6)	6	0.1	20
11	AuCl	Ox1 (6)	24	0.1	traces
12	**C** (15)	Ox1 (6)	0.5	0.1	46
13	**M** (15)	Ox1 (6)	4	1	19
14	**C** (15)	Ox1 (6)	1	1	42
15	**C** (10)	Ox1 (6)	2	0.1	24
16	**C** (5)	Ox1 (6)	6	0.1	10

[a] Reaction conditions: [**44**] = 0.1 M, temperature = 80 ºC. [b] Isolated yields.

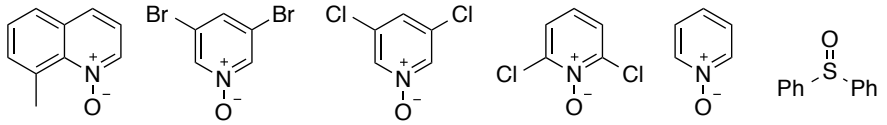

Ox1 **Ox2** **Ox3** **Ox4** **Ox5** **Ox6**

Further studies revealed that decreasing the concentration from 0.1 to 0.01 M minimized product decomposition, thus allowing us to scale up the reaction while maintaining the yield in a 40-50% range (Table 5, entries 1 and 3). However, when the reaction was performed at lower temperatures (Table 5, entries 5 and 6), we observed a considerable loss of yield. Thus, treatment of **44** with gold catalyst **C** (15 mol%) and 8-

methylquinoline *N*-oxide (6 equiv) in DCE (0.01 M) at 80 ºC for 1 h afforded 1,4,7-trindantrione (**41**) in 42% yield.

Table 5. Further optimization of the gold(I)-catalyzed oxidative cyclization of **44**

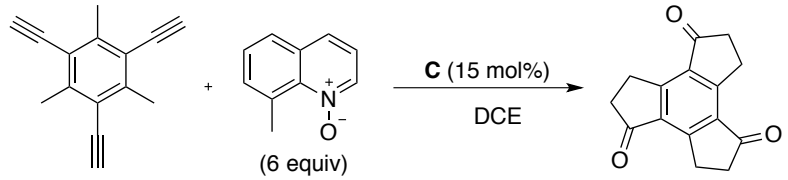

44 **41**

Entry	Time (h)	T (ºC)	[X] (M)	Scale (mmol)	Yield (%)[a]
1	0.5	80	0.1	0.1	46
2	0.5	80	1	0.1	21
3	0.5	80	0.01	0.1	52
4	1	80	0.01	2	42
5	0.5	60	0.01	0.1	28
6	0.5	40	0.01	0.1	16

[a] Isolated yields.

Triple Gold(I)-catalyzed Cyclodehydration of Aryl-substituted Allylic Alcohols

Concurrently, we were intrigued by the possibility of accessing the trisubstituted trindene core through assembly of the three five-membered rings by means of a triple cyclization. Thus, we anticipated that the gold(I)-catalyzed cyclodehydration of aryl-substituted allylic alcohols developed for the synthesis of indenes by the group of Yamamoto could afford a 2,5,8-trisilylated trindene core,[63] which could give access to the corresponding 2,5,8-trifunctionalized C_{3h}-symmetric trindene derivatives. The required substrate for this transformation was readily prepared by triple addition of 1-bromovinyltriisopropylsilane to commercially available benzene-1,3,5-tricarbaldehyde, which afforded triol **51** as a 1:1 inseparable mixture of *syn* and *anti* isomers in 84% yield (Scheme 18).

63 (a) Usanov, D. L.; Naodovic, M.; Brasholz, M.; Yamamoto, H. *Helv. Chim. Acta* **2012**, *95*, 1773–1789. (b) Usanov, D. L.; Yamamoto, H. *Org. Lett.* **2012**, *14*, 414–417.

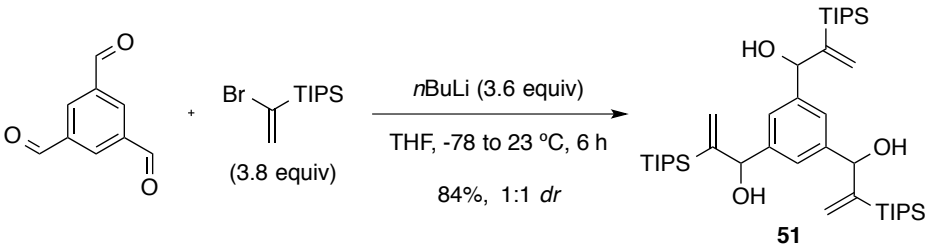

Scheme 18. Synthesis of triol **51**.

The cyclization of **51** under similar reaction conditions to those previously reported for the formation of indenes (10 mol% each of Ph_3PAuCl and $AgSbF_6$)[63] led to trindene **52** in 23% yield, together with partial cyclization products (Table 6, entry 1). The structure of **52** was further confirmed by X-ray diffraction (Figure 7).

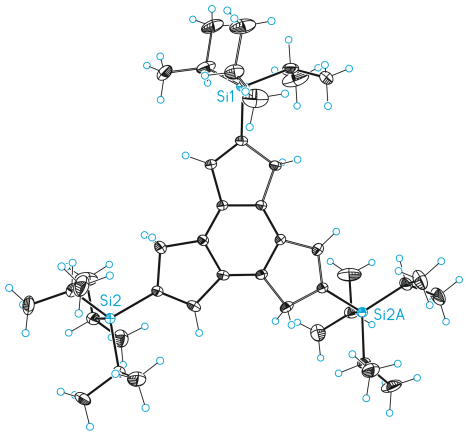

Figure 7. X-ray crystal structure of **52** (50% probability thermal ellipsoids)

In order to improve the outcome of this transformation, a variety of conditions were tested. Initial investigations were focused on the use of gold catalysts generated *in situ* (Table 6, entries 1-4).[63] Although we found that the reaction proceed slightly better with lower catalyst loadings and longer reaction times (Table 6, entry 2), **52** could only be prepared in modest yields. As expected, no cyclization was observed in the absence of LAuCl precatalysts (Table 6, entry 5).

Table 6. Optimization of the triple gold(I)-catalyzed cyclodehydration of **51**[a]

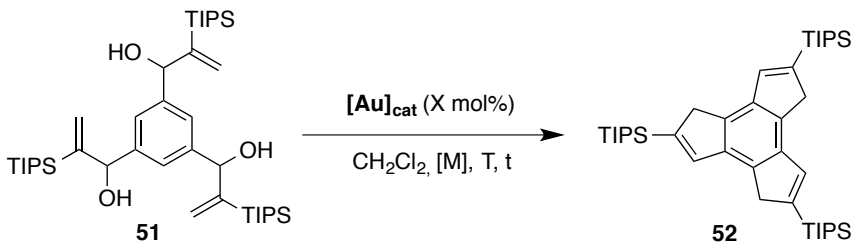

Entry	$[Au]_{cat}$ (mol%)	Additive (mol%)	Time (h)	Yield (%)[b]
1	Ph_3PAuCl (22)	$AgSbF_6$ (30)	1	23
2	Ph_3PAuCl (15)	$AgSbF_6$ (15)	5	30
3	Et_3PAuCl (20)	$AgSbF_6$ (20)	6	41
4	JohnPhosAuCl (20)	$AgSbF_6$ (20)	6	35
5	-	$AgSbF_6$ (20)	6	<2

[a] Reaction conditions: [**51**] = 0.1 M, T = 23 ºC. [b] Isolated yields.

Various cationic gold(I) complexes were also evaluated (Table 7). Interestingly, when the reaction was performed at 23 ºC (Table 7, entries 1-5), much longer reaction times were required and the product could only be obtained in poor yields. Rather, when the reaction was performed on a sealed microwave vial at 70 ºC (Table 7, entries 6-10), full conversion was achieved in 6 to 24 hours. The best results were observed with catalysts **C** and **I** (Table 7, entries 7 and 9). However, since catalyst **C** required longer reaction times, phosphite gold(I) complex **I** was selected for further optimization.

Table 7. Screening of cationic gold(I) complexes for the cyclization of **51**[a]

Entry	$[Au]_{cat}$ (mol%)	T (ºC)	Time (h)	Yield (%)[b]
1	**A** (15)	23	80	18
2	**C** (15)	23	80	<1
3	**G** (15)	23	80	9
4	**I** (15)	23	80	20
5	**M** (15)	23	80	14
6	**A** (15)	70[c]	6	38
7	**C** (15)	70[c]	24	48
8	**G** (15)	70[c]	6	39
9	**I** (15)	70[c]	6	45
10	**M** (15)	70[c]	6	32

[a] Reaction conditions: [**51**] = 0.1 M. [b] Isolated yields. [c] Performed on a sealed microwave vial.

Subsequently, we attempted to perform the reaction at lower temperatures in order to find milder reaction conditions (Table 8). At 50 ºC the gold catalyzed cyclization afforded **52** in 28% yield (Table 8, entry 1). Decreasing the concentration from 0.1 to 0.025 M proved to be beneficial for the formation of trindene **52** (Table 8, entry 3), which could be obtained in 62% yield (85% average yield for each C–C bond formation).

Table 8. Optimization of the triple gold(I)-catalyzed cyclodehydration of **51**

Entry	$[Au]_{cat}$ (mol%)	T (ºC)	[51] (M)	Time (h)	Yield (%)[a]
1	**I** (15)	50	0.1	15	28
2	**I** (15)	50	0.25	15	25
3	**I** (15)	50	0.025	15	62

[a] Isolated yields.

The subsequent selective functionalization of **52** to generate the corresponding tribromo- and triiodo- derivatives **53** and **54** proved to be nontrivial (Scheme 19), leading to complex mixtures. Therefore, this strategy for the generation of 2,5,8-trifunctionalized C_{3h}-symmetric trindene derivatives was not pursued further.

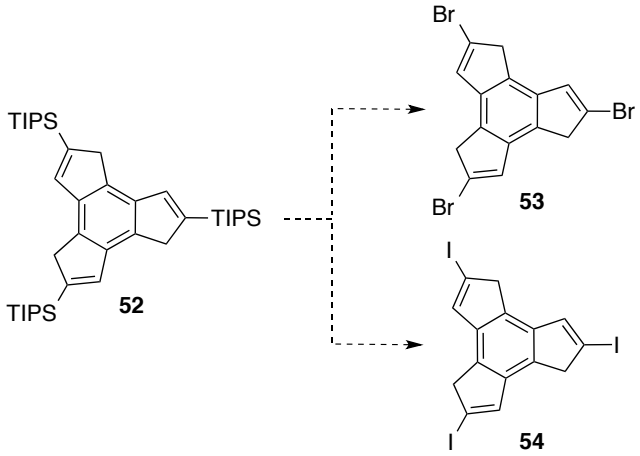

Scheme 19. Functionalization attempts of symmetric trindene **52**

Synthesis of C_{3h}-Symmetric Derivatives

With a reliable synthesis of 1,4,7-trindantrione (**41**) in hand, we focused on its application as a platform for the ready preparation of a variety of C_{3h}-symmetric derivatives with a common trindene core via triple Pd-catalyzed cross coupling reactions. To this aim, **41** was converted into the corresponding tristriflate **55** after treatment with triflic anhydride and 2,6-lutidine (Scheme 20).

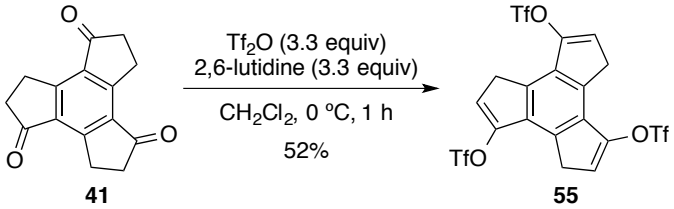

Scheme 20. Synthesis of **55** from 1,4,7- trisketone (**41**)

As illustrated in Table 9, the triple Suzuki-Miyaura coupling of **55** with aryl- and heteroarylboronic acids, as well as with a vinyl boronic ester, gave rise to derivatives **42a-j** in good to excellent yields using $Pd(PPh_3)_4$ as the catalyst. Several derivatives were prepared bearing ether (**42b**, **42j**), thioether (**42c**), aryl (**42d**), halide (**42e**) or carbonyl (**42f**) functionalities, as well as expanded aromatic frameworks (**42g**, **42i**).

Table 9. Suzuki-Miyaura coupling of **55** with aryl- and heteroarylboronic acids[a]

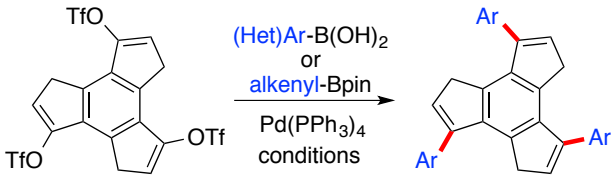

55 **42a-j**

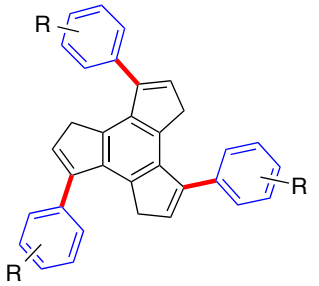

42a: R = H (87%)[a]
42b: R = *p*-OMe (91%)[a]
42c: R = *p*-SMe (87%)[b], (85%)[c]
42d: R = *p*-Ph (94%)[a]
42e: R = *p*-F (70%)[a]
42f: R = *m*-COMe (83 %)[b], (80%)[c]

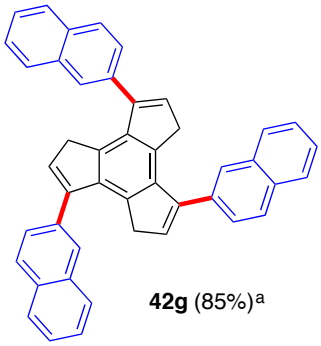

42g (85%)[a]

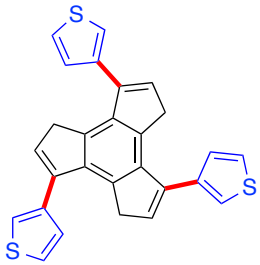

42h (30%)[c]

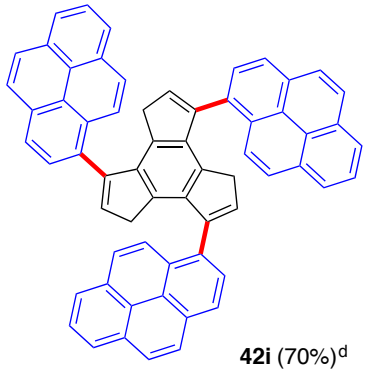

42i (70%)[d]

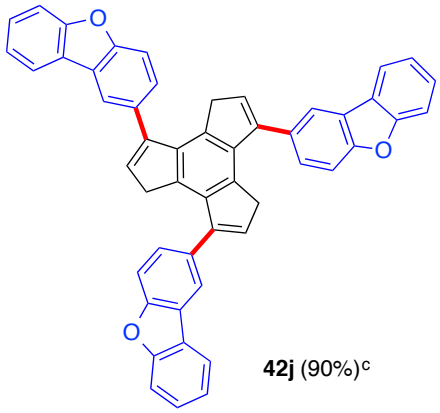

42j (90%)[c]

[a] Conditions: (a) 8 mol% catalyst, Na_2CO_3 (5 equiv), toluene-EtOH, 90 °C. (b) 15 mol% catalyst, K_3PO_4 (5 equiv), dioxane, 23 °C. (c) 15 mol% catalyst, K_3PO_4 (5 equiv), dioxane, 70 °C. (d) 15 mol% catalyst, K_3PO_4 (5 equiv), dioxane, 23 °C.

Photophysical Properties of C_{3h} Aryltrindene 42i

As a representative example we investigated the photophysical properties of 1,4,7-tris(pyrene)trindene (**42i**), which were compared with the parent pyrene.

Thus, the UV–Vis absorption and photoluminescence spectra of compound **42i** and pyrene were mesured in dilute THF solutions (c = $1.26 \cdot 10^{-5}$ M) at 25 ºC. The resulting data are summarized in Table 10.

Table 10. Absorption and emission spectral data of compound **42i** and pyrene

Compound	λ_{abs}/nm	ε_{abs}, 10^3 $mol^{-1}lcm^{-1}$	λ_{em} /nm
42i	316	29.5	381
	330	57.4	398
	346	82.9	
pyrene	306	14.0	372
	321	34.9	393
	337	56.3	

The absorption spectra of compound **42i** and pyrene in THF exhibit intense absorption bands in the UV region (Figure 8). Compound **42i** shows the characteristic pyrene absortion pattern at 316 nm, 330 nm and 346 nm. The λ_{max} at about 346 nm is attributed to the π–π* transition of the pyrene core and displays a red-shift up to 10 nm compared with the unsubstituted parent pyrene (337 nm).

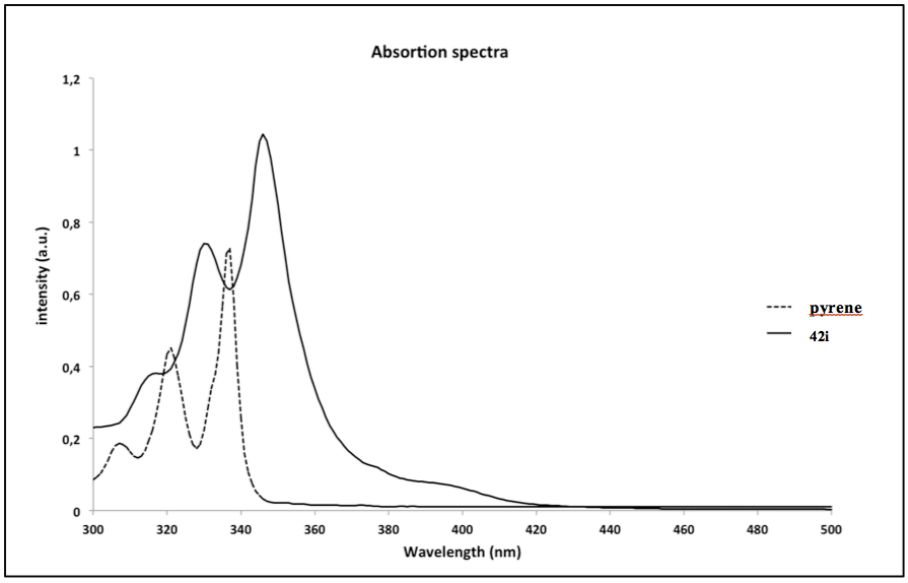

Figure 8. Absorption spectra of compound **42i** and pyrene in THF at 25 ºC

Compound **42i** shows emission at 25 ºC in a degassed THF solution with the maximum at *ca.* 381 nm (Figure 9). In this case, the vibronic fine structure typical from pyrene is not observed. The fluorescence band appears slightly red-shifted, which is consistent with the absorption spectrum of **42i** relative to that of pyrene.

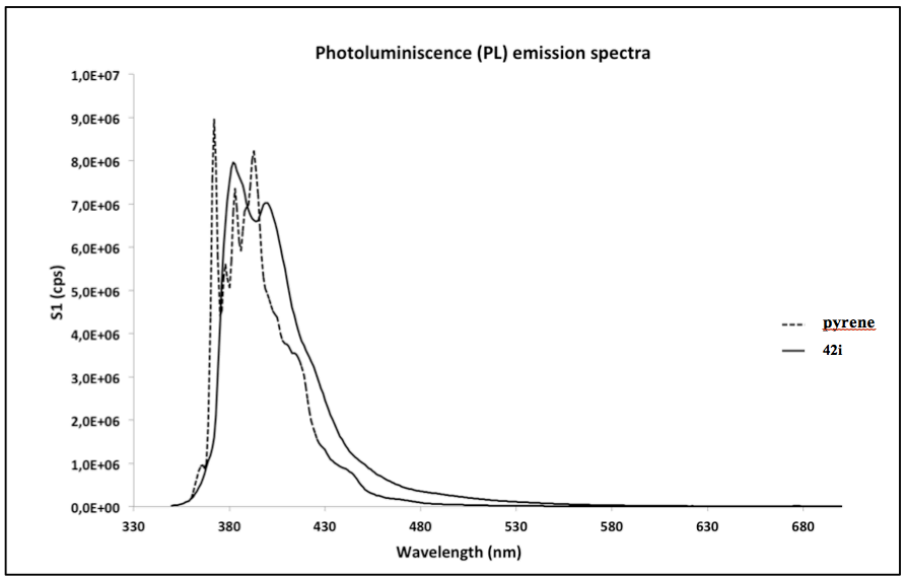

Figure 9. The emission spectra of **42i** and pyrene in degassed THF at 25ºC

Hydrogenation of 1,4,7-Triphenyltrindene (42a)

Moreover, the possibility of further derivatization of polyarenes **42** to stereoselectively prepare *syn*-trisubstituted trindane derivatives was illustrated by the hydrogenation of triphenyltrindene **42a**, which was accomplished in the presence of PtO_2 under 50 atm of H_2 for 72 h to afford selectively 1,4,7-*syn*-triphenyltrindane **56** (Table 11, entry 6), whose structure was unambiguously assured by X-ray diffraction analysis (Figure 10). Surprisingly, when the same transformation was attempted using Pd/C as the catalyst under different conditions, no reaction was observed (Table 11, entries 1–4).

Table 11. Hydrogenation of **42a**

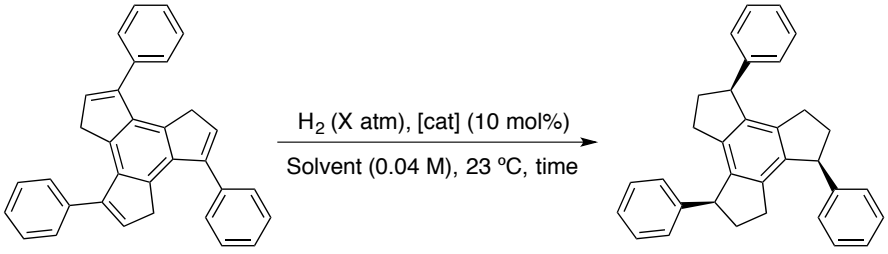

42a ***syn*-56**

Entry	[cat]	H_2 (atm)	Solvent	t (h)	Yield (%)
1	Pd/C	4	EtOAc	16	–[a]
2	Pd/C	10	EtOAc	16	–[a]
3	Pd/C	50	EtOAc	16	–[a]
4	Pd/C	50	THF	72	–[a]
5	PtO_2	50	THF	24	traces
6	PtO_2	50	THF	72	73

[a] No reaction was observed. 100% of starting material was recovered.

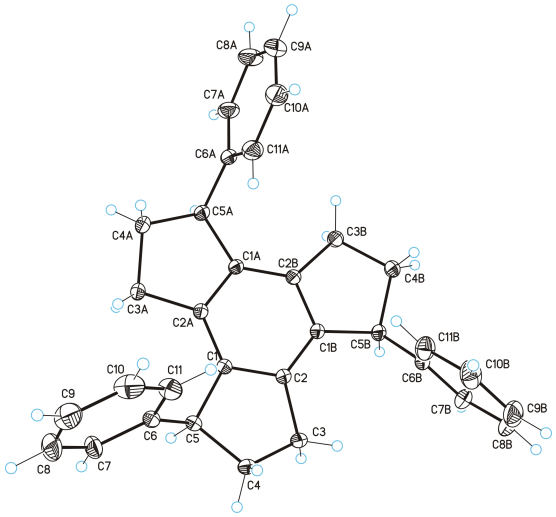

Figure 10. X-ray crystal structure of *syn*-**56** (50% probability thermal ellipsoids)

Synthesis of a New Crushed C60 (45)

As a model study, we performed the Suzuki coupling of boronic ester **57** similar to that required for the construction of a more complex C_{3h}-symmetric polyarene that features the topology of C_{60} fullerene. Hence, the synthesis of **58**, a smaller prototype of **45**, was first essayed under standard reaction conditions by coupling of **55** with 2-indenylboron nucleophile **57** (Scheme 21). Gratifyingly, the triple coupling afforded **58** in 63-68% yield.

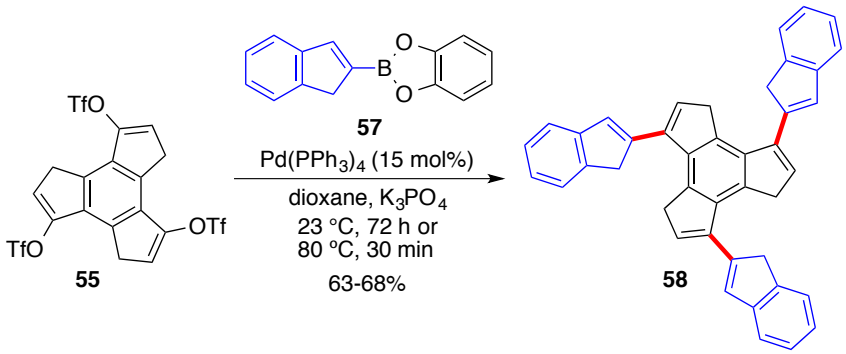

Scheme 21. Synthesis of **58** as a prototype of **45** by triple vinyl-vinyl Suzuki cross coupling

Encouraged by the formation of **58**, we decided to attempt the coupling of three 2-trindenyl units to **55**. Thus, the required alkenyl nucleophile was prepared from 1-trindanone **31** in 5 steps (Scheme 22). α-Bromination of **31** gave **59**, which was converted into alkenyl bromide **60** by reduction with $NaBH_4$ followed by acid-catalyzed dehydration in 65% yield over the 2 steps. Finally, **60** was transformed into more stable potassium trifluoroborate salt **61** in 73% overall yield by a two-step protocol.

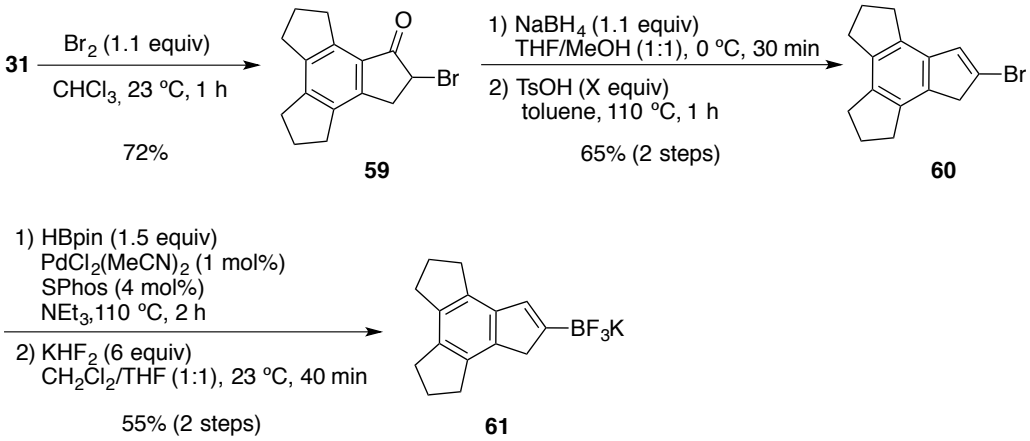

Scheme 22. Synthesis of potassium trifluoroborate **61**

The final triple coupling of tristriflate **55** with trifluoroborate **61** was carried out under the reaction conditions established for the synthesis of **58** to form **45**, which can be considered as a new crushed C60 fullerene,[43] as a white solid in 24% yield (Scheme 23). This yield could not be further improved due to the formation of trindene as a result of the protodeborylation of **61**, but nevertheless it represents a 63% average yield for each C–C bond formation.

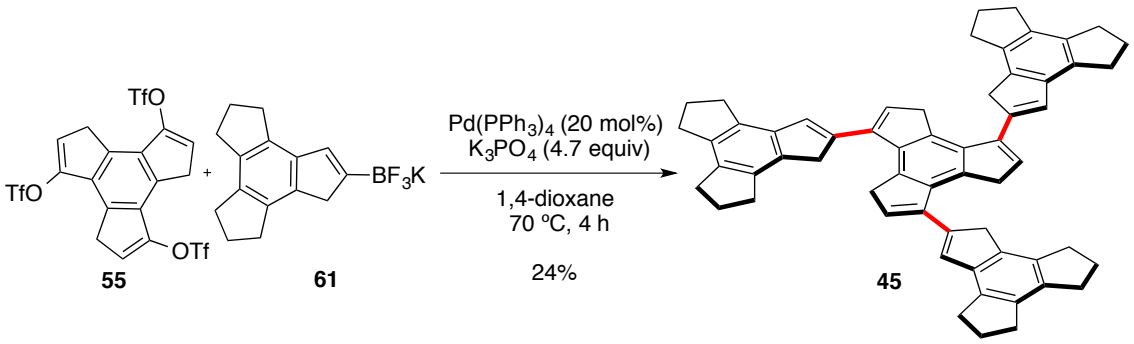

Scheme 23. Synthesis of crushed fullerene **45**

Conclusions

The C_{15} trindene core has been constructed through a triple gold(I)-catalyzed oxidative cyclization thus highlighting the proficiency of gold catalysis in the context of the construction of polycyclic structures (Scheme 24).

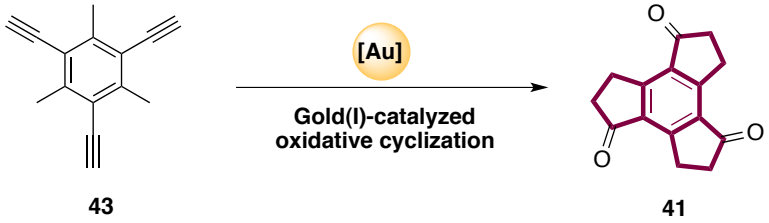

Scheme 24. Synthesis of 1,4,7-trindantrione (**41**) via gold(I)-catalyzed oxidative cyclization

1,4,7-Trindantrione (**41**) and its tristriflate (**55**) are now readily available C_{3h} C_{15} synthons that could allow accessing to a wide variety of derivatives, playing a role similar to that of truxene in the preparation of carbon-rich materials.[43,44] Moreover, we have developed a novel approach for the synthesis of C_{3h}-symmetric aryltrindenes by triple Pd-catalyzed cross-coupling reactions (Scheme 25).

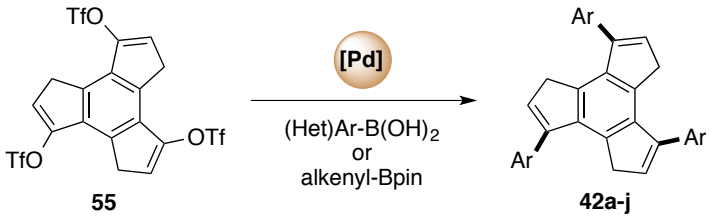

Scheme 25. Synthesis of C_{3h}-symmetric aryltrindenes via threefold Pd-coupling

This methodology has been successfully applied to the synthesis of a new trindane-based crushed C60, which features the topology of fullerene (Figure 11).

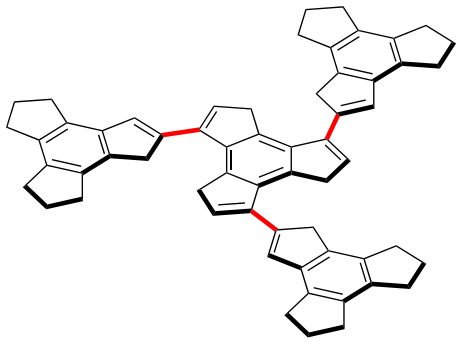

Figure 11. New trindane-based crushed C60

Experimental Part

General Methods

Unless other wise stated, reactions were performed under argon in solvents dried by passing through an activated alumina column on a PureSolv^{TM} solvent purification system (Innovative Technologies, Inc., MA). Analytical thin layer chromatography was carried out using TLC-aluminum sheets coated with 0.2 mm of silica gel (Merck GF_{234}) using UV light as the visualizing agent and an acidic solution of vanillin in ethanol as the developing agent. Chromatographic purifications were carried out using flash grade silica gel (SDS Chromatogel 60 ACC, 40-63 μm) or automated flash chromatographer CombiFlash Companion. Preparative TLC was performed on 20 cm x 20 cm silica gel plates (2.0 mm thick, catalogue number 02015, Analtech). If indicated, preparative TLC was performed on 20 cm x 20 cm aluminium oxide plates (0.25 mm thick, 90066, Fluka). Organic solutions were concentrated under reduced pressure on a Büchi rotary evaporator.

NMR spectra were recorded at 298 K (unless otherwise stated) on a Bruker Avance 300, Bruker Avance 400 Ultrashield and Bruker Avance 500 Ultrashield apparatuses. The data are reported as such: chemical shift [δ, ppm] (multiplicity, coupling constant [Hz], number of protons). The chemical shifts are given in ppm downfield from tetramethylsilane using the residual protio-solvent as internal reference (d_H = 7.26 ppm and d_C = 77.16 for $CDCl_3$). The abbreviations for multiplicities are: s (singlet), d (doublet), t (triplet), q (quartet), quin (quintet), sext (sextet), sept (septet). Mass spectra were recorded on a Waters Micromass LCT Premier (ESI), Waters Micromass GCT (EI, CI) and Bruker Daltonics Autoflex (MALDI) spectrometers. Melting points were determined using a Büchi melting point apparatus. UV-Vis measurements were carried out on a Shimadzu UV-1700PC spectrophotometer equipped with a photomultiplier detector, double beam optics, and D_2 and W light source. Fluorescence measurements were carried out on a Fluorolog Horiba Jobin Yvon spectrofluorimeter equipped with photomultiplier detector, double monochromator and Xe light source. Crystal structure determinations were carried out using a Bruker-Nonius diffractomer equipped with an APPEX 2 4K CCD area detector, a FR591 rotating anode with MoK_a radiation, Montel mirrors as monochromator and a Kryoflex low temperature device (T = –173 °C). Full-sphere data collection was used with w and j scans. *Programs used*: Data collection APEX-2, data reduction Bruker Saint V/.60A and absorption correction SADABS.

Structure Solution and Refinement: Crystal structure solution was achieved using direct methods as implement in SHELXTL and visualized using the program XP. Missing atoms were subsequently located from difference Fourier synthesis and added to the atom list. Least-squares refinement on F2 using all measured intensities was carried out using the program SHELXTL. All non-hydrogen atoms were refined including anisotropic displacement parameters.

All reagents were used as purchased and used with no further purification, unless otherwise stated.

Synthetic Procedures and Analyical Data

1,1',1''-(Benzene-1,3,5-triyl)tris(2-(triisopropylsilyl)prop-2-en-1-ol) (51)

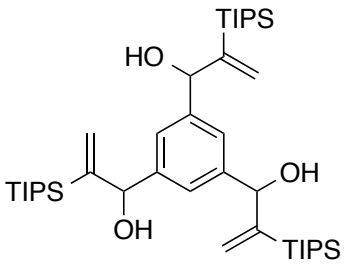

A solution of (1-bromovinyl)triisopropylsilane[63b] (2.44 g, 9.29 mmol) in anhydrous THF (30 mL) was treated dropwise with *n*-BuLi (2.5 M solution in hexanes, 3.9 mL, 9.88 mmol) at -78 ºC under argon. The mixture was left at -78 ºC for 2 h. Then, benzene-1,3,5-tricarbaldehyde (421 mg, 2.6 mmol) was carefully added in one portion. After two additional hours, the reaction was allowed to warm to room temperature and stirred for another 2 h (the mixture becomes a bright orange solution). After completion of the reaction, the crude was poured into a saturated solution of NH_4Cl and the product was extracted with ethyl acetate. The combined extracts were dried over anhydrous $MgSO_4$ and concentrated under reduced pressure. The residue was purified by column chromatography over silica gel using cyclohexane:EtOAc 9:1 as eluent to afford the product as a colorless oil (1.56 g, 84%).

Mixture of *syn* and *anti* isomers: ^{1}H NMR (400 MHz, $CDCl_3$) δ 7.30 – 7.27 (m, J = 2.9 Hz, 3H + 3H), 5.92 – 5.88 (m, 3H + 3H), 5.61 – 5.59 (m, 3H + 3H), 5.39 (s, 3H + 3H), 1.19 (sep, J = 7.3 Hz, 9H + 9H), 1.07 (d, J = 7.3 Hz, 27H + 27H), 1.02 – 0.97 (m, 27H + 27H). ^{13}C NMR (101 MHz, $CDCl_3$) δ 149.8, 149.7, 149.6, 143.3, 143.3, 129.3, 129.2, 126.3, 126.2, 125.9, 76.5, 76.4, 19.0, 18.9, 11.5. HRMS-ESI(+) *m/z* calc. for $C_{42}H_{78}NaO_3Si_3$ $[M+Na]^+$: 737.5151, found: 737.5172.

2,5,8-Tris(triisopropylsilyl)-4,7-dihydro-1*H*-cyclopenta[*e*]-*as*-indacene (52)

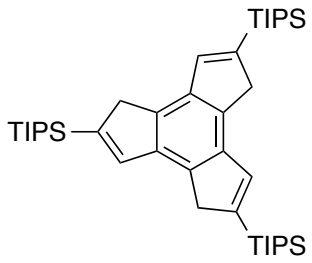

A microwave vial was charged with gold(I) catalyst **I** (41 mg, 0.035 mmol), sealed and put under argon. Then, a solution of **51** (166 mg, 0.232 mmol) in anhydrous dichloromethane (9.3 mL) was added and the resulting mixture was stirred at 50 ºC for 15 h (TLC monitoring). The reaction mixture was cooled to 23 ºC, the volatiles removed under reduced pressure and the resulting crude purified by column chromatography using cyclohexane as eluent to afford the product as a white foamy solid (78 mg, 51%).

Mp = 28–29 ºC. ^{1}H NMR (400 MHz, $CDCl_3$) δ 7.34 (t, J = 1.7 Hz, 3H), 3.69 (d, J = 1.8 Hz, 6H), 1.34 (sep, J = 7.4 Hz, 9H), 1.14 (d, J = 7.4 Hz, 54H). ^{13}C NMR (101 MHz,

$CDCl_3$) δ 143.7, 141.3, 139.7, 135.6, 43.0, 19.0, 11.7. HRMS-ESI(+) *m/z* calc. for $C_{42}H_{73}Si_3$ $[M+H]^+$: 661.5015, found: 661.5020.

2,3,5,6,8,9-Hexahydro-1*H*-cyclopenta[*e*]-*as*-indacene-1,4,7-trione (41)

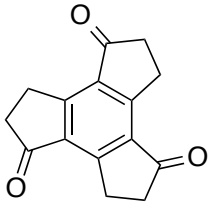

8-Methylquinoline *N*-oxide (1.91 g, 12 mmol) and gold(I) complex **C** (458 mg, 0.30 mmol) were added to a solution of 1,3,5-triethynylbenzene[62] (385 mg, 2 mmol) in DCE (200 mL, 0.01 M). After heating at 80 ºC for 1 h, the mixture was cooled down to room temperature and washed with a saturated solution of $Na_2S_2O_3$ (2x100 mL) and an aqueous solution of HCl (10% v/v, 100 mL). The organic layer was then dried over $MgSO_4$, filtered and concentrated under reduced pressure. Purification by column chromatography using cyclohexane:EtOAc 2:1 to 0:1 as eluent afforded the title compound as an off-white solid (198 mg, 42%).

Mp > 210 ºC. ^{1}H NMR (300 MHz, $CDCl_3$) δ 3.56 – 3.51 (m, 6H), 2.81 – 2.77 (m, 6H). ^{13}C NMR (101 MHz, $CDCl_3$) δ 205.6, 160.7, 134.3, 36.6, 25.9. HRMS-ESI(+) *m/z* calc. for $C_{15}H_{12}NaO_3$ $[M+Na]^+$: 263.0670, found: 263.0684.

4,7-Dihydro-1*H*-cyclopenta[*e*]-*as*-indacene-3,6,9-triyl tris(trifluoromethanesulfonate) (55)

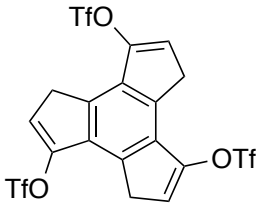

41 (90 mg, 0.375 mmol) was dissolved in anhydrous CH_2Cl_2 (11 mL) under argon and the solution was cooled down to 0 ºC. Then Tf_2O (0.21 mL, 1.24 mmol) was added dropwise followed by 2,6-lutidine (0.145 mL, 1.24 mmol), and the reaction was kept at 0 ºC for 30 min. After diluting with CH_2Cl_2 (5 mL) the mixture was washed with water (3x5 mL) and the organic layer was dried over $MgSO_4$ and concentrated under reduced pressure without heating. The product was obtained after column chromatography using cyclohexane:EtOAc 95:5 as eluent as a white solid (123 mg, 52%).

Mp = 135–137 ºC. ^{1}H NMR (300 MHz, $CDCl_3$) δ 6.52 (t, *J* = 2.4 Hz, 3H), 3.79 (d, *J* = 2.4 Hz, 6H). ^{13}C NMR (101 MHz, $CDCl_3$) δ 147.5, 133.0, 130.9, 118.8 (q, *J* = 320.9 Hz), 119.2, 33.7. ^{19}F NMR (376 MHz, $CDCl_3$) δ -73.1. HRMS-ESI(+) *m/z* calc. for $C_{18}H_8F_9O_9S_3$ $[M+H]^+$: 634.9171, found: 634.9163.

Synthesis of C_{3h} Aryltrindenes

General Procedure A

A screw-cap test-tube, equipped with a magnetic stir bar, was charged with tristriflate **55** (318 mg, 0.50 mmol), arylboronic acid (4.5 equiv) and $Pd(PPh_3)_4$ (46 mg, 0.04 mmol, 8 mol%). The vial was sealed with a teflon screw-cap and then evacuated and

backfilled with argon. Toluene (5.55 mL, 0.09 M), ethanol (2.00 mL, 0.25 M) and Na_2CO_3 2 M (2.25 mL, 9 equiv) were subsequently added and the mixture heated at 90 ºC for 40 min (TLC monitoring). The reaction was diluted with 5 mL of EtOAc and the organic phase was separated, dried over $MgSO_4$ and concentrated to dryness. The crude was adsorbed in basic Al_2O_3 and purified by flash chromatography using basic Al_2O_3 as stationary phase (cyclohexane:EtOAc 1:0 to 9:1) .

General Procedure B

A screw-cap test-tube, equipped with a magnetic stir bar, was charged with tristriflate **55** (318 mg, 0.50 mmol), arylboronic acid (5 equiv), K_3PO_4 (5 equiv) and $Pd(PPh_3)_4$ (87 mg, 0.75 mmol, 15 mol%). The vial was sealed with a teflon screw-cap, then evacuated and backfilled with argon. Deoxygenated dioxane (14.2 mL, 0.035 M) was added and the mixture was stirred at room temperature overnight. The reaction was diluted with 8 mL of EtOAc, the organic phase was separated, dried over $MgSO_4$ and concentrated to dryness. The crude was adsorbed in basic Al_2O_3 and purified by flash chromatography using basic Al_2O_3 as stationary phase (cyclohexane:EtOAc 1:0 to 9:1).

General Procedure C

A screw-cap test-tube, equipped with a magnetic stir bar, was charged with tristriflate **55** (318 mg, 0.50 mmol), arylboronic acid (5 equiv), K_3PO_4 (5 equiv) and $Pd(PPh_3)_4$ (87 mg, 0.75 mmol, 15 mol%). The vial was sealed with a teflon screw-cap, then evacuated and backfilled with argon. Deoxygenated dioxane (14.2 mL, 0.035 M) was added and stirred at 70 ºC in a preheated oil bath for 2–4 h (TLC monitoring). The reaction was diluted with 8 mL of EtOAc, the organic phase was separated, dried over $MgSO_4$ and concentrated to dryness. The crude was adsorbed in basic Al_2O_3 and purified by flash chromatography using basic Al_2O_3 as stationary phase (cyclohexane:EtOAc 1:0 to 9:1 or cyclohexane:CH_2Cl_2 9:1 to 8:2).

3,6,9-Triphenyl-4,7-dihydro-1*H*-cyclopenta[*e*]-*as*-indacene (42a)

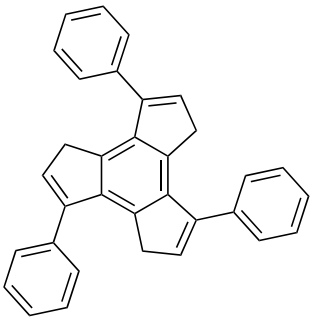

This compound was prepared in 87% yield according to the general procedure **A**, starting form tristriflate **55** and phenylboronic acid. White solid.

Mp = 210–211 ºC. ^{1}H NMR (400 MHz, $CDCl_3$) δ 7.45 – 7.38 (m, 15 H), 6.31 (t, *J* = 2.0 Hz, 3H), 3.19 (d, *J* = 2.0 Hz, 6H). ^{13}C NMR (101 MHz, $CDCl_3$) δ 145.7, 139.9, 138.3, 133.9, 132.3, 129.0, 128.1, 127.4, 38.1. HRMS-APCI(+) *m/z* calc. for $C_{33}H_{23}$ $[M+H]^+$: 419.1800, found: 419.1803.

3,6,9-Tris(4-methoxyphenyl)-4,7-dihydro-1*H*-cyclopenta[*e*]-*as*-indacene (42b)

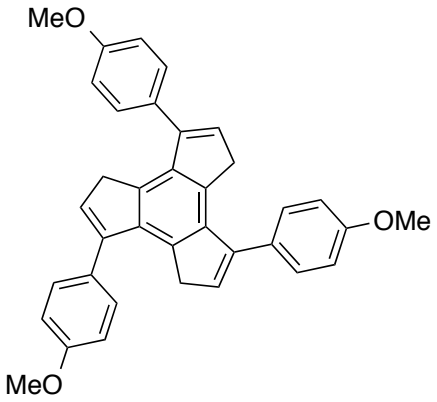

This compound was prepared in 91% yield according to the general procedure **A**, starting form tristriflate **55** and (4-methoxyphenyl)boronic acid. Off-white solid.

Mp = 219–220 ºC. ^{1}H NMR (400 MHz, $CDCl_3$) δ 7.37 (d, *J* = 8.4 Hz, 6H), 6.97 (d, *J* = 8.4 Hz, 6H), 6.28 (t, *J* = 1.8 Hz, 3H), 3.88 (s, 9H), 3.19 (d, *J* = 1.8 Hz, 6H). ^{13}C NMR (126 MHz, $CDCl_3$) δ 159.1, 145.3, 140.1, 133.9, 132.0, 130.7, 130.1, 127.6, 113.5, 55.5, 38.0. HRMS-APCI(+) *m/z* calc. for $C_{36}H_{29}O_3$ $[M+H]^+$: 509.2117, found: 509.2121.

3,6,9-Tris(4-(methylthio)phenyl)-4,7-dihydro-1*H*-cyclopenta[*e*]-*as*-indacene (42c)

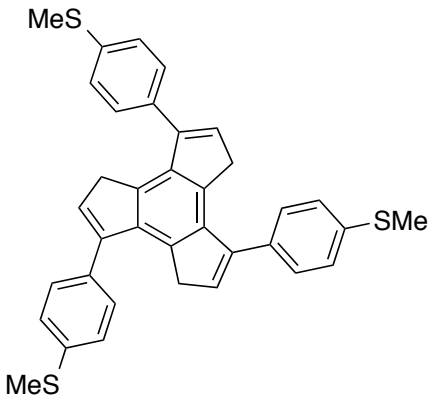

This compound was prepared in 87% yield according to the general procedure **B**, and 85% yield according to the general procedure **C** starting form tristriflate **55** and (4-(methylthio)phenyl) boronic acid. Brown solid.

Mp = 226–227 ºC. ^{1}H NMR (400 MHz, $CDCl_3$) δ 7.37 (d, *J* = 8.6 Hz, 6H), 7.32 (d, *J* = 8.3 Hz, 6H), 6.31 (t, *J* = 2.0 Hz, 3H), 3.21 (d, *J* = 2.0 Hz, 6H), 2.55 (s, 9H). ^{13}C NMR (101 MHz, $CDCl_3$) δ 145.1, 139.8, 137.6, 135.0, 139.9, 132.5, 129.4, 126.2, 38.2, 16.0. HRMS-ESI(+) *m/z* calc. for $C_{36}H_{31}S_3$ $[M+H]^+$: 559.1582, found: 559.1554.

3,6,9-Tri(biphenyl-4-yl)-4,7-dihydro-1*H*-cyclopenta[*e*]-*as*-indacene (42d)

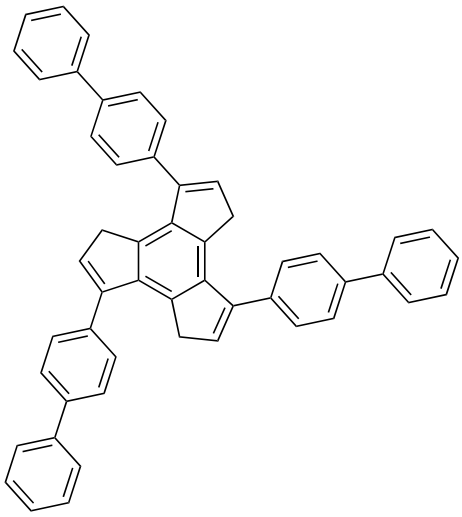

This compound was prepared in 94% yield according to the general procedure **A**, starting form tristriflate **55** and [1,1'-biphenyl]-4-ylboronic acid. White solid.

Mp = 245–246 ºC. ^{1}H NMR (400 MHz, $CDCl_3$) δ 7.72 – 7.68 (m, 12H), 7.55 (app. d, *J* = 8.0 Hz, 6H), 7.48 (app. t, *J* = 8.0 Hz, 6H), 7.38 (app. t, *J* = 6.0 Hz, 3H), 6.39 (t, *J* = 4.0 Hz, 3H), 3.31 (d, *J* = 4.0 Hz, 6H). ^{13}C NMR (101 MHz, $CDCl_3$) δ 145.4, 141.0, 140.3, 140.0, 137.3, 134.1, 132.6, 129.5, 129.0, 127.5, 127.2, 126.8, 38.4. HRMS-APCI(+) *m/z* calc. for $C_{51}H_{35}$ $[M+H]^+$: 647.2739, found: 647.2739.

3,6,9-Tris(4-fluorophenyl)-4,7-dihydro-1*H*-cyclopenta[*e*]-*as*-indacene (42e)

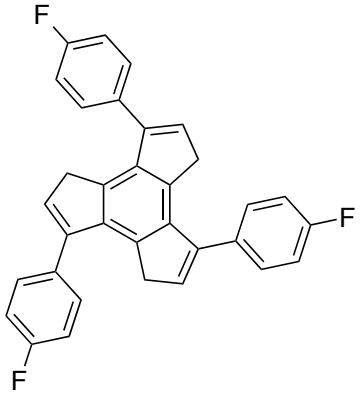

This compound was prepared in 70% of yield according to the general procedure A, starting form tristriflate **55** and (4-fluorophenyl)boronic acid. Off-white solid.

Mp = 174–176 ºC. ^{1}H NMR (500 MHz, $CDCl_3$) δ 7.43 – 7.37 (m, 6H), 7.16 – 7.10 (m, 6H), 6.32 (t, *J* = 2.1 Hz, 3H), 3.16 (d, *J* = 2.1 Hz, 6H). ^{13}C NMR (101 MHz, $CDCl_3$) δ 162.5 (d, *J* = 246 Hz), 144.7, 139.9, 134.1 (d, *J* = 3.2 Hz), 133.8, 132.6, 130.6 (d, *J* = 8 Hz), 115.1 (d, *J* = 21 Hz), 38.0. ^{19}F NMR (376 MHz, $CDCl_3$) δ -115.21. HRMS-APCI(–) *m/z* calc. for $C_{33}H_{21}F_3$ $[M–H]^-$: 473.1517, found: 473.1510.

1,1',1''-(3,3',3''-(4,7-Dihydro-1*H*-cyclopenta[*e*]-*as*-indacene-3,6,9-(triyl)tris-(benzene-3,1-diyl))triethanone (42f)

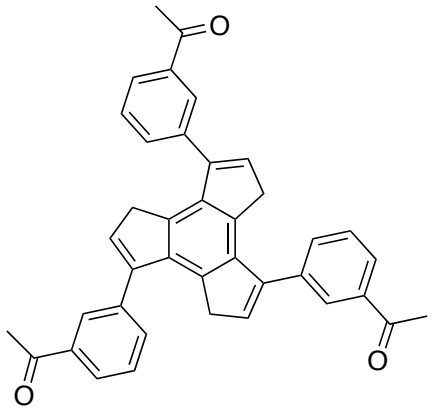

This compound was prepared in 83% yield according to the general procedure **B**, and 80% yield according to the general procedure **C** starting form tristriflate **55** and (3-acetylphenyl)boronic acid. Off-white solid.

Mp = 102–104 ºC. ^{1}H NMR (400 MHz, $CDCl_3$) δ 8.08 (t, *J* = 1.6 Hz, 3H), 8.04 (dt, *J* = 7.6, 1.6 Hz,

3H), 7.69 (dt, *J* = 7.6, 1.6 Hz, 3H), 7.58 (t, *J* = 7.6 Hz, 3H), 6.40 (t, *J* = 2.0 Hz, 3H), 3.20 (d, *J* = 2.0 Hz, 6H), 2.68 (s, 9H). ^{13}C NMR (101 MHz, $CDCl_3$) δ 198.0, 144.6, 139.5, 138.4, 136.9, 133.7, 133.4, 133.0, 128.7, 128.4, 127.4, 38.1, 26.8. HRMS-ESI(+) *m/z* calc. for $C_{39}H_{30}NaO_3$ $[M+Na]^+$: 569.2087, found: 569.2094.

3,6,9-Tri(naphthalen-2-yl)-4,7-dihydro-1*H*-cyclopenta[*e*]-*as*-indacene (42g)

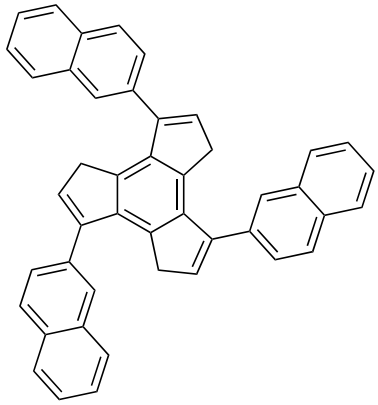

This compound was prepared in 85% yield according to the general procedure **A**, starting form tristriflate **55** and naphthalen-2-ylboronic acid. White solid.

Mp = 276–278 ºC. ^{1}H NMR (400 MHz, $CDCl_3$) δ 7.95-7.88 (m, 12H), 7.63 (dd, *J* = 7.2, 1.3 Hz, 3H), 7.58 – 7.51 (m, 6H), 6.39 (t, *J* = 2.0 Hz, 3H), 3.27 (d, *J* = 2.0 Hz, 6H). ^{13}C NMR (126 MHz, $CDCl_3$) δ 145.7, 140.1, 135.8, 134.2, 133.3, 132.9, 132.8, 128.1, 127.9, 127.6, 127.6, 127.5, 126.4, 126.0, 38.4. HRMS-APCI(+) *m/z* calc. for $C_{45}H_{29}$ $[M+H]^+$: 569.2269, found: 569.2267.

3,6,9-Tri(thiophen-3-yl)-4,7-dihydro-1*H*-cyclopenta[*e*]-*as*-indacene (42h)

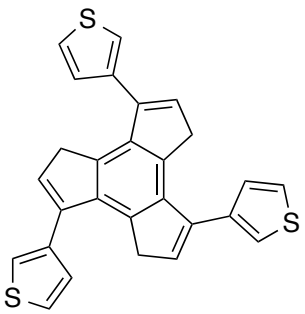

This compound was prepared in 30% of yield according to the general procedure **C**, starting form tristriflate **55** and thiophen-3-ylboronic acid. Brown dark solid.

Mp = 210–212 ºC. ^{1}H NMR (400 MHz, $CDCl_3$) δ 7.41 (dd, *J* = 4.9, 3.0 Hz, 3H), 7.29 (dd, *J* = 3.0, 1.3 Hz, 3H), 7.19 (dd, *J* = 4.9, 1.2 Hz, 3H), 6.40 (t, *J* = 2.1 Hz, 3H), 3.25 (d, *J* = 2.1 Hz, 6H). ^{13}C NMR (101 MHz, $CDCl_3$) δ 140.4, 139.8, 138.3, 133.7, 133.0, 129.2, 125.1, 122.8, 37.7. HRMS-ESI(+) *m/z* calc. for $C_{27}H_{19}S_3$ $[M+H]^+$: 439.0643, found: 439.0649.

3,6,9-Tri(pyren-2-yl)-4,7-dihydro-1*H*-cyclopenta[e]-as-indacene (42i)

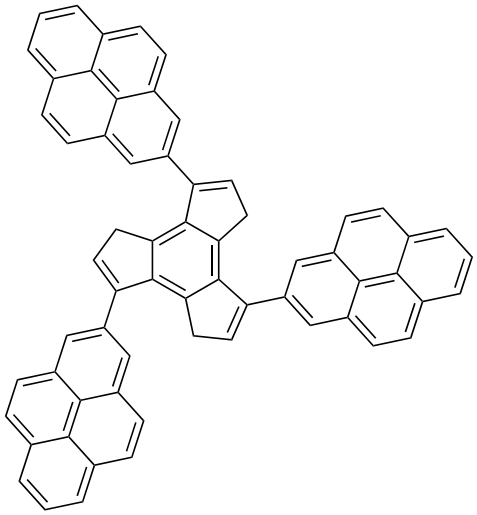

In a glovebox, anhydrous and deoxygenated dioxane (0.7 mL, 0.035 M) was added to a solid mixture of **55** (16 mg, 0.025 mmol), pyren-1-ylboronic acid (31 mg, 0.126 mmol), K_3PO_4 (27 mg, 0.126 mmol) and $Pd(PPh_3)_4$ (4 mg, 0.0038 mmol). The resulting mixture was stirred at 23 ºC overnight, then heated at 70 ºC for 1.5 h and then cooled down to room temperature and diluted with EtOAc (3 mL). After washing with water (3x5 mL) the organic layer was dried over $MgSO_4$, filtered and concentrated under reduced pressure. The product was obtained after purification by flash column chromatography using basic Al_2O_3 as the stationary phase using cyclohexane:CH_2Cl_2 9:1 to 8:2 as eluent as an off-white solid (14 mg, 70%).

Mp > 250 ºC (decomposition). ^{1}H NMR (500 MHz, $C_2D_2Cl_4$, 398K) δ 8.28-8.08 (m, 27H), 8.07-7.97 (m, 3H), 6.29 (t, *J* = 1.6 Hz, 1H), 2.95-2.66 (m, 2H). ^{13}C NMR (126 MHz, $C_2D_2Cl_4$, 398K) δ 143.7, 141.0, 133.9, 133.7, 133.6, 131.5, 131.1, 130.8, 129.8, 127.4, 127.3, 127.2, 127.1, 125.8, 125.7, 124.9, 124.8, 124. 8, 124.2, 37.3. *Note: One carbon signal missing due to overlapping*. HRMS-APCI(+) *m/z* calc. for $C_{63}H_{35}$ $[M+H]^+$: 791.2739, found: 791.2708.

3,6,9-Tris(dibenzo[*b,d*]furan-2-yl)-4,7-dihydro-1*H*-cyclopenta[*e*]-*as*-indacene (42j)

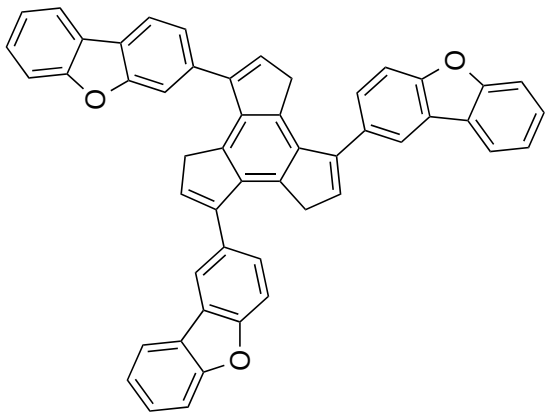

This compound was prepared in 90% yield according to the general procedure **C**, starting form tristriflate **55** and dibenzo[*b,d*]furan-4-ylboronic acid. Off-white solid.

Mp = 192–194 ºC. ^{1}H NMR (500 MHz, $CDCl_3$) δ 8.04 (app. dt, *J* = 7.2, 2.0 Hz, 6H), 7.56 (d, *J* = 8.4 Hz, 3H), 7.49-7.43 (m, 9H), 7.39 (dt, *J* = 7.5, 1.0 Hz, 3H), 6.42 (t, *J* = 2.0 Hz, 3H), 3.08 (d, *J* = 2.0 Hz, 6H). ^{13}C NMR (101 MHz, $CDCl_3$) δ 156.3, 154.3, 140.2, 139.9, 134.1, 134.0, 128.5, 127.3, 124.5, 124.3, 123.0, 122.9, 122.8, 120.8, 120.1, 112.3, 37.1. HRMS-APCI(+) *m/z* calc. for $C_{51}H_{29}O_3$ $[M+H]^+$: 689.2117, found: 689.2102.

Hydrogenation of 1,4,7-triphenyltrindene (42a)

(1*R,4*R**,7*R**)-1,4,7-Triphenyl-2,3,4,5,6,7,8,9-octahydro-1*H*-cyclopenta[*e*]-*as*-indacene (*syn*-56)**

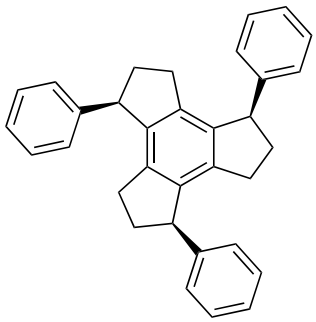

A mixture of **42a** (56 mg, 0.133 mmol) and PtO_2 (3 mg, 0.014 mmol) in THF (HPLC grade, 3 ml) was placed in a 25 ml autoclave equipped with a magnetic stirrer bar. The autoclave was purged three times with hydrogen and pressurized at 50 atm. After 72 h the excess hydrogen gas was released. The solution was then filtered through a celite pad and concentrated under reduced pressure without heating. The product was purified by flash chromatography using cyclohexane:EtOAc 96:4 as eluent to yield the title compound as a colorless oil (41 mg, 73%). The product precipitated as a white solid after treatment with hexane.

Mp = 131-132 ºC. ^{1}H NMR (400 MHz, $CDCl_3$) δ 7.39-7.02 (m, 15H), 4.31 (dd, *J* = 8.6, 5.3 Hz, 3H), 2.62-2.44 (m, 6H), 2.44-2.31 (m, 3H), 2.00-1.80 (m, 3H). ^{13}C NMR (101 MHz, $CDCl_3$) δ 146.1, 140.9, 139.9, 128.5, 127.9, 126.0, 50.5, 36.8, 29.9. HRMS-MALDI(+) *m/z* calc. for $C_{33}H_{30}Na$ $[M+Na]^+$: 449.2240, found: 449.2223.

2-(1*H*-Inden-2-yl)benzo[d][1,3,2]dioxaborole (57)

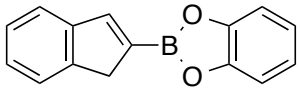

In a one neck round bottom flask, adapted with a dean stark trap, were placed 2-indenylboronic (1.60 g, 10.0 mmol), catechol (1.1 g, 10.0 mmol), toluene (166.7 mL, 0.06 M) and ethanol (16.7 mL, 0.6 M). The mixture was refluxed for 4 h and evaporated to dryness to yield a brown solid (2.30 g, 98 %) corresponding to desired product.

Note: Small impurities are always observed by NMR due to its prompt decomposition. Therefore, we recommend to recrystallize (CH_2Cl_2/pentane) this compound just before use.

Mp = 124.5–126 ºC. ^{1}H NMR (400 MHz, $CDCl_3$) δ 7.93 (t, *J* = 2.0 Hz, 1H), 7.59 (app. t, *J* = 8.0 Hz, 2H), 7.37 – 7.32 (m, 2H), 7.29 (app. dd, *J* = 5.9, 3.4 Hz, 2H), 7.12 (app. dd, *J* = 5.9, 3.3 Hz, 2H), 3.78 (d, *J* = 2.0 Hz, 2H). ^{13}C NMR (101 MHz, $CDCl_3$) δ 148.5, 148.3, 147.2, 144.7, 126.9, 126.8, 124.3, 122.9, 122.6, 112.6, 41.3 (one peak missing due to overlapping). HRMS-APCI(+) *m/z* calc. for $C_{15}H_{11}BO_2$ $[M]^+$: 233.0852, found: 233.0841.

3,6,9-Tri(1*H*-inden-2-yl)-4,7-dihydro-1*H*-cyclopenta[*e*]-*as*-indacene (58)

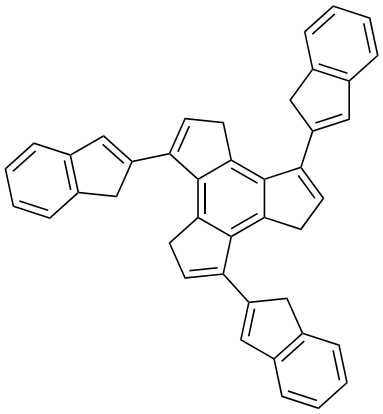

In a 100 mL dry schlenk flask, were placed tristriflate **55** (1.45g, 2.28 mmol), **57** (2.13 g, 9.12 mmol), $Pd(PPh_3)_4$ (0.39 g, 0.342 mmol, 15 mol%), K_3PO_4 (2.42 g, 11.4 mmol) and dry, deoxygenated dioxane (76 mL). The mixture was stirred 72 h at room temperature under argon. The reaction was transferred to a 500 mL flask and diluted with ethyl acetate (100 mL) and water (100 mL). The organic phase was washed several times with water, then dried over $MgSO_4$ and evaporated to dryness to get a black solid. The solid was dissolved in chloroform and filtered through a small silica gel bed that was previously neutralized with a solution of 30% (Et_3N/Hex). The filtrate was evaporated to dryness and precipitated from acetone, to get a brown-dark solid (1.07 g, 68 %) of the desired compound.

Note: Alternatively, this compound could be prepared following the previously described procedure stirring the mixture at 80 ºC for 30 min under argon.

Mp > 350 ºC. ^{1}H NMR (400 MHz, $CDCl_3$) δ 7.51 (d, *J* = 7.4 Hz, 3H), 7.46 (d, *J* = 7.5 Hz, 3H), 7.33 (t, *J* = 7.7 Hz, 3H), 7.23 (t, *J* = 7.5 Hz, 3H), 7.00 (app. s, 3H), 6.48 (t, *J* = 2.2 Hz, 3H), 3.79 (app. s, 6H), 3.60 (d, *J* = 2.2 Hz, 6H). ^{13}C NMR (101 MHz, $CDCl_3$) δ 145.5, 143.5, 143.2, 141.7, 139.7, 134.2, 133.0, 129.9, 126.8, 124.8, 123.8, 121.1, 43.3, 38.8. HRMS-MALDI(+) *m/z* calc. for $C_{42}H_{31}$ $[M+H]^+$: 535.2420, found: 535.2430.

Synthesis of New Crushed C60

2-Bromo-2,3,4,5,6,7,8,9-octahydro-1*H*-cyclopenta[*e*]-*as*-indacen-1-one (59)

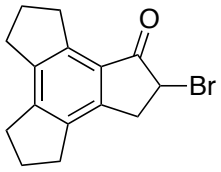

A solution of Br_2 (0.53 mL, 10.36 mmol) in $CHCl_3$ (80 mL) was added dropwise to a solution of **31**[8] (2.00 g, 9.42 mmol) in $CHCl_3$ (100 mL) at room temperature. After 1 h stirring at room temperature, the volatiles were removed under reduced pressure and the crude purified by flash chromatography using cyclohexane:EtOAc 98:2 as eluent to afford the product as a pale yellow solid (1.97 g, 72%).

Mp = 158–160 ºC. ^{1}H NMR (400 MHz, $CDCl_3$) δ 4.63 (dd, *J* = 7.5, 3.1, 1H), 3.69 (dd, *J* = 18.0, 7.5 Hz, 1H), 3.32 – 3.17 (m, 3H), 2.94 – 2.78 (m, 6H), 2.25 – 2.10 (m, 4H). ^{13}C NMR (101 MHz, $CDCl_3$) δ 199.8, 148.9, 145.1, 142.9, 141.1, 139.0, 127.8, 45.4, 36.9, 32.1, 31.1, 30.5, 29.9, 25.4, 25.1. HRMS-ESI(+) *m/z* calc. for $C_{15}H_{15}BrNaO$ $[M+Na]^+$: 313.0198, found: 313.0217.

8-Bromo-2,3,4,5,6,7-hexahydro-1*H*-cyclopenta[*e*]-*as*-indacene (60)

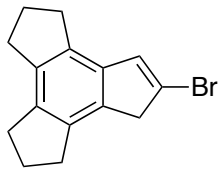

59 (2.31 g, 7.93 mmol) was dissolved in 80 mL of a 1:1 MeOH / THF solution and cooled to 0 ºC. $NaBH_4$ (0.33 g, 8.73 mmol) was then added in portions and the reaction was stirred for 30 min. Then the reaction was quenched with H_2O (50 mL) and the volatiles were evaporated. The remaining aqueous phase was extracted with CH_2Cl_2 (2x40 mL) and the combined organic layers dried over $MgSO_4$, filtered and concentrated to dryness. The resulting crude halohydrine was suspended in toluene (60 mL) and *p*-toluenesulfonic acid monohydrate (0.15 g, 0.793 mmol) together with Na_2SO_4 (100 mg) were added. The mixture was refluxed for 30 min and after cooling down to room temperature, washed with H_2O (40 mL), dried over $MgSO_4$, filtered and concentrated *in vacuo*. Purification by flash chromatography over silica gel, using cyclohexane as eluent gave the product as a white solid (1.41 g, 65%).

Mp = 139–141 ºC. ^{1}H NMR (400 MHz, $CDCl_3$) δ 6.94 (t, *J* = 1.7 Hz, 1H), 3.48 (dt, *J* = 2.0, 1.0 Hz, 2H), 2.93 (t, *J* = 7.4 Hz, 2H), 2.88 – 2.80 (m, 6H), 2.13 (p, *J* = 7.4 Hz, 4H). ^{13}C NMR (101 MHz, $CDCl_3$) δ 138.8, 138.0, 137.2, 136.7, 136.0, 134.0, 131.9, 123.4, 44.4, 31.4, 31.4, 31.0, 30.9, 25.8, 25.6. HRMS-ESI(+) *m/z* calc. for $C_{15}H_{15}BrNa$ $[M+Na]^+$: 297.0249, found: 297.0249.

Trifluoro(4,5,6,7,8,9-hexahydro-1*H*-cyclopenta[*e*]-*as*-indacen-2-yl)-λ^4-borane, potassium salt (61)

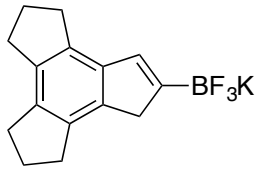

An oven-dried microwave vial was charged with **60** (1.33 g, 4.83 mmol), $PdCl_2(CH_3CN)_2$ (13 mg, 0.048 mmol) and SPhos (79 mg, 0.193 mmol). The vial was capped and then evacuated and backfilled with Ar. Anhydrous 1,4-dioxane (4.8 mL) was added followed by anhydrous NEt_3 (2.02 mL, 14.50 mmol) and HBpin (1.05 mL, 7.25 mmol). The reaction mixture was heated at 110 °C for 2 h and then allowed to cool down to room temperature. The reaction mixture was filtered through a thin pad of alumina and then concentrated under reduced pressure. The crude pinacol borane was directly dissolved in 3 mL of a 1:1 mixture of CH_2Cl_2/THF mixture. Then aqueous KHF_2 4.5 M (4.8 mL, 28.98 mmol) was added in one portion. The reaction mixture is stirred for 40 min and then the solvent was removed to complete dryness. Boiling acetone (3x20 mL) was added directly to the crude and the remaining inorganic salts were filtered off. The acetone was evaporated, and the resulting solid was triturated with pentane to yield the product as a pale yellow solid (0.80 g, yield over two steps = 55%).

Mp = 270–272 ºC. ^{1}H NMR (500 MHz, Acetone-d_6) δ 6.68 (s, 1H), 3.15 (s, 2H), 2.90 (t, J = 7.4 Hz, 2H), 2.82 (t, J = 7.5 Hz, 2H), 2.77 (app. q, J = 6.6 Hz, 4H), 2.09 – 2.07 (bs, 4H). ^{13}C NMR (126 MHz, Acetone-d_6) δ 143.6, 140.9, 137.6, 137.2, 134.7, 133.5, 129.9, 129.8, 41.7, 32.3, 32.1, 32.0, 31.9, 26.8, 26.7. ^{19}F NMR (471 MHz, Acetone-d_6) δ -133.96. HRMS-ESI(–) *m/z* calc. for $C_{15}H_{15}BF_3$ $[M–K]^-$: 263.1224, found: 263.1210.

7'-(4,5,6,7,8,9-Hexahydro-1*H*-cyclopenta[*e*]-*as*-indacen-2-yl)-4,4'',5,5'',6,6',6'',7,7'', 8,8'',9,9',9''-tetradecahydro-1*H*,1''*H*,3'*H*-2,1':4',2''-tercyclopenta[*e*]-*as*-indacene (45)

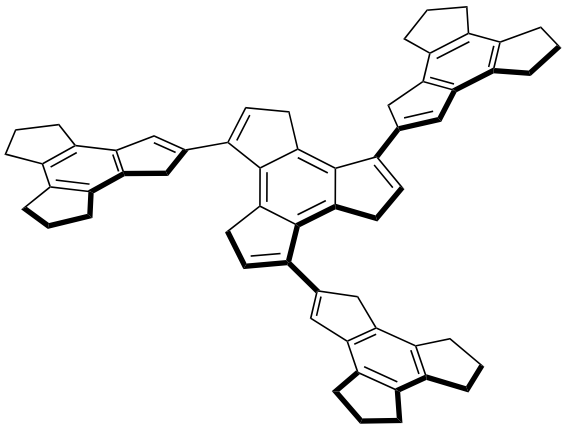

In a glovebox, anhydrous and deoxygenated dioxane (1.05 mL, 0.03 M) was added to a solid mixture of **55** (20 mg, 0.03 mmol), **61** (43 mg, 0.14 mmol), anhydrous K_3PO_4 (30 mg, 0.14 mmol) and $Pd(PPh_3)_4$ (6 mg, 0.005 mmol). The resulting mixture was heated at 70 ºC for 4 h and then cooled down to room temperature and diluted with EtOAc (3 mL). After washing with water (3x5 mL) the organic layer was dried over $MgSO_4$, filtered and concentrated under reduced pressure. The product was obtained after purification by preparative TLC using cyclohexane:CH_2Cl_2 8:2 as eluent as a white solid (6 mg, 24%). Mp > 220 ºC (decomposition). ^{1}H NMR (500 MHz, $CDCl_3$) δ 7.00 (t, J = 2.0 Hz, 3H), 6.44 (t, J = 2.0 Hz, 3H), 3.67 (s, 6H), 3.59 (d, J = 2.0 Hz, 6H), 3.06 (t, J = 7.3 Hz, 6H), 2.98 – 2.87 (m, 18H), 2.23 – 2.13 (m, 12H). ^{13}C NMR (101 MHz, $CDCl_3$) δ 142.4, 142.2, 139.8, 139.5, 138.8, 137.2, 137.0, 136.6, 134.7, 134.3, 132.4, 128.6, 42.0, 38.9, 31.5, 31.5, 31.2, 31.1, 25.9, 25.8. HRMS-MALDI(+) *m/z* calc. for $C_{60}H_{54}$ $[M]^+$: 775.4226, found: 775.4237.

Crystallographic Data

2,5,8-Tris(triisopropylsilyl)-4,7-dihydro-1*H*-cyclopenta[*e*]-*as*-indacene (52)

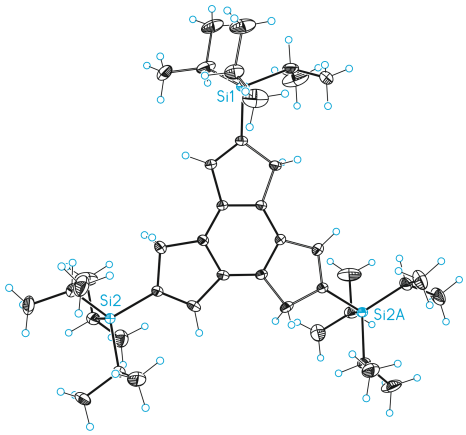

Table T12. Crystal data and structure refinement for **52**.

Empirical formula	C42H72Si3
Formula weight	661.26
Temperature	100(2) K
Wavelength	0.71073 Å
Crystal system	Monoclinic
Space group	P2(1)/m
Unit cell dimensions	
a = 8.7755(3)Å	α = 90°.
b = 27.3542(9)Å	β = 98.5066(8)°.
c = 8.7914(3)Å	γ = 90°.
Volume	2087.13(12) $Å^3$
Z	2
Density (calculated)	1.052 Mg/m^3
Absorption coefficient	0.140 mm^{-1}
F(000)	732
Crystal size	0.30 x 0.20 x 0.10 mm^3
Theta range for data collection	2.342 to 30.630°.
Index ranges	-11<=h<=12,-35<=k<=39,-12<=l<=7
Reflections collected	19427
Independent reflections	6210[R(int) = 0.0188]
Completeness to theta =30.630°	94.3%
Absorption correction	Multi-scan
Max. and min. transmission	0.986 and 0.758
Refinement method	Full-matrix least-squares on F^2
Data / restraints / parameters	6210/ 190/ 268
Goodness-of-fit on F^2	1.035
Final R indices [I>2sigma(I)]	R1 = 0.0398, wR2 = 0.1038
R indices (all data)	R1 = 0.0449, wR2 = 0.1079
Largest diff. peak and hole	0.500 and -0.302 $e.Å^{-3}$

Table T13. Bond lengths [Å] and angles [°] for **52**.

Bond lengths

Si1-C12	1.873(2)	C5-C5#1	1.3914(18)
Si1-C1	1.8740(12)	C5-C6	1.478(11)
Si1-C9	1.874(2)	C5-C6'	1.494(11)
Si1-C15	1.915(2)	C6-C7	1.377(4)
Si1-C15#1	1.915(2)	C6'-C7	1.504(4)
Si2-C7	1.8691(9)	C7-C8'	1.384(4)
Si2-C22	1.8914(10)	C7-C8	1.509(4)
Si2-C18	1.8955(11)	C9-C11	1.520(3)
Si2-C25	1.9015(12)	C9-C10	1.547(3)
C1-C2#1	1.387(4)	C12-C14	1.544(3)
C1-C2	1.387(4)	C12-C13	1.567(12)
C1-C2'	1.503(4)	C15-C17	1.485(11)
C1-C2'#1	1.503(4)	C15-C16	1.533(4)
C2-C3	1.479(11)	C18-C19	1.5287(19)
C2'-C3	1.496(11)	C18-C20	1.5346(15)
C3-C4	1.3932(12)	C22-C23	1.5298(18)
C3-C3#1	1.4062(17)	C22-C24	1.5369(15)
C4-C5	1.4088(12)	C25-C27	1.5286(17)
C4-C8'	1.462(10)	C25-C26	1.5334(16)
C4-C8	1.513(11)		

Angles

C12-Si1-C1	109.94(8)	C1-C2'-C3	104.0(6)
C12-Si1-C9	112.02(12)	C4-C3-C3#1	120.02(5)
C1-Si1-C9	105.97(8)	C4-C3-C2	134.1(2)
C12-Si1-C15	106.63(13)	C3-C3-C2#1	105.9(2)
C1-Si1-C15	110.94(6)	C4-C3-C2'	129.19(18)
C9-Si1-C15	111.40(12)	C3-C3-C2'#1	110.78(17)
C12-Si1-C15#1	46.53(13)	C3-C4-C5	119.98(8)
C1-Si1-C15#1	110.94(6)	C3-C4-C8'	134.4(2)
C9-Si1-C15#1	67.37(12)	C5-C4-C8'	105.6(2)
C15-Si1-C15#1	136.38(13)	C3-C4-C8	128.80(18)
C7-Si2-C22	108.42(4)	C5-C4-C8	111.19(18)
C7-Si2-C18	107.97(4)	C5-C5-C4#1	120.00(5)
C22-Si2-C18	116.09(5)	C5-C5-C6#1	134.4(2)
C7-Si2-C25	108.07(5)	C4-C5-C6	105.5(2)
C22-Si2-C25	107.89(5)	C5-C5-C6'#1	129.02(18)
C18-Si2-C25	108.15(5)	C4-C5-C6'	110.86(19)
C2-C1-C2#1	106.1(10)	C7-C6-C5	111.5(7)
C2'-C1-C2'#1	110.3(9)	C7-C6'-C5	103.9(6)
C2-C1-Si1#1	126.6(5)	C8'-C7-C6'	107.7(6)
C2-C1-Si1	126.6(5)	C6-C7-C8	109.0(6)
C2'-C1-Si1	124.7(4)	C6-C7-Si2	127.1(5)
C2'-C1-Si1#1	124.7(4)	C8'-C7-Si2	127.3(5)
C1-C2-C3	111.0(6)	C6'-C7-Si2	124.7(4)

C8-C7-Si2	123.8(4)	C16-C15-Si1	114.8(2)
C7-C8-C4	102.7(5)	C19-C18-C20	110.14(11)
C7-C8'-C4	112.0(6)	C19-C18-Si2	114.40(8)
C11-C9-C10	110.3(2)	C20-C18-Si2	114.02(8)
C11-C9-Si1	114.92(17)	C23-C22-C24	110.44(11)
C10-C9-Si1	113.93(18)	C23-C22-Si2	115.38(8)
C14-C12-C13	110.9(4)	C24-C22-Si2	112.88(8)
C14-C12-Si1	114.61(18)	C27-C25-C26	110.45(12)
C13-C12-Si1	111.5(4)	C27-C25-Si2	112.17(8)
C17-C15-C16	112.2(5)	C26-C25-Si2	111.72(8)
C17-C15-Si1	112.0(4)		

Table T14. Torsion angles [°] for **52**

C12-Si1-C1-C2_a#1	129.4(6)	C3#1-C3-C4-C8'	-175.1(5)
C9-Si1-C1-C2#1	-109.3(6)	C2-C3-C4-C8'	5.3(8)
C15-Si1-C1-C2#1	11.7(6)	C2'-C3-C4-C8'	3.4(8)
C15#1-Si1-C1-C2#1	179.3(6)	C3#1-C3-C4-C8	-177.0(5)
C12-Si1-C1-C2	-61.6(6)	C2-C3-C4-C8	3.4(8)
C9-Si1-C1-C2	59.7(6)	C2'-C3-C4-C8	1.4(7)
C15-Si1-C1-C2	-179.3(6)	C3-C4-C5-C5#1	-0.83(11)
C15#1-Si1-C1-C2	-11.7(6)	C8'-C4-C5-C5#1	176.1(4)
C12-Si1-C1-C2'	-59.3(5)	C8-C4-C5-C5#1	177.4(4)
C9-Si1-C1-C2'	61.9(5)	C3-C4-C5-C6	-177.6(4)
C15-Si1-C1-C2'	-177.0(5)	C8'-C4-C5-C6	-0.6(6)
C15#1-Si1-C1-C2'	-9.5(5)	C8-C4-C5-C6	0.6(6)
C12-Si1-C1-C2'#1	127.2(5)	C3-C4-C5-C6'	-177.2(4)
C9-Si1-C1-C2'#1	-111.6(5)	C8'-C4-C5-C6'	-0.2(6)
C15-Si1-C1-C2'#1	9.5(5)	C8-C4-C5-C6'	1.0(6)
C15#1-Si1-C1-C2'#1	177.0(5)	C5#1-C5-C6-C7	-174.9(2)
C2#1-C1-C2-C3	-0.9(12)	C4-C5-C6-C7	1.2(7)
C2'-C1-C2-C3	143(19)	C6'-C5-C6-C7	-175(9)
C2'#1-C1-C2-C3	0.7(3)	C5#1-C5-C6'-C7	-175.54(19)
Si1-C1-C2-C3	-171.8(3)	C4-C5-C6'-C7	0.4(7)
C2#1-C1-C2'-C3	1.6(3)	C6-C5-C6'-C7	5(8)
C2-C1-C2'-C3	-35(18)	C5-C6-C7-C8'	-1.2(8)
C2'#1-C1-C2'-C3	3.2(11)	C5-C6-C7-C6'	168(21)
Si1-C1-C2'-C3	-171.1(3)	C5-C6-C7-C8	-2.5(8)
C1-C2-C3-C4	-179.8(3)	C5-C6-C7-Si2	172.9(3)
C1-C2-C3-C3#1	0.6(7)	C5-C6'-C7-C6	-11(20)
C1-C2-C3-C2'	-162(9)	C5-C6'-C7-C8'	-0.4(8)
C1-C2'-C3-C4	179.5(2)	C5-C6'-C7-C8	-1.7(8)
C1-C2'-C3-C3#1	-2.0(7)	C5-C6'-C7-Si2	173.4(2)
C1-C2'-C3-C2	16(8)	C22-Si2-C7-C6	28.2(5)
C3#1-C3-C4-C5	0.83(11)	C18-Si2-C7-C6	154.7(5)
C2-C3-C4-C5	-178.7(6)	C25-Si2-C7-C6	-88.5(5)
C2'-C3-C4-C5	179.3(5)	C22-Si2-C7-C8'	-159.0(5)

C18-Si2-C7-C8'	-32.4(5)	C15#1-Si1-C9-C11	146.3(2)
C25-Si2-C7-C8'	84.3(5)	C12-Si1-C9-C10	-71.6(2)
C22-Si2-C7-C6'	28.4(5)	C1-Si1-C9-C10	168.55(19)
C18-Si2-C7-C6'	155.0(5)	C15-Si1-C9-C10	47.8(2)
C25-Si2-C7-C6'	-88.3(5)	C15#1-Si1-C9-C10	-85.0(2)
C22-Si2-C7-C8	-157.1(4)	C1-Si1-C12-C14	-160.90(18)
C18-Si2-C7-C8	-30.5(5)	C9-Si1-C12-C14	81.6(2)
C25-Si2-C7-C8	86.2(5)	C15-Si1-C12-C14	-40.6(2)
C6-C7-C8-C4	2.6(7)	C15#1-Si1-C12-C14	98.7(2)
C8'-C7-C8-C4	-16(11)	C1-Si1-C12-C13	72.1(5)
C6'-C7-C8-C4	2.2(7)	C9-Si1-C12-C13	-45.4(5)
Si2-C7-C8-C4	-172.9(2)	C15-Si1-C12-C13	-167.6(5)
C3-C4-C8-C7	176.05(19)	C15#1-Si1-C12-C13	-28.3(5)
C5-C4-C8-C7	-2.0(6)	C7-Si2-C18-C19	-62.57(10)
C8'-C4-C8-C7	10(7)	C22-Si2-C18-C19	59.36(10)
C6-C7-C8'-C4	0.8(8)	C25-Si2-C18-C19	-179.28(9)
C6'-C7-C8'-C4	0.3(8)	C7-Si2-C18-C20	169.40(9)
C8-C7-C8'-C4	162(12)	C22-Si2-C18-C20	-68.68(11)
Si2-C7-C8'-C4	-173.3(3)	C25-Si2-C18-C20	52.68(11)
C3-C4-C8'-C7	176.3(2)	C7-Si2-C22-C23	59.88(9)
C5-C4-C8'-C7	-0.1(7)	C18-Si2-C22-C23	-61.80(10)
C8-C4-C8'-C7	-168(8)	C25-Si2-C22-C23	176.70(8)
C12-Si1-C9-C11	159.8(2)	C7-Si2-C22-C24	-171.81(10)
C1-Si1-C9-C11	39.9(2)	C18-Si2-C22-C24	66.50(12)
C15-Si1-C9-C11	-80.9(2)	C25-Si2-C22-C24	-55.00(11)

(1*R,4*R**,7*R**)-1,4,7-Triphenyl-2,3,4,5,6,7,8,9-octahydro-1*H*-cyclopenta[*e*]-*as*-indacene (*syn*-56)**

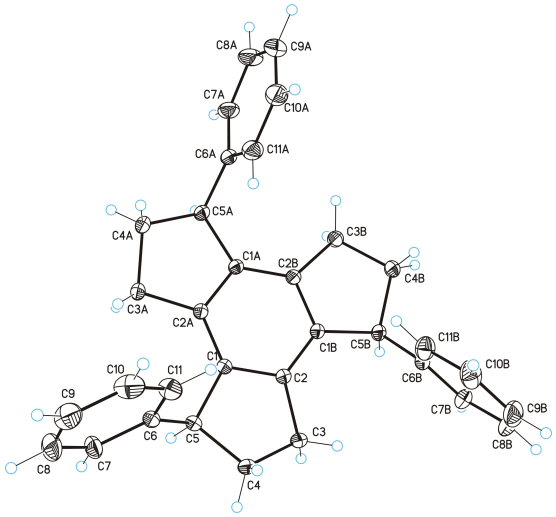

Table T15. Crystal data and structure refinement for ***syn*-56**.

Empirical formula	C66H60
Formula weight	853.14
Temperature	100(2)K
Wavelength	0.71073 Å
Crystal system	Trigonal
Space group	R3c
Unit cell dimensions	
a = 14.034(3) Å	α= 90.00 °.
b = 14.034(3) Å	β = 90.00 °.
c = 20.209(5) Å	γ = 120.00 °.
Volume	3446.9(14) $Å^3$
Z	3
Density (calculated)	1.233 Mg/m^3
Absorption coefficient	0.069 mm^{-1}
F(000)	1368
Crystal size	0.20 x 0.20 x 0.20 mm^3
Theta range for data collection	2.62 to 37.56 °.
Index ranges	-23 <=h<=23 ,-23 <=k<=22 ,-34 <=l<=33
Reflections collected	14190
Independent reflections	3605 [R(int) = 0.0522]
Completeness to theta =37.56 °	0.937 %
Absorption correction	Empirical
Max. and min. transmission	0.9863 and 0.9863
Refinement method	Full-matrix least-squares on F^2
Data / restraints / parameters	3605 / 1 / 100
Goodness-of-fit on F^2	0.861
Final R indices [I>2sigma(I)]	R1 = 0.0403 , wR2 = 0.1048
R indices (all data)	R1 = 0.0442 , wR2 = 0.1075
Largest diff. peak and hole	0.406 and -0.285 $e.Å^{-3}$

Table T16. Bond lengths [Å] and angles [°] for ***syn*-56**

Bond lengths

C1-C2#1	1.3955(11)	C6-C7	1.3918(12)
C1-C2	1.4035(11)	C6-C11	1.3941(11)
C1-C5	1.5178(11)	C4-C3	1.5421(12)
C2-C1#2	1.3955(11)	C11-C10	1.3928(14)
C2-C3	1.5109(11)	C7-C8	1.3917(14)
C5-C6	1.5129(11)	C9-C10	1.3828(19)
C5-C4	1.5596(12)	C9-C8	1.3881(19)

Angles

C2-C1-C2#1	120.16(7)	C2-C1-C5	111.13(6)
C2-C1-C5#1	128.67(6)	C1-C2-C1#2	119.84(7)

C1-C2-C3#2	129.31(7)	C3-C4-C5	106.59(6)
C1-C2-C3	110.76(6)	C2-C3-C4	103.35(6)
C6-C5-C1	115.64(6)	C10-C11-C6	120.64(9)
C6-C5-C4	111.60(6)	C8-C7-C6	120.82(9)
C1-C5-C4	102.69(6)	C10-C9-C8	119.09(9)
C7-C6-C11	118.37(7)	C9-C8-C7	120.43(11)
C7-C6-C5	121.18(7)	C9-C10-C11	120.64(9)
C11-C6-C5	120.35(7)		

Table T17. Torsion angles [°] for ***syn*-56**

C2#1-C1-C2-C1#2	1.15(13)	C1-C5-C4-C3	-21.76(7)
C5-C1-C2-C1#2	178.99(5)	C1#2-C2-C3-C4	167.65(7)
C2#1-C1-C2-C3	-175.73(5)	C1-C2-C3-C4	-15.85(7)
C5-C1-C2-C3	2.11(8)	C5-C4-C3-C2	23.04(7)
C2#1-C1-C5-C6	-48.23(10)	C7-C6-C11-C10	-0.50(14)
C2-C1-C5-C6	134.17(7)	C5-C6-C11-C10	-176.89(9)
C2#1-C1-C5-C4	-170.01(7)	C11-C6-C7-C8	-0.24(14)
C2-C1-C5-C4	12.39(7)	C5-C6-C7-C8	176.11(9)
C1-C5-C6-C7	136.45(8)	C10-C9-C8-C7	-1.02(18)
C4-C5-C6-C7	-106.67(9)	C6-C7-C8-C9	1.01(17)
C1-C5-C6-C11	-47.26(10)	C8-C9-C10-C11	0.28(18)
C4-C5-C6-C11	69.62(9)	C6-C11-C10-C9	0.48(16)
C6-C5-C4-C3	-146.25(6)		

Chapter II:

Diastereoselective Gold(I)-Catalyzed [2+2+2] Cycloaddition of Oxo-1,5-Enynes

Introduction

As mentioned in the **General Introduction**, the cycloisomerization of 1,n-enynes catalyzed by gold(I) has been extensively studied over the last decade.[1,2,3] Several nucleophiles have been used to trap different gold intermediates giving rise to complex architectures from relatively simple starting materials. So far, a number of methodologies based on the intra- or intermolecular reactions of enynes with carbonyl compounds in the presence of gold(I) catalysts have been developed. Those processes constitute a powerful tool for the construction of complex hetero- and carbocycles, including core scaffolds of biologically active natural products.

Oxo-1,6-enynes react in the presence of gold(I) complexes to give oxatricyclic compounds through a formal [2+2+2] alkyne/alkene/carbonyl cycloaddition process

---

1 (a) Zhang, L.; Sun, J.; Kozmin, S. A. *Adv. Synth. Catal*. **2006**, *348*, 2271–2296. (b) Fürstner, A.; Davies, P. W. *Angew. Chem. Int. Ed.* **2007**, *46*, 3410–3449. (c) Hashmi, A. S. K. *Chem. Rev*. **2007***, 107*, 3180–3211. (d) Li, Z.; Brouwer, C.; He, C. *Chem. Rev.* **2008**, *108*, 3239–3265. (e) Jiménez-Núñez, E.; Echavarren, A. M. *Chem. Rev.* **2008**, *108*, 3326–3350. (f) Gorin, D. J.; Sherry, B. D.; Toste, F. D. *Chem. Rev*. **2008**, *108*, 3351–3378. (g) Michelet, V.; Toullec, P. Y.; Genêt, J.-P. *Angew. Chem. Int. Ed.* **2008**, *47*, 4268–4315. (h) Aubert, C.; Fensterbank, L.; Garcia, P.; Malacria, M.; Simonneau, A. *Chem. Rev*. **2011**, *111*, 1954–1993. (i) Krause, N.; Winter, C. *Chem. Rev*. **2011**, *111*, 1994–2009. (j) Obradors, C.; Echavarren, A. M. *Acc. Chem. Res*. **2014**, *47*, 902–912. (k) Fensterbank, L.; Malacria, M. *Acc. Chem. Res*. **2014**, *47*, 953–965. (l) Dorel, R.; Echavarren, A. M. *Chem. Rev*. **2015**, *115*, 9028–9072.

2 Reviews of total synthesis of natural products by using gold(I) catalysis: (a) Hashmi, A. S. K.; Rudolph, M. *Chem. Soc. Rev*. **2008**, *37*, 1766–1775. (b) Rudolph, M.; Hashmi, A. S. K. *Chem. Commun*. **2011**, *47*, 6536–6544. (c) Rudolph, M.; Hashmi, A. S. K. *Chem. Soc. Rev*. **2012**, *41*, 2448–2462. (d) Fürstner, A. *Acc. Chem. Res*. **2014**, *47*, 925–938. (e) Zhang, Y.; Luo, T.; Yang, Z. *Nat. Prod. Rep.* **2014**, *31*, 489–503.

3 Work from our group on the total synthesis of terpenoids by using gold(I) catalysis: (a) Jiménez-Núñez, E.; Molawi, K.; Echavarren, A. M. *Chem. Commun*. **2009**, 7327–7329. (b) Molawi, K.; Delpont, N.; Echavarren, A. M. *Angew. Chem. Int. Ed.* **2010**, *49*, 3517–3519. (c) Gaydou, M.; Miller, R. E.; Delpont, N.; Ceccon, J.; Echavarren, A. M. *Angew. Chem. Int. Ed.* **2013**, *52*, 6396–6399. (d) Carreras, J.; Livendahl, M.; McGonigal, P. R.; Echavarren, A. M. *Angew. Chem. Int. Ed.* **2014**, *53*, 4896–4899.

(Scheme 1).[4] Thus, the cyclization of 1,6-enyne bearing a carbonyl moiety **1** using AuCl leads to tricyclic scaffold **2** in 84% yield (50:1 *dr*), together with diene **3** as a minor side product.

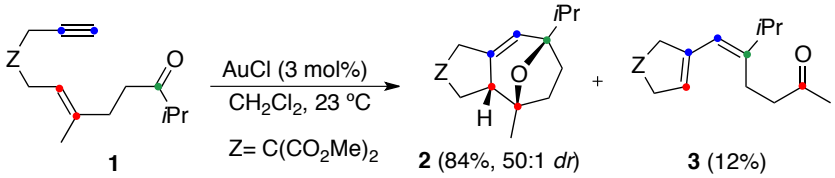

1 **2** (84%, 50:1 *dr*) **3** (12%)

Scheme 1. Intramolecular [2+2+2] cycloaddition of 1,6-enynes bearing a carbonyl group

The transformation presumably proceeds by attack of the carbonyl on the cyclopropyl gold carbene intermediate **4**, thus forming a five-membered oxonium cation **5** stereospecifically (Scheme 2).[4] This intermediate undergoes a Prins-type cyclization to give **6**, which after deauration leads to the final oxatricyclic derivative **7** (orange route). Simultaneous ring opening could explain the formation of minor epimer **8** (violet route) and the carbonyl compound **9** (blue route).

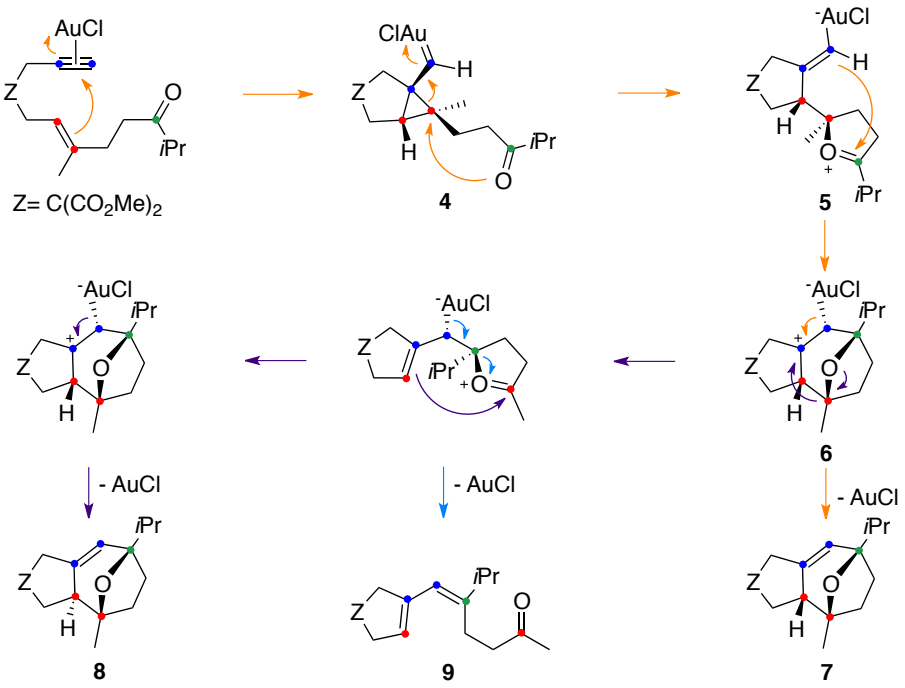

Scheme 2. Proposed mechanism of the intramolecular [2+2+2] cycloaddition of 1,6-enynes with carbonyl group

4 Jiménez-Núñez, E.; Claverie, C. K.; Nieto-Oberhuber, C.; Echavarren, A. M. *Angew. Chem. Int. Ed.* **2006**, *45,* 5452–5455**.**

In a similar vein, terminal alkynes and 5-oxoalkenes undergo a [2+2+2] cycloaddition reaction by intermolecular reaction of the alkyne and the alkene followed by intramolecular attack of the carbonyl group to form [3.2.1]oxabicycles **10** (Scheme 3).[5,6]

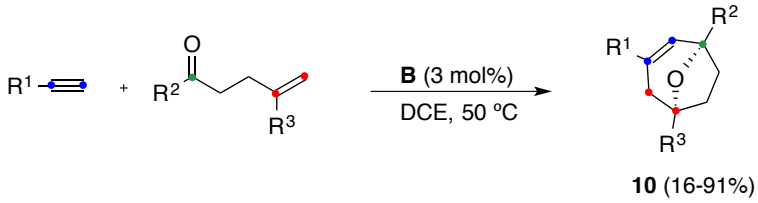

Scheme 3. Intermolecular [2+2+2] cycloaddition of terminal alkynes with oxoalkenes

The proposed catalytic cycle based on DFT calculations (M06 functional) revealed a stepwise formation of the C–C and C–O bonds (Scheme 4).[5] Thus, complex **11** suffered nucleophilic attack from the oxoalkene in the rate-determining step of the process (free activation energy of 15.9 kcal/mol). The *anti* cyclopropyl gold carbene **12** was formed regio- and stereoselectively and underwent nucleophilic attack of the carbonyl group at the most substituted position to generate the oxonium cation **13**. Subsequent Prins-type cyclization led to benzylic carbocation **14** and, finally, to **15** by deauration and ligand exchange between **10** and phenylacetylene.

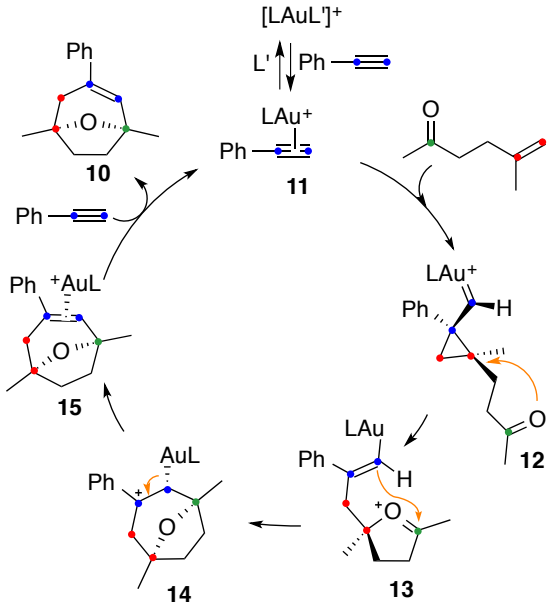

Scheme 4. Catalytic cycle for the intermolecular gold(I)-catalyzed [2+2+2] cycloaddition of terminal alkynes with oxoalkenes based on DFT calculations[7]

5 Obradors, C.; Echavarren, A. M. *Chem.–Eur. J.* **2013**, *19*, 3547–3551.

6 Muratore, M. E.; Homs, A.; Obradors, C.; Echavarren, A. M. *Chem. Asian J.* **2014**, *9*, 3066–3082.

Very recently, our group reported a similar transformation involving simple oxo-1,7-allenenes to afford bicyclo[6.3.0]undecane ring systems.[8] As an example, 11-oxo-1,7-allenene **16** reacted with IPr-gold(I) cationic complex **G** to give **17** in 71% yield as single diastereomer (Scheme 5). This transformation presumably occurs through oxonium cation **18**, which undergoes an *endo*-selective Prins cyclization to generate intermediate **19**. In the case of 1,1-dialkyl-substituted alkenes, such as **21**, seven-membered ring systems **22** are formed (via intermediate **20)** as a consequence of an *exo*-selective Prins cyclization.

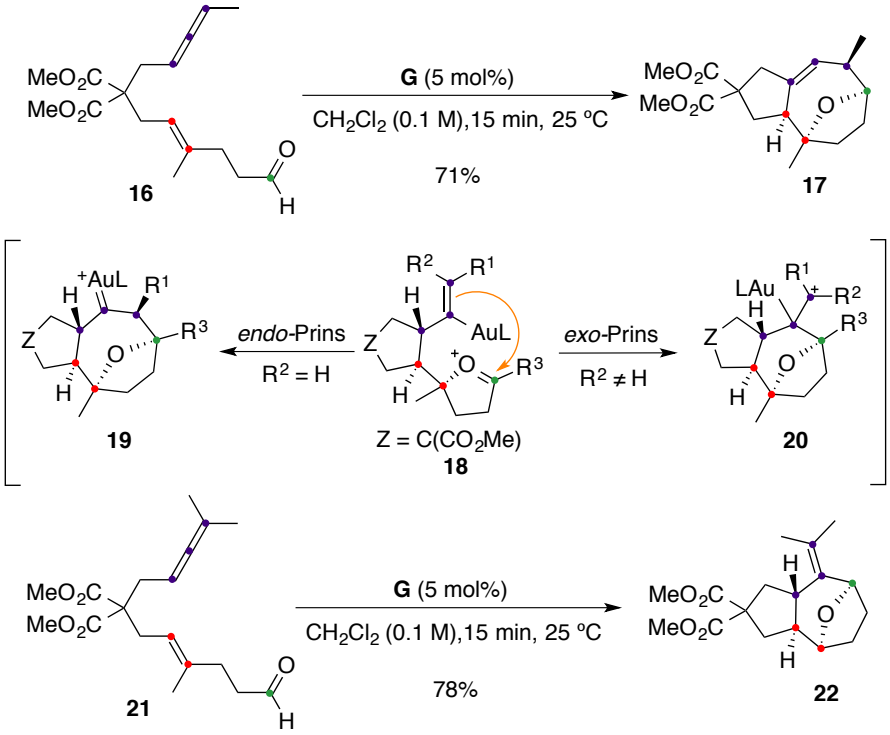

Scheme 5. Gold(I)-catalyzed intramolecular cycloaddition of 11-oxo-1,7-allenenes

This reaction can also be carried out intermolecularly between 1,7-allenenes with aliphatic or aromatic aldehydes. Thus, hexahydro-1*H*-cyclopenta[*c*]oxepines **23** can be prepared in moderate to good yields as mixture of diastereomers (Scheme 6).[8]

7 DFT calculations: M06, 6-31G(d) (C,H,P,O), SDD (Au), CH_2Cl_2, L= PMe_3.

8 Jiménez, T.; Carreras, J.; Ceccon, J.; Echavarren, A. M. *Org. Lett*. **2016**, 18, 1410–1413.

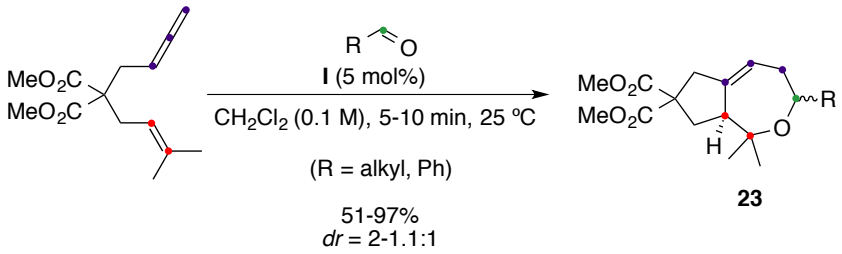

Scheme 6. Gold(I)-catalyzed intermolecular cycloaddition of 1,7-allenenes with aldehydes

The related gold(I)-catalyzed intermolecular reaction between allenamides and oxoalkenes forms seven- to nine-membered rings.[9] Thus, for example, allenamide **24** reacts with carbonyl-tethered alkene **25** and phosphite gold catalyst **I** to provide 8-oxabicyclo[3.2.1]octane **26** in 87% yield (Scheme 7).

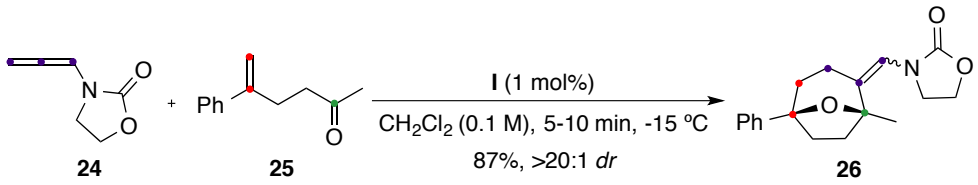

Scheme 7. Gold(I)-catalyzed cascade cycloaddition between allenamide **24** and oxoalkene **25**

Finally, 2,6-disubstituted tetrahydropyrans can be stereoselectively assembled through a fully intermolecular gold(I)-catalyzed [2+2+2] cycloaddition reaction involving three different π–unsaturated components, namely an allene, an alkene, and an aldehyde.[10] Thus, the cycloaddition of allenamide **24** and benzaldehyde with 3-methyl-1*H*-indene provided the corresponding tetrahydropyran **27** in 69% yield with complete stereoselectivity (Scheme 8). The proposed mechanism involves the formation of an intermediate of type **28**, followed by nucleophilic attack of the carbonyl group to give intermediate **29**, which undergoes a Prins-like cyclization to generate **27**.

9 Faustino, H.; Alonso, I.; Mascareñas, J. L. *Angew. Chem. Int. Ed.* **2013**, *52*, 6526–6530.

10 Faustino, H.; Varela, I.; Mascareñas, J. L.; López, F. *Chem. Sci.* **2015**, *6*, 2903–2908.

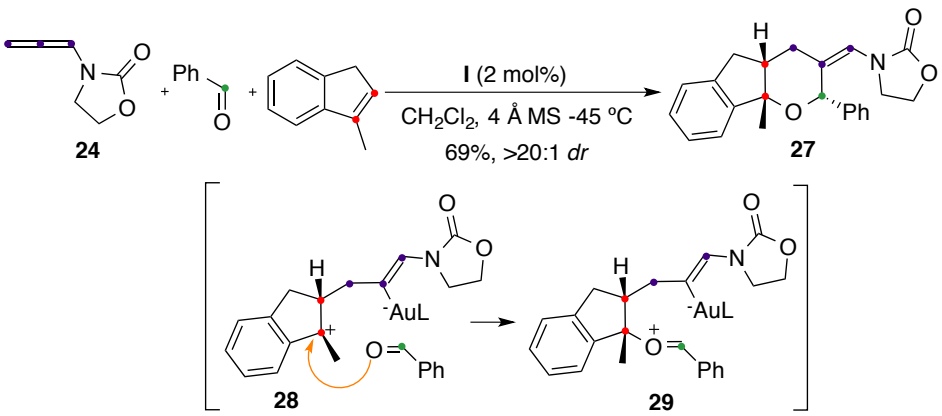

Scheme 8. Fully intermolecular gold(I)-catalyzed [2+2+2] cycloaddition

The synthetic potential of the [2+2+2] alkyne/alkene/carbonyl cycloaddition has been exploited for the synthesis of several oxygen-bridged sesquiterpenoids. Thus, this methodology was applied for the stereoselective synthesis of (+)-orientalol F starting from oxo-1,6-enyne **30**, which reacted with cationic gold catalyst **A** to generate oxatricyclic derivative **31** (Scheme 9).[3a]

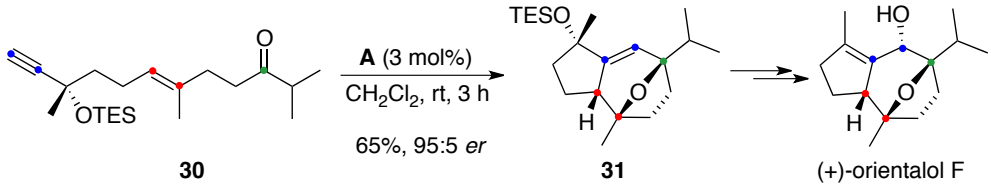

Scheme 9. Gold(I)-catalyzed synthesis of (+)-orientalol F

Likewise, the enantioselective synthesis of (–)-englerin A[3b, 11] constitutes another representative example (Scheme 10). The gold(I)-catalyzed cyclization of ketoenyne **32a** bearing an unprotected alcohol group at the stereogenic allylic position lead to key oxatricyclic diol **33** in a single step.[3b] A closely similar synthetic route was reported simultaneously starting from oxoenyne **32b** and using AuCl as catalyst.[11]

11 Zhou, Q.; Chen, X.; Ma, D. *Angew. Chem., Int. Ed.* **2010**, *49*, 3513–3516.

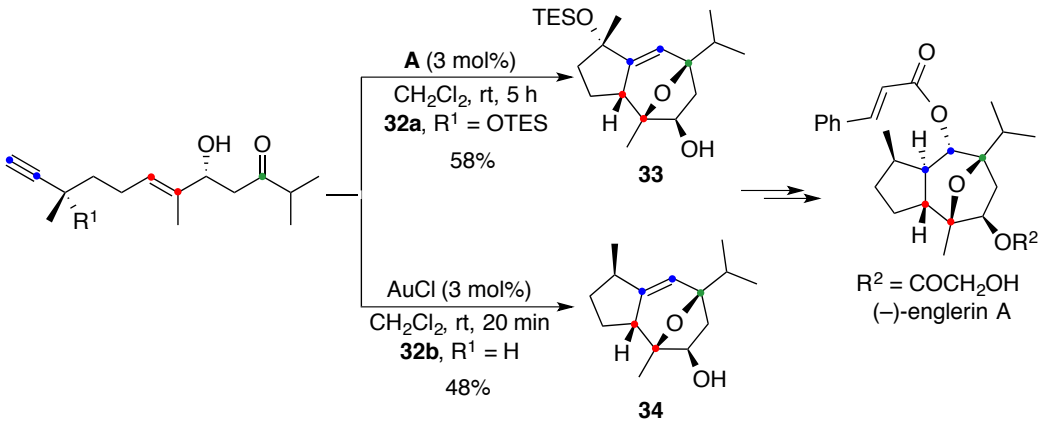

Scheme 10. Enantioselective synthesis of (–)-englerin A

We envisaged that other naturally occurring compounds, such as isovelerenol[12] and bakkenolide III[13] with an octahydro-1*H*-indene core (Figure 1) could be accessed starting from adequately functionalized oxo-1,5-enynes.[1,14]

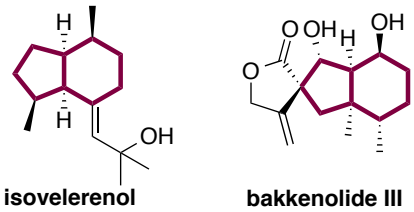

Figure 1. Naturally occurring sesquiterpenes with an octahydro-1*H*-indene structure

In a preliminary study, (*E*)- and (*Z*)-enynals **35** bearing a phenylsulfonyl group at the tether were found to undergo an analogous cycloaddition reaction cascade to form oxatricyclic adducts (Scheme 11).[14] Surprisingly, the cyclization of substrate (*E*)-**35** was found to be poorly stereoselective yielding *syn*-**36** and *anti*-**36** in ratios that ranged from 1:1.5 to 3-4:1, whereas good stereoselectivities were achieved in the transformation of (*Z*)-**35** into *anti*-**36** (20-30:1*dr*).

12 Kobayashi, M.; Yasuzawa, T.; Kyogoku, Y.; Kido, M.; Kitagawa, I. *Chem. Pharm. Bull.* **1982**, *30*, 3431–3434.

13 Jiang, C.-H.; Bhattachrayya, A.; Sha, C.-K. *Org. Lett.* **2007**, *9*, 3241–3243, and references therein.

14 Huguet, N.; Echavarren, A. M. *Synlett* **2012**, 49–53.

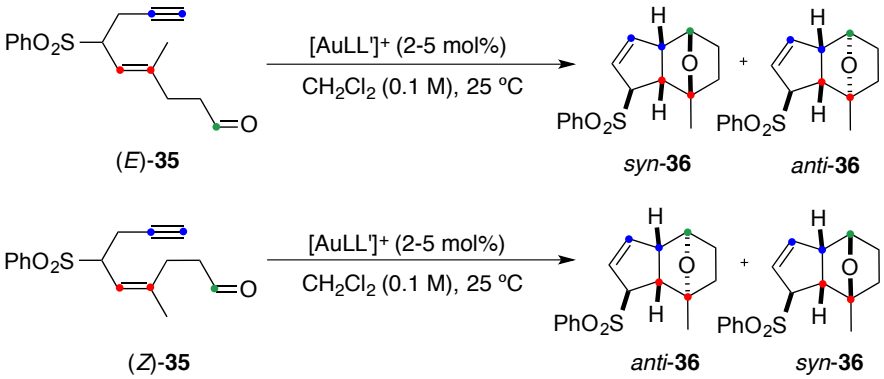

Scheme 11. Gold-catalyzed reaction of (*E*)- and (*Z*)-enynals **35**

It was argued that these results could be explained if a stepwise process was occurring through diastereomeric intermediates that could undergo intramolecular nucleophilic attack of the carbonyl group by inversion or retention of the configuration.[14]

Objectives

The intramolecular gold-catalyzed [2+2+2] cycloaddition of oxo-1,6-enynes and oxo-1,7-allenenes developed in our group proved to proceed with excellent diastereoselectivity, providing access to a single diasteromer in most cases. However, the preliminary results obtained for oxo-1,5-enynes demonstrated that the control of the diastereoselectivity could be more challenging with these substrates.[14]

In this context, we decided to investigate the stereoselectivity in an analogous transformation of other differently substituted substrates. In particular, we focused our attention on studying the reactivity of *O*-protected homopropargylic and allylic oxo-1,5-enynes (**37**) to build oxatricyclic derivatives **38**.

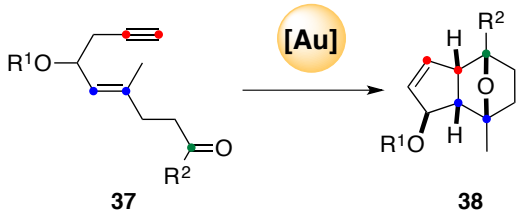

Scheme 12. Intramolecular gold-catalyzed [2+2+2] cycloaddition of oxo-1,5-enynes **37**

A theoretical study was performed to support the proposed mechanism of this transformation and to explain its overall stereoselectivity.

Results and Discussion

Synthesis of *O*-protected Homopropargylic and Allylic Oxo-1,5-enynes

A wide variety of (*Z*)- and (*E*)-oxo-1,5-enynes bearing protected homopropargylic alcohols were prepared in five to seven steps through a linear synthetic route starting from commercially available nerol and geraniol, respectively (Schemes 13-17).

Firstly, the required (*Z*)-6,10-dimethylundeca-5,9-dien-1-yn-4-ol ((*Z*)-**39**) and (*E*)-6,10-dimethylundeca-5,9-dien-1-yn-4-ol ((*E*)-**39**) were readily prepared by oxidization with Dess-Martin periodinane (DMP) and propargylation to form secondary alcohols (*Z*)- and (*E*)-**39** in good yields according to literature procedures (Scheme 13).[15]

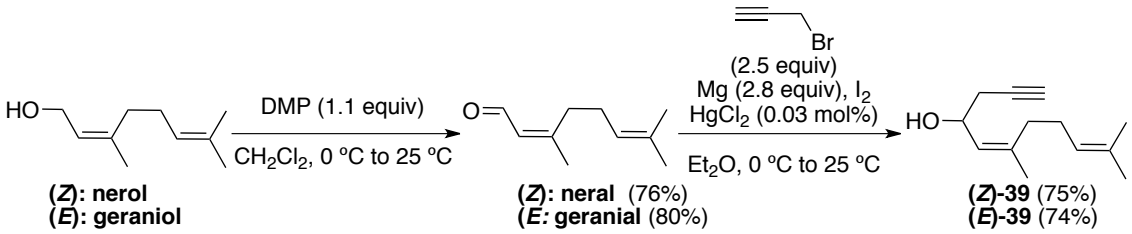

Scheme 13. Synthesis of allylic homopropargylic alcohols (*Z*)- and (*E*)-**39**

Protection of secondary alcohol (*Z*)-**39** with benzoyl chloride in pyridine gave benzoate (*Z*)-**40a** in 84% yield (Scheme 14). Alternatively, (*Z*)-**39** was converted into its TBS-ether (*Z*)-**40b** under standard conditions. Then, dihydroxylation of (*Z*)-**40a-b** with AD-mix-α followed by treatment with a suspension of sodium periodate supported in SiO_2[16] provided *O*-protected 1,5-enynals (*Z*)-**37a** and (*Z*)-**37b** in excellent yields.

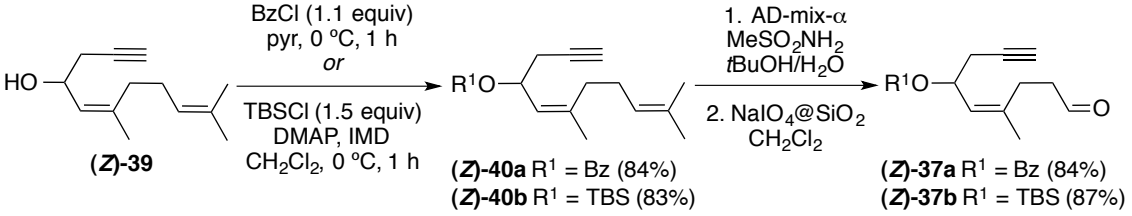

Scheme 14. Synthesis of 1,5-enynals (*Z*)-**37a** and (*Z*)-**37b**

15 (a) Wilson, M. S.; Woo, J. C. S; Dake; G. R. *J. Org. Chem.* **2006**, *71*, 4237–4245. (b) Yang, M.; Hongbo Dong, H.; Jiang, J; Wang, M. *Molecules* **2015**, *20*, 21023–21036.

16 Zhong, Y.; Shing, T. *J. Org. Chem.* **1997**, *62*, 2622–2624.

Keto-1,5-enynes (*Z*)-**37c-j** were prepared from (*Z*)-**37a** or (*Z*)-**37b** through a conventional two-step sequence by the addition of different Grignard reagents followed by Dess-Martin oxidation of the resulting secondary alcohols (Scheme 15).[17]

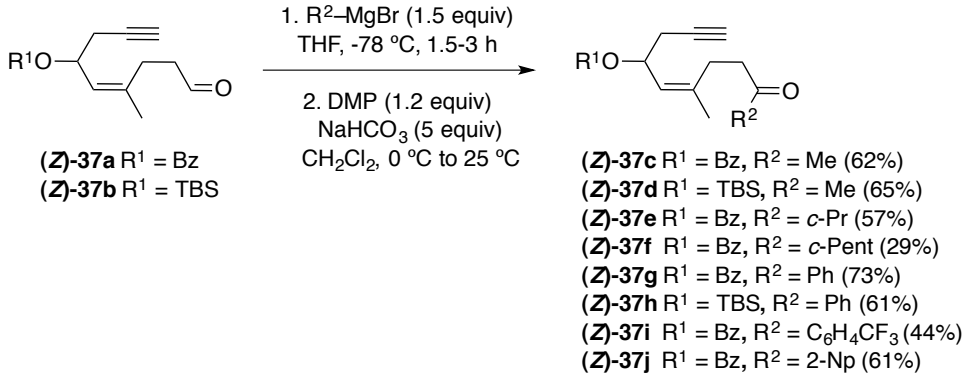

Scheme 15. Synthesis of keto-1,5-enynes (*Z*)-**37**

An analogous synthetic route was used for the synthesis of (*E*)-1,5-enynals (Scheme 16). Additionally, trimethylsilyl (TES) and methoxymethyl acetal (MOM) protected allylic homopropargylic enynals (*E*)-**37k** and (*E*)-**37l** could also be prepared in good yields. The corresponding precursors (*E*)-**40k** and (*E*)-**40l** were obtained under standard conditions using TESCl and MOMCl, respectively.

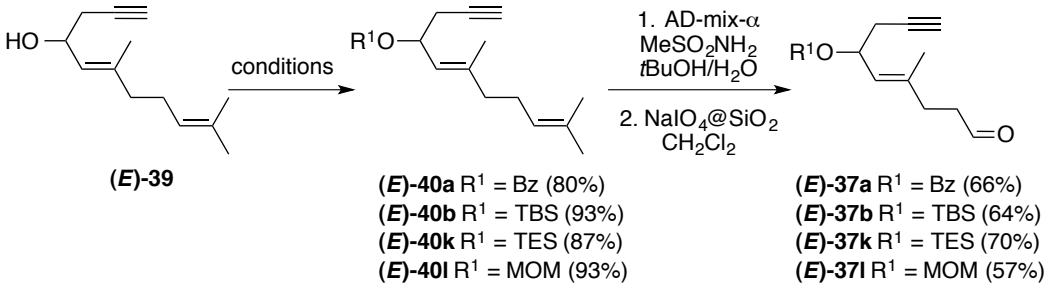

Scheme 16. Synthesis of (*E*)-1,5-enynals[18]

Finally, various benzoate (Bz) and *tert*-butylsilyl (TBS) protected (*E*)-keto-1,5-enynes were synthesized via Grignard addition/Dess-Martin oxidation starting from (*E*)-**37a** or (*E*)-**37b** in moderate to good yields (Scheme 17).[17]

17 In some cases, the isolation of alcohol intermediate **S1** was necessary. See experimental section of this chapter for more details.

18 Reagents and conditions for alcohol protection: R^1 = Bz: BzCl (1.1 equiv), pyr; R^1 = TBS: TBSCl (1.5 equiv), DMAP, IMD, CH_2Cl_2; R^1 = TES: TESCl (1.5 equiv), DMAP, IMD, CH_2Cl_2; R^1 = MOM: MOMCl (1.5 equiv), DIPEA (3 equiv), CH_2Cl_2.

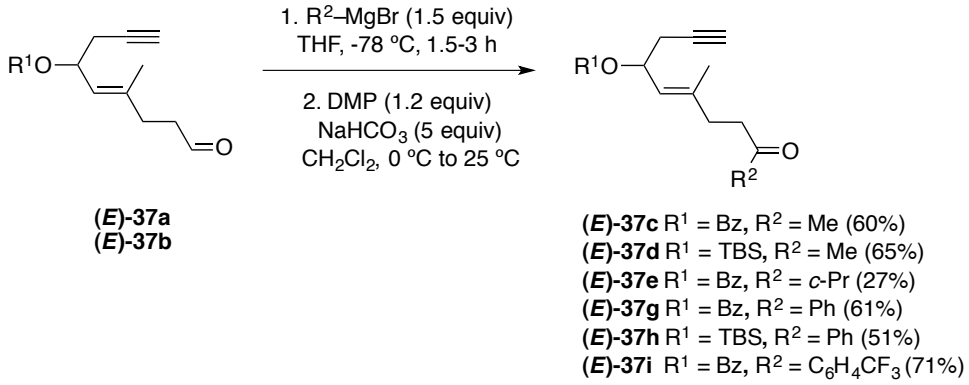

Scheme 17. Synthesis of keto-1,5-enynes (*E*)-**37c-e** and (*E*)-**37g-i**

Optimization of the [2+2+2] Cycloaddition

First, we investigated the reaction of (*Z*)-6-methyl-9-oxonon-5-en-1-yn-4-yl benzoate ((*Z*)-**37a**) as the model substrate, using 5 mol% of commercially available cationic JohnPhos-gold(I) catalyst **A** at 25 °C in CH_2Cl_2. Under these conditions, we observed complete conversion of (*Z*)-**37a** to afford the cyclization product *anti*-**38a** in moderate yield (Table 1, entry 1) together with uncharacterized decomposition products.

Various solvents were evaluated in order to find the optimum conditions. Whereas no cycloisomerization was observed in THF, DME, DMSO, DMF, MeCN, or MeOH (Table 1, entries 2 to 7), the reaction proceeded in chlorinated or aromatic solvents (Table 1, entries 8 to 13). When the reaction was performed in Et_2O or EtOAc the yields were very low (Table 1, entries 14 to 15). The best results were observed in toluene (Table 1, entry 11) giving rise to *anti*-**38a** in higher yield. Thus, toluene was selected as the solvent for further optimization.

Table 1. Screening of solvents for the [2+2+2] cycloaddition

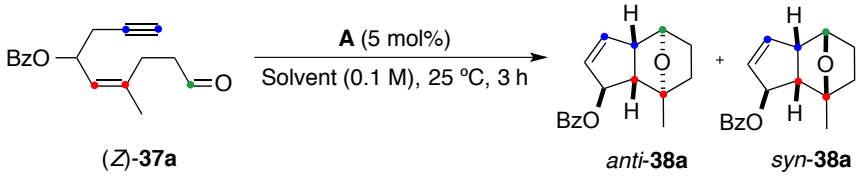

Entry	Solvent	Yield (%)[a]	Ratio *anti/syn*
1	CH_2Cl_2	55	93:7
2	THF	0[b]	–
3	DME	0[b]	–
4	DMSO	<1 (<7)[c]	–
5	DMF	0	–

6	MeCN	<3 (20)[c]	n.d.
7	MeOH	0[d]	–
8	DCE	46	91:9
9	$CDCl_3$	62	91:9
10	Benzene	64	89:11
11	Toluene	66	92:8
12	$PhCF_3$	41 (95)[c]	89:11
13	PhCl	36	88:12
14	Et_2O	21 (65)[c]	n.d.
15	EtOAc	16 (70)[c]	n.d.

n.d. = diasteromeric ratio not determined. [a] Crude analyzed by ^{1}H NMR spectroscopy using mesitylene as internal standard, yields referred to oxatricycle *anti*-**38a**. [b] Only decomposition observed. [c] % of conversion, 100% if not otherwise stated. [d] Exclusive addition of methanol to the ketone as well as the dimethyl acetal formation on the aldehyde.

Efforts to improve this cyclization cascade using other gold catalysts were unsuccessful. Lower yields were obtained with catalysts **C**, **E**, **G**, **H** and **I** (Table 2, entries 3-7). Thus, the use of NHC or phosphite ligands as well as other counterions (BAr_4^{F-}) has an adverse influence on this transformation. Furthermore, no cycloisomerization was observed with neutral gold complex **M** (Table 2, entry 8). Although the reaction proceeded well with gold catalyst **B** (Table 2, entry 2), the use of sterically hindered phosphines resulted in a decrease in selectivity.

Table 2. Screening of catalysts for the [2+2+2] cycloaddition[a]

Entry	[Au]	t (h)	Yield (%)[b]	Ratio *anti/syn*
1	**A**	3	66	92:8
2	**B**	2	66	81:19
3	**C**	3	25 (90)[c]	68:32
4	**E**	3	6 (50)[c]	n.d.
5	**G**	2	29 (80)[c]	65:35
6	**H**	2	32 (95)[c]	73:27
7	**I**	3	12	n.d.
8	**M**	2	<1 (<5)[c]	n.d.

n.d. = diasteromeric ratio not determined. [a] Reaction of (Z)-**37a** with 5 mol% of **[Au]** catalyst in toluene (0.1 M) at 25 ºC. [b] Crude analyzed by ^{1}H NMR

spectroscopy using mesitylene as internal standard, yields referred to oxatricycle *anti*-**38a**. [c] % of conversion, 100% if not otherwise stated.

Decreasing the concentration from 0.1 to 0.01 M substantially improved the reaction yield while maintaining the selectivity (Table 3, entries 1-3). Further studies revealed that longer reaction times did not have any detrimental influence on the outcome of the transformation (Table 3, entry 5) and that performing the reaction at lower temperature did not improve the stereoselectivity (Table 3, entry 4).

Table 3. Effect of concentration, temperature and reaction time[a]

Entry	[M]	t (h)	T (ºC)	Yield (%)[b]	Ratio *anti/syn*
1	0.1	3	25	66	92:8
2	0.05	2	25	66	90:10
3[c]	0.01	6	25	83	92:8
4	0.01	24	0	83	92:8
5	0.01	15	25	88	91:9

[a] Reaction of (*Z*)-**37a** with 5 mol% of catalyst **A** in toluene. [b] Crude analyzed by ^{1}H NMR spectroscopy using mesitylene as internal standard, yields referred to oxatricycle *anti*-**38a**.

Under the optimized conditions, the cyclization of (*Z*)-**37a** led to the formation of *anti*-**38a** in 90% isolated yield (92:8 *dr*). The configuration of the major isomer could be confirmed by X-ray diffraction (Figure 2, *anti*-**38a**).

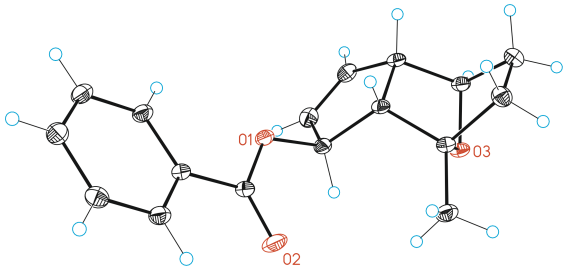

Figure 2. ORTEP representations of *anti*-**38a** with 50% probability of the thermal ellipsoids

Scope of the [2+2+2] Cycloaddition

Having the optimal conditions in hand, we sought to evaluate the generality of the reaction. In general, moderate to good yields (38−90%) of the corresponding oxatricyclic adducts *anti*-**38a-j**, *syn*-**38a-e**, *syn*-**38g-I** and *syn*-**38k-l** were obtained (Tables 4 and 5).

All the studied (*Z*)-1,5-enynes **37a-j** cyclized with good to high diastereoselectivities

(Table 4). The size of the substituent attached to the carbonyl group (R^2 in Table 4) did not seem to have a clear influence on the stereoselectivity. However, the bulkier TBS protecting group of the alcohol usually improved the overall diastereoselectivity of the formal cycloaddition compared to the benzoate.

Table 4. Gold-catalyzed cyclization of (*Z*)-oxo-1,5-enynes

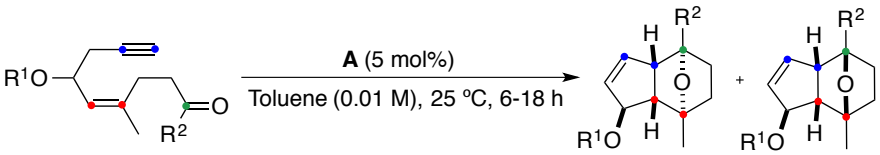

(Z)-**37** *anti*-**38** *syn*-**38**

Entry	Enyne	R^1	R^2	Yield 38 (%)[a]	Ratio *anti/syn*
1	(*Z*)-**37a**	Bz	H	**38a** (90)	92:8 (91:9)[b]
2	(*Z*)-**37b**	TBS	H	**38b** (58)	>98:2 (83:17)[b]
3	(*Z*)-**37c**	Bz	Me	**38c** (79; 55[c])	83:17 (83:17)[b]
4	(*Z*)-**37d**	TBS	Me	**38d** (70)	>98:2 (>98:2)[b]
5	(*Z*)-**37e**	Bz	*c*-Pr	**38e** (74)	89:11 (83:17)[b]
6	(*Z*)-**37f**	Bz	*c*-Pent	**38f** (68)	85:15 (84:16)[b]
7	(*Z*)- **37g**	Bz	Ph	**38g** (88; 69[d])	93:7 (91:9)[b]
8	(*Z*)- **37h**	TBS	Ph	**38h** 61[d]	>98:2 (93:7)[b]
9	(*Z*)- **37i**	Bz	$C_6H_4CF_3$	**38i** 65	>98:2 (87:13)[b]
10	(*Z*)- **37j**	Bz	2-Np[e]	**38j** 56[d]	>98:2 (93:7)[b]

[a] Product yields are reported after purification. [b] Crude *dr* determined by ^{1}H NMR spectroscopy. [c] Result of crystallization (*dr* ≥98:2). [d] Result of crystallization (*dr* >98:2). [e] 2-Np = 2-naphthyl.

The high stereoselectivities observed with (*Z*)-enynes are in agreement with the previous observations for the related transformation developed in our group.[14] These oxatricycles were formed in generally good yields and the major isomer may, in most cases, be isolated in virtually diastereomerically pure form by standard chromatographic methods or by crystallization. This allowed us to obtain the crystal structures of three derivatives, confirming that the major isomer formed in all cases has the same relative configuration, regardless of the nature of R^1 and R^2 (Figures 2-4).

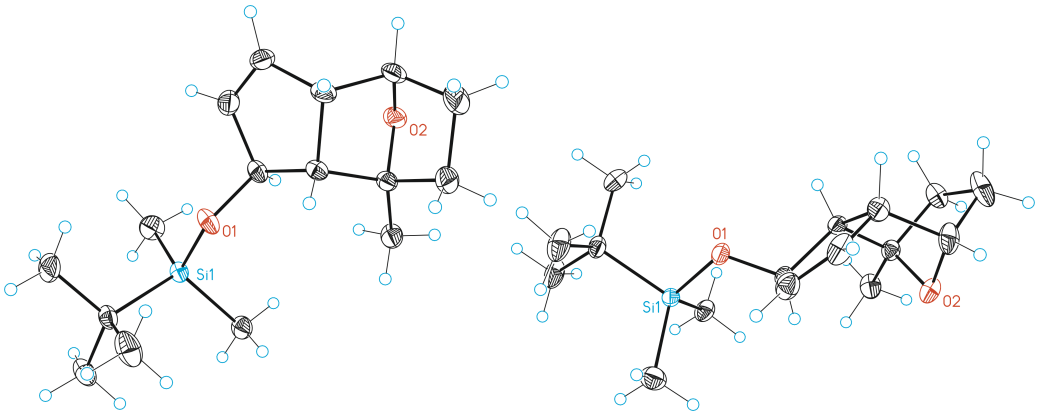

Figure 3. ORTEP representations of *anti*-**38b** with 50% of probability of the thermal ellipsoids

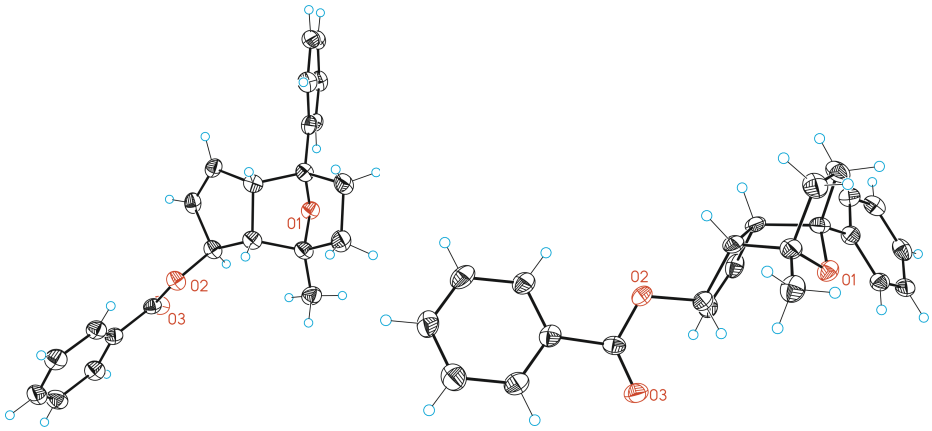

Figure 4. ORTEP representations of *anti*-**38g** with 50% of probability of the thermal ellipsoids

Interestingly, the cyclization of (*E*)-enynals **37a-b**, **37k-l** also proceeded with excellent stereoselectivity to give the expected oxatricyclic products *syn*-**38a-b**, *syn*-**38k-l** in satisfactory yields (Table 5, entries 1-2 and 9-10). Additionally, other (*E*)-keto-1,5-enynes **37c-i** were also examined (Table 5). Different trends were observed depending on the nature of the protecting group. Thus, alkyl- ((*E*)-**37d**) and aryl-substituted ((*E*)-**37h**) TBS-protected keto-1,5-enynes led to the formation of cyclized derivatives (Table 5, entries 4 and 7) in good yield and with high selectivity. In contrast, benzoate-protected 1,5-enynes bearing bulky substituents on the ketone (Table 5, entries 5, 6 and 8) afforded the expected products, albeit with moderate yields and lower diastereoselectivity.

Table 5. Gold-catalyzed cyclization of (*E*)-oxo-1,5-enynes

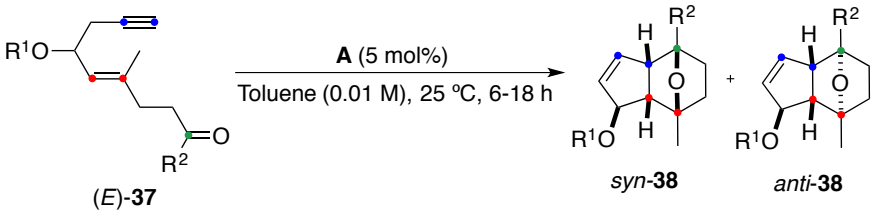

Entry	Enyne	R^1	R^2	Yield 38 (%)[a]	Ratio *syn/anti*
1	(*E*)-**37a**	Bz	H	**38a** (83)	93:7 (93:7)[d]
2	(*E*)- **37b**	TBS	H	**38b** (82)	>99:1 (99:1)[d]
3[b]	(*E*)- **37c**	Bz	Me	**38c** (78)	88:12 (89:11)[d]
4	(*E*)- **37d**	TBS	Me	**38d** (75)	97:3 (99:1)[d]
5[b]	(*E*)- **37e**	Bz	*c*-Pr	**38e** (52)	82:18 (87:13)[d]
6[b]	(*E*)- **37g**	Bz	Ph	**38g** (38; 20[e])	57:43 (58:42)[d]
7	(*E*)- **37h**	TBS	Ph	**38h** (90)	>99:1 (96:4)[d]
8	(*E*)- **37i**	Bz	$C_6H_4CF_3$	**38i** (48)	91:9 (83:17)[d]
9	(*E*)- **37k**	TES	H	**38k** (71)	>99:1 (95:5)[d]
10[e]	(*E*)- **37l**	MOM	H	**38l** (81)	>99:1 (99:1)[d]

[a] Product yields and *dr* are reported after purification. [b] Reaction at 30 °C. [c] Reaction at 40 °C.
[d] Crude *dr* determined by ^{1}H NMR spectroscopy. [e] Result of crystallization (*dr* 56:44).

The relative configurations of these compounds were assigned by analogy to that of *syn*-**38c,** which was established by X-ray crystallography (Figure 5, *syn*-**38c**).

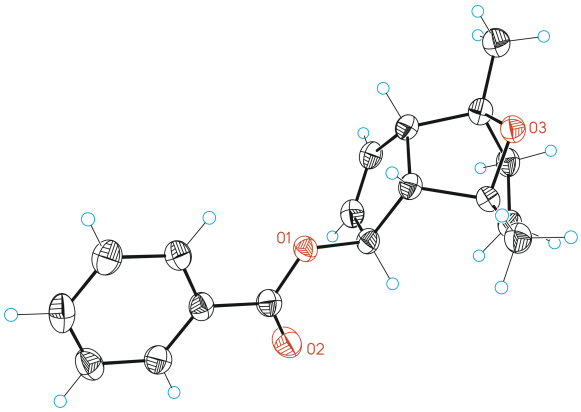

Figure 5. ORTEP representations of *syn*-**38c** with 50% probability of the thermal ellipsoids

Mechanistic proposal

We propose a mechanism for the formation of the oxatricyclic derivative *syn*-**38** starting from (*E*)-**37** initiated by activation of the alkyne to form a cyclopropyl gold(I)-carbene **41** followed by the intramolecular attack of the carbonyl group to generate the oxocarbenium intermediate **42** (Scheme 18). Intermediate **42** could form a second C–C bond through a Prins-type reaction with the alkenyl metal leading to carbene-like intermediate **43**, which is reminiscent of the mechanism for the gold(I)-catalyzed reaction of oxo-1,6-enynes. A final hydrogen shift followed by deauration would lead to product *syn*-**38**. The formation of the minor stereoisomer *anti*-**38** from (*E*)-**37** is consistent with the existence of another competitive stepwise process. Thus, the nucleophilic attack of the carbonyl group on the opposite face of intermediate **41** (*syn* to the breaking cyclopropane C–C bond) would lead to oxocarbenium **44**, which undergoes an analogous sequence (Prins-type cyclization, hydrogen shift and deauration) to generate the minor diastereomer *anti*-**38**.

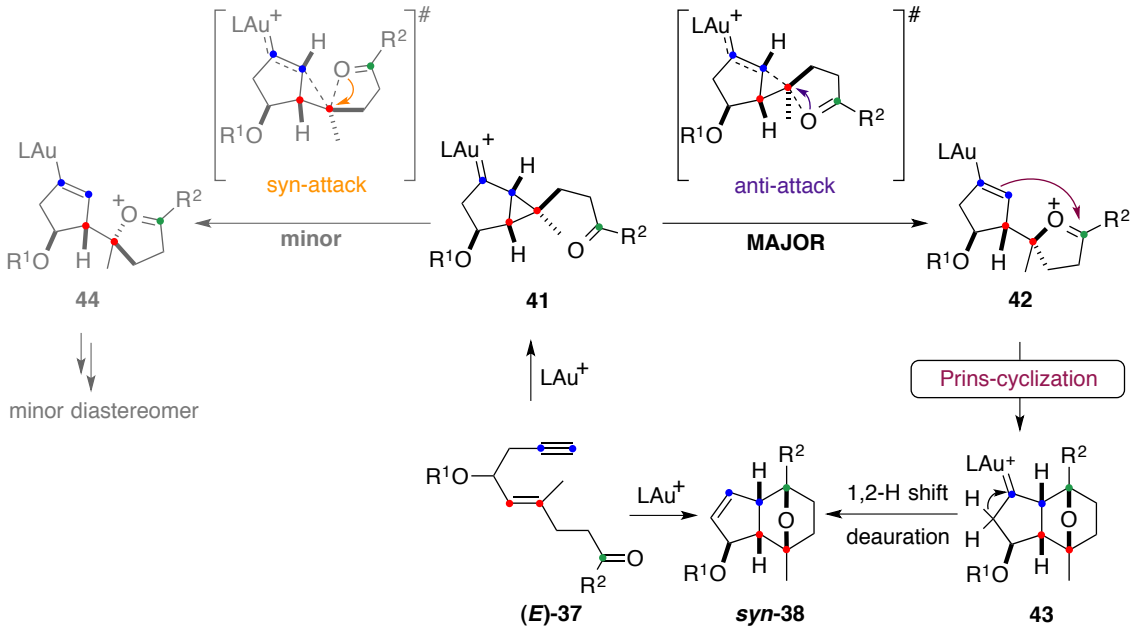

Scheme 18. Proposed mechanism of the formal [2+2+2] cycloaddition of oxo-1,5-enyne (*E*)-**37**

The mechanistic proposal outlined in Scheme 18 is supported by DFT calculations at the M06, 6-31G(d) (C, H, P, O) and SDD (Au) level, taking into account the solvent effect (toluene) and employing PMe_3 as the phosphine ligand (Figure 6).

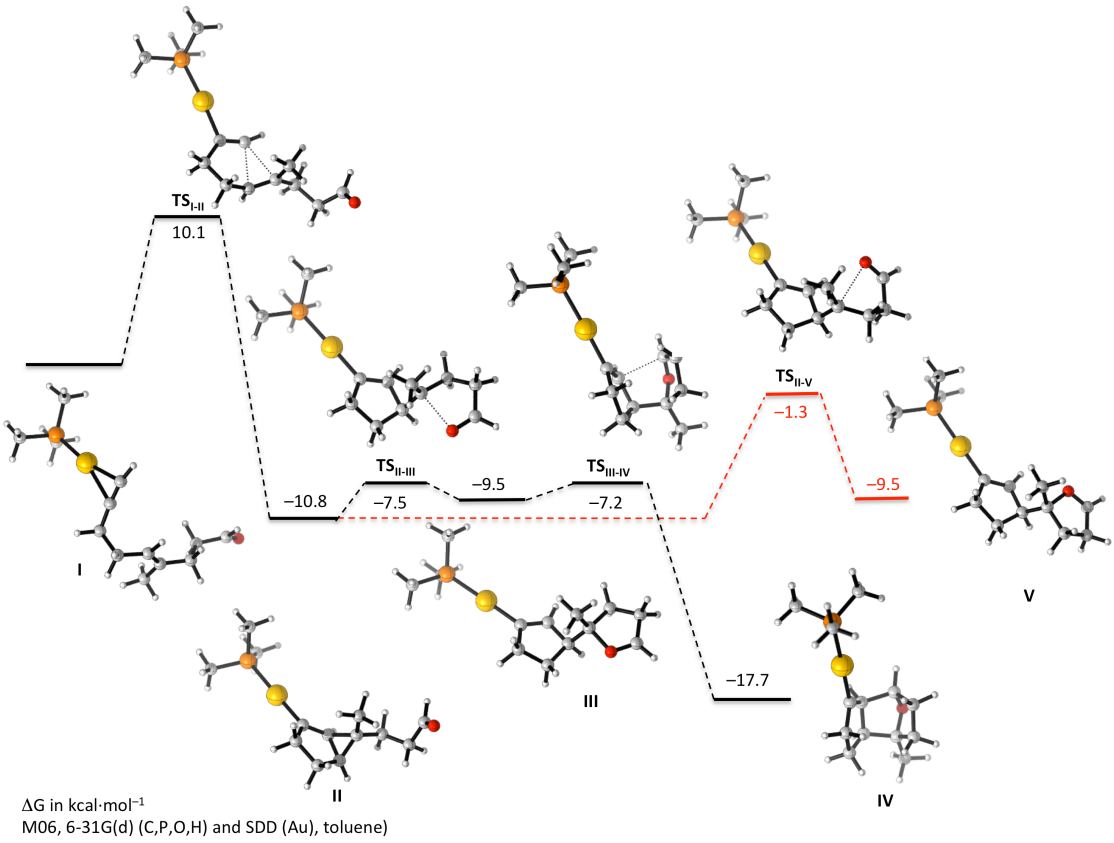

Figure 6. Energy profiles for the competitive reaction pathways of gold(I) complex **I**.

This study shows that the first cyclization giving rise to intermediate **II** (corresponding to **41** in Scheme 18) has the highest activation energy. It would thus be the rate-determining step if the ligand exchange equilibrium that regenerates the entering reactive species **I** from the final substrate-gold(I) complex is not considered. The calculated energy differences for the two competitive transition states **TS$_{II-III}$** (1.3 kcal·mol^{-1}) and **TS$_{II-V}$** (9.5 kcal·mol^{-1}) show that the formation of oxocarbenium intermediate **III** is kinetically more favoured than the formation of **V**, which is in general agreement with our experimental findings. Our calculations further support the existence of a discrete intermediate **II** in the cyclization of the 1,5-enyne,[19] which undergoes intramolecular nucleophilic opening to form preferentially intermediate **III** by an overall *anti*-type attack**.**

19 López-Carrillo, V.; Huguet, N.; Mosquera, Á.; Echavarren, A. M. *Chem.–Eur. J.* **2011**, *17*, 10972–10978.

Synthesis of crown ether 45

Intriguingly, treatment of 1,5-enyne (*E*)-**37l** with cationic JohnPhos-gold(I) catalyst **A** (3 mol%) in CH_2Cl_2 instead of toluene at 0 ºC led to the isolation of unexpected crown ether **45** in moderate yield (Table 6, entry 2). Lower yields were obtained when the reaction was carried out at higher temperature or using cationic catalyst **G** (Table 6, entries 1 and 3). The structure of this compound was confirmed by X-ray diffraction (Figure 7).

Table 6. Synthesis of crown ether **45**

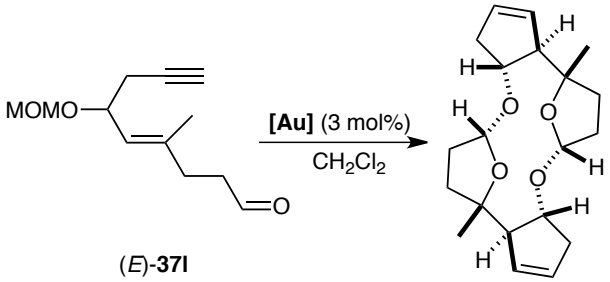

(*E*)-**37l** **45**

Entry	[Au]	T (ºC)	t (h)	Yield (%)[b]
1	**A**	23	3	8
2	**A**	0	15	49
3	**G**	0	15	9

[a] Reaction of (Z)-**37l** with 3 mol% of **[Au]** catalyst in CH_2Cl_2 (0.1 M).
[b] Isolated yields.

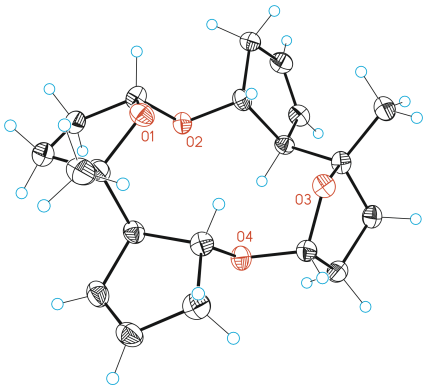

Figure 7. ORTEP representation of crown ether **45** with 50% probability of the thermal ellipsoids

The formation of **45** can be rationalized by the bimolecular reaction of two oxocarbenium intermediates **42**, in which the protecting group has been cleaved under the reaction conditions (Scheme 19).

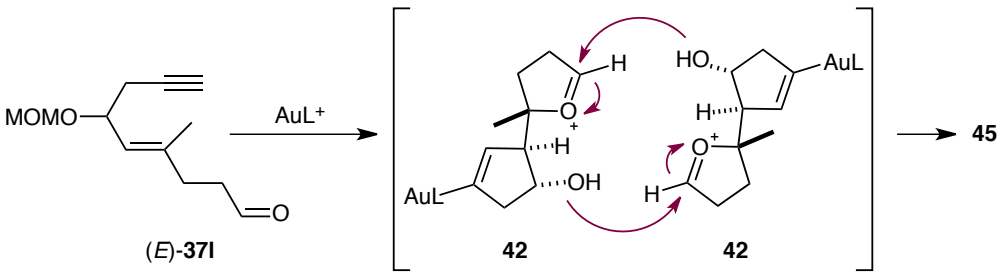

Scheme 19. Gold(I)-catalyzed reaction of oxo-enyne (*E*)-**37l** to give crown ether **45** and proposed mechanism

Conclusions

We have extended the scope of the intramolecular gold(I)-catalyzed formal [2+2+2] cycloaddition reaction to *O*-protected homopropargylic and allylic oxo-1,5-enynes. Undesired side reactions could be almost completely suppressed by carrying out the reaction in anhydrous toluene instead of chlorinated solvents and at higher dilution. Furthermore, under the optimized reaction conditions, the cyclization of (*Z*)- and (*E*)-isomers takes place with moderate to excellent yield (38-90%) and increased selectivity in most of the cases, providing access to substituted octahydro-1*H*-indenes.

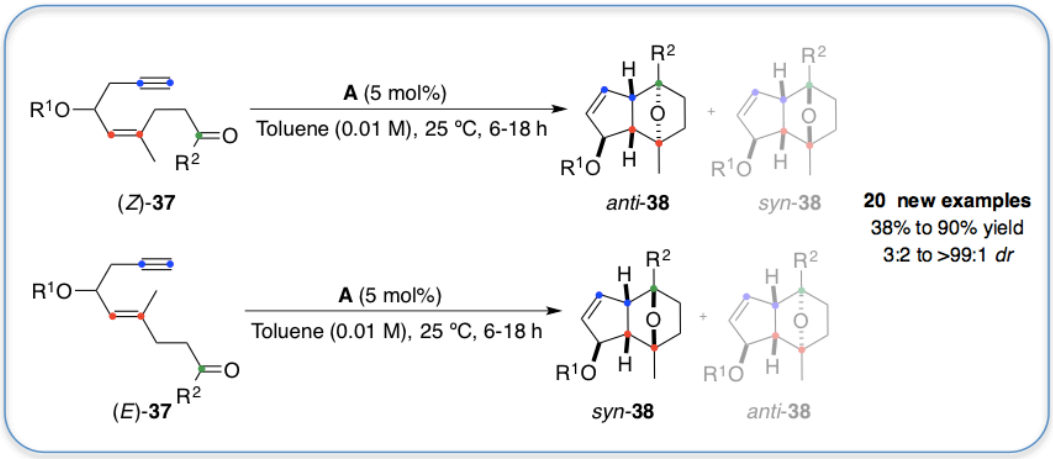

A theoretical study of the mechanism of this transformation has been performed. According with our DFT calculations, after the formation of the cyclopropyl gold(I)-carbene, the nucleophilic attack of the carbonyl group can take place by two competitive pathways that can explain the observed lack of complete stereoselectivity. The subsequent Prins-type cyclization (only one possible mode of cyclization in each scenario) followed by hydrogen shift and deauration lead to the observed diastereomeric oxatricycles.

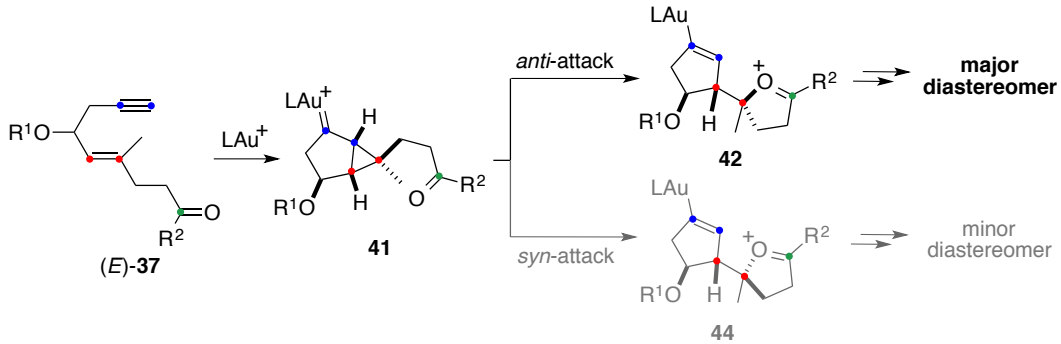

The evaluation of the biological properties of these new compounds is currently underway (Eli Lilly, Open Innovation Drug Discovery (OIDD)). Future developments will aim at exploring the reactivity of other functionalized oxoenynes as well as developing asymmetric alternatives, either on enantioenriched substrates or employing a chiral gold(I) catalyst for the reaction of achiral substrates.

Experimental Part

General Methods

Unless other wise stated, reactions were performed under argon in solvents dried by passing through an activated alumina column on a PureSolv^{TM} solvent purification system (Innovative Technologies, Inc., MA). Analytical thin layer chromatography was carried out using TLC-aluminum sheets coated with 0.2 mm of silica gel (Merck GF_{234}) using UV light as the visualizing agent and an acidic solution of vanillin in ethanol as the developing agent. Chromatographic purifications were carried out using flash grade silica gel (SDS Chromatogel 60 ACC, 40-63 μm) or automated flash chromatographer CombiFlash Companion. Preparative TLC was performed on 20 cm x 20 cm silica gel plates (2.0 mm thick, catalogue number 02015, Analtech). If indicated, preparative TLC was performed on 20 cm x 20 cm aluminium oxide plates (0.25 mm thick, 90066, Fluka). Organic solutions were concentrated under reduced pressure on a Büchi rotary evaporator.

NMR spectra were recorded at 298 K (unless otherwise stated) on a Bruker Avance 300, Bruker Avance 400 Ultrashield and Bruker Avance 500 Ultrashield apparatuses. The data are reported as such: chemical shift [δ, ppm] (multiplicity, coupling constant [Hz], number of protons). The chemical shifts are given in ppm downfield from tetramethylsilane using the residual protio-solvent as internal reference (d_H = 7.26 ppm and d_C = 77.16 for $CDCl_3$). The abbreviations for multiplicities are: s (singlet), d (doublet), t (triplet), q (quartet), quin (quintet), sext (sextet), sept (septet). Mass spectra were recorded on a Waters Micromass LCT Premier (ESI), Waters Micromass GCT (EI, CI) and Bruker Daltonics Autoflex (MALDI) spectrometers. Melting points were determined using a Büchi melting point apparatus.

Crystal structure determinations were carried out using a Bruker-Nonius diffractomer equipped with an APPEX 2 4K CCD area detector, a FR591 rotating anode with MoK_a radiation, Montel mirrors as monochromator and a Kryoflex low temperature device (T = –173 °C). Full-sphere data collection was used with w and j scans. *Programs used*: Data collection APEX-2, data reduction Bruker Saint V/.60A and absorption correction SADABS. Structure Solution and Refinement: Crystal structure solution was achieved using direct methods as implement in SHELXTL and visualized using the program XP. Missing atoms were subsequently located from difference Fourier synthesis and added to the atom list. Least-squares refinement on F2 using all measured intensities was

carried out using the program SHELXTL. All non-hydrogen atoms were refined including anisotropic displacement parameters.

All reagents were used as purchased and used with no further purification, unless otherwise stated.

All calculations were performed with DFT using the M06 functional as implemented in Gaussian 09.[20] The 6-31G(d) basis set[21,22] was used for all atoms except gold, which was treated with SDD and the associated effective core potential.[23] The solvent effect was taken into account using the polarizable continuum model (IEF-PCM, solvent = toluene) as implemented in Gaussian 09.[24,25,26,27] Frequency calculations were performed to characterize the stationary points as minima.

---

20 Frisch, M. J.; Trucks, G. W.; Schlegel, H. B.; Scuseria, G. E.; Robb, M. A.; Cheeseman, J. R.; Scalmani, G.; Barone, V.; Mennucci, B.; Petersson, G. A.; Nakatsuji, H.; Caricato, M.; Li, X.; Hratchian, H. P.; Izmaylov, A. F.; Bloino, J.; Zheng, G.; Sonnenberg, J. L.; Hada, M.; Ehara, M.; Toyota, K.; Fukuda, R.; Hasegawa, J.; Ishida, M.; Nakajima, T.; Honda, Y.; Kitao, O.; Nakai, H.; Vreven, T. ; Montgomery (Jr.), J. A.; Peralta, J. E.; Ogliaro, F.; Bearpark, M.; Heyd, J. J.; Brothers, E.; Kudin, K. N.; Staroverov, K. N.; Kobayashi, R.; Normand, J.; Raghavachari, K.; Rendell, A.; Burant, J. C.; Iyengar, S. S.; Tomasi, J.; Cossi, M.; Rega, N.; Millam, N. J.; Klene, M.; Knox, J. E.; Cross, J. B.; Bakken, V.; Adamo, C.; Jaramillo, J.; Gomperts, R.; Stratmann, R. E.; Yazyev, O.; Austin, A. J.; Cammi, R.; Pomelli, C.; Ochterski, J. W.; Martin, R. L.; Morokuma, K.; Zakrzewski, V. G.; Voth, G. A.; Salvador, P.; Dannenberg, J. J.; Dapprich, S.; Daniels, A. D.; Farkas, O.; Foresman, J. B.; Ortiz, J. V.; Cioslowski, J.; Fox, D. J.; Gaussian 09, revision 02; Gaussian, Inc.: Wallingford, CT, **2009**.

21 Francl, M. M.; Pietro, W. J.; Hehre, W. J.; Binkley, J. S.; Gordon, M. S.; Defrees, D. J.; Pople, J. A. *J. Chem. Phys*. **1982**, *77*, 3654–3665.

22 Hehre, W. J. ; Ditchfield, R. ; Pople, J. A. *J. Chem. Phys*. **1972**, *56*, 2257–2261.

23 Andrae, D.; Haussermann, U.; Dolg, M. Stoll, H.; Preuss, H. *Theor. Chim. Acta* **1990**, *77*, 123–141.

24 Cances, E.; Mennucci, B.; Tomasi, J. *J. Chem. Phys*. **1997**, *107*, 3032–3041.

25 Cossi, M.; Barone, V.; Mennucci, B.; Tomasi, J. *Chem. Phys. Lett*. **1998***, 286*, 253–260.

26 Mennucci, B.; Tomasi, J. *J. Chem. Phys.* **1997**, *106*, 5151–5158.

27 Miertus, S.; Tomasi, J. *Chem. Phys*. **1982**, *65*, 239–245.

Synthetic Procedures and Analyical Data

General procedure for the preparation of allylic homopropargylic protected alcohols

(*E*)-6,10-Dimethylundeca-5,9-dien-1-yn-4-ol ((*E*)-**39**) and (*Z*)-6,10-dimethylundeca-5,9-dien-1-yn-4-ol ((*Z*)-**39**) were prepared according to known literature procedures.[15] Spectroscopic data were in agreement with those reported.

Preparation of benzoic esters of 39 (40a)

In a dry round-bottom flask under argon, **39** (1 equiv) was dissolved in pyridine (1 M solution) and the solution was cooled to 0 °C. Benzoyl chloride (1.1 equiv) was added slowly dropwise. The mixture was stirred at 0 °C for 1 h upon which time TLC indicated full conversion of **39**. The suspension was poured over 3-5% aqueous HCl (10 volumes of pyridine) and extracted with diethyl ether (2 × volume $HCl_{aq.}$). The combined ethereal extracts were washed with 3-5% aqueous HCl (5 × ½ initial volume $HCl_{aq.}$), the washed organic phase dried over Na_2SO_4 and the filtrate concentrated. The crude material was purified by column chromatography on silica gel eluting with pentane/diethyl ether 98:2 to 9:1 or cyclohexane/ethyl acetate 95:5 to 9:1.

(*E*)-6,10-Dimethylundeca-5,9-dien-1-yn-4-yl benzoate ((*E*)-40a)

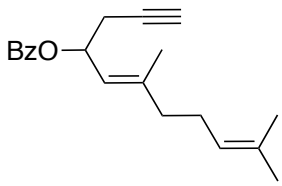

Prepared on 3.0 g scale from (*E*)-**39**. The product was isolated as a pale yellow oil (3.70 g, 80%).

^{1}H NMR (400 MHz, $CDCl_3$) δ 8.08 – 8.03 (m, 2H), 7.58 – 7.52 (m, 1H), 7.46 – 7.40 (m, 2H), 5.87 (dt, *J* = 9.1, 6.1 Hz, 1H), 5.35 (dq, *J* = 9.1, 1.3 Hz, 1H), 5.08 (tq, *J* = 5.4, 1.6 Hz, 1H), 2.71 – 2.55 (m, 2H), 2.16 – 2.02 (m, 4H), 1.98 (t, *J* = 2.6 Hz, 1H), 1.82 (d, *J* = 1.4 Hz, 3H), 1.65 (d, *J* = 1.4 Hz, 3H), 1.59 (app. s, 3H). ^{13}C NMR (101 MHz, $CDCl_3$) δ 165.9, 142.3, 133.0, 131.9, 130.6, 129.8 (2C), 128.4 (2C), 123.8, 122.0, 79.9, 70.3, 69.7, 39.7, 26.4, 25.8, 25.3, 17.9, 17.2. HRMS-ESI(+) *m/z* calc. for $C_{20}H_{24}O_2Na$ $[M+Na]^+$: 319.1669, found: 319.1666.

(*Z*)-6,10-Dimethylundeca-5,9-dien-1-yn-4-yl benzoate ((*Z*)-40a)

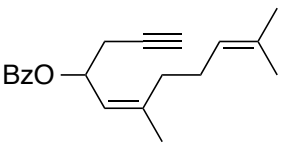

Prepared on 2.5 g scale from (*Z*)-**39**. The product was isolated as a pale yellow oil (2.90 g, 84%).

^{1}H NMR (500 MHz, $CDCl_3$) δ 8.09 – 8.04 (m, 2H), 7.55 (ddt, *J* = 8.8, 7.0, 1.4 Hz, 1H), 7.46 – 7.41 (m, 2H), 5.88 (dt, *J* = 9.4, 5.9 Hz, 1H), 5.40 (dd, *J* = 9.4, 1.6 Hz, 1H), 5.14 (ddt, *J* = 7.1, 4.2, 1.6 Hz, 1H), 2.63 (dd, *J* = 6.0, 2.7 Hz, 2H), 2.42 – 2.33 (m, 1H), 2.21 – 2.08 (m, 3H), 2.00 (t, *J* = 2.6 Hz, 1H), 1.79 (d, *J* = 1.4 Hz, 3H), 1.67 (s, 3H), 1.61 (s, 3H). ^{13}C NMR (126 MHz, $CDCl_3$) δ 165.8, 142.7, 133.0, 132.3,

130.7, 129.8 (2C), 128.4 (2C), 123.9, 122.6, 80.0, 70.4, 69.3, 32.9, 26.7, 25.8, 25.5, 23.6, 17.8. HRMS-ESI(+) *m/z* calc. for $C_{20}H_{24}O_2Na$ $[M+Na]^+$: 319.1669, found: 319.1673.

Preparation of TBS ether of 39 (40b)

In a dry round-bottom flask under argon, **39** (1 equiv) was dissolved in CH_2Cl_2 (0.3-0.6 M solution) and the solution was cooled to 0 °C. Imidazole (1.8-2 equiv) and DMAP (*ca.* 1-5 mol %) were added followed by the addition of TBS-Cl (1.5 equiv) (solid or as a solution in CH_2Cl_2 (3.78 M)). The mixture was then allowed to warm to 25 °C and stirred for 2-6 h upon which time TLC indicated full conversion of **39**. The suspension was poured on brine (3 volumes of CH_2Cl_2) and the organic layer collected. The aqueous layer was re-extracted with CH_2Cl_2 (2 × ½ volume brine). The combined organic extracts were washed with brine (½ initial volume brine), the washed organic phase dried over Na_2SO_4 or $MgSO_4$ and the filtrate concentrated. The crude material was purified by column chromatography on silica gel eluting with pentane/diethyl ether 100:0 to 95:5 or cyclohexane/ethyl acetate 95:5 to afford the pure TBS ether.

(*E*)-*tert*-Butyl((6,10-dimethylundeca-5,9-dien-1-yn-4-yl)oxy)dimethylsilane ((*E*)-40b)

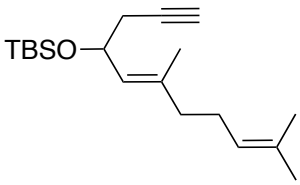

Prepared on 1.5 g scale from (*E*)-**39**. The product was isolated as a pale yellow oil (2.24 g, 93%).

^{1}H NMR (500 MHz, $CDCl_3$) δ 5.16 (dq, *J* = 8.7, 1.4 Hz, 1H), 5.10 (ddq, *J* = 8.4, 5.6, 1.4 Hz, 1H), 4.53 (dt, *J* = 8.7, 6.4 Hz, 1H), 2.38 (ddd, *J* = 16.5, 6.6, 2.7 Hz, 1H), 2.27 (ddd, *J* = 16.5, 6.3, 2.7 Hz, 1H), 2.09 (app. q, *J* = 7.3 Hz, 2H), 2.03 – 1.98 (m, 2H), 1.92 (t, *J* = 2.7 Hz, 1H), 1.67 (s, 3H), 1.66 (d, *J* = 1.3 Hz, 3H), 1.60 (s, 3H), 0.88 (s, 9H), 0.06 (s, 3H), 0.04 (s, 3H). ^{13}C NMR (126 MHz, $CDCl_3$) δ 136.4, 131.7, 128.0, 124.2, 82.0, 69.3, 68.6, 39.6, 28.7, 26.4, 26.0 (3C), 25.8, 18.4, 17.8, 16.9, –4.2, –4.6. HRMS-ESI(+) *m/z* calc. for $C_{19}H_{34}OSiNa$ $[M+Na]^+$: 329.2271, found: 329.2270.

(*Z*)-*tert*-Butyl((6,10-dimethylundeca-5,9-dien-1-yn-4-yl)oxy)dimethylsilane ((*Z*)-40b)

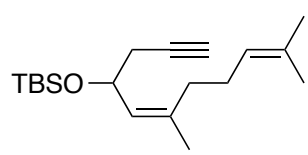

Prepared on 2.5 g scale from (Z)-**39**. The product was isolated as a pale yellow oil (3.20 g, 83%).

^{1}H NMR (400 MHz, $CDCl_3$) δ 5.16 (app. d, *J* = 8.7 Hz, 1H), 5.11 (app. tdd, *J* = 5.1, 2.8, 1.4 Hz, 1H), 4.53 (ddd, *J* = 8.8, 6.7, 5.9 Hz, 1H), 2.37 (ddd, *J* = 16.5, 6.7, 2.6 Hz, 1H), 2.26 (ddd, *J* = 16.5, 5.9, 2.7 Hz, 1H), 2.19 – 1.96 (m, 4H),

1.93 (t, *J* = 2.6 Hz, 1H), 1.71 (d, *J* = 1.4 Hz, 3H), 1.69 (s, 3H), 1.62 (s, 3H), 0.88 (s, 9H), 0.07 (s, 3H), 0.03 (s, 3H). ^{13}C NMR (101 MHz, $CDCl_3$) δ 136.6, 132.1, 128.7, 124.2, 82.1, 69.4, 68.2, 32.7, 29.0, 26.7, 26.0 (3C), 25.8, 23.2, 18.3, 17.8, –4.1, –4.5. HRMS-ESI(+) *m/z* calc. for $C_{19}H_{34}OSiNa$ $[M+Na]^+$: 329.2271, found: 329.2268.

Preparation of TES ether of 39 (40c)

In a dry round-bottom flask under argon, **39** (1 equiv) was dissolved in CH_2Cl_2 (0.3 M solution) and the solution was cooled to 0 °C. Imidazole (2 equiv) and DMAP (1.11 equiv) were added followed by the addition of TESCl (1.5 equiv). The mixture was then allowed to warm to 25 °C and stirred for 1 hour upon which time TLC indicated full conversion of **39**. The suspension was poured on brine (3 volumes of CH_2Cl_2) and the organic layer collected. The aqueous layer was re-extracted with CH_2Cl_2 (2 × ½ volume brine). The combined organic extracts were washed with brine (½ initial volume brine), the dried organic layer dried over $MgSO_4$ and the filtrate concentrated. The crude material was purified by column chromatography on silica gel eluting with pentane/diethyl ether 90:10.

(*E*)-((6,10-Dimethylundeca-5,9-dien-1-yn-4-yl)oxy)triethylsilane ((*E*)-40k)

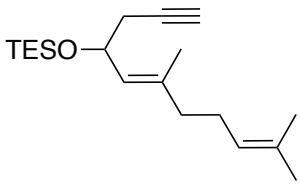

Prepared on 579 mg scale from (*E*)-**39**. The product was isolated as a pale yellow oil (795 mg, 87%).

^{1}H NMR (500 MHz, $CDCl_3$) δ 5.19 (dq, *J* = 8.7, 1.3 Hz, 1H), 5.10 (ddq, *J* = 8.4, 5.7, 1.4 Hz, 1H), 4.53 (dt, *J* = 8.7, 6.4 Hz, 1H), 2.41 (ddd, *J* = 16.5, 6.2, 2.7 Hz, 1H), 2.29 (ddd, *J* = 16.5, 6.6, 2.7 Hz, 1H), 2.13 – 2.06 (m, 2H), 2.03 – 1.98 (m, 2H), 1.92 (t, *J* = 2.6 Hz, 1H), 1.68 – 1.66 (m, 6H), 1.60 (s, 3H), 0.95 (t, *J* = 7.9 Hz, 9H), 0.59 (q, *J* = 7.9 Hz, 6H). ^{13}C NMR (126 MHz, $CDCl_3$) δ 136.7, 131.7, 127.8, 124.2, 81.8, 69.4, 68.2, 39.7, 28.8, 26.4, 25.8, 17.8, 16.9, 6.9 (3C), 5.0 (3C). HRMS-ESI(+) *m/z* calc. for $C_{19}H_{34}OSiNa$ $[M+Na]^+$: 329.2271, found: 329.2272.

Preparation of MOM ether of 39 (40l)

In a dry round-bottom flask under argon, **39** (1 equiv) was dissolved in CH_2Cl_2 (0.3 M solution) and the solution was cooled to 0 °C. *N,N*-Diisopropylethylamine (3 equiv) was added followed by the addition of MOMCl (3 equiv). The mixture was then allowed to warm to 25 °C and stirred for 2 h upon which time TLC indicated full conversion of **39**. The suspension was poured on brine (3 volumes of CH_2Cl_2) and the organic layer collected. The aqueous layer was re-extracted with CH_2Cl_2 (2 × ½ volume brine). The combined organic extracts were washed with brine (½ initial volume brine), the washed

organic phase dried over $MgSO_4$ and the filtrate concentrated. The crude material was purified by column chromatography on silica gel eluting with pentane/diethyl ether 9:1 to 8:2.

(*E*)-4-(Methoxymethoxy)-6,10-dimethylundeca-5,9-dien-1-yne ((*E*)-40l)

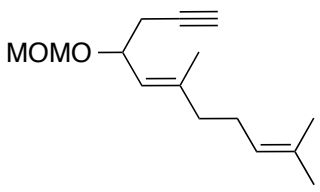

Prepared on 579 mg scale from (*E*)-**39**. The product was isolated as a pale yellow oil (657 mg, 93%).

^{1}H NMR (400 MHz, $CDCl_3$) δ 5.13 – 5.04 (m, 2H), 4.67 (d, *J* = 6.7 Hz, 1H), 4.55 – 4.47 (m, 2H), 3.39 (s, 3H), 2.48 (ddd, J = 16.7, 6.5, 2.6 Hz, 1H), 2.41 (ddd, J = 16.7, 5.9, 2.7 Hz, 1H), 2.15 – 2.02 (m, 4H), 1.98 (t, *J* = 2.6 Hz, 1H), 1.70 (d, *J* = 1.4 Hz, 3H), 1.67 (app. d, *J* = 1.4 Hz, 3H), 1.60 (s, 3H). ^{13}C NMR (101 MHz, $CDCl_3$) 141.7, 131.9, 124.0, 123.6, 93.4, 81.3, 69.9, 69.6, 55.5, 39.8, 26.4, 25.9, 25.8, 17.8, 16.8. HRMS-ESI(+) *m/z* calc. for $C_{15}H_{24}O_2Na$ $[M+Na]^+$: 259.1669, found: 259.1668.

General Procedure for the preparation of aldehydes from 40 (37)

In a dry round-bottom flask under argon, AD-mix-α (1.4 g per mmol of **40**) and methylsulfonamide (1 equiv) were dissolved in *t*BuOH/H_2O 1:1 (15 mL per mmol of **40**) and the solution was cooled to 0 °C. **40** (1 equiv) was added slowly as a solution in *t*BuOH (0.5 mL per mmol). The mixture was stirred at 0 °C for 5 min then allowed to warm to 25 °C and stirred for 16 hours. TLC indicated full conversion of **40** into the diol. The suspension was quenched by addition of a saturated solution of Na_2SO_3 (15 mL per mmol) and then solid Na_2SO_3 (2 g per mmol). The resulting mixture was stirred at 25 °C for 1 hour, then poured on brine (5 volumes of *t*BuOH) and extracted with ethyl acetate (4 × volume *t*BuOH). The combined organic extracts were washed with a saturated solution of Na_2SO_3 (15 mL per mmol) (2 × volume *t*BuOH) and a saturated solution of $NaHCO_3$ (volume *t*BuOH), dried over Na_2SO_4 and concentrated. The crude diol was redissolved in HPLC grade CH_2Cl_2 (20 mL per mmol) and the solution cooled to 0 °C and $NaIO_4@SiO_2$[16] (2 g per mmol) was added. The suspension was stirred at 25 °C for 1.5-3 h upon which time TLC indicated full conversion of the diol. The solids were filtered off on a pad of Celite and washed with diethyl ether (3 × 10 mL per mmol) and the filtrate concentrated. The resulting crude aldehyde was purified by column chromatography on silica gel eluting with pentane/diethyl ether 98:2 to 9:1 or cyclohexane/ethyl acetate 90:10 to 80:20 to afford the pure aldehyde.

(*E*)-6-Methyl-9-oxonon-5-en-1-yn-4-yl benzoate ((*E*)-37a)

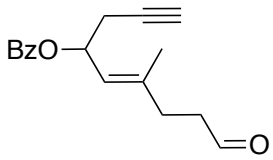

Prepared on 2.63 g scale from (*E*)-**40a**. The product was isolated as a pale yellow oil (1.59 g, 66%).

^{1}H NMR (400 MHz, $CDCl_3$) δ 9.77 (t, *J* = 1.7 Hz, 1H), 8.07 – 8.02 (m, 2H), 7.56 (ddt, *J* = 8.7, 6.9, 1.3 Hz, 1H), 7.47 – 7.40 (m, 2H), 5.84 (dt, *J* = 9.0, 6.1 Hz, 1H), 5.38 (ddq, *J* = 9.1, 2.7, 1.4 Hz, 1H), 2.70 – 2.55 (m, 4H), 2.42 – 2.36 (m, 2H), 1.99 (t, *J* = 2.7 Hz, 1H), 1.85 (d, *J* = 1.3 Hz, 3H). ^{13}C NMR (101 MHz, $CDCl_3$) δ 201.8, 165.8, 140.4, 133.1, 130.4, 129.8 (2C), 128.5 (2C), 122.8, 79.5, 70.5, 69.4, 41.9, 31.7, 25.2, 17.4. HRMS-ESI(+) *m/z* calc. for $C_{18}H_{22}O_4Na$ $[M+CH_3OH+Na]^+$: 325.1410, found: 325.1403.

(*Z*)-6-Methyl-9-oxonon-5-en-1-yn-4-yl benzoate ((*Z*)-37a)

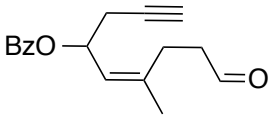

Prepared on 2.5 g scale from (*Z*)-**40a**. The product was isolated as a pale yellow solid (2.90 g, 84%).

Mp = 33–35 °C. ^{1}H NMR (500 MHz, $CDCl_3$) δ 9.81 (t, *J* = 1.2 Hz, 1H), 8.06 – 8.02 (m, 2H), 7.58 – 7.53 (m, 1H), 7.46 – 7.41 (m, 2H), 5.86 (dt, *J* = 9.4, 6.1 Hz, 1H), 5.38 (app. dd, *J* = 9.4, 1.5 Hz, 1H), 2.70 – 2.53 (m, 6H), 2.01 (t, *J* = 2.6 Hz, 1H), 1.77 (d, *J* = 1.4 Hz, 3H). ^{13}C NMR (126 MHz, $CDCl_3$) δ 201.7, 165.8, 140.6, 133.1, 130.4, 129.8 (2C), 128.5 (2C), 123.9, 79.7, 70.7, 69.2, 42.3, 25.3, 25.1, 23.3. HRMS-ESI(+) *m/z* calc. for $C_{17}H_{18}O_3Na^+$ $[M+Na]^+$: 293.1148, found: 293.1154 (also observed: *m/z* calc. for $C_{18}H_{22}O_4Na$ $[M+MeOH+Na]^+$: 325.1410, found: 325.1423).

(*E*)-6-((*tert*-Butyldimethylsilyl)oxy)-4-methylnon-4-en-8-ynal ((*E*)-37b)

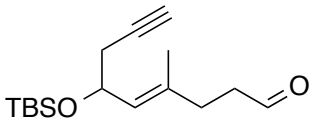

Prepared on 2.24 g scale from (*E*)-**40b**. The product was isolated as a pale yellow oil (1.314 g, 64%).

^{1}H NMR (400 MHz, $CDCl_3$) δ 9.78 (t, *J* = 1.8 Hz, 1H), 5.19 (dq, *J* = 8.7, 1.3 Hz, 1H), 4.52 (dt, *J* = 8.6, 6.5 Hz, 1H), 2.58 – 2.51 (m, 2H), 2.43–2.31 (m, 3H), 2.27 (ddd, *J* = 16.5, 6.7, 2.7 Hz, 1H), 1.92 (t, *J* = 2.7 Hz, 1H), 1.69 (d, *J* = 1.4 Hz, 3H), 0.87 (s, 9H), 0.06 (s, 3H), 0.02 (s, 3H). ^{13}C NMR (101 MHz, $CDCl_3$) δ 202.1, 134.7, 128.8, 81.6, 69.6, 68.4, 42.0, 31.7, 28.6, 25.9 (3C), 18.3, 17.1, –4.3, –4.6. HRMS-ESI(+) *m/z* calc. for $C_{16}H_{28}O_2SiNa$ $[M+Na]^+$: 303.1751, found: 303.1744.

(*Z*)-6-((*tert*-Butyldimethylsilyl)oxy)-4-methylnon-4-en-8-ynal ((*Z*)-37b)

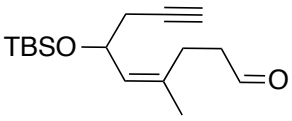

Prepared on 3.0 g scale from (*Z*)-**40b**. The product was isolated as a pale yellow oil (2.40 g, 87%).

^{1}H NMR (500 MHz, $CDCl_3$) δ 9.80 (t, *J* = 1.5 Hz, 1H), 5.20 (app. dd, *J* = 8.8, 1.4 Hz, 1H), 4.52 (ddd, *J* = 8.9, 6.9, 6.0 Hz, 1H), 2.58 – 2.53 (m, 2H), 2.51 – 2.44 (m, 1H), 2.40 (ddd, *J* = 16.5, 6.0, 2.7 Hz, 1H), 2.35 – 2.24 (m, 2H), 1.93 (t, *J* = 2.6 Hz, 1H), 1.70 (d, *J* = 1.4 Hz, 3H), 0.86 (s, 9H), 0.06 (s, 3H), 0.02 (s, 3H). ^{13}C NMR (126 MHz, $CDCl_3$) δ 201.7, 134.6, 129.9, 81.8, 69.8, 68.0, 42.5, 28.9, 25.9 (3C), 24.7, 23.0, 18.3, –4.2, –4.5. HRMS-ESI(+) *m/z* calc. for $C_{16}H_{28}O_2SiNa$ $[M+Na]^+$: 303.1751, found: 303.1752 (also observed: *m/z* calc. for $C_{17}H_{32}O_{3Si}Na$ $[M+MeOH+Na]^+$: 335.2013, found: 335.2025.

(*E*)-4-Methyl-6-((triethylsilyl)oxy)non-4-en-8-ynal ((*E*)-37k)

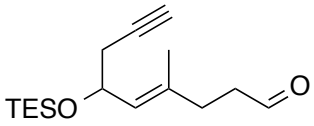

Prepared on 790 mg scale from (*E*)-**40k**. The product was isolated as a pale yellow oil (506 mg, 70%).

^{1}H NMR (500 MHz, $CDCl_3$) δ 9.78 (t, *J* = 1.7 Hz, 1H), 5.24 – 5.19 (m, 1H), 4.53 (ddd, *J* = 8.7, 7.0, 5.9 Hz, 1H), 2.55 (ddd, *J* = 8.0, 6.9, 1.6 Hz, 2H), 2.41 (ddd, J = 16.4, 5.9, 2.6 Hz, 1H), 2.36 – 2.32 (m, 2H), 2.29 (ddd, J = 16.5, 7.1, 2.7 Hz, 1H), 1.92 (t, *J* = 2.7 Hz, 1H), 1.70 (d, *J* = 1.3 Hz, 3H), 0.94 (t, *J* = 7.9 Hz, 9H), 0.58 (q, *J* = 7.7 Hz, 6H). ^{13}C NMR (126 MHz, $CDCl_3$) δ 202.1, 134.9, 128.7, 81.4, 69.6, 68.0, 42.0, 31.7, 28.7, 17.2, 6.9 (3C), 5.0 (3C). HRMS-ESI(+) *m/z* calc. for $C_{16}H_{28}O_2SiNa$ $[M+Na]^+$: 303.1751, found: 303.1756.

(*E*)-6-(Methoxymethoxy)-4-methylnon-4-en-8-ynal ((*E*)-37l)

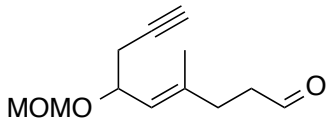

Prepared on 650 mg scale from (*E*)-**40l**. The product was isolated as a pale yellow oil (385 mg, 57%).

^{1}H NMR (400 MHz, $CDCl_3$) δ 9.77 (t, *J* = 1.7 Hz, 1H), 5.17 – 5.12 (m, 1H), 4.62 (d, *J* = 6.8 Hz, 1H), 4.55 – 4.46 (m, 2H), 3.38 (s, 3H), 2.60 – 2.53 (m, 2H), 2.47 (ddd, *J* = 16.7, 6.2, 2.7 Hz, 1H), 2.44 – 2.35 (m, 3H), 1.98 (t, *J* = 2.6 Hz, 1H), 1.73 (d, *J* = 1.4 Hz, 3H). ^{13}C NMR (101 MHz, $CDCl_3$) δ 201.9, 139.6, 124.5, 93.6, 80.9, 69.8, 69.8, 55.5, 42.0, 31.8, 25.7, 17.1. HRMS-ESI(+) *m/z* calc. for $C_{12}H_{18}O_3Na$ $[M+Na]^+$: 233.1148, found: 233.1158.

General Procedure for the preparation of ketones (37c-j)

Depending on the polarity of the alcohol intermediate **S1** (and the ease of purification), one of the two following methods was used for the preparation of ketones **37c-j**.

Method A

In a dry flask under argon, corresponding aldehyde (**37a-b**) (1 equiv) was dissolved in anhydrous THF (*ca.* 4 mL per mmol) and the solution was cooled to -78 °C. A solution of Grignard reagent RMgX (1.5 equiv) was added slowly at -78 °C. The mixture was stirred at -78 °C for 1.5-3 h upon which time a milky suspension was observed. The

suspension was quenched by addition of a saturated aqueous solution of NH_4Cl (*ca.* 5 mL per mmol) at -78 °C, then allowed to warm to 25 °C stirring vigorously. It was then poured on brine (70 mL per mmol) and extracted with diethyl ether (3 × 40 mL per mmol). The combined ethereal extracts were dried over Na_2SO_4 and concentrated. The crude material was purified by column chromatography on silica gel eluting with cyclohexane/ethyl acetate to afford the alcohol as a mixture of diastereomers (the unreacted aldehyde can be recovered and recycled at this stage).

The pure alcohol was redissolved in CH_2Cl_2 (*ca.* 10 mL per mmol) and the solution cooled to 0 °C and $NaHCO_3$ (5 equiv) and Dess-Martin periodinane (1.2 equiv) were added sequentially. The mixture was stirred at 0 °C for 1-2 h then 25 °C for 1-2 h upon which time TLC showed full conversion of the alcohol to the less polar ketone. The mixture was either quenched by addition of a saturated solution of sodium thiosulfate and extracted with CH_2Cl_2 or diluted with pentane (2-3 × volume CH_2Cl_2) and filtered. The resulting crude product was purified by chromatography on silica gel eluting with cyclohexane/ethyl acetate to afford the title ketones.

Method B

In a dry flask under argon, corresponding aldehyde (**37a-b**) (1 equiv) was dissolved in anhydrous THF (*ca.* 4 mL per mmol) and the solution was cooled to -78 °C. A solution of Grignard reagent RMgX (1.5 equiv) was added slowly at -78 °C. The mixture was stirred at -78 °C for 1.5-3 h upon which time a milky suspension was observed. The suspension was quenched by addition of a saturated aqueous solution of NH_4Cl (*ca.* 5 mL per mmol) at -78 °C, then allowed to warm to 25 °C stirring vigorously. It was then poured on brine (70 mL per mmol) and extracted with diethyl ether (3 × 40 mL per mmol). The combined ethereal extracts were dried over Na_2SO_4 and concentrated. The crude alcohol (containing the unreacted starting aldehyde) was redissolved in CH_2Cl_2 (*ca.* 10 mL per mmol) and the solution cooled to 0 °C and $NaHCO_3$ (5 equiv) and Dess-Martin periodinane (1.2 equiv) were added sequentially. The mixture was stirred at 0 °C for 1-2 h then 25 °C for 1-2 h upon which time TLC showed full conversion of the alcohol to the less polar ketone. The mixture was either quenched by addition of a saturated solution of sodium thiosulfate and extracted with CH_2Cl_2 or diluted with pentane (2–3 × volume CH_2Cl_2) and filtered. The resulting crude product was purified by chromatography on silica gel eluting with cyclohexane/ethyl acetate to afford the title ketones (the unreacted aldehyde can be recovered and recycled).

(*E*)-9-Hydroxy-6-methyldec-5-en-1-yn-4-yl benzoate ((*E*)-S1c)

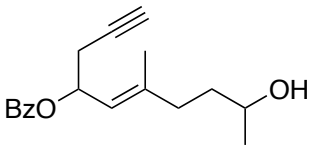

Prepared on 300 mg scale from (*E*)-**37a** according to method **A** and using a commercial solution of MeMgBr in Et_2O (3 M). The product was purified by silica gel column chromatography eluting with cyclohexane/ethyl acetate 4:1 to 3:1 and obtained as a colorless oil (221 mg, 70%, *ca.* 1:1 *dr*). **Note**: in the proton assignments below '1H + 1H' refers to a signal accounting for one proton of each diastereomer; likewise, '1C + 1C' refers to a signal accounting for one carbon of each diastereomer.

^{1}H NMR (400 MHz, $CDCl_3$) 8.07 – 8.02 (m, 2H + 2H), 7.58 – 7.52 (m, 1H + 1H), 7.47 – 7.40 (m, 2H + 2H), 5.89 – 5.81 (m, 1H + 1H), 5.39 (app. d quin, J = 9.0, 1.4 Hz, 1H + 1H), 3.80 (app. sept, J = 5.7 Hz, 1H + 1H), 2.71 – 2.56 (m, 2H + 2H), 2.24 – 2.06 (m, 2H + 2H), 1.99 and 1.99 (q, J = 2.5 Hz, 1H + 1H), 1.84 (s, 3H + 3H), 1.63 – 1.55 (m, 2H + 2H), 1.20 (d, J = 6.2 Hz, 3H + 3H). ^{13}C NMR (101 MHz, $CDCl_3$) δ 165.9, 165.9, 142.4 (1C + 1C), 133.0 (1C + 1C), 130.7 (1C + 1C), 129.8 (2C + 2C), 128.5 (2C + 2C), 122.3, 122.3, 79.8, 79.8, 70.4, 70.4, 69.7, 69.7, 68.0, 67.9, 37.2, 37.2, 36.1, 36.0, 25.3 (1C + 1C), 23.7, 23.7, 17.2 (1C + 1C). HRMS-ESI(+) *m/z* calc. for $C_{18}H_{22}O_3Na$ $[M+Na]^+$: 309.1461, found: 309.1457.

(*E*)-6-Methyl-9-oxodec-5-en-1-yn-4-yl benzoate ((*E*)-37c)

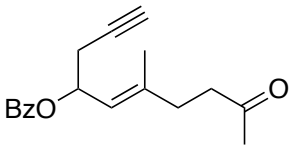

Prepared on 221 mg scale from (*E*)-**S1c** according to method **A**. The product was purified by silica gel column chromatography eluting with cyclohexane/ethyl acetate 9:1 to 4:1 to afford a colorless oil (186 mg, 85%); 60% yield over 2 steps.

^{1}H NMR (400 MHz, $CDCl_3$) δ 8.06 – 8.02 (m, 2H), 7.55 (ddt, J = 8.0, 6.9, 1.4 Hz, 1H), 7.48 – 7.40 (m, 2H), 5.84 (dt, J = 9.0, 6.1 Hz, 1H), 5.38 – 5.32 (m, 1H), 2.69 – 2.53 (m, 4H), 2.36 – 2.29 (m, 2H), 2.15 (s, 3H), 1.99 (t, J = 2.6 Hz, 1H), 1.83 (d, J = 1.4 Hz, 3H). ^{13}C NMR (101 MHz, $CDCl_3$) δ 208.1, 165.8, 141.0, 133.1, 130.5, 129.8 (2C), 128.5 (2C), 122.4, 79.7, 70.4, 69.5, 41.9, 33.4, 30.1, 25.2, 17.4. HRMS-ESI(+) *m/z* calc. for $C_{18}H_{20}O_3Na$ $[M+Na]^+$: 307.1305, found: 307.1306.

(*Z*)-9-Hydroxy-6-methyldec-5-en-1-yn-4-yl benzoate ((*Z*)-S1c)

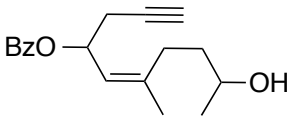

Prepared on 300 mg scale from (*Z*)-**37a** according to method **A** and using a commercial solution of MeMgBr in Et_2O (3 M). The product was purified by silica gel column chromatography

eluting with cyclohexane/ethyl acetate 85:15 to 7:3 and obtained as a colorless oil (208 mg, 65%, *ca.* 1.15:1 *dr*; 80% brsm) (plus 55 mg of recovered aldehyde, 18%).

^{1}H NMR (500 MHz, $CDCl_3$) δ 8.07 – 8.03 (m, 2H *major* + 2H *minor*), 7.58 – 7.52 (m, 1H *major* + 1H *minor*), 7.46 – 7.40 (m, 2H *major* + 2H *minor*), 5.92 (app. dt, *J* = 9.3, 6.1 Hz, 1H *major* + 1H *minor*), 5.38 – 5.32 (m, 1H *major* + 1H *minor*), 3.84 – 3.73 (m, 1H *major* + 1H *minor*), 2.70 – 2.56 (m, 2H *major* + 2H *minor*), 2.50 (dt, *J* = 13.6, 8.2 Hz, 1H *major*), 2.38 (ddd, *J* = 13.5, 10.0, 5.6 Hz, 1H *minor*), 2.30 (ddd, *J* = 13.4, 9.8, 6.7 Hz, 1H *minor*), 2.19 (ddd, *J* = 13.7, 8.0, 5.7 Hz, 1H *major*), 2.00 and 2.00 (two t, *J* = 2.6 Hz, 1H *major* + 1H *minor*), 1.78 (d, *J* = 1.4 Hz, 3H *minor*), 1.76 (d, *J* = 1.4 Hz, 3H *major*), 1.66 – 1.50 (m, 2H *major* + 2H *minor*), 1.20 (d, *J* = 6.2 Hz, 3H *minor*), 1.19 (d, *J* = 6.2 Hz, 3H *major*). ^{13}C NMR (126 MHz, $CDCl_3$) δ 166.1, 165.9, 143.0, 142.1, 133.2, 133.1, 130.5, 130.4, 129.9 (2C one diastereomer), 129.8 (2C one diastereomer), 128.5 (2C one diastereomer), 128.4 (2C one diastereomer), 123.2, 122.6, 79.9, 79,8, 70.5, 70.5, 69.7, 69.3, 68.0, 66.6, 37.7, 36.9, 29.2, 28.5, 25.6, 25.4, 23.9, 23.7, 23.5, 23.2. HRMS-ESI(+) *m/z* calc. for $C_{18}H_{22}O_3Na$ $[M+Na]^+$: 309.1461, found: 309.1451.

(*Z*)-6-Methyl-9-oxodec-5-en-1-yn-4-yl benzoate ((*Z*)-37c)

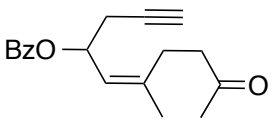

Prepared on 190 mg scale from (*Z*)-**S1c** according to method **A**. The product was purified by silica gel column chromatography eluting with cyclohexane/ethyl acetate 4:1 to afford a colorless oil (179 mg, 95%); 62% yield over 2 steps (76% based on recovered starting material).

^{1}H NMR (400 MHz, $CDCl_3$) δ 8.07 – 8.01 (m, 2H), 7.58 – 7.51 (m, 1H), 7.47 – 7.39 (m, 2H), 5.85 (dt, *J* = 9.3, 6.1 Hz, 1H), 5.39 – 5.33 (m, 1H), 2.70 – 2.41 (m, 6H), 2.14 (s, 3H), 2.00 (t, *J* = 2.7 Hz, 1H), 1.74 (d, *J* = 1.5 Hz, 3H). ^{13}C NMR (101 MHz, $CDCl_3$) δ 208.0, 165.7, 141.1, 133.0, 130.5, 129.8 (2C), 128.4 (2C), 123.5, 79.8, 70.5, 69.3, 42.0, 30.0, 26.8, 25.3, 23.3. HRMS-ESI(+) *m/z* calc. for $C_{18}H_{20}O_3Na$ $[M+Na]^+$: 307.1305, found: 307.1304.

(*E*)-7-((*tert*-Butyldimethylsilyl)oxy)-5-methyldec-5-en-9-yn-2-ol ((*E*)-S1d)

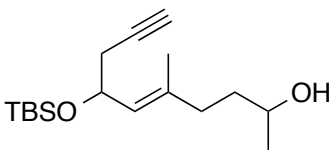

Prepared on 500 mg scale of (*E*)-**37b** according to method **A** and using a commercial solution of MeMgBr in Et_2O (3 M). Purified by silica gel column chromatography eluting with cyclohexane/ethyl acetate 95:5 to 9:1 and obtained as a colorless oil (470 mg, 89%, *ca.* 1:1 *dr*). **Note**: in the proton assignments below '1H + 1H' refers to a signal accounting for one proton of each diastereomer; likewise, '1C + 1C' refers to a signal accounting for one carbon of each diastereomer.

^{1}H NMR (500 MHz, $CDCl_3$) δ 5.20 (app. d quin, *J* = 8.6, 1.3 Hz, 1H + 1H), 4.53 (app. dt, *J* = 8.6, 6.5 Hz, 1H + 1H), 3.80 (app. sext *J* = 6.4 Hz, 1H + 1H), 2.40 (app. ddd, *J* = 16.5, 6.2, 2.6 Hz, 1H + 1H), 2.28 (app. ddd, *J* = 16.5, 6.7, 2.6 Hz, 1H + 1H), 2.15 – 2.02 (m, 2H + 2H), 1.92 and 1.91 (two t, *J* = 2.6 Hz, 1H + 1H), 1.69 (d, *J* = 1.4 Hz, 3H one dia) and 1.68 (d, *J* = 1.4 Hz, 3H other dia), 1.64 – 1.50 (m, 2H + 2H), 1.20 (d, *J* = 0.6 Hz, 3H one dia) and 1.19 (d, *J* = 0.6 Hz, 3H other dia), 0.87 (s, 9H + 9H), 0.06 (s, 3H + 3H), 0.03 (s, 3H + 3H). ^{13}C NMR (126 MHz, $CDCl_3$) δ 136.6, 136.4, 128.2 (1C + 1C), 81.8, 81.8, 69.5, 69.4, 68.4 (1C + 1C), 68.2, 67.8, 37.2, 37.2, 36.2, 35.9, 28.7, 28.7, 26.0 (3C + 3C), 23.6 (1C + 1C), 18.3 (1C + 1C), 17.0 (1C + 1C), –4.2, –4.2, –4.6 (1C + 1C). HRMS-ESI(+) *m/z* calc. for $C_{17}H_{32}O_2SiNa$ $[M+Na]^+$: 319.2064, found: 319.2072.

(*E*)-7-((*tert*-Butyldimethylsilyl)oxy)-5-methyldec-5-en-9-yn-2-one ((*E*)-37d)

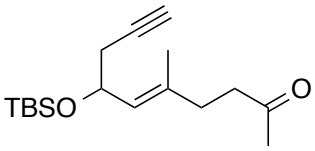

Prepared on 470 mg scale from (*E*)-**S1d** according to method **A**. The product was purified by silica gel column chromatography eluting with cyclohexane/ethyl acetate 9:1 to afford a colorless oil (339 mg, 73%); 65% yield over 2 steps.

^{1}H NMR (500 MHz, $CDCl_3$) δ 5.15 (app. d sept, *J* = 8.6, 1.4 Hz, 1H), 4.51 (dt, *J* = 8.6, 6.5 Hz, 1H), 2.57 – 2.51 (m, 2H), 2.38 (ddd, *J* = 16.5, 6.3, 2.6 Hz, 1H), 2.30 – 2.22 (m, 3H), 2.15 (s, 3H), 1.91 (t, *J* = 2.6 Hz, 1H), 1.67 (d, *J* = 1.3 Hz, 3H), 0.87 (s, 9H), 0.05 (s, 3H), 0.02 (s, 3H). ^{13}C NMR (126 MHz, $CDCl_3$) δ 208.3, 135.3, 128.3, 81.7, 69.5, 68.4, 42.1, 33.3, 30.0, 28.7, 26.0 (3C), 18.3, 17.2, –4.2, –4.6. HRMS-ESI(+) *m/z* calc. for $C_{17}H_{30}O_2SiNa$ $[M+Na]^+$: 317.1907, found: 317.1909.

(*Z*)-7-((*tert*-Butyldimethylsilyl)oxy)-5-methyldec-5-en-9-yn-2-ol ((*Z*)-S1d)

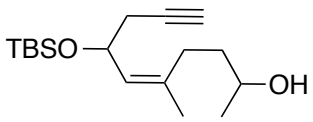

Prepared on 300 mg scale from (*Z*)-**37b** according to method **A** and using a commercial solution of MeMgBr in Et_2O (3 M). The product was purified by silica gel column chromatography eluting with cyclohexane/ethyl acetate 95:5 to 9:1 and obtained as a colorless oil (220 mg, 69%, *ca.* 1.35:1 *dr* – 81% brsm) (plus 45 mg of recovered aldehyde, 15%).

^{1}H NMR (500 MHz, $CDCl_3$) δ 5.20 – 5.14 (m, 1H *major* + 1H *minor*), 4.59 – 4.52 (m, 1H *major* + 1H *minor*), 3.83 – 3.75 (m, 1H *major* + 1H *minor*), 2.43 – 2.36 (m, 1H *major* + 1H *minor*), 2.32 – 2.19 (m, 2H *major* + 2H *minor*), 2.13 – 2.02 (m, 1H *major* + 1H *minor*), 1.94 and 1.93 (two t, *J* = 2.7 Hz, 1H *major* + 1H *minor*), 1.72 (d, *J* = 1.4 Hz, 3H *minor*), 1.71 (d, *J* = 1.4 Hz, 3H *major*), 1.59 – 1.51 (m, 2H *major* + 2H *minor*), 1.21 and 1.21 (two d, *J* = 6.2 Hz, 3H *minor* + 3H *minor*), 0.87 (s, 9H *minor*), 0.87 (s, 9H

major), 0.06 (s, 3H *major* + 3H *minor*), 0.04 (s, 3H *minor*), 0.03 (s, 3H *major*). ^{13}C NMR (126 MHz, $CDCl_3$) δ 136.7, 136.6, 128.8, 128.7, 82.1, 82.0, 69.7, 69.6, 68.3, 68.1, 68.0, 67.8, 37.7, 37.4, 29.0, 29.0, 28.9, 28.7, 26.0 (3C *major* + 3C *minor*), 23.9, 23.8, 23.3, 23.3, 18.3 (1C *major* + 1C *minor*), –4.1 (1C *major* + 1C *minor*), –4.5, –4.5. HRMS-ESI(+) *m/z* calc. for $C_{17}H_{32}O_2SiNa$ $[M+Na]^+$: 319.2064, found: 319.2074.

(*Z*)-7-((*tert*-Butyldimethylsilyl)oxy)-5-methyldec-5-en-9-yn-2-one ((*Z*)-37d)

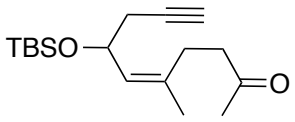

Prepared on 205 mg scale from (*Z*)-**S1d** according to method **A**, purified by silica gel column chromatography eluting with cyclohexane/ethyl acetate 95:5 to 9:1 to afford a colorless oil (193 mg, 93%); 65% yield over 2 steps (75% based on recovered starting material).

^{1}H NMR (500 MHz, $CDCl_3$) δ 5.20 – 5.15 (m, 1H), 4.52 (dt, *J* = 8.8, 6.4 Hz, 1H), 2.53 (app. t, *J* = 7.9 Hz, 2H), 2.44 – 2.34 (m, 2H), 2.30 – 2.23 (m, 2H), 2.15 (s, 3H), 1.92 (t, *J* = 2.6 Hz, 1H), 1.68 (d, *J* = 1.4 Hz, 3H), 0.86 (s, 9H), 0.06 (s, 3H), 0.02 (s, 3H). ^{13}C NMR (126 MHz, $CDCl_3$) δ 208.0, 135.2, 129.5, 81.9, 69.6, 68.0, 42.2, 30.1, 28.9, 26.4, 25.9 (3C), 23.1, 18.3, –4.2, –4.5. HRMS-ESI(+) *m/z* calc. for $C_{17}H_{30}O_2SiNa$ $[M+Na]^+$: 317.1907, found: 317.1906.

(*E*)-9-Cyclopropyl-9-hydroxy-6-methylnon-5-en-1-yn-4-yl benzoate ((*E*)-S1e)

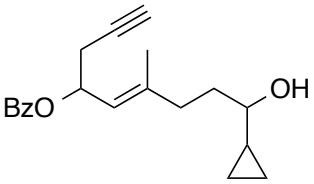

Prepared on 268 mg scale from (*E*)-**37a** according to method **A** and using a freshly prepared solution of *c*-C_3H_5MgBr in Et_2O (~0.4 M). The product was purified by silica gel column chromatography eluting with cyclohexane/ethyl acetate 8:2 obtained as a colorless oil (116 mg, 37%, *ca.* 1:1 *dr*). **Note**: in the proton assignments below '1H + 1H' refers to a signal accounting for one proton of each diastereomer; likewise, '1C + 1C' refers to a signal accounting for one carbon of each diastereomer.

^{1}H NMR (400 MHz, $CDCl_3$) δ 8.07 – 8.02 (m, 2H + 2H), 7.55 (app. t, *J* = 7.2 Hz, 1H + 1H), 7.43 (app. t, *J* = 7.8 Hz, 2H + 2H), 5.86 (app. dtd, *J* = 8.9, 6.1, 1.5 Hz, 1H + 1H), 5.39 (app. d, *J* = 9.2 Hz, 1H + 1H), 2.85 (app. quin, *J* = 6.4 Hz, 1H + 1H), 2.70 – 2.56 (m, 2H + 2H), 2.29 – 2.10 (m, 2H + 2H), 2.00 – 1.96 (m, 1H + 1H), 1.84 (s, 3H + 3H), 1.79 – 1.70 (m, 2H + 2H), 0.96 – 0.85 (m, 1H + 1H), 0.57 – 0.45 (m, 2H + 2H), 0.30 – 0.16 (m, 2H + 2H). ^{13}C NMR (101 MHz, $CDCl_3$) δ 165.9, 165.9, 142.5, 142.4, 133.0 (1C + 1C), 130.6, 130.6, 129.8 (2C + 2C), 128.5 (2C + 2C), 122.1, 122.0, 79.8, 79.8, 76.5, 76.4, 70.4, 70.3, 69.7 (1C + 1C), 35.8, 35.8, 35.2, 35.1, 25.3, 25.3, 18.1, 18.1,

17.3, 17.3, 2.9, 2.9, 2.7, 2.7. HRMS-ESI(+) *m/z* calc. for $C_{20}H_{24}O_3Na$ $[M+Na]^+$: 335.1618, found: 335.1614.

(*E*)-9-Cyclopropyl-6-methyl-9-oxonon-5-en-1-yn-4-yl benzoate ((*E*)-37e)

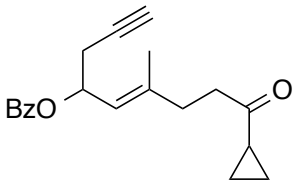

Prepared on 115 mg scale from (*E*)-**S1e** according to method **A**. The product was purified by silica gel column chromatography eluting with cyclohexane/ethyl acetate 8:2 to afford a colorless oil (84 mg, 73%); 27% yield over 2 steps.

^{1}H NMR (500 MHz, $CDCl_3$) δ 8.07 – 8.02 (m, 2H), 7.58 – 7.53 (m, 1H), 7.46 – 7.41 (m, 2H), 5.85 (dt, *J* = 9.1, 6.1 Hz, 1H), 5.39 – 5.35 (m, 1H), 2.72 – 2.67 (m, 2H), 2.67 – 2.57 (m, 2H), 2.36 (td, *J* = 7.7, 1.3 Hz, 2H), 1.98 (t, *J* = 2.6 Hz, 1H), 1.92 (tt, *J* = 7.8, 4.5 Hz, 1H), 1.84 (d, *J* = 1.4 Hz, 3H), 1.04 – 0.96 (m, 2H), 0.90 – 0.80 (m, 2H). ^{13}C NMR (126 MHz, $CDCl_3$) δ 210.2, 165.9, 141.2, 133.1, 130.5, 129.8 (2C), 128.5 (2C), 122.3, 79.7, 70.4, 69.5, 41.8, 33.6, 25.2, 20.6, 17.4, 10.9, 10.9. HRMS-ESI(+) *m/z* calc. for $C_{20}H_{22}O_3Na$ $[M+Na]^+$: 333.1461, found: 333.1450.

(*Z*)-9-Cyclopropyl-9-hydroxy-6-methylnon-5-en-1-yn-4-yl benzoate ((*Z*)-S1e)

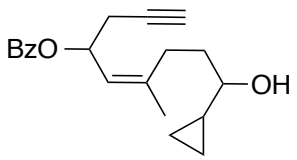

Prepared on 300 mg scale from (*Z*)-**37a** according to method **A** and using a freshly prepared solution of *c*-C_3H_5MgBr in Et_2O (~0.4 M). The product was purified by silica gel column chromatography eluting with cyclohexane/ethyl acetate 9:1 to 3:1 and obtained as a colorless oil (230 mg, 66%, *ca.* 4:3 *dr*; 80% based on recovered starting material) (plus 51 mg of recovered starting material, 17%).

^{1}H NMR (500 MHz, $CDCl_3$) δ 8.07 – 8.02 (m, 2H *major* + 2H *minor*), 7.58 – 7.52 (m, 1H *major* + 1H *minor*), 7.46 – 7.40 (m, 2H *major* + 2H *minor*), 5.96 – 5.89 (m, 1H *major* + 1H *minor*), 5.39 – 5.33 (m, 1H *major* + 1H *minor*), 2.92 – 2.82 (m, 1H *major* + 1H *minor*), 2.69 – 2.57 (m, 2H *major* + 2H *minor*), 2.53 (dt, *J* = 13.5, 8.3 Hz, 1H *major*), 2.50 – 2.33 (m, 2H *minor*), 2.22 (ddd, *J* = 13.5, 8.5, 5.3 Hz, 1H *major*), 2.00 and 1.99 (two t, *J* = 2.7 Hz, 1H *major* + 1H *minor*), 1.87 – 1.62 (m, 3+2H *major* + 3+2H *minor*), 0.95 – 0.86 (m, 1H *major* + 1H *minor*), 0.55 – 0.43 (m, 3H *major* + 1H *minor*), 0.31 – 0.23 (m, 1H *major* + 1H *minor*), 0.23 – 0.17 (m, 1H *minor*), 0.17 – 0.12 (m, 1H *minor*). ^{13}C NMR (126 MHz, $CDCl_3$) δ 166.1, 165.9, 143.2, 142.3, 133.1, 133.0, 130.6, 130.5, 129.9 (2C one diastereomer), 129.8 (2C one diastereomer), 128.5 (2C one diastereomer), 128.4 (2C one diastereomer), 123.1, 122.6, 80.0, 79.8, 76.3, 75.5, 70.5, 70.4, 69.7, 69.3, 35.6, 35.0, 29.0, 28.7, 25.6, 25.4, 23.5, 23.3, 18.1, 17.9, 2.8, 2.7, 2.7, 2.6. HRMS-ESI(+) *m/z* calc. for $C_{20}H_{24}O_3Na$ $[M+Na]^+$: 335.1618, found: 335.1620.

(*Z*)-9-Cyclopropyl-6-methyl-9-oxonon-5-en-1-yn-4-yl benzoate ((*Z*)-37e)

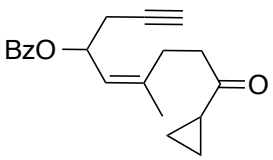

Prepared on 215 mg scale from (*Z*)-**S1e** according to method **A**. The product was purified by silica gel column chromatography eluting with cyclohexane/ethyl acetate 9:1 to afford a colorless oil (184 mg, 86%); 57% yield over 2 steps (69% based on recovered starting material).

^{1}H NMR (500 MHz, $CDCl_3$) δ 8.07 – 8.02 (m, 2H), 7.57 – 7.52 (m, 1H), 7.46 – 7.40 (m, 2H), 5.86 (dt, *J* = 9.3, 6.0 Hz, 1H), 5.40 – 5.35 (m, 1H), 2.75 (ddd, *J* = 16.7, 9.7, 5.9 Hz, 1H), 2.71 – 2.59 (m, 3H), 2.56 (dddd, *J* = 13.7, 9.7, 5.9, 0.7 Hz, 1H), 2.49 (dddd, *J* = 13.8, 9.7, 6.0, 0.8 Hz, 1H), 2.00 (t, *J* = 2.7 Hz, 1H), 1.93 (tt, *J* = 7.8, 4.6 Hz, 1H), 1.76 (d, *J* = 1.4 Hz, 3H), 1.04 – 1.00 (m, 2H), 0.88 – 0.83 (m, 2H). ^{13}C NMR (126 MHz, $CDCl_3$) δ 210.1, 165.8, 141.3, 133.0, 130.5, 129.8 (2C), 128.4 (2C), 123.4, 79.9, 70.5, 69.3, 41.8, 27.0, 25.4, 23.4, 20.5, 10.9 (2C). HRMS-ESI(+) *m/z* calc. for $C_{20}H_{22}O_3Na$ $[M+Na]^+$: 333.1461, found: 333.1458.

(*Z*)-9-Cyclopentyl-6-methyl-9-oxonon-5-en-1-yn-4-yl benzoate ((*Z*)-37f)

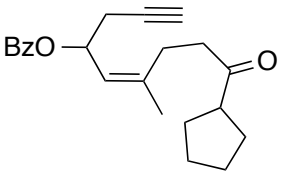

Prepared on 300 mg scale from (*Z*)-**37a** according to method **B** and using a freshly prepared solution of *c*-C_5H_9MgBr in Et_2O (~1.2 M). The product was purified by silica gel column chromatography eluting with cyclohexane/ethyl acetate 95:5 to 4:1 and isolated as a colorless oil (109 mg, 29% over 2 steps; 59% based on recovered starting material) (plus 184 mg of recovered aldehyde, 61%).

^{1}H NMR (500 MHz, $CDCl_3$) δ 8.06 – 8.02 (m, 2H), 7.54 (ddt, *J* = 8.8, 7.0, 1.4 Hz, 1H), 7.45 – 7.40 (m, 2H), 5.85 (dt, *J* = 9.3, 6.0 Hz, 1H), 5.37 (dd, *J* = 9.2, 1.5 Hz, 1H), 2.89 – 2.81 (m, 1H), 2.68 – 2.41 (m, 6H), 2.00 (t, *J* = 2.7 Hz, 1H), 1.84 – 1.49 (m, 11H). ^{13}C NMR (126 MHz, $CDCl_3$) δ 212.4, 165.7, 141.5, 133.0, 130.6, 129.8 (2C), 128.4 (2C), 123.3, 79.9, 70.5, 69.3, 51.5, 40.1, 29.0, 29.0, 26.9, 26.1, 26.1, 25.3, 23.4. HRMS-ESI(+) *m/z* calc. for $C_{22}H_{26}O_3Na$ $[M+Na]^+$: 361.1774, found: 361.1767.

(*E*)-6-Methyl-9-oxo-9-phenylnon-5-en-1-yn-4-yl benzoate ((*E*)-37g)

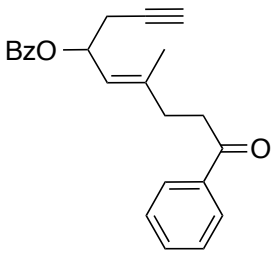

Prepared on 300 mg scale from (*E*)-**37a** according to method **B** and using a commercial solution of PhMgBr in Et_2O (3 M). The product was purified by silica gel column chromatography eluting with cyclohexane/ethyl acetate 4:1 to 3:1 isolated as a colorless oil (233 mg, 61% over 2 steps).

^{1}H NMR (300 MHz, $CDCl_3$) δ 8.10 – 8.03 (m, 2H), 8.00 – 7.93 (m, 2H), 7.61 – 7.53 (m, 2H), 7.51 – 7.41 (m, 4H), 5.89 (dt, *J* = 9.0, 6.1 Hz, 1H), 5.43 (app. dq, *J* = 9.1, 1.3 Hz, 1H), 3.17 – 3.08 (m, 2H), 2.64 (dt, *J* = 5.8, 2.5 Hz, 2H), 2.56 – 2.47 (m, 2H), 1.98 (t, *J* = 2.4 Hz, 1H), 1.91 (s, 3H). ^{13}C NMR (126 MHz, $CDCl_3$) δ 199.6, 165.9, 141.3, 137.1, 133.2, 133.1, 130.5, 129.8 (2C), 128.7 (2C), 128.5 (2C), 128.2 (2C), 122.5, 79.7, 70.4, 69.5, 37.0, 33.9, 25.2, 17.5. HRMS-ESI(+) *m/z* calc. for $C_{23}H_{22}O_3Na$ $[M+Na]^+$: 369.1461, found: 369.1449.

(*Z*)-6-Methyl-9-oxo-9-phenylnon-5-en-1-yn-4-yl benzoate ((*Z*)-37g)

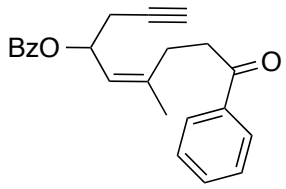

Prepared on 300 mg scale from (*Z*)-**37a** according to method **B** and using a commercial solution of PhMgBr in Et_2O (3 M). The product was purified by silica gel column chromatography eluting with cyclohexane/ethyl acetate 95:5 to 9:1 and isolated as a colorless solid (279 mg, 73% over 2 steps).

Mp = 40–43 °C. ^{1}H NMR (500 MHz, $CDCl_3$) δ 8.07 – 8.02 (m, 2H), 7.99 – 7.93 (m, 2H), 7.58 – 7.51 (m, 2H), 7.48 – 7.39 (m, 4H), 5.88 (dt, *J* = 9.3, 6.0 Hz, 1H), 5.41 (app. d, *J* = 9.9 Hz, 1H), 3.21 (ddd, *J* = 17.0, 9.6, 5.7 Hz, 1H), 3.09 (ddd, *J* = 17.0, 9.7, 6.1 Hz, 1H), 2.75 – 2.60 (m, 4H), 2.00 (t, *J* = 2.6 Hz, 1H), 1.82 (d, *J* = 1.4 Hz, 3H). ^{13}C NMR (126 MHz, $CDCl_3$) δ 199.6, 165.7, 141.3, 137.0, 133.1, 133.0, 130.5, 129.8 (2C), 128.7 (2C), 128.4 (2C), 128.2 (2C), 123.6, 79.9, 70.5, 69.4, 37.1, 27.3, 25.4, 23.5. HRMS-ESI(+) *m/z* calc. for $C_{23}H_{22}O_3Na$ $[M+Na]^+$: 369.1461, found: 369.1469.

(*E*)-6-((*tert*-Butyldimethylsilyl)oxy)-4-methyl-1-phenylnon-4-en-8-yn-1-one ((*E*)-37h)

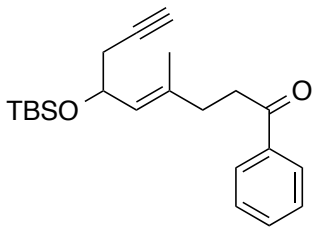

Prepared on 309 mg scale from (*E*)-**37b** according to method **B** and using a commercial solution of PhMgBr in Et_2O (3 M). The product was purified by silica gel column chromatography eluting with cyclohexane/ethyl acetate 4:1 to 3:1 isolated as a colorless oil (201 mg, 51% over 2 steps).

^{1}H NMR (500 MHz, $CDCl_3$) δ 7.98 – 7.93 (m, 2H), 7.59 – 7.54 (m, 1H), 7.49 – 7.44 (m, 2H), 5.21 (app. dq, *J* = 8.6, 1.3 Hz, 1H), 4.54 (dt, *J* = 8.6, 6.5 Hz, 1H), 3.11 – 3.06 (m, 2H), 2.46 – 2.41 (m, 2H), 2.39 (ddd, J = 16.5, 6.5, 2.7 Hz, 1H), 2.27 (ddd, 16.5, 6.4, 2.7 Hz, 1H), 1.91 (t, *J* = 2.6 Hz, 1H), 1.74 (d, *J* = 1.3 Hz, 3H), 0.87 (s, 9H), 0.07 (s, 3H), 0.03 (s, 3H). ^{13}C NMR (126 MHz, $CDCl_3$) δ 199.7, 137.1, 135.5, 133.1, 128.7 (2C), 128.4, 128.2 (2C), 81.8, 69.5, 68.5, 37.1, 33.8, 28.7, 26.0 (3C), 18.4, 17.3, –4.2, –4.6. HRMS-ESI(+) *m/z* calc. for $C_{22}H_{32}O_2SiNa$ $[M+Na]^+$: 379.2064, found: 369.2057.

(*Z*)-7-((*tert*-Butyldimethylsilyl)oxy)-4-methyl-1phenylnon-4-en-8-yn-1-one ((*Z*)-37h)

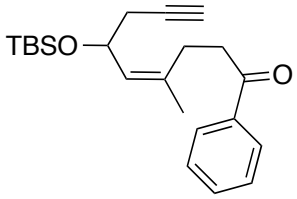

Prepared on 300 mg scale from (*Z*)-**37b** according to method **B** and using a commercial solution of PhMgBr in Et_2O (3 M). The product was purified by silica gel column chromatography eluting with cyclohexane/ethyl acetate 95:5 to 9:1 and isolated as a pale yellow oil (232 mg, 61% over 2 steps) (plus 75 mg of aldehyde recovered, 25%; 81% based on recovered starting material).

^{1}H NMR (500 MHz, $CDCl_3$) δ 7.99 – 7.93 (m, 2H), 7.60 – 7.54 (m, 1H), 7.50 – 7.44 (m, 2H), 5.25 – 5.20 (m, 1H), 4.57 (dt, *J* = 8.8, 6.4 Hz, 1H), 3.15 – 3.02 (m, 2H), 2.65 – 2.57 (m, 1H), 2.46 – 2.37 (m, 2H), 2.30 (ddd, *J* = 16.5, 6.7, 2.7 Hz, 1H), 1.91 (t, *J* = 2.6 Hz, 1H), 1.77 (d, *J* = 1.4 Hz, 3H), 0.87 (s, 9H), 0.07 (s, 3H), 0.04 (s, 3H). ^{13}C NMR (126 MHz, $CDCl_3$) δ 199.6, 137.0, 135.5, 133.2, 129.6, 128.8 (2C), 128.1 (2C), 82.0, 69.7, 68.1, 37.3, 28.9, 26.9, 26.0 (3C), 23.3, 18.3, –4.1, –4.5. HRMS-ESI(+) *m/z* calc. for $C_{22}H_{32}O_2SiNa$ $[M+Na]^+$: 379.2064, found: 379.2069.

(*E*)-6-Methyl-9-oxo-9-(4-(trifluoromethyl)phenyl)non-5-en-1-yn-4-yl benzoate ((*E*)-37i)

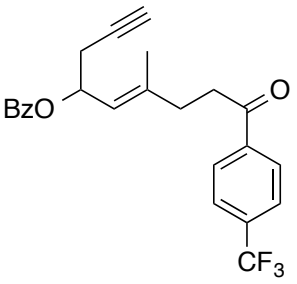

Prepared on 300 mg scale from (*E*)-**37a** according to method **B** and using a freshly prepared solution of 4-CF_3-C_6H_4MgBr in Et_2O (~0.8 M). The product was purified by silica gel column chromatography eluting with pentane/diethyl ether 95:5 to 9:1 and isolated as a pale yellow solid (324 mg, 71% over 2 steps).

^{1}H NMR (400 MHz, $CDCl_3$) δ 8.06 – 8.02 (m, 4H), 7.73 – 7.69 (m, 2H), 7.59 – 7.53 (m, 1H), 7.47 – 7.41 (m, 2H), 5.86 (dt, *J* = 9.0, 6.1 Hz, 1H), 5.40 (app. dq, *J* = 9.1, 1.3 Hz, 1H), 3.16 – 3.10 (m, 2H), 2.69 – 2.57 (m, 2H), 2.54 – 2.48 (m, 2H), 1.97 (t, *J* = 2.6 Hz, 1H), 1.89 (d, *J* = 1.3 Hz, 3H). ^{13}C NMR (126 MHz,

$CDCl_3$) δ 198.6, 165.8, 140.8, 139.7 (app. d, J_{C-F} = 1.0 Hz), 134.5 (app. d, J_{C-F} = 32.5 Hz), 133.1, 130.4, 129.8 (2C), 128.5 (4C), 125.8 (q, J_{C-F} = 3.7 Hz, 2C), 123.7 (q, J_{C-F} = 273.4 Hz), 122.8, 79.6, 70.5, 69.5, 37.3, 33.6, 25.2, 17.5. ^{19}F NMR (376 MHz, $CDCl_3$) δ –62.83. HRMS-ESI(+) *m/z* calc. for $C_{24}H_{21}F_3O_3Na$ $[M+Na]^+$: 437.1335, found: 437.1333.

(*Z*)-6-Methyl-9-oxo-9-(4-(trifluoromethyl)phenyl)non-5-en-1-yn-4-yl benzoate ((*Z*)-37i)

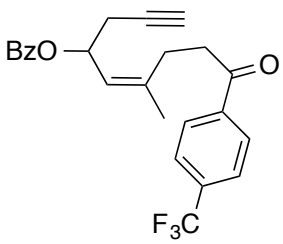

Prepared on 300 mg scale from (*Z*)-**37a** according to method **B** and using a freshly prepared solution of 4-CF_3-C_6H_4MgBr in Et_2O (~0.8 M). The product was purified by silica gel column chromatography eluting with pentane/diethyl ether 95:5 to 9:1 and isolated as a pale yellow solid (204 mg, 44% over 2 steps).

Mp = 42–44 °C. ^{1}H NMR (400 MHz, $CDCl_3$) δ 8.10 – 8.00 (m, 4H), 7.71 (app. d, *J* = 8.1 Hz, 2H), 7.58 – 7.51 (m, 1H), 7.46 – 7.38 (m, 2H), 5.87 (dt, *J* = 9.4, 6.1 Hz, 1H), 5.42 (app. dd, *J* = 9.4, 1.5 Hz, 1H), 3.26 (ddd, *J* = 17.2, 9.3, 6.0 Hz, 1H), 3.09 (ddd, *J* = 17.2, 9.1, 6.7 Hz, 1H), 2.75 – 2.59 (m, 4H), 2.01 (t, *J* = 2.6 Hz, 1H), 1.82 (d, *J* = 1.4 Hz, 3H). ^{13}C NMR (101 MHz, $CDCl_3$) δ 198.6, 165.8, 141.0, 139.6 (app. d, J_{C-F} = 1.1 Hz), 134.4 (q, J_{C-F} = 32.6 Hz), 133.1, 130.4, 129.8 (2C), 128.6 (2C), 128.5 (2C), 125.8 (q, J_{C-F} = 3.7 Hz, 2C), 123.9, 123.8 (q, J_{C-F} = 272.7 Hz), 79.8, 70.6, 69.4, 37.4, 27.1, 25.3, 23.5. ^{19}F NMR (376 MHz, $CDCl_3$) δ –63.19. HRMS-ESI(+) *m/z* calc. for $C_{24}H_{21}O_3F_3Na$ $[M+Na]^+$: 437.1335, found: 437.1337.

(*Z*)-6-Methyl-9-(naphthalene-2-yl)-9-oxonon-5-en-1-yn-4-yl benzoate ((*Z*)-37j)

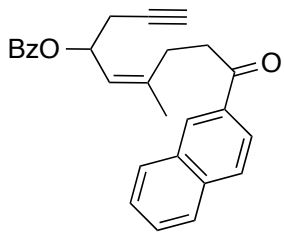

Prepared on 300 mg scale from (*Z*)-**37a** according to method **B** and using a freshly prepared solution of 2-naphthyl-MgBr in Et_2O (~0.4 M). The product was purified by silica gel column chromatography eluting with cyclohexane/ethyl acetate 9:1 to 3:1 and isolated as a pale yellow solid (269 mg, 61% over 2 steps).

Mp = 74–77 °C. ^{1}H NMR (500 MHz, $CDCl_3$) δ 8.52 (d, *J* = 1.7 Hz, 1H), 8.08 – 8.02 (m, 3H), 7.96 (d, *J* = 8.0 Hz, 1H), 7.91 – 7.85 (m, 2H), 7.60 (ddd, *J* = 8.2, 6.9, 1.4 Hz, 1H), 7.57 – 7.51 (m, 2H), 7.44 – 7.39 (m, 2H), 5.93 (dt, *J* = 9.3, 6.1 Hz, 1H), 5.44 (dd, *J* = 9.4, 1.6 Hz, 1H), 3.37 (ddd, *J* = 16.7, 8.7, 6.7 Hz, 1H), 3.21 (ddd, *J* = 16.7, 9.0, 6.9 Hz, 1H), 2.74 (app. ddd, *J* = 8.6, 6.5, 1.8 Hz, 2H), 2.71 – 2.62 (m, 2H), 2.01 (t, *J* = 2.6 Hz, 1H), 1.86 (d, *J* = 1.4 Hz, 3H). ^{13}C NMR (126 MHz, $CDCl_3$) δ 199.6, 165.8, 141.4,

135.7, 134.3, 133.0, 132.7, 130.5, 130.0, 129.8 (2C), 129.8, 128.6, 128.5, 128.5 (2C), 127.9, 126.8, 124.0, 123.6, 79.9, 70.6, 69.5, 37.2, 27.6, 25.4, 23.6. HRMS-ESI(+) *m/z* calc. for $C_{27}H_{24}O_3Na$ $[M+Na]^+$: 419.1618, found: 419.1613.

Standard procedure for the cyclization of aldehydes and ketones

A round-bottom flask was charged with the oxoenyne substrate (**37**) and the flask was placed in a glovebox. In the glovebox, the substrate was dissolved with toluene (0.01 M solution) and a stock solution of gold catalyst **A** (5 mol % in CH_2Cl_2 [1/35 volume of toluene]) was added in one portion to the vigorously stirred solution. The resulting mixture was stirred at 25 °C for the indicated time. It was then removed from the glovebox and quenched by addition of QuadraPure™ resin (*ca.* 10 mg per 0.1 mmol) and the suspension stirred vigorously for 15–60 min. It was then filtered on a sintered funnel and the volatiles were removed *in vacuo*. The crude material was redissolved in $CDCl_3$ and the internal standard added to measure the NMR yields and diastereomeric ratios. All the material was then collected and purified according to the details provided for each compound below.

(1*R,3a*R**,4*R**,7*S**,7a*R**)-7-Methyl-3a,4,5,6,7,7a-hexahydro-1*H*-4,7-epoxyinden-1-yl benzoate (*syn*-38a)**

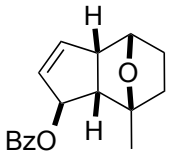

Performed on 0.21 mmol scale from (*E*)-**37a** (59 mg) with stirring for 16 h at 25 °C. Crude ^{1}H NMR yield = 81% (83:8 *dr*, *ca.* 10:1). Purified by preparative silica gel TLC eluting with cyclohexane/CH_2Cl_2/ethyl acetate 80:15:5 and isolated as a pale yellow solid (49 mg, 0.181 mmol, 83%, 93:7 *dr*).

Mp = 81–83 °C. ^{1}H NMR (400 MHz, $CDCl_3$) δ 8.05 – 8.00 (m, 2H), 7.58 – 7.52 (m, 1H), 7.46 – 7.40 (m, 2H), 6.07 (ddd, *J* = 5.7, 2.2, 1.0 Hz, 1H), 5.92 (dtd, *J* = 5.7, 2.1, 0.6 Hz, 1H), 5.77 (tt, *J* = 2.5, 1.2 Hz, 1H), 4.58 – 4.53 (m, 1H), 3.64 – 3.57 (m, 1H), 2.55 (dddd, *J* = 9.2, 2.3, 1.4, 0.6 Hz, 1H), 1.74 – 1.62 (m, 2H), 1.61 (s, 3H), 1.57 – 1.49 (m, 1H), 1.45 – 1.35 (m, 1H). ^{13}C NMR (101 MHz, $CDCl_3$) δ 166.7, 139.9, 133.1, 130.9, 130.5, 129.8 (2C), 128.5 (2C), 85.8, 79.9, 78.9, 59.4, 56.2, 30.9, 28.5, 21.4. HRMS-ESI(+) *m/z* calc. for $C_{17}H_{18}O_3Na$ $[M+Na]^+$: 293.1148, found: 293.1151.

(1*R,3a*R**,4*S**,7*R**,7a*R**)-7-Methyl-3a,4,5,6,7,7a-hexahydro-1*H*-4,7-epoxyinden-1-yl benzoate (*anti*-38a)**

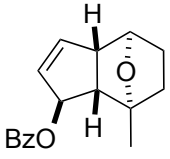

Performed on 0.37 mmol scale from (*Z*)-**37a** (100 mg) with stirring for 6 h at 25 °C. Crude ^{1}H NMR yield = 91% (91:9 *dr*, yield of combined

diastereomers). Purified by preparative silica gel TLC eluting with cyclohexane/CH_2Cl_2/ethyl acetate 80:15:5 and isolated as a pale yellow oil (82 mg, 0.30 mmol, 82%, 97:3 *dr*). This compound was crystallized from CH_2Cl_2/pentane to obtain single crystals suitable for X-ray diffraction.

Mp = 75–77 °C. ^{1}H NMR (500 MHz, $CDCl_3$) δ 8.05 – 7.99 (m, 2H), 7.54 (ddt, *J* = 7.9, 6.9, 1.3 Hz, 1H), 7.45 – 7.39 (m, 2H), 6.00 (ddd, *J* = 5.5, 2.2, 0.9 Hz, 1H), 5.97 – 5.92 (m, 2H), 4.19 (d, *J* = 5.1 Hz, 1H), 3.15 (dq, *J* = 6.5, 2.1 Hz, 1H), 2.32 (dd, *J* = 6.9, 1.7 Hz, 1H), 1.87 (ddt, *J* = 12.9, 11.3, 5.4 Hz, 1H), 1.68 (s, 3H), 1.65 – 1.51 (m, 3H). ^{13}C NMR (126 MHz, $CDCl_3$) δ 166.3, 137.7, 133.0, 131.6, 130.6, 129.7 (2C), 128.4 (2C), 84.5, 81.9, 78.1, 57.5, 56.2, 36.5, 31.1, 18.4. HRMS-ESI(+) *m/z* calc. for $C_{17}H_{18}O_3Na$ $[M+Na]^+$: 293.1148, found: 293.1157.

tert-Butyldimethyl(((1*R,3a*R**,4*R**,7*S**,7a*R**)-7-methyl-3a,4,5,6,7,7a-hexahydro-1*H*-4,7-epoxyinden-1-yl)oxy)silane (*syn*-38b)**

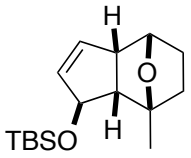

Performed on 0.203 mmol scale from (*E*)-**37b** (57 mg) with stirring for 16 h at 25 °C. Crude ^{1}H NMR yield = 82% (99:1 *dr*). Purified by silica gel column chromatography eluting with cyclohexane/CH_2Cl_2/ethyl acetate 80:15:5 and isolated as a pale yellow oil (48 mg, 0.170 mmol, 82%, >99:1 *dr*).

^{1}H NMR (500 MHz, $CDCl_3$) δ 5.81 (ddd, *J* = 5.6, 2.2, 0.9 Hz, 1H), 5.71 (dt, *J* = 5.7, 2.0 Hz, 1H), 4.62 – 4.59 (m, 1H), 4.47 (t, *J* = 5.6 Hz, 1H), 3.56 – 3.51 (m, 1H), 2.35 (dt, *J* = 9.3, 1.7 Hz, 1H), 1.64 – 1.53 (m, 1H), 1.51 (s, 3H), 1.49 – 1.41 (m, 2H), 1.32 – 1.23 (m, 1H), 0.88 (s, 9H), 0.08 (s, 3H), 0.08 (s, 3H). ^{13}C NMR (126 MHz, $CDCl_3$) δ 136.0, 134.8, 85.6, 79.1, 76.9, 62.6, 56.0, 30.8, 28.4, 26.1 (3C), 21.7, 18.3, –4.1, –4.3. HRMS-APCI(+) *m/z* calc. for $C_{16}H_{29}O_2Si$ $[M+H]^+$: 281.1931, found: 281.1929.

tert-Butyldimethyl(((1*R,3a*R**,4*S**,7*R**,7a*R**)-7-methyl-3a,4,5,6,7,7a-hexahydro-1*H*-4,7-epoxyinden-1-yl)oxy)silane (*anti*-38b)**

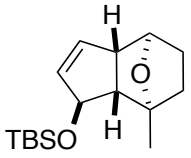

Performed on 0.37 mmol scale from (*Z*)-**37b** (104 mg) by addition of solid gold catalyst **A** (5 mol%) to a toluene solution (0.01 M) of (*Z*)-**37b**, with stirring for 14 h at 25 °C. Crude ^{1}H NMR yield = 73% (83:17 *dr*, yield of combined diastereomers). Purified by silica gel column chromatography eluting with pentane/diethyl ether 95:5 and isolated as a pale yellow oil (57 mg, 0.20 mmol, 58%, ≥ 97:3 *dr*) [minor diastereomer *syn*-**38b** (12 mg) was also isolated, 12%]

^{1}H NMR (400 MHz, $CDCl_3$) δ 5.76 (app. s, 2H), 4.80 – 4.76 (m, 1H), 4.10 (d, *J* = 5.0 Hz, 1H), 3.05 (dd, *J* = 6.9, 2.3 Hz, 1H), 2.09 (dd, *J* = 6.9, 2.0 Hz, 1H), 1.85 – 1.75 (m, 1H), 1.63 – 1.46 (m, 6H), 0.89 (s, 9H), 0.10 (s 3H), 0.08 (s, 3H). ^{13}C NMR (101 MHz, $CDCl_3$) δ 135.8, 133.8, 84.3, 79.2, 78.6, 59.8, 57.3, 36.5, 31.2, 26.0 (3C), 18.6, 18.2, –3.9, –4.3. HRMS-ESI(+) *m/z* calc. for $C_{16}H_{28}O_2SiNa$ $[M+Na]^+$: 303.1751, found: 303.1748.

Triethyl(((1*R,3a*R**,4*R**,7*S**,7a*R**)-7-methyl-3a,4,5,6,7,7a-hexahydro-1H-4,7-epoxyinden-1-yl)oxy)silane (*syn*-38k)**

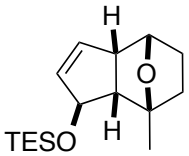

Performed on 0.20 mmol scale from (*E*)-**37k** (56 mg) with stirring for 44 h at 25 °C. Crude ^{1}H NMR yield = 84% (95:5 *dr*). Purified by silica gel column chromatography eluting with cyclohexane/CH_2Cl_2/ethyl acetate 80:15:5 and isolated as a pale yellow oil (34 mg, 0.142 mmol, 71%, >99:1 *dr*).

^{1}H NMR (500 MHz, $CDCl_3$) δ 5.83 (ddd, *J* = 5.6, 2.2, 0.9 Hz, 1H), 5.72 (dtd, *J* = 5.7, 2.0, 0.6 Hz, 1H), 4.58 (app. tt, *J* = 2.3, 1.2 Hz, 1H), 4.48 (t, *J* = 5.7 Hz, 1H), 3.58 – 3.52 (m, 1H), 2.37 (d, *J* = 9.3 Hz, 1H), 1.65 – 1.55 (m, 1H), 1.52 (s, 3H), 1.50 – 1.40 (m, 2H), 1.33 – 1.26 (m, 1H), 0.96 (t, *J* = 7.9 Hz, 9H), 0.61 (q, *J* = 7.9 Hz, 6H). ^{13}C NMR (101 MHz, $CDCl_3$) δ 136.2, 134.7, 85.6, 79.1, 76.5, 62.5, 55.9, 30.8, 28.5, 21.6, 6.9 (3C), 5.0 (3C). HRMS-ESI(+) *m/z* calc. for $C_{16}H_{28}O_2SiNa$ $[M+Na]^+$: 303.1751, found: 303.1751.

(1*R,3a*R**,4*R**,7*S**,7a*R**)-1-(Methoxymethoxy)-7-methyl-3a,4,5,6,7,7a-hexahydro-1H-4,7-epoxyindene (*syn*-38l)**

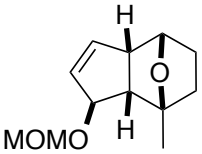

Performed on 0.20 mmol scale from (*E*)-**37l** (42 mg) with stirring for 24 h at 40 °C. Crude ^{1}H NMR yield = 82% (>99:1 *dr*). Purified by silica gel column chromatography eluting with cyclohexane/CH_2Cl_2/ethyl acetate 80:15:5 and isolated as a pale yellow oil (34 mg, 0.161 mmol, 81%, >99:1 *dr*).

^{1}H NMR (500 MHz, $CDCl_3$) δ 5.91 (ddd, *J* = 5.7, 2.2, 1.1 Hz, 1H), 5.82 (dt, *J* = 5.7, 2.3 Hz, 1H), 4.68 – 4.63 (m, 2H), 4.51 – 4.47 (m, 2H), 3.54 – 3.48 (m, 1H), 3.35 (s, 3H), 2.43 (dt, *J* = 9.4, 1.9 Hz, 1H), 1.64 – 1.57 (m, 1H), 1.51 (s, 3H), 1.50 – 1.43 (m, 2H), 1.32 – 1.25 (m, 1H). ^{13}C NMR (126 MHz, $CDCl_3$) δ 137.9, 132.4, 95.3, 85.5, 81.4, 79.1, 59.7, 55.9, 55.3, 30.7, 28.4, 21.1. HRMS-ESI(+) *m/z* calc. for $C_{12}H_{18}O_3Na$ $[M+Na]^+$: 233.1148, found: 233.1143.

(1*R,3a*R**,4*R**,7*S**,7a*R**)-4,7-Dimethyl-3a,4,5,6,7,7a-hexahydro-1*H*-4,7-epoxyinden-1-yl benzoate (*syn*-38c)**

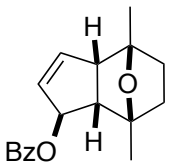

Performed on 0.2 mmol scale from (*E*)-**37c** (56 mg) with stirring for 17 h at 30 °C. Crude ^{1}H NMR yield = 87% (89:11 *dr*, yield of combined diastereomers). Purified by preparative silica gel TLC eluting with cyclohexane/CH_2Cl_2/ethyl acetate 80:15:5 and isolated as a pale yellow oil (44 mg, 0.154 mmol, 78%, 88:12 *dr*). Further purification by preparative silica gel TLC eluting twice with cyclohexane/CH_2Cl_2/ethyl acetate 80:15:5 resulted in the isolation of a pale yellow oil (20 mg, 0.071 mmol, 36%, >99:1 *dr*).

^{1}H NMR (500 MHz, $CDCl_3$) δ 8.04 – 8.01 (m, 2H), 7.56 – 7.52 (m, 1H), 7.45 – 7.40 (m, 2H), 6.06 (ddd, *J* = 5.6, 2.2, 1.0 Hz, 1H), 5.92 (dtd, *J* = 5.6, 2.1, 0.6 Hz, 1H), 5.77 (tt, *J* = 2.4, 1.2 Hz, 1H), 3.28 (d quin, *J* = 9.2, 2.0 Hz, 1H), 2.65 (dt, *J* = 9.3, 1.8 Hz, 1H), 1.72 – 1.66 (m, 1H), 1.64 – 1.57 (m, 1H), 1.56 (s, 3H), 1.53 (ddd, *J* = 12.1, 3.4, 2.2 Hz, 1H), 1.50 (s, 3H), 1.48 – 1.43 (m, 1H). ^{13}C NMR (101 MHz, $CDCl_3$) δ 166.6, 139.7, 133.0, 130.8, 130.6, 129.7 (2C), 128.4 (2C), 85.9, 85.5, 80.5, 61.8, 60.5, 34.6, 32.6, 21.8, 21.6. HRMS-ESI(+) *m/z* calc. for $C_{18}H_{20}O_3Na$ $[M+Na]^+$: 307.1305, found: 307.1297.

(1*R,3a*R**,4*S**,7*R**,7a*R**)-4,7-Dimethyl-3a,4,5,6,7,7a-hexahydro-1*H*-4,7-epoxyinden-1-yl benzoate (*anti*-38c)**

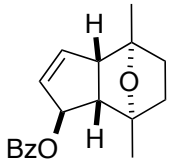

Performed on 0.25 mmol scale from (*Z*)-**37k** (71 mg) with stirring for 18 h at 25 °C. Crude ^{1}H NMR yield = 89% (83:17 *dr*, yield of combined diastereomers). Purified by column chromatography on silica gel eluting with cyclohexane/CH_2Cl_2/ethyl acetate 80:15:5 and isolated as a pale yellow solid (56 mg, 0.197 mmol, 79%, 83:17 *dr*). Further crystallization from diethyl ether/pentane afforded 39 mg of colorless solid (55%, ≥ 98:2 *dr*) (plus 17 mg of pale yellow oil, 24%, 56:44 *dr*).

Mp = 79–81 °C. ^{1}H NMR (500 MHz, $CDCl_3$) δ 8.05 – 8.00 (m, 2H), 7.54 (ddt, *J* = 7.8, 6.9, 1.3 Hz, 1H), 7.45 – 7.39 (m, 2H), 6.02 – 5.98 (m, 2H), 5.98 – 5.95 (m, 1H), 3.13 – 3.08 (m, 1H), 2.43 (dd, *J* = 6.8, 1.9 Hz, 1H), 1.74 – 1.60 (m, 7H), 1.38 (s, 3H). ^{13}C NMR (126 MHz, $CDCl_3$) δ 166.3, 136.5, 133.0, 132.2, 130.7, 129.7 (2C), 128.4 (2C), 84.3, 84.2, 82.1, 60.0, 57.7, 38.6, 38.1, 18.8, 18.5. HRMS-ESI(+) *m/z* calc. for $C_{18}H_{20}O_3Na$ $[M+Na]^+$: 307.1305, found: 307.1298.

tert-Butyl(((1*R,3a*R**,4*R**,7*S**,7a*R**)-4,7-dimethyl-3a,4,5,6,7,7a-hexahydro-1*H*-4,7-epoxyinden-1-yl)oxy)dimethylsilane (*syn*-38d)**

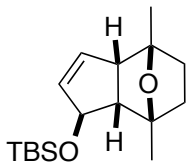

Performed on 0.217 mmol scale from (*E*)-**37d** (64 mg) with stirring for 17 h at 25 °C. Crude ^{1}H NMR yield = 97% (>99:1 *dr*). The product was further purified by silica gel column chromatography eluting with cyclohexane/CH_2Cl_2/ethyl acetate 80:15:5 and isolated as a pale yellow oil (41 mg, 0.141 mmol, 65%, >99:1 *dr*).

^{1}H NMR (500 MHz, $CDCl_3$) δ 5.81 (ddd, *J* = 5.6, 2.2, 0.9 Hz, 1H), 5.71 (dtd, *J* = 5.6, 2.0, 0.6 Hz, 1H), 4.61 – 4.60 (m, 1H), 3.22 (dd, *J* = 9.5, 2.0 Hz, 1H), 2.46 (d, *J* = 9.4 Hz, 1H), 1.55 – 1.50 (m, 2H), 1.47 (s, 3H), 1.45 (s, 3H), 1.41 – 1.37 (m, 2H), 0.88 (s, 9H), 0.08 (s, 3H), 0.08 (s, 3H). ^{13}C NMR (126 MHz, $CDCl_3$) δ 135.9, 134.7, 86.0, 85.3, 77.6, 63.8, 61.6, 34.6, 32.5, 26.1 (3C), 21.9, 21.8, 18.3, –4.1, –4.2. HRMS-ESI(+) *m/z* calc. for $C_{17}H_{30}O_2SiNa$ $[M+Na]^+$: 317.1907, found: 317.1896.

tert-Butyl(((1*R,3a*S**,4*S**,7*R**,7a*R**)-4,7-dimethyl-3a,4,5,6,7,7a-hexahydro-1*H*-4,7-epoxyinden-1-yl)oxy)dimethylsilane (*anti*-38d)**

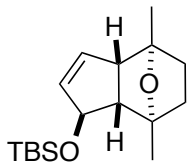

Performed on 0.3 mmol scale from (*Z*)-**37d** (88 mg) with stirring for 18 h at 25 °C. Crude ^{1}H NMR yield = 74% (>98:2 *dr*). Purified by silica gel column chromatography eluting with pentane/diethyl ether 95:5 and isolated as a pale yellow oil (62 mg, 0.211 mmol, 70%, > 98:2 *dr*).

^{1}H NMR (500 MHz, $CDCl_3$) δ 5.79 (dt, *J* = 5.7, 1.9 Hz, 1H), 5.74 (ddd, *J* = 5.7, 2.4, 1.2 Hz, 1H), 4.80 (dq, *J* = 2.2, 1.1 Hz, 1H), 3.00 (dq, *J* = 6.7, 2.0 Hz, 1H), 2.18 (dd, *J* = 7.1, 2.2 Hz, 1H), 1.71 – 1.53 (m, 4H), 1.51 (s, 3H), 1.31 (s, 3H), 0.88 (s, 9H), 0.09 (s 3H), 0.08 (s, 3H). ^{13}C NMR (126 MHz, $CDCl_3$) δ 136.4, 132.5, 84.5, 84.1, 79.4, 61.4, 59.7, 38.5, 38.2, 26.0 (3C), 18.9, 18.5, 18.2, –3.9, –4.3. HRMS-ESI(+) *m/z* calc. for $C_{17}H_{30}O_2SiNa$ $[M+Na]^+$: 317.1907, found: 317.1904.

(1*R,3a*R**,4*S**,7*S**,7a*R**)-4-Cyclopropyl-7-methyl-3a,4,5,6,7,7a-hexahydro-1*H*-4,7-epoxyinden-1-yl benzoate (*syn*-38e)**

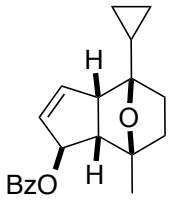

Performed on 0.2 mmol scale from (*E*)-**37e** (62 mg) with stirring for 15 h at 25 °C. Crude ^{1}H NMR yield = 54% (80:20 *dr*, yield of combined diastereomers, 77% conversion). Purified by preparative silica gel TLC eluting with cyclohexane/CH_2Cl_2/ethyl acetate 85:15:5 and isolated as a pale yellow oil (32 mg, 0.103 mmol, 52%, 82:18 *dr*).

^{1}H NMR (500 MHz, $CDCl_3$) δ 8.05 – 7.99 (m, 2H + 2H *minor*), 7.57 – 7.51 (m, 1H + 1H *minor*), 7.45 – 7.40 (m, 2H + 2H *minor*), 6.05 (ddd, *J* = 5.7, 2.1, 1.0 Hz, 1H), 5.93 –

5.89 (m, 1H), 5.76 (tt, *J* = 2.4, 1.2 Hz, 1H), 3.30 (d quin, *J* = 9.0, 2.1 Hz, 1H), 2.62 (dt, *J* = 9.3, 1.7 Hz, 1H), 1.70 – 1.62 (m, 1H + 1H *minor*), 1.54 (s, 3H), 1.50 – 1.34 (m, 3H + 3H *minor*), 1.24 – 1.16 (m, 1H), 0.60 – 0.52 (m, 2H + 1H *minor*), 0.53 – 0.46 (m, 1H + 2H *minor*), 0.45 – 0.37 (m, 1H). ^{13}C NMR (101 MHz, $CDCl_3$) δ 166.6, 140.3, 133.0, 130.7, 129.7 (2C), 128.5 (2C), 88.8, 84.9, 80.3, 60.1, 59.8, 31.8, 31.2, 21.6, 14.9, 1.5, 1.5. Note: *one carbon could not be detected due to overlap of signals*. HRMS-ESI(+) *m/z* calc. for $C_{20}H_{22}O_3Na$ $[M+Na]^+$: 333.1461, found: 333.1464.

(1*R,3a*R**,4*R**,7*R**,7a*R**)-4-Cyclopropyl-7-methyl-3a,4,5,6,7,7a-hexahydro-1*H*-4,7-epoxyinden-1-yl benzoate (*anti*-38e)**

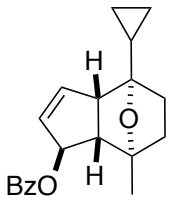

Performed on 0.2 mmol scale from (*Z*)-**37e** (62 mg) with stirring for 18 h at 25 °C. Crude ^{1}H NMR yield = 83% (87:13 *dr*, yield of combined diastereomers). Purified by preparative silica gel TLC eluting with cyclohexane/CH_2Cl_2/ethyl acetate 85:12:3 and isolated as a pale yellow oil (46 mg, 0.148 mmol, 74%, 89:11 *dr*).

^{1}H NMR (500 MHz, $CDCl_3$) δ 8.05 – 8.00 (m, 2H + 2H *minor*), 7.57 – 7.52 (m, 1H + 1H *minor*), 7.45 – 7.40 (m, 2H + 2H *minor*), 6.18 (app. dq, *J* = 4.9, 2.2 Hz, 1H), 5.99 – 5.95 (m, 2H), 3.22 – 3.18 (m, 1H), 2.43 (dd, *J* = 6.9, 1.8 Hz, 1H), 1.67 (ddd, *J* = 12.0, 9.2, 5.0 Hz, 1H), 1.63 – 1.55 (m, 4H + 3H *minor*), 1.46 (td, *J* = 11.7, 4.9 Hz, 1H + 2H *minor*), 1.39 (ddd, *J* = 11.6, 9.2, 4.8 Hz, 1H + 1H *minor*), 1.08 (tt, *J* = 8.5, 5.4 Hz, 1H), 0.60 – 0.54 (m, 1H + 2H *minor*), 0.53 – 0.49 (m, 2H), 0.33 – 0.28 (m, 1H). ^{13}C NMR (126 MHz, $CDCl_3$) δ 166.3, 136.8, 133.0, 131.6, 130.7, 129.7 (2C), 128.4 (2C), 86.9, 83.7, 82.3, 60.6, 57.6, 37.6, 32.7, 18.7, 12.2, 2.2, 1.4. HRMS-ESI(+) *m/z* calc. for $C_{20}H_{21}O_3Na$ $[M+Na]^+$: 333.1461, found: 333.1461.

(1*R,3a*R**,4*R**,7*R**,7a*R**)-4-Cyclopentyl-7-methyl-3a,4,5,6,7,7a-hexahydro-1*H*-4,7-epoxyinden-1-yl benzoate (*anti*-38f)**

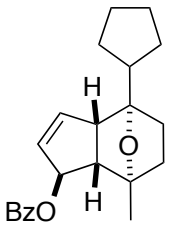

Performed on 0.2 mmol scale from (*Z*)-**37f** (68 mg) with stirring for 18 h at 25 °C. Crude ^{1}H NMR yield = 78% (84:16 *dr*, yield of combined diastereomers). Purified by preparative silica gel TLC eluting with cyclohexane/CH_2Cl_2/ethyl acetate 85:12:3 and isolated as a pale yellow oil (46 mg, 0.136 mmol, 68%, 85:15 *dr*). **Note**: since the diastereomeric counterpart of this tricycle was not prepared, the distinguishable data for the minor diastereomer are also given below.

^{1}H NMR (500 MHz, $CDCl_3$) δ 8.04 – 8.00 (m, 2H + 2H *minor*), 7.57 – 7.51 (m, 1H + 1H *minor*), 7.45 – 7.39 (m, 2H + 2H *minor*), 6.07 (ddd, *J* = 5.6, 2.2, 1.0 Hz, 1H *minor*),

6.06 – 6.03 (m, 1H), 6.00 – 5.95 (m, 2H), 5.92 – 5.89 (m, 1H *minor*), 5.76 (tt, *J* = 2.4, 1.2 Hz, 1H *minor*), 3.40 – 3.35 (m, 1H *minor*), 3.19 (td, *J* = 4.2, 2.1 Hz, 1H), 2.68 (dt, *J* = 9.2, 1.7 Hz, 1H *minor*), 2.44 (dd, *J* = 6.9, 1.9 Hz, 1H), 2.30 (app. quin, *J* = 8.7 Hz, 1H *minor*), 2.20 (quin, *J* = 8.1 Hz, 1H), 1.86 (app. ddq, *J* = 15.6, 8.0, 3.8 Hz, 1H), 1.83 – 1.35 (m, 13H + 13H *minor*), 1.35 – 1.24 (m, 1H + 2H *minor*). ^{13}C NMR (126 MHz, $CDCl_3$) δ 166.3, 136.6, 132.9, 132.0, 130.7, 129.7 (2C), 128.4 (2C), 89.7, 83.8, 82.3, 60.0, 57.6, 41.0, 37.9, 30.1, 28.9, 27.5, 26.4, 26.2, 18.8. [signals for *anti*-38f: 166.6, 141.0, 133.0, 130.6, 129.7, 91.0, 84.6, 80.2, 60.4, 59.3, 45.0, 32.1, 30.6, 28.3, 28.1, 26.0, 21.6.] HRMS-ESI(+) *m/z* calc. for $C_{22}H_{26}O_3Na$ $[M+Na]^+$: 361.1774, found: 361.1774.

(1*R,3a*R**,4*R**,7*S**,7a*R**)-7-Methyl-4-phenyl-3a,4,5,6,7,7a-hexahydro-1*H*-4,7-epoxyinden-1-yl benzoate (*syn*-38g)**

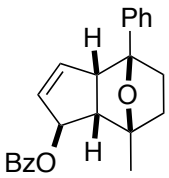

Performed on 0.2 mmol scale from (*E*)-**37g** (64 mg) with stirring for 15 h at 30 °C. Crude ^{1}H NMR yield = 72% (58:42 *dr*, yield of combined diastereomers). Purified by preparative silica gel TLC eluting with cyclohexane/CH_2Cl_2/ethyl acetate 80:15:5 and isolated as an off-white solid (35 mg, 0.102 mmol, 50%, 57:43 *dr*).

Mp = 94–98 °C. ^{1}H NMR (500 MHz, $CDCl_3$) 8.05 – 8.02 (m, 2H + 2H *minor*), 7.58 – 7.53 (m, 1H + 1H *minor*), 7.45 – 7.41 (m, 3H + 2H *minor*), 7.39 – 7.35 (m, 2H), 7.34 – 7.32 (m, 1H + 4H *minor*), 7.31 – 7.27 (m, 1H), 6.24 (ddd, *J* = 5.6, 2.2, 1.0 Hz, 1H), 6.03 – 6.00 (m, 1H), 5.85 (d quin, *J* = 2.5, 1.2 Hz, 1H), 3.59 (d quin, *J* = 9.2, 2.1 Hz, 1H), 2.79 (dt, *J* = 9.4, 1.8 Hz, 1H), 2.10 – 2.02 (m, 1H), 1.88 – 1.77 (m, 2H + 2H *minor*), 1.68 (s, 3H), 1.67 – 1.61 (m, 1H). ^{13}C NMR (101 MHz, $CDCl_3$) δ 166.7, 143.0, 139.8, 133.1, 131.4, 130.5, 129.8 (2C), 128.5 (2C), 128.5 (2C), 127.4, 125.2 (2C), 89.4, 85.7, 80.3, 63.2, 60.3, 35.0, 32.3, 21.7. HRMS-ESI(+) *m/z* calc. for $C_{23}H_{22}O_3Na$ $[M+Na]^+$: 369.1461, found: 369.1450.

(1*R,3a*R**,4*S**,7*R**,7a*R**)-7-Methyl-4-phenyl-3a,4,5,6,7,7a-hexahydro-1*H*-4,7-epoxyinden-1-yl benzoate (*anti*-38g)**

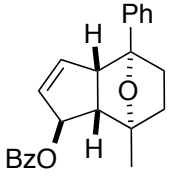

Performed on 0.2 mmol scale from (*Z*)-**37g** (69 mg) with stirring for 14 h at 25 °C. Crude ^{1}H NMR yield = 90% (91:9 *dr*, yield of combined diastereomers). Purified by column chromatography on silica gel eluting with cyclohexane/ethyl acetate 95:5 and isolated as a colorless solid (61 mg, 0.176 mmol, 88%, 93:7 *dr*). Further crystallization from CH_2Cl_2 (200 μL) + diethyl ether (200 μL) + pentane (1 mL), first at 4 °C for 2 h then at – 30 °C for 24 hours, gave

30 mg of colorless needles (43%, >98:2 *dr*). The filtrate was recrystallized from CH_2Cl_2 (100 μL) + diethyl ether (200 μL) + pentane (1.2 mL) to give a second crop of 18 mg of colorless solid (26%, >98:2 *dr*). Overall yield after crystallization was 69% (>98:2 *dr*). Mp = 137–138 °C. ^{1}H NMR (400 MHz, $CDCl_3$) δ 8.07 – 8.01 (m, 2H), 7.58 – 7.52 (m, 1H), 7.47 – 7.40 (m, 2H), 7.37 – 7.30 (m, 4H), 7.29 – 7.22 (m, 1H), 6.06 (dt, *J* = 3.4, 1.7 Hz, 1H), 5.89 (dt, *J* = 5.7, 2.1 Hz, 1H), 5.45 (ddd, *J* = 5.7, 2.3, 1.2 Hz, 1H), 3.52 (dq, *J* = 6.7, 2.2 Hz, 1H), 2.55 (dd, *J* = 6.7, 1.8 Hz, 1H), 2.24 – 2.15 (m, 1H), 1.97 – 1.79 (m, 3H), 1.77 (s, 3H). ^{13}C NMR (101 MHz, $CDCl_3$) δ 166.3, 140.9, 137.2, 133.0, 131.5, 130.6, 129.7 (2C), 128.4 (2C), 128.2 (2C), 127.0, 125.4 (2C), 87.9, 84.4, 82.3, 61.6, 57.4, 38.4, 38.2, 18.8. HRMS-ESI(+) *m/z* calc. for $C_{23}H_{22}O_3Na$ $[M+Na]^+$: 369.1461, found: 369.1459.

tert-Butyldimethyl(((1*R,3a*R**,4*R**,7*S**,7a*R**)-7-methyl-4-phenyl-3a,4,5,6,7,7a-hexahydro-1*H*-4,7-epoxyinden-1-yl)oxy)silane (*syn*-38h)**

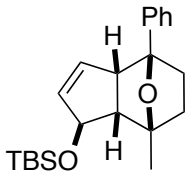

Performed on 0.2 mmol scale from (*E*)-**37h** (71 mg) with stirring for 15 h at 25 °C. Crude ^{1}H NMR yield = 98% (>96:4 *dr*). Purified by silica gel column chromatography eluting with cyclohexane/ CH_2Cl_2/ethyl acetate 80:17:3 to 80:15:5 and isolated as a pale yellow oil (64 mg, 0.181 mmol, 90%, 99:1 *dr*).

^{1}H NMR (400 MHz, $CDCl_3$) δ 7.44 – 7.39 (m, 2H), 7.38 – 7.32 (m, 2H), 7.29 – 7.24 (m, 1H), 6.00 (ddd, *J* = 5.6, 2.2, 0.9 Hz, 1H), 5.84 – 5.80 (m, 1H), 4.70 (tt, *J* = 2.3, 1.2 Hz, 1H), 3.54 (d quin, *J* = 9.4, 2.0 Hz, 1H), 2.60 (dt, *J* = 9.4, 1.7 Hz, 1H), 1.99 (app. ddd, *J* = 12.4, 9.3, 4.1 Hz, 1H), 1.76 – 1.61 (m, 2H), 1.61 (s, 3H), 1.58 – 1.51 (m, 1H), 0.91 (s, 9H), 0.12 (s, 3H), 0.11 (s, 3H). ^{13}C NMR (101 MHz, $CDCl_3$) δ 143.3, 136.0, 135.4, 128.4 (2C), 127.2, 125.1 (2C), 89.5, 85.4, 77.5, 63.6, 63.0, 35.1, 32.3, 26.1 (3C), 22.0, 18.4, –4.1, –4.2. HRMS-ESI(+) *m/z* calc. for $C_{22}H_{32}O_2SiNa$ $[M+Na]^+$: 379.2064, found: 379.2071.

tert-Butyldimethyl(((1*R,3a*R**,4*S**,7*R**,7a*R**)-7-methyl-4-phenyl-3a,4,5,6,7,7a-hexahydro-1*H*-4,7-epoxyinden-1-yl)oxy)silane (*anti*-38h)**

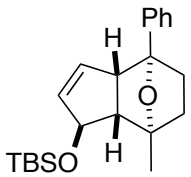

Performed on 0.2 mmol scale from (*Z*)-**37h** (71 mg) with stirring for 18 h at 25 °C. Crude ^{1}H NMR yield = 77% (>98:2 *dr*). Purified by silica gel column chromatography eluting with pentane/diethyl ether 95:5 and isolated as an off-white solid (58 mg). Crystallization from hot pentane gave analytically pure material (44 mg, 0.122 mmol, 61%, > 98:2 *dr*).

Mp = 72–75 °C. ^{1}H NMR (500 MHz, $CDCl_3$) δ 7.35 – 7.27 (m, 4H), 7.26 – 7.19 (m, 1H), 5.68 (dt, *J* = 5.7, 2.0 Hz, 1H), 5.21 (ddd, *J* = 5.7, 2.4, 1.2 Hz, 1H), 4.91 (dq, *J* = 3.3, 1.9, 1.2 Hz, 1H), 3.43 (dq, *J* = 6.8, 2.2 Hz, 1H), 2.31 (dd, *J* = 7.0, 2.0 Hz, 1H), 2.14 (ddd, *J* = 10.6, 8.6, 3.9 Hz, 1H), 1.89 – 1.72 (m, 3H), 1.64 (s, 3H), 0.90 (s, 9H), 0.12 (s, 3H), 0.10 (s, 3H). ^{13}C NMR (126 MHz, $CDCl_3$) δ 141.2, 135.7, 133.2, 128.2 (2C), 126.8, 125.4 (2C), 88.2, 84.3, 79.6, 61.3, 61.1, 38.5, 38.4, 26.1 (3C), 19.0, 18.2, –3.9, –4.2. HRMS-ESI(+) *m/z* calc. for $C_{22}H_{32}O_2SiNa$ $[M+Na]^+$: 379.2064, found: 379.2067.

(1*R,3a*R**,4*R**,7*S**,7a*R**)-7-Methyl-4-(4-(trifluoromethyl)phenyl)-3a,4,5,6,7,7a-hexahydro-1*H*-4,7-epoxyinden-1-yl benzoate (*syn*-38i)**

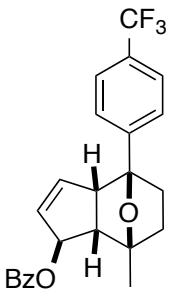

Performed on 0.2 mmol scale from (*E*)-**37i** (82 mg) with stirring for 17 h at 25 °C. Crude ^{1}H NMR yield = 78% (83:17 *dr*, yield of combined diastereomers). Purified by preparative silica gel TLC eluting with cyclohexane/CH_2Cl_2/ethyl acetate 85:15:5 and isolated as a pale yellow oil (40 mg, 0.096 mmol, 48%, >98:2 *dr*).

^{1}H NMR (400 MHz, $CDCl_3$) δ 8.06 – 8.01 (m, 2H + 2H *minor*), 7.66 – 7.60 (m, 2H + 2H *minor*), 7.59 – 7.52 (m, 3H + 1H *minor*), 7.47 – 7.40 (m, 2H + 4H *minor*), 6.23 (ddd, *J* = 5.7, 2.1, 1.0 Hz, 1H), 6.05 (dt, *J* = 5.6, 2.1 Hz, 1H), 5.85 (sept, *J* = 1.3 Hz, 1H), 3.54 (d quin, *J* = 8.8, 2.2 Hz, 1H), 2.80 (dt, *J* = 9.2, 1.7 Hz, 1H), 2.13 – 2.04 (m, 1H), 1.90 – 1.81 (m, 1H + 3H *minor*), 1.80 – 1.64 (m, 5H + 3H *minor*). ^{13}C NMR (101 MHz, $CDCl_3$) δ 166.6, 147.0 (app. d, J_{C-F} = 1.1 Hz), 139.2, 133.2, 132.0, 130.4, 129.8 (2C), 129.6 (q, J_{C-F} = 32.4 Hz), 128.5 (2C), 125.5 (q, J_{C-F} = 4.0 Hz, 2C), 125.5 (2C), 124.3 (q, J_{C-F} = 271.9 Hz), 89.0, 86.0, 80.1, 63.2, 60.4, 34.9, 32.3, 21.6. ^{19}F NMR (376 MHz, $CDCl_3$) δ –62.55. HRMS-ESI(+) *m/z* calc. for $C_{24}H_{21}O_3F_3Na$ $[M+Na]^+$: 437.1335, found: 437.1342.

(1*R,3a*R**,4*S**,7*R**,7a*R**)-7-Methyl-4-(4-(trifluoromethyl)phenyl)-3a,4,5,6,7,7a-hexahydro-1*H*-4,7-epoxyinden-1-yl benzoate (*anti*-38i)**

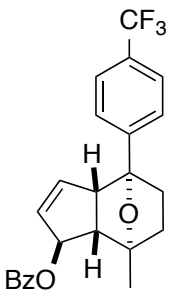

Performed on 0.2 mmol scale from (*Z*)-**37i** (100 mg) with stirring for 17 h at 25 °C. Crude ^{1}H NMR yield = 99% (86:14 *dr*, yield of combined diastereomers). Purified by preparative silica gel TLC eluting with cyclohexane/CH_2Cl_2/ethyl acetate 85:12:3 and isolated as a colorless solid (54 mg, 0.13 mmol, 65%, >98:2 *dr*) (22 mg of a fraction containing a 57:43 *dr* mixture of diastereomers was also collected, 27%).

Mp = 108–110 °C. ^{1}H NMR (400 MHz, $CDCl_3$) δ 8.06 – 8.01 (m, 2H), 7.60 (app. d, *J* = 8.2 Hz, 2H), 7.55 (ddt, *J* = 8.7, 6.9, 1.4 Hz, 1H), 7.48 – 7.40 (m, 4H), 6.05 (app. dt, *J* = 3.2, 1.8 Hz, 1H), 5.91 (dt, *J* = 5.7, 2.1 Hz, 1H), 5.38 (ddd, *J* = 5.7, 2.3, 1.2 Hz, 1H), 3.53 (dq, *J* = 6.7, 2.2 Hz, 1H), 2.58 (dd, *J* = 6.8, 1.8 Hz, 1H), 2.25 – 2.17 (m, 1H), 1.94 – 1.80 (m, 3H), 1.77 (s, 3H). ^{13}C NMR (101 MHz, $CDCl_3$) δ 166.3, 144.9 (app. d, J_{C-F} = 1.1 Hz), 136.4, 133.1, 132.1, 130.6, 129.7 (2C), 129.3 (q, J_{C-F} = 32.3 Hz), 128.5 (2C), 125.9 (2C), 125.2 (q, J_{C-F} = 3.8 Hz, 2C), 124.4 (q, J_{C-F} = 271.9 Hz), 87.6, 84.8, 82.1, 61.6, 57.6, 38.3, 38.1, 18.7. ^{19}F NMR (376 MHz, $CDCl_3$) δ –63.53. HRMS-ESI(+) *m/z* calc. for $C_{24}H_{21}O_3F_3Na$ $[M+Na]^+$: 437.1335, found: 437.1338.

(1*R,3a*R**,4*S**,7*R**,7a*R**)-7-Methyl-4-(naphthalen-2-yl)-3a,4,5,6,7,7a-hexahydro-1*H*-4,7-epoxyinden-1-yl benzoate (*anti*-38j)**

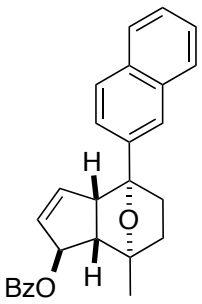

Performed on 0.2 mmol scale from (*Z*)-**37j** (79 mg) with stirring for 17 h at 25 °C. Crude ^{1}H NMR yield = 78% (94:6 *dr*). Purified by preparative silica gel TLC eluting with cyclohexane/CH_2Cl_2/ethyl acetate 85:12:3 and isolated as a pale yellow oil that solidified on standing.

Further crystallization from CH_2Cl_2 (200 µL) + diethyl ether (200 µL) + pentane (1.2 mL), first at 4 °C for 2 h then at -30 °C for 16 hours, gave 33 mg of colorless solid (42%, >98:2 *dr*). The filtrate was recrystallized from CH_2Cl_2 (100 µL) + diethyl ether (100 µL) + pentane (0.8 mL) to give a second crop of 11 mg of colorless solid (14%, >98:2 *dr*). Overall yield after crystallization 56% (>98:2 *dr*).

Mp = 125–126 °C. ^{1}H NMR (400 MHz, $CDCl_3$) δ 8.09 – 8.02 (m, 2H), 7.89 – 7.80 (m, 4H), 7.59 – 7.53 (m, 1H), 7.52 – 7.40 (m, 5H), 6.14 – 6.09 (m, 1H), 5.90 (dt, *J* = 5.7, 2.1 Hz, 1H), 5.44 (ddd, *J* = 5.8, 2.1, 1.1 Hz, 1H), 3.62 (dq, *J* = 6.7, 2.2 Hz, 1H), 2.61 (dd, *J* = 6.7, 1.8 Hz, 1H), 2.30 (ddd, *J* = 11.3, 8.5, 4.9 Hz, 1H), 1.99 (td, *J* = 11.7, 5.1 Hz, 1H), 1.95 – 1.85 (m, 2H), 1.83 (s, 3H). ^{13}C NMR (101 MHz, $CDCl_3$) δ 166.3, 138.4, 137.2, 133.3, 133.0, 132.6, 131.6, 130.7, 129.7 (2C), 128.5 (2C), 128.2, 128.0, 127.8, 126.2, 125.8, 123.9, 123.8, 88.1, 84.6, 82.3, 61.6, 57.6, 38.5, 38.4, 18.9. HRMS-ESI(+) *m/z* calc. for $C_{27}H_{24}O_3Na$ $[M+Na]^+$: 419.1618, found: 419.1614.

Crown ether 45

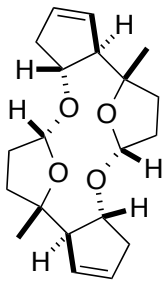

A solution of (*E*)-**37l** (20 mg, 0.1 mmol) and gold catalyst **A** (3 mol%) in anhydrous CH_2Cl_2 (1 mL) was stirred at 0 °C for 10 h. It was then quenched by addition of Et_3N (5 μL) and the solvent was removed in vacuo (at 25 °C). The crude material was purified by silica gel column chromatography eluting with cyclohexane/ethyl acetate 90:10 and isolated as a white solid (8 mg, 0.024 mmol, 49%). **Note**: *the reaction was performed under air atmosphere.*

Mp = 258–260°C. ^{1}H NMR (500 MHz, $CDCl_3$) δ 5.83 – 5.79 (m, 2H), 5.63 (app. ddd, *J* = 5.6, 4.3, 2.5 Hz, 2H), 5.33 (dd, *J* = 6.1, 2.6 Hz, 2H), 4.72 (d, *J* = 6.0 Hz, 2H), 3.27 (app. q, *J* = 2.1 Hz, 2H), 2.63 (ddt, *J* = 17.8, 8.2, 2.2 Hz, 2H), 2.35 (dt, *J* = 17.9, 2.1 Hz, 2H), 2.28 – 2.19 (m, 2H), 2.13 – 2.07 (m, 2H), 2.06 – 1.98 (m, 2H), 1.64 – 1.54 (m, 2H), 1.02 (s, 6H). ^{13}C NMR (126 MHz, $CDCl_3$) δ 131.1 (2C), 130.6 (2C), 102.4 (2C), 85.3 (2C), 76.1 (2C), 63.6 (2C), 40.6 (2C), 36.6 (2C), 33.1 (2C), 22.2 (2C). HRMS-ESI(+) *m/z* calc. $C_{20}H_{28}O_4Na$ $[M+Na]^+$: 355.1880, found: 355.1868.

Crystallographic Data

(1*R**,3a*R**,4*S**,7*R**,7a*R**)-7-Methyl-3a,4,5,6,7,7a-hexahydro-1*H*-4,7-epoxyinden-1-yl benzoate (*anti*-38a)

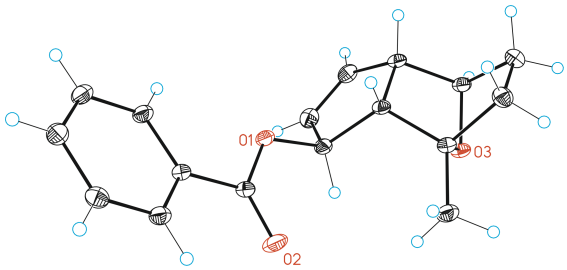

Table T7. Crystal data and structure refinement for *anti*-**38a**

Identification code	mo_MMu1322_0m
Empirical formula	C17H18O3
Formula weight	270.31
Temperature	100(2) K
Wavelength	0.71073 Å
Crystal system	Triclinic
Space group	P-1
Unit cell dimensions	
a = 8.3651(6)Å	α = 99.6589(18)°.
b = 8.4760(6)Å	β = 96.413(2)°.
c = 9.7723(7)Å	γ = 96.7245(18)°.
Volume	672.23(8) $Å^3$
Z	2
Density (calculated)	1.335 Mg/m^3
Absorption coefficient	0.091 mm^{-1}
F(000)	288
Crystal size	0.30 x 0.25 x 0.07 mm^3
Theta range for data collection	2.133 to 32.435°.
Index ranges	-9<=h<=12,-12<=k<=10,-13<=l<=14
Reflections collected	8446
Independent reflections	4216[R(int) = 0.0377]
Completeness to theta =32.435°	87.1%
Absorption correction	Empirical
Max. and min. transmission	0.994 and 0.676
Refinement method	Full-matrix least-squares on F^2
Data / restraints / parameters	4216/ 0/ 182
Goodness-of-fit on F^2	1.084
Final R indices [I>2sigma(I)]	R1 = 0.0513, wR2 = 0.1428
R indices (all data)	R1 = 0.0535, wR2 = 0.1454
Largest diff. peak and hole	0.519 and -0.463 $e.Å^{-3}$

Table T8. Bond lengths [Å] and angles [°] for *anti*-**38a**

Bond lengths			
O1-C11	1.3417(12)	C6-C7	1.5486(15)
O1-C1	1.4657(11)	C7-C8	1.5509(14)
O2-C11	1.2136(11)	C8-C10	1.5104(13)
O3-C5	1.4450(11)	C8-C9	1.5458(13)
O3-C8	1.4516(11)	C11-C12	1.4925(13)
C1-C2	1.4975(14)	C12-C13	1.3939(13)
C1-C9	1.5457(13)	C12-C17	1.3971(12)
C2-C3	1.3297(15)	C13-C14	1.3910(13)
C3-C4	1.4988(14)	C14-C15	1.3950(14)
C4-C5	1.5476(13)	C15-C16	1.3901(15)
C4-C9	1.5630(13)	C16-C17	1.3918(13)
C5-C6	1.5303(14)		
Angles			
C11-O1-C1	118.23(7)	O3-C8-C7	102.50(8)
C5-O3-C8	97.02(6)	C10-C8-C7	114.19(8)
O1-C1-C2	107.66(7)	C9-C8-C7	108.30(7)
O1-C1-C9	110.63(7)	C1-C9-C8	115.64(7)
C2-C1-C9	105.27(8)	C1-C9-C4	105.34(8)
C3-C2-C1	112.15(9)	C8-C9-C4	100.95(7)
C2-C3-C4	112.67(9)	O2-C11-O1	124.52(9)
C3-C4-C5	113.55(8)	O2-C11-C12	124.11(9)
C3-C4-C9	104.43(8)	O1-C11-C12	111.35(7)
C5-C4-C9	101.44(7)	C13-C12-C17	120.05(9)
O3-C5-C6	102.38(8)	C13-C12-C11	118.42(8)
O3-C5-C4	103.23(7)	C17-C12-C11	121.45(9)
C6-C5-C4	108.94(8)	C14-C13-C12	119.85(8)
C5-C6-C7	100.40(8)	C13-C14-C15	120.13(9)
C6-C7-C8	102.62(8)	C16-C15-C14	119.93(9)
O3-C8-C10	110.65(7)	C15-C16-C17	120.18(9)
O3-C8-C9	100.99(7)	C16-C17-C12	119.80(9)
C10-C8-C9	118.29(8)		

Table T9. Torsion angles [°] for *anti*-**38a**

C11-O1-C1-C2	140.16(9)	C8-O3-C5-C4	-54.81(8)
C11-O1-C1-C9	-105.31(9)	C3-C4-C5-O3	-82.22(9)
O1-C1-C2-C3	119.91(9)	C9-C4-C5-O3	29.23(9)
C9-C1-C2-C3	1.87(10)	C3-C4-C5-C6	169.52(8)
C1-C2-C3-C4	0.65(11)	C9-C4-C5-C6	-79.04(9)
C2-C3-C4-C5	106.76(9)	O3-C5-C6-C7	-39.50(9)
C2-C3-C4-C9	-2.84(10)	C4-C5-C6-C7	69.34(9)
C8-O3-C5-C6	58.32(8)	C5-C6-C7-C8	6.26(9)

C5-O3-C8-C10	-175.19(8)	C5-C4-C9-C1	-114.48(7)
C5-O3-C8-C9	58.72(8)	C3-C4-C9-C8	124.42(7)
C5-O3-C8-C7	-53.04(8)	C5-C4-C9-C8	6.19(8)
C6-C7-C8-O3	28.37(9)	C1-O1-C11-O2	-0.25(15)
C6-C7-C8-C10	148.08(8)	C1-O1-C11-C12	177.85(8)
C6-C7-C8-C9	-77.83(9)	O2-C11-C12-C13	14.74(15)
O1-C1-C9-C8	130.04(8)	O1-C11-C12-C13	-163.37(9)
C2-C1-C9-C8	-113.93(8)	O2-C11-C12-C17	-168.46(10)
O1-C1-C9-C4	-119.46(7)	O1-C11-C12-C17	13.44(13)
C2-C1-C9-C4	-3.43(8)	C17-C12-C13-C14	-2.13(15)
O3-C8-C9-C1	73.51(9)	C11-C12-C13-C14	174.72(9)
C10-C8-C9-C1	-47.33(12)	C12-C13-C14-C15	0.99(15)
C7-C8-C9-C1	-179.25(8)	C13-C14-C15-C16	1.04(16)
O3-C8-C9-C4	-39.56(8)	C14-C15-C16-C17	-1.94(16)
C10-C8-C9-C4	-160.39(8)	C15-C16-C17-C12	0.79(16)
C7-C8-C9-C4	67.69(9)	C13-C12-C17-C16	1.24(15)
C3-C4-C9-C1	3.75(8)	C11-C12-C17-C16	-175.51(9)

tert-Butyldimethyl(((1*R,3a*R**,4*S**,7*R**,7a*R**)-7-methyl-3a,4,5,6,7,7a-hexahydro-1*H*-4,7-epoxyinden-1-yl)oxy)silane (*anti*-38b)**

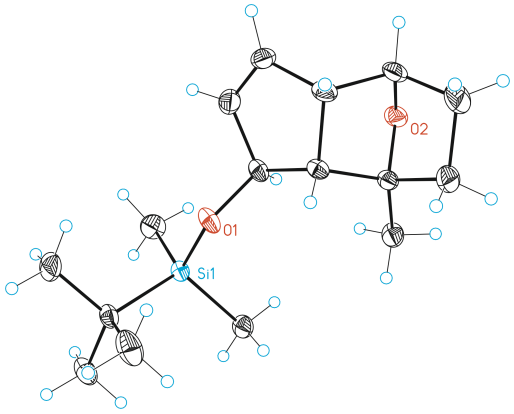

Table T10. Crystal data and structure refinement for *anti*-**38b**

Identification code	mo_MMu1335D_0m
Empirical formula	C16H28O2Si
Formula weight	280.47
Temperature	100(2) K
Wavelength	0.71073 Å
Crystal system	Monoclinic
Space group	P2(1)/n
Unit cell dimensions	
a = 6.6228(4)Å	α= 90°.
b = 10.6004(7)Å	β = 97.220(2)°.
c = 23.5812(14)Å	γ = 90°.
Volume	1642.37(18) Å^3

Z	4
Density (calculated)	1.134 Mg/m^3
Absorption coefficient	0.140 mm^{-1}
F(000)	616
Crystal size	0.30 x 0.15 x 0.04 mm^3
Theta range for data collection	1.741 to 30.095°.
Index ranges	-6<=h<=9,-14<=k<=14,-31<=l<=32
Reflections collected	18867
Independent reflections	4272[R(int) = 0.0461]
Completeness to theta =30.095°	88.4%
Absorption correction	Empirical
Max. and min. transmission	0.994 and 0.76
Refinement method	Full-matrix least-squares on F^2
Data / restraints / parameters	4272/ 0/ 178
Goodness-of-fit on F^2	1.069
Final R indices [I>2sigma(I)]	R1 = 0.0406, wR2 = 0.1032
R indices (all data)	R1 = 0.0523, wR2 = 0.1099
Largest diff. peak and hole	0.445 and -0.286 $e.Å^{-3}$

Table T11. Bond lengths [Å] and angles [°] for *anti*-**38b**

Bond lengths			
Si1-O1	1.6550(9)	C4-C5	1.5480(18)
Si1-C12	1.8596(13)	C4-C9	1.5650(17)
Si1-C11	1.8615(15)	C5-C6	1.520(2)
Si1-C13	1.8855(13)	C6-C7	1.545(2)
O1-C1	1.4390(14)	C7-C8	1.5442(18)
O2-C5	1.4409(16)	C8-C10	1.5021(17)
O2-C8	1.4555(16)	C8-C9	1.5422(17)
C1-C2	1.499(2)	C13-C14	1.533(2)
C1-C9	1.5469(17)	C13-C16	1.5334(19)
C2-C3	1.324(2)	C13-C15	1.5360(18)
C3-C4	1.494(2)		
Angles			
O1-Si1-C12	110.94(6)	C3-C2-C1	112.61(13)
O1-Si1-C11	111.11(6)	C2-C3-C4	113.02(12)
C12-Si1-C11	107.82(7)	C3-C4-C5	115.10(12)
O1-Si1-C13	103.53(5)	C3-C4-C9	103.76(10)
C12-Si1-C13	112.02(6)	C5-C4-C9	100.99(10)
C11-Si1-C13	111.46(6)	O2-C5-C6	102.24(11)
C1-O1-Si1	124.32(8)	O2-C5-C4	103.45(10)
C5-O2-C8	96.83(10)	C6-C5-C4	109.34(13)
O1-C1-C2	111.26(10)	C5-C6-C7	100.74(11)
O1-C1-C9	111.06(10)	C8-C7-C6	102.43(12)
C2-C1-C9	104.27(10)	O2-C8-C10	111.13(10)

O2-C8-C9	100.67(10)	C1-C9-C4	105.97(10)
C10-C8-C9	117.88(10)	C14-C13-C16	109.38(12)
O2-C8-C7	102.23(10)	C14-C13-C15	108.91(12)
C10-C8-C7	113.85(11)	C16-C13-C15	108.48(11)
C9-C8-C7	109.18(10)	C14-C13-Si1	110.18(9)
C8-C9-C1	115.11(10)	C16-C13-Si1	108.71(9)
C8-C9-C4	101.20(9)	C15-C13-Si1	111.15(9)

Table T12. Torsion angles [°] for *anti*-**38b**

C12-Si1-O1-C1	-67.47(11)	C6-C7-C8-C9	77.16(13)
C11-Si1-O1-C1	52.45(12)	O2-C8-C9-C1	-73.84(12)
C13-Si1-O1-C1	172.20(10)	C10-C8-C9-C1	47.13(16)
Si1-O1-C1-C2	-111.05(11)	C7-C8-C9-C1	179.07(11)
Si1-O1-C1-C9	133.27(9)	O2-C8-C9-C4	39.90(11)
O1-C1-C2-C3	-123.80(13)	C10-C8-C9-C4	160.88(12)
C9-C1-C2-C3	-4.00(15)	C7-C8-C9-C4	-67.19(12)
C1-C2-C3-C4	0.36(17)	O1-C1-C9-C8	-123.37(11)
C2-C3-C4-C5	-105.96(14)	C2-C1-C9-C8	116.70(12)
C2-C3-C4-C9	3.40(15)	O1-C1-C9-C4	125.69(10)
C8-O2-C5-C6	-58.47(12)	C2-C1-C9-C4	5.77(12)
C8-O2-C5-C4	55.14(12)	C3-C4-C9-C8	-126.01(11)
C3-C4-C5-O2	81.70(14)	C5-C4-C9-C8	-6.51(13)
C9-C4-C5-O2	-29.31(13)	C3-C4-C9-C1	-5.57(13)
C3-C4-C5-C6	-169.93(11)	C5-C4-C9-C1	113.94(11)
C9-C4-C5-C6	79.05(12)	O1-Si1-C13-C14	49.58(11)
O2-C5-C6-C7	39.48(14)	C12-Si1-C13-C14	-70.01(11)
C4-C5-C6-C7	-69.70(14)	C11-Si1-C13-C14	169.09(10)
C5-C6-C7-C8	-5.86(15)	O1-Si1-C13-C16	-70.27(10)
C5-O2-C8-C10	175.33(11)	C12-Si1-C13-C16	170.13(9)
C5-O2-C8-C9	-59.01(11)	C11-Si1-C13-C16	49.23(11)
C5-O2-C8-C7	53.50(11)	O1-Si1-C13-C15	170.40(10)
C6-C7-C8-O2	-28.87(13)	C12-Si1-C13-C15	50.81(12)
C6-C7-C8-C10	-148.81(12)	C11-Si1-C13-C15	-70.10(12)

(1*R,3a*R**,4*R**,7*S**,7a*R**)-4,7-Dimethyl-3a,4,5,6,7,7a-hexahydro-1*H*-4,7-epoxyinden-1-yl benzoate (*syn*-38c)**

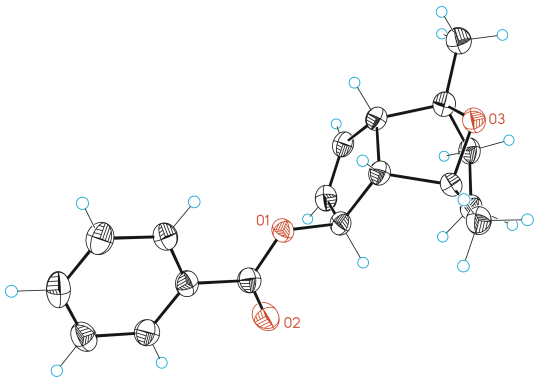

Table T13. Crystal data and structure refinement for *syn*-**38c**

Identification code	mo_PCR_O208-b_0m
Empirical formula	C18H20O3
Formula weight	284.34
Temperature	100(2) K
Wavelength	0.71073 Å
Crystal system	Triclinic
Space group	P-1
Unit cell dimensions	
a = 5.8663(10)Å	α= 78.624(5)°.
b = 10.9320(18)Å	β = 79.886(5)°.
c = 12.288(2)Å	γ = 75.951(5)°.
Volume	742.7(2) $Å^3$
Z	2
Density (calculated)	1.272 Mg/m^3
Absorption coefficient	0.085 mm^{-1}
F(000)	304
Crystal size	0.18 x 0.07 x 0.04 mm^3
Theta range for data collection	1.706 to 26.493°.
Index ranges	-7<=h<=7,-13<=k<=13,-15<=l<=14
Reflections collected	7440
Independent reflections	2997[R(int) = 0.0578]
Completeness to theta =26.493°	97.299995%
Absorption correction	Multi-scan
Max. and min. transmission	0.997 and 0.653
Refinement method	Full-matrix least-squares on F^2
Data / restraints / parameters	2997/ 0/ 192
Goodness-of-fit on F^2	1.034
Final R indices [I>2sigma(I)]	R1 = 0.0572, wR2 = 0.1490
R indices (all data)	R1 = 0.0927, wR2 = 0.1705
Largest diff. peak and hole	0.299 and -0.256 $e.Å^{-3}$

Table T14. Bond lengths [Å] and angles [°] for *syn*-**38c**

Bond lengths

C1-O2	1.211(3)	C8-C9	1.509(3)
C1-O1	1.339(3)	C8-C16	1.527(3)
C1-C2	1.489(3)	C9-C10	1.315(4)
C2-C7	1.388(4)	C10-C11	1.500(3)
C2-C3	1.392(3)	C11-C16	1.554(3)
C3-C4	1.385(3)	C11-C12	1.563(3)
C4-C5	1.382(4)	C12-O3	1.454(3)
C5-C6	1.385(4)	C12-C17	1.502(4)
C6-C7	1.388(3)	C12-C13	1.534(3)
C8-O1	1.472(2)	C13-C14	1.537(4)

C14-C15	1.545(3)	C15-C18	1.501(3)
C15-O3	1.451(3)	C15-C16	1.546(3)

Angles

O2-C1-O1	123.9(2)	O3-C12-C17	110.1(2)
O2-C1-C2	123.7(2)	O3-C12-C13	100.96(19)
O1-C1-C2	112.4(2)	C17-C12-C13	116.1(2)
C7-C2-C3	119.5(2)	O3-C12-C11	101.05(17)
C7-C2-C1	118.4(2)	C17-C12-C11	116.3(2)
C3-C2-C1	122.1(2)	C13-C12-C11	110.1(2)
C4-C3-C2	120.1(2)	C12-C13-C14	101.82(18)
C5-C4-C3	120.3(3)	C13-C14-C15	102.5(2)
C4-C5-C6	119.9(2)	O3-C15-C18	109.93(19)
C5-C6-C7	120.1(3)	O3-C15-C14	102.01(18)
C2-C7-C6	120.1(2)	C18-C15-C14	116.4(2)
O1-C8-C9	109.40(18)	O3-C15-C16	100.19(18)
O1-C8-C16	107.39(17)	C18-C15-C16	115.82(19)
C9-C8-C16	104.2(2)	C14-C15-C16	110.27(19)
C10-C9-C8	112.0(2)	C8-C16-C15	117.10(19)
C9-C10-C11	113.2(2)	C8-C16-C11	106.75(19)
C10-C11-C16	103.3(2)	C15-C16-C11	101.42(18)
C10-C11-C12	117.43(18)	C1-O1-C8	115.99(17)
C16-C11-C12	102.03(18)	C15-O3-C12	97.88(17)

Table T15. Torsion angles [°] for *syn*-**38c**

O2-C1-C2-C7	-0.2(4)	C16-C11-C12-C13	75.8(2)
O1-C1-C2-C7	178.5(2)	O3-C12-C13-C14	37.8(2)
O2-C1-C2-C3	-178.5(2)	C17-C12-C13-C14	156.8(2)
O1-C1-C2-C3	0.1(3)	C11-C12-C13-C14	-68.4(2)
C7-C2-C3-C4	-2.5(4)	C12-C13-C14-C15	-4.9(2)
C1-C2-C3-C4	175.8(2)	C13-C14-C15-O3	-29.5(2)
C2-C3-C4-C5	1.1(4)	C13-C14-C15-C18	-149.2(2)
C3-C4-C5-C6	1.0(4)	C13-C14-C15-C16	76.2(2)
C4-C5-C6-C7	-1.7(4)	O1-C8-C16-C15	138.63(19)
C3-C2-C7-C6	1.8(4)	C9-C8-C16-C15	-105.4(2)
C1-C2-C7-C6	-176.6(2)	O1-C8-C16-C11	-108.65(19)
C5-C6-C7-C2	0.3(4)	C9-C8-C16-C11	7.3(2)
O1-C8-C9-C10	108.0(2)	O3-C15-C16-C8	154.55(18)
C16-C8-C9-C10	-6.6(3)	C18-C15-C16-C8	-87.3(3)
C8-C9-C10-C11	3.0(3)	C14-C15-C16-C8	47.6(3)
C9-C10-C11-C16	1.9(3)	O3-C15-C16-C11	38.9(2)
C9-C10-C11-C12	113.2(2)	C18-C15-C16-C11	157.0(2)
C10-C11-C12-O3	-142.3(2)	C14-C15-C16-C11	-68.1(2)
C16-C11-C12-O3	-30.3(2)	C10-C11-C16-C8	-5.8(2)
C10-C11-C12-C17	98.5(3)	C12-C11-C16-C8	-128.09(18)
C16-C11-C12-C17	-149.4(2)	C10-C11-C16-C15	117.30(19)
C10-C11-C12-C13	-36.2(3)	C12-C11-C16-C15	-5.0(2)

O2-C1-O1-C8	1.6(3)	C14-C15-O3-C12	53.89(19)
C2-C1-O1-C8	-177.01(18)	C16-C15-O3-C12	-59.56(18)
C9-C8-O1-C1	80.5(2)	C17-C12-O3-C15	179.43(18)
C16-C8-O1-C1	-166.98(19)	C13-C12-O3-C15	-57.36(19)
C18-C15-O3-C12	178.03(17)	C11-C12-O3-C15	55.9(2)

tert-Butyldimethyl(((1*R,3a*R**,4*S**,7*R**,7a*R**)-7-methyl-4-phenyl-3a,4,5,6,7,7a-hexahydro-1*H*-4,7-epoxyinden-1-yl)oxy)silane (*anti*-38g)**

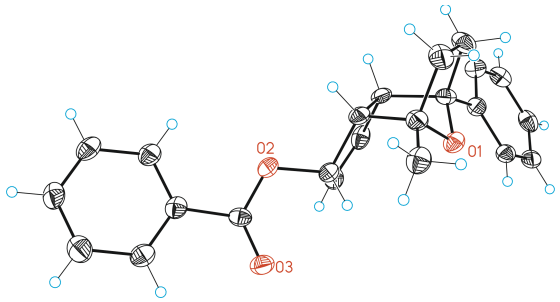

Table T16. Crystal data and structure refinement for *anti*-**38g**

Identification code	MMu1340B_twin1_hklf4
Empirical formula	C23H22O3
Formula weight	346.40
Temperature	100(2) K
Wavelength	0.71073 Å
Crystal system	Monoclinic
Space group	P2(1)/n
Unit cell dimensions	
a = 5.9424(6)Å	α= 90°.
b = 10.1276(10)Å	β = 91.195(9)°.
c = 30.051(3)Å	γ = 90°.
Volume	1808.1(3) $Å^3$
Z	4
Density (calculated)	1.273 Mg/m^3
Absorption coefficient	0.083 mm^{-1}
F(000)	736
Crystal size	? x ? x ? mm^3
Theta range for data collection	2.122 to 29.247°.
Index ranges	-7<=h<=7,-12<=k<=13,-40<=l<=40
Reflections collected	21609
Independent reflections	4378[R(int) = 0.1719]
Completeness to theta =29.247°	89.1%
Absorption correction	Multi-scan
Max. and min. transmission	0.999 and 0.768
Refinement method	Full-matrix least-squares on F^2
Data / restraints / parameters	4378/ 0/ 236
Goodness-of-fit on F^2	0.918
Final R indices [I>2sigma(I)]	R1 = 0.0771, wR2 = 0.1749

R indices (all data)	R1 = 0.1372, wR2 = 0.1971
Largest diff. peak and hole	0.399 and -0.535 e.Å^{-3}

Table T17. Bond lengths [Å] and angles [°] for *anti*-3**8g**

Bond lengths			
C1-O1	1.441(3)	C10-C11	1.391(4)
C1-C10	1.508(4)	C10-C15	1.395(4)
C1-C9	1.537(4)	C11-C12	1.377(4)
C1-C2	1.564(4)	C12-C13	1.389(4)
C2-C3	1.488(4)	C13-C14	1.376(4)
C2-C6	1.565(4)	C14-C15	1.389(4)
C3-C4	1.321(4)	C17-O3	1.207(3)
C4-C5	1.491(4)	C17-O2	1.331(3)
C5-O2	1.475(3)	C17-C18	1.501(4)
C5-C6	1.540(4)	C18-C19	1.385(4)
C6-C7	1.541(4)	C18-C23	1.388(4)
C7-O1	1.452(3)	C19-C20	1.403(4)
C7-C16	1.499(4)	C20-C21	1.363(4)
C7-C8	1.531(4)	C21-C22	1.384(4)
C8-C9	1.543(4)	C22-C23	1.401(4)
Angles			
O1-C1-C10	111.8(2)	C7-C8-C9	103.0(2)
O1-C1-C9	102.8(2)	C1-C9-C8	100.8(2)
C10-C1-C9	115.8(2)	C11-C10-C15	118.5(3)
O1-C1-C2	101.97(19)	C11-C10-C1	119.5(2)
C10-C1-C2	115.0(2)	C15-C10-C1	122.0(2)
C9-C1-C2	107.9(2)	C12-C11-C10	120.8(3)
C3-C2-C1	114.9(2)	C11-C12-C13	120.5(3)
C3-C2-C6	104.5(2)	C14-C13-C12	119.2(3)
C1-C2-C6	101.0(2)	C13-C14-C15	120.7(3)
C4-C3-C2	113.4(2)	C14-C15-C10	120.3(3)
C3-C4-C5	111.4(2)	O3-C17-O2	125.0(2)
O2-C5-C4	110.4(2)	O3-C17-C18	123.1(3)
O2-C5-C6	108.27(19)	O2-C17-C18	111.8(2)
C4-C5-C6	106.1(2)	C19-C18-C23	120.2(3)
C5-C6-C7	115.9(2)	C19-C18-C17	117.6(2)
C5-C6-C2	104.6(2)	C23-C18-C17	122.2(3)
C7-C6-C2	101.7(2)	C18-C19-C20	119.4(3)
O1-C7-C16	111.3(2)	C21-C20-C19	120.1(3)
O1-C7-C8	102.9(2)	C20-C21-C22	121.2(3)
C16-C7-C8	114.2(2)	C21-C22-C23	119.1(3)
O1-C7-C6	100.71(19)	C18-C23-C22	119.9(3)
C16-C7-C6	117.6(2)	C1-O1-C7	97.63(19)
C8-C7-C6	108.3(2)	C17-O2-C5	116.2(2)

Table T18. Torsion angles [°] for *anti*-**38g**

O1-C1-C2-C3	-80.6(3)	C2-C1-C10-C11	68.1(3)
C10-C1-C2-C3	40.6(3)	O1-C1-C10-C15	3.1(3)
C9-C1-C2-C3	171.5(2)	C9-C1-C10-C15	120.5(3)
O1-C1-C2-C6	31.2(2)	C2-C1-C10-C15	-112.5(3)
C10-C1-C2-C6	152.3(2)	C15-C10-C11-C12	1.1(4)
C9-C1-C2-C6	-76.7(2)	C1-C10-C11-C12	-179.5(2)
C1-C2-C3-C4	107.4(3)	C10-C11-C12-C13	-1.7(4)
C6-C2-C3-C4	-2.3(3)	C11-C12-C13-C14	1.2(4)
C2-C3-C4-C5	0.8(3)	C12-C13-C14-C15	-0.2(4)
C3-C4-C5-O2	118.2(3)	C13-C14-C15-C10	-0.4(4)
C3-C4-C5-C6	1.1(3)	C11-C10-C15-C14	-0.1(4)
O2-C5-C6-C7	128.1(2)	C1-C10-C15-C14	-179.4(2)
C4-C5-C6-C7	-113.4(2)	O3-C17-C18-C19	14.5(4)
O2-C5-C6-C2	-120.9(2)	O2-C17-C18-C19	-166.3(2)
C4-C5-C6-C2	-2.4(3)	O3-C17-C18-C23	-165.1(2)
C3-C2-C6-C5	2.8(3)	O2-C17-C18-C23	14.1(3)
C1-C2-C6-C5	-116.8(2)	C23-C18-C19-C20	1.4(4)
C3-C2-C6-C7	123.7(2)	C17-C18-C19-C20	-178.2(2)
C1-C2-C6-C7	4.2(2)	C18-C19-C20-C21	0.1(4)
C5-C6-C7-O1	74.8(2)	C19-C20-C21-C22	-0.6(4)
C2-C6-C7-O1	-37.9(2)	C20-C21-C22-C23	-0.3(4)
C5-C6-C7-C16	-46.3(3)	C19-C18-C23-C22	-2.4(4)
C2-C6-C7-C16	-159.0(2)	C17-C18-C23-C22	177.2(2)
C5-C6-C7-C8	-177.6(2)	C21-C22-C23-C18	1.9(4)
C2-C6-C7-C8	69.7(2)	C10-C1-O1-C7	-179.5(2)
O1-C7-C8-C9	29.9(3)	C9-C1-O1-C7	55.6(2)
C16-C7-C8-C9	150.7(2)	C2-C1-O1-C7	-56.2(2)
C6-C7-C8-C9	-76.1(3)	C16-C7-O1-C1	-175.5(2)
O1-C1-C9-C8	-36.2(3)	C8-C7-O1-C1	-52.8(2)
C10-C1-C9-C8	-158.5(2)	C6-C7-O1-C1	59.0(2)
C2-C1-C9-C8	71.1(3)	O3-C17-O2-C5	1.0(4)
C7-C8-C9-C1	3.4(3)	C18-C17-O2-C5	-178.1(2)
O1-C1-C10-C11	-176.2(2)	C4-C5-O2-C17	90.2(3)
C9-C1-C10-C11	-58.9(3)	C6-C5-O2-C17	-154.0(2)

Crown Ether 45

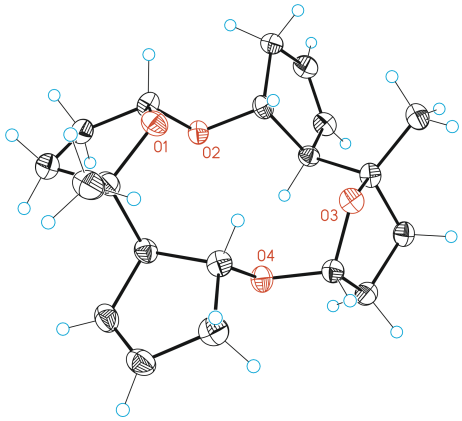

Table T19. Crystal data and structure refinement for **45**

Identification code	mo_PCRO031P1
Empirical formula	C20H28O4
Formula weight	332.42
Temperature	100(2) K
Wavelength	0.71073 Å
Crystal system	Monoclinic
Space group	P2(1)/c
Unit cell dimensions	
a = 10.6396(12) Å	α= 90.00 °.
b = 19.486(3) Å	β = 112.385(4) °.
c = 8.9289(10) Å	γ = 90.00 °.
Volume	1711.6(3) Å3
Z	4
Density (calculated)	1.290 Mg/m3
Absorption coefficient	0.088 mm-1
F(000)	720
Crystal size	0.02 x 0.01 x 0.002 mm3
Theta range for data collection	2.07 to 25.37 °.
Index ranges	-12 <=h<=12 ,-23 <=k<=22 ,-10 <=l<=10
Reflections collected	22094
Independent reflections	3136 [R(int) = 0.0848]
Completeness to theta =25.37 °	99.7%
Absorption correction	Empirical
Max. and min. transmission	0.9998 and 0.9982
Refinement method	Full-matrix least-squares on F2
Data / restraints / parameters	3136 / 0 / 219
Goodness-of-fit on F2	1.077
Final R indices [I>2sigma(I)]	R1 = 0.0466 , wR2 = 0.1018
R indices (all data)	R1 = 0.1125 , wR2 = 0.1238
Largest diff. peak and hole	0.251 and -0.236 e.Å-3

Table T20. Bond lengths [Å] and angles [°] for **45**

Bond lengths			
C1-O1	1.460(3)	C10-C11	1.544(3)
C1-C5	1.513(3)	C11-O3	1.454(3)
C1-C2	1.525(3)	C11-C15	1.518(3)
C1-C20	1.550(3)	C11-C12	1.532(3)
C2-C3	1.529(3)	C12-C13	1.530(3)
C3-C4	1.524(3)	C13-C14	1.528(3)
C4-O2	1.410(3)	C14-O4	1.410(3)
C4-O1	1.423(3)	C14-O3	1.425(3)
C6-O2	1.441(3)	C16-O4	1.444(3)
C6-C10	1.535(3)	C16-C20	1.535(3)
C6-C7	1.552(3)	C16-C17	1.546(3)
C7-C8	1.498(3)	C17-C18	1.498(4)
C8-C9	1.316(3)	C18-C19	1.319(4)
C9-C10	1.506(3)	C19-C20	1.503(3)
Angles			
O1-C1-C5	105.93(19)	C15-C11-C12	112.95(19)
O1-C1-C2	102.29(18)	O3-C11-C10	109.72(17)
C5-C1-C2	114.1(2)	C15-C11-C10	112.32(19)
O1-C1-C20	109.62(18)	C12-C11-C10	111.9(2)
C5-C1-C20	112.8(2)	C13-C12-C11	103.78(18)
C2-C1-C20	111.4(2)	C14-C13-C12	104.42(19)
C1-C2-C3	103.83(19)	O4-C14-O3	112.01(17)
C4-C3-C2	104.5(2)	O4-C14-C13	108.1(2)
O2-C4-O1	111.53(18)	O3-C14-C13	106.92(18)
O2-C4-C3	108.6(2)	O4-C16-C20	106.73(19)
O1-C4-C3	106.89(19)	O4-C16-C17	110.67(18)
O2-C6-C10	106.57(18)	C20-C16-C17	106.29(19)
O2-C6-C7	110.47(19)	C18-C17-C16	103.2(2)
C10-C6-C7	106.26(19)	C19-C18-C17	112.4(2)
C8-C7-C6	102.94(19)	C18-C19-C20	112.5(2)
C9-C8-C7	112.7(2)	C19-C20-C16	103.17(19)
C8-C9-C10	112.5(2)	C19-C20-C1	113.08(19)
C9-C10-C6	103.20(18)	C16-C20-C1	113.8(2)
C9-C10-C11	113.27(19)	C4-O1-C1	109.07(18)
C6-C10-C11	114.3(2)	C4-O2-C6	113.83(18)
O3-C11-C15	106.98(19)	C14-O3-C11	109.13(18)
O3-C11-C12	102.32(17)	C14-O4-C16	113.28(18)

Table T21. Torsion angles [°] for **45**

O1-C1-C2-C3	34.8(2)	C1-C2-C3-C4	-22.5(2)
C5-C1-C2-C3	148.7(2)	C2-C3-C4-O2	122.0(2)
C20-C1-C2-C3	-82.2(2)	C2-C3-C4-O1	1.5(2)

O2-C6-C7-C8	-100.3(2)	O4-C16-C20-C19	103.1(2)
C10-C6-C7-C8	14.9(2)	C17-C16-C20-C19	-15.1(2)
C6-C7-C8-C9	-9.8(3)	O4-C16-C20-C1	-134.05(19)
C7-C8-C9-C10	0.4(3)	C17-C16-C20-C1	107.8(2)
C8-C9-C10-C6	9.3(3)	O1-C1-C20-C19	171.37(19)
C8-C9-C10-C11	-114.9(2)	C5-C1-C20-C19	53.6(3)
O2-C6-C10-C9	103.1(2)	C2-C1-C20-C19	-76.1(3)
C7-C6-C10-C9	-14.7(2)	O1-C1-C20-C16	54.1(3)
O2-C6-C10-C11	-133.43(19)	C5-C1-C20-C16	-63.7(3)
C7-C6-C10-C11	108.7(2)	C2-C1-C20-C16	166.58(19)
C9-C10-C11-O3	171.58(19)	O2-C4-O1-C1	-96.9(2)
C6-C10-C11-O3	53.7(2)	C3-C4-O1-C1	21.7(2)
C9-C10-C11-C15	52.7(3)	C5-C1-O1-C4	-155.40(18)
C6-C10-C11-C15	-65.1(3)	C2-C1-O1-C4	-35.7(2)
C9-C10-C11-C12	-75.5(2)	C20-C1-O1-C4	82.6(2)
C6-C10-C11-C12	166.60(18)	O1-C4-O2-C6	-67.2(2)
O3-C11-C12-C13	34.8(2)	C3-C4-O2-C6	175.22(18)
C15-C11-C12-C13	149.5(2)	C10-C6-O2-C4	161.36(18)
C10-C11-C12-C13	-82.6(2)	C7-C6-O2-C4	-83.6(2)
C11-C12-C13-C14	-22.1(2)	O4-C14-O3-C11	-96.2(2)
C12-C13-C14-O4	121.93(19)	C13-C14-O3-C11	22.1(2)
C12-C13-C14-O3	1.2(2)	C15-C11-O3-C14	-154.79(18)
O4-C16-C17-C18	-100.9(2)	C12-C11-O3-C14	-35.8(2)
C20-C16-C17-C18	14.6(2)	C10-C11-O3-C14	83.1(2)
C16-C17-C18-C19	-8.7(3)	O3-C14-O4-C16	-67.3(2)
C17-C18-C19-C20	-1.1(3)	C13-C14-O4-C16	175.14(18)
C18-C19-C20-C16	10.4(3)	C20-C16-O4-C14	161.42(18)
C18-C19-C20-C1	-112.9(2)	C17-C16-O4-C14	-83.3(2)

DFT Calculations

Cartesian Coordinates (in Å)

Table T22: Optimized geometry for **I**

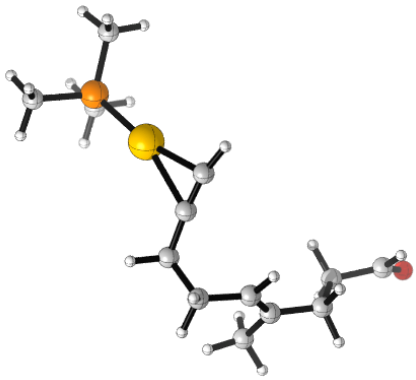

Free energy G = -1060.601557 Hartree/particle.

C	-3.38036300	-1.75231700	-0.30282300	C	-0.99589100	-1.98703100	0.52592700
C	-4.22247800	-1.03509100	0.45397400	H	-0.26131300	-2.70738300	0.91318700
C	-0.45788000	-1.33164100	-0.66033700	H	-1.16416900	-1.23427500	1.31059400
H	-3.44158600	-1.63744500	-1.38824300	C	-2.32865900	-2.69586100	0.19652400
C	-0.09980500	-0.81950500	-1.72060200	H	-2.13566700	-3.47873600	-0.54886400
H	-0.02117800	-0.49190000	-2.74212600	H	-2.64461800	-3.21030800	1.11345200
Au	1.59943500	-0.14485100	-0.40738400	C	-4.24741100	-1.07524300	1.95193800
P	3.54190900	0.76036300	0.51362000	H	-3.83136600	-0.15116200	2.38050800
C	3.24690200	1.79681300	1.97884400	H	-5.27983000	-1.14822900	2.32240900
H	4.19935000	2.19732000	2.34959600	H	-3.68049700	-1.91380300	2.37177900
H	2.58607000	2.62988400	1.71545300	C	-5.22128300	-0.11051600	-0.18395200
H	2.77219900	1.20808800	2.77097700	H	-5.16078200	-0.19458300	-1.27983400
C	4.75335800	-0.49517700	1.02850300	H	-6.24006600	-0.42322700	0.09899600
H	5.03877800	-1.11015400	0.16785000	C	-5.02731400	1.35327900	0.22159400
H	5.64864000	-0.00534800	1.43287700	H	-3.98253400	1.64485900	0.01452100
H	4.31959600	-1.14440800	1.79672100	H	-5.21238200	1.52692800	1.28927000
C	4.43157100	1.83347700	-0.65613300	C	-5.90831600	2.27985000	-0.56888000
H	3.80058400	2.68251800	-0.94083600	H	-5.95790400	2.04682400	-1.66211800
H	5.34946800	2.20858200	-0.18500700	O	-6.51687100	3.21333900	-0.10643400
H	4.69555900	1.27081900	-1.55809900				

Table T23: Optimized geometry for $\mathbf{TS_{I\text{-}II}}$

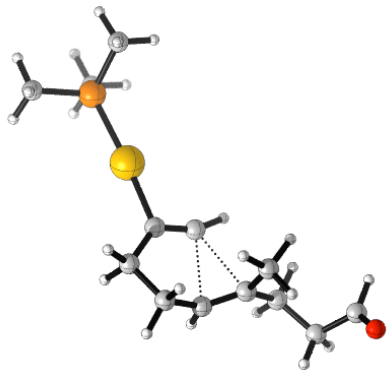

Free energy G = -1060.585505 Hartree/particle.

C	-0.82244400	2.33953400	0.09624900	H	-4.02821800	-0.30280500	-2.11249300
C	-0.46839200	0.90675700	-0.08723800	C	4.31189800	-1.40210300	-1.47597100
C	-1.24909300	-0.05674700	-0.37689000	C	4.91670600	0.77651200	0.31415100
C	-3.65647400	0.28656000	-0.08641300	C	4.11906300	-1.78266000	1.38104800
C	-3.05390500	1.43265700	-0.50916300	H	5.36368500	-1.69965900	-1.37534800
C	-2.35361900	2.43372500	0.33313100	H	3.70439500	-2.29078100	-1.67907500
C	-4.29489800	-0.62579200	-1.09815400	H	4.21353000	-0.71045700	-2.32002800
C	-3.82047600	-0.11015300	1.34636300	H	5.94583500	0.39485900	0.32773200
Au	1.50630600	0.12060600	-0.02461000	H	4.81605500	1.51122400	-0.49205500
P	3.74225200	-0.59253500	0.05380900	H	4.70511100	1.27312800	1.26741400
H	-0.26526800	2.80971700	0.91500100	H	5.18288000	-2.05256300	1.35211700
H	-0.53538500	2.87364300	-0.82163200	H	3.88819500	-1.33956000	2.35610300
H	-2.68710900	3.44792600	0.07900600	H	3.51560900	-2.68841700	1.25632900
H	-2.56179600	2.28090000	1.39793700	C	-5.82446900	-0.68342700	-0.96686800
H	-3.06201000	1.63512300	-1.58425500	H	-6.23170900	-1.08705500	-1.90726900
H	-1.49108900	-1.06635000	-0.66927500	H	-6.26230800	0.31248100	-0.81856400
H	-3.61618600	-1.18256200	1.47767200	C	-6.29984400	-1.59976300	0.12763200
H	-3.16932300	0.44067100	2.03045800	H	-5.82519300	-2.61377700	0.11302300
H	-4.85838200	0.05595000	1.67020900	O	-7.12539800	-1.31043000	0.95787400
H	-3.89437200	-1.64867700	-0.97620800				

Table T24: Optimized geometry for **II**

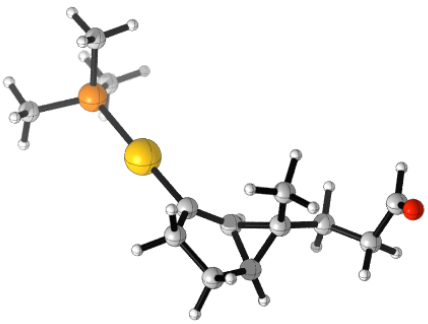

Free energy G = -1060.618707 Hartree/particle.

C	-1.03924600	2.13452500	0.72018400	H	-3.61521900	-0.56096100	-2.19291900
C	-0.59093600	0.96697100	-0.08037500	C	3.96216800	-1.77448900	-1.31839100
C	-1.62567600	0.50839200	-0.90454000	C	4.85898200	0.59761100	0.05671200
C	-3.05206900	0.12517100	-0.23659700	C	3.84995100	-1.64361600	1.55596600
C	-2.87011100	1.47267000	-0.73931400	H	4.98679400	-2.14826700	-1.19444100
C	-2.44557900	2.54613400	0.23930700	H	3.27066300	-2.62439400	-1.33497600
C	-3.77912300	-0.84832800	-1.14650400	H	3.88600400	-1.24436600	-2.27422900
C	-3.13631100	-0.20829000	1.22869100	H	5.83875100	0.10765000	0.12693300
Au	1.32742300	0.22527500	-0.03819000	H	4.81912800	1.19005100	-0.86385100
P	3.53387700	-0.65453400	0.05589800	H	4.73338900	1.27184500	0.91100100
H	-0.93872200	1.92482900	1.79843400	H	4.87500600	-2.03577700	1.53835300
H	-0.30760500	2.94113200	0.55113400	H	3.71832700	-1.02217400	2.44860900
H	-2.41350900	3.52054400	-0.25890600	H	3.14507200	-2.48083900	1.60755800
H	-3.15979000	2.63259100	1.06812700	C	-5.28568600	-0.88075800	-0.86749500
H	-3.37294000	1.75111100	-1.66626500	H	-5.78620800	-1.29369600	-1.75756200
H	-1.42912000	-0.09124200	-1.79085800	H	-5.69739500	0.12365900	-0.69735100
H	-2.87596000	-1.26019900	1.40316700	C	-5.67211300	-1.77465400	0.27962800
H	-2.49697700	0.40557000	1.86835500	H	-5.21085100	-2.79343900	0.23892000
H	-4.16886100	-0.05557800	1.57161800	O	-6.42077500	-1.46335100	1.17254300
H	-3.35382600	-1.85796300	-1.02630200				

Table T25: Optimized geometry for $\mathbf{TS_{II\text{-}III}}$

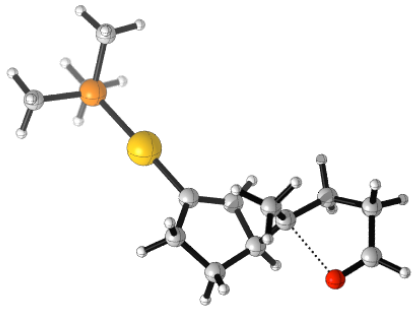

Free energy G = -1060.61346 Hartree/particle.

C	1.18177900	-1.95027400	0.39918700	H	3.45731500	-0.75031200	-1.75979300
C	0.61245400	-0.68640600	-0.19333100	H	1.47571800	0.94342100	-1.36960900
C	1.58085000	-0.00161400	-0.83997000	H	3.84698400	0.93269000	2.13297600
C	3.54306300	0.21960500	0.12175800	H	2.43440500	-0.11416900	1.91091900
C	2.94744600	-0.74256900	-0.78858700	H	4.04481900	-0.82647800	1.90194900
C	2.58008200	-2.11468400	-0.23078100	H	3.32195800	2.31245000	-0.07419200
C	4.01032700	1.52890900	-0.42594700	H	3.96249700	1.51357500	-1.52206700
C	3.47010500	0.05669100	1.59638600	C	-4.50745800	0.73651900	-1.50884000
Au	-1.37936500	-0.15567800	-0.07387100	C	-4.72362000	-0.84014900	0.88376400
P	-3.67540700	0.42438900	0.08642200	C	-4.01691900	1.93712700	1.05164400
H	1.21117700	-1.86996900	1.49993900	H	-5.56004900	0.99895900	-1.34079100
H	0.53645000	-2.81506100	0.19615400	H	-4.01033600	1.55970200	-2.03418800
H	2.52932200	-2.82004000	-1.06827800	H	-4.45609000	-0.15864000	-2.13845500
H	3.33783100	-2.50139800	0.46242100	H	-5.76712500	-0.50074900	0.92069000

H	-4.67006000	-1.77944200	0.32196500	H	5.46579300	2.28449000	1.05009000
H	-4.36938500	-1.02569400	1.90404400	H	5.86388300	2.66457800	-0.60898400
H	-5.09709300	2.13092700	1.08476200	C	6.27177800	0.64572900	0.00734700
H	-3.64080100	1.81959000	2.07404100	H	7.37137200	0.75238400	0.05777800
H	-3.51156200	2.79370300	0.59155300	O	5.75469500	-0.45385300	-0.03000400
C	5.43117800	1.88095800	0.02513100				

Table T26: Optimized geometry for **III**

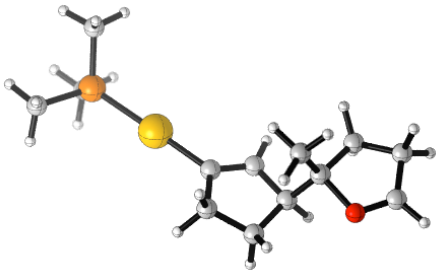

Free energy G = -1060.616754 Hartree/particle.

C	1.19018700	-1.92839800	0.32234500	H	3.96540400	1.67526300	-1.41539400
C	0.60775900	-0.64599500	-0.23199300	C	-4.54158700	0.70654400	-1.49758500
C	1.58411300	0.07530400	-0.81109500	C	-4.72581300	-0.88807200	0.88082200
C	3.84640200	0.21590500	0.18517000	C	-4.07496700	1.89659000	1.06744300
C	2.94940200	-0.58774800	-0.73757000	H	-5.59779500	0.95216200	-1.32616900
C	2.61167300	-2.01153100	-0.26542100	H	-4.05811400	1.53936400	-2.02067000
C	4.21446600	1.60053600	-0.35002900	H	-4.47757500	-0.18424700	-2.13242200
C	3.50088900	0.19594200	1.65073400	H	-5.77437700	-0.56519200	0.92463300
Au	-1.38589200	-0.14366200	-0.08044300	H	-4.65967100	-1.82143800	0.31040300
P	-3.69435600	0.39767700	0.09216000	H	-4.36507800	-1.07886100	1.89793900
H	1.19283800	-1.89163200	1.42470700	H	-5.15933000	2.06638800	1.10054900
H	0.58762200	-2.80824900	0.05842400	H	-3.69716300	1.78063300	2.08951800
H	2.60819300	-2.66795600	-1.14430900	H	-3.58775400	2.76767700	0.61481000
H	3.35325200	-2.42764300	0.42978600	C	5.72726600	1.73067600	-0.15774200
H	3.45256700	-0.59494000	-1.72001400	H	6.02226100	2.24776300	0.77203600
H	1.45553300	1.05055100	-1.28407500	H	6.26233700	2.25059200	-0.96181800
H	4.19155400	0.81539300	2.23751200	C	6.16227200	0.33438200	-0.03544700
H	2.49007100	0.60515600	1.76573200	H	7.19020500	-0.03657300	-0.05750800
H	3.51031500	-0.82090300	2.05711100	O	5.25319100	-0.50162400	0.13157700
H	3.65763200	2.37899600	0.18140300				

Table T27: Optimized geometry for $\mathbf{TS_{III\text{-}IV}}$

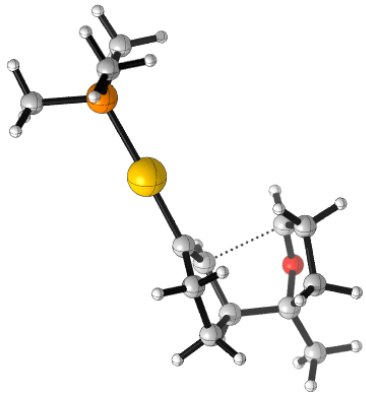

Free energy G = -1060.612966 Hartree/particle.

C	1.55990900	-1.69685900	0.85141000	H	3.62105600	-0.21639400	1.94907300
C	0.89685800	-0.75635300	-0.11963700	C	-4.46041600	-0.86328100	-0.93398900
C	1.83918000	-0.30487900	-0.99807800	C	-4.15370500	0.28544100	1.68073000
C	4.14148800	0.26225900	-0.12737500	C	-3.86223000	1.93476200	-0.65689300
C	3.22770200	-0.84877900	-0.72397700	H	-5.51523700	-0.56670600	-0.86594200
C	2.94227000	-2.00874700	0.24684700	H	-4.15511000	-0.86962800	-1.98634500
C	3.81870700	0.65370800	1.31910600	H	-4.34499700	-1.87673100	-0.53337900
C	5.59829700	0.07056200	-0.42875300	H	-5.22432600	0.52185200	1.62438500
Au	-1.09699600	-0.23798300	-0.05532300	H	-4.02806300	-0.70374200	2.13516200
P	-3.41405400	0.29588900	0.01173700	H	-3.65543200	1.02520300	2.31705200
H	1.60301900	-1.23602000	1.85493900	H	-4.94622100	2.09139000	-0.58259900
H	0.95741900	-2.60514500	0.99275800	H	-3.34665900	2.72256500	-0.09630600
H	2.88059700	-2.93787300	-0.33184000	H	-3.56195600	2.00183200	-1.70856700
H	3.73037900	-2.16165900	0.99643500	C	2.61007300	1.59522700	1.19555600
H	3.71906000	-1.19958300	-1.64245100	H	2.78300500	2.57245100	1.67426900
H	1.60695000	0.23759800	-1.91506800	H	1.66446800	1.21669600	1.59496400
H	6.20213100	0.90577900	-0.05589300	C	2.57184700	1.82317600	-0.26964700
H	5.94264300	-0.84834300	0.06297400	H	1.90257100	2.49516600	-0.80655500
H	5.76435400	-0.03975900	-1.50638200	O	3.65213800	1.47186900	-0.86746900
H	4.67688900	1.18104600	1.75176000				

Table T28: Optimized geometry for **IV**

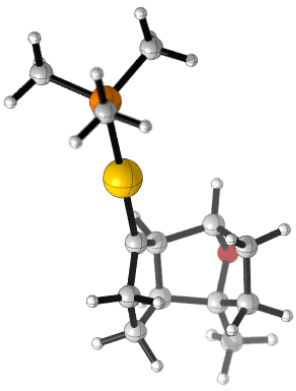

Free energy G = -1060.6298 Hartree/particle.

C	1.56182000	-1.82303200	0.65505800	H	3.49153500	-0.18410300	1.98627600
C	0.92103000	-0.75264300	-0.12785300	C	-4.34382800	-0.46484800	-1.31753900
C	1.93493100	-0.07308900	-0.92296200	C	-4.21380200	-0.22893900	1.55472200
C	4.11839000	0.38217600	-0.05664200	C	-3.74524300	2.08494900	-0.10518200
C	3.29888000	-0.76494000	-0.69451800	H	-5.40279100	-0.19229200	-1.22279100
C	2.99855200	-2.01226900	0.14342100	H	-3.97037100	-0.12369100	-2.28954200
C	3.62598400	0.70884400	1.36376200	H	-4.24758900	-1.55516600	-1.26884500
C	5.60625600	0.26490400	-0.21722900	H	-5.27576900	0.04651800	1.52055700
Au	-1.06256100	-0.24914100	-0.05303700	H	-4.12839100	-1.31550600	1.66681400
P	-3.37864700	0.30364100	0.02442200	H	-3.74607700	0.24922400	2.42249100
H	1.49240700	-1.48677500	1.71083700	H	-4.82963300	2.24837700	-0.05924900
H	0.94377400	-2.73460500	0.65864400	H	-3.26645000	2.62734900	0.71747200
H	3.04577900	-2.91060700	-0.48246100	H	-3.36263000	2.47886100	-1.05329400
H	3.71743500	-2.16255500	0.95881600	C	2.31925900	1.48175400	1.08774000
H	3.77869600	-1.02303000	-1.64661800	H	2.40390300	2.52832100	1.40017800
H	1.60602900	0.01837100	-1.96889700	H	1.42793300	1.06554000	1.57801300
H	6.11112000	1.15786700	0.17016300	C	2.26435900	1.41364900	-0.43850200
H	5.97645700	-0.60642000	0.33901500	H	1.65834500	2.17024600	-0.94302100
H	5.87651900	0.13954900	-1.27284800	O	3.60996700	1.50621200	-0.81427400
H	4.36253200	1.34322900	1.87041900				

Table T29: Optimized geometry for **TS_{II-V}**

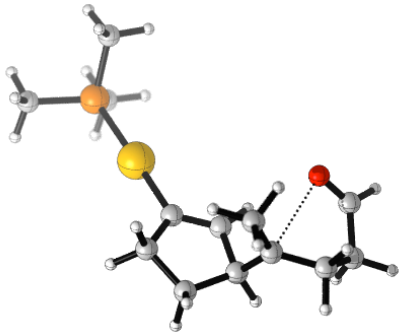

Free energy G = -1060.603562 Hartree/particle.

C	1.16987400	-2.29236900	0.05346300	H	0.52125500	-3.03727800	-0.42664400
C	0.72635900	-0.88463800	-0.23272300	H	2.64223200	-2.86148900	-1.45323900
C	1.76726500	-0.12302000	-0.60220200	H	3.28108300	-2.96395500	0.18158600
C	3.94205500	-0.39850600	0.39067400	H	3.59706600	-0.78465500	-1.65035400
C	3.10415800	-0.92248400	-0.67760100	H	1.76222000	0.93850500	-0.83298000
C	2.61787000	-2.37926800	-0.46866500	H	3.76715700	0.18659800	2.41375000
C	5.18610500	0.33649300	0.06370100	H	2.72260200	-1.20629000	1.97581200
C	3.68408300	-0.71914500	1.80055300	H	4.49523800	-1.38741300	2.13947800
Au	-1.22793200	-0.22634500	-0.09485200	H	5.82241800	-0.40066900	-0.45813800
P	-3.48043900	0.49216600	0.09528900	H	5.70801700	0.63902800	0.97966000
H	1.10232100	-2.50020300	1.13392800	C	-4.12093100	1.45135100	-1.32056500

C	-4.68750500	-0.86765300	0.27525800	H	-3.56552400	1.03434100	2.45936500
C	-3.81993300	1.56425500	1.53455800	H	-3.20810700	2.47144900	1.47659100
H	-5.16406300	1.74314400	-1.14118100	C	5.01153400	1.54718000	-0.85236600
H	-3.51539700	2.35285100	-1.46668200	H	4.60919200	1.27722400	-1.84243400
H	-4.06893800	0.84710400	-2.23319100	H	5.97870600	2.02737300	-1.04666500
H	-5.70405100	-0.46581000	0.37810200	C	4.05443400	2.50824500	-0.21423400
H	-4.64601200	-1.51919800	-0.60480600	H	4.02881400	3.54320400	-0.60902900
H	-4.44554600	-1.46604800	1.16086600	O	3.32015500	2.15781700	0.68383700
H	-4.88091600	1.84578700	1.56042100				

Table T30: Optimized geometry for **V**

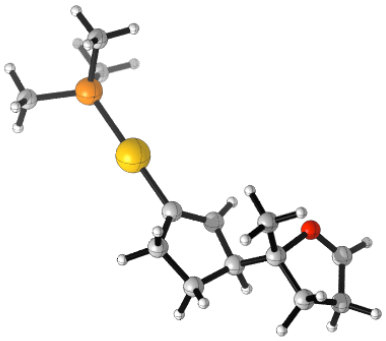

Free energy G = -1060.616739 Hartree/particle.

C	-1.21897400	1.99847400	0.13128600	H	-5.85461800	0.39754600	1.30752400
C	-0.64030900	0.65663800	-0.26166900	C	4.23475900	-1.66339400	-1.10251200
C	-1.63094500	-0.14931000	-0.68391300	C	4.83049200	0.97429700	-0.15305800
C	-3.91088500	-0.07248600	0.45244300	C	4.15203300	-1.09759600	1.70769100
C	-2.99975100	0.49102400	-0.63760800	H	5.29925400	-1.88037600	-0.94328900
C	-2.67069000	1.97938100	-0.38388900	H	3.65736800	-2.58686600	-0.98110700
C	-5.37835400	0.34381700	0.32152700	H	4.09076100	-1.29761500	-2.12541500
C	-3.36165700	-0.04242700	1.84897600	H	5.86464900	0.61557700	-0.06477900
Au	1.35586200	0.16837400	-0.09919100	H	4.68579900	1.41501100	-1.14589100
P	3.65586000	-0.40496800	0.09028000	H	4.65316600	1.75142300	0.59902100
H	-1.16673400	2.12377100	1.22559000	H	5.22051000	-1.35052000	1.70413400
H	-0.65143100	2.83921200	-0.29029100	H	3.95890500	-0.36543500	2.49989500
H	-2.73385900	2.51164700	-1.34074300	H	3.56874300	-2.00022400	1.92202300
H	-3.37744800	2.47586100	0.29622800	C	-6.04458300	-0.74169600	-0.52886500
H	-3.54587200	0.37388200	-1.59159500	H	-6.13542900	-0.48838500	-1.59925500
H	-1.50455100	-1.18251600	-1.01011500	H	-7.05391700	-1.03623200	-0.21452400
H	-3.99476100	-0.61866700	2.53359500	C	-5.10673900	-1.86378300	-0.42214700
H	-2.33737700	-0.42874900	1.87948800	H	-5.26776300	-2.88918100	-0.76448200
H	-3.35157900	0.99744600	2.19922400	O	-4.00574300	-1.60156300	0.10025600
H	-5.45528300	1.33126500	-0.14493000				

Chapter III:

Gold(I)-Catalyzed Synthesis of Natural Products: Studies Towards the Synthesis of Pycnanthuquinones and Carexanes

Introduction

Gold Catalysis in Total synthesis

Gold chemistry constitutes a powerful tool for the construction of complex polycyclic skeletons from relatively simple substrates under mild reaction conditions. The notable chemo-, regio- and stereoselectivities of these processes, combined with high functional group compatibility and atom economy, have led to the development of new creative disconnections for target molecules. The application of gold catalysis in the total synthesis of natural products and molecules with pharmaceutical interest has grown during the last decade along with the discovery of novel methodologies and catalysts.[1]

As illustrative examples, (–)-mersicarpine,[2] (–)-GSK1360707[3] and gomerone C[4] have been recently synthesized using gold catalysis in the key step (Scheme 1). The alkaloid (–)-mersicarpine was isolated from the *Kopsia* species of plants and features an atypical tetracyclic structure with a seven-membered cyclic imine. A gold-catalyzed hydroamination of alkynes was used to build the indole core. In the second case, the antidepressive drug candidate (–)-GSK1360707 was obtained via enantioselective cycloisomerization of 1,6-enynes using a chiral phosphoramidite gold catalyst. Lastly, gomerone C was isolated from the red algae *Laurencia majuscula* found at the southern coast of La Gomera. The tricyclic core skeleton was prepared via gold-catalyzed conia-ene reaction of chlorinated silyl enol ether **1**.

---

1 (a) Rudolph, M.; Hashmi, A. S. K. *Chem. Soc. Rev.* **2008**, *37*, 1766–1775. (b) Rudolph, M.; Hashmi, A. S. K. *Chem. Soc. Rev.* **2012**, *41*, 2448–2462. (c) Zhang, Y.; Luo, T.; Yang, Z. *Nat. Prod. Rep.* **2014**, *31*, 489–503. (d) Pflästerer, D.; Hashmi, A. S. K. *Chem. Soc. Rev.* **2016**, *45*, 1331–1367.

2 Nakajima, R.; Ogino, T.; Yokoshima, S.; Fukuyama, T. *J. Am. Chem. Soc.* **2010**, *132*, 1236–1237.

3 Teller, H.; Fürstner, A. *Chem.–Eur. J.* **2011**, *17*, 7764–7767.

4 Huwyler, N.; Carreira, E. M. *Angew. Chem. Int. Ed.* **2012**, *51*, 13066–13069.

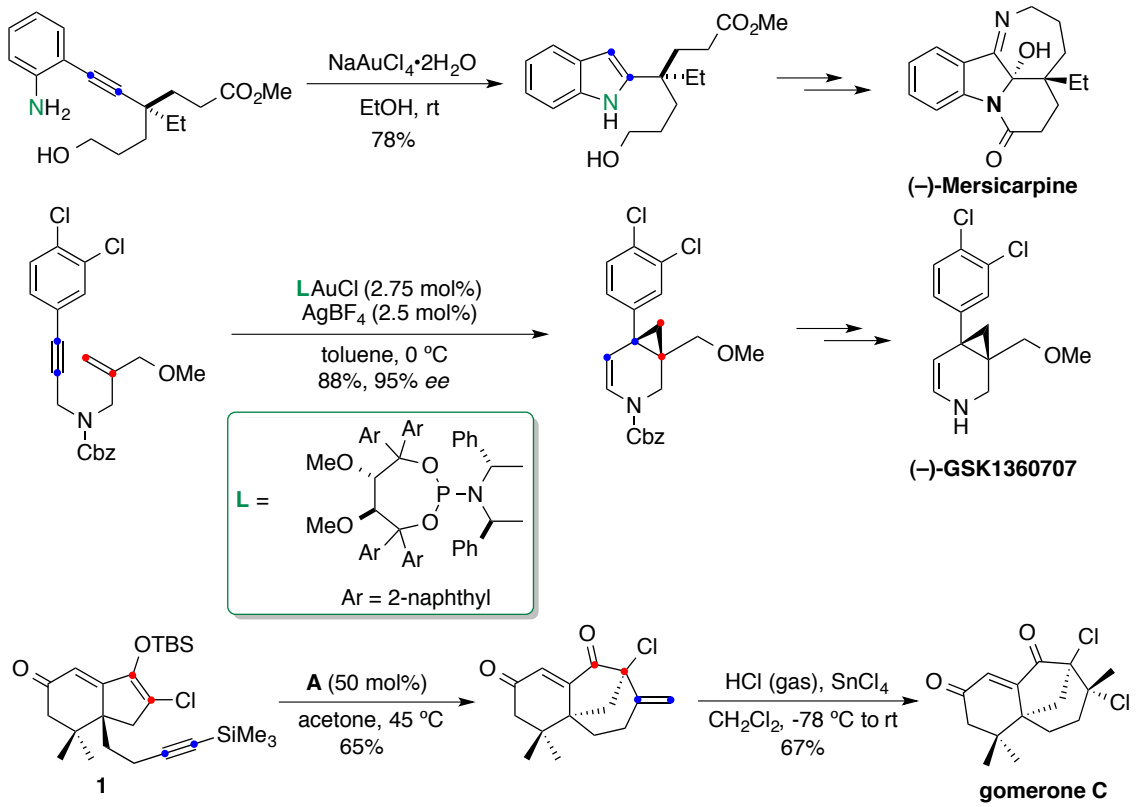

Scheme 1. Natural products synthesized via gold catalysis

Our group has also contributed significantly in this field, which has resulted in total syntheses of several bioactive sesquiterpenes (Figure 1). An emblematic example is the synthesis of (–)-englerin A,[5] in which the oxatricyclic skeleton was built through a formal [2+2+2] alkyne/alkene/carbonyl gold(I)-catalyzed cycloaddition reaction. Also remarkable is the synthesis of the antiviral (+)-schisanwilsonene A,[6] isolated from the plant *Schisandra wilsoniana*. In this case, the key step involved a fully stereoselective tandem cyclization/1,5-migration/intermolecular cyclopropanation. Likewise, the short synthesis of (–)-epiglobulol, (–)-4α,7α-aromadendranediol, and (–)-4β,7α-aromadendranediol was achieved using a stereodivergent gold(I)-catalyzed cascade reaction.[7]

5 Molawi, K.; Delpont, N.; Echavarren, A. M. *Angew. Chem. Int. Ed.* **2010**, *49*, 3517–3519.

6 Gaydou, M.; Miller, R.E.; Delpont, N.; Ceccon, J.; Echavarren, A. M. *Angew. Chem. Int. Ed.* **2013**, *52*, 6396–6399.

7 Carreras, J.; Livendahl, M.; McGonigal, P. R.; Echavarren, A. M. *Angew. Chem. Int. Ed.* **2014**, *53*, 4896–4899.

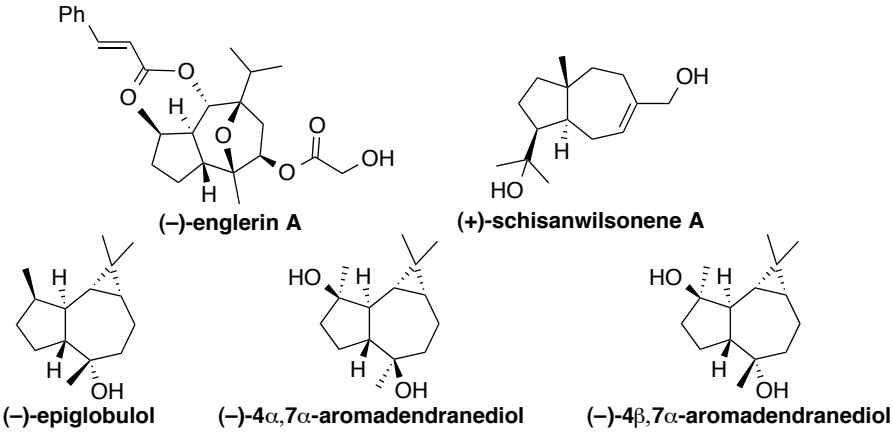

Figure 1. Examples of bioactive sesquiterpenes synthesized by our group using gold catalysis

More recent examples include the syntheses of (+)-rumphellaone A and (+)-hushinone[8] by using a diastereoselective gold(I)-catalyzed [2+2] macrocyclization, as well as the synthesis of lundurines A−C[9] through the key intermediate **2**, which was prepared through a gold(I)-catalyzed intramolecular hydroarylation reaction (Scheme 2).

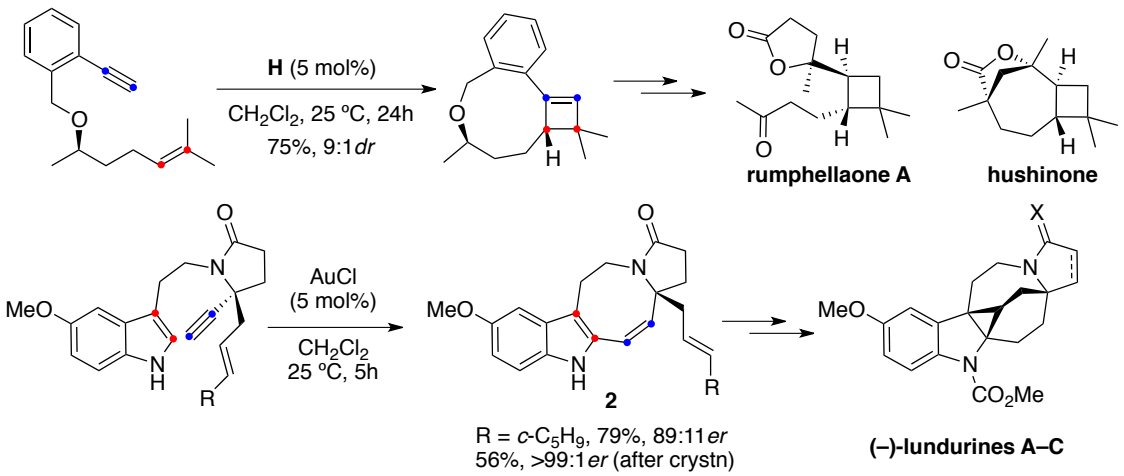

Scheme 2. Recent examples reported by our group on the application of gold catalysis

The gold(I)-catalyzed oxidative cyclization has also been applied on the synthesis of several natural compounds. Although the majority of these products have been prepared by intermolecular alkyne oxidation, as in the case of pimprinine and its congener WS-

8 Ranieri, B.; Obradors, C.; Mato, M.; Echavarren, A. M. *Org. Lett.* **2016**, *18*, 1614–1617.

9 Kirillova, M. S.; Muratore, M. E.; Dorel, R.; Echavarren, A. M. *J. Am. Chem. Soc.* **2016**, *138*, 3671–3674.

30581B (Scheme 3),[10] the oxygen transfer can also take place intramolecularly. Thus, for example, alkyne **3** was converted into the corresponding *N*-oxide that underwent oxidative cyclization to generate quinolizidine **4**, a key intermediate in the synthesis of alkaloid (±)-decinine.[11]

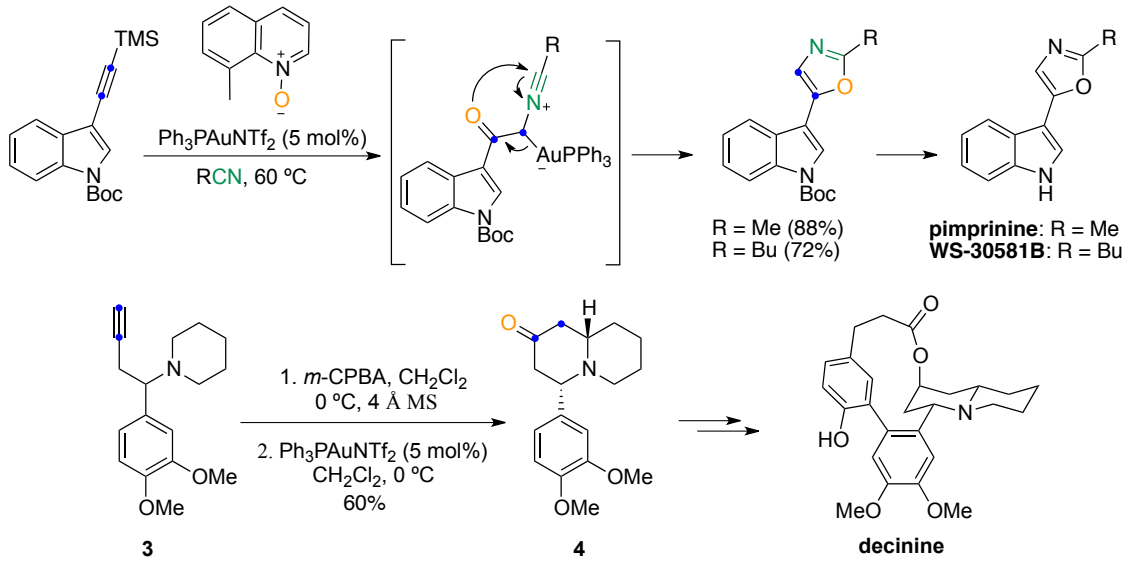

Scheme 3. Selected examples of natural products synthesized via gold(I)-catalyzed oxidative cyclization

More recently, the gold(I) mediated oxidative cycloisomerization of 1,5-enynes was used as a key step in the first enantioselective total synthesis of (–)-nardoaristolone B, a natural sesquiterpene isolated from the roots of *Nardostachys chinensis* Batal (Scheme 4).[12]

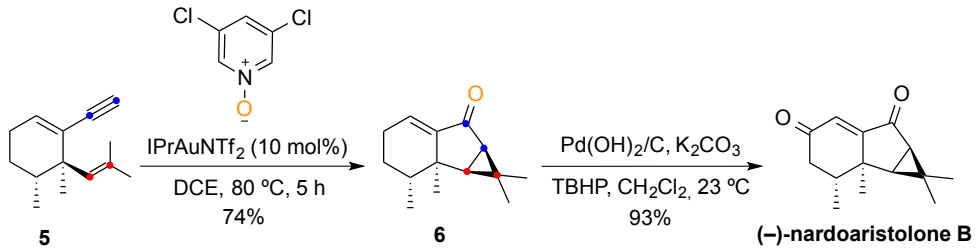

Scheme 4. Synthesis of (–)-nardoaristolone B via gold(I)-catalyzed oxidative cycloisomerization

10 Yundong, W.; Yuejun, O.; Pengcheng, Q.; Weimin, H.; Jiannan, X. *Acta Chim. Sin.* **2012**, *70*, 1367–1370.

11 Shan, Z.-H.; Liu, J.; Xu, L.-M.; Tang, Y.-F.; Chen, J.-H.; Yang, Z. *Org. Lett.* **2012**, *14*, 3712–3715.

12 Homs, A.; Muratore, M. E.; Echavarren, A. M. *Org. Lett*. **2015**, *17*, 461–463.

Pycnanthuquinones

Pycnanthuquinone C is the simplest of the pycnanthuquinones, a family of natural products that has been isolated from very different biological sources (Figure 2).

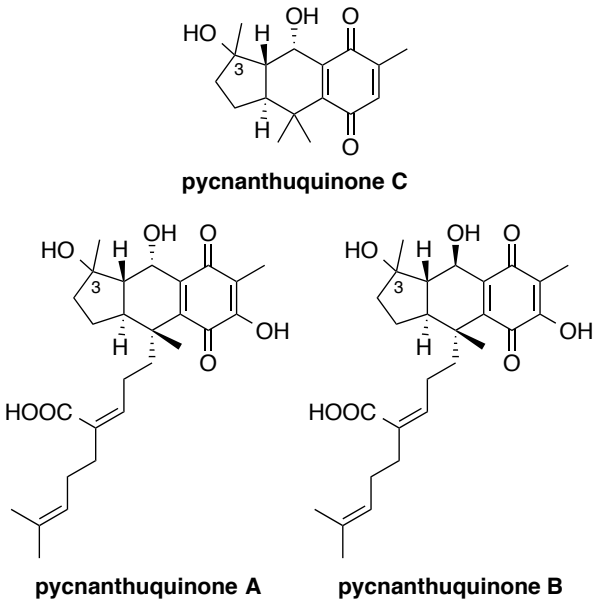

Figure 2. Structures of the pycnanthuquinone natural product family

The more complex pycnanthuquinones A and B have been found in *Pycnanthus angolensis,* a West African tree used in traditional African medicine, in the search for compounds that have antihyperglycemic activity (Figure 3).[13] Posterior investigation of the brown alga *Cystophora harveyi* led to the isolation of pycnanthuquinone C.[14]

Figure 3. *Pycnanthus angolensis* (left) and *Cystophora harveyi* (right)

13 Fort, D. M.; Ubillas, R. P.; Mendez, C. D.; Jolad, S. D.; Inman, W. D.; Carney, J. R.; Chen, J. L.; Ianiro, T. T.; Hasbun, C.; Bruening, R. C.; Luo, J.; Reed, M. J.; Iwu, M.; Carlson, T. J.; King, S. R.; Bierer, D. E.; Cooper, R. *J. Org. Chem.* **2000**, *65*, 6534–6539.

14 Laird, D. W.; Poole, R.; Wikström, M.; van Altena, I. A. *J. Nat. Prod.* **2007**, *70*, 671–674.

Despite the efforts to elucidate completely the configuration of these meroterpenoids, the use of spectroscopic methods only allowed to the assignment of the ring junction as *trans* and the relative configuration of C-1 and C-2, while the relative configuration with respect to C-3 could not be determined.

In 2010, the group of Trauner reported a three-step, protecting-group-free synthesis of unnatural (−)-pycnanthuquinone C through a vinyl quinone Diels–Alder (VQDA) process (Scheme 5).[15] This synthesis provided strong evidence for the formation of the pycnanthuquinone skeleton through a biosynthetic cycloaddition.

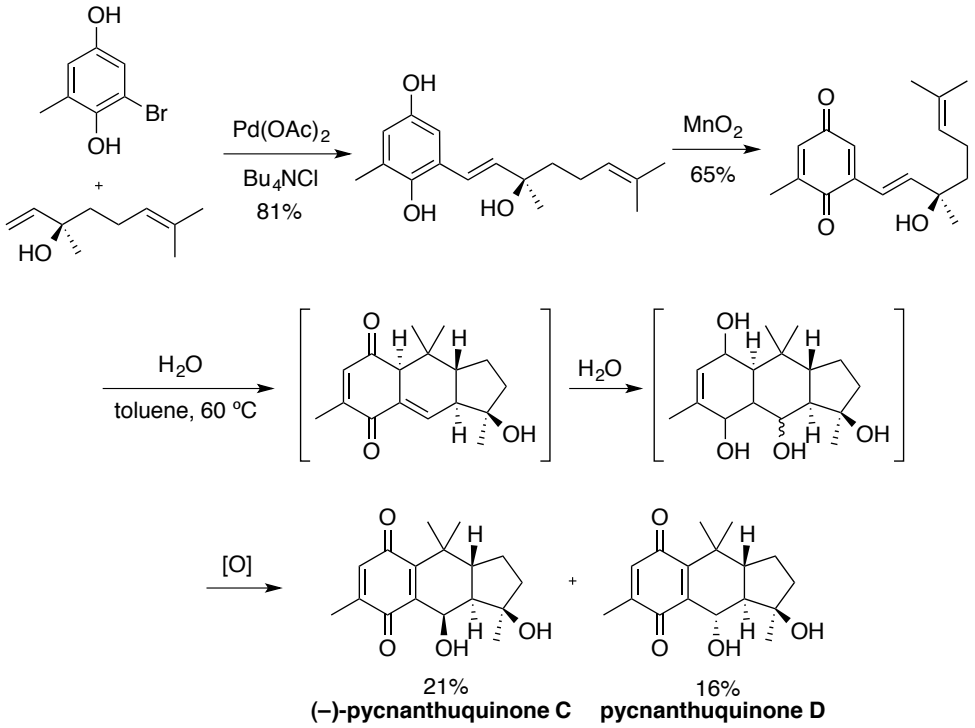

Scheme 5. Biomimetic synthesis of (–)-pycnanthuquinone C and pycnanthuquinone D

Despite the importance of these biologically active terpenoids and the singularity of this linear fused 5,6,6-ring core, this biomimetic synthesis constitutes the only example reported in the literature to our days.

Therefore, we considered we could use an intramolecular gold(I)-catalyzed [4+2] cycloaddition reaction for the construction of the 5,6,6-tricyclic skeleton of the pycnanthuquinones (Scheme 6). As mentioned in the **General Introduction**, 1,6-enynes bearing an aryl group react stereospecifically with gold(I) catalysts to afford

15 Löbermann, F.; Mayer, P.; Trauner, D. *Angew. Chem. Int. Ed.* **2010**, *49*, 6199–6202.

tricyclic products resulting from a formal intramolecular [4+2] cycloaddition.[16] Interestingly, this transformation proceeds under mild conditions and various electron donating and electron withdrawing substituents at several positions of the arene are well tolerated.

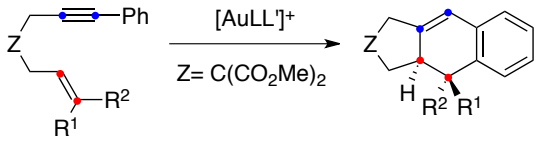

Scheme 6. Intramolecular gold(I)-catalyzed [4+2] cycloaddition reaction

According to the proposed mechanism, once the cyclopropyl gold(I) carbene **8** is formed, a Friedel-Crafts-type reaction takes place leading to intermediate **10**. Final aromatization and protodemetalation give access to tricyclic products **12** (Scheme 7).

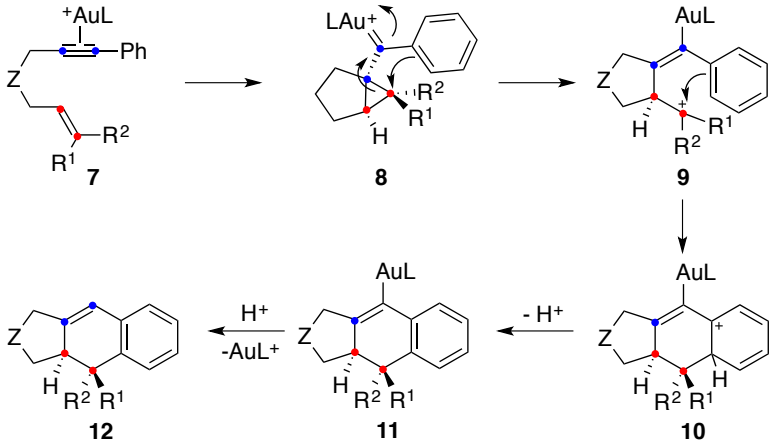

Scheme 7. Proposed mechanism for the formal [4+2] cycloaddition reaction of 1,6-arylenynes

To date, several strategies have been explored towards the synthesis of (+)-pycnanthuquinone C. Initial investigations were focused on the intramolecular gold(I)-catalyzed [4+2] cycloaddition reaction of 1,6-arylenynes differing on the substitution at C-3 (Schemes 8-10).[17] Firstly, 1,6-enyne **13** bearing no functional groups at this position was examined (Scheme 8). After treatment of **13** with cationic gold(I) catalyst **D**, tricyclic precursor **14** was obtained stereospecifically in quantitative yield. Despite the efforts to functionalize **14**, the most advanced intermediate that could be obtained

16 Nieto-Oberhuber, C.; Pérez-Galán, P.; Herrero-Gómez, E.; Lauterbach, T.; Rodríguez, C.; López, S.; Bour, C.; Rosellón, A.; Cárdenas, D. J.; Echavarren, A. M. *J. Am. Chem. Soc.* **2008**, *130*, 269–279.

17 Pérez-Galán, P.; Lauterbach, T. ICIQ PhD Thesis 2008, unpublished results.

through this approach was the quinone adduct **16** with the skeleton of the natural product**.** As illustrated in Scheme 8, **16** was prepared via hydrogenation of the double bond followed by oxidation with ceric ammonium nitrate (CAN).

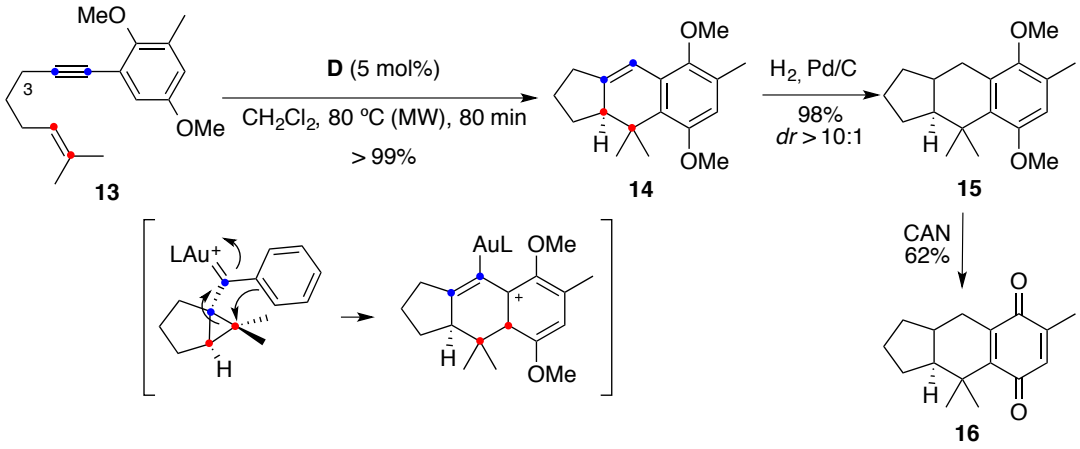

Scheme 8. Strategy 1: toward the synthesis of pycnanthuquinone C

Later, the gold(I)-catalyzed cyclization of higher functionalized 1,6-arylenynes was also examined. Unfortunately, substrates with secondary alcohols at the propargylic position failed to give the expected [4+2] cycloaddition product. As an example, arylenyne **17** reacted with cationic gold complex **D** leading to 1,3-diene **18** through a 6-*endo-dig* cyclization with migration of the OR group (Scheme 9).

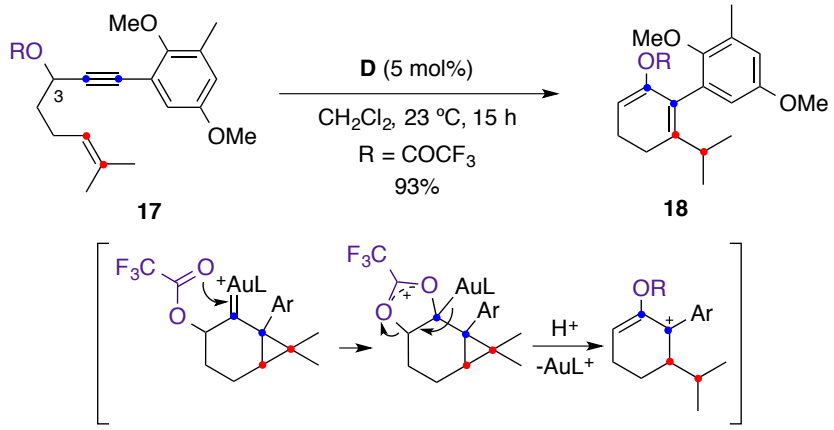

Scheme 9. Strategy 2: toward the synthesis of pycnanthuquinone C

On the other hand, arylenyne **19** bearing a tertiary alcohol at the propargylic position led to the unexpected formation of bicyclic product **20**. As illustrated in Scheme 10, this transformation occurs through the intramolecular trapping of cyclopropyl gold intermediate **21** to generate **22**.

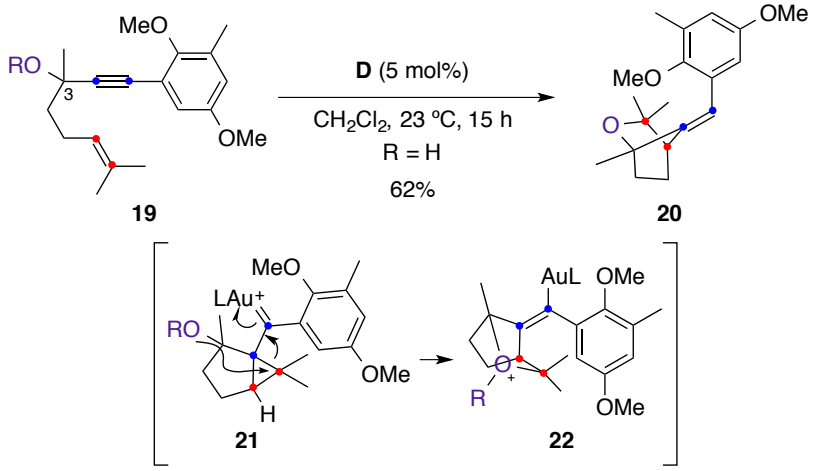

Scheme 10. Strategy 3: toward the synthesis of pycnanthuquinone C

Protection of the hydroxyl group with MOM, methyl, TEM, PMB, *tert*-butyl acetate or $COCF_3$, failed to give any tricyclic product in the presence of gold catalysts. Additionally, 1,6-enynes bearing different substituents on the aryl moiety were also examined.[18] Interestingly, after treatment of 1,6-arylenyne **23** with gold complex **D** four different tricyclic products could be obtained, albeit in low yield (Scheme 11).

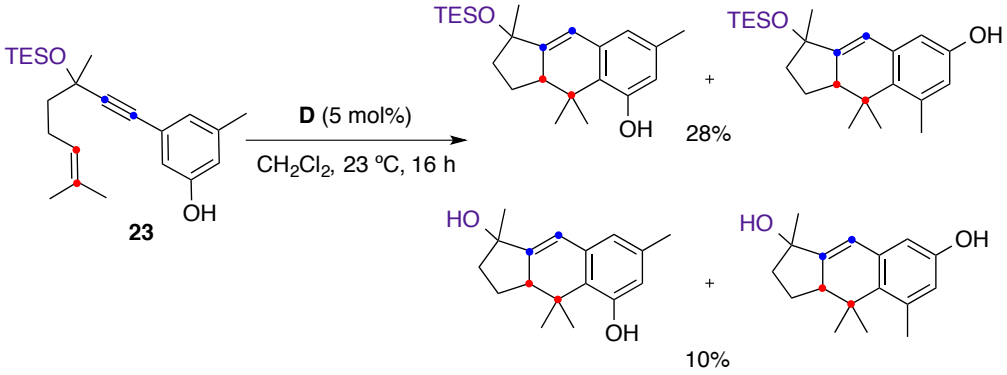

Scheme 11. Cyclization of 1,6-arylenyne **23**

In parallel, an alternative approach based on the intramolecular gold(I)-catalyzed [4+2] cycloaddition of 1,5-benzylenynes [19] was applied for the synthesis of tricyclic intermediate **25** (Scheme 12).[20] Thus, 1,5-benzylenyne **24** reacted with gold(I) catalyst **A** to generate stereospecifically **25** in 95% yield.

18 Huguet, N.; McGonigal, P. R. ICIQ 2010, unpublished results.

19 López-Carrillo, V.; Huguet, N.; Mosquera, Á.; Echavarren, A. M. *Chem.–Eur. J.* **2011**, *17*, 10972–10978.

20 Huguet, N. ICIQ PhD Thesis 2013, unpublished results.

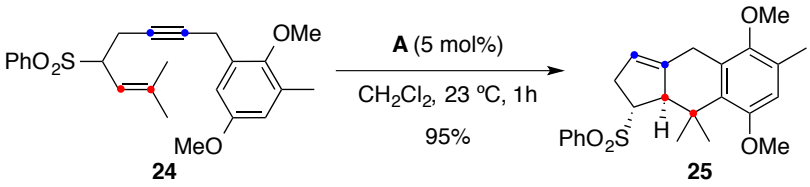

Scheme 12. Gold(I)-catalyzed cyclization of 1,5-benzylenyne **24**

As shown in Scheme 13, further studies were performed in order to functionalize the tricyclic precursor **25**. However, all the attempts to convert deoxypycnanthuquinone C **26** into pycnanthuquinone C failed. Likewise, initial desulfurization of **25** led to intermediate **27**, which unfortunately could not be transformed into the desired product.

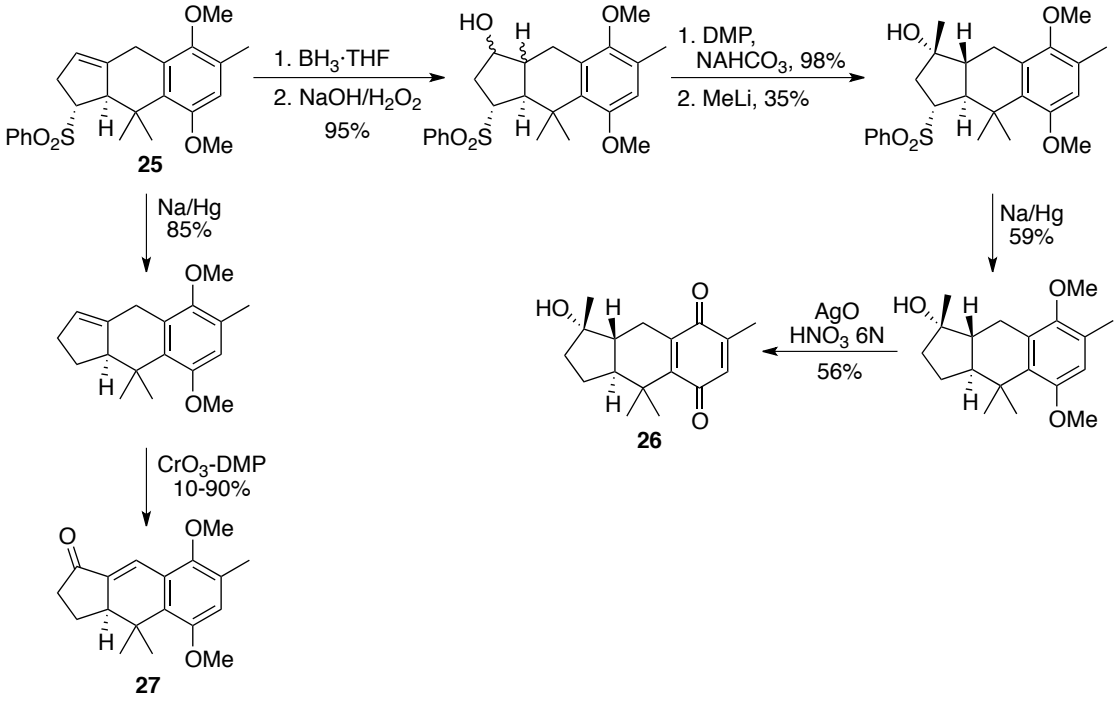

Scheme 13. Studies on the functionalization of tricyclic intermediate **25**

The Carexane Natural Product Family

The carexanes are a series of secondary metabolites present in the leaves of *Carex distachya* (Figure 4), an herbaceous plant found in the Mediterranean bush.[21]

Figure 4. *Carex distachya*

Although the first three carexanes (carexanes A-C) were isolated in small quantities by Fiorentino and coworkers in 2005,[21] further investigations on the same source led to the isolation of an increased number of novel compounds featuring either bicyclic or tetracyclic skeletons (Figure 5).[22,23,24,25] Structure elucidation of all these compounds was achieved on the basis of their spectroscopic properties.

These biologically active compounds and their biosynthetic derivatives (such as distachyasin) have been shown to enhance growth of *Carex distachya,*[22] serve as a phytotoxin to other plant species,[23] and possess antioxidant capabilities analogous to other plant flavonoids.[24]

---

21 D'Abrosca, B.; Fiorentino, A.; Golino, A.; Monaco, P.; Oriano, P.; Pacifico, S. *Tetrahedron Lett.* **2005**, *46*, 5269–5272.

22 Fiorentino, A.; D'Abrosca, B.; Pacifico, S.; Natale, A.; Monaco, P. *Phytochemistry* **2006**, *67*, 971–977.

23 (a) Fiorentino, A.; D'Abrosca, B.; Izzo, A.; Pacifico, S.; Monaco, P. *Tetrahedron* **2006**, *62*, 3259–3265. (b) Fiorentino, A.; D'Abrosca, B.; Pacifico, S.; Izzo, A.; Letizia, M.; Esposito, A.; Monaco, P. *Biochem. Syst. Ecol.* **2008**, *36*, 691–698.

24 Fiorentino, A.; D'Abrosca, B.; Pacifico, S.; Iacovino, R.; Mastellone, C.; Di Blasio, B.; Monaco, P. *Bioorg. Med. Chem. Lett.* **2006**, *16*, 6096–6101.

25 Fiorentino, A.; D'Abrosca, B.; Pacifico, S.; Iacovino, R.; Izzo, A.; Uzzo, P.; Russo, A.; Di Blasio, B.; Monaco, P. *Tetrahedron* **2008**, *64*, 7782–7786.

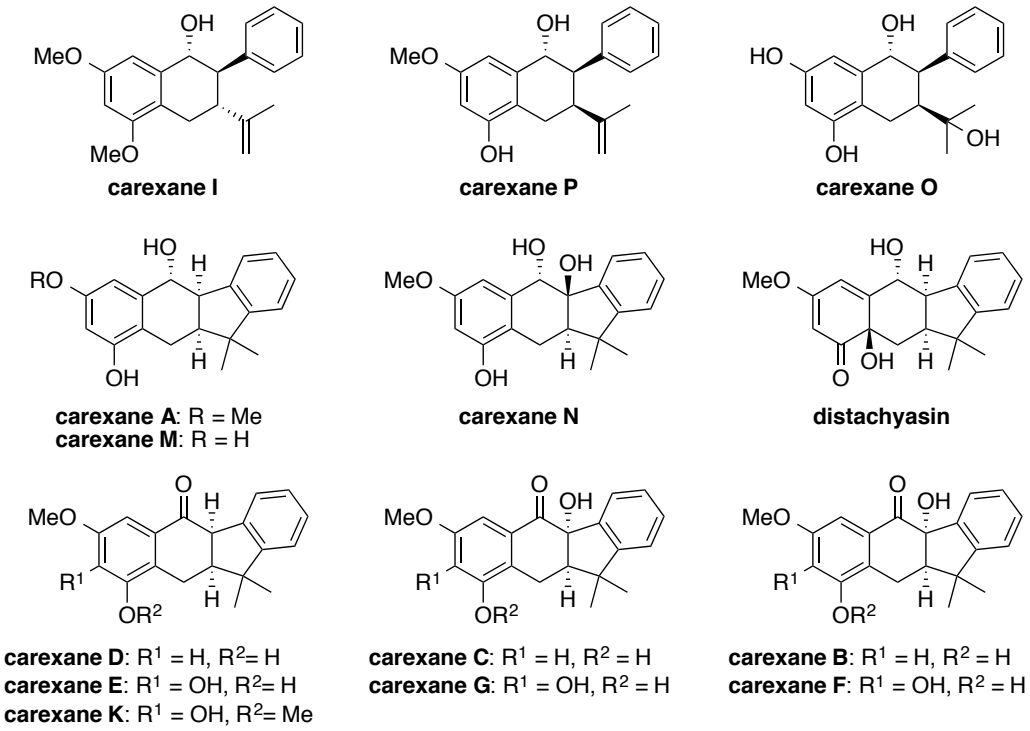

Figure 5. Structures of the carexane natural product family[26]

It has been suggested that these compounds probably originate biosynthetically by the prenylation of a stilbene precursor, cyclization and successive modification, as illustrated in Scheme 14.

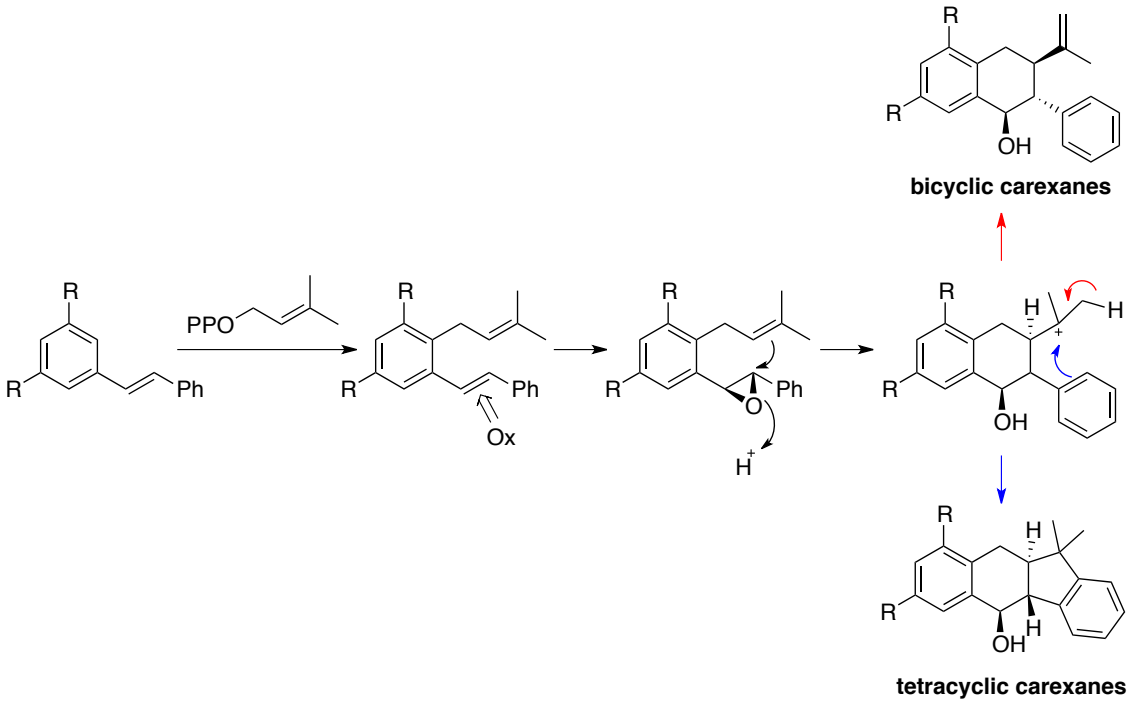

Scheme 14. Biosynthetic pathway proposed for the carexanes

26 The structure of carexane I is represented as it was initially assigned (see ref. 22).

To date, no total synthesis of any member of this group of natural products has been reported.

Objectives

As part of our investigations on the application of gold catalysis for the synthesis of biologicaly active molecules, we focused our attention on two families of natural products: the pycnanthuquinones and the carexanes.

Inspired by the easy accessibility of 5,6,6-tricyclic compounds through the gold(I)-catalyzed [4+2] cycloaddition reaction of arylenynes, we decided to apply this general method as the key step towards the synthesis of (+)-pycnanthuquinone C (Scheme 15). Our studies focused on the use of functionalized 1,6-arylenynes, which would allow the development of an asymmetric approach starting from the enantiomerically pure enyne. Thus, a wide range of substrates, differing on the substitution at C-3 and at the aryl ring could be conceived to provide the core carbon skeleton.

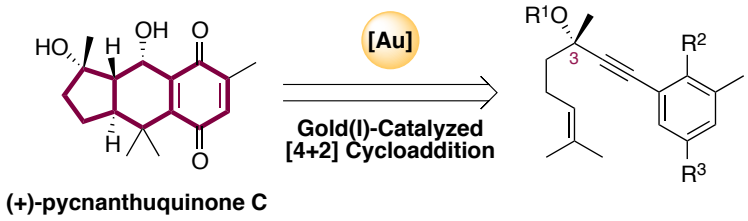

Scheme 15. Proposed synthesis of the 5,6,6-tricyclic core of (+)-pycnanthuquinone C

On the other hand, we envisioned an enantioselective gold(I)-catalyzed alkoxy-cyclization of 1,6-enynes as the key step for the ready access to the common bicyclic core of carexanes via a 6-*endo*-*dig* cyclization (Scheme 16). Further functionalization would lead to the preparation of the complete family of bicyclic and tetracyclic natural products for the first time.

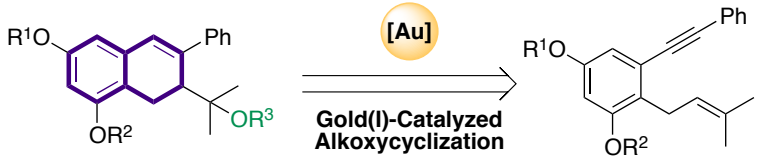

Scheme 16. Proposed synthesis of the bicyclic scaffold of carexanes

Results and Discussion

Studies Towards the Synthesis of Pycnanthuquinone C

Gold(I)-Catalyzed [4+2] Cycloaddition of Functionalized 1,6-Arylenynes

As mentioned in the introduction of this chapter, several strategies have been explored in our group towards the synthesis of (+)-pycnanthuquinone C. These strategies relied on the application of a gold(I)-catalyzed [4+2] cycloaddition reaction to build the 5,6,6-tricyclic skeleton and subsequent functionalization of the carbocyclic core. However, although in many cases the gold catalyzed transformation proceeded satisfactorily, further functionalization was problematic and any case would require an excessive number of steps.

Therefore, we envisaged that the use of functionalized 1,6-arylenynes **29** could lead to the preparation of more advanced intermediate **28** in a single step, reducing the number of subsequent functionalization steps (Scheme 17). Moreover, this strategy would allow the development of an enantioselective synthesis of (+)-pycnanthuquinone C from readily available enantiomerically enriched enynes with a propargylic stereocenter.

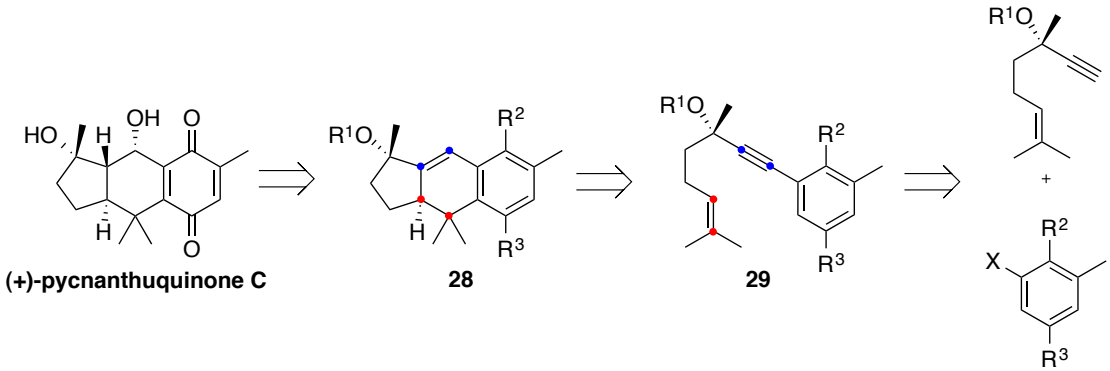

Scheme 17. Retrosynthetic analysis for (+)-pycnanthuquinone C

In a preliminary study developed in our laboratory, 1,6-arylenynes bearing a tertiary alcohol (**19a**) or a protected hydroxyl group at the propargylic position (**19b**) were found to undergo unexpected cyclizations in the presence of gold catalysts, failing to give any tricyclic product (Figure 6). Therefore, other 1,6-arylenynes bearing TES or Ac protected aryls such as **30a** or **30b** were also examined. Unfortunately, no conversion or deprotection of the TES or acetate groups was observed after treatment with gold(I) or gold(III) complexes. Cyclization of less substituted arylenynes **23a-c** was also studied. Whereas enyne **23b** failed to give any product, **23a** and **23c** led to mixtures of desired tricyclic adducts, albeit in low yield.

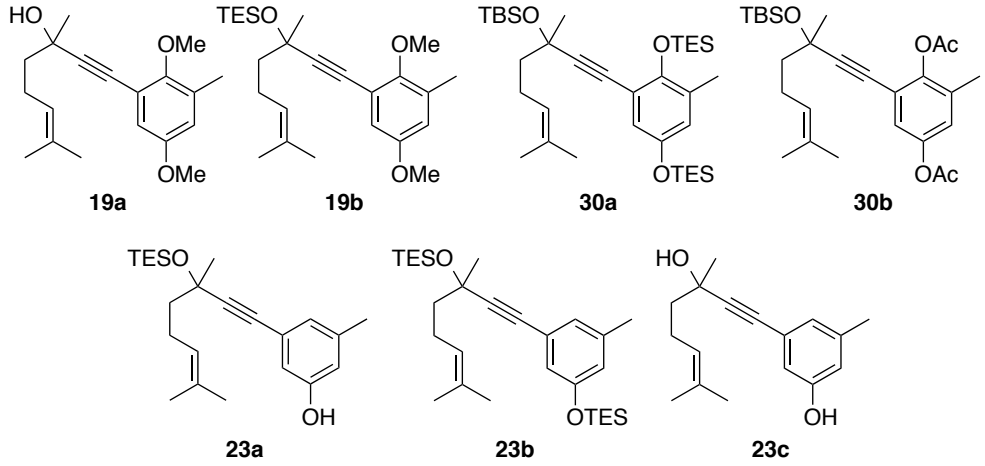

Figure 6. Previously examined highly functionalized 1,6-arylenynes

Encouraged by these results, a wide variety of substrates differing on the substitution at C-3 and at the aryl ring were synthesized employing cross coupling methodologies.

Synthesis of Functionalized 1,6-Arylenynes

The synthesis of the racemic 1,6-enyne **32** was carried out through a previously reported procedure starting with commercially available 6-methylhept-5-en-2-one by addition of ethynyl magnesium bromide and MOM protection (Scheme 18).[27] Subsequent stannylation of the alkyne led to **33**.

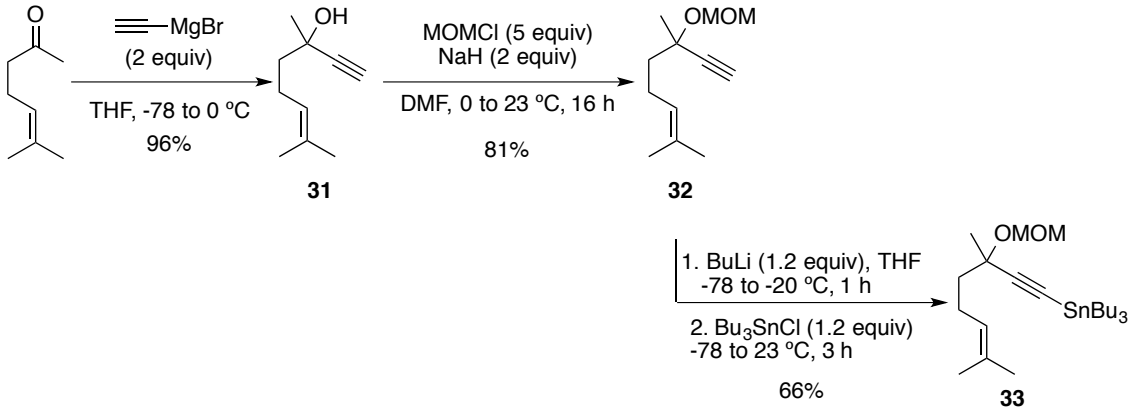

Scheme 18. Synthesis of 1,6-enynes **31**, **32** and **33**

On the other hand, various arene partners were prepared following different synthetic routes, depending on the required substitution at the aryl ring. The synthesis of 2,5-symmetric substituted 1-bromoarene **37** started by bromination of commercial available

27 Trost, B. M.; Toste, F. D. *J. Am. Chem. Soc.* **2002**, *124*, 5025–5036.

o-cresol to give **34** in 99% yield (Scheme 19).[28] Then, oxidation of **34** with CrO_3 afforded 1,4-benzoquinone **35** (95% yield), which was reduced with $Na_2S_2O_4$ to give hydroquinone **36** in excellent yield. Final MOM protection led to the desired coupling partner **37** in 61% yield.

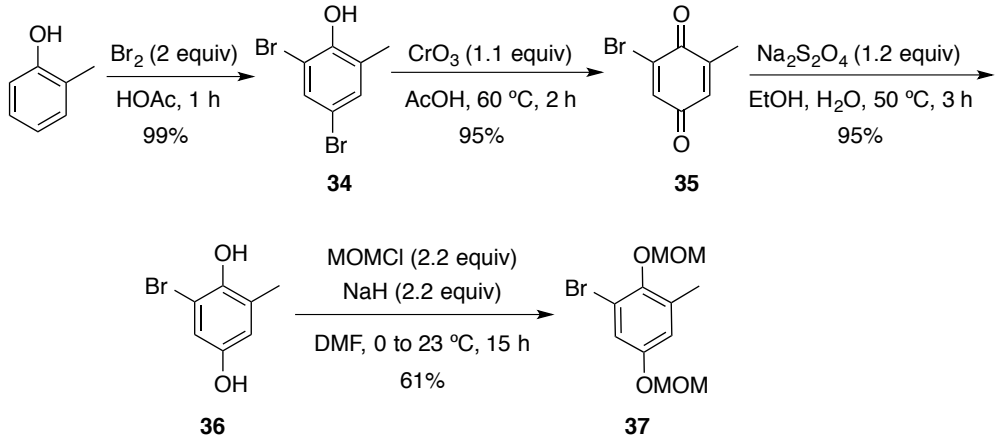

Scheme 19. Synthesis of 2,5-symmetric substituted 1-bromoarene **37**

On the other hand, different substituted aryl chlorides were prepared to gain further insight into the influence of the electron density of the aromatic counterpart on the gold(I)-catalyzed cyclization. Thus, 5-chloro substituted 1-bromoarenes **39** and **40** were prepared in two steps from commercially available 4-chloro-2-methylphenol via bromination[28] and subsequent protection of phenol (Scheme 20).

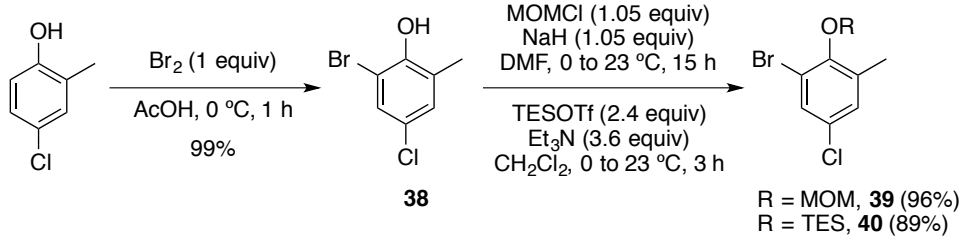

Scheme 20. Synthesis of 5-chloro substituted 1-bromoarenes **39** and **40**

2-Chloro substituted bromoarenes **42** and **43** could be prepared starting from commercially available 1-bromo-2-chloro-3-methylbenzene (Scheme 21). Thus, phenol **42** was synthesized via iridium-catalyzed regioselective C–H borylation/oxone oxidation in 64% yield (over two steps).[29] Protection of the phenol as the MOM

28 Maloney, D. J.; Hecht, S. M. *Org. Lett*. **2005**, 19, 4297–4300.

29 (a) Norberg, A. M.; Smith III, M. R.; Maleczka Jr, R. E. *Synthesis* **2011**, 857–859. (b) Partridge, B. M.; Hartwig, J. F. *Org.Lett.* **2013**, *1*, 140–143.

derivative led to **43** in good yield.

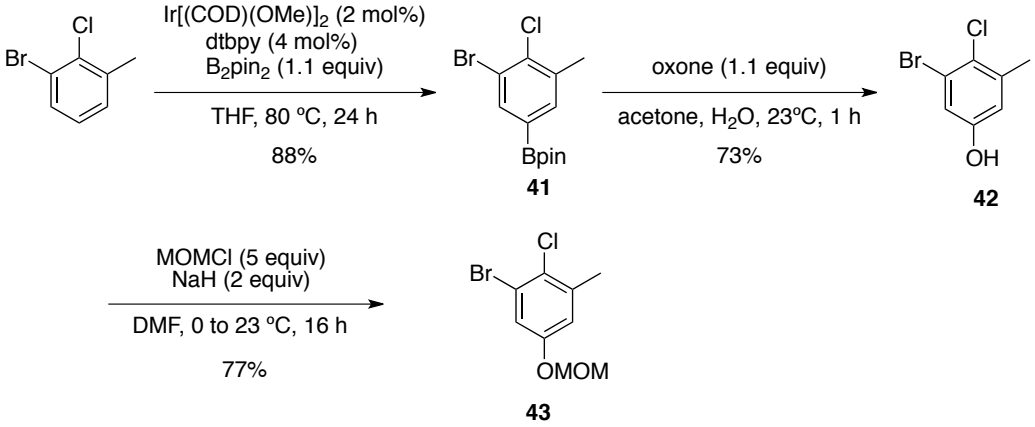

Scheme 21. Synthesis of 2-chloro substituted bromoarenes **42** and **43**

Less substituted arylbromide **45** was prepared in two steps form *o*-cresol (Scheme 22). Bromination with 1 equiv of *N*-bromosuccinimide led to the quantitative formation of intermediate **44**.[30] Then, MOM protection under standard conditions afforded **45** in excellent yield.

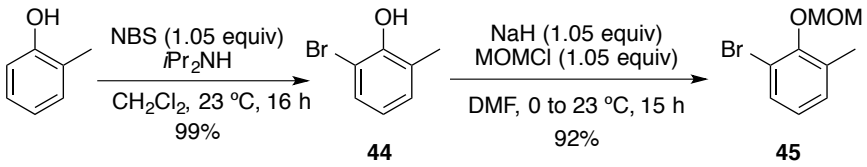

Scheme 22. Synthesis of arylbromide **45**

The cyclization precursors were prepared by Stille cross-coupling in moderate to excellent yields as indicated in Table 1.

30 Velder, J.; Robert, T.; Weidner, I.; Neudörfl, J.-M.; Lex, J.; Schmalz, H.-G. *Adv. Synth. Catal.* **2008**, 350, 1309–1315.

Table 1. Synthesis of 1,6-arylenynes **29a-f**

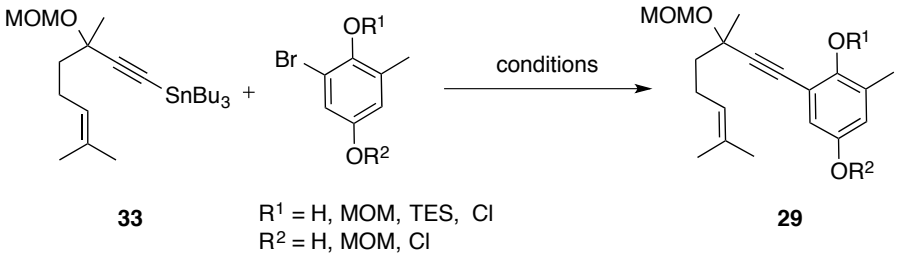

33 R^1 = H, MOM, TES, Cl; R^2 = H, MOM, Cl **29**

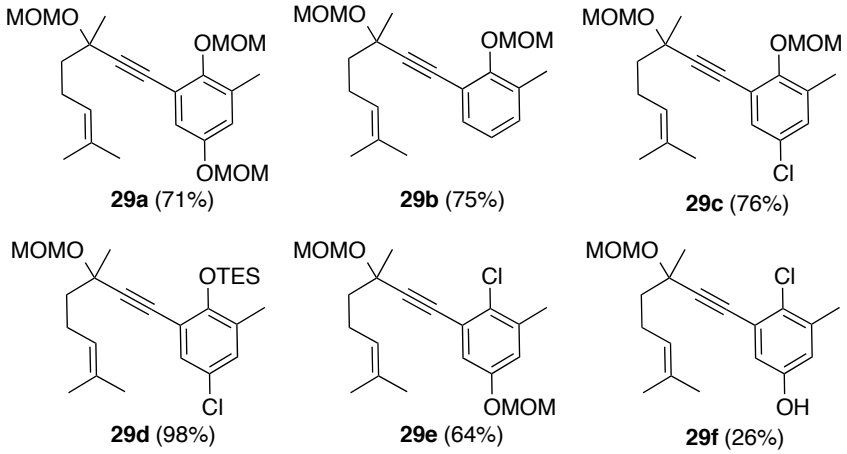

Conditions: stannane (1.1 equiv), arene (1 equiv), 10 mol% $Pd(PPh_3)_4$,, toluene (0.1M), 110 °C, 16 h.

Additionally, silyl deprotection of **29d** with TBAF in CH_2Cl_2 afforded arylenyne **29g** in 92% yield (Scheme 23).

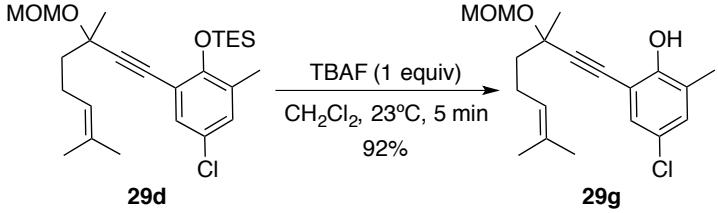

29d **29g**

Scheme 23. Synthesis of 1,6-arylenyne **29g**

Finally, arylenyne **29h** was prepared by Sonogashira coupling of 1,6-enyne **31** and bromoaryne **42** in 74% yield (Scheme 24).

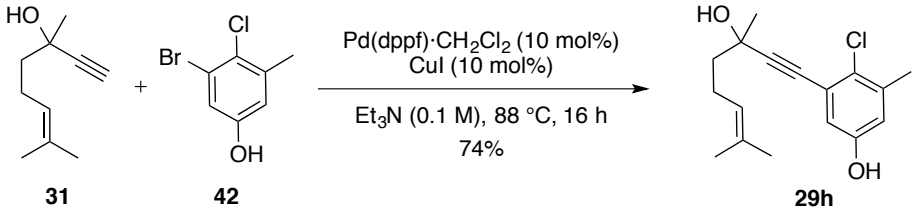

31 **42** **29h**

Scheme 24. Synthesis of 1,6-arylenyne **29h** via Sonogashira coupling

Studies on the Cyclization of Functionalized 1,6-Arylenynes

The cyclization of these new substrates was investigated in the presence of gold(I) complexes **A-C**, **G-I**, platinum (II) complex **P** and $PtCl_2$ (Scheme 25). The results of our extensive investigations will be briefly discussed.

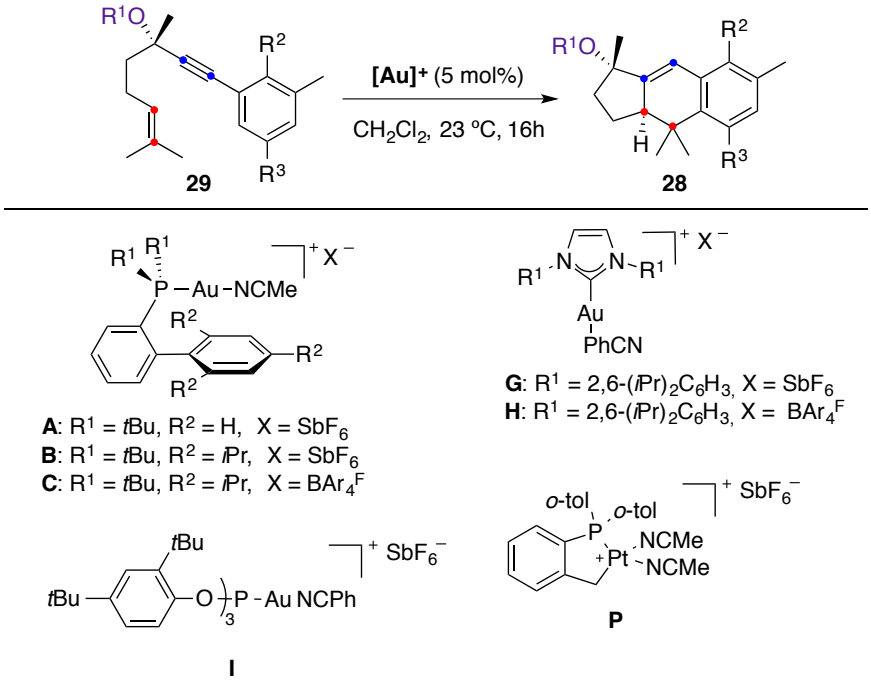

Scheme 25. Studies on the gold(I)-catalyzed [4+2] cycloaddition reaction

Under the usual reaction conditions, treatment of 1,6-arylenynes bearing a tertiary alcohol (**29h**) or a MOM protected hydroxyl group at the propargylic position (**29a-29g**) with phosphine-gold(I) complexes **A-C** gave complex mixtures. Complete decomposition was observed when the reactions were carried out in the presence phosphite-gold(I) complex **I** or gold(I) complexes bearing NHC ligands (**G, H**). No cyclization was observed when the reactions were carried out in the presence of platinum catalyst **P** or $PtCl_2$, even when the reaction temperature was increased to 50 ºC.

Interestingly, treatment of 1,6-arylenyne **29h** with gold(I) complex **G** led to the isolation of tricyclic adduct **46**, in which the tertiary hydroxyl group was eliminated, together with oxocycle **47** (Scheme 26). Unfortunately, competitive degradation of the starting material could not be avoided.

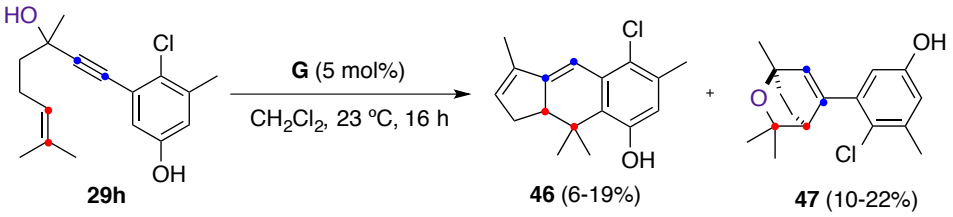

Scheme 26. Gold(I)-catalyzed [4+2] cycloaddition reaction of **29h**

The structure of oxocycle **47** could be confirmed by X-Ray diffraction (Figure 7).

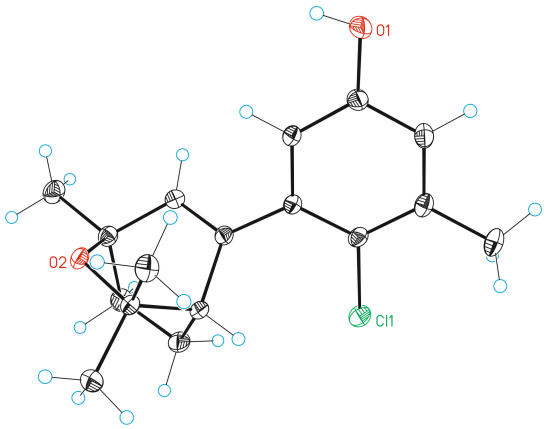

Figure 7. ORTEP representations of **47** with 50% probability of the thermal ellipsoids

The proposed mechanism for the formation of byproduct **47** is illustrated in Scheme 27. Accordingly, gold(I)-activated arylenyne **48** undergoes an initial 6-*endo-dig* cyclization followed by hydroxyl migration (through intermediate **49**) to generate **50**, which after protodeauration would lead to oxoadduct **47**.

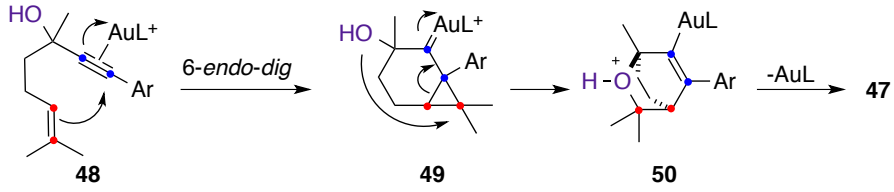

Scheme 27. Proposed mechanism for the formation of **47**

Unfortunately, no significant increment in the yield to **46** was observed by changing the catalyst loading, the concentration, the temperature or the reaction time (Table 2, entries 1-7). Likewise, when the reaction was performed in other solvents (Table 2, entries 8-13), product **46** could be isolated, albeit in poor yield.

Table 2. Optimization of gold(I)-catalyzed [4+2] cycloaddition of **29h**

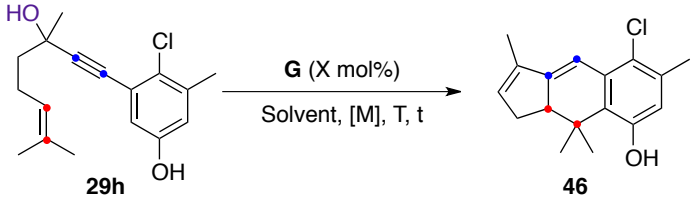

29h **46**

Entry	G (mol %)	Solvent	[M]	T (ºC)	Time (h)	Yield (%)[a]
1	3	CH_2Cl_2	0.1	23	4	19
2	5	CH_2Cl_2	0.1	23	4	15
3	3	CH_2Cl_2	0.05	23	4	9
4	5	CH_2Cl_2	0.05	23	4	13
5	3	CH_2Cl_2	0.1	0	46	15
6	5	CH_2Cl_2	0.1	0	46	8
7	5	CH_2Cl_2	0.1	50	3	-[b]
8	3	acetone	0.1	23	13	17
9	3	MeCN	0.1	23	13	-[c]
10	3	THF	0.1	23	13	8
11	3	toluene	0.1	23	13	5
12	3	DMF	0.1	23	22	-[c]
13	3	DMSO	0.1	23	22	-[c]

[a] Isolated yield. [b] Decomposition. [c] No conversion.

Thus, considering the difficulties to prevent the alkoxy(hydroxyl) group migration or elimination processes, this strategy for the synthesis of (+)-pycnanthuquinone C was abandoned.

Gold(I)-Catalyzed [4+2] Cycloaddition of Less Functionalized 1,6-Arylenynes

We considered an alternative approach based on the gold(I)-catalyzed [4+2] cycloaddition of arylenyne **52** (Scheme 28). We reasoned that this new substrate would undergo cyclization without suffering other competing processes to form **51**, which could be functionalized to obtain (+)-pycnanthuquinone C.

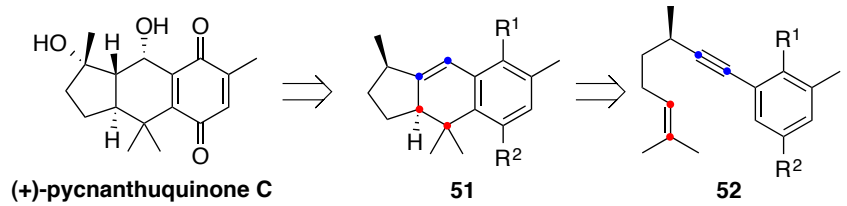

Scheme 28. Retrosynthetic analysis for (+)-pycnanthuquinone C

Synthesis of Less Functionalized 1,6-Arylenyne

The synthesis of the racemic enyne **54** was carried out through a previously two-step reported procedure starting with commercially available 2,6-dimethyl-5-heptenal (Scheme 29). [31] Thus, reaction of this aldehyde with dibromomethylene triphenylphosphorane afforded dibromide **53**. Subsequent treatment with 2 equiv of butyllithium and final addition of water gave volatile **54** in 38 % overall yield.

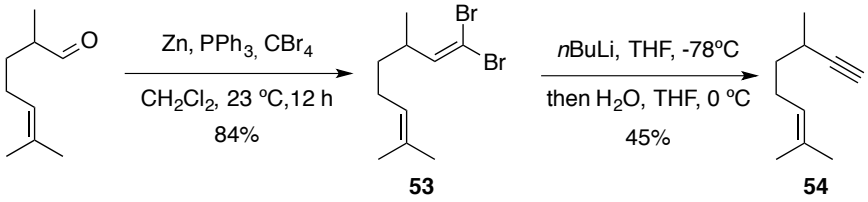

Scheme 29. Synthesis of 1,6-enyne **54**

The preparation of the arene partner **58** for the Sonogashira reaction started by the iodination of *o*-cresol with NIS to form diiodoarene **55** (Scheme 30). Further oxidation of **55** with CrO_3 afforded 1,4-benzoquinone **56** (75% yield), which was reduced with Na_2SO_4 to **57** and methylated with Me_2SO_4 to give iodoarene **58** in moderate yield (39%, over 2 steps).

31 Snider, B. B.; Killinger, T. A. *J. Org. Chem.* **1978**, *43*, 2161–2164.

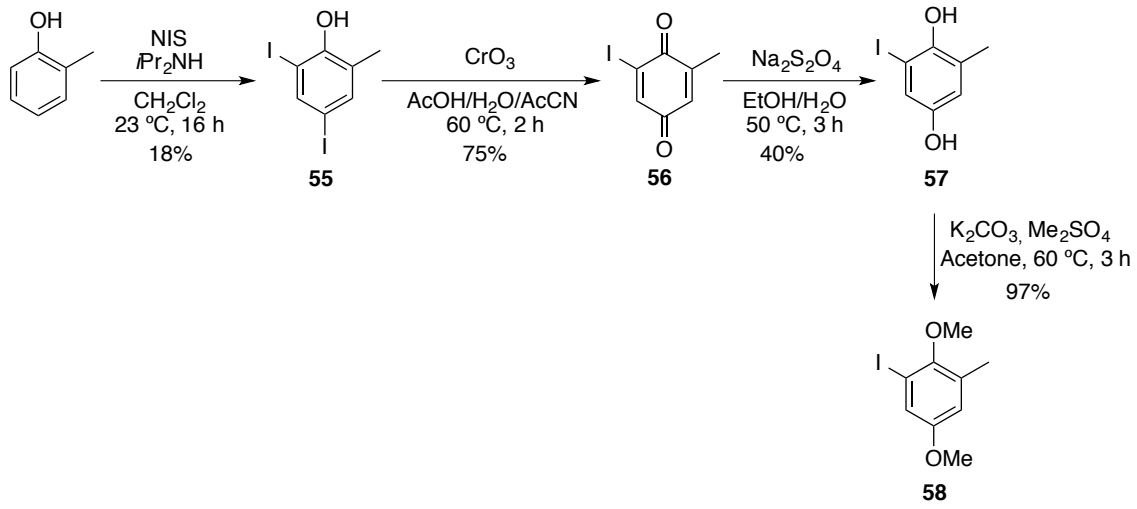

Scheme 30. Synthesis of iodoarene **58**

The precursor for the gold(I)-catalyzed cyclization was obtained in 73% yield by Sonogashira coupling of 1,6-enyne **54** and iodoarene **58** under standard conditions (Scheme 31).

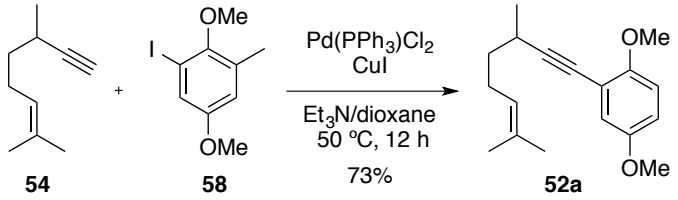

Scheme 31. Synthesis of arylenyne **52a**

Studies on the Gold(I)-Catalyzed Cyclization of 1,6-Arylenyne 52a

Exposing enyne **52a** to the cationic gold(I) complex **G** in CH_2Cl_2 led to the formation of linear fused 5,6,6-tricyclic product **51a** in 74% yield as a 9:1 mixture of inseparable diastereomers (Scheme 32). In contrast, decomposition of the starting material was observed after treatment with gold complexes bearing phosphine (**A**) or phosphite (**I**) ligands.

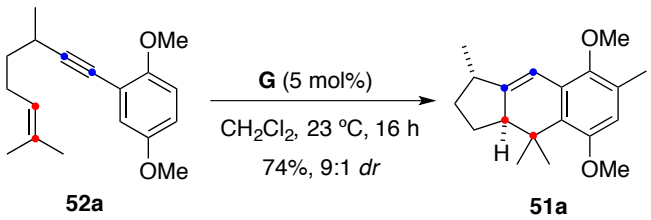

Scheme 32. Gold(I)-catalyzed [4+2] cycloaddition of 1,6-enyne **52a**

The structure and the relative configuration of the major isomer **51a** was confirmed by X-ray diffraction (Figure 8).

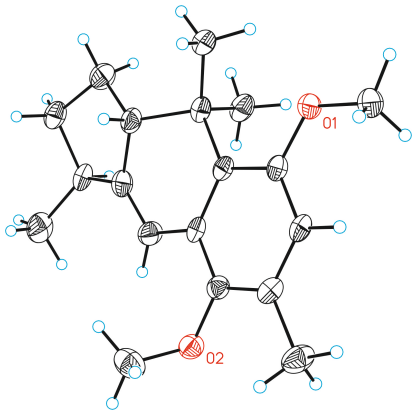

Figure 8. ORTEP representations of **51a** with 50% probability of the thermal ellipsoids.

Studies on the Functionalization of Tricyclic Intermediate 51a

At that point we focused our attention on the functionalization of tricyclic intermediate **51a**. Considering our previous studies, different strategies were proposed in order to complete the synthesis of pycnanthuquinone C (Scheme 33).

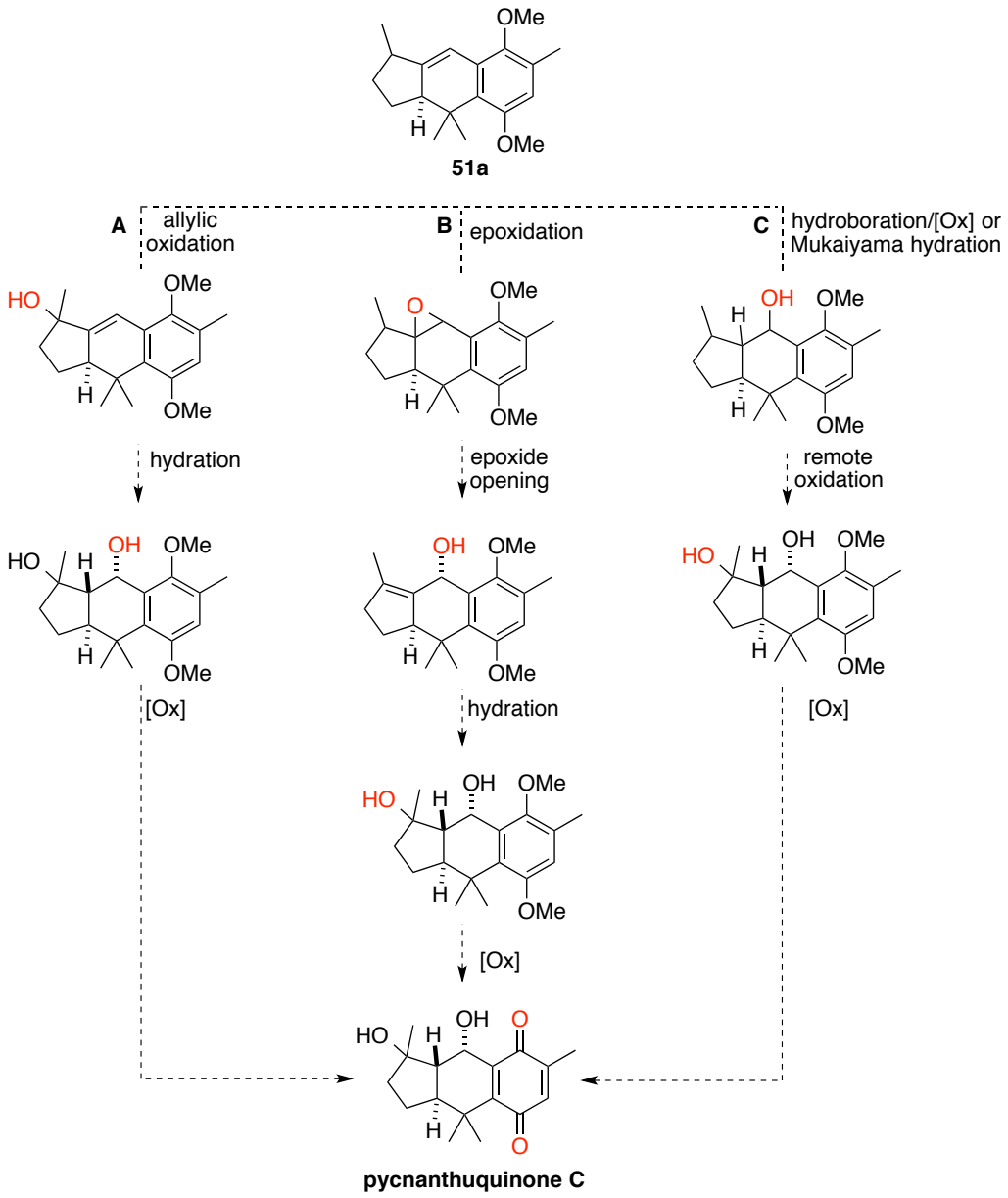

Scheme 33. Proposed strategies towards the synthesis of pycnanthuquinone C from **51a**

Initial attempts focused on the allylic oxidation of **51a** (Table 3).[32,33] Disappointingly, either no reaction or formation of undesired product **60** was observed in most of the cases. Given that the formation of over-oxidized product **60** seemed more favoured than the required intermediate **59**, alternative functionalization strategies were explored.

32 For a review on allylic oxidations in natural product synthesis: Nakamura, A.; Nakada, M. *Synthesis* **2013**, *45*, 1421–1451.

33 (a) Carruters, W.; Coldham, I. *Modern Methods of Organic Synthesis*, 6.1.3, 374–377. (b) Shing, T. K. M.; Yeung; Su, P. L. *Org. Lett.* **2006**, *8*, 3149–3151.

Table 3. Allylic oxidation of **51a**

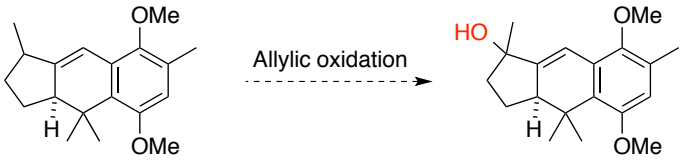

51a **59**

Entry	Reagent (equiv)	Conditions	Outcome
1	SeO_2 (0.2) aq. TBHP 70% (2)	CH_2Cl_2 (0.1 M) 0 to 23 ºC, 17 h	–[a]
2	SeO_2 (1)	CH_2Cl_2 (0.1 M) 0 ºC, 4 h	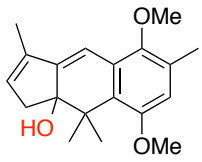 **60**
3	SeO_2 (1.1)	EtOH (0.1 M) 23 ºC, 48 h	–[a]
4	SeO_2 (2)	CH_2Cl_2 (0.1 M) 23 ºC, 1 h	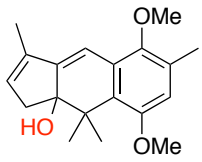 **60**
5	$Mn(ac)_3 \cdot H_2O$ (0.1) TBHP 6M in decane (2)	EtOAc (0.1 M), 3 Å MS 23 ºC, 23 h	–[a]
6	DDQ (3)	CH_2Cl_2/H_2O (3:1) 0 ºC, 0.75 h	Complex mixture

The progress of the reaction was monitored by TLC. [a] No conversion.

On the other hand, epoxidation of the double bond was attempted under a variety of conditions (Table 4).[34] Exclusive formation of rearranged ketone **62** was observed after treatment with *m*-CPBA (Table 4, entry 1). This unexpected compound most likely arises from the opening of intermediate epoxide **61** in an acid-catalyzed reaction. Unfortunately, when *m*-CPBA was used in combination with $NaHCO_3$ only decomposition was observed (Table 4, entry 2). Likewise, other epoxidation methods failed to give the desired epoxide.

34 Kürti, L.; Czakó, B. *Strategic Applications of Named Reactions in Organic Synthesis*, Elsevier Inc. **2005**, 222–223 and 362–363.

Table 4. Epoxidation of **51a**

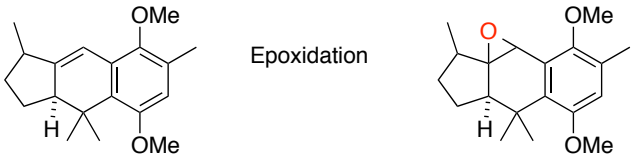

51a **61**

Entry	Reagent (equiv)	Conditions	Outcome (yield%)[a]
1	*m*-CPBA (2.2)	CH_2Cl_2 (0.1 M) 0 to 23ºC, 1 h	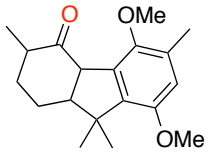 **62** (50%)
2	*m*-CPBA (1.1)/$NaHCO_3$ (1.5)	CH_2Cl_2 (0.1 M), 23 ºC, 1.5 h	Decomposition
3	NBS (1.2)	THF/H_2O (2:1), 23 ºC, 20 h	Decomposition

The progress of the reaction was monitored by TLC. [a] Isolated yield.

We also examined the possibility of accessing to intermediate **63** via Mukaiyama reduction-hydration (Table 5).[35,36] We reasoned that the formation of most stable benzylic radical intermediate would led selectively to desired product **63**. However, either starting material was recovered unchanged or total decomposition was observed.

Table 5. Mukaiyama hydration of **51a**

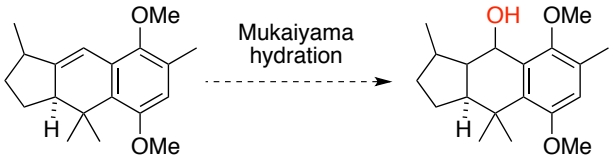

51a **63**

Entry	Reagent (equiv)	Conditions	Outcome
1	$Co(acac)_3/PhSiH_3$	THF, O_2 (air balloon), 25 ºC, 15 h	–[a]
2	$Co(acac)_3/PhSiH_3$	THF, O_2 (air balloon), 60 ºC, 15 h	Decomposition
3	$Co(acac)_3/PhSiH_3$	*i*PrOH, O_2 (air balloon), 25 ºC, 15 h	–[a]
4	$Co(acac)_3/PhSiH_3$	*i*PrOH, O_2 (air balloon), 60 ºC, 9 h	–[a]

35 (a) Mukaiyama, T.; Yamada, T. *Bull. Chem. Soc. Jpn.* **1995**, *68*, 17–35. (b) Mukaiyama, T.; Isayama, S.; Inoki, S.; Kato, K.; Yamada, T. Takai, T. *Chem. Lett.* **1989**, *3*, 449–452. (c) Inoki, S.; Kato, K.; Takai, T.; Isayama, S.; Yamada, T.; Mukaiyama, T. *Chem. Lett.* **1989**, *3*, 515–518. (d) Isayama, S.; Mukaiyama, T. *Chem. Lett.* **1989**, *6,* 1071–1074. (e) Inoki, S.; Isayama, S.; Mukaiyama, T. *Chem. Lett. 1990*, 1869–1872.

36 For a general review: Hoffmann, R. W. *Chem. Soc. Rev.* **2016**, *45*, 577–583.

5	$Mn(acac)_2/PhSiH_3$	*i*PrOH, O_2 (air balloon), 23 ºC, 60 h	–[a]

The progress of the reaction was monitored by TLC. [a] No conversion.

Hydroboration[37] of tricyclic precursor **51a** using BH_3 in THF followed by oxidation with $NaOH/H_2O_2$ afforded the desired secondary alcohol **63a-b** in 64% yield as a 1:1 mixture of inseparable diastereomers together with an unidentified by-product (Scheme 34).

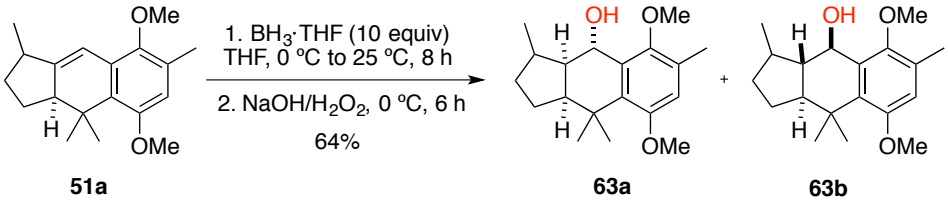

51a **63a** **63b**

Scheme 34. Hydroboration of **51a**

Nevertheless, we continued our studies with the inseparable mixture of alcohols, turning our attention on the synthesis of α,β–unsaturated ketone **65** (Scheme 35).[38] We reasoned that by accessing to this intermediate the control of the stereoselectivity could be more easily addressed.

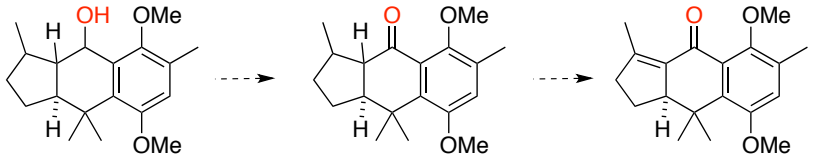

63 **64** **65**

Scheme 35. Oxidation of **63**

Oxidation to the corresponding ketone **64** was achieved using Dess-Martin periodinane in 50% yield (Scheme 36). However, attempts to convert **64** into the α,β–unsaturated ketone **65** only led to decomposition of the starting compound.

37 Corey, E. J.; Gavai, A. V. *Tetrahedron Lett*. **1988**, *29*, 3201-3204

38 Carvalho, J. F. S.; Silva, M. M. C.; Moreira, J. N.; Simões, S.; Sá e Melo, M. L. *J. Med. Chem*. **2011**, *54,* 6375–6393.

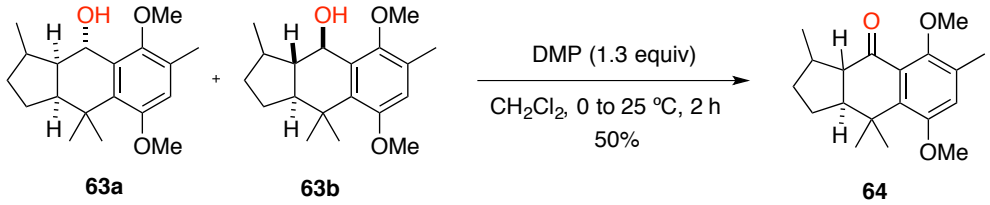

Scheme 36. Oxidation of **63**

We considered an alternative approach for the functionalization of cyclization product **51a** starting with the oxidation of the aromatic system to the corresponding quinone **66** (Scheme 37).

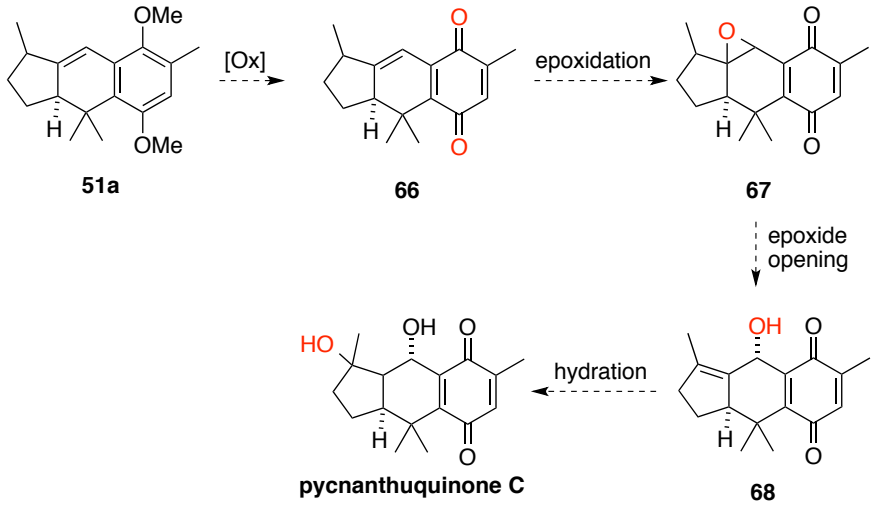

Scheme 37. Alternative functionalization strategy of cyclization product **51a**

As shown in Table 6, the oxidation of the aromatic system was attempted with various oxidants.[39] Although no product formation was observed when ceric ammonium nitrate (CAN) (Table 6, entries 1 and 2) or $PhI(O_2CF_3)_2$ (Table 6, entry 3) were used, quinone **66** could be obtained in 30% yield after treatment with AgO and nitric acid (Table 6, entry 4).[40]

Table 6. Synthesis of quinone **66**

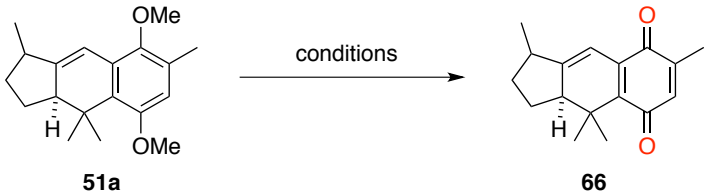

39 Love, B. E.; Bonner-Stewart, J.; Forrest, L. A. *Synlett* **2009**, *5*, 813–817.

40 Harrowven, D. C.; Tyte, M. J. *Tetrahedron Lett.* **2001**, *42*, 8709–8711.

Entry	Reagent (equiv)	Conditions	Outcome (yield%)[a]
1	CAN (2.3)	MeCN/H_2O (1:1), 0 to 25 ºC, 0.5 h	–[b]
2	CAN (2.3)	MeCN/H_2O (1:1), 25 ºC, 16 h	Decomposition
3	$PhI(O_2CF_3)_2$ (4)	H_2O/MeOH (4:1), 25 ºC, 1 h	Decomposition
4	AgO (4.2), HNO_3 6 N	Dioxane, 25 ºC, 3 h	**66** (30%)

The progress of the reaction was monitored by TLC. [a] Isolated yield. [b] No conversion.

Subsequent epoxidation of quinone **66** was achieved in moderate yield using *m*-CPBA in combination with $NaHCO_3$ in CH_2Cl_2 at low temperature (Scheme 38).

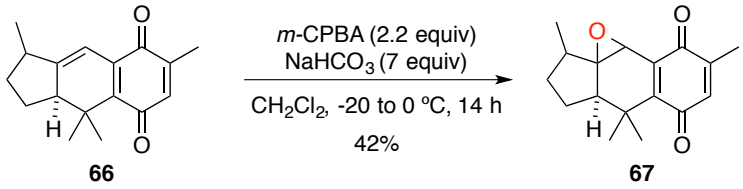

Scheme 38. Epoxidation of **66**

The opening of epoxide **67** was essayed using different bases (Table 7).[41] Unfortunately, treatment of **67** with Et_2NLi, LiTMP or LDA led to complete decomposition of starting material.

Table 7. Studies on the epoxide opening

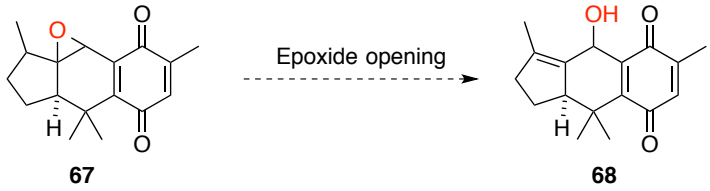

Entry	Reagent (equiv)	Conditions	Outcome
1	Et_2NLi (2.5)	THF, -20 ºC, 15 min	Decomposition
2	LiTMP (4)	Benzene, 0 to 25 ºC, 2.5 h	Decomposition
3	LDA (4)	Et_2O, 25 ºC, 2 h	Decomposition

41 (a) Yasuda, A.; Tanaka, S.; Oshima, K.; Yamamoto, H.; Nozaki, H. *J. Am. Chem. Soc.* **1974**, *96*, 6513–6514. (b) Heathcock, C. H.; Mahaim, C.; Schlecht, M. F.; Utawanit, T. *J. Org. Chem.* **1984**, *49*, 3264–3274.

Studies Towards the Synthesis of Carexanes

As mentioned in the introduction of this chapter, the carexanes are a large family of natural products featuring either a tetralin or a 6,6,5,6-tetracyclic skeleton decorated with phenols and phenolic ethers.

We rationalize that a common scaffold of all these compounds could be accessed through a selective gold(I)-catalyzed 6-*endo-dig* cyclization of enyne **73**, which could be trapped with an external nucleophile or further eliminated to afford dihydronaphthalene derivatives **69** or **70**, respectively (Scheme 39). Moreover, intermediate **72** could undergo a subsequent Friedel-Crafts reaction leading to a fused 6,6,5,6-tetracyclic product **71**. The gold(I)-catalyzed precursor **73** would be easily prepared from commercially available 3,5-dimethoxybenzaldehyde and prenyl bromide.

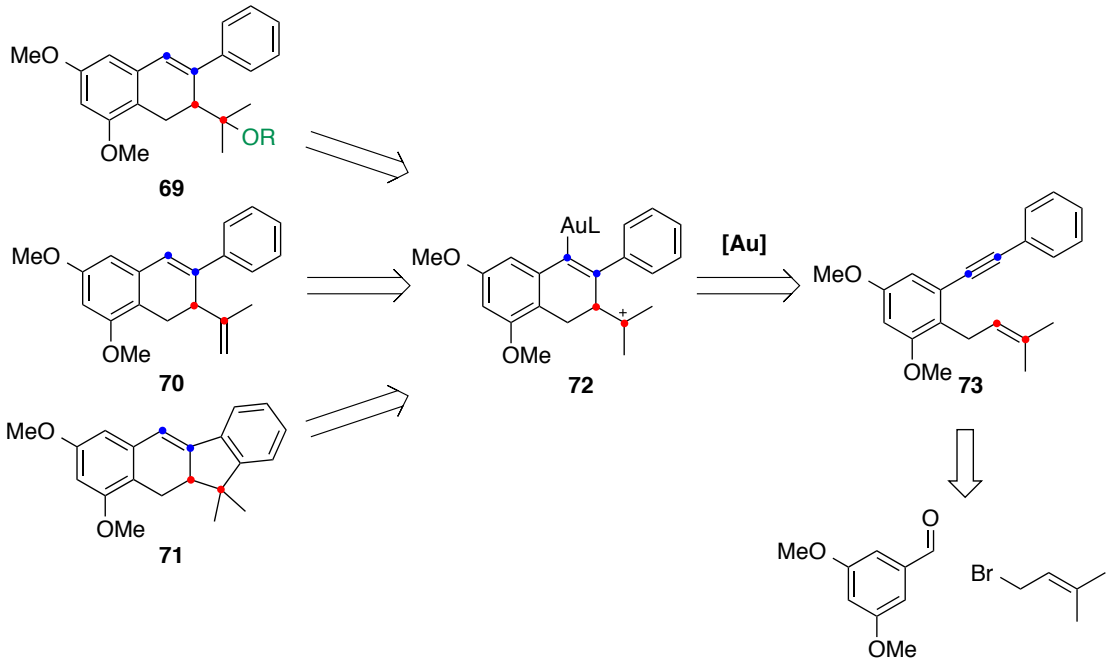

Scheme 39. Retrosynthetic analysis for the carexanes

Synthesis of 1,6-Enyne 73

The synthesis of required 1,6-enyne **73** was completed in 4 steps starting from 3,5-dimethoxybenzaldehyde (Scheme 40). Initial bromination was carried out with NBS according to a reported procedure.[42] Then, aldehyde **74** was converted into the corresponding acetylene **75** in 87% yield using the modified Seyferth-Gilbert homologation. Subsequent Sonogashira coupling with iodobenzene led to **76** in 84%

42 Gadakh, S. K.; Sudalai, A. *Tetrahedron Lett.* **2016**, 57, 25–28.

yield. Finally, prenylation of **76** was accomplished by treatment with *n*-butyllithium, TMEDA and CuI followed by addition of prenyl bromide to afford enyne **73** in 65% yield.

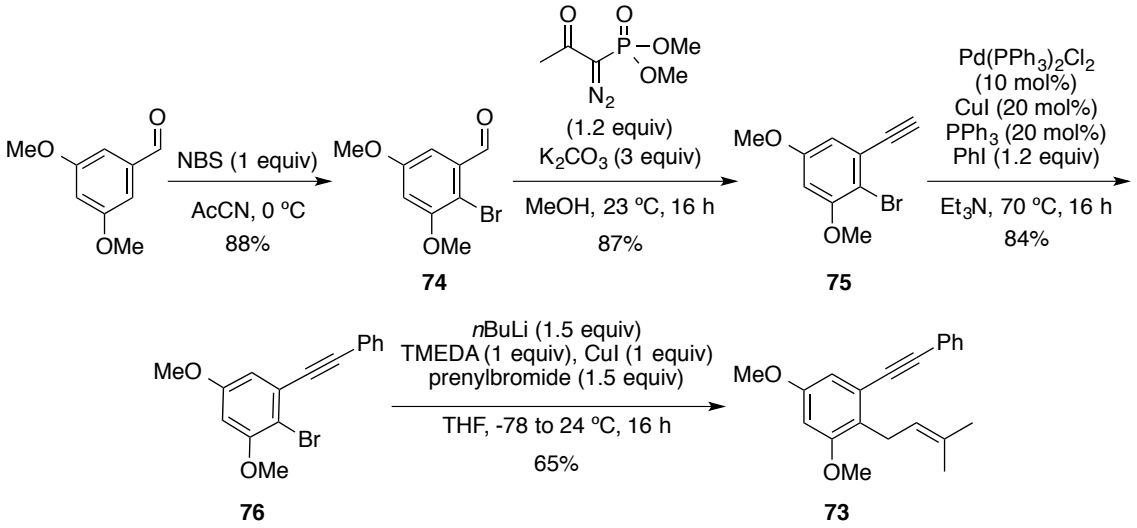

Scheme 40. Synthesis of 1,6-enyne **73**

Studies on the Gold(I)-Catalyzed Cyclization

We investigated the reaction of enyne **73** using 5 mol% of various gold(I) complexes at 25 °C in CH_2Cl_2 (Table 8). Under these conditions, we observed the formation of up to four products in different ratios depending on the nature of the catalyst used.

Thus, treatment with commercially available cationic JohnPhos-gold(I) catalyst **A** led to the exclusive formation of hydroxyl-substituted dihydronaphthalene derivative **69a** in 69% yield (Table 8, entry 1). The use of more sterically hindered phosphine *t*BuXPhos in combination with BAr_4^{F-} counterion resulted in the isolation of tetracycle **77** in 54% yield (Table 8, entry 2). In the presence of catalyst **K**, the same tetracyclic derivative could be isolated, albeit in lower yield (Table 8, entry 3). Unfortunately, partial decomposition of the starting material was always observed. Interestingly, when the reaction was performed in the presence of catalyst **G**, bearing an NHC ligand and SbF_6^- as counterion, exclusive formation of naphthalene derivative **78** was observed in a remarkable yield (Table 8, entry 4). Analogous complex with BAr_4^{F-} anion afforded mixtures of the four products (Table 8, entry 5). On the other hand, the use of phosphite ligands (Table 8, entry 6) or more donating phosphines (Table 8, entry 7) had an adverse influence on the selectivity of this transformation. Likewise, treatment with

neutral gold complex $IPrAuNf_2$ (**M**) (Table 8, entry 8) or gold(I) catalyst **J** (Table 8, entry 9) gave rise to complex mixtures of these four compounds.

Table 8. Gold(I)-catalyzed cyclization of 1,6-enyne **73**

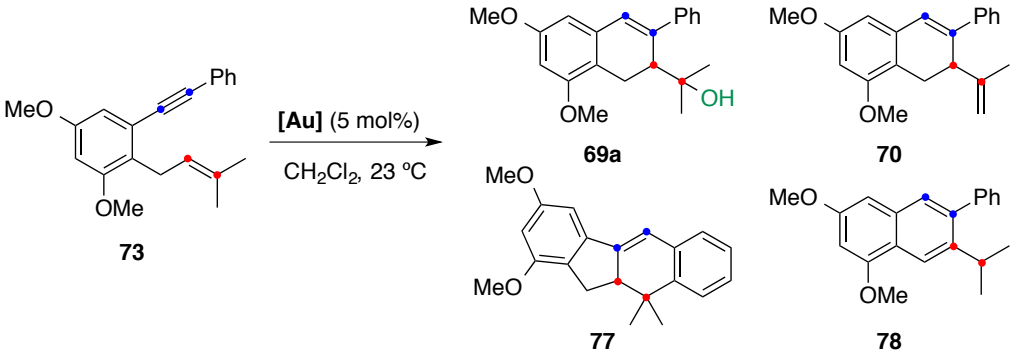

Entry[a]	[Au]	t (h)	Conversion (%)	69a (yield,%)	70 (yield,%)	77 (yield,%)	78 (yield,%)
1	**A**	16	>99	69[b]	–	–	–
2	**C**	36	>99	12[b]	–	54[b]	–
3	**K**	36	>80	–	–	36[b]	–
4	**G**	24	>99	–	–	–	72[b]
5	**H**	24	>99	18	5	12	8
6	**I**	4.5	>99	17	17	17	17
7	**L**	24	80	15	15	30	12
8	**M**	5	>99	13	16	13	17
9	**J**	24	77	6	5	32	14

[a] Determined by ^1H NMR using 1,4-diacetylbenzene as internal standard. [b] Isolated yield.

Additionally, other Lewis acids such as $PtCl_2$, $GaCl_3$, $InBr_3$, InI_3, $Cu(OTf)_2$, $BiCl_3$, and $ZrCl_4$ were tested but formation of similar complex mixtures were observed in all the cases.

As initially conceived, compounds **69a** and **70** would arise from a 6-*endo* cyclization through common intermediate **72** (Scheme 41). Then, subsequent hydroxyl addition would lead to dihydronaphthalene derivative **69a** (green route), whilst proton elimination would afford **70** (blue route). Moreover, intermediate **72** could undergo a 1,3–H shift to form benzylic carbocation **80** (orange route), which after proton elimination would give rise to naphthalene derivative **78**. On the other hand, the

tetracyclic product **77** would derive from an initial 5-*exo* cyclization followed by a Friedel-Crafts-type process (red route).

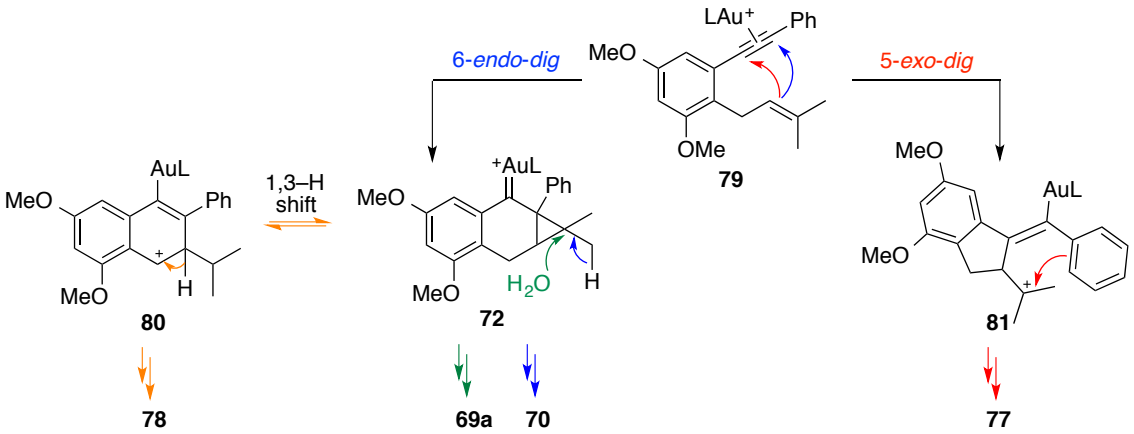

Scheme 41. Proposed mechanism for the gold(I)-catalyzed cyclization of gold(I)-activated 1,6-enyne **79**

Several conditions were assayed to promote the intramolecular Friedel-Crafts alkylation reaction of dihydronaphthalene derivative **69a** (Scheme 42). However, treatment of **69a** with $AlCl_3$, $FeCl_3$, TfOH, *p*TSOH·H_2O, H_3PO_4, $Bi(OTf)_3$, or $BF_3{\cdot}Et_2O$ led to the exclusive formation of naphthalene derivative **78**.

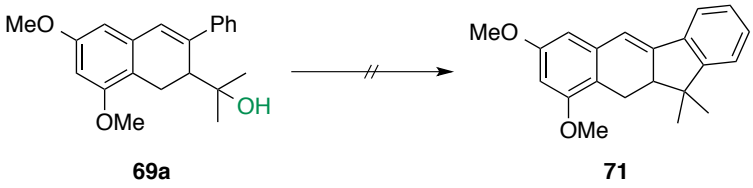

Scheme 42. Studies on the Friedel-Crafts reaction of **69a**

We tried the epoxidation of **77** to access to the rearranged ketone **82** through an analogous process to that observed during the studies towards the synthesis of pycnanthuquinone C (Scheme 43).[43]

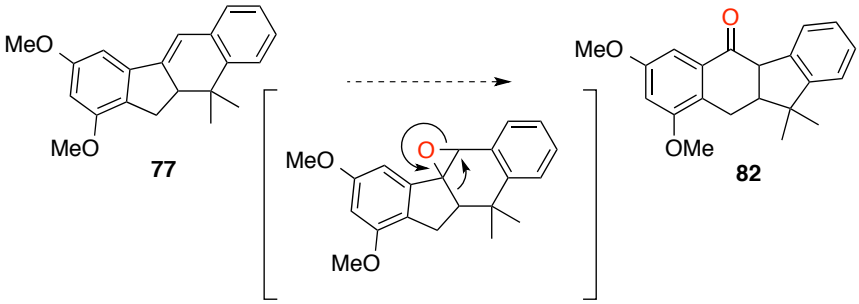

Scheme 43. Studies on the epoxidation of **77**

43 For previous studies regarding the synthesis of pycnanthuquinone C see table 4.

Therefore, epoxidation of the double bond was attempted under different conditions. However, either complete decomposition (Table 9, entries 1-2) or recovery of unreacted starting material (Table 9, entries 3-8) was observed.

Table 9. Screening conditions for epoxidation of **77**

Entry	Reagent (equiv)	Conditions	Outcome
1	*m*-CPBA (2)	CH_2Cl_2, 23 ºC, 6 h	Decomposition
2	*m*-CPBA (1.5)	CH_2Cl_2, 0 to 23 ºC, 20 h	Decomposition
3	*m*-CPBA (1.3), $NaHCO_3$ (3)	H_2O/CH_2Cl_2 (1:1), 23 ºC, 15 h	–[a]
4	*m*-CPBA (1.3), $NaHCO_3$ (3)	H_2O/CH_2Cl_2 (1:1), 40 ºC, 7 d	–[a]
5	oxone (1.3), $NaHCO_3$ (3)	H_2O/CH_2Cl_2 (1:1), 23 ºC, 15 h	–[a]
6	oxone (1.3), $NaHCO_3$ (3)	H_2O/CH_2Cl_2 (1:1), 40 ºC, 7 d	–[a]
7	oxone (1.3)	acetone/CH_2Cl_2 (1:1), 23 ºC, 15 h	–[a]
8	oxone (1.3)	acetone/CH_2Cl_2 (1:1), 40 ºC, 7 d	–[a]

[a] Only starting material was recovered.

The gold(I)-catalyzed oxidative cyclization of enyne **73** was also investigated. Thus, several amine-*N*-oxides were tested in combination with gold(I) catalyst IPrAuNTf$_2$ (**M**) at 23 ºC in CH_2Cl_2. Although complex reaction mixtures were obtained in most cases, after treatment with 8-methylquinoline *N*-oxide exclusive formation of compound **83** in 79% yield was observed (Scheme 44). Our mechanistic proposal involves the formation of α-oxo gold(I) carbene **84**, which undergoes a 1,5–H shift to generate allyl carbocation **85**. Subsequent attack of the carbonyl group would afford **86**, which after protodeauration gives **83**.

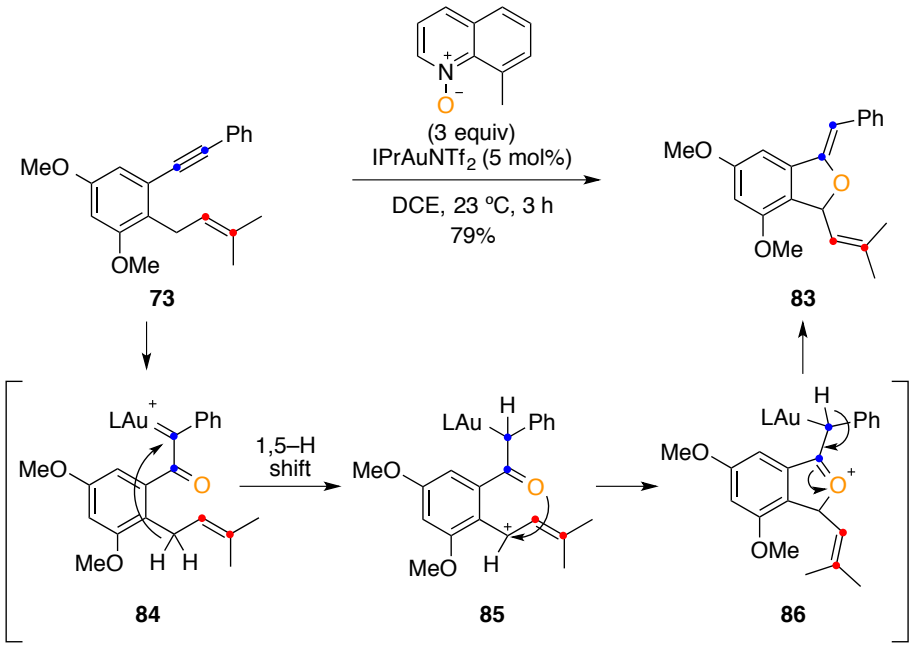

Scheme 44. Gold(I)-catalyzed oxidative cyclization of **73**

In parallel, we decided to expand the scope of the gold(I)-catalyzed alkoxy(hydroxy) cyclization of **73**. We reasoned that by using a bulkier nucleophile, we could access to a protected ether product, which could be further functionalized while minimizing undesired side reactions. Furthermore, we hypothesized that for the studies on the asymmetric version of this transformation, the use of larger nucleophiles may lead to an increased enantioselectivity. Thus, several alcohols were used to trap the proposed cationic intermediate **72** leading to the corresponding dihydronaphthalene derivatives **69** in moderate yield (Table 10, entries 1-3 and 7). Bulky nucleophiles such as *tert*-butanol (Table 10, entry 4) and triisopropylsilyl alcohol (Table 10, entry 5) gave primarily the elimination product **70**.

Table 10. Gold(I)-catalyzed alkoxy(hydroxy)cyclization of **73**

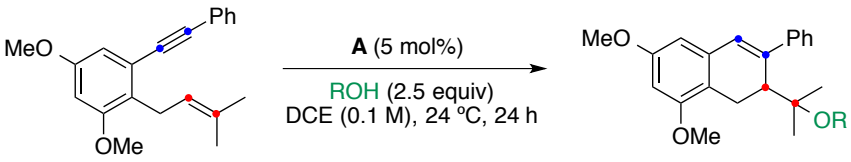

73 **69**

Entry	ROH	Product	Yield (%)[a]
1	H_2O	**69a**	69
2	MeOH	**69b**	51
3	*i*PrOH	**69c**	56
4	*t*BuOH	**69d**	–[b]
5	TIPSOH	**69e**	–[b]
6	PMBOH	**69f**	–
7	allyl alcohol	**69g**	53

[a] Isolated yield. [b] Exclusive formation of product **70**.

Studies on the Enantioselective Gold(I)-Catalyzed 6-*endo* Cyclization

All the studies on the development of the enantioselective gold(I)-catalyzed 6-*endo* alkoxy(hydroxy)cyclization were performed in the Cellex High Throughput Experimentation unit (HTE).

Initially, to determine the optimal reaction conditions for the formation of **69a**, two different set-ups were examined: (A) *in situ* generation of the catalyst followed by the addition of the substrate, and (B) *in situ* generation of the catalyst in the presence of the substrate. Additionally, two different additives ($NaBAR_4^F$ *vs.* $AgSbF_6$) for the generation of the catalyst were evaluated, as well as the amount of nucleophile added (0, 2.5 or 5 equiv).

The best results were obtained by employing conditions A in combination with 2.5 equiv of nucleophile. Although the use of both couterions led to very similar results, $AgSbF_6$ was selected for the generation of the catalyst to prevent potential solubility issues. Subsequently, we essayed several chiral gold complexes in the gold(I)-catalyzed cyclization of 1,6-enyne **73** following our optimized protocol (Scheme 45, Figures 9-11).

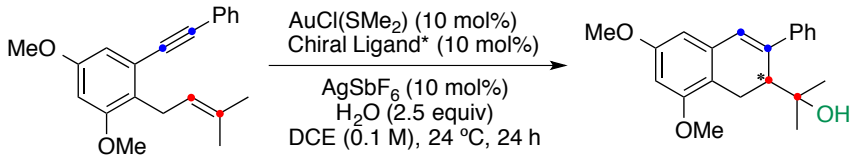

73 **69a**

Scheme 45. Initial screenings for the enantioselective hydroxycyclization of **73**

Although our initial screening of various chiral bisphosphine, phosphoramidite and phosphite ligands resulted in very low enantioselectivities (Figure 9), we could observe formation of desired product with modest enantioselectivity when PhanePhos ligand (*R*)-**L8** was used (Figure 9, entry B3). Likewise, bisphosphine ligands (*R*,*R*)-**L7**, (*S*)-**L14**, (*R*,S_P)-**L17**, (*R*,*R*)-**L18** were found to induce some enantioselectivity (Figure 9, entries B2, C3, C6, D1, respectively). Therefore, we expanded the study to other chiral ligands featuring related JosiPhos, MeO-BiPhep and DuPhos bis-phosphine scaffolds (Figures 10 and 11).

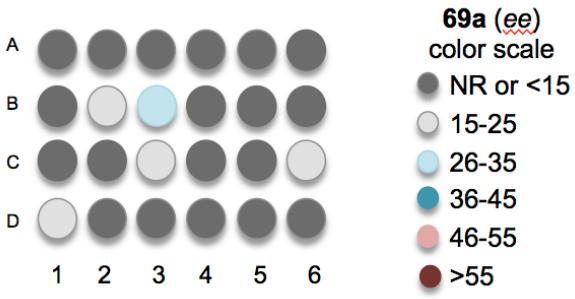

	1	2	3	4	5	6
A	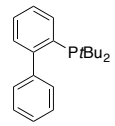 **L0**	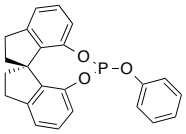 (*R*)-**L1**	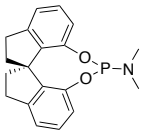 (*R*)-**L2**	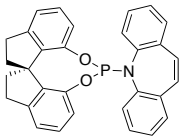 (*X*)-**L3**	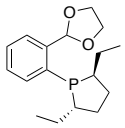 (*S,S*)-**L4**	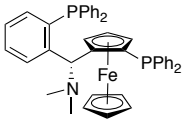 (R_p,*R*)-**L5**
B	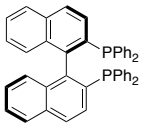 (*R*)-**L6**	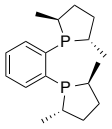 (*R,R*)-**L7**	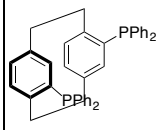 (*R*)-**L8**	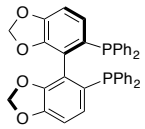 (*R*)-**L9**	 (*R,R*)-**L10**	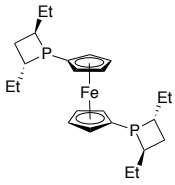 (*R,R*)-**L11**
C	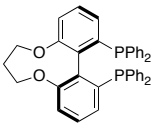 (*R*)-**L12**	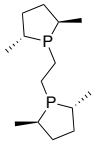 (*R,R*)-**L13**	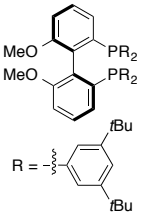 (*S*)-**L14**	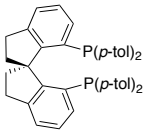 (*R*)-**L15**	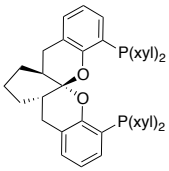 (*S*)-**L16**	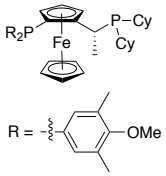 (*R*,S_P)-**L17**
D	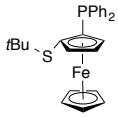 (*R,R*)-**L18**	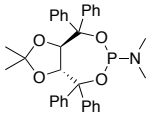 (*R,R*)-**L19**	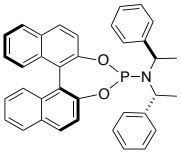 (*S*)-**L20**	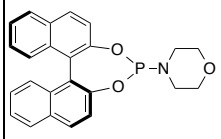 (*S*)-**L21**	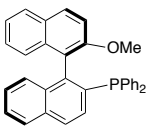 (*R*)-**L22**	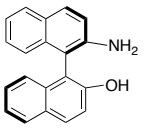 (*R*)-**L23**

Figure 9. Initial screening for the enantioselective hydroxycyclization of **73**

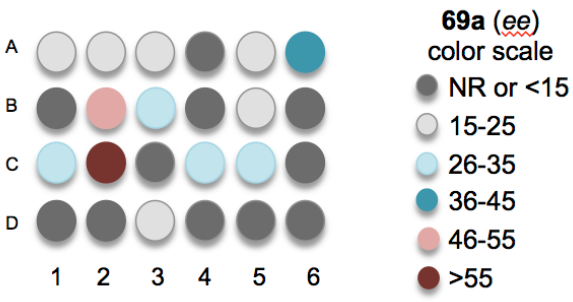

	1	2	3	4	5	6
A	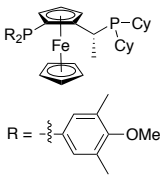 (R,S_P)-**L17**	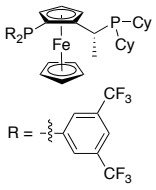 (R,S_P)-**L24**	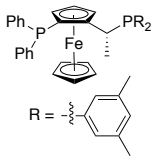 (R,S_P)-**L25**	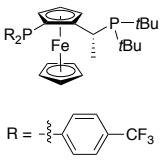 (R,S_P)-**L26**	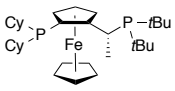 (R,S_P)-**L27**	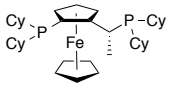 (R,S_P)-**L28**
B	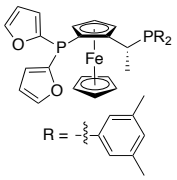 (R,S_P)-**L29**	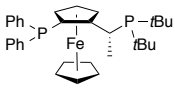 (R,S_P)-**L30**	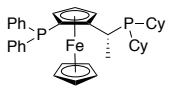 (R,S_P)-**L31**	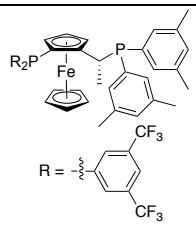 (R,S_P)-**L32**	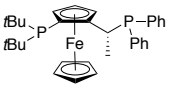 (R,S_P)-**L33**	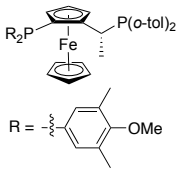 (R,S_P)-**L34**
C	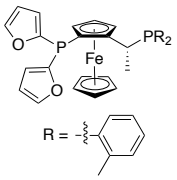 (R,S_P)-**L35**	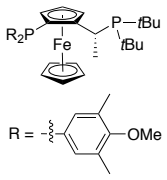 (R,S_P)-**L36**	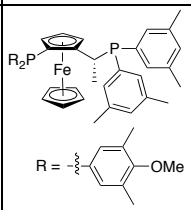 (R,S_P)-**L37**	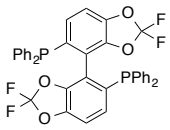 (R)-**L38**	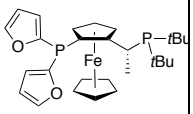 (R,S_P)-**L39**	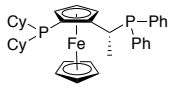 (R,S_P)-**L40**
D	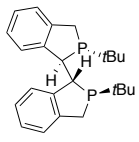 (R,R,S,S)-**L40**	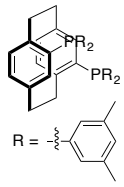 (R)-**L41**	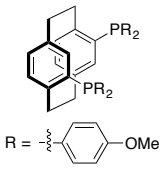 (S)-**L42**	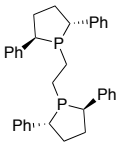 (R,R)-**L43**	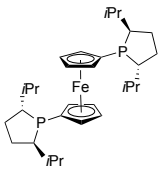 (S,S)-**L44**	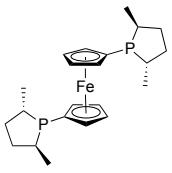 (S,S)-**L45**

Figure 10. Initial screening for the enantioselective hydroxycyclization of **73**

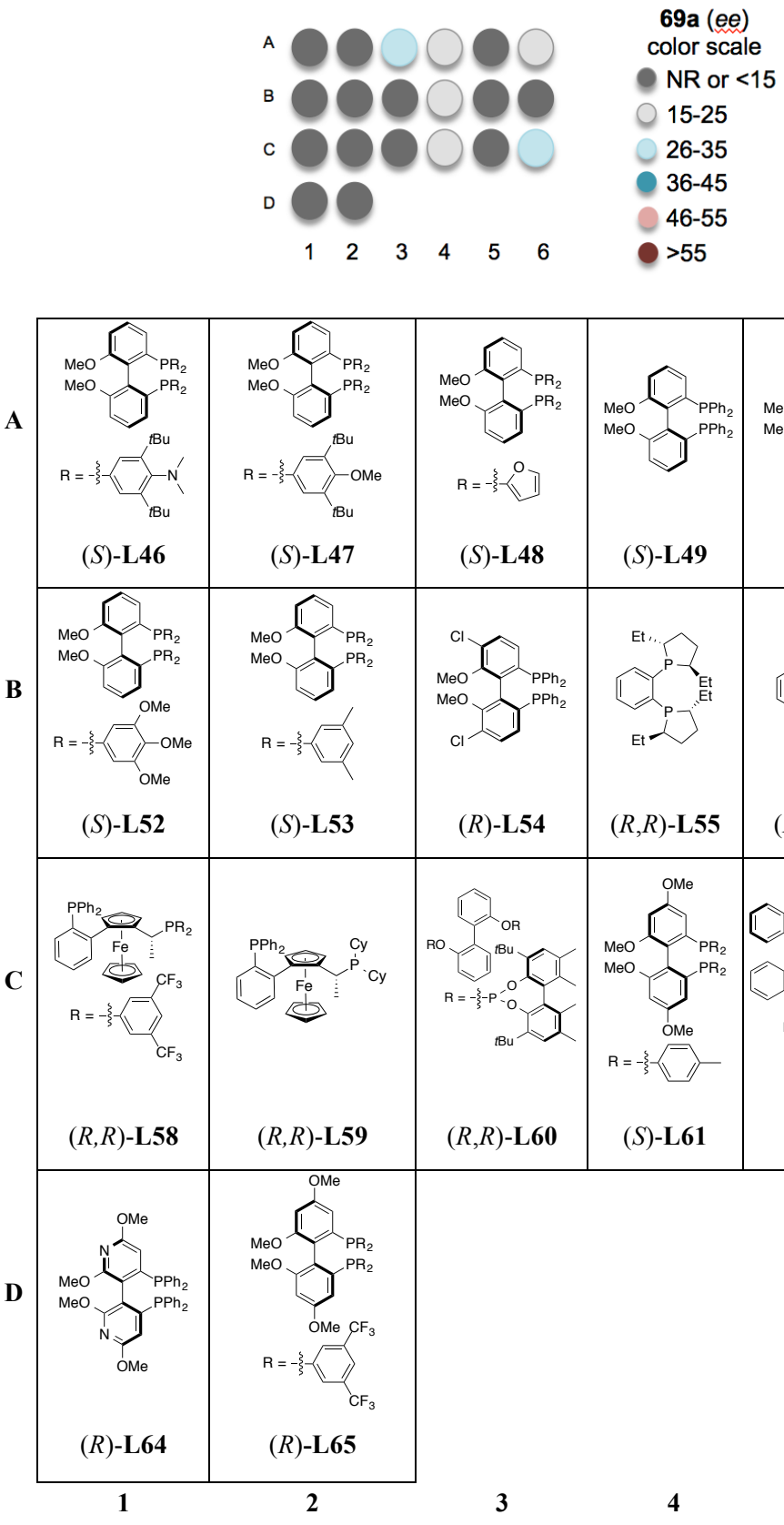

Figure 11. Initial screening for the enantioselective hydroxycyclization of **73**

Interestingly, JosiPhos bidentate ligands (R,S_P)-**L36** and (R,S_P)-**L30** were able to produce enantioenriched dihydronaphthalene derivative **69a** with -60% and -49% *ee*, respectively (Figure 10, entries C2 and B2). However, in the vast majority of the cases, the induced enantioselectivities still rather poor.

In order to improve enantioinduction, we chose to modify the nucleophile used to trap the proposed cationic intermediate. We hypothesized that by utilizing a bulkier nucleophile, we may observe increased enantioselectivity.

Therefore, JosiPhos (R,S_P)-**L36** and MeO-BiPhep (S)-**L48** ligands were selected to continue the screening for the formation of enantioenriched **69** using different nucleophiles (H_2O, MeOH, *i*PrOH). Additionally, the counterion (BAR_4^{F-} *vs*. SbF_6^-) and mol% of counterion (10 *vs*. 20) were evaluated (Table 11).

Table 11. Enantioselective gold(I)-catalyzed cyclization of **73**

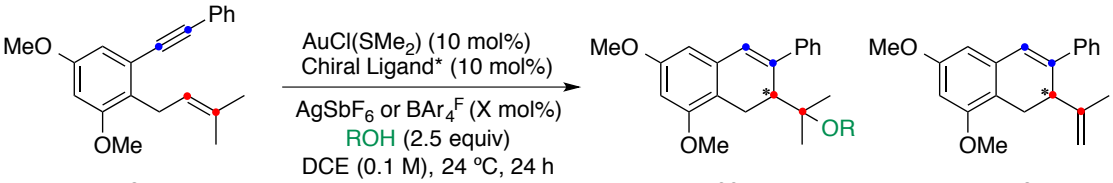

73 **69** **70**

Entry	Ligand	ROH	Counteranion	mol%	*ee* 69(%)[a]	*ee* 70(%)[a]
1	L36	H_2O	$AgSbF_6$	10	-62	-62
2	L36	H_2O	$NaBAr_4^F$	10	-19	-34
3	L36	H_2O	$AgSbF_6$	20	-71	-68
4	L36	H_2O	$NaBAr_4^F$	20	-9	-15
5	L36	MeOH	$AgSbF_6$	10	-26	-61
6	L36	MeOH	$NaBAr_4^F$	10	4	-39
7	L36	MeOH	$AgSbF_6$	20	15	-59
8	L36	MeOH	$NaBAr_4^F$	20	44	-48
9	L36	*i*PrOH	$AgSbF_6$	10	–	-61
10	L36	*i*PrOH	$NaBAr_4^F$	10	13	–
11	L36	*i*PrOH	$AgSbF_6$	20	–	-67
12	L36	*i*PrOH	$NaBAr_4^F$	20	13	–
13	L48	H_2O	$AgSbF_6$	10	16	24
14	L48	H_2O	$NaBAr_4^F$	10	31	45
15	L48	H_2O	$AgSbF_6$	20	-16	24

16	L48	H_2O	$NaBAr_4^F$	20	30	47
17	L48	MeOH	$AgSbF_6$	10	55	37
18	L48	MeOH	$NaBAr_4^F$	10	76	42
19	L48	MeOH	$AgSbF_6$	20	59	34
20	L48	MeOH	$NaBAr_4^F$	20	57	42
21	L48	*i*PrOH	$AgSbF_6$	10	–	37
22	L48	*i*PrOH	$NaBAr_4^F$	10	-24	19
23	L48	*i*PrOH	$AgSbF_6$	20	–	37
24	L48	*i*PrOH	$NaBAr_4^F$	20	–	37

[a] *ee* determined by UPC[2] (UltraPerformance Convergence Chromatography)

As shown in Table 11, using JosiPhos (R,S_P)-**L36** ligand and water as a nucleophile, $AgSbF_6$ was found to be a better chloride scavenger, leading to cleaner reaction mixtures. By increasing the amount of choride scavenger from 10 to 20 mol% (Table 11, entries 1 and 3), enantioenriched dihydronaphthalene **69a** was obtained with -71% *ee*. Contrary, when methanol was used as nucleophile, the best results were obtained when the reaction was performed with 20 mol% of $NaBar_4^F$ (Table 11, entry 8). Isopropanol was found to be significantly less reactive than water or methanol. The best enantioselectivities were obtained for the elimination product **70** using SbF_6^- as counterion (Table 11, entries 9 and 11). When the reaction was performed with MeO-BiPhep (*S*)-**L48** ligand, methanol proved to be the best nucleophile, leading to the enantioenriched cycloaddition product **69b** with a range from 55 to 76% of *ee* (Table 11, entries 17-20). On the other hand, the use of water or isopropanol under these conditions was found to be less convenient (Table 11, entries 13-16 and 21-24). Furthermore, increasing the amount of chloride scavenger did not seem to have a clear effect on the outcome of the reaction.

Despite these encouraging results, concurrent studies to functionalize those dihydronaphthalene derivatives revealed that subsequent alkoxy deprotection would be non-trivial. Therefore, we turned our attention to the use of allyl alcohol as nucleophile, since a wide variety of conditions could be applied for the removal of the resulting allyl ether. Thus, we select the best ligands for the generation of hydroxycyclization product, (*R*)-**L8,** (R,S_P)-**L30,** (R,S_P)-**L36,** (*S*)-**L48** and (*R*,*R*)-**L55**, to perform our screening.

As shown in Table 12, the best results were obtained when the reaction was performed using JosiPhos ligand (*R*,S_P)-**L36** and 10 mol% of $AgSbF_6$ (Table 12, entry 9). Under these conditions, alkoxycyclization product **69g** was obtained in 39% yield with -47% *ee*. In addition, moderate enantioselectivities were also obtained with JosiPhos (*R*,S_P)-**L30** and MeO-BiPhep (*S*)-**L48** ligands (Table 12, entries 5-6 and 13-14).

Table 12. Enantioselective gold(I)-catalyzed cyclization of **73** with allyl alcohol as nucleophile

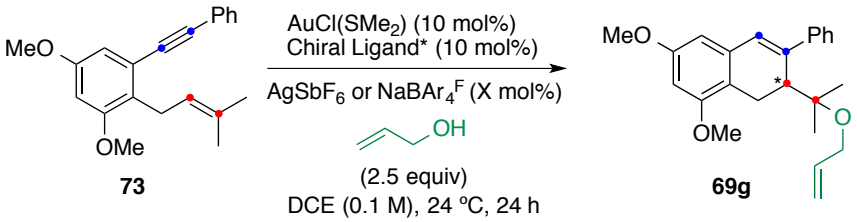

Entry	Ligand	Counteranion	mol%	*ee* 69g(%)[a]	GC Yield (%)
1	L8	$AgSbF_6$	10	17	12
2	L8	$AgSbF_6$	20	9	26
3	L8	$NaBAr_4^F$	10	8	4
4	L8	$NaBAr_4^F$	20	48	5
5	L30	$AgSbF_6$	10	-37	37
6	L30	$AgSbF_6$	20	-21	23
7	L30	$NaBAr_4^F$	10	4	10
8	L30	$NaBAr_4^F$	20	–	17
9	L36	$AgSbF_6$	10	-47	39
10	L36	$AgSbF_6$	20	-33	29
11	L36	$NaBAr_4^F$	10	-8	9
12	L36	$NaBAr_4^F$	20	-34	19
13	L48	$AgSbF_6$	10	35	37
14	L48	$AgSbF_6$	20	37	31
15	L48	$NaBAr_4^F$	10	–	2
16	L48	$NaBAr_4^F$	20	40	4
17	L55	$AgSbF_6$	10	33	26
18	L55	$AgSbF_6$	20	46	17
19	L55	$NaBAr_4^F$	10	36	6
20	L55	$NaBAr_4^F$	20	44	19

[a] *ee* determined by UPLC or by UPC[2]

Next, the cyclization **73** was studied in twelve solvents with different dielectric constants to evaluate their effect on this transformation. This new screening was performed using the best previously examined chiral ligands (*R*,*S*P)-**L30,** (*R*,*S*P)-**L36** and (*S*)-**L48**, $AgSbF_6$ (10 mol%) as chloride scavenger and allyl alcohol (2.5 equiv) as nucleophile (Table 13).

Table 13. Solvent screening on the enantioselective gold(I)-catalyzed cyclization of **73**

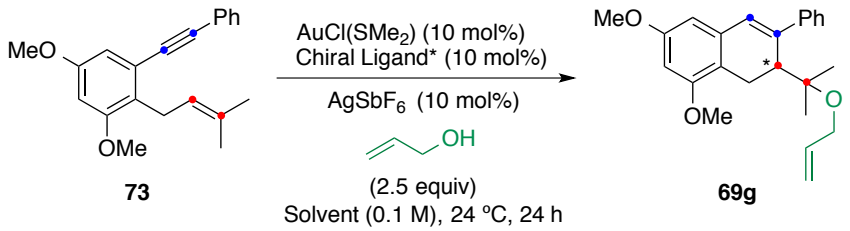

Solvent	Entry	L*	*ee*(%)[a]	Entry	L*	*ee*(%)[a]	Entry	L*	*ee*(%)[a]
Ph	1	L30	-42(44)	13	L36	-56(44)	25	L48	20(8)
$PhCH_3$	2	L30	-34(41)	14	L36	-54(46)	26	L48	28(10)
$CHCl_3$	3	L30	-43(37)	15	L36	-53(36)	27	L48	16(13)
PhCl	4	L30	-41(40)	16	L36	-54(39)	28	L48	25(10)
EtOAc	5	L30	-39(33)	17	L36	-70(13)	29	L48	31(7)
CH_2Cl_2	6	L30	-44(38)	18	L36	-58(39)	30	L48	18(10)
THF	7	L30	-44(40)	19	L36	-57(52)	31	L48	–
$PhCF_3$	8	L30	-43(37)	20	L36	-60(36)	32	L48	29(14)
DCE	9	L30	-38(44)	21	L36	-67(40)	33	L48	22(12)
Allyl alcohol	10	L30	-52(39)	22	L36	-63(34)	34	L48	28(9)
DMF	11	L30	–	23	L36	–	35	L48	–
DMSO	12	L30	–	24	L36	–	36	L48	–

[a] *ee* determined by UPC2. % GC yield in brackets

Surprisingly, when the reaction was carried out in the presence of JosiPhos ligands (*R*,*S*P)-**L30** and (*R*,*S*P)-**L36**, many solvents (including moderately coordinating solvents such as THF) allowed the reaction to proceed in reasonable yield and enantiomeric excess. Thus, ligand (*R*,*S*P)-**L30** afforded **69g** with *ee* values in a range from -38 to -52% (Table 13, entries 1 to 10). The use of allyl alcohol as solvent proved to be beneficial (Table 13, entry 10). Likewise, the use of (*R*,*S*P)-**L36** resulted in slightly better yields and higher enantioselectivities (-53 to -70% *ee*) (Table 13, entries 13 to 22). In this case, THF and 1,2-dichloroethane (DCE) were found to be the best solvents (Table 13, entries 7 and 9). Rather, in the presence of ligand (*S*)-**L48**, the cyclization proceeded with low yields (7 to 14%) and poor enantioselectivities (16-31%) (Table 13,

entries 25-34). Finally, when the reaction was performed in DMF and DMSO, no alkoxycyclization was observed regardless of the ligand used (Table 13, entries 11-12, 23-24 and 35-36).

From this preliminary study, the best reaction conditions involve the use of 10 mol% of $AgSbF_6$ as chloride scavenger, allyl alcohol as a nucleophile, and JosiPhos ligand (R,S_P)-**L36** in DCE (-67% *ee*, 40% yield). Work on the optimization of these results is now in progress.[44]

Synthesis of the Racemic Carexane I

Concurrently, we continued towards the total synthesis of racemic carexane I (Figure 12). Although the relative configuration of this compound was initially assigned as H7/H8 *trans* and H8/H16 *trans*,[22,45] it was later revised on the basis of the X-ray diffraction analysis of parent tetracyclic carexane D.[25] Accordingly, it was proposed that all the carexanes with a tetrahydronaphthalene skeleton feature a *trans/cis* configuration between the substituents in H-7/H-8 and H-8/H16, respectively. However, to date there is no total synthesis nor crystalline structure of any of the carexanes featuring a tetrahydronaphthalene core that secure this hypothesis.

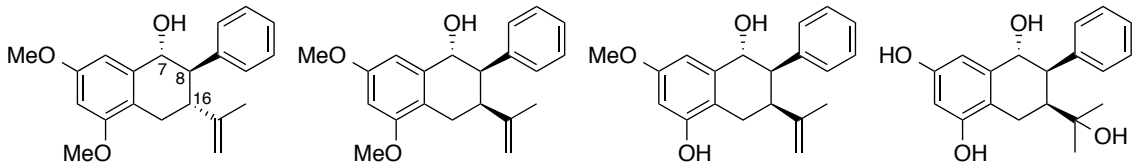

Figure 12. Carexanes I, P and O

We focus our initial investigations on finding the optimal conditions for the dehydration of **69a**. We reasoned that this transformation could be challenging due to the tendency of dihydronaphathalene derivative **69a** to generate undesired naphthalene **78**. After screening, the best results were obtained when **69a** was treated with $POCl_3$ in pyridine at 23 ºC for 1 h to afford **70** in 66% yield (Scheme 46). Notably, formation of **78** was not observed.

44 Currently under development by Joan G. Mayans at the ICIQ.

45 The numbering of the atoms follows that of the publications on the isolation of these natural products.

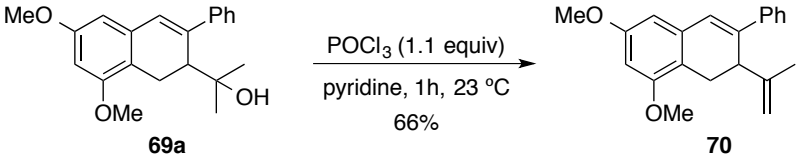

Scheme 46. Studies on the elimination of tertiary alcohol of **69a**

On the other hand, hydroboration of dihydronaphthalene derivative using BH_3 in THF followed by oxidation with $NaOH/H_2O_2$ afforded the desired secondary alcohols **87a** and **87b** in 62% yield and 4.3:1 *dr* (Scheme 47).[46] Both diastereomers could be readily separated by column chromatography.

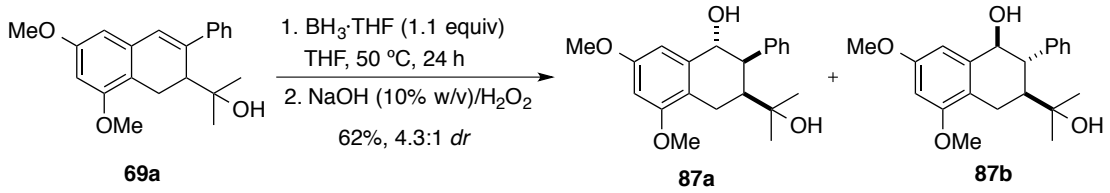

Scheme 47. Hydroboration-oxidation of **69a**

Presumably, the hydroboration reaction proceeds by preferential addition from the face opposite to the bulky substituent at C-16, which explains the formation of **87a** as the major isomer. The relative configuration of both isomers was determined by NMR spectroscopy and assigned by comparison with the reported data of isolated carexane O (Table 14).[25] Additionally, we calculated the optimized structures of the corresponding compounds using DFT analysis (M06, 6-31 G(d,p) (C,H,O)) (Figure 13).

Thus, the observed coupling constants of the H-7 and H-8 protons for **87a** were in agreement with dihedral angles of about 60º or 110º as in the case of isolated carexane O (Table 14). In the minimized structures of **87a** and carexane O, the H-7 and H-8 protons showed a dihedral angle H(7)–C(7)–C(8)–H(8) of -78.7(7)º and -78.2(3)º, respectively (Figure 13). The torsion angles H(8)–C(8)–C(16)–H(16) were -61.0(8)º in both cases. Thus, corresponding to a *trans* orientation among the H-7 and H-8 protons and *cis* orientation among the H-8 and H-16 protons. In the case of **87b**, higher *J* values were observed for the H-7 and H-8 protons (*J* = 6.0 Hz), and the H-8 and H-16 (*J* = 3.2

46 Jackman, H.; Marsden, S. P.; Shapland, P.; Barrett, S. *Org. Lett.* **2007**, *9*, 5179–5182.

Hz). These values are in good accordance with a *trans/trans* orientation between H-7, H-8 and H-16 protons.[47]

Table 14. Comparison with NMR data of **87a**, **87b** with isolated carexane O[25,a]

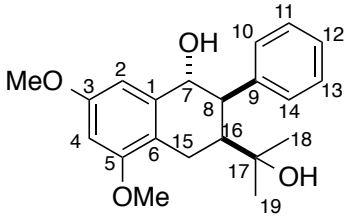

Position	^{1}H NMR of 87a δ (ppm)	^{1}H NMR of 87b δ (ppm)	^{1}H NMR of isolated carexane O δ (ppm)
1	–	–	–
2	–	–	–
3	–	–	–
4	6.50 *d* (2.4)	6.46 *d* (2.3)	6.31 *d* (0.9)
5	–	–	–
6	6.52 *d* (2.4)	6.76 *dd* (2.5, 1.0)	6.31 *d* (0.9)
7	4.47 *d* (1.8)	5.06 *d* (6.0)	4.38 *d* (1.8)
8	3.49 app. *dt* (3.3, 1.4)	3.71 *dd* (6.3, 3.2)	3.46 br *s*
9	–	–	–
10	6.99 – 6.95 *m*	7.06 – 7.03 *m*	6.99 *ov*
11	7.15 – 7.11 *m*	7.15 –7.10 *m*	7.13 *ov*
12	7.15 – 7.11 *m*	7.15 –7.10 *m*	7.13 *ov*
13	7.15 – 7.11 *m*	7.15 –7.10 *m*	7.13 *ov*
14	6.99 – 6.95 *m*	7.06 – 7.03 *m*	6.99 *ov*
15	3.04 *dd* (16.6, 4.1)	2.99 *dd* (17.6, 5.5)	2.98 *dd* (14.5, 5.8)
	2.43 *dd* (16.7, 13.0)	2.56 *ddd* (17.7, 12.9, 1.7)	2.38 *m*
16	2.50 *ddd* (13.0, 4.2, 3.4)	2.25 *ddd* (12.9, 5.5, 3.1)	2.47 *m*
17	–	–	–
18	0.90 *s*	0.89 *s*	0.92 *s*
19	1.16 *s*	1.08 *s*	1.14 *s*
OMe	3.79 *s*	3.78 *s*	–
OMe	3.86 *s*	3.85 *s*	–

[a] ^{1}H NMR spectra in CD_3OD at 25 ºC. The couplings (Hz) are reported in brackets.

47 The lowest-energy conformation found for compound **87b** has H-7, H-8 and H-16 protons in axial position (the difference between these two conformations is ΔG^o = 5.3 kcal·mol^{-1}). However, this conformation is not in agreement with the experimental data.

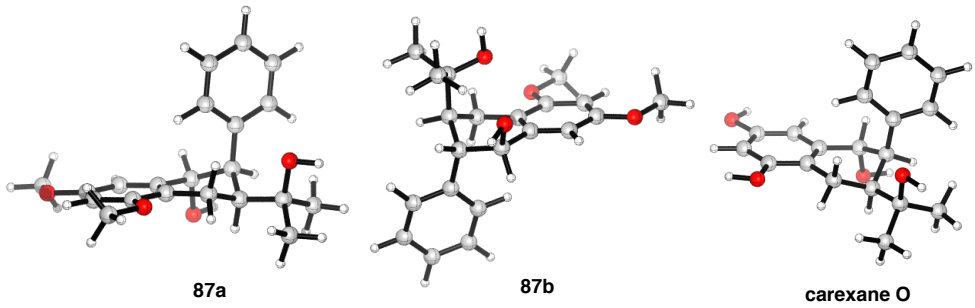

Figure 13. Optimized structures of **87a**, **87b** and isolated carexane O. DFT calculations (M06/6-31G(d,p)).

Therefore, we continue our investigations with the major isomer **87a**, which already has the proposed relative configuration at all the stereogenic centers. However, attempts to perform the dehydration of tertiary alcohol **87a** using $POCl_3$ in pyridine only led to the formation of an unidentified compound for which was tentatively assigned an oxo-brigded structure (Scheme 48).

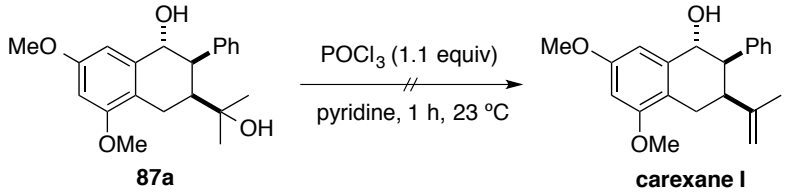

Scheme 48. Studies on the dehydration of tertiary alcohol of **87a**

On that account, we decided to convert the secondary alcohol into the corresponding ketone prior to attempt the elimination of tertiary alcohol (Scheme 49). The best results were obtained when **87a** was treated with Dess-Martin periodinane (DMP) in combination with $NaHCO_3$ to obtain ketone **88** in 81% yield. Treatment with pyridinum chlorochromate (PCC)[48] also afforded **88**, albeit in 50% yield.

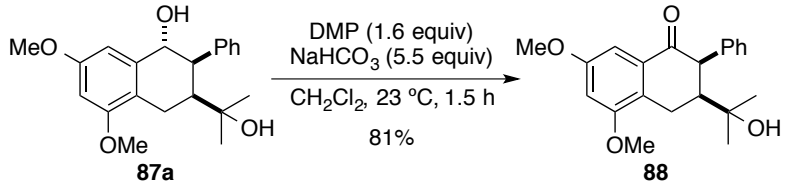

Scheme 49. Synthesis of ketone **88**

48 Liu, Y.; Cheng, L.-J.; Yue, H.-T.; Che, W.; Xie, J.-H.; Zhou, Q.-L. *Chem. Sci.* **2016**, *7*, 4725–4729.

We intended the dehydration of **88** with $POCl_3$ under the optimized conditions used to synthesize **70** (see Scheme 46). However, complete decomposition of starting material was observed. Fortunately, treatment with Burgess reagent in CH_2Cl_2 afforded **89** in 94% yield (Scheme 50),[48] which could be further reduced with $LiAlH_4$ to afford *epi*-carexane I in 93% yield.

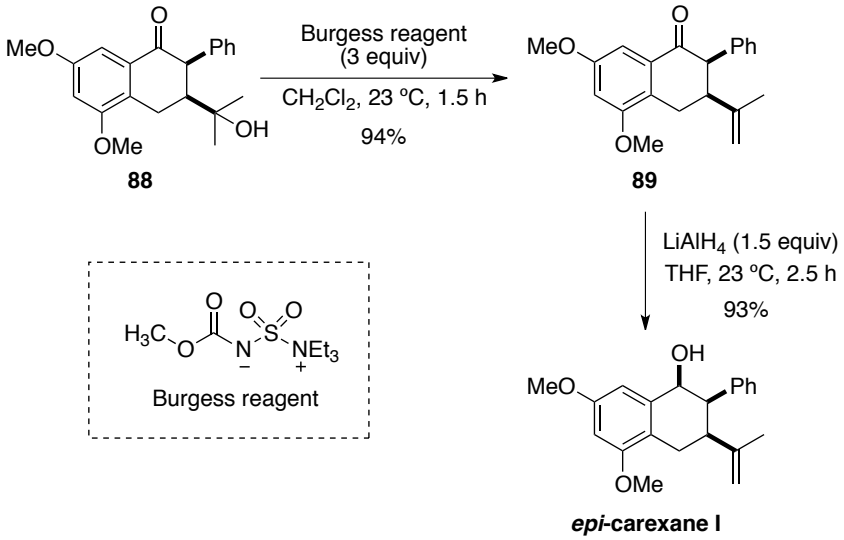

Scheme 50. Studies towards the synthesis of carexane I

The synthesis of carexane I was accomplished from diol **87a** by selective TIPS protection of the secondary alcohol to afford silyl ether **90**, followed by dehydration of the tertiary alcohol and final silyl deprotection of **91** employing TBAF (Scheme 51).

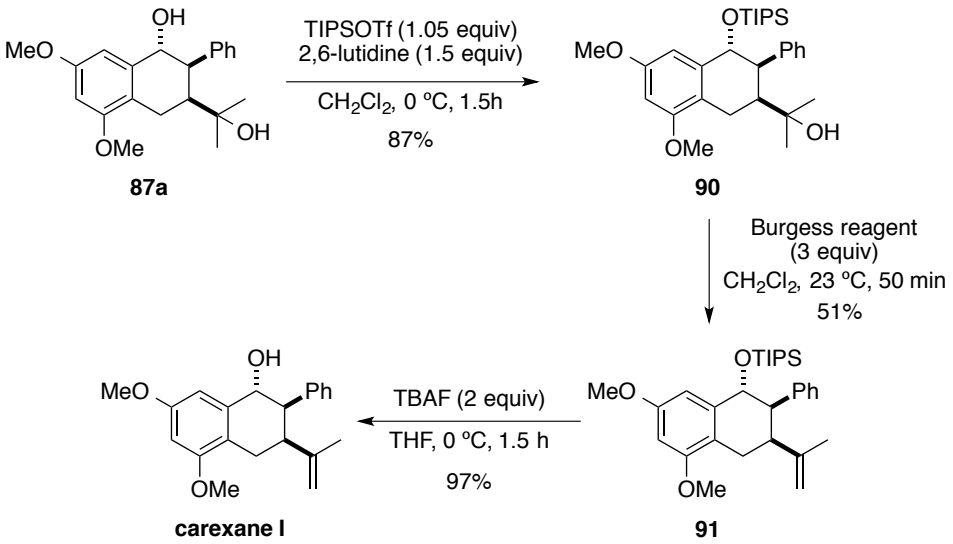

Scheme 51. Synthesis of carexane I

Additionally, the structure and relative configuration of carexane I were confirmed by X-ray diffraction (Figure 14).

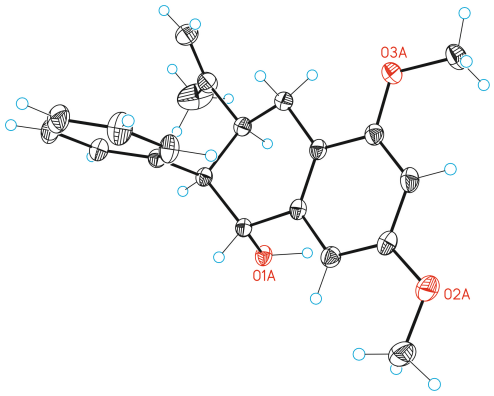

Figure 14. ORTEP representations of synthesized carexane I with 50% probability of the thermal ellipsoids

As anticipated, our data and the reported data for carexane I were in agreement with a *trans*/cis orientation of H–7, H-8 and H-16 protons, which further confirm the initial hypothesis (Tables 14 and 15).

Table 14. Comparison with NMR data of isolated carexane I[a]

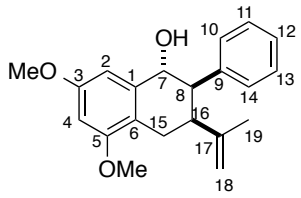

Position	^{1}H NMR of synthesized carexane I δ (ppm)	^{1}H NMR of isolated carexane I[22] δ (ppm)
1	–	–
2	–	–
3	–	–
4	6.45 *d* (2.4)	6.45 *d* (2.4)
5	–	–
6	6.61 *d* (2.4)	6.61 *d* (2.4)
7	4.88 *d* (2.6)	4.88 *d* (2.7)
8	3.42 *t* (3.1)	3.42 *t* (3.0)
9	–	–
10	6.90 –6.83 *m*	6.86 *m*
11	7.18 – 7.12 *m*	7.14 *m*
12	7.18 – 7.12 *m*	7.14 *m*
13	7.18 – 7.12 *m*	7.14 *m*
14	6.90 –6.83 *m*	6.86 *m*
15	2.78 *dd* (17.3, 4.5)	2.78 *dd* (17.7, 4.8)
	2.29 *dd* (17.3, 12.0)	2.29 *dd* (17.7, 12.3)
16	2.91 *dt* (12.1, 3.9)	2.91 *dt* (11.7, 3.0)
17	–	–
18	4.81 *s*	4.81 *s*
	4.47 *s*	4.47 *s*
19	1.79 *s*	1.79 *s*
OMe	3.82 *s*	3.80 *s*
OMe	3.84 *s*	3.81 *s*

[a] ^{1}H NMR spectra in $CDCl_3$ at 25 ºC. The couplings (Hz) are reported in brackets.

Table 15. Comparison with NMR data of isolated carexane I[22,49]

	Synthesized carexane I		Isolated carexane I	
Position	**^{1}H NMR δ (ppm)**	**^{13}C NMR δ (ppm)**	**^{1}H NMR δ (ppm)**	**^{13}C NMR δ (ppm)**
1	–	140.0	–	140.0
2	–	120.2	–	120.2
3	–	159.2	–	159.1
4	6.49 *d* (2.4)	98.8	6.48 *d* (2.4)	98.0
5	–	160.6	–	160.5
6	6.63 *d* (2.4)	106.5	6.62 *d* (2.4)	106.5
7	4.76 *d* (2.2)	7.2	4.76 *d* (2.7)	73.2
8	3.37 *dd* (3.6, 2.2)	51.4	3.53 *dd* (3.3, 2.7)	51.4
9	–	140.6	–	140.6
10	6.85 –6.80 *m*	129.9	6.82 *m*	129.9
11	7.12 – 7.08 *m*	128.6	7.09 *m*	128.6
12	7.12 – 7.08 *m*	127.4	7.09 *m*	127.4
13	7.12 – 7.08 *m*	128.6	7.09 *m*	128.6
14	6.85 –6.80 *m*	129.9	6.82 *m*	129.9
15	2.70 *dd* (17.2, 4.6)	24.1	2.69 *dd* (17.4, 4.5)	24.1
	2.20 *dd* (17.3, 12.3)		2.21 *dd* (17.4, 12.3)	
16	2.95 *dt* (12.7, 4.2)	40.8	2.94 *dt* (12.3, 3.3)	40.5
17	–	147.9	–	147.9
18	4.77 app. *s*	111.7	4.75 *s*	111.7
	4.42 *s*		4.44 *s*	
19	1.80 *s*	22.9	1.79 *s*	22.8
OMe	3.81 *s*	55.8	3.81 *s*	55.7
OMe	3.82 *s*	55.9	3.82 *s*	55.8

[a] NMR spectra in CD_3OD at 25 ºC. The couplings (Hz) are reported in brackets.

49 When the NMR spectra were performed in CD_3OD at 25 ºC, two small discrepancies were observed between the reported data and our data: ^{1}H-NMR signal corresponding to H-8 (δ 3.53 *vs*. 3.37 ppm) and ^{13}C-NMR signal corresponding to C-4 (δ 98.0 *vs*. 98.8 ppm).

Conclusions

We have prepared the required 5,6,6-tricyclic core of the pycnanthuquinone C **51a** in good yield by a [4+2] gold(I)-catalyzed cycloaddition reaction of 1,6-enyne **52a** (Scheme 51).

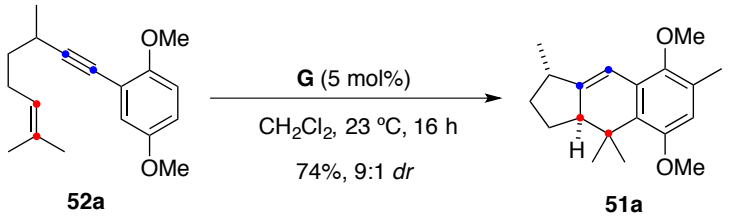

Scheme 51. Studies towards the synthesis of pycnanthuquinone C

Among the different strategies explored to functionalize **51a**, the oxidation of tricyclic intermediate to the corresponding quinone was found to be crucial to perform the subsequent epoxidation step (Scheme 52). However, further investigations are still required in order to access to the natural product.

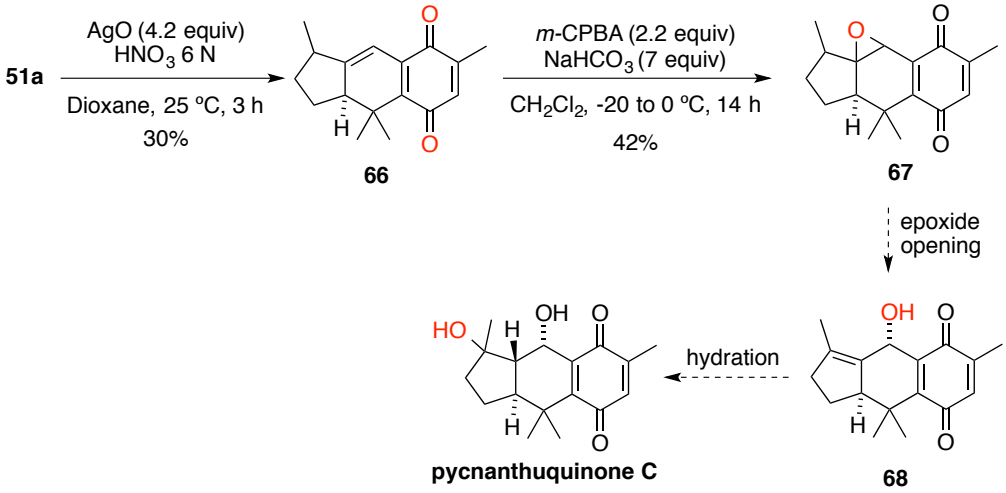

Scheme 52. Studies on the functionalization of tricyclic intermediate **51a**

We have also developed an enantioselective gold(I)-catalyzed 6-*endo*-*dig* cyclization for the ready access to the common bicyclic core of carexanes. After the evaluation of a number of chiral gold(I) complexes and different reaction conditions, the corresponding enantioenriched dihydronaphthalene derivative **69g** could be obtained with moderate yield (40%) and *ee* values (*ca*. 67%) (Scheme 53).

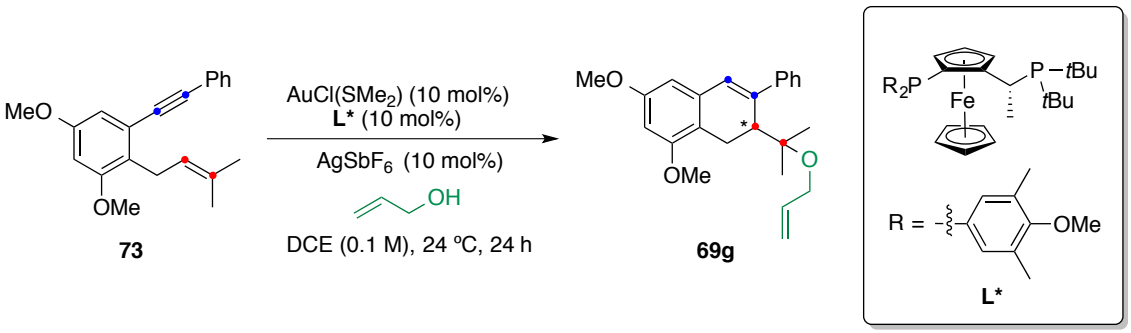

Scheme 53. Enantioselective gold(I)-catalyzed 6-*endo-dig* cyclization of **73**

We accomplished the first total synthesis of racemic carexane I in 4 steps from dihydronaphthalene derivative **69a** in 18% overall yield (Scheme 54). Future work will involve the optimization of these steps, the preparation of carexanes O and P, and the development of the enantioselective synthesis.

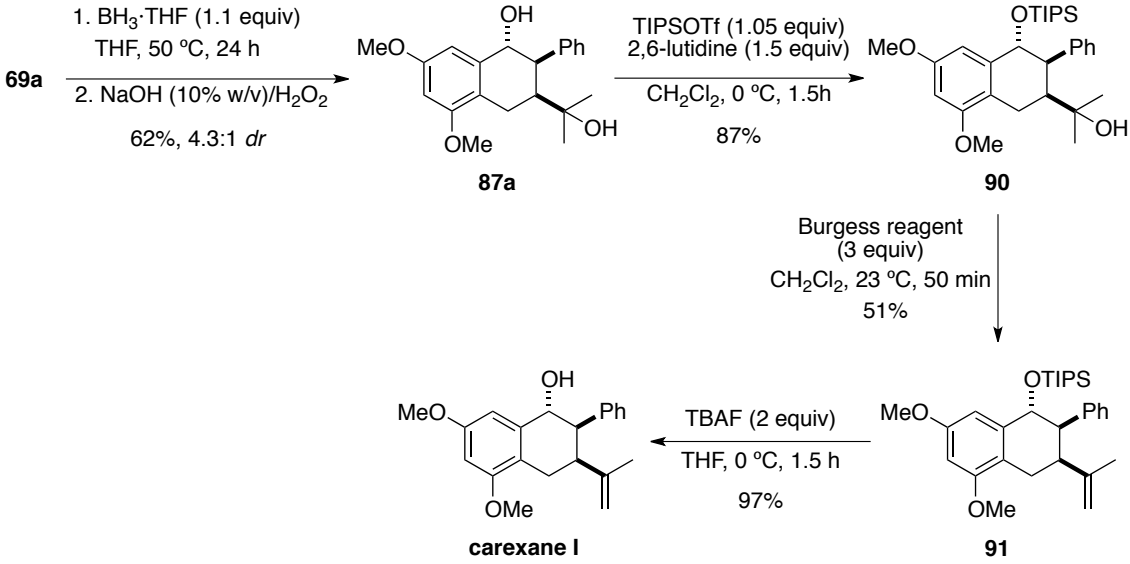

Scheme 54. Synthesis of carexane I

Experimental Part

General Methods

Unless other wise stated, reactions were performed under argon in solvents dried by passing through an activated alumina column on a PureSolv^{TM} solvent purification system (Innovative Technologies, Inc., MA). Analytical thin layer chromatography was carried out using TLC-aluminum sheets coated with 0.2 mm of silica gel (Merck GF_{234}) using UV light as the visualizing agent and an acidic solution of vanillin in ethanol as the developing agent. Chromatographic purifications were carried out using flash grade silica gel (SDS Chromatogel 60 ACC, 40-63 μm) or automated flash chromatographer CombiFlash Companion. Preparative TLC was performed on 20 cm x 20 cm silica gel plates (2.0 mm thick, catalogue number 02015, Analtech). If indicated, preparative TLC was performed on 20 cm x 20 cm aluminium oxide plates (0.25 mm thick, 90066, Fluka). Organic solutions were concentrated under reduced pressure on a Büchi rotary evaporator.

NMR spectra were recorded at 298 K (unless otherwise stated) on a Bruker Avance 300, Bruker Avance 400 Ultrashield and Bruker Avance 500 Ultrashield apparatuses. The data are reported as such: chemical shift [δ, ppm] (multiplicity, coupling constant [Hz], number of protons). The chemical shifts are given in ppm downfield from tetramethylsilane using the residual protio-solvent as internal reference (d_H = 7.26 ppm and d_C = 77.16 for $CDCl_3$). The abbreviations for multiplicities are: s (singlet), d (doublet), t (triplet), q (quartet), quin (quintet), sext (sextet), sept (septet). Mass spectra were recorded on a Waters Micromass LCT Premier (ESI), Waters Micromass GCT (EI, CI) and Bruker Daltonics Autoflex (MALDI) spectrometers. GCMS analysis were performed in a Agilent Technologies Instrument (5977A Series GC/MSD System). Melting points were determined using a Büchi melting point apparatus.

Crystal structure determinations were carried out using a Bruker-Nonius diffractomer equipped with an APPEX 2 4K CCD area detector, a FR591 rotating anode with MoK_a radiation, Montel mirrors as monochromator and a Kryoflex low temperature device (T = –173 °C). Full-sphere data collection was used with w and j scans. *Programs used*: Data collection APEX-2, data reduction Bruker Saint V/.60A and absorption correction SADABS. Structure Solution and Refinement: Crystal structure solution was achieved using direct methods as implement in SHELXTL and visualized using the program XP. Missing atoms were subsequently located from difference Fourier synthesis and added to the atom list. Least-squares refinement on F2 using all measured intensities was

carried out using the program SHELXTL. All non-hydrogen atoms were refined including anisotropic displacement parameters.

All reagents were used as purchased and used with no further purification, unless otherwise stated.

All calculations were performed with DFT using the M06 functional as implemented in Gaussian 09.[50] The 6-31G(d,p) basis set was used for all atoms (C,H,O).[51] Frequency calculations were performed to characterize the stationary points as minima.

50 Frisch, M. J.; Trucks, G. W.; Schlegel, H. B.; Scuseria, G. E.; Robb, M. A.; Cheeseman, J. R.; Scalmani, G.; Barone, V.; Mennucci, B.; Petersson, G. A.; Nakatsuji, H.; Caricato, M.; Li, X.; Hratchian, H. P.; Izmaylov, A. F.; Bloino, J.; Zheng, G.; Sonnenberg, J. L.; Hada, M.; Ehara, M.; Toyota, K.; Fukuda, R.; Hasegawa, J.; Ishida, M.; Nakajima, T.; Honda, Y.; Kitao, O.; Nakai, H.; Vreven, T. ; Montgomery (Jr.), J. A.; Peralta, J. E.; Ogliaro, F.; Bearpark, M.; Heyd, J. J.; Brothers, E.; Kudin, K. N.; Staroverov, K. N.; Kobayashi, R.; Normand, J.; Raghavachari, K.; Rendell, A.; Burant, J. C.; Iyengar, S. S.; Tomasi, J.; Cossi, M.; Rega, N.; Millam, N. J.; Klene, M.; Knox, J. E.; Cross, J. B.; Bakken, V.; Adamo, C.; Jaramillo, J.; Gomperts, R.; Stratmann, R. E.; Yazyev, O.; Austin, A. J.; Cammi, R.; Pomelli, C.; Ochterski, J. W.; Martin, R. L.; Morokuma, K.; Zakrzewski, V. G.; Voth, G. A.; Salvador, P.; Dannenberg, J. J.; Dapprich, S.; Daniels, A. D.; Farkas, O.; Foresman, J. B.; Ortiz, J. V.; Cioslowski, J.; Fox, D. J.; Gaussian 09, revision 02; Gaussian, Inc.: Wallingford, CT, **2009**.

51 Hehre, W. J.; Ditchfield, R.; Pople, J. A. *J. Chem. Phys.* **1972**, *56*, 2257–2261.

Synthetic Procedures and Analyical Data

3-(Methoxymethoxy)-3,7-dimethyloct-6-en-1-yne (32)

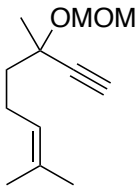

To a suspension of NaH (60% in oil, 1.16 g, 29.1 mmol) in dry DMF (30 mL), was added a solution of **31**[27] (2.22 g, 14.55 mmol) in dry DMF (30 mL) at 0 ºC. After stirring for 30 minutes, MOMCl (5.86 g, 72.75 mmol) was added carefully and the resulting mixture was warmed to 23 ºC. After 17 hours, the reaction was treated with H_2O and extracted with ethyl acetate (3 x 100 mL). The combined organic phases were washed with water and brine, dried over $MgSO_4$. The crude was purified by flash chromatography over silica gel using cyclohexane:EtOAc 95:5 as eluent to afford the compound (1.68 g, 59%) as a colorless oil.

^{1}H NMR (400 MHz, $CDCl_3$) δ 5.12 (tdq, *J* = 7.2, 2.8, 1.4 Hz, 1H), 4.99 (d, *J* = 7.0 Hz, 1H), 4.82 (d, *J* = 7.0 Hz, 1H), 3.39 (s, 3H), 2.50 (s, 1H), 2.25 – 2.08 (m, 2H), 1.81 – 1.72 (m, 1H), 1.71 – 1.63 (m, 1H), 1.71 – 1.64 (m, 4H), 1.50 (s, 3H). ^{13}C NMR (101 MHz, $CDCl_3$) δ 131.9, 123.7, 93.1, 84.7, 73.9, 73.8, 55.6, 42.6, 27.9, 25.7, 23.1, 17.6. GCMS-ESI(+) *m/z* calc. for $C_{12}H_{20}O_2$ $[M]^+$: 196.2, found: 196.2.

Tributyl(3-(methoxymethoxy)-3,7-dimethyloct-6-en-1-yn-1-yl)stannane (33)

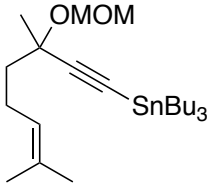

*n*BuLi (4.1 mL, 10.27 mmol; 2.5 M in hexanes) was added to a solution of 1,6-enyne **32** (1.68 g, 8.56 mmol) in dry THF (75 mL) at -78 ºC and the resulting mixture was allowed to warm up to -20 ºC within 2 hour. The reaction mixture was cooled to -78 ºC and tributylchlorostannane (3.34 g, 10.27 mmol) in 11 mL of THF. After complete addition, the solution was allowed to reach 23 ºC. After 16 hours, the reaction was treated with H_2O and extracted with ethyl acetate (3 x 150 mL). The combined organic phases were washed with water and brine, dried over $MgSO_4$. The crude was purified by flash chromatography over silica gel using cyclohexane as eluent to afford **33** (2.75 g, 66%) as a colorless oil.

^{1}H NMR (500 MHz, $CDCl_3$) δ 5.13 (tdt, *J* = 7.3, 2.9, 1.4 Hz, 1H), 5.04 (d, *J* = 6.7 Hz, 1H), 4.83 (d, *J* = 6.7 Hz, 1H), 3.38 (s, 3H), 2.24 – 2.11 (m, 2H), 1.78 – 1.70 (m, 1H), 1.69 – 1.67 (m, 3H), 1.66 – 1.60 (m, 4H), 1.59 – 1.52 (m, 6H), 1.47 (s, 3H), 1.37 – 1.30 (m, 6H), 1.00 – 0.95 (m, 6H), 0.90 (t, *J* = 7.3 Hz, 10H). ^{13}C NMR (126 MHz, $CDCl_3$) δ 131.7, 124.3, 111.0, 93.3, 88.6, 74.9, 55.7, 43.1, 29.1 (3C), 28.5, 27.1 (3C), 25.8, 23.7, 17.8, 13.8 (3C), 11.2 (3C). HRMS-ESI(+) *m/z* calc. for $C_{24}H_{46}O_2Sn$ $[M+Na]^+$: 509.2412, found: 509.2389.

1-Bromo-5-chloro-2-(methoxymethoxy)-3-methylbenzene (39)

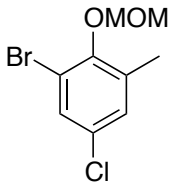

To a solution of phenol **38**[28] (1.0 g, 4.52 mmol) in DMF (20 mL) was added NaH (60% in oil, 0.19 g, 4.75 mmol) portionwise at 0 ºC. After stirring for 30 minutes, MOMCl was added (0.38 g, 4.75 mmol) and the resulting mixture was warmed to 23 ºC and was stirred for 2 hours. The reaction was quenched with H_2O and extracted with ethyl acetate (3 x 100 mL). The combined organic phases were washed with water and brine, dried over $MgSO_4$. The crude was purified by flash chromatography over silica gel using 8:2 cyclohexane:EtOAc as eluent to afford the title compound (1.15 g, 96%) as a colorless oil.

^{1}H NMR (400 MHz, $CDCl_3$) δ 7.40 – 7.38 (m, 1H), 7.13 – 7.11 (m, 1H), 5.05 (s, 2H), 3.63 (s, 3H), 2.33 (bs, 3H). ^{13}C NMR (101 MHz, $CDCl_3$) δ 152.3, 135.2, 130.6, 130.3, 129.9, 117.9, 99.9, 58.0, 17.5. GCMS-ESI(+) *m/z* calc. for $C_9H_{10}BrClO_2$ $[M]^+$: 265.5, found: 266.0.

(2-Bromo-4-chloro-6-methylphenoxy)triethylsilane (40)

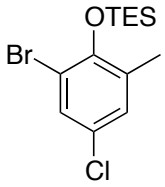

A solution of phenol **38**[28] (0.5 g, 2.26 mmol), TESOTf (0.62 mL, 2.71 mmol), NEt_3 (0.56 mL, 4.07 mmol) in DCM (15 mL) was stirred at 23 ºC for 6 hours. The reaction was quenched with H_2O and extracted with ethyl acetate (3 x 100 mL). The combined organic phases were washed with water and brine, dried over $MgSO_4$. The crude was purified by flash chromatography over silica gel using 10:1 cyclohexane:EtOAc as eluent to afford the title compound (0.639 g, 89%) as a colorless oil.

^{1}H NMR (400 MHz, $CDCl_3$) δ 7.34 (dd, *J* = 2.7, 0.7 Hz, 1H), 7.05 (dq, *J* = 2.5, 0.7 Hz, 1H), 2.23 (t, *J* = 0.7 Hz, 3H), 1.01 – 0.96 (m, 9H), 0.87 – 0.79 (m, 6H). ^{13}C NMR (101 MHz, $CDCl_3$) δ 150.9, 131.9, 130.2, 129.9, 126.4, 115.6, 18.1, 6.9 (3C), 6.0 (3C). GCMS-ESI(+) *m/z* calc. for $C_{13}H_{20}BrClOSi$ $[M]^+$: 335.7, found: 336.1.

2-(3-Bromo-4-chloro-5-methylphenyl)-4,4,5,5-tetramethyl-1,3,2-dioxaborolane (41)

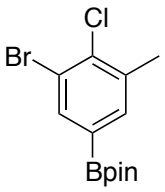

A solution of 1-bromo-2-chloro-3-methylbenzene (5.0 g, 24.33 mmol), $[Ir(COD)(OMe)]_2$ (323 mg, 0.487 mmol), dtbpy (261 mg, 0.97 mmol), B_2pin_2 (7.7 g, 29.20 mmol) in dry and degassed THF (75 mL) was heated at 80 ºC for 24 h. The reaction was treated with H_2O and extracted with ethyl acetate (3 x 150 mL). The combined organic phases were washed with water and brine, dried over $MgSO_4$. The crude was purified by flash

chromatography over silica gel using cyclohexane:EtOAc 9:1 as eluent to afford the compound (6.65 g, 83%) as a white solid**.**

Mp = 81–82 ºC. ^{1}H NMR (400 MHz, $CDCl_3$) δ 7.88 (dd, *J* = 1.4, 0.7 Hz, 1H), 7.58 (dq, *J* = 1.4, 0.8 Hz, 1H), 2.43 (app. t, *J* = 0.7 Hz, 3H), 1.34 (s, 12H). ^{13}C NMR (100 MHz, $CDCl_3$) δ 137.9, 137.9, 137.4, 137.3, 135.7, 122.9, 84.3 (2C), 24.8 (4C), 21.3. GCMS-ESI(+) *m/z* calc. for $C_{13}H_{17}BBrClO_2$ $[M]^+$: 331.4, found: 332.0.

3-Bromo-4-chloro-5-methylphenol (42)

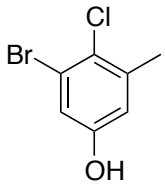

To a solution of **41** (6.65 g, 20.06 mmol) in acetone (80 mL) was carefully added a solution of oxone (14 g, 22.77 mmol) in water (80 mL) over 1 hour. After complete addition, the solution was stirred for an additional 30 min at 23 ºC. The reaction was quenched with $NaHSO_3$ solution (40% w/p) and extracted with ether (3 x 150 mL). The combined organic phases were washed with water and brine, dried over $MgSO_4$. The crude was purified by flash chromatography over silica gel using cyclohexane:EtOAc 8:2 as eluent to afford the compound (3.7 g, 83%) as a white solid.

Mp = 110–111 ºC. ^{1}H NMR (400 MHz, $CDCl_3$) δ 6.99 (d, *J* = 2.9 Hz, 1H), 6.69 (app. dd, *J* = 2.9, 0.8 Hz, 1H), 4.90 (br s, 1H), 2.37 (s, 3H). ^{13}C NMR (101 MHz, $CDCl_3$) δ 154.0, 139.3, 126.4, 123.1, 118.4, 117.2, 21.9. GCMS-ESI(+) *m/z* calc. for C_7H_6BrClO $[M]^+$: 221.5, found: 222.0.

1-Bromo-2-chloro-5-(methoxymethoxy)-3-methylbenzene (43)

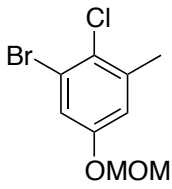

To a solution of phenol **42** (0.11 g, 0.498 mmol) in DMF (5 mL) was added NaH (60% in oil, 21 mg, 0.523 mmol) portionwise at 0 ºC. After stirring for 30 minutes, MOMCl was added (42 mg, 0.523 mmol) and the resulting mixture was warmed to 23 ºC and was stirred for 2 hours. The reaction was treated with H_2O and extracted with ethyl acetate (3 x 20 mL). The combined organic phases were washed with water and brine, dried over $MgSO_4$. The crude was purified by flash chromatography over silica gel using cyclohexane:EtOAc 5:1 as eluent to afford the compound (0.20 g, 95%) as a yellow oil.

^{1}H NMR (400 MHz, $CDCl_3$) δ 7.19 (dq, *J* = 2.9, 0.6 Hz, 1H), 6.88 (dq, *J* = 2.9, 0.7 Hz, 1H), 5.12 (s, 2H), 3.46 (s, 3H), 2.40 (t, *J* = 0.6 Hz, 3H). ^{13}C NMR (101 MHz, $CDCl_3$) δ 155.6, 139.0, 127.5, 123.1, 119.3, 118.1, 94.7, 56.3, 22.1. GCMS-ESI(+) *m/z* calc. for $C_9H_{10}BrClO_2$ $[M]^+$: 265.5, found: 266.0.

1-Bromo-2-(methoxymethoxy)-3-methylbenzene (45)

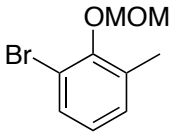

To a solution of phenol **44**[30] (0.5 g, 2.67 mmol) in DMF (20 mL) was added NaH (60% in oil, 0.11 g, 2.81 mmol) portionwise at 0 ºC. After stirring for 30 minutes, MOMCl was added (0.22 g, 2.81 mmol) and the resulting mixture was warmed to 23 ºC and was stirred for 2 hours. The reaction was quenched with H_2O and extracted with ethyl acetate (3 x 100 mL). The combined organic phases were washed with water and brine, dried over $MgSO_4$. The crude was purified by flash chromatography over silica gel using cyclohexane:EtOAc 95:5 as eluent to afford the compound (569 mg, 92%) as a colorless oil.

^{1}H NMR (400 MHz, $CDCl_3$) δ 7.41 – 7.37 (m, 1H), 7.12 (ddq, *J* = 7.6, 1.6, 0.7 Hz, 1H), 6.90 (t, *J* = 7.8 Hz, 1H), 5.08 (s, 2H), 3.65 (s, 3H), 2.36 (s, 3H). ^{13}C NMR (101 MHz, $CDCl_3$) δ 153.3, 134.0, 131.2, 130.5, 125.6, 117.5, 99.7, 57.9, 17.5. GCMS-ESI(+) *m/z* calc. for $C_9H_{11}BrO_2$ $[M]^+$: 231.1, found: 230.1.

General procedure for the preparation of arylenynes 29a-f via Stille coupling

A solution of stannane **33** (1 or 1.1 equiv) and bromoarene (1 equiv), $Pd(PPh_3)_4$ (5 mol%) in degassed toluene (0.1 M) was heated to 110 ºC for 16 hours. The reaction was treated with NH_4Cl and extracted with ethyl acetate. The combined organic phases were washed with water and brine, dried over $MgSO_4$. The crude was purified by flash chromatography over silica gel using cyclohexane:EtOAc as eluent to afford the title compound.

2,5-Bis(methoxymethoxy)-1-(3-(methoxymethoxy)-3,7-dimethyloct-6-en-1-yn-1-yl)-3-methylbenzene (29a)

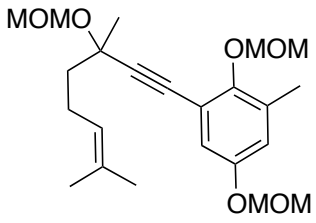

Prepared on from stannane **33** (0.35 g, 0.73 mmol) and bromoarene **37** (0.21 g, 0.73 mmol) according to the general procedure described above. The product was purified by silica gel column chromatography eluting with cyclohexane/ethyl acetate 9:1 to 8:2 and obtained as a colorless oil (208 mg, 71%).

^{1}H NMR (400 MHz, $CDCl_3$) δ 6.92 (d, *J* = 3.0 Hz, 1H), 6.84 – 6.82 (m, 1H), 5.17 – 5.12 (m, 3H), 5.10 (s, 2H), 5.05 (d, *J* = 7.0 Hz, 1H), 4.87 (d, *J* = 7.0 Hz, 1H), 3.58 (s, 3H), 3.46 (s, 3H), 3.41 (s, 3H), 2.29 (s, 3H), 2.27 – 2.16 (m, 2H), 1.85 (ddd, *J* = 13.5, 10.6, 6.1 Hz, 1H), 1.76 (ddd, *J* = 13.5, 10.9, 6.0 Hz, 1H), 1.69 (d, *J* = 0.7 Hz, 3H), 1.63 (s, 3H), 1.58 (s, 3H). ^{13}C NMR (101 MHz, $CDCl_3$) δ 152.9, 152.3, 133.1, 132.0, 124.0,

119.9, 118.5, 116.9, 99.8, 94.9, 94.2, 93.4, 82.8, 74.7, 57.7, 56.1, 55.8, 42.9, 28.0, 25.8, 23.5, 17.8, 17.2. GCMS-ESI(+) *m/z* calc. for $C_{23}H_{34}O_6$ $[M]^+$: 406.5, found: 406.3.

2-(Methoxymethoxy)-1-(3-(methoxymethoxy)-3,7-dimethyloct-6-en-1-yn-1-yl)-3-methylbenzene (29b)

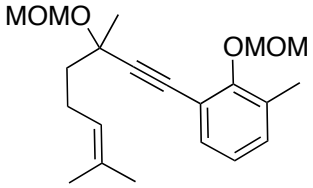

Prepared on from stannane **33** (0.49 g, 1.0 mmol) and bromoarene **45** (0.23 g, 1.0 mmol) according to the general procedure described above. The product was purified by silica gel column chromatography eluting with cyclohexane/ethyl acetate 9:1 and obtained as a colorless oil (0.261 g, 75%).

^{1}H NMR (400 MHz, $CDCl_3$) δ 7.27 – 7.24 (m, 1H), 7.16 – 7.11 (m, 1H), 6.95 (t, *J* = 7.6 Hz, 1H), 5.22 (s, 2H), 5.18 – 5.12 (m, 1H), 5.06 (d, *J* = 7.0 Hz, 1H), 4.88 (d, *J* = 7.0 Hz, 1H), 3.59 (s, 3H), 3.41 (s, 3H), 2.32 (s, 3H), 2.28 – 2.18 (m, 2H), 1.86 (ddd, *J* = 13.5, 10.5, 6.1 Hz, 1H), 1.76 (ddd, *J* = 13.5, 11.0, 6.0 Hz, 1H), 1.69 (d, *J* = 1.1 Hz, 3H), 1.63 (s, 3H), 1.58 (s, 3H). ^{13}C NMR (101 MHz, $CDCl_3$) δ 157.4, 132.0, 132.0, 131.7, 131.6, 124.0, 123.9, 116.3, 99.6, 94.2, 93.4 83.0, 74.7, 57.7, 55.8, 43.0, 28.1, 25.8, 23.5, 17.8, 16.9. GCMS-ESI(+) *m/z* calc. for $C_{21}H_{30}O_4$ $[M]^+$: 346.5, found: 346.2.

5-Chloro-2-(methoxymethoxy)-1-(3-(methoxymethoxy)-3,7-dimethyloct-6-en-1-yn-1-yl)-3-methylbenzene (29c)

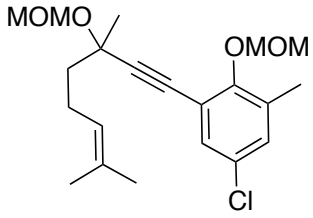

Prepared on from stannane **33** (0.35 g, 0.73 mmol) and bromoarene **39** (0.63 g, 2.5 mmol) according to the general procedure described above. The product was purified by silica gel column chromatography eluting with cyclohexane/ethyl acetate 8:2 and obtained as a colorless oil (719 mg, 76%).

^{1}H NMR (400 MHz, $CDCl_3$) δ 7.22 (dd, *J* = 2.6, 0.6 Hz, 1H), 7.12 (dt, *J* = 2.7, 0.7 Hz, 1H), 5.19 (s, 2H), 5.17 – 5.11 (m, 1H), 5.03 (d, *J* = 7.0 Hz, 1H), 4.86 (d, *J* = 7.0 Hz, 1H), 3.57 (s, 3H), 3.41 (s, 3H), 2.30 – 2.28 (m, 3H), 2.26 – 2.16 (m, 2H), 1.85 (ddd, *J* = 13.5, 10.6, 6.0 Hz, 1H), 1.75 (ddd, *J* = 13.5, 11.0, 5.9 Hz, 1H), 1.69 (q, *J* = 1.2 Hz, 3H), 1.63 (s, 3H), 1.57 (s, 3H). ^{13}C NMR (101 MHz, $CDCl_3$) δ 156.1, 133.8, 132.1, 131.3, 131.0, 128.6, 123.9, 117.7, 99.7, 95.4, 93.4, 81.8, 74.6, 57.8, 55.8, 42.9, 28.0, 25.8, 23.5, 17.8, 16.9. GCMS-ESI(+) *m/z* calc. for $C_{21}H_{29}ClO_4$ $[M]^+$: 380.9, found: 380.2.

(4-Chloro-2-(3-(methoxymethoxy)-3,7-dimethyloct-6-en-1-yn-1-yl)-6-methylphenoxy)triethylsilane (29d)

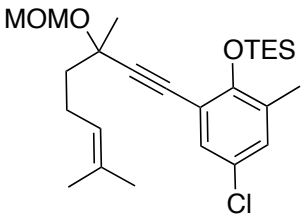

Prepared on from stannane **33** (0.90 g, 1.87 mmol) and bromoarene **40** (0.6 g, 1.87 mmol) according to the general procedure described above. The product was purified by silica gel column chromatography eluting with cyclohexane/ethyl acetate 9:1 and obtained as a colorless oil (801 mg, 98%).

^{1}H NMR (400 MHz, $CDCl_3$) δ 7.18 (dd, *J* = 2.8, 0.7 Hz, 1H), 7.05 (dd, *J* = 2.7, 0.7 Hz, 1H), 5.14 (tdt, *J* = 7.2, 2.9, 1.5 Hz, 1H), 5.03 (d, *J* = 7.0 Hz, 1H), 4.87 (d, *J* = 7.0 Hz, 1H), 3.41 (s, 3H), 2.29 – 2.19 (m, 2H), 2.18 (t, *J* = 0.7 Hz, 3H), 1.91 – 1.73 (m, 2H), 1.69 (d, *J* = 1.0 Hz, 3H), 1.63 (s, 3H), 1.58 (s, 3H), 0.99 – 0.93 (m, 9H), 0.86 – 0.78 (m, 6H). ^{13}C NMR (101 MHz, $CDCl_3$) δ 153.7, 132.0, 131.4, 131.2, 131.1, 125.7, 124.0, 116.4, 94.5, 93.3, 83.1, 74.8, 55.8, 42.9, 27.7, 25.8, 23.4, 17.8, 17.4, 6.9 (3C), 5.8 (3C). GCMS-ESI(+) *m/z* calc. for $C_{25}H_{39}ClO_3Si$ $[M]^+$: 451.1, found: 450.3.

2-Chloro-5-(methoxymethoxy)-1-(3-(methoxymethoxy)-3,7-dimethyloct-6-en-1-yn-1-yl)-3-methylbenzene (29e)

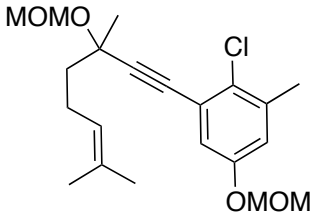

Prepared on from stannane **33** (0.58 g, 1.19 mmol) and bromoarene **43** (266 mg, 1 mmol) according to the general procedure described above. The product was purified by silica gel column chromatography eluting with cyclohexane/ethyl acetate 95:5 and obtained as a colorless oil (240 mg, 64%).

^{1}H NMR (500 MHz, $CDCl_3$) δ 7.01 – 6.99 (m, 1H), 6.89 (dt, *J* = 2.9, 0.7 Hz, 1H), 5.16 (tdt, *J* = 7.2, 2.9, 1.5 Hz, 1H), 5.12 (s, 2H), 5.11 (d, *J* = 6.9 Hz, 1H), 4.91 (d, *J* = 6.9 Hz, 1H), 3.46 (s, 3H), 3.42 (s, 3H), 2.34 (t, *J* = 0.6 Hz, 3H), 2.31 – 2.20 (m, 2H), 1.88 (ddd, *J* = 13.5, 10.9, 5.8 Hz, 1H), 1.77 (ddd, *J* = 13.5, 11.1, 5.8 Hz, 1H), 1.69 (q, *J* = 1.3 Hz, 3H), 1.64 (bs, 3H), 1.60 (s, 3H). ^{13}C NMR (75 MHz, $CDCl_3$) δ 155.0, 137.9, 132.0, 129.2, 124.1, 123.5, 119.4, 118.3, 95.0, 94.6, 93.5, 83.5, 74.7, 56.2, 55.8, 42.9, 28.0, 25.9, 23.5, 21.0, 17.8. GCMS-ESI(+) *m/z* calc. for $C_{21}H_{29}ClO_4$ $[M]^+$: 380.9, found: 380.1.

4-Chloro-3-(3-(methoxymethoxy)-3,7-dimethyloct-6-en-1-yn-1-yl)-5-methylphenol (29f)

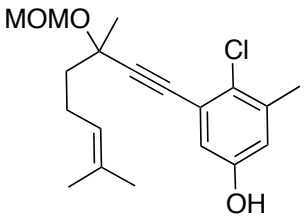

Prepared on from stannane **33** (2.7 g, 5.6 mmol) and bromoarene **42** (1.13 g, 5.1 mmol) according to the general procedure described above. The product was purified by silica gel column chromatography eluting with cyclohexane/ethyl acetate 9:1 and obtained as colorless oil (430 mg, 26%).

^{1}H NMR (400 MHz, $CDCl_3$) δ 6.80 – 6.76 (m, 1H), 6.71 – 6.68 (m, 1H), 5.19 – 5.09 (m, 2H), 4.94 – 4.89 (m, 1H), 3.44 – 3.41 (m, 3H), 2.33 – 2.29 (m, 3H), 2.31 – 2.19 (m, 2H), 1.87 (ddd, *J* = 13.5, 10.6, 6.1 Hz, 1H), 1.76 (ddd, *J* = 13.4, 10.9, 6.1 Hz, 1H), 1.69 (q, *J* = 1.2 Hz, 3H), 1.64 (s, 3H), 1.59 (s, 5H). ^{13}C NMR (101 MHz, $CDCl_3$) δ 153.5, 138.0, 132.0, 127.8, 124.0, 123.5, 118.5, 117.5, 94.8, 93.4, 83.6, 74.8, 55.8, 42.9, 28.1, 25.9, 23.6, 20.9, 17.9. GCMS-ESI(+) *m/z* calc. for $C_{19}H_{25}ClO_3$ $[M]^+$: 336.9, found: 336.1.

4-Chloro-2-(3-(methoxymethoxy)-3,7-dimethyloct-6-en-1-yn-1-yl)-6-methylphenol (29g)

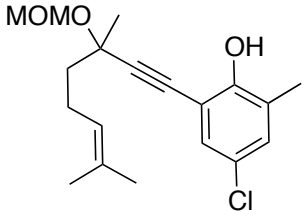

To a solution of **29d** (0.35 g, 0.80 mmol) in THF (10 mL) was added a solution of TBAF (1.0 M, 1.2 mL, 1.2 mmol) and stirred for 30 min at 23 ºC. The reaction was quenched with NH_4Cl and extracted with ethyl acetate. The combined organic phases were washed with water and brine, dried over $MgSO_4$. The crude was purified by flash chromatography over silica gel using cyclohexane:EtOAc 5:1 as eluent to afford the title compound (137 mg, 51%) as a yellow oil.

^{1}H NMR (400 MHz, $CDCl_3$) δ 7.75 (s, 1H), 7.06 (dd, *J* = 2.6, 0.7 Hz, 1H), 7.04 (dd, *J* = 2.6, 0.9 Hz, 1H), 5.14 (dddt, *J* = 7.2, 5.8, 2.9, 1.4 Hz, 1H), 5.06 (d, *J* = 7.9 Hz, 1H), 4.88 (d, *J* = 7.9 Hz, 1H), 3.52 (s, 3H), 2.30 – 2.13 (m, 5H), 1.81 (ddd, *J* = 13.6, 10.7, 5.9 Hz, 1H), 1.77 – 1.71 (m, 1H), 1.69 (q, *J* = 1.2 Hz, 3H), 1.63 (d, *J* = 1.4 Hz, 3H), 1.53 (s, 3H). ^{13}C NMR (101 MHz, $CDCl_3$) δ 155.4, 132.4, 131.3, 127.6, 126.6, 123.6, 123.6, 109.7, 97.2, 92.5, 80.4, 73.8, 55.6, 42.5, 27.8, 25.8, 23.5, 17.8, 16.2. GCMS-ESI(+) *m/z* calc. for $C_{19}H_{25}ClO_3$ $[M]^+$: 336.9, found: 336.1.

4-Chloro-3-(3-hydroxy-3,7-dimethyloct-6-en-1-yn-1-yl)-5-methylphenol (29h)

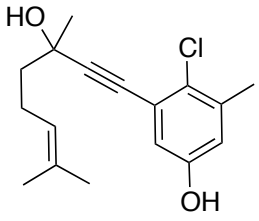

A microwave vial was charged with $Pd(dppf)Cl_2{\cdot}CH_2Cl_2$ (5 mol%) and CuI (10 mol%), sealed and put under argon. Then, a solution of 1,6-enyne **32** (1.0 g, 6.57 mmol) and bromoarene **42** (1.46 g, 6.57 mmol) in degassed NEt_3 (0.1 M) was added, and the resulting mixture was stirred for 16 h at 90 ºC. The reaction was treated with NH_4Cl and extracted with ethyl acetate. The combined organic phases were washed with water and brine, dried over $MgSO_4$. The crude was purified by flash chromatography over silica gel using cyclohexane:EtOAc 7:3 and obtained as a beige solid (1.43 g, 74%).

Mp 98–99 ºC. ^{1}H NMR (400 MHz, $CDCl_3$) δ 6.80 (d, *J* = 2.8 Hz, 1H), 6.70 (dd, *J* = 3.0, 0.8 Hz, 1H), 5.20 (ddt, *J* = 8.0, 6.6, 1.5 Hz, 1H), 2.48 – 2.35 (m, 1H), 2.32 (s, 3H), 2.31 – 2.22 (m, 1H), 1.81 (dd, *J* = 8.9, 7.1 Hz, 2H), 1.70 (q, *J* = 1.2 Hz, 3H), 1.67 (s, 3H), 1.60 (s, 3H). ^{13}C NMR (101 MHz, $CDCl_3$) δ 153.5, 138.1, 132.9, 127.9, 123.9, 123.5, 118.5, 117.5, 97.4, 81.1, 69.4, 43.5, 29.9, 25.9, 24.0, 20.9, 18.0. GCMS-ESI(+) *m/z* calc. for $C_{17}H_{21}ClO_2$ $[M]^+$: 292.8, found: 292.2.

5-Chloro-3,6,9,9-tetramethyl-9,9a-dihydro-1*H*-cyclopenta[*b*]naphthalen-8-ol (46)

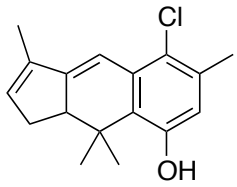

To a solution of enyne **29h** (397 mg, 1.36 mmol) in 13.6 mL of acetone was added gold catalyst **G** (38 mg, 0.04 mmol). The resulting mixture was stirred for 13 h at 23 ºC (TLC monitoring). The crude was concentrated under vacuum and purified by flash chromatography over silica gel using cyclohexane:EtOAc 8:2 as eluent to afford the compound **46** (44 mg, 12% yield) as yellow oil.

^{1}H NMR (300 MHz, $CDCl_3$) δ 6.62 (d, *J* = 2.9 Hz, 1H), 6.43 (s, 1H), 6.05 – 6.01 (m, 1H), 2.96 – 2.88 (m, 1H), 2.59 – 2.45 (m, 1H), 2.43 – 2.30 (m, 1H), 2.28 (d, *J* = 0.7 Hz, 3H), 1.93 – 1.90 (m, 3H), 1.66 (s, 3H), 0.93 (s, 3H). ^{13}C NMR (126 MHz, $CDCl_3$) δ 152.2, 152.1, 139.7, 137.1, 135.2, 135.1, 128.3, 124.5, 117.5, 110.2, 49.0, 38.6, 32.2, 27.2, 20.4, 18.5, 12.4. GCMS-ESI(+) *m/z* calc. for $C_{17}H_{19}ClO$ $[M]^+$: 274.8, found: 274.1.

4-Chloro-3-methyl-5-((1*R,4*S**)-1,3,3-trimethyl-2-oxabicyclo[2.2.2]oct-5-en-5-yl)phenol (47)**

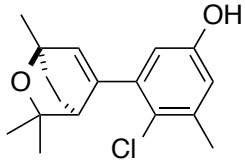

To a solution of enyne **29h** (397 mg, 1.36 mmol) in 13.6 mL of CH_2Cl_2 was added gold catalyst **G** (38 mg, 0.04 mmol). The

resulting mixture was stirred for 13 h at 23 ºC (TLC monitoring). The crude was concentrated under vacuum and purified by flash chromatography over silica gel using cyclohexane:EtOAc 8:2 as eluent to afford the compound **47** (60 mg, 15% yield) in yield as a yellow solid.

Mp = 155–157 ºC. ^{1}H NMR (500 MHz, $CDCl_3$) δ 7.82 (s, 1H), 6.74 – 6.71 (m, 2H), 6.23 (d, *J* = 1.8 Hz, 1H), 2.84 (dt, *J* = 3.5, 2.1 Hz, 1H), 2.35 (s, 3H), 2.23 – 2.12 (m, 2H), 2.17 (s, 3H), 1.99 – 1.89 (m, 2H), 1.48 (s, 3H), 1.38 (s, 3H), 1.00 (s, 3H). ^{13}C NMR (101 MHz, $CDCl_3$) δ 155.3, 148.8, 140.6, 138.5, 133.0, 117.8, 115.0, 76.4, 73.4, 44.1, 32.0, 31.1, 29.2, 28.3, 24.3, 21.0, 20.3. GCMS-ESI(+) *m/z* calc. for $C_{17}H_{21}ClO_2$ $[M]^+$: 292.8, found: 292.2.

2-Iodo-6-methylbenzene-1,4-diol (57)

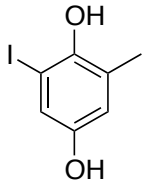

To a suspension containing **56**[28] (250 mg, 1.01 mmol) in ethanol (4 mL) and water (1 mL) $Na_2S_2O_4$ (211 mg, 1.21 mmol) was added at 50 ºC. After 1.5 h the reaction mixture was concentrated under reduced pressure, diluted with ethyl acetate, washed with water and brine, dried over $MgSO_4$ and concentrated. The crude was purified by flash chromatography over silica gel using cyclohexane:EtOAc 8:2 as eluent to afford the compound (98 mg, 40%) as an off-white solid.

Mp = 110–111 ºC. ^{1}H NMR (400 MHz, $CDCl_3$) δ 6.99 (dq, *J* = 3.0, 0.6 Hz, 1H), 6.63 (dp, *J* = 2.8, 0.7 Hz, 1H), 4.91 (d, *J* = 0.6 Hz, 1H), 4.39 (s, 1H), 2.26 (t, *J* = 0.7 Hz, 3H). ^{13}C NMR (126 MHz, $CDCl_3$) δ 149.5, 147.5, 125.5, 121.7, 118.9, 85.2, 17.5. HRMS-ESI(-) *m/z* calc. for $C_7H_6IO_2$ $[M–H]^–$: 248.9418, found: 248.9417.

1-Iodo-2,5-dimethoxy-3-methylbenzene (58)

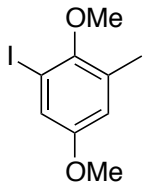

To a solution of **57** (83 mg, 0.33 mmol) in acetone (7.2 mL) dimethylsulfate (0.14 mL, 1.44 mmol) and K_2CO_3 (199 mg, 1.44 mmol) were added. The reaction mixture was heated to 60 ºC for 3 h, cooled to room temperature and filtered. The filtrate was concentrated under reduced pressure. The crude was purified by flash chromatography over silica gel using cyclohexane:EtOAc 95:5 as eluent to afford the compound (88 mg, 97%) as a colorless oil.

^{1}H NMR (500 MHz, $CDCl_3$) δ 7.12 (dd, *J* = 3.1, 0.7 Hz, 1H), 6.70 (dq, *J* = 3.0, 0.7 Hz, 1H), 3.74 (s, 3H), 3.73 (s, 3H), 2.31 (t, *J* = 0.6 Hz, 3H). ^{13}C NMR (126 MHz, $CDCl_3$) δ 156.3, 152.2, 132.5, 121.5, 117.5, 91.7, 60. 6, 55.8, 17.5. GCMS-ESI(+) *m/z* calc. for $C_9H_{11}IO_2$ $[M]^+$: 278.1, found: 278.0.

2-(3,7-Dimethyloct-6-en-1-yn-1-yl)-1,4-dimethoxybenzene (52a)

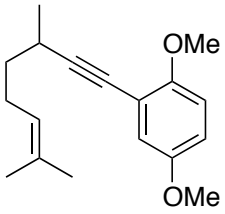

A microwave vial was charged with $Pd(PPh_3)_2Cl_2$ (9 mg, 0.013 mmol) and CuI (5 mg, 0.026 mmol), sealed and put under argon. Then, a solution of 1,6-enyne **54**[31] (72 mg, 0.52 mmol) and iodoarene **58** (73 mg, 0.26 mmol) in degassed dioxane (0.6 mL) and Et_3N (0.3 mL) were added, and the resulting mixture was stirred for 12 h at 50 ºC. The reaction was treated with H_2O and extracted with ethyl acetate. The combined organic phases were washed with water and brine, dried over $MgSO_4$. The crude was purified by preparatory thin layer chromatography (silica gel) using cyclohexane: EtOAc 98:2 as eluent to afford the title compound (59 mg, 73%) as yellow oil.

Note: when the reaction was performed in gram scale the purification was carried out by flash chromatography over silica gel using cyclohexane:EtOAc 98:2 as eluent.

^{1}H NMR (300 MHz, $CDCl_3$) δ 6.73 (d, *J* = 3.1 Hz, 1H), 6.65 (dd, *J* = 3.3, 0.9 Hz, 1H), 5.19 – 5.10 (m, 1H), 3.83 (s, 3H), 3.74 (s, 3H), 2.76 – 2.64 (m, 1H), 2.28 – 2.13 (m, 5H), 1.70 (q, *J* = 1.3 Hz, 3H), 1.64 (s, 3H), 1.62 – 1.47 (m, 2H), 1.28 (d, *J* = 6.9 Hz, 3H). ^{13}C NMR (75 MHz, $CDCl_3$) δ 155.0, 153.6, 132.3, 132.2, 124.2, 118.1, 117.0, 115.0, 98.8, 77.3, 60.6, 55.7, 37.3, 26.5, 26.6, 25.9, 21.1, 17.9, 16.5. HRMS-ESI(-) *m/z* calc. for $C_{18}H_{23}O_2$ $[M–H]^–$: 271.1704, found: 271.1713.

(1*R,3a*R**)-5,8-Dimethoxy-1,4,4,7-tetramethyl-2,3,3a,4-tetrahydro-1*H*-cyclopenta[*b*]naphthalene (51a)**

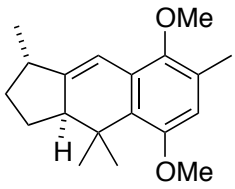

To a solution of enyne **52a** (517 mg, 1.8 mmol) in 1 mL of CH_2Cl_2 was added gold catalyst **G** (83 mg, 0.09 mmol). The resulting mixture was stirred for 22 h at 23 ºC (TLC monitoring). The crude was concentrated under vacuum and purified by flash column chromatography over silica gel using cyclohexane:EtOAc 99:1 as eluent to afford the compound (408 mg, 79%, 9:1 *dr*) as yellow oil.

^{1}H NMR (400 MHz, $CDCl_3$) δ 6.57 (s, 1H), 6.47 (t, *J* = 3.1 Hz, 1H), 3.79 (s, 3H), 3.69 (s, 3H), 2.64 – 2.53 (m, 2H), 2.27 (s, 3H), 2.09 – 2.00 (m, 1H), 1.94 – 1.87 (m, 1H), 1.61 (s, 3H), 1.55 – 1.46 (m, 1H), 1.26 (d, *J* = 6.6 Hz, 3H), 1.24 – 1.16 (m, 1H), 0.94 (s, 3H). ^{13}C NMR (101 MHz, $CDCl_3$) δ 154.5, 152.4, 148.4, 131.3, 129.8, 128.9, 113.1, 111.4, 60.9, 56.0, 52.2, 39.3, 38.0, 34.1, 27.6, 25.9, 19.6, 18.6, 16.0. HRMS-ESI(+) *m/z* calc. for $C_{19}H_{26}NaO_2$ $[M+Na]^+$: 309.1825, found: 309.1827.

3,6,9,9-Tetramethyl-9,9a-dihydro-1*H*-cyclopenta[*b*]naphthalene-5,8,9a-triol (60)

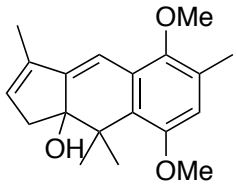

To a solution of **51a** (47 mg, 0.164 mmol) in CH_2Cl_2 (1.5 mL) was added selenium dioxide (111 mg, 0.30 mmol). The resulting mixture was stirred for 1 h at 23 ºC (TLC monitoring). The crude was purified directly by preparatory thin layer chromatography (silica gel) using cyclohexane:EtOAc 8:2 as the eluent to afford the title compound **60** (28 mg, 56%) as an orange oil.

^{1}H NMR (400 MHz, $CDCl_3$) δ 6.65 – 6.63 (m, 1H), 6.58 (s, 1H), 5.78 – 5.75 (m, 1H), 3.81 (s, 3H), 3.71 (s, 3H), 2.66 (d, *J* = 2.8 Hz, 2H), 2.27 (s, 3H), 1.56 (s, 3H), 1.51 – 1.48 (m, 6H). ^{13}C NMR (101 MHz, $CDCl_3$) δ 154.5, 150.8, 150.8, 148.8, 129.3 (2C), 127.7, 124.8, 113.1, 109.2, 77.7, 61.3, 55.6, 48.8, 37.1, 30.9, 30.5, 28.1, 16.1. GCMS-ESI(+) *m/z* calc. for $C_{19}H_{24}O_3$ $[M]^+$: 300.4, found: 300.1.

5,8-Dimethoxy-3,6,9,9-tetramethyl-2,3,9,9a-tetrahydro-1*H*-fluoren-4(4a*H*)-one (62)

To a solution of **51a** (43 mg, 0.149 mmol) in CH_2Cl_2 (1.5 mL) was added *m*-CPBA (56 mg, 0.327 mmol) at 0 ºC. The resulting mixture was allowed to reach 23 ºC and was stirred for 1 h (TLC monitoring). The mixture was filtered through a celite plug and concentrated under reduced pressure. Then, it was purified by preparatory thin layer chromatography (silica gel) using cycloehexane: EtOAc 9:1 as the eluent to afford the title compound (22 mg, 50%) as a pale yellow oil.

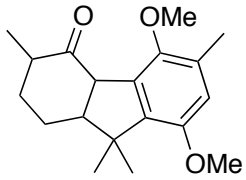

^{1}H NMR (400 MHz, $CDCl_3$) δ 6.59 (s, 1H), 3.79 (s, 3H), 3.67 (s, 3H), 3.37 – 3.34 (m, 1H), 2.50 – 2.40 (m, 1H), 2.27 (s, 3H), 2.23 – 2.15 (m, 1H), 2.09 (dt, *J* = 4.6, 2.5 Hz, 1H), 1.96 (tt, *J* = 14.3, 4.5 Hz, 1H), 1.71 (tt, *J* = 14.3, 5.0 Hz, 1H), 1.64 –1.60 (m, 1H), 1.60 (s, 3H), 1.23 (s, 3H), 1.12 (d, *J* = 7.3 Hz, 3H). ^{13}C NMR (101 MHz, $CDCl_3$) δ 216.8, 153.6, 149.1, 133.1, 131.5, 129.5, 112.9, 61.0, 60.0, 55.5, 54.3, 43.3, 41.1, 30.0, 26.8, 25.3, 23.6, 18.1, 16.4. HRMS-ESI(+) *m/z* calc. for $C_{19}H_{26}NaO_3$ $[M+Na]^+$: 325.1774, found: 325.1770.

(3*R,3a*S**,4*R**,9a*R**)-5,8-dimethoxy-3,6,9,9-tetramethyl-2,3,3a,4,9,9a-hexahydro-1*H*-cyclopenta[*b*]naphthalen-4-ol** and **(3*R**,3a*R**,4*S**,9a*R**)-5,8-dimethoxy-3,6,9,9-tetramethyl-2,3,3a,4,9,9a-hexahydro-1*H*-cyclopenta[*b*]naphthalen-4-ol (63a and 63b)**

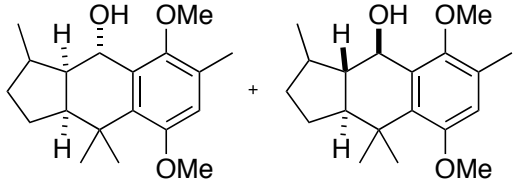

To a solution **51a** (70 mg, 0.25 mmol) in dry THF (5 mL) borane tetrahydrofuran complex

(2.5 mL, 2.5 mmol, 1 M in THF) was added dropwise at 0 ºC. The reaction mixture was allowed to reach 25 ºC. After 8 hours, the mixture was cooled to 0 ºC and 1 mL of 10% aqueous NaOH was added drop wise followed by 1 mL of a solution of 30% H_2O_2 solution. The mixture was stirred for 6 h at 0 ºC. Then, the reaction was treated with water and extracted with ethyl acetate. To the combined organic phases was added a sat. aqueous solution of $Na_2S_2O_3$. The resulting mixture was stirred for 40 min, then washed with water, brine and dried over $MgSO_4$. The crude was purified by flash chromatography over silica gel using cyclohexane:EtOAc 80:20 as eluent to afford a mixture of inseparable alcohols (47 mg, 63%, 1.1:1 *dr*) as a yellow oil. *Note: an inseparable byproduct was observed together with the mixture of the two alcohols, however the corresponding signals have not been listed below.*

One isomer: ^{1}H NMR (300 MHz, $CDCl_3$) δ 6.62 (s, 1H), 4.59 (dd, *J* = 7.2, 1.7 Hz, 1H), 4.23 (d, *J* = 1.7 Hz, 1H), 3.77 (s, 3H), 3.75 (s, 3H), 2.41 – 2.31 (m, 1H), 2.26 (s, 3H), 2.16 – 1.61 (m, 5H), 1.54 – 1.45 (m, 1H), 1.37 (s, 3H), 1.25 (s, 3H), 1.09 (d, *J* = 7.1 Hz, 3H). GCMS-ESI(+) *m/z* calc. for $C_{19}H_{26}O_3$ $[M]^+$: 304.4, found: 304.2.

Other isomer: ^{1}H NMR (300 MHz, $CDCl_3$) δ 6.61 (s, 1H), 4.90 (dd, *J* = 10.0, 1.1 Hz, 1H), 4.82 (d, *J* = 1.1 Hz, 1H), 3.80 (s, 3H), 3.78 (s, 3H), 2.56 – 2.44 (m, 1H), 2.26 (s, 3H), 2.16 – 1.61 (m, 5H), 1.54 – 1.45 (m, 1H), 1.43 (s, 3H), 1.39 (s, 3H), 1.05 (d, *J* = 7.2 Hz, 3H). GCMS-EI(+) *m/z* calc. for $C_{19}H_{26}O_3$ $[M]^+$: 304.4, found: 304.2.

(3*R,9a*R**)-5,8-Dimethoxy-3,6,9,9-tetramethyl-3,3a,9,9a-tetrahydro-1*H*-cyclopenta[*b*]naphthalen-4(2*H*)-one (64)**

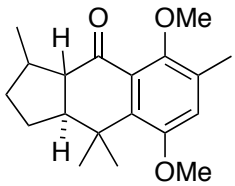

To a solution of the inseparable mixture of alcohols **63a** and **63b** (12 mg, 0.039 mmol) in CH_2Cl_2 (2 mL), DMP (23 mg, 0.054 mmol) was added at 0 ºC. The resulting mixture was allowed to reach 23 ºC and was stirred for 2 h (TLC monitoring). The crude was purified directly by preparatory thin layer chromatography (silica gel) using cyclohexane: EtOAc 9:1 as the eluent to afford the title compound **64** (6 mg, 50%) as a pale yellow oil.

^{1}H NMR (300 MHz, $CDCl_3$) δ 6.83 (s, 1H), 3.77 (s, 3H), 3.74 (s, 3H), 2.57 (dd, *J* = 9.9, 7.3 Hz, 1H), 2.30 – 2.20 (m, 5H), 1.92 – 1.68 (m, 4H), 1.50 (s, 3H), 1.26 (s, 3H), 1.20 – 1.14 (m, 3H). GCMS-ESI(+) *m/z* calc. for $C_{19}H_{26}O_3$ $[M]^+$: 302.4, found: 302.2.

(1*R,3a*R**)-1,4,4,7-Tetramethyl-2,3,3a,4-tetrahydro-1*H*-cyclopenta[*b*]naphthalene-5,8-dione (66)**

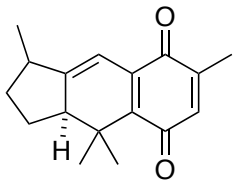

To a solution of **51a** (39 mg, 0.14 mmol) and AgO (73 mg, 0.59 mmol) in dioxane (2 mL), HNO_3 6 N (0.23 mL, 1.40 mmol) was added. The reaction was stirred at 23ºC for 3 hours. Additional 35 mg (0.3 mmol) of AgO were added and the mixture was stirred for 2 hours. The crude was concentrated and purified by flash chromatography over silica gel using cyclohexane:EtOAc 9:1 as eluent to afford the title compound (11 mg, 30%) as an orange oil.

^{1}H NMR (500 MHz, $CDCl_3$) δ 6.46 – 6.42 (m, 2H), 2.61 – 2.54 (m, 1H), 2.53 – 2.47 (m, 1H), 2.09 – 2.02 (m, 1H), 2.00 (d, *J* = 1.6 Hz, 3H), 1.90 – 1.82 (m, 1H), 1.53 – 1.49 (m, 4H), 1.49 – 1.41 (m, 1H), 1.23 (d, *J* = 6.8 Hz, 3H), 0.88 (s, 3H). ^{13}C NMR (126 MHz, $CDCl_3$) δ 188.2, 187.8, 161.9, 142.9, 141.8, 138.1, 135.6, 109.6, 52.6, 40.3, 37.1, 33.5, 26.4, 24.9, 18.0, 17.9, 15.3. GCMS-ESI(+) *m/z* calc. for $C_{17}H_{20}O_2$ $[M]^+$: 256.3, found: 256.1.

(2*R,4a*S**)-2,5,5,8-Tetramethyl-3,4,4a,5-tetrahydrocyclopenta[2,3]naphtho[1,2-*b*]oxirene-6,9(2*H*,9b*H*)-dione (67)**

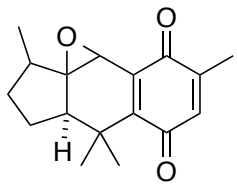

To a solution of **66** (10 mg, 0.039 mmol) in CH_2Cl_2 (1 mL), *m*-CPBA (15 mg, 0.086 mmol) and $NaHCO_3$ (18 mg, 0.21 mmol) were added at -20 ºC. The mixture was allowed to reach 0 ºC and was stirred for 24 hours. Then, the reaction mixture was treated with water and extracted with CH_2Cl_2. The combined organic phases were washed with a sat. solution of $Na_2S_2O_3$, a sat. solution of $NaHCO_3$, water and brine, dried over $MgSO_4$ and concentrated under reduced pressure. The crude was purified by flash chromatography over silica gel using cyclohexane:EtOAc 9:1 to 8:2 as eluent to afford the title compound (4 mg, 27%).

^{1}H NMR (500 MHz, $CDCl_3$) δ 6.51 (q, *J* = 1.6 Hz, 1H), 3.83 (s, 1H), 2.44 – 2.19 (m, 1H), 2.13 – 2.06 (m, 1H), 2.04 (d, *J* = 1.5 Hz, 4H), 2.01 – 1.92 (m, 2H), 1.54 – 1.43 (m, 1H), 1.34 (s, 3H), 1.17 (s, 3H), 0.96 (d, *J* = 6.5 Hz, 3H). ^{13}C NMR (75 MHz, $CDCl_3$) δ 187.7, 187.3, 152.8, 144.2, 138.6, 135.3, 77.4, 69.0, 49.9, 48.3, 37.7, 36.8, 32.0, 27.2, 27.1, 25.2, 24.8, 15.3, 13.9. GCMS-ESI(+) *m/z* calc. for $C_{17}H_{20}O_3$ $[M]^+$: 272.3, found: 272.1.

2-Bromo-1-ethynyl-3,5-dimethoxybenzene (75)

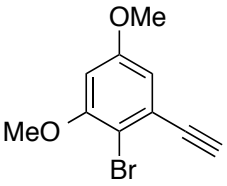

To a solution of aldehyde **74**[42] (1.35 g, 5.51 mmol) in MeOH (100 mL) was added freshly prepared Ohira Bestmann reagent (1.27 g, 6.61 mmol) followed by K_2CO_3 (2.28 g, 16.53 mmol). The resulting mixture was stirred overnight at 23 ºC (the reaction time was shorter, it was stirred overnight for convenience). After completion, the reaction was quenched with H_2O and extracted with EtOAc (3 x 150 mL). The combined organic phases were washed with water and brine, dried over $MgSO_4$. The crude was purified by flash chromatography over silica gel using cyclohexane:EtOAc 95:5 as eluent to afford the compound (1.20 g, 87%) as a pink oil.

^{1}H NMR (500 MHz, $CDCl_3$) δ 6.69 (d, *J* = 2.8 Hz, 1H), 6.49 (d, *J* = 2.7 Hz, 1H), 3.86 (s, 3H), 3.79 (s, 3H), 3.36 (s, 1H). ^{13}C NMR (126 MHz, $CDCl_3$) δ 159.5, 157.1, 125.6, 109.6, 106.76, 101.3, 82.3, 81.7, 56.5, 55.8. HRMS-ESI(+) *m/z* calc. for $C_{10}H_{10}BrO_2$ $[M+H]^+$: 240.9859, found: 240.9863.

2-Bromo-1,5-dimethoxy-3-(phenylethynyl)benzene (76)

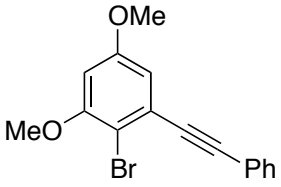

Two necked flask was charged with $Pd(PPh_3)_2Cl_2$ (349 mg, 0.498 mmol), CuI (189 mg, 0.996 mmol), PPh_3 (261 mg, 0.996 mmol) and put under argon. Then, 15 mL of degassed Et_3N were added. To this mixture was added a solution of alkyne **75** (1.20 g, 4.98 mmol) and iodobenzene (0.67 mL, 5.97 mmol) in degassed Et_3N (35 mL). The resulting mixture was stirred overnight at 70 ºC. After cooling at 23 ºC, H_2O was carefully added and extracted with EtOAc (3 x 150 mL). The combined organic phases were washed with water and brine, dried over $MgSO_4$. The crude was purified by flash chromatography over silica gel using cyclohexane:EtOAc 97:3 as eluent to afford the compound (1.53 g, 96%) as a yellow oil.

^{1}H NMR (300 MHz, $CDCl_3$) δ 7.62 – 7.56 (m, 2H), 7.39 – 7.33 (m, 3H), 6.73 (d, *J* = 2.7 Hz, 1H), 6.48 (d, *J* = 2.7 Hz, 1H), 3.89 (s, 3H), 3.83 (s, 3H). ^{13}C NMR (75 MHz, $CDCl_3$) δ 159.5, 157.1, 131.9 (2C), 128.8, 128.5 (2C), 126.7, 123.0, 108.7, 106.7, 100.8, 93.9, 88.5, 6.5, 55.8. HRMS-ESI(+) *m/z* calc. for $C_{16}H_{14}BrO_2$ $[M+H]^+$: 317.0172, found: 317.0172.

1,5-Dimethoxy-2-(3-methylbut-2-en-1-yl)-3-(phenylethynyl)benzene (73)

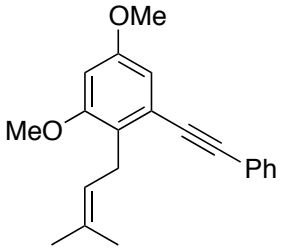

A two necked flask was charged with **76** (1.53 g, 4.82 mmol) in 20 mL of anhydrous THF. The solution was cooled at -78 ºC and 3 mL of *n*BuLi (2.5 M in hexanes) were added dropwise and stirred for 15 minutes. TMEDA (0.73 mL, 4.82 mmol) was then added and stirred for 15 minutes. CuI (0.917 g, 4.82 mmol) was added in one portion and the mixture was stirred for additional 20 minutes. Finally, prenylbromide (0.83 mL, 7.23 mmol) was added. The resulting mixture was stirred overnight while it was allowed to warm to 23 ºC slowly. The suspension was carefully quenched by addition of a saturated aqueous solution of NH_4Cl and extracted with EtOAc (3 x 150 mL). The combined organic phases were washed with water and brine, dried over $MgSO_4$ and concentrated. The crude was purified by flash chromatography over silica gel using cyclohexane:EtOAc 98:2 as eluent to afford the compound (0.96 g, 65%) as a yellow oil.

^{1}H NMR (400 MHz, $CDCl_3$) δ 7.55 – 7.51 (m, 2H), 7.38 – 7.32 (m, 3H), 6.65 (d, *J* = 2.5 Hz, 1H), 6.46 (d, *J* = 2.5 Hz, 1H), 5.27 (app. dddt, *J* = 7.1, 5.7, 2.9, 1.4 Hz, 1H), 3.81 (d, J = 2.0 Hz, 6H), 3.55 (d, *J* = 7.1 Hz, 3H), 1.80 (s, 3H), 1.68 (d, *J* = 1.1 Hz, 3H). ^{13}C NMR (101 MHz, $CDCl_3$) δ 158.5, 131.7 (2C), 131.4, 128.5 (2C), 128.3, 125.8, 123.7, 123.0, 107.5, 100.2, 92.4, 88.9, 55.8, 55.6, 27.3, 26.0, 18.2. HRMS-ESI(+) *m/z* calc. for $C_{21}H_{23}O_2$ $[M+H]^+$: 307.1693, found: 307.1680.

2-(6,8-Dimethoxy-3-phenyl-1,2-dihydronaphthalen-2-yl)propan-2-ol (69a)

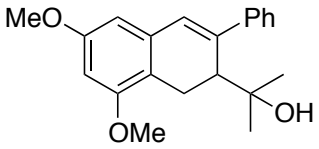

To a solution of enyne **73** (15 mg, 0.05 mmol) in 0.5 mL of CH_2Cl_2 were added 2 μL of H_2O (0.11 mmol) followed by gold catalyst **A** (2 mg, 0.0025). The resulting mixture was stirred for 16 h at 23 ºC (TLC monitoring). The crude was concentrated under vacuum and purified by flash column chromatography over silica gel using cyclohexane:EtOAc 9:1 to 7:3 as eluent to afford the title compound (10 mg, 69%) as yellow oil.

^{1}H NMR (400 MHz, $CDCl_3$) δ 7.59 – 7.55 (m, 2H), 7.43 – 7.38 (m, 2H), 7.33 – 7.29 (m, 1H), 6.81 (s, 1H), 6.40 (q, *J* = 2.4 Hz, 2H), 3.85 (d, *J* = 9.2 Hz, 6H), 3.60 (d, *J* = 16.9 Hz, 1H), 3.16 (dd, *J* = 8.3, 1.2 Hz, 1H), 2.79 (dd, *J* = 17.0, 8.2 Hz, 1H), 1.04 (s, 3H), 0.95 (s, 3H). ^{13}C NMR (101 MHz, $CDCl_3$) δ 159.1, 156.9, 143.3, 141.0, 136.0, 128.8 (2C), 128.0, 127.4, 126.7 (2C), 115.1, 103.4, 98.1, 75.3, 55.7, 55.5, 45.3, 28.8, 27.9, 22.8. HRMS-ESI(+) *m/z* calc. for $C_{21}H_{24}NaO_3$ $[M+Na]^+$: 347.1618, found: 347.1626.

1,3-Dimethoxy-10,10-dimethyl-10a,11-dihydro-10*H*-benzo[*b*]fluorine (77)

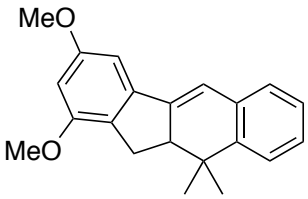

To a solution of enyne **73** (143 mg, 0.47 mmol) in 4.6 mL of CH_2Cl_2 was added gold catalyst **C** (36 mg, 0.023 mmol). The resulting mixture was stirred for 21 h at 23 ºC (TLC monitoring). The crude was concentrated under vacuum and purified by preparatory thin layer chromatography (silica gel) using cyclohexane:EtOAc 9:1 as eluent to afford the title compound (79 mg, 55%) as a yellow oil.

^{1}H NMR (400 MHz, $CDCl_3$) δ 7.39 – 7.35 (m, 1H), 7.23 – 7.15 (m, 3H), 6.82 (d, *J* = 3.0 Hz, 1H), 6.71 (d, *J* = 2.1 Hz, 1H), 6.39 (d, *J* = 2.0 Hz, 1H), 3.87 (s, 3H), 3.85 (s, 3H), 3.13 (ddd, *J* = 9.1, 6.3, 3.0 Hz, 1H), 3.04 (dd, *J* = 16.1, 8.8 Hz, 1H), 2.80 (dd, *J* = 16.1, 6.3 Hz, 1H), 1.53 (s, 3H), 0.95 (s, 3H). ^{13}C NMR (101 MHz, $CDCl_3$) δ 160.9, 157.2, 146.1, 144.9, 141.8, 134.4, 127.7, 127.3, 127.1, 126.4, 123.9, 115.9, 99.3, 95.9, 55.8, 55.5, 48.9, 37.3, 27.8, 25.6, 21.9. GCMS-ESI(+) *m/z* calc. for $C_{21}H_{22}O_2$ $[M]^+$: 306.4, found: 302.2.

7-Isopropyl-1,3-dimethoxy-6-phenylnaphthalene (78)

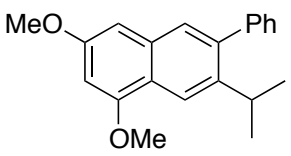

To a solution of enyne **73** (15 mg, 0.05 mmol) in 0.5 mL of CH_2Cl_2 was added gold catalyst **G** (2 mg, 0.0025 mmol). The resulting mixture was stirred for 24 h at 23 ºC (TLC monitoring). The crude was concentrated under vacuum and purified by preparatory thin layer chromatography (silica gel) using cyclohexane:EtOAc 9:1 as eluent to afford the title compound (11 mg, 72%).

^{1}H NMR (400 MHz, $CDCl_3$) δ 8.12 (s, 1H), 7.49 (s, 1H), 7.46 – 7.40 (m, 2H), 7.40 – 7.35 (m, 3H), 6.68 (d, *J* = 2.3 Hz, 1H), 6.48 (d, *J* = 2.2 Hz, 1H), 4.00 (s, 3H), 3.89 (s, 3H), 3.17 – 3.09 (m, 1H), 1.23 (s, 3H), 1.21 (s, 3H). ^{13}C NMR (101 MHz, $CDCl_3$) δ 158.1, 156.4, 142.3, 140.6, 133.1, 132.2, 129.6 (2C), 128.1 (2C), 127.5, 126.9, 121.5, 118.2, 97.6, 97.6, 55.7, 55.5, 29.7, 24.7 (2C). GCMS-ESI(+) *m/z* calc. for $C_{21}H_{22}O_2$ $[M]^+$: 306.4, found: 302.2.

(*Z*)-1-Benzylidene-4,6-dimethoxy-3-(2-methylprop-1-en-1-yl)-1,3-dihydroisobenzofuran (83)

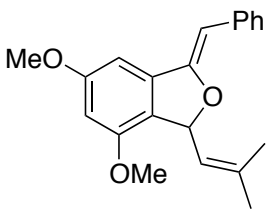

8-Methylquinoline *N*-oxide (50 mg, 0.31 mmol) and gold(I) complex **M** (5 mg, 0.0052 mmol) were added to a solution of **73** (32 mg, 1.04 mmol) in DCE (1 mL, 0.1 M). After stirring at 23 ºC for 3 h, the crude was concentrated under vacuum and

purified by preparatory thin layer chromatography (silica gel) using cyclohexane:EtOAc 85:15 as eluent to afford the title compound (27 mg, 79%) as a yellow oil.

^{1}H NMR (300 MHz, $CDCl_3$) δ 7.76 – 7.69 (m, 2H), 7.35 – 7.28 (m, 2H), 7.16 – 7.08 (m, 1H), 6.61 (d, *J* = 1.9 Hz, 1H), 6.39 (d, *J* = 1.9 Hz, 1H), 6.29 (d, *J* = 8.7 Hz, 1H), 5.82 (s, 1H), 5.19 – 5.13 (m, 1H), 3.87 (s, 3H), 3.79 (s, 3H), 1.93 (d, *J* = 1.3 Hz, 3H), 1.79 (d, *J* = 1.4 Hz, 3H). ^{13}C NMR (75 MHz, $CDCl_3$) δ 162.0, 156.0, 155.4, 143.0, 137.5, 136.7, 128.5, 127.9, 125.2, 122.6, 99.9, 95.9, 94.7, 82.3, 77.4, 55.9, 55.6, 26.1, 18.7. GCMS-ESI(+) *m/z* calc. for $C_{21}H_{22}O_3$ $[M]^+$: 322.4, found: 322.2.

6,8-Dimethoxy-2-(2-methoxypropan-2-yl)-3-phenyl-1,2-dihydronaphthalene (69b)

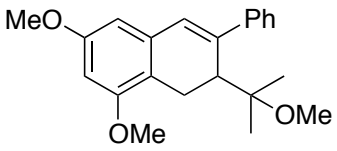

To a solution of 31 mg of enyne **73** (0.1 mmol) and 10.1 μL methanol (0.25 mmol) in 1 mL of 1,2-dichloroethane was added gold catalyst **A** (3 mg, 0.004 mmol). The resulting mixture was stirred for 17-24 h at 24 ºC until the reaction was complete (TLC monitoring). The crude mixture was quenched with the addition of Quadpure MPA 100–400 μm, filtered, concentrated under vacuum, and purified by preparatory thin layer chromatography (silica gel) using pentane:Et_2O 19:1 as eluent to afford the title compound (17 mg, 51%) as a pale yellow/white oily foam.

Note: Reaction was run in a sealed microwave vessel inside the glovebox with dry, deoxygenated methanol.

^{1}H NMR (500 MHz, $CDCl_3$) δ 7.55 – 7.49 (m, 2H), 7.43 – 7.34 (m, 2H), 7.33 – 7.25 (m, 1H), 6.72 (s, 1H), 6.38 (dd, *J* = 14.9, 2.3 Hz, 2H), 3.85 (d, *J* = 10.8 Hz, 6H), 3.63 (d, *J* = 17.0 Hz, 1H), 3.35 – 3.29 (m, 1H), 3.16 (s, 3H), 2.70 (dd, *J* = 17.0, 8.7 Hz, 1H), 0.89 (s, 3H), 0.73 (s, 3H). ^{13}C NMR (126 MHz, $CDCl_3$) δ 158.8, 156.8, 143.8, 141.1, 135.8, 128.5, 128.4, 126.9, 126.6, 115.8, 103.2, 97.9, 79.0, 55.6, 55.3, 48.9, 41.1, 29.7, 24.8, 22.5, 21.6. HRMS-ESI(+) *m/z* calc. for $C_{22}H_{27}O_3$ $[M+H]^+$: 339.1955, found: 339.1958.

2-(2-Isopropoxypropan-2-yl)-6,8-dimethoxy-3-phenyl-1,2-dihydronaphthalene (69c)

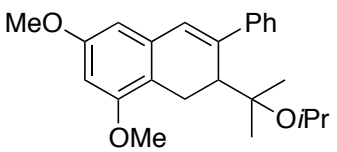

To a solution of 30 mg of enyne **73** (0.1 mmol) and 19.2 μL of isopropanol (0.25 mmol) in 1 mL of 1,2-dichloroethane was added gold catalyst **A** (3 mg, 0.004 mmol). The resulting mixture was stirred for 17-24 h at 24 ºC until the reaction was complete (TLC monitoring). The crude mixture was quenched with the addition of Quadpure MPA 100–400 μm, filtered, concentrated under vacuum, and purified by preparatory thin

layer chromatography (silica gel) using pentane:Et_2O 19:1 as the eluent to afford the title compound **69c** (20 mg, 56%) as a pale yellow/white oily foam.

Note: Reaction was run in a sealed microwave vessel inside the glovebox with dry, deoxygenated methanol.

^{1}H NMR (500 MHz, $CDCl_3$) δ 7.57 – 7.51 (m, 2H), 7.38 (dd, *J* = 8.3, 7.0 Hz, 2H), 7.33 – 7.25 (m, 1H), 6.72 (s, 1H), 6.37 (dd, *J* = 16.4, 2.3 Hz, 2H), 3.85 (d, *J* = 7.4 Hz, 6H), 3.81 – 3.71 (m, 1H), 3.22 (dd, *J* = 8.7, 1.0 Hz, 1H), 2.67 (dd, *J* = 17.0, 8.7 Hz, 1H), 1.10 (dd, *J* = 22.1, 6.1 Hz, 6H), 0.85 (s, 3H), 0.73 (s, 3H).^{13}C NMR (126 MHz, $CDCl_3$) δ 158.7, 156.8, 144.0, 141.2, 135.9, 128.3 (2C), 126.9 (2C), 126.7, 116.2, 103.1, 97.9, 79.7, 77.2, 63.0, 55.6, 55.3, 42.9, 26.1, 25.1, 24.9, 22.9, 21.9. HRMS-ESI(+) *m/z* calc. for $C_{24}H_{31}O_3$ $[M+H]^+$: 367.2268, found: 367.2272.

2-(2-(Allyloxy)propan-2-yl)-6,8-dimethoxy-3-phenyl-1,2-dihydronaphthalene (69g)

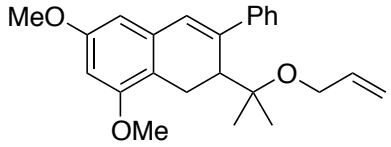

To a solution of 61 mg of enyne **73** (0.2 mmol) and 17.0 μL of allyl alcohol (0.5 mmol) in 1 mL of 1,2-dichloroethane was added gold catalyst **A** (57 mg, 0.008 mmol). The resulting mixture was stirred for 17-24 h at 24 ºC until the reaction was complete (TLC monitoring). The crude mixture was quenched with the addition of Quadpure MPA 100–400 μm, filtered, concentrated under vacuum, and purified by preparatory thin layer chromatography (silica gel) using pentane:Et_2O 19:1 as the eluent to afford the title compound **69g** (39 mg, 53%) as a pale yellow/white oily foam.

Note: Reaction was run in a sealed microwave vessel inside the glovebox with dry, deoxygenated methanol.

^{1}H NMR (500 MHz, $CDCl_3$) δ 7.56 – 7.50 (m, 2H), 7.42 – 7.35 (m, 2H), 7.33 – 7.25 (m, 1H), 6.73 (s, 1H), 6.42 – 6.35 (m, 2H), 5.77 (ddt, *J* = 17.2, 10.5, 5.3 Hz, 1H), 5.19 (dq, *J* = 17.2, 1.7 Hz, 1H), 5.07 (dq, *J* = 10.4, 1.6 Hz, 1H), 3.93 – 3.78 (m, 7H), 3.69 (dd, *J* = 16.9, 1.1 Hz, 1H), 3.33 (dd, *J* = 8.6, 1.1 Hz, 1H), 2.71 (dd, *J* = 17.0, 8.6 Hz, 1H), 0.95 (s, 3H), 0.78 (s, 3H). ^{13}C NMR (126 MHz, $CDCl_3$) δ 158.8, 156.8, 143.9, 141.3, 136.0, 135.9, 128.4 (2C), 128.4, 126.9 (2C), 126.7, 115.8, 115.4, 103.2, 97.9, 79.3, 62.5, 55.6, 55.3, 42.0, 25.2, 23.0, 21.9. HRMS-ESI(+) *m/z* calc. for $C_{24}H_{29}O_3$ $[M+H]^+$: 365.2111, found: 365.2115.

6,8-Dimethoxy-3-phenyl-2-(prop-1-en-2-yl)-1,2-dihydronaphthalene (70)

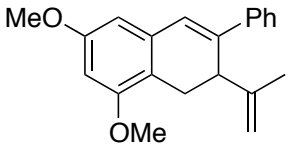

To a solution of **69a** (12 mg, 0.037 mmol) in 1 mL of pyridine was added $POCl_3$ (5 μL, 0.041 mmol). The resulting mixture

was stirred for 1 h at 23 ºC (TLC monitoring). The reaction was treated with water and extracted with EtOAc. The combined organic phases were washed with water and brine, dried over $MgSO_4$. The crude was purified by flash chromatography over silica gel using cyclohexane:EtOAc 95:5 as eluent to afford the compound (8 mg, 66%) as a yellow oil.

^{1}H NMR (500 MHz, $CDCl_3$) δ 7.55 – 7.52 (m, 2H), 7.37 – 7.32 (m, 2H), 7.28 – 7.24 (m, 1H), 6.92 (s, 1H), 6.38 (d, *J* = 2.4 Hz, 1H), 6.37 (d, *J* = 2.4 Hz, 1H), 4.75 – 4.72 (m, 1H), 4.71 – 4.68 (m, 1H), 3.82 (s, 3H), 3.81 (s, 3H), 3.46 (dd, *J* = 7.9, 2.3 Hz, 1H), 3.28 (dd, *J* = 16.3, 2.2 Hz, 1H), 2.81 (dd, *J* = 16.3, 7.9 Hz, 1H), 1.75 (s, 3H). ^{13}C NMR (101 MHz, $CDCl_3$) δ 158.9, 157.5, 144.5, 140.7, 140.5, 135.8, 128.3 (2C), 127.3, 125.7 (2C), 125.3, 113.7, 111.9, 103.5, 97.9, 55.6, 55.3, 43.4, 25.6, 21.3. GCMS-ESI(+) *m/z* calc. for $C_{21}H_{22}O_2$ $[M]^+$: 306.4, found: 306.2.

(1*R,2*R**,3*S**)-3-(2-Hydroxypropan-2-yl)-5,7-dimethoxy-2-phenyl-1,2,3,4-tetrahydronaphthalen-1-ol (87a) and (1*R**,2*R**,3*R**)-3-(2-hydroxypropan-2-yl)-5,7-dimethoxy-2-phenyl-1,2,3,4-tetrahydronaphthalen-1-ol (87b)**

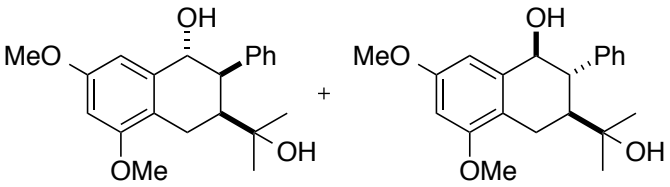

87a **87b**

To a solution **69a** (329 mg, 1.01 mmol) in dry THF (22 mL) borane tetrahydrofuran complex (5 mL, 5.05 mmol, 1 M in THF) was added dropwise at 23 ºC. The reaction mixture was warmed to reach 50 ºC and was stirred for 36 hours. After cooling to 23 ºC, 1.2 mL of 10% aqueous NaOH was added dropwise followed by 2.4 mL of a solution of 30% H_2O_2 solution. The mixture was stirred for 2 hours at 23 ºC. The reaction was treated with water and extracted with EtOAc. The combined organic phases were washed with sat. solution of $Na_2S_2O_3$, water and brine, dried over $MgSO_4$. The crude was purified by preparatory thin layer chromatography (silica gel) using cyclohexane:EtOAc 1:1 as the eluent to afford the title compounds **87a** and **87b** as white solids (62%, 4.3:1 *dr*).

Major isomer (87a) *(178 mg, 52% yield)*: Mp = 76-78 ºC. ^{1}H NMR (500 MHz, $CDCl_3$) δ 7.20 – 7.14 (m, 2H), 7.04 – 6.99 (m, 1H), 6.47 (d, *J* = 2.4 Hz, 1H), 6.45 (d, *J* = 2.5 Hz, 1H), 4.59 (d, *J* = 2.0 Hz, 1H), 3.86 (s, 3H), 3.79 (s, 3H), 3.61 – 3.58 (m, 1H), 3.03 (dd, *J* = 17.8, 5.3 Hz, 1H), 2.60 (dd, *J* = 17.8, 12.8 Hz, 1H), 2.43 (ddd, *J* = 12.8, 5.3, 3.7 Hz, 1H), 2.06 (bs, 1H), 1.65 (bs, 1H), 1.24 (s, 3H), 1.18 (s, 3H). ^{13}C NMR (126 MHz, $CDCl_3$) δ 159.3, 158.3, 140.3, 138.2, 129.7 (2C), 128.8 (2C), 127.1, 119.4, 105.1, 98.5,

74.4, 73.3, 55.5, 55.5, 47.6, 42.5, 29.1, 28.3, 20.5. HRMS-ESI(+) *m/z* calc. for HRMS-ESI(+) *m/z* calc. for $C_{21}H_{26}NaO_4$ $[M+Na]^+$: 365.1723, found: 365.1730.

Minor isomer (87b) *(40 mg, 11% yield)*: Mp = 67–68 ºC. ^{1}H NMR (400 MHz, $CDCl_3$) δ 7.27 – 7.21 (m, 3H), 7.16 – 7.09 (m, 2H), 6.82 (d, *J* = 2.5 Hz, 1H), 6.44 (d, *J* = 2.4 Hz, 1H), 5.05 (d, *J* = 5.7 Hz, 1H), 3.88 (s, 3H), 3.86 – 3.83 (m, 1H), 3.83 (s, 3H), 3.02 (dd, *J* = 17.9, 5.8 Hz, 1H), 2.74 (ddd, *J* = 18.0, 12.6, 1.6 Hz, 1H), 2.26 (ddd, *J* = 12.5, 5.9, 3.4 Hz, 1H), 1.24 (s, 3H), 1.17 (s, 3H). ^{13}C NMR (101 MHz, $CDCl_3$) δ 159.4, 157.8, 141.1, 137.6, 131.3, 131.3, 129.2, 127.7, 117.5, 101.5, 97.5, 73.3, 73.1, 55.5, 55.5, 47.5, 47.1, 29.1, 28.1, 21.2. HRMS-ESI(+) *m/z* calc. for $C_{21}H_{26}NaO_4$ $[M+Na]^+$: 365.1723, found: 365.1710.

(2*R,3*S**)-3-(2-Hydroxypropan-2-yl)-5,7-dimethoxy-2-phenyl-3,4-dihydronaphthalen-1(2*H*)-one (88)**

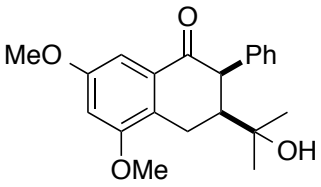

To a solution of alcohol **87a** (30 mg, 0.088 mmol) in CH_2Cl_2 (1 mL), DMP (60 mg, 0.14 mmol) and $NaHCO_3$ (41 mg, 0.485 mmol) were added at 23 ºC. The resulting mixture was stirred for 1.5 hours (TLC monitoring). The reaction was treated with water and saturated aqueous solution of $Na_2S_2O_3$, and extracted with CH_2Cl_2. The combined organic phases were washed with a sat. solution of $Na_2S_2O_3$, water and brine, dried over $MgSO_4$. The crude was purified by preparatory thin layer chromatography (silica gel) using cyclohexane:EtOAc 2:3 as eluent to afford the title compound (24 mg, 81%) as a pale yellow oil.

^{1}H NMR (300 MHz, $CDCl_3$) δ 7.25 – 7.13 (m, 6H), 6.71 (d, *J* = 2.5 Hz, 1H), 4.19 (d, *J* = 4.4 Hz, 1H), 3.89 (s, 3H), 3.83 (s, 3H), 3.23 (dd, *J* = 18.1, 4.7 Hz, 1H), 2.93 (dd, *J* = 18.1, 12.5 Hz, 1H), 2.42 (dt, *J* = 12.4, 4.6 Hz, 1H), 1.19 (s, 6H). ^{13}C NMR (75 MHz, $CDCl_3$) δ 197.6, 159.3, 158.3, 136.3, 133.4, 129.8 (2C), 129.2 (2C), 127.6, 126.8, 104.5, 100.9, 73.1, 55.9, 55.7, 54.7, 48.7, 28.6, 28.2, 20.6. GCMS-ESI(+) *m/z* calc. for $C_{21}H_{24}O_4$ $[M]^+$: 340.4, found: 340.2.

(2*R,3*S**)-5,7-Dimethoxy-2-phenyl-3-(prop-1-en-2-yl)-1,2,3,4-tetrahydronaphthalen-1-ol (89)**

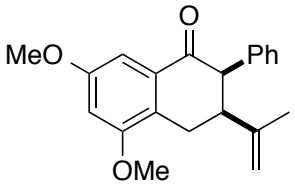

To a solution of ketone **88** (7 mg, 0.021 mmol) in THF (1 mL), burgess reagent (22 mg, 0.091 mmol) was added at 23 ºC. The resulting mixture was stirred for 2.5 hours (TLC monitoring).

Then, the reaction was treated with water and extracted with EtOAc. The combined organic phases were washed with water and brine, dried over $MgSO_4$. The crude product was used without further purification in the following step (6 mg, 93%).

^{1}H NMR (500 MHz, $CDCl_3$) δ 7.26 (d, *J* = 2.5 Hz, 1H), 7.23 – 7.19 (m, 3H), 7.02 – 6.97 (m, 2H), 6.72 (d, *J* = 2.5 Hz, 1H), 4.86 (dq, *J* = 2.0, 1.4 Hz, 1H), 4.58 (s, 1H), 4.07 (d, *J* = 4.3 Hz, 1H), 3.90 (s, 3H), 3.89 (s, 3H), 3.07 – 2.99 (m, 2H), 2.74 (dd, *J* = 18.2, 12.8 Hz, 1H), 1.78 (s, 3H). ^{13}C NMR (126 MHz, $CDCl_3$) δ 198.8, 159.3, 158.2, 144.7, 135.8, 134.0, 128.7 (2C), 128.3 (2C), 127.2, 126.7, 112.8, 104.6, 100.6, 56.0, 55.9, 55.8, 45.9, 23.1, 22.4. GCMS-ESI(+) *m/z* calc. for $C_{21}H_{24}O_3$ $[M]^+$: 322.1, found: 322.4.

(1*R,2*S**,3*R**)-5,7-Dimethoxy-2-phenyl-3-(prop-1-en-2-yl)-1,2,3,4-tetrahydronaphthalen-1-ol (*epi*-carexane I)**

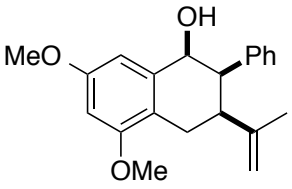

A flame-dried round bottom flask was charged with $LiAlH_4$ (3 mg, 0.34 mmol) and put under argon atmosphere. Then, a solution of **89** (6 mg, 0.018 mmol) in THF (1.5 mL) was added dropwise at 0 ºC. The resulting mixture was stirred for 1 h (TLC monitoring). Then, the reaction was treated with water and extracted with EtOAc. The combined organic phases were washed with water and brine, dried over $MgSO_4$. The crude was concentrated directly to afford the title compound (6 mg, 93%) as a pale yellow oil.

^{1}H NMR (400 MHz, $CDCl_3$) δ 7.21 – 7.15 (m, 3H), 7.00 – 6.94 (m, 2H), 6.42 (dd, *J* = 6.2, 3.2 Hz, 1H), 5.21 – 5.12 (m, 1H), 4.76 (s, 1H), 4.49 (s, 1H), 3.84 (s, 3H), 3.83 (s, 3H), 2.78 (dd, *J* = 8.2, 3.9 Hz, 1H), 2.76 – 2.73 (m, 1H), 2.48 (ddd, *J* = 18.1, 13.5, 1.8 Hz, 1H), 1.76 (s, 3H). ^{13}C NMR (101 MHz, $CDCl_3$) δ 159.4, 157.7, 146.0, 141.4, 136.5, 130.4, 128.5, 127.2, 117.8, 111.6, 101.6, 97.5, 72.6, 55.6, 49.7, 44.3, 29.9, 23.3, 22.6. GCMS-ESI(+) *m/z* calc. for $C_{21}H_{24}O_3$ $[M]^+$: 324.4, found: 324.2.

2-((2*R,3*S**,4*S**)-6,8-Dimethoxy-3-phenyl-4-((triisopropylsilyl)oxy)-1,2,3,4-tetrahydronaphthalen-2-yl)propan-2-ol (90)**

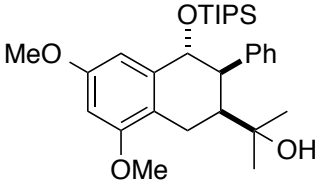

To a solution of **87a** (30 mg, 0.088 mmol) in anhydrous CH_2Cl_2 (1.2 mL), 2,6-lutidine (15 µL, 0.132 mmol) and TIPSOTf (25 µL, 0.092 mmol) were added dropwise at 0 ºC. The resulting mixture was stirred for 1.5 h at the same temperature. Upon completion, the reaction was treated with water and extracted with CH_2Cl_2. The combined organic phases were washed with brine and dried over $MgSO_4$. The crude was purified by flash chromatography over silica gel using

cyclohexane:EtOAc 9:1 to 8:2 as eluent to afford the desired compound (38 mg, 87%) as a colorless oil.

^{1}H NMR (500 MHz, $CDCl_3$) δ 7.18 – 7.14 (m, 3H), 6.98 – 6.95 (m, 2H), 6.44 (d, *J* = 2.4 Hz, 1H), 6.39 (d, *J* = 2.4 Hz, 1H), 4.69 (d, *J* = 2.0 Hz, 1H), 3.85 (s, 3H), 3.77 (s, 3H), 3.57 (t, *J* = 2.7 Hz, 1H), 3.02 (dd, *J* = 16.1, 3.9 Hz, 1H), 2.68 – 2.56 (m, 2H), 1.25 (s, 3H), 1.21 (s, 3H), 1.19 – 1.13 (m, 3H), 1.10 (d, *J* = 7.0 Hz, 9H), 1.07 (d, *J* = 7.0 Hz, 9H). ^{13}C NMR (126 MHz, $CDCl_3$) δ 158.5, 158.1, 140.3, 138.5, 129.9 (2C), 128.9 (2C), 127.0, 119.4, 105.9, 98.0, 74.9, 73.4, 55.4, 55.3, 49.1, 29.1, 28.5, 20.7, 18.5 (3C), 18.5 (3C), 17.9, 13.0 (3C). HRMS-ESI(+) *m/z* calc. for $C_{30}H_{46}NaO_4Si$ $[M+Na]^+$: 521.3058, found: 521.3060.

(((1*R,2*R**,3*S**)-5,7-Dimethoxy-2-phenyl-3-(prop-1-en-2-yl)-1,2,3,4-tetrahydronaphthalen-1-yl)oxy)triisopropylsilane (91)**

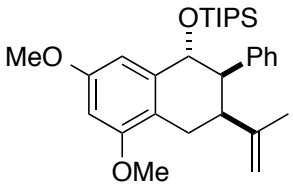

To a solution of **90** (34 mg, 0.068 mmol) in THF (2.5 mL), burgess reagent (49 mg, 0.2047 mmol) was added at 23 ºC. The resulting mixture was stirred for 50 min (TLC monitoring). Then, the reaction was treated with water and extracted with EtOAc. The combined organic phases were washed with water and brine, dried over $MgSO_4$. The crude product was purified by flash chromatography over silica gel using cyclohexane:EtOAc 95:5 as eluent to afford the compound (17 mg, 51%) as a yellow oil.

^{1}H NMR (400 MHz, $CDCl_3$) δ 7.14 – 7.09 (m, 3H), 6.81 – 6.77 (m, 2H), 6.53 (d, *J* = 2.4 Hz, 1H), 6.42 (d, *J* = 2.4 Hz, 1H), 4.95 (d, *J* = 1.7 Hz, 1H), 4.80 (t, *J* = 1.8 Hz, 1H), 4.49 (s, 1H), 3.82 (s, 3H), 3.81 (s, 3H), 3.43 – 3.37 (m, 1H), 3.14 (dt, *J* = 13.3, 4.3 Hz, 1H), 2.74 (dd, *J* = 17.3, 4.6 Hz, 1H), 2.23 (dd, *J* = 17.3, 13.0 Hz, 1H), 1.81 (s, 3H), 1.22 – 1.14 (m, 3H), 1.11 (d, *J* = 6.9 Hz, 9H), 1.09 (d, *J* = 7.0 Hz, 9H). ^{13}C NMR (101 MHz, $CDCl_3$) δ 158.6, 157.9, 146.9, 139.3, 139.2, 129.1 (2C), 127.8 (2C), 126.4, 119.4, 111.4, 105.6, 98.0, 73.7, 55.5, 55.4, 51.2, 39.1, 23.0, 22.7, 18.5 (3C), 18.5 (3C), 13.1 (3C). GCMS-ESI(+) *m/z* calc. for $C_{30}H_{44}NaO_3Si$ $[M+Na]^+$: 503.2952, found: 503.2951.

(1*R,2*R**,3*S**)-5,7-Dimethoxy-2-phenyl-3-(prop-1-en-2-yl)-1,2,3,4-tetrahydronaphthalen-1-ol (Carexane I)**

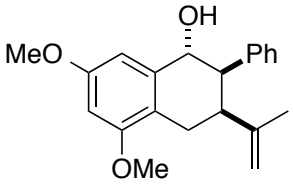

A solution of **91** (17 mg, 0.0350 mmol) in anhydrous THF (3 mL) was treated with 1 M solution of TBAF (70 μL, 0.0699 mmol) at 0ºC under Ar. After 1.5 h, the crude was concentrated

upon addition of fluorisil and was purified by flash chromatography over silica gel using cyclohexane:EtOAc 9:1 to 7:3 as eluent to afford the compound (11 mg, 97 %) as off-white solid.

Mp = 128-130 ºC. ^{1}H NMR (300 MHz, $CDCl_3$) δ 7.18 – 7.12 (m, 3H), 6.90 – 6.83 (m, 2H), 6.61 (d, *J* = 2.4 Hz, 1H), 6.45 (d, *J* = 2.4 Hz, 1H), 4.88 (d, *J* = 2.6 Hz, 1H), 4.81 (t, *J* = 1.6 Hz, 1H), 4.47 (s, 1H), 3.84 (s, 3H), 3.82 (s, 3H), 3.42 (t, *J* = 3.1 Hz, 1H), 2.91 (dt, *J* = 12.1, 3.9 Hz, 1H), 2.78 (dd, *J* = 17.3, 4.5 Hz, 1H), 2.29 (dd, *J* = 17.3, 12.0 Hz, 1H), 2.01 (s, 1H), 1.79 (s, 3H). ^{13}C NMR (75 MHz, $CDCl_3$) δ 159.2, 157.9, 146.2, 138.9, 138.8, 128.9 (2C), 127.7 (2C), 126.4, 119.2, 111.7, 104.3, 98.3, 72.5, 55.4 (2C), 49.6, 39.8, 23.0, 22.70. HRMS-ESI(+) *m/z* calc. for $C_{21}H_{24}NaO_3$ $[M+Na]^+$: 347.1618, found: 347.1609.

Crystallographic Data

4-Chloro-3-methyl-5-((1*R**,4*S**)-1,3,3-trimethyl-2-oxabicyclo[2.2.2]oct-5-en-5-yl)phenol (47)

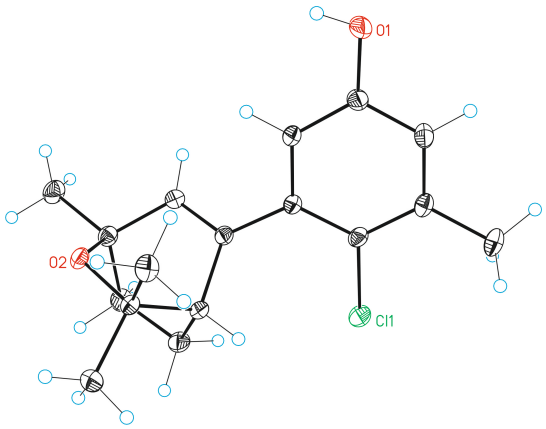

Table T16. Crystal data and structure refinement for **47**

Identification code	mo_PCR134P4_0m
Empirical formula	C17H21ClO2
Formula weight	292.79
Temperature	100(2) K
Wavelength	0.71073 Å
Crystal system	Triclinic
Space group	P-1
Unit cell dimensions	
a = 7.5694(7)Å	α = 62.329(3)°.
b = 10.7335(10)Å	β = 71.973(3)°.
c = 10.9019(11)Å	γ = 84.508(3)°.
Volume	744.71(13) Å3
Z	2
Density (calculated)	1.306 Mg/m3
Absorption coefficient	0.256 mm-1
F(000)	312
Crystal size	1.00 x 0.45 x 0.45 mm3
Theta range for data collection	2.146 to 30.904°.
Index ranges	-10<=h<=10,-14<=k<=13,-15<=l<=15
Reflections collected	11500
Independent reflections	4083[R(int) = 0.0322]
Completeness to theta =30.904°	86.799995%
Absorption correction	Multi-scan
Max. and min. transmission	0.894 and 0.769
Refinement method	Full-matrix least-squares on F2
Data / restraints / parameters	4083/ 0/ 186
Goodness-of-fit on F2	1.054
Final R indices [I>2sigma(I)]	R1 = 0.0373, wR2 = 0.0994
R indices (all data)	R1 = 0.0420, wR2 = 0.1036
Largest diff. peak and hole	0.440 and -0.378 e.Å-3

Table T17. Bond lengths [Å] and angles [°] for **47**

Bond lengths			
Cl1-C2	1.7455(12)	C5-C6	1.3919(14)
O1-C5	1.3609(14)	C8-C9	1.3418(14)
O2-C14	1.4641(12)	C8-C13	1.5174(14)
O2-C10	1.4714(13)	C9-C10	1.5033(15)
C1-C6	1.3990(15)	C10-C15	1.5162(15)
C1-C2	1.4004(14)	C10-C11	1.5311(17)
C1-C8	1.4812(14)	C11-C12	1.5507(16)
C2-C3	1.4004(15)	C12-C13	1.5448(16)
C3-C4	1.3878(17)	C13-C14	1.5520(15)
C3-C7	1.5046(15)	C14-C16	1.5241(15)
C4-C5	1.3938(15)	C14-C17	1.5264(16)
Angles			
C14-O2-C10	113.88(8)	C8-C9-C10	114.45(9)
C6-C1-C2	118.07(9)	O2-C10-C9	106.82(8)
C6-C1-C8	117.32(9)	O2-C10-C15	105.89(9)
C2-C1-C8	124.60(10)	C9-C10-C15	113.42(9)
C3-C2-C1	121.98(10)	O2-C10-C11	106.73(9)
C3-C2-Cl1	118.35(8)	C9-C10-C11	109.69(9)
C1-C2-Cl1	119.66(8)	C15-C10-C11	113.74(9)
C4-C3-C2	118.28(10)	C10-C11-C12	109.10(9)
C4-C3-C7	120.01(10)	C13-C12-C11	108.03(9)
C2-C3-C7	121.69(11)	C8-C13-C12	107.62(9)
C3-C4-C5	121.10(10)	C8-C13-C14	107.20(9)
O1-C5-C6	122.43(10)	C12-C13-C14	109.43(8)
O1-C5-C4	117.85(10)	O2-C14-C16	107.51(8)
C6-C5-C4	119.72(10)	O2-C14-C17	108.07(9)
C5-C6-C1	120.82(10)	C16-C14-C17	109.75(9)
C9-C8-C1	123.45(10)	O2-C14-C13	107.74(8)
C9-C8-C13	112.13(9)	C16-C14-C13	112.47(9)
C1-C8-C13	123.94(9)	C17-C14-C13	111.12(8)

Table T18. Torsion angles [°] for **47**

C6-C1-C2-C3	-0.1(4)	C7-C3-C4-C5	-176.94(10)
C6-C1-C2-C3	-0.30(16)	C3-C4-C5-O1	179.77(10)
C8-C1-C2-C3	-179.44(10)	C3-C4-C5-C6	-0.31(17)
C6-C1-C2-Cl1	-178.66(8)	O1-C5-C6-C1	178.61(10)
C8-C1-C2-Cl1	2.20(15)	C4-C5-C6-C1	-1.30(16)
C1-C2-C3-C4	-1.24(16)	C2-C1-C6-C5	1.59(16)
Cl1-C2-C3-C4	177.14(8)	C8-C1-C6-C5	-179.21(10)
C1-C2-C3-C7	177.22(10)	C6-C1-C8-C9	43.84(15)
Cl1-C2-C3-C7	-4.40(14)	C2-C1-C8-C9	-137.02(12)
C2-C3-C4-C5	1.55(16)	C6-C1-C8-C13	-127.61(11)

C2-C1-C8-C13	51.53(16)	C1-C8-C13-C12	-129.29(11)
C1-C8-C9-C10	-169.75(10)	C9-C8-C13-C14	-59.22(12)
C13-C8-C9-C10	2.60(14)	C1-C8-C13-C14	113.08(11)
C14-O2-C10-C9	-57.09(11)	C11-C12-C13-C8	-61.68(11)
C14-O2-C10-C15	-178.28(8)	C11-C12-C13-C14	54.49(11)
C14-O2-C10-C11	60.20(10)	C10-O2-C14-C16	-119.17(10)
C8-C9-C10-O2	55.79(12)	C10-O2-C14-C17	122.42(9)
C8-C9-C10-C15	172.07(10)	C10-O2-C14-C13	2.27(11)
C8-C9-C10-C11	-59.53(13)	C8-C13-C14-O2	55.03(10)
O2-C10-C11-C12	-64.74(11)	C12-C13-C14-O2	-61.41(11)
C9-C10-C11-C12	50.65(12)	C8-C13-C14-C16	173.33(9)
C15-C10-C11-C12	178.87(9)	C12-C13-C14-C16	56.90(11)
C10-C11-C12-C13	7.32(13)	C8-C13-C14-C17	-63.18(11)
C9-C8-C13-C12	58.40(12)	C12-C13-C14-C17	-179.62(9)

(1*R,3a*R**)-5,8-Dimethoxy-1,4,4,7-tetramethyl-2,3,3a,4-tetrahydro-1*H*-cyclopenta[*b*]-naphthalene (51a)**

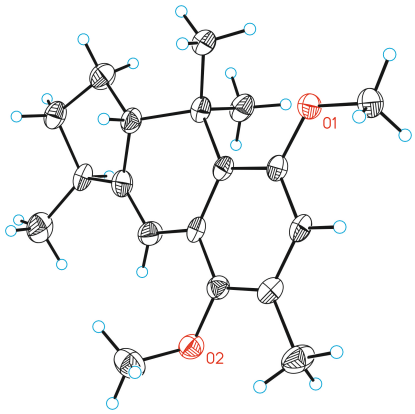

Table T19. Crystal data and structure refinement for **51a**

Identification code	mo_PCR_P309P_0m
Empirical formula	C19H26O2
Formula weight	286.40
Temperature	100(2) K
Wavelength	0.71073 Å
Crystal system	Monoclinic
Space group	P2(1)/n
Unit cell dimensions	
a = 14.191(2)Å	α= 90°.
b = 7.1381(12)Å	β = 108.401(5)°.
c = 16.826(3)Å	γ = 90°.
Volume	1617.3(4) Å3
Z	4
Density (calculated)	1.176 Mg/m3
Absorption coefficient	0.074 mm-1
F(000)	624
Crystal size	0.15 x 0.03 x 0.02 mm3

Theta range for data collection	2.551 to 27.241°.
Index ranges	-17<=h<=18,-8<=k<=6,-21<=l<=15
Reflections collected	10219
Independent reflections	3225[R(int) = 0.0484]
Completeness to theta =27.241°	88.9%
Absorption correction	Multi-scan
Max. and min. transmission	0.999 and 0.87
Refinement method	Full-matrix least-squares on F2
Data / restraints / parameters	3225/ 98/ 213
Goodness-of-fit on F2	1.028
Final R indices [I>2sigma(I)]	R1 = 0.0600, wR2 = 0.1437
R indices (all data)	R1 = 0.1112, wR2 = 0.1669
Largest diff. peak and hole	0.202 and -0.210 e.Å-3

Table T20. Bond lengths [Å] and angles [°] for **51a**

Bond lengths

C1-C2	1.383(3)	C10-C18	1.537(3)
C1-C6	1.392(3)	C10-C11	1.547(4)
C1-O2	1.404(3)	C11-C15	1.512(4)
C2-C3	1.391(3)	C11-C12	1.538(3)
C2-C8	1.503(4)	C12-C13'	1.518(10)
C3-C4	1.389(3)	C12-C13	1.528(4)
C4-O1	1.379(3)	C13-C14	1.534(4)
C4-C5	1.410(3)	C14-C19	1.514(4)
C5-C6	1.419(3)	C14-C15	1.526(4)
C5-C10	1.543(3)	C13'-C14'	1.513(10)
C6-C16	1.466(3)	C14'-C19	1.511(9)
C7-O2	1.427(3)	C14'-C15	1.524(9)
C9-O1	1.422(3)	C15-C16	1.317(4)
C10-C17	1.537(3)		

Angles

C2-C1-C6	122.8(2)	C1-C6-C16	119.2(2)
C2-C1-O2	117.9(2)	C5-C6-C16	120.2(2)
C6-C1-O2	119.2(2)	C17-C10-C18	108.9(2)
C1-C2-C3	117.0(2)	C17-C10-C5	106.7(2)
C1-C2-C8	121.6(2)	C18-C10-C5	115.28(19)
C3-C2-C8	121.4(2)	C17-C10-C11	111.9(2)
C4-C3-C2	121.7(2)	C18-C10-C11	106.6(2)
O1-C4-C3	121.5(2)	C5-C10-C11	107.5(2)
O1-C4-C5	116.8(2)	C15-C11-C12	104.1(2)
C3-C4-C5	121.7(2)	C15-C11-C10	112.3(2)
C4-C5-C6	116.2(2)	C12-C11-C10	118.8(2)
C4-C5-C10	124.4(2)	C13'-C12-C11	105.4(7)
C6-C5-C10	119.0(2)	C13-C12-C11	103.7(2)
C1-C6-C5	120.5(2)	C12-C13-C14	105.5(3)

C19-C14-C15	113.7(2)	C16-C15-C14'	132.6(5)
C19-C14-C13	116.1(3)	C11-C15-C14'	100.8(4)
C15-C14-C13	102.0(2)	C16-C15-C14	129.3(2)
C14'-C13'-C12	102.0(8)	C11-C15-C14	110.8(2)
C19-C14'-C13'	120.8(10)	C15-C16-C6	120.3(2)
C19-C14'-C15	114.0(7)	C4-O1-C9	117.88(19)
C13'-C14'-C15	99.2(11)	C1-O2-C7	112.42(19)
C16-C15-C11	119.9(2)		

Table T21. Torsion angles [°] for **51a**

C6-C1-C2-C3	-0.1(4)	C10-C11-C12-C13'	132.0(10)
O2-C1-C2-C3	177.1(2)	C15-C11-C12-C13	28.1(3)
C6-C1-C2-C8	-177.5(2)	C10-C11-C12-C13	153.9(2)
O2-C1-C2-C8	-0.3(4)	C11-C12-C13-C14	-38.4(3)
C1-C2-C3-C4	-0.1(4)	C12-C13-C14-C19	156.4(2)
C8-C2-C3-C4	177.3(2)	C12-C13-C14-C15	32.3(3)
C2-C3-C4-O1	-176.4(2)	C11-C12-C13'-C14'	26.1(16)
C2-C3-C4-C5	1.9(4)	C12-C13'-C14'-C19	-173.2(10)
O1-C4-C5-C6	175.1(2)	C12-C13'-C14'-C15	-48.0(16)
C3-C4-C5-C6	-3.4(3)	C12-C11-C15-C16	169.7(3)
O1-C4-C5-C10	2.4(3)	C10-C11-C15-C16	39.9(3)
C3-C4-C5-C10	-176.1(2)	C12-C11-C15-C14'	-35.7(8)
C2-C1-C6-C5	-1.5(4)	C10-C11-C15-C14'	-165.5(7)
O2-C1-C6-C5	-178.7(2)	C12-C11-C15-C14	-8.4(3)
C2-C1-C6-C16	174.4(2)	C10-C11-C15-C14	-138.2(2)
O2-C1-C6-C16	-2.8(3)	C19-C14'-C15-C16	-28.5(17)
C4-C5-C6-C1	3.1(3)	C13'-C14'-C15-C16	-158.3(8)
C10-C5-C6-C1	176.2(2)	C19-C14'-C15-C11	-178.2(10)
C4-C5-C6-C16	-172.7(2)	C13'-C14'-C15-C11	52.1(11)
C10-C5-C6-C16	0.4(3)	C19-C14-C15-C16	41.9(4)
C4-C5-C10-C17	84.9(3)	C13-C14-C15-C16	167.6(3)
C6-C5-C10-C17	-87.6(3)	C19-C14-C15-C11	-140.3(3)
C4-C5-C10-C18	-36.2(3)	C13-C14-C15-C11	-14.6(3)
C6-C5-C10-C18	151.3(2)	C11-C15-C16-C6	-4.2(4)
C4-C5-C10-C11	-154.9(2)	C14'-C15-C16-C6	-149.3(10)
C6-C5-C10-C11	32.6(3)	C14-C15-C16-C6	173.4(3)
C17-C10-C11-C15	65.9(3)	C1-C6-C16-C15	167.0(3)
C18-C10-C11-C15	-175.1(2)	C5-C6-C16-C15	-17.1(4)
C5-C10-C11-C15	-50.9(3)	C3-C4-O1-C9	-0.2(3)
C17-C10-C11-C12	-55.8(3)	C5-C4-O1-C9	-178.7(2)
C18-C10-C11-C12	63.2(3)	C2-C1-O2-C7	99.8(3)
C5-C10-C11-C12	-172.6(2)	C6-C1-O2-C7	-82.9(3)
C15-C11-C12-C13'	6.2(10)		

Carexane I

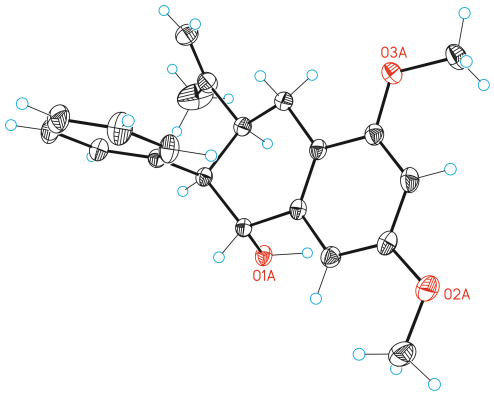

Table T22. Crystal data and structure refinement for **carexane I**

Identification code	mo_PCR_C173_05
Empirical formula	C22.25H27O3
Formula weight	342.44
Temperature	100(2) K
Wavelength	0.71073 Å
Crystal system	Triclinic
Space group	P-1
Unit cell dimensions	
a = 10.6353(6)Å	α= 107.8335(15)°.
b = 13.0254(7)Å	β = 104.6754(16)°.
c = 15.5365(9)Å	γ = 98.9253(16)°.
Volume	1917.66(19) Å3
Z	4
Density (calculated)	1.186 Mg/m3
Absorption coefficient	0.077 mm-1
F(000)	738
Crystal size	0.18 x 0.12 x 0.06 mm3
Theta range for data collection	1.697 to 30.184°.
Index ranges	-14<=h<=13,-18<=k<=17,0<=l<=21
Reflections collected	18580
Independent reflections	18580[R(int) =?]
Completeness to theta =30.184°	83.8%
Absorption correction	Multi-scan
Max. and min. transmission	0.995 and 0.765
Refinement method	Full-matrix least-squares on F2
Data / restraints / parameters	18580/ 7/ 495
Goodness-of-fit on F2	1.029
Final R indices [I>2sigma(I)]	R1 = 0.0531, wR2 = 0.1447
R indices (all data)	R1 = 0.0667, wR2 = 0.1556
Largest diff. peak and hole	0.792 and -0.260 e.Å-3

Table T23. Bond lengths [Å] and angles [°] for **carexane I**

Bond lengths			
O1A-C8A	1.4491(17)	O2B-C20B	1.416(2)
O2A-C11A	1.3703(18)	O3B-C13B	1.3745(18)
O2A-C20A	1.429(2)	O3B-C21B	1.4270(19)
O3A-C13A	1.3702(17)	C1B-C6B	1.394(2)
O3A-C21A	1.4272(18)	C1B-C2B	1.395(2)
C1A-C6A	1.391(2)	C1B-C7B	1.5160(18)
C1A-C2A	1.394(2)	C2B-C3B	1.390(2)
C1A-C7A	1.517(2)	C3B-C4B	1.384(3)
C2A-C3A	1.388(2)	C4B-C5B	1.381(3)
C3A-C4A	1.386(3)	C5B-C6B	1.395(2)
C4A-C5A	1.383(3)	C7B-C8B	1.5338(19)
C5A-C6A	1.389(2)	C7B-C16B	1.557(2)
C7A-C8A	1.5286(19)	C8B-C9B	1.5170(19)
C7A-C16A	1.5558(19)	C9B-C14B	1.389(2)
C8A-C9A	1.5188(19)	C9B-C10B	1.402(2)
C9A-C14A	1.3882(19)	C10B-C11B	1.382(2)
C9A-C10A	1.406(2)	C11B-C12B	1.395(2)
C10A-C11A	1.384(2)	C12B-C13B	1.377(2)
C11A-C12A	1.399(2)	C13B-C14B	1.410(2)
C12A-C13A	1.382(2)	C14B-C15B	1.5075(19)
C13A-C14A	1.4141(19)	C15B-C16B	1.528(2)
C14A-C15A	1.5071(19)	C16B-C17B	1.518(2)
C15A-C16A	1.526(2)	C17B-C18B	1.343(2)
C16A-C17A	1.515(2)	C17B-C19B	1.489(2)
C17A-C18A	1.328(2)	C1S-C2S	1.502(7)
C17A-C19A	1.492(3)	C2S-C3S	1.510(8)
O1B-C8B	1.4438(16)	C3S-C4S	1.532(7)
O2B-C11B	1.3756(17)	C4S-C5S	1.530(8)
Angles			
C11A-O2A-C20A	116.37(12)	O1A-C8A-C7A	108.20(11)
C13A-O3A-C21A	117.06(12)	C9A-C8A-C7A	114.51(11)
C6A-C1A-C2A	117.94(14)	C14A-C9A-C10A	121.47(13)
C6A-C1A-C7A	119.20(13)	C14A-C9A-C8A	121.35(12)
C2A-C1A-C7A	122.85(13)	C10A-C9A-C8A	117.12(12)
C3A-C2A-C1A	120.82(15)	C11A-C10A-C9A	119.23(13)
C4A-C3A-C2A	120.35(16)	O2A-C11A-C10A	124.52(14)
C5A-C4A-C3A	119.60(15)	O2A-C11A-C12A	114.92(13)
C4A-C5A-C6A	119.79(15)	C10A-C11A-C12A	120.56(14)
C5A-C6A-C1A	121.48(15)	C13A-C12A-C11A	119.52(13)
C1A-C7A-C8A	113.10(11)	O3A-C13A-C12A	123.50(13)
C1A-C7A-C16A	113.83(11)	O3A-C13A-C14A	115.12(13)
C8A-C7A-C16A	109.22(11)	C12A-C13A-C14A	121.37(13)
O1A-C8A-C9A	109.28(11)	C9A-C14A-C13A	117.84(13)

C9A-C14A-C15A	122.53(12)	C14B-C9B-C10B	121.41(13)
C13A-C14A-C15A	119.60(12)	C14B-C9B-C8B	121.10(13)
C14A-C15A-C16A	112.46(11)	C10B-C9B-C8B	117.26(12)
C17A-C16A-C15A	113.85(12)	C11B-C10B-C9B	119.13(13)
C17A-C16A-C7A	111.67(12)	O2B-C11B-C10B	124.95(14)
C15A-C16A-C7A	111.48(11)	O2B-C11B-C12B	114.24(13)
C18A-C17A-C19A	121.11(16)	C10B-C11B-C12B	120.80(13)
C18A-C17A-C16A	123.39(15)	C13B-C12B-C11B	119.28(13)
C19A-C17A-C16A	115.43(15)	O3B-C13B-C12B	123.31(13)
C11B-O2B-C20B	116.88(12)	O3B-C13B-C14B	115.06(13)
C13B-O3B-C21B	116.57(13)	C12B-C13B-C14B	121.63(13)
C6B-C1B-C2B	118.22(13)	C9B-C14B-C13B	117.70(13)
C6B-C1B-C7B	122.78(13)	C9B-C14B-C15B	121.98(12)
C2B-C1B-C7B	119.00(13)	C13B-C14B-C15B	120.30(13)
C3B-C2B-C1B	121.27(15)	C14B-C15B-C16B	112.51(11)
C4B-C3B-C2B	119.87(15)	C17B-C16B-C15B	114.10(12)
C5B-C4B-C3B	119.63(15)	C17B-C16B-C7B	112.15(11)
C4B-C5B-C6B	120.64(16)	C15B-C16B-C7B	110.82(12)
C1B-C6B-C5B	120.36(15)	C18B-C17B-C19B	120.79(15)
C1B-C7B-C8B	113.56(12)	C18B-C17B-C16B	123.40(14)
C1B-C7B-C16B	114.06(11)	C19B-C17B-C16B	115.80(13)
C8B-C7B-C16B	109.63(11)	C1S-C2S-C3S	114.0(5)
O1B-C8B-C9B	106.77(11)	C2S-C3S-C4S	114.2(4)
O1B-C8B-C7B	106.69(11)	C5S-C4S-C3S	110.6(4)
C9B-C8B-C7B	115.47(11)		

Table T24. Torsion angles [°] for **carexane I**

C6A-C1A-C2A-C3A	-1.4(2)	C7A-C8A-C9A-C10A	164.47(12)
C7A-C1A-C2A-C3A	179.20(14)	C14A-C9A-C10A-C11A	-0.3(2)
C1A-C2A-C3A-C4A	0.2(3)	C8A-C9A-C10A-C11A	176.91(13)
C2A-C3A-C4A-C5A	1.0(3)	C20A-O2A-C11A-C10A	-6.9(2)
C3A-C4A-C5A-C6A	-1.0(2)	C20A-O2A-C11A-C12A	173.44(14)
C4A-C5A-C6A-C1A	-0.3(2)	C9A-C10A-C11A-O2A	-179.34(14)
C2A-C1A-C6A-C5A	1.4(2)	C9A-C10A-C11A-C12A	0.3(2)
C7A-C1A-C6A-C5A	-179.13(13)	O2A-C11A-C12A-C13A	179.29(14)
C6A-C1A-C7A-C8A	-134.04(13)	C10A-C11A-C12A-C13A	-0.4(2)
C2A-C1A-C7A-C8A	45.40(18)	C21A-O3A-C13A-C12A	14.9(2)
C6A-C1A-C7A-C16A	100.53(15)	C21A-O3A-C13A-C14A	-166.04(13)
C2A-C1A-C7A-C16A	-80.04(17)	C11A-C12A-C13A-O3A	179.48(13)
C1A-C7A-C8A-O1A	154.63(11)	C11A-C12A-C13A-C14A	0.5(2)
C16A-C7A-C8A-O1A	-77.49(13)	C10A-C9A-C14A-C13A	0.4(2)
C1A-C7A-C8A-C9A	-83.23(14)	C8A-C9A-C14A-C13A	-176.69(13)
C16A-C7A-C8A-C9A	44.65(16)	C10A-C9A-C14A-C15A	-177.52(13)
O1A-C8A-C9A-C14A	103.26(14)	C8A-C9A-C14A-C15A	5.4(2)
C7A-C8A-C9A-C14A	-18.29(19)	O3A-C13A-C14A-C9A	-179.58(12)
O1A-C8A-C9A-C10A	-73.98(15)	C12A-C13A-C14A-C9A	-0.5(2)

O3A-C13A-C14A-C15A	-1.6(2)	C14B-C9B-C10B-C11B	2.4(2)
C12A-C13A-C14A-C15A	177.50(14)	C8B-C9B-C10B-C11B	-172.18(12)
C9A-C14A-C15A-C16A	-20.52(19)	C20B-O2B-C11B-C10B	9.3(2)
C13A-C14A-C15A-C16A	161.57(13)	C20B-O2B-C11B-C12B	-171.40(14)
C14A-C15A-C16A-C17A	175.42(12)	C9B-C10B-C11B-O2B	177.96(13)
C14A-C15A-C16A-C7A	47.99(16)	C9B-C10B-C11B-C12B	-1.3(2)
C1A-C7A-C16A-C17A	-61.82(16)	O2B-C11B-C12B-C13B	-179.91(13)
C8A-C7A-C16A-C17A	170.71(12)	C10B-C11B-C12B-C13B	-0.6(2)
C1A-C7A-C16A-C15A	66.79(15)	C21B-O3B-C13B-C12B	-2.3(2)
C8A-C7A-C16A-C15A	-60.68(15)	C21B-O3B-C13B-C14B	177.25(14)
C15A-C16A-C17A-C18A	-33.9(2)	C11B-C12B-C13B-O3B	-179.01(13)
C7A-C16A-C17A-C18A	93.47(17)	C11B-C12B-C13B-C14B	1.4(2)
C15A-C16A-C17A-C19A	149.15(16)	C10B-C9B-C14B-C13B	-1.6(2)
C7A-C16A-C17A-C19A	-83.51(19)	C8B-C9B-C14B-C13B	172.80(12)
C6B-C1B-C2B-C3B	0.7(2)	C10B-C9B-C14B-C15B	177.04(12)
C7B-C1B-C2B-C3B	-179.52(14)	C8B-C9B-C14B-C15B	-8.6(2)
C1B-C2B-C3B-C4B	0.1(2)	O3B-C13B-C14B-C9B	-179.96(12)
C2B-C3B-C4B-C5B	-0.8(3)	C12B-C13B-C14B-C9B	-0.4(2)
C3B-C4B-C5B-C6B	0.6(3)	O3B-C13B-C14B-C15B	1.41(19)
C2B-C1B-C6B-C5B	-0.9(2)	C12B-C13B-C14B-C15B	-178.99(13)
C7B-C1B-C6B-C5B	179.33(15)	C9B-C14B-C15B-C16B	25.75(18)
C4B-C5B-C6B-C1B	0.3(3)	C13B-C14B-C15B-C16B	-155.68(13)
C6B-C1B-C7B-C8B	-43.12(19)	C14B-C15B-C16B-C17B	-178.63(11)
C2B-C1B-C7B-C8B	137.14(14)	C14B-C15B-C16B-C7B	-50.89(15)
C6B-C1B-C7B-C16B	83.47(17)	C1B-C7B-C16B-C17B	59.59(16)
C2B-C1B-C7B-C16B	-96.27(16)	C8B-C7B-C16B-C17B	-171.80(11)
C1B-C7B-C8B-O1B	-154.67(11)	C1B-C7B-C16B-C15B	-69.21(15)
C16B-C7B-C8B-O1B	76.45(13)	C8B-C7B-C16B-C15B	59.40(14)
C1B-C7B-C8B-C9B	86.88(14)	C15B-C16B-C17B-C18B	23.2(2)
C16B-C7B-C8B-C9B	-42.01(15)	C7B-C16B-C17B-C18B	-103.81(17)
O1B-C8B-C9B-C14B	-100.99(14)	C15B-C16B-C17B-C19B	-156.25(13)
C7B-C8B-C9B-C14B	17.42(18)	C7B-C16B-C17B-C19B	76.69(16)
O1B-C8B-C9B-C10B	73.60(15)	C1S-C2S-C3S-C4S	-178.8(7)
C7B-C8B-C9B-C10B	-167.99(12)	C2S-C3S-C4S-C5S	-175.5(8)

DFT Calculations

Cartesian Coordinates (in Å)

Table T25: Optimized geometry for **87a**

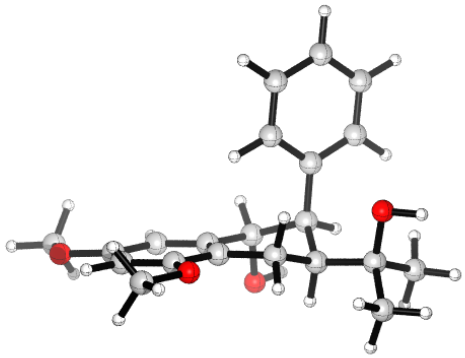

Free energy G = -1101.296506 Hartree/particle.

C	-2.18494000	1.20623200	-0.82886300	H	0.02331400	-1.24536100	-1.26513200
C	-1.04774400	0.71654700	-0.10036100	C	2.84976400	-2.91423200	-2.25792200
C	-1.22170000	-0.38481600	0.74867700	H	4.69470900	-3.03950500	-1.10866200
C	-2.48450900	-0.99846700	0.91309000	H	0.88553700	-2.62726700	-3.14845300
C	-3.60035400	-0.50183300	0.20764900	H	3.22757800	-3.53179700	-3.08817200
C	-3.44727400	0.60560100	-0.67333600	H	0.88922400	1.47385600	1.80900400
H	-2.56922600	-1.85078800	1.59843800	C	2.69686300	1.76190900	0.62870900
H	-4.33579500	0.95873800	-1.21071500	C	2.51717400	3.32374900	0.59850400
O	-4.91562600	-0.99925600	0.27164100	H	3.50659100	3.81363300	0.56777000
O	-1.90088000	2.29860300	-1.66821900	H	1.94775200	3.63399700	-0.29265600
C	-0.05026200	-0.95747700	1.58247100	H	1.98489100	3.66675300	1.50223100
H	-0.08355200	-2.07594300	1.50460900	C	3.68067700	1.43243800	1.80802000
C	1.37193700	-0.48264300	1.07550200	H	4.60681100	2.02409400	1.69909500
H	2.07338300	-0.66700200	1.91449100	H	3.21340300	1.69064900	2.77405800
C	1.29835700	1.06855700	0.85898300	H	3.94962300	0.36435800	1.81410800
C	0.30551500	1.40980800	-0.28478800	O	3.20739000	1.27721000	-0.64602300
H	0.76427400	1.12178400	-1.25330000	H	4.09623200	1.77507600	-0.70842600
H	0.13813600	2.50223400	-0.32144700	C	-5.04458000	-2.12880000	1.18643400
O	-0.29263700	-0.51835400	2.95481800	H	-4.42100900	-2.99752500	0.87372900
H	0.46249700	-0.99237800	3.45358100	H	-4.77533500	-1.85672500	2.23270100
C	1.87450600	-1.31826900	-0.12057900	H	-6.11407800	-2.42374100	1.15523600
C	3.18346400	-1.85166000	-0.09484900	C	-3.07702600	2.78764100	-2.37955700
C	1.05718700	-1.61956300	-1.23242600	H	-3.51696400	2.01223700	-3.04765600
C	3.66979700	-2.63723100	-1.15136400	H	-3.86941600	3.14882800	-1.68457400
H	3.83206200	-1.65012600	0.77241400	H	-2.72493800	3.63857300	-2.99900200
C	1.54120300	-2.40620400	-2.29082900				

Table T26: Optimized geometry for **87b**

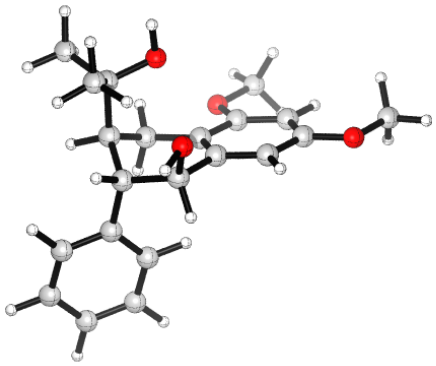

Free energy G = -1101.300940 Hartree/particle.

C	2.02596900	0.22847100	1.17607000	H	-2.39243700	-1.34866000	1.06228700
C	0.77814600	0.00174300	0.51610200	O	-0.35389500	-0.98829600	-2.70534300
C	0.70742100	0.21816500	-0.87386500	H	-1.13911700	-0.81974300	-3.33580000
C	1.83788400	0.63401400	-1.59865300	C	-2.61141300	0.91143400	-0.27688400
C	3.07406400	0.84453100	-0.94208900	C	-4.00836200	0.81674400	-0.08893400
C	3.17100900	0.64664400	0.45787700	C	-1.97692200	2.13772200	0.01396100
H	1.77452000	0.78861400	-2.68586400	C	-4.75354000	1.91424200	0.36864500
H	4.11947400	0.81281400	0.97624500	H	-4.51427800	-0.13755200	-0.30991900
O	4.12372900	1.25818400	-1.78635300	C	-2.72105000	3.23840000	0.47212600
O	1.98649600	0.00096900	2.56591100	H	-0.88710500	2.23484200	-0.11110100
C	5.38232100	1.44901900	-1.07620700	C	-4.11033000	3.13184200	0.64965200
H	5.74537500	0.51046000	-0.59775900	H	-5.84309000	1.82076100	0.50448600
H	6.11846000	1.76667100	-1.84377200	H	-2.20878200	4.18858400	0.69372300
H	5.31303400	2.24162200	-0.29588400	H	-4.69201300	3.99623900	1.00732000
C	3.28052400	0.17276400	3.21312700	C	-0.96099900	-2.70203600	0.12753700
H	3.11732100	-0.06651400	4.28465400	C	-1.44403200	-3.65983100	1.27742000
H	4.05408400	-0.51695000	2.80420900	H	-2.54563200	-3.72738800	1.28519400
H	3.65810700	1.21839700	3.13428800	H	-1.03252300	-4.67315800	1.12235200
C	-0.60444700	0.02500200	-1.67030400	H	-1.10213900	-3.28657700	2.25794300
H	-0.83660700	0.99979200	-2.17063800	C	-1.50899600	-3.21407800	-1.24359800
C	-0.42138600	-0.47932600	1.34001900	H	-1.18884300	-4.25922300	-1.40118600
H	-0.05498900	-1.13817400	2.14981500	H	-2.61140300	-3.18201600	-1.26799600
H	-0.91968500	0.38534900	1.82495300	H	-1.07640200	-2.55466100	-2.02879700
C	-1.84531700	-0.33935000	-0.76536400	O	0.49798800	-2.66913400	0.09024900
H	-2.55512400	-0.90891700	-1.39775100	H	0.70457900	-3.61364600	-0.23682700
C	-1.46376500	-1.23357300	0.46671800				

Table T27: Optimized geometry for **87b'**

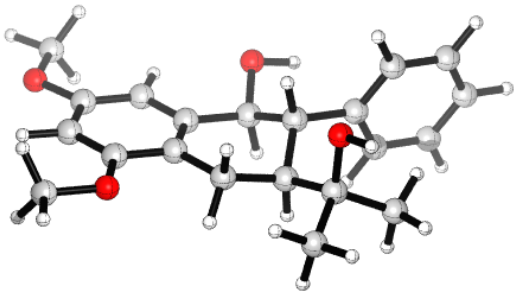

Free energy G = -1101.292473 Hartree/particle.

C	-2.95557500	1.10008100	-0.00252000	H	-0.75896400	2.50107200	0.79379700
C	-1.59901900	0.64333800	0.10053500	O	0.13954700	-2.55324800	-0.36288900
C	-1.36310200	-0.73360100	0.16208200	H	1.11625100	-2.80736200	-0.21032000
C	-2.41766000	-1.67134800	0.12795800	C	2.53615700	-0.85128500	-0.14429800
C	-3.74854500	-1.21537300	0.02651100	C	3.34401800	-1.02079600	-1.28970400
C	-4.01962400	0.18057500	-0.03368600	C	3.03376700	-1.29180500	1.10419400
H	-2.15931300	-2.73704500	0.16332800	C	4.62165200	-1.59647600	-1.18980000
H	-5.06694100	0.49696300	-0.11121300	H	2.96359900	-0.68013400	-2.26645400
O	-4.90104700	-2.02272400	-0.02020700	C	4.30921600	-1.86824800	1.20530200
O	-3.08401300	2.50027100	-0.06777000	H	2.42160600	-1.15851100	2.01041400
C	-4.58444300	-3.44647200	0.02127900	C	5.10781400	-2.02071400	0.05831400
H	-4.05991300	-3.73349800	0.96135100	H	5.24265500	-1.71551500	-2.09229900
H	5.55861400	-3.97627900	-0.02432900	H	4.68595500	-2.19942900	2.18650500
H	-3.95822200	-3.76400000	-0.84366100	H	6.10953000	-2.47220500	0.13791300
C	4.47218500	2.93670300	-0.16456200	C	2.02768700	2.22714900	0.04746000
H	-4.44016700	4.04551500	-0.20198400	C	1.58655400	3.66227400	0.51973500
H	-4.96887100	2.55892200	-1.08749100	H	0.69704100	4.00993900	-0.02920600
H	-5.07619800	2.62220400	0.71717400	H	1.36405500	3.65583400	1.60072700
C	0.07880500	-1.26344500	0.30115000	H	2.40726200	4.37856800	0.33893300
H	0.30212000	-1.36596500	1.39823300	C	3.42581500	1.95870900	0.71718500
C	1.13330800	-0.22949100	-0.27242600	H	3.30229600	1.79327300	1.80111200
H	0.92351600	-0.06993100	-1.34853100	H	3.92174600	1.08134000	0.27679900
C	0.94063600	1.14633100	0.45671400	H	4.07838100	2.83753000	0.57169000
H	1.01359600	0.98644500	1.55236700	O	2.10840200	2.15898700	-1.40677400
C	-0.47988600	1.68804500	0.09661300	H	2.78214400	2.89907500	-1.60693300
H	-0.42000300	2.14198800	-0.91500500				

Table T28: Optimized geometry for **carexane O**

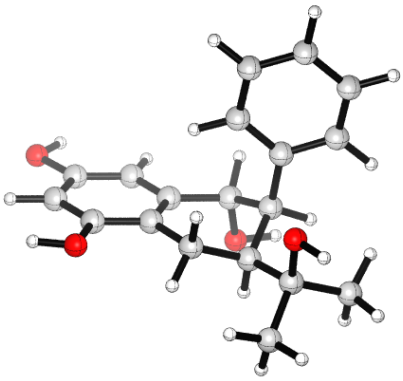

Free energy G = -1023.74374 Hartree/particle.

C	2.38008000	-0.45923900	1.44608000
C	1.21007400	-0.11913200	0.69398900
C	1.18464100	-0.44683900	-0.67180300
C	2.28338900	-1.07447900	-1.29463500
C	3.43947100	-1.39347300	-0.54589000
C	3.48541900	-1.08734100	0.83688100
H	2.24201800	-1.30447900	-2.37081300
H	4.38324300	-1.34020000	1.42115300
O	4.56514100	-2.01321200	-1.10139500
O	2.36135000	-0.13145900	2.80654000
C	-0.02409500	-0.09720600	-1.56960600
H	-0.32234000	-1.02317900	-2.12688000
C	-1.29443800	0.37917100	-0.76640300
H	-1.91600100	0.98274200	-1.45958700
C	-0.97299900	1.26399000	0.48724100
H	-1.92351900	1.36183900	1.05214500
C	0.04443500	0.55358000	1.42460900
H	-0.49292300	-0.20820900	2.02626600
H	0.43546700	1.30670600	2.13719500
O	0.46253500	0.90109300	-2.53023400
H	-0.38615600	1.11763300	-3.05326300
C	-2.16723000	-0.81709900	-0.32117200
C	-3.56180900	-0.62877100	-0.20161300
C	-1.62516400	-2.07723500	0.00556200
C	-4.39656200	-1.67314700	0.22418500
H	-3.99148100	0.35661000	-0.44761800
C	-2.45964200	-3.12442800	0.43270100
H	-0.53819300	-2.23909300	-0.06859900
C	-3.84600200	-2.92716400	0.54166800
H	-5.48307500	-1.51004800	0.30880000
H	-2.02108700	-4.10357900	0.68438400
H	-4.49833900	-3.74967000	0.87562300
C	-0.54206000	2.75229400	0.18392400
C	0.85958800	2.86426000	-0.49166500
H	1.06143200	3.91794300	-0.75280600
H	1.64123000	2.51146000	0.20093000
H	0.86302000	2.23196300	-1.40901900
C	-1.60338300	3.45180400	-0.73993900
H	-2.62884900	3.25060300	-0.38419800
H	-1.43532100	4.54353500	-0.73073500
H	-1.50729600	3.10379500	-1.78251600
O	-0.54891400	3.37260100	1.51025600
H	-0.14716900	4.28753600	1.30244400
H	4.30665800	-2.12161300	-2.08092800
H	3.27549300	-0.44174700	3.13199000

Chapter IV:

α,β-Unsaturated Gold(I)-Carbenes by Tandem Cyclization and 1,5-Alkoxy Migration of 1,6-Enynes: Computational Studies

Introduction

As mentioned in the **General Introduction**, gold carbenes have been often proposed as intermediates in many gold-catalyzed transformations.[1] The structure of these species can be understood in the context of the bonding model developed by Toste and Goddard.[2] Accordingly, a three-centered-four-electron σ-hyperbond must be formed between the metal centre and both ligand and substrate.

Two resonances are often proposed: carbene **1** with a gold-carbon double bond, and carbocation **2** with a gold-carbon single bond (Scheme 1). However, a more precise representation would be a "half double-bond" model **3**, which denotes a partial contribution of both σ and π-bonding to the gold-carbon interaction. Considering the competition between ligand and substrate for the electron density of gold, strongly σ-donating and weakly π-acidic ligands are expected to increase the carbene-like reactivity.

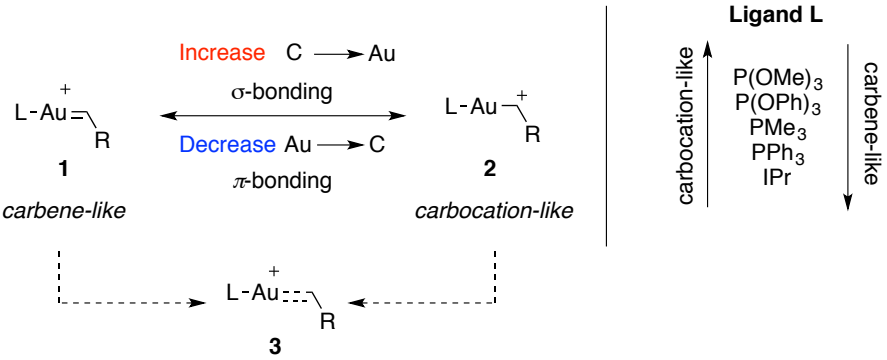

Scheme 1. Nature of gold(I)-carbenes bonding

Much effort has been devoted to study the bonding nature of these gold-carbenes, revealing the importance of ligand tuning to obtain the desired reactivity in every specific gold(I)-catalyzed reaction.[1]

1 For a recent discussion on the nature of the carbene-like intermediates, see: Harris, R. J.; Widenhoefer, R. A. *Chem. Soc. Rev.* **2016**, 45, 4533–4551.

2 Benitez, D.; Shapiro, N. D.; Tkatchouk, E.; Wang, Y.; Goddard, W. A.; Toste, F. D. *Nat. Chem.* **2009**, *1*, 482–486.

To date, several methods for the generation of gold carbenes have been reported. One of the most extended strategies relies on the decomposition of diazo compounds,[3] albeit limited applicability of the resulting carbene species has been observed (Scheme 2, eq. 1). As safer surrogates for diazo carbonyl compounds, alkynes serve as precursors to versatile α-oxo gold carbenes in the presence of a suitable oxidant (eq. 2).[4] Gold(I) carbenes have also been generated from 7-substituted-cycloheptatrienes via retro-Büchner reaction promoted by cationic gold(I) complexes (eq. 3).[5] Other alternatives include the ring cleavage of cyclopropenes[6] to give vinyl gold(I) carbene intermediates (eq. 4) or the use of propargylic carboxylates (eq. 5),[7] which undergo a 1,2-acyloxy

3 (a) Fructos, M. R.; Belderrain, T. R.; de Frémont, P.; Scott, N. M.; Nolan, S. P.; Díaz-Requejo, M. M.; Pérez, P. J. *Angew. Chem. Int. Ed.* **2005**, *44*, 5284–5288. (b) Prieto, A.; Fructos, M. R.; Díaz-Requejo, M. M.; Pérez, P. J.; Pérez-Galán, P.; Delpont, N.; Echavarren, A. M. *Tetrahedron* **2009**, *65*, 1790–1793. (c) Rivilla, I.; Gómez-Emeterio, B. P.; Fructos, M. R.; Díaz-Requejo, M. M.; Pérez, P. J. *Organometallics* **2011**, *30*, 2855–2860. (d) Pérez, P. J.; Díaz-Requejo, M. M.; Rivilla, I. *Beilstein J. Org. Chem.* **2011**, *7*, 653–657. (e) Yu, Z.; Ma, B.; Chen, M.; Wu, H.-H.; Liu, L.; Zhang, J. *J. Am. Chem. Soc.* **2014**, *136*, 6904–6907.

4 For a general review, see: Zhang, L. *Acc. Chem. Res.* **2014**, *47*, 877–888.

5 Solorio-Alvarado, C. R.; Wang, Y.; Echavarren, A. M. *J. Am. Chem. Soc.* **2011**, *133*, 11952–11955.

6 (a) Hadfield, M. S.; Bauer, J. T.; Glen, P. E.; Lee, A.-L. *Org. Biomol. Chem.* **2010**, *8*, 4090–4095. (b) For review on gold(I) catalyzed transformations of cyclopropenes: Miege, F.; Meyer, C.; Cossy. J. *Beilstein. J. Org. Chem.* **2011**, *7*, 717–734.

7 For reviews and lead references on gold-catalyzed propargylic carboxylate rearrangement: (a) Gorin, D. J.; Dubé, P.; Toste, F. D. *J. Am. Chem. Soc.* **2006**, *128*, 14480–14481. (b) Marco-Contelles, J.; Soriano, E. *Chem.–Eur. J.* **2007**, *13*, 1350–1357. (c) Amijs, C. H. M.; López-Carrillo, V.; Echavarren, A. M. *Org. Lett.* **2007**, *9*, 4021–4024. (d) Correa, A.; Marion, N.; Fensterbank, L.; Malacria, M.; Nolan, S. P.; Cavallo, L. *Angew. Chem. Int. Ed.* **2008**, *47*, 718–721. (e) Li, G.; Zhang, G.; Zhang, L. *J. Am. Chem. Soc.* **2008**, *130*, 3740–3741. (f) Shapiro, N. D.; Toste, F. D. *J. Am. Chem. Soc.* **2008**, *130*, 9244–9245 (g) Shapiro, N. D.; Shi, Y.; Toste, F. D. *J. Am. Chem. Soc.* **2009**, *131*, 11654–11655. (h) Wang, S.; Zhang, G.; Zhang, L. *Synlett* **2010**, 692–706. (i) de Haro, T.; Gómez-Bengoa, E.; Cribiú, R.; Huang, X.; Nevado, C. *Chem.–Eur. J.* **2012**, *18*, 6811–6824. (j) Shiroodi, R. K.; Gevorgyan, V. *Chem. Soc. Rev.* **2013**, *42*, 4991–5001.

migration of the neighboring carboxylate moiety. These highly reactive species can be trapped intra- or intermolecularly by a range of nucleophiles.

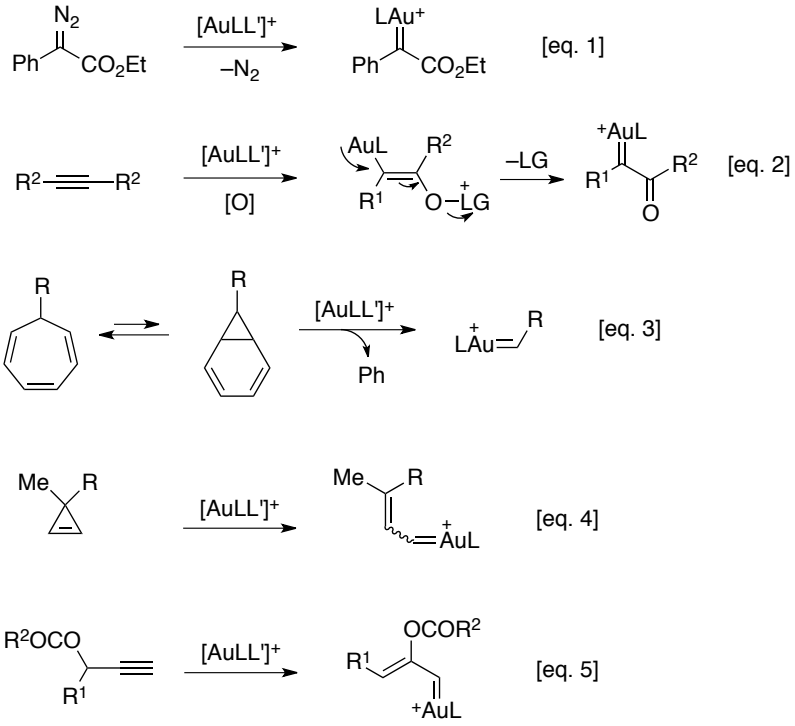

Scheme 2. Common methods for the generation of gold(I)-carbenes

Very recently, our group has reported a novel method for the generation of well-defined gold carbenoids [$LAuCH_2Cl$] bearing bulky ligands, which upon chloride abstraction act as gold carbene equivalents in solution (Scheme 3).[8]

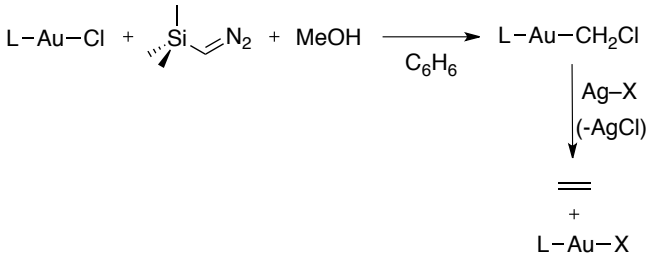

Scheme 3. Generation of gold carbenes from gold(I) carbenoids by chloride abstraction

As explained in the **General Introduction**, gold(I)-catalyzed cyclizations of 1,n-enynes proceed through intermediates that can be considered as highly distorted gold(I) carbenes,[9] which present different reactivity toward many functional groups. We

8 Sarria-Toro, J. M.; García-Morales, C.; Raducan, M.; Smirnova, E. S.; Echavarren, A. M. *Angew. Chem. Int. Ed.* **2017**, *56*, 1859–1863.

9 Jiménez-Núñez, E.; Echavarren, A. M. *Chem. Rev.* **2008**, *108*, 3326–3350.

recently found that 1,6-enynes such as **4** bearing propargyl alcohols, ethers, or silyl ethers react with gold(I) catalysts through the usual type of highly delocalized cyclopropyl gold(I) intermediates **5**,[1] which then undergo a new type of 1,5-migration of the OR groups to generate species **6**[10] that we postulated as intermediate between *α,β*-unsaturated gold(I)-carbenes and gold(I)-stabilized allyl cations (Scheme 4).[1,11] In the presence of carbon nucleophiles such as indole or furans, products **7**[10] or trienes such as **8**[12] were obtained by Friedel-Crafts-type reactions. Intermediates **6** can also react with electron-rich alkenes to form the corresponding cyclopropanes,[10] a reaction which is also characteristic of gold(I) carbenes **6**.[3b,5,13] Furthermore, we demonstrated the potential of this tandem cyclization/1,5-OR migration/cyclopropanation to form products **9** that were key intermediates in the first total synthesis of the natural sesquiterpene (+)-schisanwilsonene A (**10**).[14]

10 Jiménez-Núñez, E.; Raducan, M.; Lauterbach, T.; Molawi, K.; Solorio, C. R.; Echavarren, A. M. *Angew. Chem. Int. Ed.* **2009**, *48*, 6152–6155.

11 Wang, Y.; Muratore, M. E.; Echavarren, A. M. *Chem.–Eur. J.* **2015**, *21*, 7332–7339.

12 Leboeuf, D.; Gaydou, M.; Wang, Y.; Echavarren, A. M. *Org. Chem. Front.* **2014**, *1*, 759–764.

13 (a) Nieto-Oberhuber, C.; López, S.; Muñoz, M. P.; Jiménez-Núñez, E.; Buñuel, E.; Cárdenas, D. J.; Echavarren, A. M. *Chem.–Eur. J.* **2006**, *12*, 1694–1702. (b) Pérez-Galán, P.; Herrero-Gómez, E.; Hog, D. T.; Martin, N. J. A.; Maseras, F.; Echavarren, A. M. *Chem. Sci.* **2011**, *2*, 141–149.

14 Gaydou, M.; Miller, R. E.; Delpont, N.; Ceccon, J.; Echavarren, A. M. *Angew. Chem. Int. Ed.* **2013**, *52*, 6396–6399.

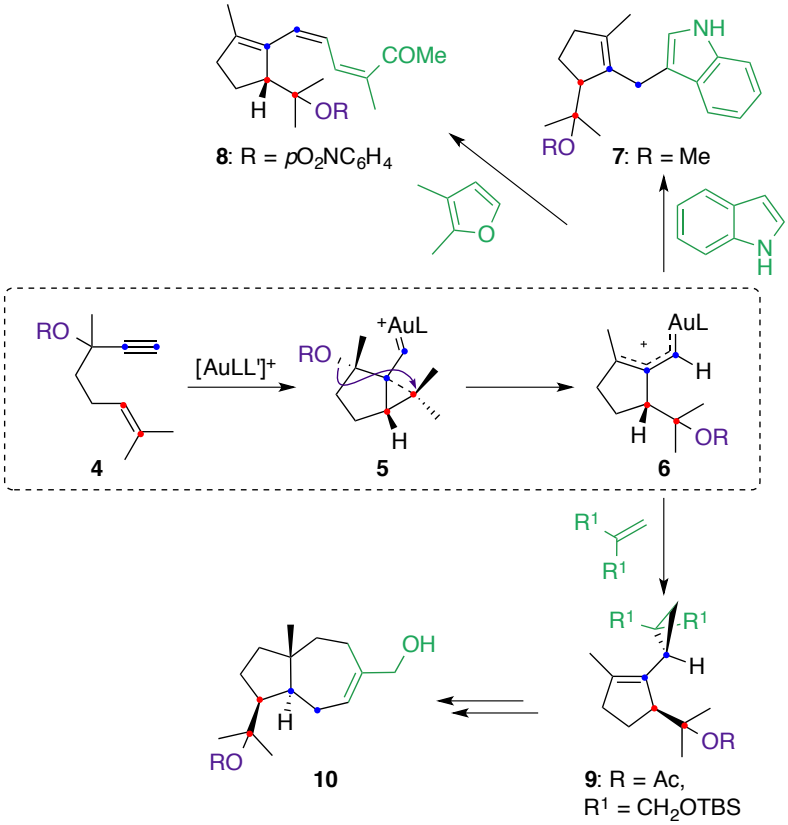

Scheme 4. Intermolecular trapping of the intermediates of the gold-catalyzed cyclization/1,5-OR migration of enynes **4**

This type of gold(I)-catalyzed 1,5-migration has been found to compete with 1,2- and 1,3-migrations of propargylic carboxylate groups.[15] Related processes have been found in the gold(I)-catalyzed reactions of dienynes **11**, which upon cyclization/1,5-OR migration, react intramolecularly with the alkene on the side chain to form stereoselectively hexahydroazulenes **13**.[10] These compounds were the key intermediates in the total synthesis of the sesquiterpernes (–)-epiglobulol (**14**) and (–)-4*β*,7*α*-aromadendranediol (**15**) (Scheme 5).[16] Alternatively, when the gold(I)-catalyzed reaction was performed in the presence of allyl alcohol, this external nucleophile reacted to give **16**, which underwent intramolecular cyclopropanation to give rise finally to the sesquiterpene (–)-4*α*,7*α*-aromadendranediol (**17**).

15 (a) Wang, S.; Zhang, G.; Zhang, L. *Synlett*, **2010**, 692–706. (b) Shu, X.-Z.; Shu, D.; Schienebeck, C. M.; Tang, W. *Chem. Soc. Rev.* **2012**, *41*, 7698–7711.

16 Carreras, J.; Livendahl, M.; McGonigal, P. R.; Echavarren, A. M. *Angew. Chem. Int. Ed.* **2014**, *53*, 4896–4899.

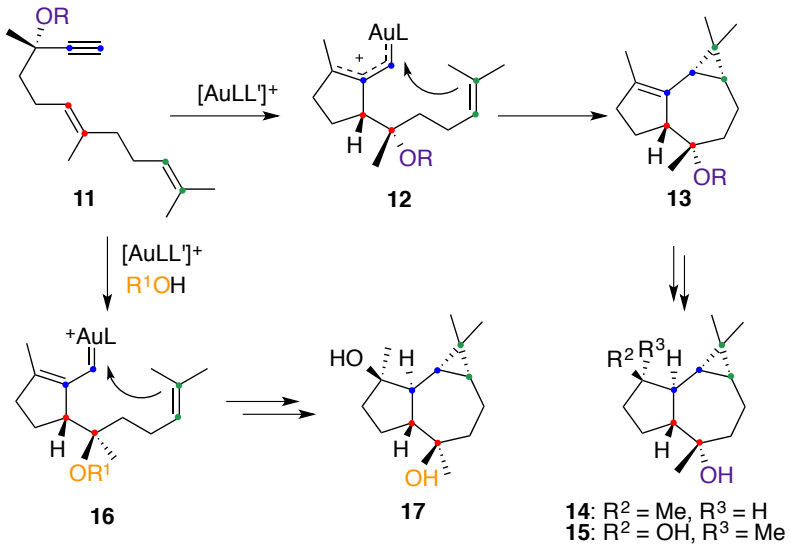

Scheme 5. Intramolecular trapping of the intermediates of the gold-catalyzed cyclization/1,5-OR migration of dienynes **11**

The proposed mechanism for these inter- and intramolecular reactions was based on the isolation of diverse products but not on a rigorous study of this intriguing process and its several possible competitive cycloisomerization pathways.

More recently, we found that 1,3-dicarbonyl compounds and *β*-ketoesters can also be used as the C-nucleophiles to trap the putative *α,β*-unsaturated gold(I)-carbenes **6** leading to products of formal alkylation (Scheme 6).[17] Interestingly, among the examined migrating OR groups, *p*-nitrophenyl (PNP) ether gave the best results. In addition, the use of less electrophilic catalysts with more donating NHC ligands, which has been proposed to enhance the carbene-like character of the intermediates in gold(I)-catalyzed reactions, proved to be beneficial.

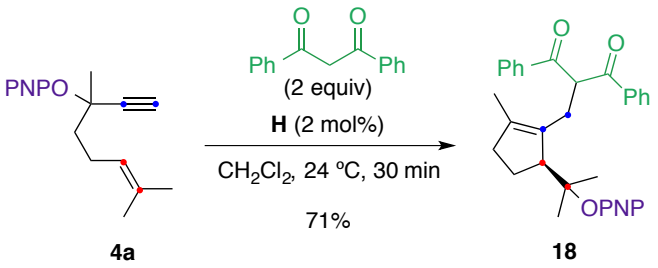

Scheme 6. Gold(I)-catalyzed reaction of 1,6-enyne **4a** with 1,3-diphenyl-1,3-propandione

17 Calleja, P.; Pablo, O.; Ranieri, B.; Gaydou, M.; Pitaval, A.; Moreno, M.; Raducan, M.; Echavarren, A. M. *Chem.–Eur. J.* **2016**, *22*, 13613–13618.

Furthermore, the 1,5-migration sequence could be expanded to other type of trapping agents such as silanes (Figure 1).[18] *p*-Nitrophenyl ether **4a** undergoes an analogous tandem cyclization/1,5-OR migration/intermolecular cyclopropanation with different olefins such as cyclohexene to form cyclopropanes **19** in good yield.[17] Interestingly, the electron-rich heterocycles also undergo cyclopropanation, which is in contrast to what we observed previously for indole, which gave product **7** after formal alkylation at C-3 (Scheme 4).

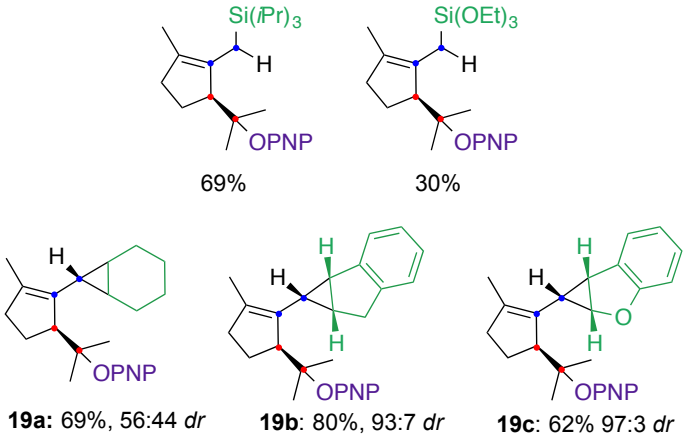

Figure 1. Gold(I)-catalyzed reaction of 1,6-enyne **4a** with different trapping agents

Interestingly, enynes **20** with tertiary propargyl hydroxyl or trimethylsilyloxy groups and different aryl groups at the alkene reacted with catalyst **A** to give *endo*-type single cleavage rearrangement products **21** under very mild conditions (Table 1).[17] By contrast, the reaction of the corresponding methyl ethers or substrates bearing phenyl or aryl groups with electron-donating substituents only led to complex reaction mixtures.

18 Studies performed by Morgane Gaydou, ICIQ PhD Thesis 2014, unpublished results.

Table 1. Gold(I)-catalyzed reaction of 1,6-enynes **20** to give six-membered ring products **21**.

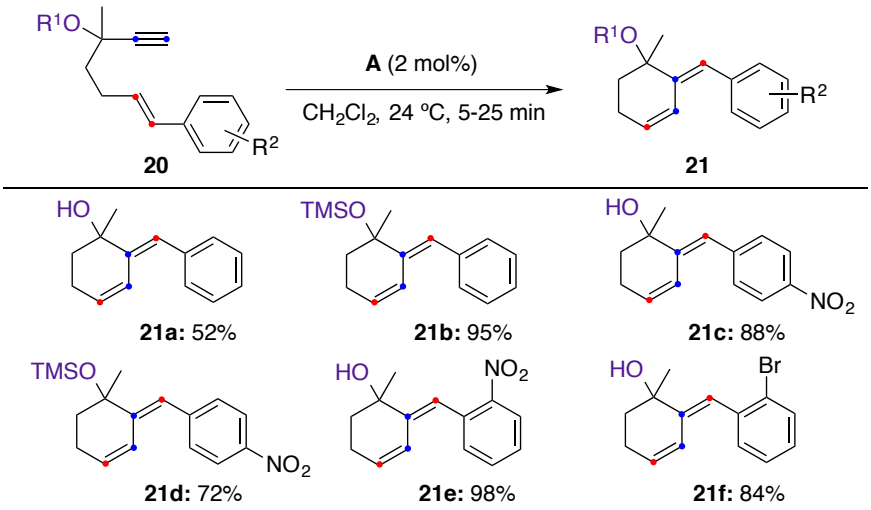

However, these are not the only exceptions to the rule that have been observed experimentally. Indeed, alcohol **22a** also reacted in the presence of catalyst **A** without migration of the OH group to give **23**, the analogous product of an *endo*-type single cleavage rearrangement (Scheme 7).[17] On the other hand, enyne **22b** reacts with methanol to give stereoselectively **24** in which the migration of the benzyloxy group has not taken place.[19]

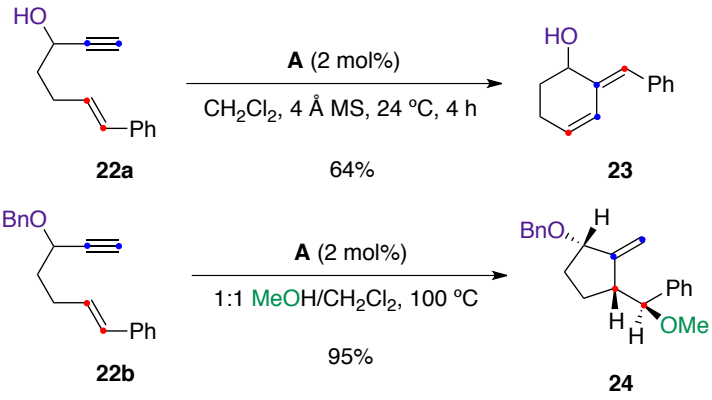

Scheme 7. Gold(I)-catalyzed cyclization of 1,6-enynes **22** without OR migration

Finally, the reaction of 1,6-enyne **25a** bearing an electron-rich *p*-methoxyphenyl propargylic amine undergoes a gold(I)-catalyzed intramolecular hydroarylation with the terminal alkyne to afford **26**, whilst PNP derivative **25b** gave cycloadduct **27** as the major product (Scheme 8).[17]

19 Jiménez-Núñez, E.; Molawi, K.; Echavarren, A. M. *Chem. Commun.* **2009**, 7327–7329.

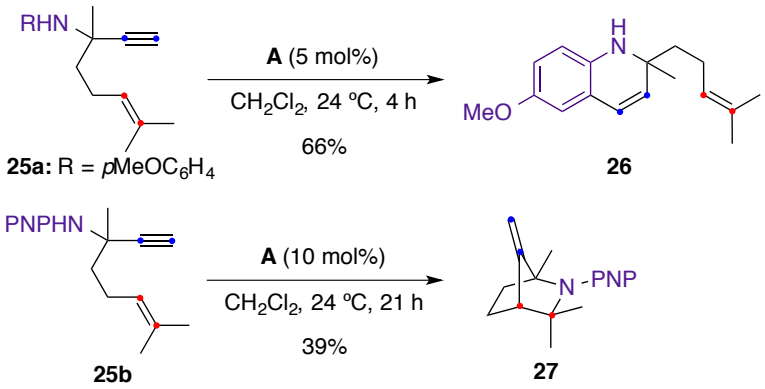

Scheme 8. Gold(I)-catalyzed cyclization of 1,6-enynes **25** with a propargylic amine

Objectives

Since the discovery of the formation of gold(I)-carbenes through a new type of intramolecular 1,5-migration of propargylic alkoxy groups,[10] much effort has been devoted in our group to expand the scope of this transformation by using a range of trapping agents (Scheme 9). Intriguingly, in some cases a skeletal rearrangement has been found to take place preferentially to form unexpected six-membered ring compounds. However, no rigorous study of this process and its various possible competitive cycloisomerization pathways had been done.

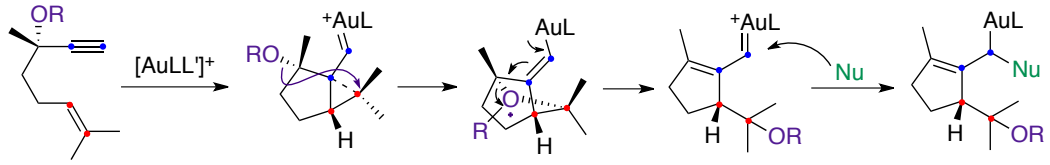

Scheme 9. Gold(I)-catalyzed 1,5-migration of 1,6-enyne **4**

We therefore performed a detailed computational study to understand the mechanisms of these complex transformations. We planned to investigate the evolution of 1,6-enynes bearing different substituents at the propargylic position and at the alkene as model substrates of the gold(I)-catalyzed 1,5-migration reaction (Figure 2).

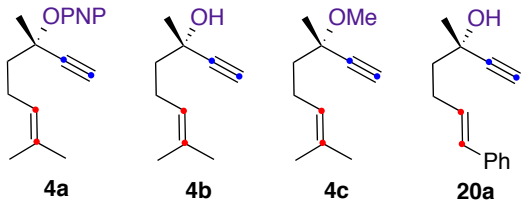

Figure 2. Selected 1,6-enynes to perform the computational study

Results and Discussion

Computational Studies on the 1,5-Alkoxy Migration of 1,6-Enynes 4a, 4b and 4c.

We focused our investigations on the gold(I) catalyzed skeletal rearrangements of different model 1,6-enynes prone to undergo intramolecular 1,5-migration in the absence of external nucleophiles.

Density Functional Theory (DFT) was the method of choice, since it has been successfully applied to similar studies.[20] With the aim to select the adequate conditions to perform our computational study, different parameters (functional, basis set and solvent model) were evaluated considering the theoretical work already developed on gold(I)-catalyzed reactions of enynes.[21] Thus, hybrid functionals B3LYP, M06 and wB97XD were tested,[22] in combination with basis sets 6-31G(d,p) (C, P, O, H) and SDD(Au), and IEF-PCM or SMD as solvation models.[23] Additionally, the effect of a larger basis set 6-311++G(d,p) (C, P, O, H) was also examined. Finally, PMe_3 was selected as an initial model to replace bulky phosphines.

As shown in Table 2, DFT calculations indicate that upon activation of the alkyne with gold(I) (**Ib**), cyclopropyl gold(I) carbene **IIb** is formed preferentially via an exocyclic rearrangement. The alternative 6-*endo-dig* pathway is less kinetically favored in all the cases, regardless the functional, basis set, or solvent model used (Table 2, conditions A-G, $\mathbf{TS_{1b}}$ *vs.* $\mathbf{TS_{2b}}$).

20 DFT-studies of Au(I)-alkyne complexes: (a) Wu, J.; Kroll, P.; Dias, H. V. R. *Inorg. Chem.* **2009**, *48*, 423–425. (b) Shapiro, N. D.; Toste, F. D. *Proc. Nat. Acad. Sci.* **2008**, *105*, 2779–2782.

21 For a review on DFT calculations in coordination chemistry, see: Tsipis, A. C. *Coord. Chem. Rev.* **2014**, 272, 1–29.

22 Faza, O. N.; Rodríguez, R. S.; López, C. S. *Theor. Chem. Acc.* **2011**, *128*, 647–661 and references therein.

23 Tomasi, J.; Mennucci, B.; Cammi, R. *Chem. Rev.* **2005**, *105*, 2999–3093.

Table 2. Reaction pathways and energy values calculated for the the initial cyclization of **Ib**: exocyclic *vs*. endocyclic process

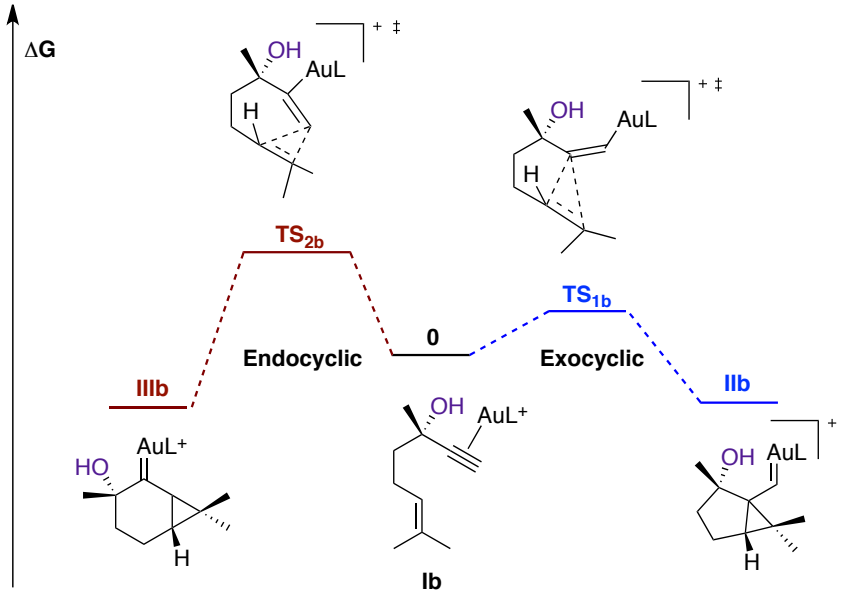

Conditions	A	B	C	D	E	F	G
Functional	**B3LYP**	**B3LYP**	**B3LYP**	**M06**	**M06**	**M06**	**wB97XD**
Basis set	**6-31G(d,p)**	**6-31G(d,p)**	**6-311++G(d,p)**	**6-31G(d,p)**	**6-31G(d,p)**	**6-311++G(d,p)**	**6-31G(d,p)**
Solvent	**IEF-PCM**	**SMD**	**IEF-PCM**	**IEF-PCM**	**SMD**	**IEF-PCM**	**IEF-PCM**
Ib	0.0	0.0	0.0	0.0	0.0	0.0	0.0
TS_{1b}	3.6	6.9	8.3	5.6	7.9	7.3	8.7
IIb	-1.1	2.6	5.9	-4.9	-2.2	0.4	-4.1
TS_{2b}	7.4	10.7	11.8	10.0	11.2	10.6	12.2
IIIb	-3.1	11.8	3.5	-6.1	-5.4	-1.3	-4.9

ΔG energies are given in kcal·mol^{-1}.

After the formation of cyclopropyl gold(I) carbene **IIb**, two possible evolution pathways have been considered: a) migration of the alkoxy moiety to the cationic center, and b) competitive skeletal rearrangement (without OR migration) to afford the corresponding single-cleavage rearrangement product (Table 3).

In order to discriminate between these two processes while maintaining the consistency with the experimental data, the selection of the appropriate functional proved to be crucial. Indeed, other studies have shown that different functionals could lead to very distinct results, even to reverse scenarios.[24]

24 (a) Nava, P.; Hagebaum-Reignier, D. Humbel, S. *ChemPhysChem*, **2012**, *13*, 2090–2096. (b) Yang, L.; Fang, R. *J. Mol. Catal. A: Chem.* **2013**, 379, 197–206. (c) Hansmann, M. M.; Rominger, F.; Hashmi, A. S. K. *Chem. Sci.* **2013**, *4*, 1552–1559.

According to our theoretical studies, the migration of the OR group in complex **IIb** proceeds stepwise via oxonium bridge **IVb**, which then leads to 1,5-migration product **VIb** though a very low barrier transition state $\mathbf{TS_{5b}}$. On the other hand, the alternative evolution of **IIb** to single-cleavage rearrangement product **Vb** was found to be thermodynamically the most favorable pathway.[25]

When functional B3LYP was used, the 1,5-migration was found to be kinetically more favorable as $\mathbf{TS_{4b}}$ has higher energy than $\mathbf{TS_{3b}}$, which is in agreement with the experimental results (Table 3, conditions A-C). However, hybrid functionals M06 or wB97XD were less consistent with our system (Table 3, conditions D-G). On the other hand, both model solvents led to very similar trends, albeit IEF-PCM system gave slightly lower energy values. Finally, modification of the basis set did not lead to remarkable differences. As expected, higher energy values were observed when 6-311++G(d,p) (C, P, O, H) was used, albeit the computational trend was maintained in all the cases.

Table 3. Alternative reaction pathways for the evolution of **IIb** and energy values: 1,5-migration *vs*. single-cleavage rearrangement

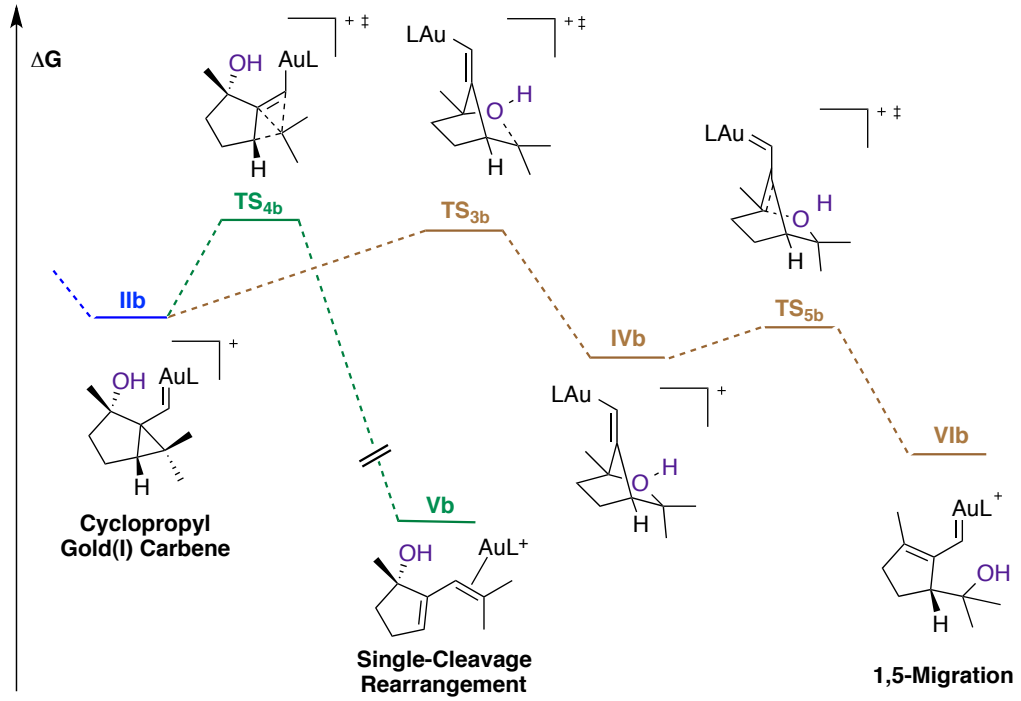

25 For an important mechanistic study on isomerization of 1,6-enynes catalyzed by $InCl_3$ that also leads to this type of products, see: Zhuo, L.-G.; Zhang, J.-J.; Yu, Z.-X. *J. Org. Chem.* **2012**, *77*, 8527–8540.

Conditions	A	B	C	D	E	F	G
Functional	**B3LYP**	**B3LYP**	**B3LYP**	**M06**	**M06**	**M06**	**wB97XD**
Basis set	**6-31G(d,p)**	**6-31G(d,p)**	**6-311++G(d,p)**	**6-31G(d,p)**	**6-31G(d,p)**	**6-311++G(d,p)**	**6-31G(d,p)**
Solvent	**IEF-PCM**	**SMD**	**IEF-PCM**	**IEF-PCM**	**SMD**	**IEF-PCM**	**IEF-PCM**
TS_{3b}	2.1	5.5	8.3	1.7	2.4	4.6	3.4
IVb	-6.6	-3.8	2.2	-7.4	-5.4	-0.8	-9.2
TS_{5b}	-6.6	-4.0	1.8	-6.5	-5.0	-1.4	-8.0
VIb	-15.7	-12.3	-10.1	-14.8	-13.5	-12.3	-15.6
TS_{4b}	6.7	9.2	15.0	-1.4	0.1	4.1	-1.3
Vb	-37.5	-35.5	-30.7	-38.1	-37.3	-36.2	-39.4

ΔG energies are given in kcal·mol^{-1}. The energy values are referred to gold(I) complex **Ib**.

Consistently with all these data, the subsequent studies were performed at the B3LYP/6-31G(d,p) (C, H, P, O), SDD(Au) level taking into account solvent effect of CH_2Cl_2 (IEF-PCM) and employing PMe_3 as the phosphine, unless otherwise stated.

In Scheme 10 the complete profile picture for the cyclization of 1,6-enyne **4b** is represented using the optimized parameters.

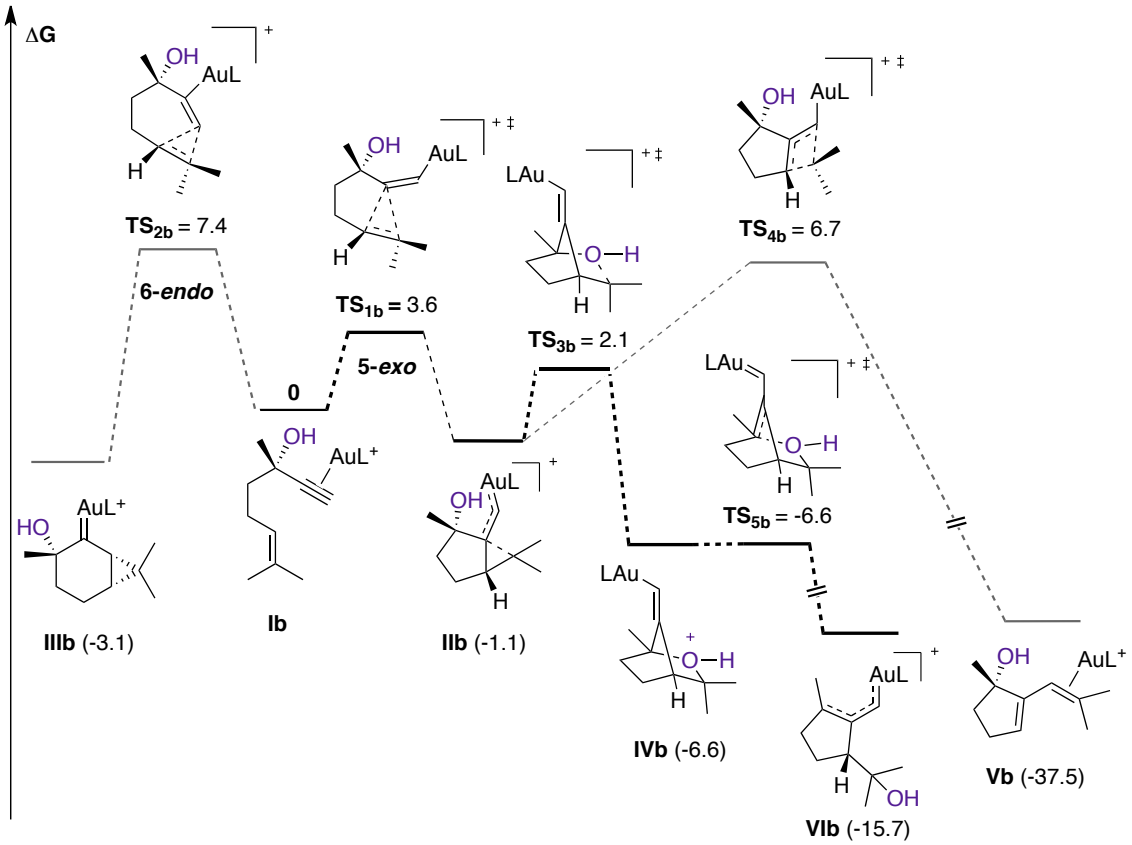

Scheme 10. Reaction pathways and energies calculated for the cyclization of **Ib** using the optimized parameters, ΔG energies are given in kcal·mol^{-1}

As illustrated in Figure 3, the calculated structure for minimum **VIb** shows very similar C–C bond distances of 1.41 and 1.39 Å. The Au–C bond distance is 2.04 Å, which might correspond to a single metal-carbon bond and is similar to that found in well-characterized heteroatom-stabilized gold(I) carbenes. Overall, the calculated structure fits better with a gold(I)-stabilized allylic cation.

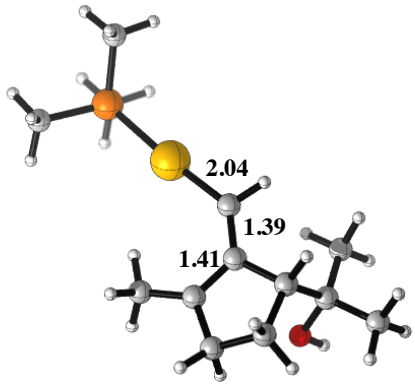

Figure 3. Computed structure for minimum **VIb** (Scheme 10) bond distances are in Å

Furthermore, we sought to evaluate the possible ligand effect for the computed trends of gold(I)-complex **Ib** (Table 4). The same reactivity trends are observed for gold(I) complexes bearing PMe_3, the bulkier PPh_3 phosphine or the model NHC ligand 1,3-dimethylimidazol-2-ylidene.

Table 4. Evaluation on the ligand effect for gold(I) complex **Ib**

Ligand	PMe_3	PPh_3	NHC
Ib	0.0	0.0	0.0
TS_{1b}	3.6	5.8	9.5
IIb	-1.1	-1.5	1.6
TS_{2b}	7.4	9.3	11.3
IIIb	-3.1	-2.5	0.1
TS_{3b}	2.1	4.4	7.9
IVb	-6.6	-4.3	-2.3
TS_{5b}	-6.6	-5.1	-0.7
VIb	-15.7	-13.9	-13.3
TS_{4b}	6.7	7.0	11.0
Vb	-37.5	-35.4	-33.1

ΔG energies are given in kcal·mol^{-1}.

The reaction profile for the gold(I) complex **Ic** was found to be very similar to the previous case (Scheme 11). Thus, after the formation of cyclopropyl gold(I) carbene

IIc, migration of the OR group takes place stepwise through cyclic intermediate **IVc**, although the cleavage occurs through a very low activation barrier (E_a = 0.1 kcal·mol^{-1}). Moreover, the difference between the activation energies of 1,5-migration and single-cleavage rearrangement process is roughly 6.2 kcal·mol^{-1}, favoring the formation of migration products.

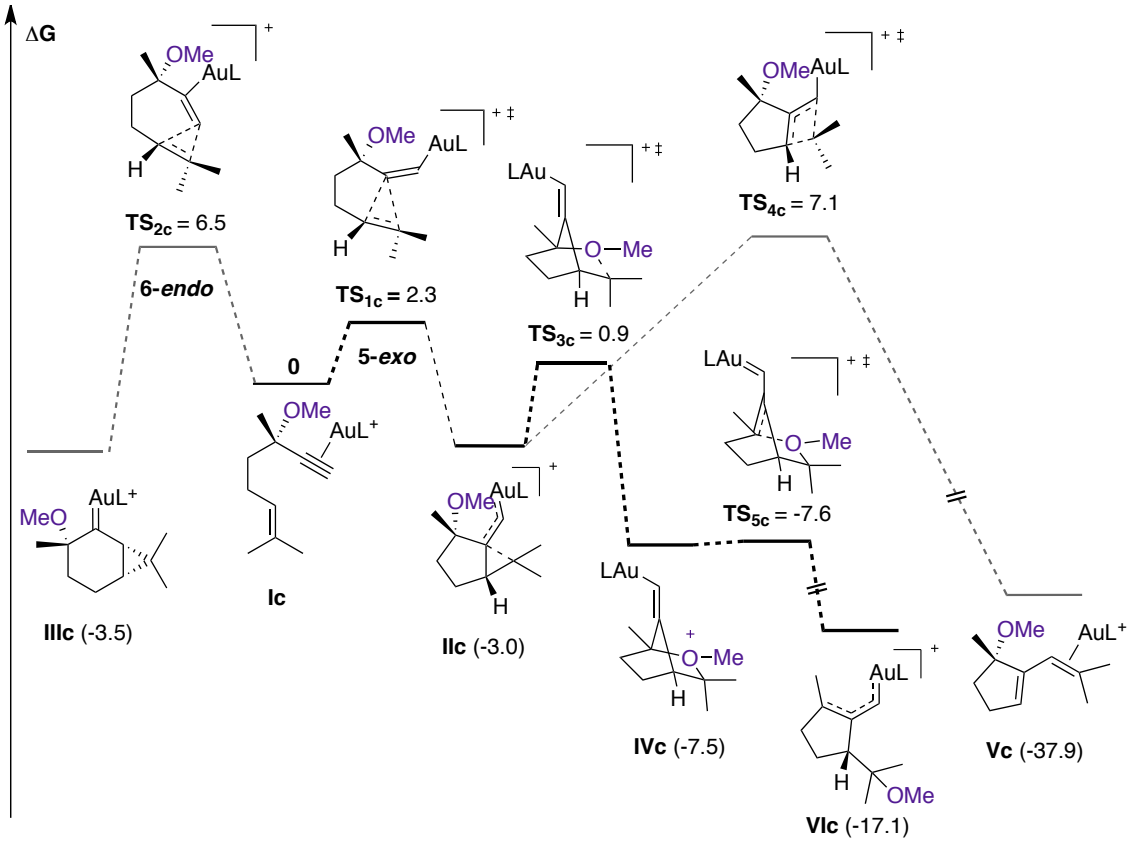

Scheme 11. Reaction pathways and energies for the cyclization of **Ic** calculated under optimized conditions, L = PMe_3, ΔG energies are given in kcal·mol^{-1}

Next, we examined computationally the evolution of enyne **Ia** coordinated with AuL^+ (L = PMe_3). Analogously to the previous examples, **Ia** reacted preferentially through a 5-*exo*-*dig* pathway to form **IIa** (Scheme 12). Remarkably, the subsequent alkoxy migration proceeds in a direct manner through **TS$_{3a}$** (E_a = 5 kcal·mol^{-1}) to afford allyl cation **VIa**, bypassing the formation of cyclic oxonium bridge intermediate. In addition, DFT calculations showed that the transformation of **IIa** to **Va** occurs with a high activation barrier (E_a = 12 kcal·mol^{-1}). Thus, this preferential migration of the alkoxy group is consistent with the high selectivity found experimentally.

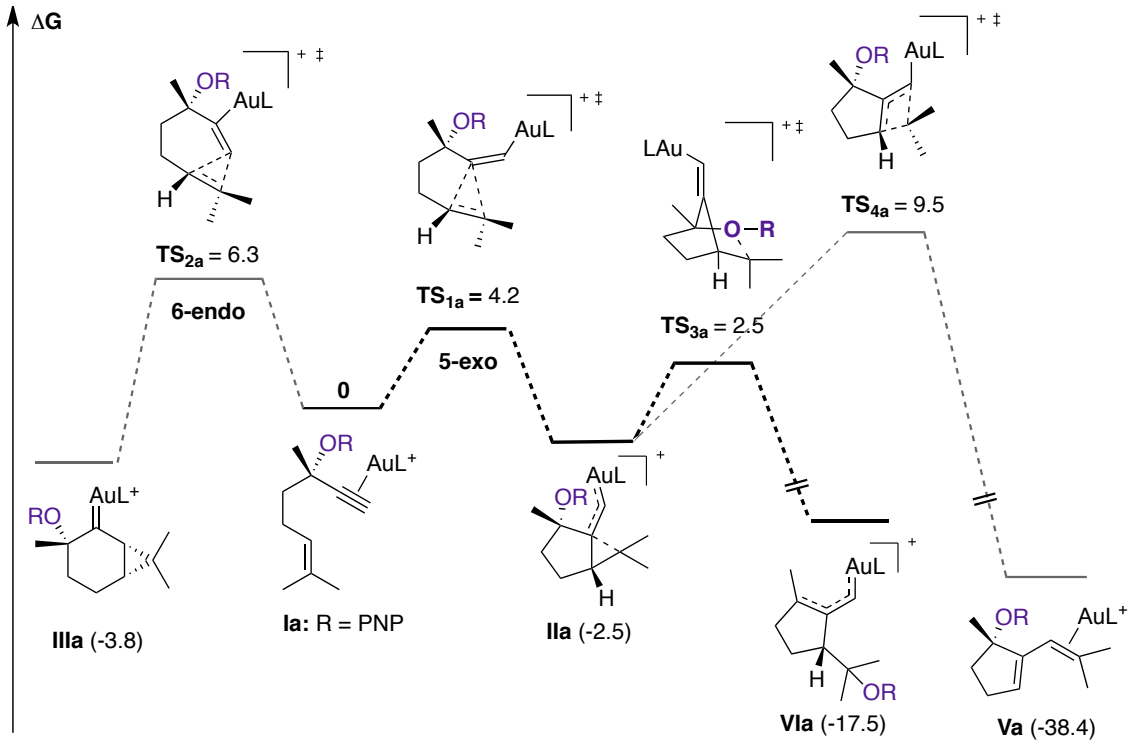

Scheme 12. Reaction pathways and energies for the cyclization of **Ia** calculated under optimized conditions, L = PMe_3, ΔG energies are given in kcal·mol^{-1}

Exception to the rule

As mentioned in the introduction of this chapter, the gold(I)-catalyzed cyclization of 1,6-enynes **20** led to the exclusive formation of six-membered ring dienes **21**, products of an apparent endocyclic skeletal rearrangement.[26,27] Previous investigations developed in our group indicate that the rearrangement of 1,6-enynes leading to this kind of products could be considered as a variant of the single cleavage mechanism in which the endocyclic cyclopropane bond undergoes cleavage to afford a ring expanded

26 Nieto-Oberhuber, C.; López, S.; Jiménez-Núñez, E.; Echavarren, A. M. *Chem.–Eur. J.* **2006**, *12*, 5916–5923.

27 (a) Soriano, E.; Ballesteros, P.; Marco-Contelles, J. *J. Org. Chem.* **2004**, *69*, 8018–8023. (b) Soriano, E.; Ballesteros, P.; Marco-Contelles, J. *Organometallics* **2005**, *24*, 3172–3181. (c) Soriano, E.; Ballesteros, P.; Marco-Contelles, J. *Organometallics* **2005**, *24*, 3182–3191. (d) Soriano, E. Marco-Contelles, J. *J. Org. Chem.* **2005**, *70*, 9345–9353.

product.[28] Moreover, several labeling experiments were found to be consistent with this mechanistic proposal.[29]

Despite of this precedents, DFT calculations for the reaction of gold(I) complex **Id** led to much less clear cut results (Schemes 13 and 14). The 5-*exo-dig* pathway leading to **IId** was again more favorable than the 6-*endo-dig* cyclization to form **IIId** (Scheme 13). However, the proposed opening of cyclopropyl gold(I)-carbene **IId** with cleavage of the endocyclic cyclopropane bond to form six-membered ring intermediate **IVd**, which upon metal elimination would afford corresponding diene **21** (via intermediate **VIId**), requires a high energy barrier (E_a = 14.7 kcal·mol^{-1}).

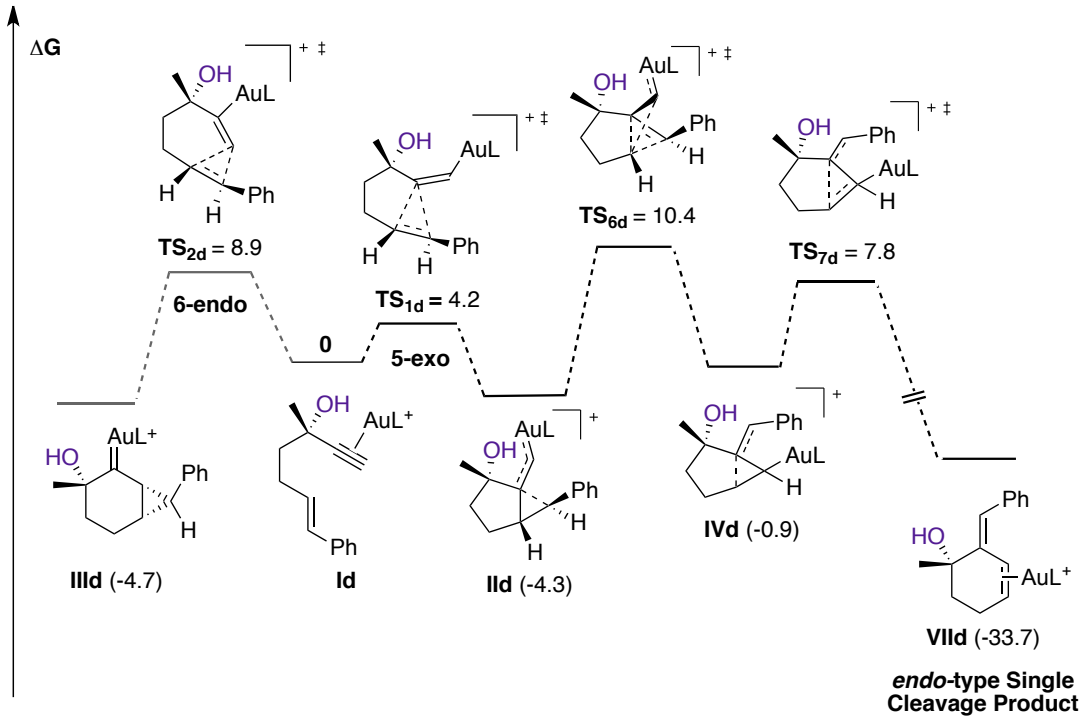

Scheme 13. Reaction pathways and energies calculated for the proposed *endo*-type single cleavage mechanism, ΔG energies are given in kcal·mol^{-1}.

Likewise, the *exo*-single cleavage rearrangement of intermediate **IId** through $\mathbf{TS_{4d}}$ also involves a high activation energy (Scheme 14). By contrast, the 1,5-migration of **IId** through oxonium bridge **IVd** to form **VId** was found to be the kinetically most

28 Cabello, N.; Jiménez-Núñez, E.; Buñuel, E.; Cárdenas, D. J.; Echavarren A. M. *Eur. J. Org. Chem.* **2007**, 4217–4223.

29 (a) Nieto-Oberhuber, C.; Muñoz, M. P.; López, S.; Jiménez-Núñez, E.; Nevado, C.; Herrero-Gómez, E.; Raducan, M.; Echavarren, A. M. *Chem.–Eur. J.* **2006**, *12*, 1677–1693. (b) Faller, J. W.; Fontaine, P. P. *J. Organomet. Chem.* **2006**, *691*, 1912–1918.

favorable pathway with a $\mathbf{TS_{3d}}$ = 3.0 kcal·mol^{-1}, although this was not observed experimentally.

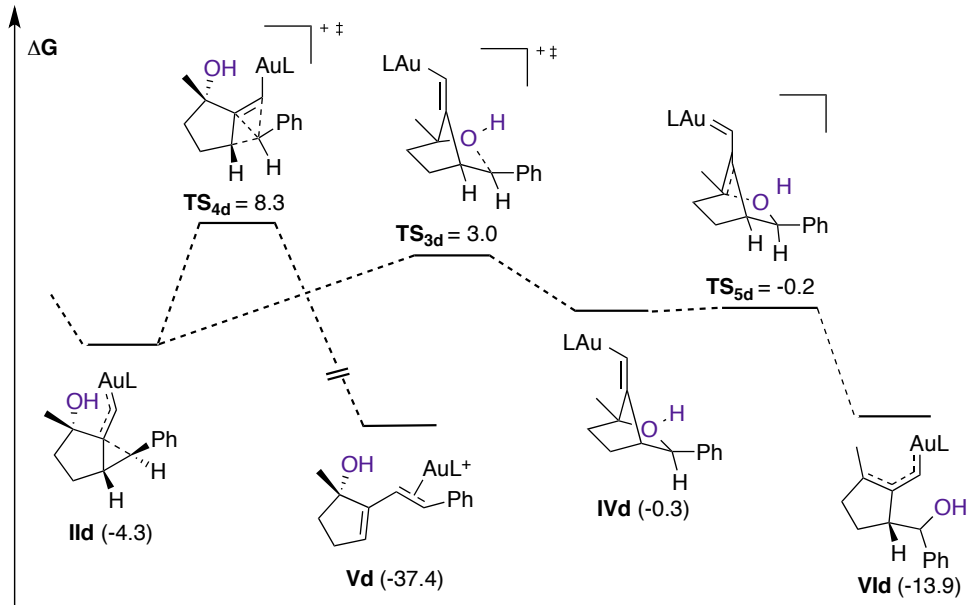

Scheme 14. Reaction pathways and energies for the cyclization of **Id**, L = PMe_3, ΔG energies are given in kcal·mol^{-1}

Therefore, additional mechanistic work would be still required to understand why in cases in which propargyl group does not migrate an *endo*-type single-cleavage rearrangement is the most favorable reaction pathway. The fact that products of 1,5-migration or single-cleavage rearrangement derived from complexes **Id** were not observed could be also attributed to the limitations of DFT calculations in complex mechanistic scenarios of this type.

Conclusions

According to our computational studies, upon activation of alkyne with gold(I), *α,β*-unsaturated gold(I)-carbenes are formed preferentially via an exocyclic rearrangement. However, these intermediates evolve differently depending on the substitution pattern of starting 1,6-enyne. Thus, whereas in the case of PNP-protected intermediate, the migration of the alkoxy moiety to the cationic center proceeds in a direct manner, the migration of alkoxy moiety in complexes **Ib** and **Ic** proceeds stepwise through bicyclic intermediates, which lead to the corresponding allyl gold cations. These results are in agreement with our experimental observations, in which among the various migrating groups, *p*-nitrophenyl ether was found to give the best results.

On the other hand, DFT calculations for the reaction of gold(I) complex **Id** led to less straightforward results. Although the 5-*exo-dig* pathway was again more favorable than the 6-*endo-dig* cyclization, the formation of 1,5-migration product was found to be the kinetically most favorable pathway, which is not consistent with the experimental results. Therefore, additional mechanistic work will be required to understand why in cases in which propargyl group does not migrate an *endo*-type single-cleavage rearrangement is the most favorable reaction pathway.

Experimental Part

DFT Calculations

Otherwise stated, calculations were performed with DFT using the B3LYP functional as implemented in Gaussian 09.[30] The 6-31G(d,p)[31] basis set was used for all atoms (C, H, O, P, N) except gold, which was treated with SDD and the associated effective core potential[32]. The solvent effect was taken into account using the polarizable continuum model in particular IEF-PCM as implemented in Gaussian 09.[33] The stationary points were characterized by vibrational analysis. Transition states were identified by the presence of one imaginary frequency while minima by a full set of real frequencies. The connectivity of the transition states was confirmed by relaxing each transition state towards both the reactant and the product. Reported energies ($kcal \cdot mol^{-1}$) are free energies (G) in solution, computed at 298 K and 1 atm.

---

30 Frisch, M. J.; Trucks, G. W.; Schlegel, H. B.; Scuseria, G. E.; Robb, M. A.; Cheeseman, J. R.; Scalmani, G.; Barone, V.; Mennucci, B.; Petersson, G. A.; Nakatsuji, H.; Caricato, M.; Li, X.; Hratchian, H. P.; Izmaylov, A. F.; Bloino, J.; Zheng, G.; Sonnenberg, J. L.; Hada, M.; Ehara, M.; Toyota, K.; Fukuda, R.; Hasegawa, J.; Ishida, M.; Nakajima, T.; Honda, Y.; Kitao, O.; Nakai, H.; Vreven, T.; Montgomery (Jr.), J. A.; Peralta, J. E.; Ogliaro, F.; Bearpark, M.; Heyd, J. J.; Brothers, E.; Kudin, K. N.; Staroverov, K. N.; Kobayashi, R.; Normand, J.; Raghavachari, K.; Rendell, A.; Burant, J. C.; Iyengar, S. S.; Tomasi, J.; Cossi, M.; Rega, N.; Millam, N. J.; Klene, M.; Knox, J. E.; Cross, J. B.; Bakken, V.; Adamo, C.; Jaramillo, J.; Gomperts, R.; Stratmann, R. E.; Yazyev, O.; Austin, A. J.; Cammi, R.; Pomelli, C.; Ochterski, J. W.; Martin, R. L.; Morokuma, K.; Zakrzewski, V. G.; Voth, G. A.; Salvador, P.; Dannenberg, J. J.; Dapprich, S.; Daniels, A. D.; Farkas, O.; Foresman, J. B.; Ortiz, J. V.; Cioslowski, J.; Fox, D. J.; Gaussian 09, revision 02; Gaussian, Inc.: Wallingford, CT, 2009.

31 Hehre, W. J.; Ditchfield, R.; Pople, J. A. *J. Chem. Phys.* **1972**, *56*, 2257–2261.

32 Andrae, D.; Haussermann, U.; Dolg, M.; Stoll, H.; Preuss, H. *Theor. Chim. Acta* **1990**, *77*, 123–141.

33 (a) Cances, E.; Mennucci, B.; Tomasi, J. *J. Chem. Phys.* **1997**, *107*, 3032–3041. (b) Cossi, M.; Barone, V.; Mennucci, B.; Tomasi, J. *Chem. Phys. Lett.* **1998**, *286*, 253–260. (c) Mennucci, B.; Tomasi, J. J. *Chem. Phys.* **1997**, *106*, 5151–5158. (d) Miertus, S.; Tomasi, J. *J. Chem. Phys*. **1982**, *65*, 239–245.

For the optimization studies, functionals M06 [34] and wB97XD, [35] basis set 6-311++G(d,p)[36] and SMD solvation model[37] were also tested.

34 Zhao, Y.; Truhlar, D. G. *Theor. Chem. Acc.* **2008***, 120*, 215–241.

35 Chai, J.-D.; Head-Gordon, M. *J. Chem. Phys.* **2009**, *131*, 174105–174113.

36 (a) Krishnan, R.; Binkley, J. S.; Seeger, R.; Pople, J. A. *J. Chem. Phys.* **1980**, *72*, 650–654. (b) Frisch, M. J.; Pople, J. A.; Binkley, J. S. *J. Chem. Phys.* **1984**, *80*, 3265–3269.

37 Marenich, A. V.; Cramer, C. J.; Truhlar, D. G. *J. Phys. Chem. B*, **2009**, *113*, 6378–6396.

Cartesian Coordinates (in Å)

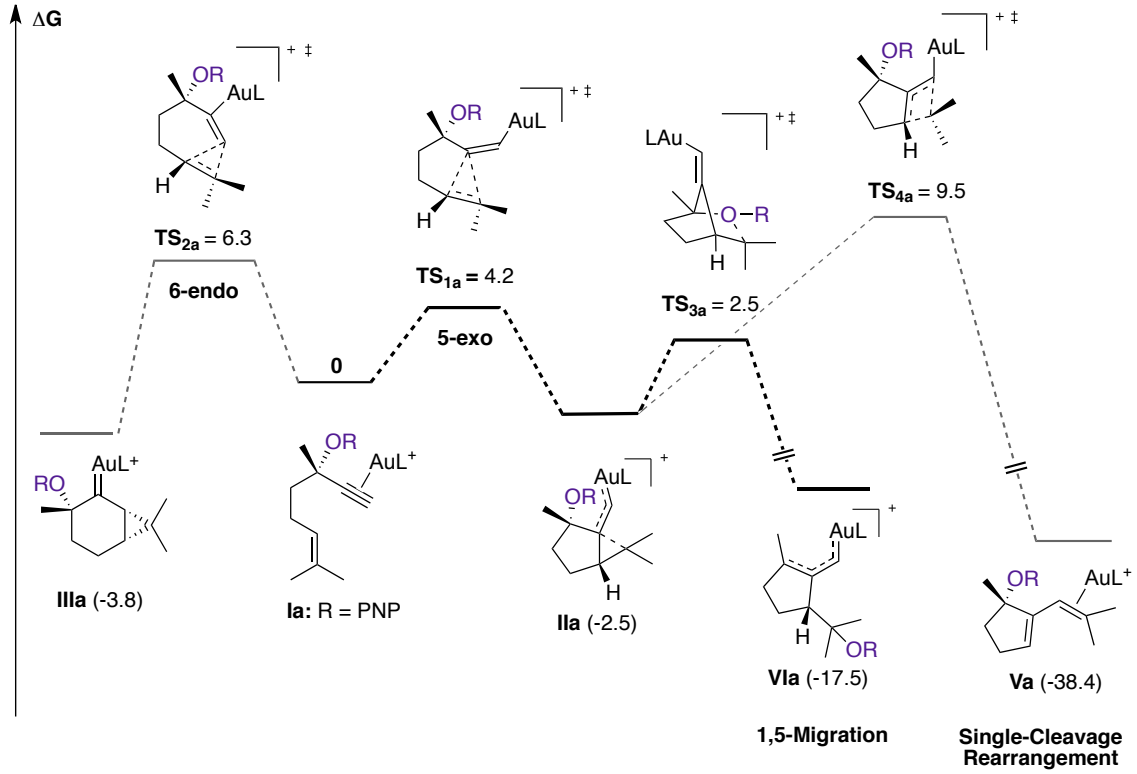

Scheme 15. Reaction pathways and energies for the cyclization of **Ia**, L= PMe_3, ΔG energies are given in kcal·mol^{-1}

Table T5: Optimized geometry for **Ia**

Free energy G = -1497.830742 Hartree/particle.

C	0.81486500	0.32324500	1.35721700
C	0.83460400	-0.97447100	2.18561000
H	1.33140400	-0.77102700	3.13711800
H	-0.19059700	-1.29422600	2.38791600
H	1.35548700	-1.78965500	1.68410800
O	2.13638900	0.89225800	1.21903900
C	0.02279200	1.40915600	2.12985100
H	-1.00394400	1.04769500	2.25732300
H	0.47648100	1.43501400	3.12562700
C	0.02364700	2.83625900	1.54414600
H	-0.22826200	3.50393900	2.38020300
H	1.04044800	3.10019500	1.24601400
C	-0.97013200	3.07716800	0.43747400
H	-1.99856900	2.81336400	0.69347300
C	-0.75929500	3.62099000	-0.77294200
C	0.58316800	4.06731600	-1.29747900
H	1.40904100	3.85482500	-0.61677500
H	0.80067800	3.57932800	-2.25638300
H	0.57869600	5.14692500	-1.49584700
C	-1.90621200	3.83708300	-1.73196400
H	-1.74294100	3.28919700	-2.66988700
H	-2.86185900	3.51547900	-1.30797100
H	-1.99496700	4.89618900	-2.00691900
C	0.26297700	0.08186600	-0.01130300
C	0.04115700	-0.10373300	-1.20708100
H	0.05529300	-0.19032600	-2.27575000
P	-4.19148500	-1.23404300	0.02207000
C	-4.65029900	-2.67561500	-1.01181600
H	-4.51462000	-2.42855500	-2.06705200
H	-4.01193700	-3.52576600	-0.76171400
H	-5.69629700	-2.93946700	-0.83172500
C	-4.55464600	-1.72060900	1.75140100
H	-3.90485700	-2.54735400	2.04615200
H	-4.37650800	-0.87308100	2.41703900
H	-5.59980600	-2.03275300	1.83276400
C	-5.40063900	0.07947500	-0.38928000
H	-5.23249700	0.94722500	0.25229300
H	-5.27660200	0.37999600	-1.43205200
H	-6.41771100	-0.29320000	-0.23707800
Au	-1.97559300	-0.58524300	-0.28935700

C	3.23260200	0.25450400	0.71443900	C	5.62757900	-0.77582300	-0.23441000
C	4.44292900	0.92725300	0.96628200	H	6.57815000	0.92378400	0.68420100
C	3.23423300	-0.93870800	-0.02497900	H	4.45936800	-2.37162000	-1.06831400
C	5.64047300	0.41742200	0.49458200	N	6.88317400	-1.32204500	-0.73313000
H	4.41622300	1.84830700	1.53747000	O	6.84625700	-2.37705400	-1.37322400
C	4.43842700	-1.45269600	-0.49652800	O	7.92281400	-0.70245200	-0.49116200
H	2.31957300	-1.46776000	-0.25069500				

Table 6: Optimized geometry for **TS_{1a}**

Free energy G = -1497.824114 Hartree/particle.

C	-1.13405200	-1.68214200	1.41242600	C	3.12450100	3.04612000	0.36218500
C	-0.31641100	-0.84361200	2.42016800	H	2.52343800	3.34965900	-0.49795100
H	-0.91754100	-0.73220200	3.32603300	H	2.49592900	3.06237500	1.25557600
H	0.61091500	-1.36214000	2.66909500	H	3.95433700	3.74719400	0.49007800
H	-0.07264700	0.14582700	2.03351000	C	4.84531000	1.00518600	1.54030900
O	-2.43688300	-1.09751000	1.17995300	H	4.24230800	0.99337600	2.45118600
C	-1.46292400	-3.06013300	2.02577800	H	5.32145200	0.02948400	1.41922800
H	-0.51594500	-3.55610000	2.2614730	H	5.61597800	1.77666100	1.62517800
H	-2.00034600	-2.89817900	2.96435500	C	4.90901200	1.48436600	-1.33586400
C	-2.29080500	-3.91276600	1.04844700	H	5.39739900	0.52258200	-1.50804200
H	-2.35764800	-4.93286000	1.44343300	H	4.34525300	1.75911700	-2.23031600
H	-3.30683300	-3.52043200	0.98969800	H	5.66795500	2.24653000	-1.13679100
C	-1.62314500	-3.93343300	-0.29558500	Au	2.08162600	-0.24299000	-0.21470200
H	-0.70139400	-4.51193100	-0.34609200	C	-2.67838300	0.17403500	0.75158900
C	-2.08576600	-3.40600000	-1.46473500	C	-4.00130400	0.60440800	0.96649700
C	-3.38669200	-2.66912900	-1.62470800	C	-1.76050700	1.02308400	0.11286700
H	-3.92167200	-2.51766100	-0.68847300	C	-4.40482600	1.86492900	0.56006600
H	-3.21420700	-1.68949800	-2.08524600	H	-4.69255000	-0.06955400	1.45981400
H	-4.03676600	-3.22417400	-2.31231400	C	-2.16500600	2.29154100	-0.29215400
C	-1.29535300	-3.58184700	-2.73122500	H	-0.74498500	0.71156700	-0.08541700
H	-1.05457200	-2.60904800	-3.17919300	C	-3.47685000	2.70344000	-0.06544500
H	-0.37069100	-4.14206500	-2.57327900	H	-5.41798700	2.20896900	0.72376600
H	-1.89405800	-4.12063200	-3.47602600	H	-1.47174700	2.96021300	-0.78656800
C	-0.36112300	-1.87763200	0.15787000	N	-3.88957000	4.03433700	-0.49067400
C	0.61414300	-1.71938800	-0.63915400	O	-3.04993700	4.75960900	-1.03261200
H	0.83682900	-2.24522000	-1.56088300	O	-5.05915100	4.37256300	-0.28793000
P	3.76848100	1.34870000	0.09460200				

Table 7: Optimized geometry for **IIa**

Free energy G = -1497.834746 Hartree/particle.

C	-0.46037500	4.32710200	-1.20903900	C	-0.34803600	1.10040500	-2.17821100
C	0.78028600	3.94621900	-0.40061000	H	0.32996100	0.26101500	-2.00588300
C	-0.58671200	1.87727500	-0.87495200	H	-1.28422700	0.71965200	-2.59067000
C	-1.44750200	3.14992400	-1.10367800	H	0.10491600	1.76296000	-2.92114400
H	-0.89591900	5.26914900	-0.86440300	C	0.77653500	2.36945400	-0.33659700
H	-0.14834800	4.47584400	-2.24627800	C	1.84001000	1.59250000	-0.00121200
H	-2.05096700	3.07359600	-2.01031500	H	2.71286700	2.14423500	0.34651700
H	-2.13802300	3.28594100	-0.26971800	P	2.48689300	-2.77859900	-0.04014800

C	1.67814600	-3.68000800	-1.42268100
H	1.90520100	-4.74860100	-1.36728600
H	0.59614000	-3.53762300	-1.36845300
H	2.03611100	-3.28360400	-2.37600800
C	4.26699400	-3.21238300	-0.18286000
H	4.66891000	-2.80080200	-1.11191300
H	4.81654500	-2.78061100	0.65706000
H	4.39838300	-4.29825600	-0.18140400
C	1.91663800	-3.64762200	1.47546700
H	2.41493700	-3.22266800	2.35014900
H	0.83792200	-3.51553700	1.58813600
H	2.14530400	-4.71539600	1.41101900
Au	2.08536300	-0.44578000	-0.03307400
O	-1.12114900	1.00532700	0.16100300
C	0.72986600	3.84710600	1.04630900
C	1.98145400	4.07994700	1.82860500
H	1.86461600	5.09672700	2.23561900
H	2.07550100	3.40838500	2.68502200
H	2.88986600	4.07372400	1.22705800
C	-0.53591400	3.78083000	1.85166800
H	-1.11168600	2.87583800	1.65497200
H	-0.30832500	3.81244500	2.91787200
H	-1.16987600	4.64007500	1.60003400
H	1.71646500	4.35480000	-0.77630200
C	-2.30512600	0.34247200	0.08530900
C	-3.31770200	0.55609800	-0.86607200
C	-2.49604800	-0.61517600	1.10232400
C	-4.49264800	-0.18584100	-0.80296200
H	-3.21159400	1.29291700	-1.64904100
C	-3.66604000	-1.35149300	1.16669600
H	-1.70806300	-0.76083600	1.83303500
C	-4.65947700	-1.13243700	0.20637700
H	-5.28100400	-0.03191600	-1.52873800
H	-3.82096000	-2.09026100	1.94261300
N	-5.89131200	-1.90503200	0.26385100
O	-6.75261200	-1.69552500	-0.59606400
O	-6.01607400	-2.73437100	1.17047200

Table 8: Optimized geometry for **TS_{3a}**

Free energy G = -1497.826759 Hartree/particle.

C	-1.34208800	-4.19587700	0.57980000
C	-1.27804700	-3.30555100	-0.67344700
C	-0.98706800	-1.80110100	1.15371200
C	-1.27114300	-3.19517500	1.76799800
H	-2.21832100	-4.84594200	0.61498700
H	-0.46414000	-4.84571600	0.57692000
H	-0.45864900	-3.45771500	2.44928700
H	-2.19275000	-3.15719200	2.35415000
C	-0.26995900	-0.86918800	2.11463500
H	-0.07863900	0.11878700	1.69604400
H	-0.86359500	-0.75828800	3.02700600
H	0.69230400	-1.31144700	2.38143700
C	-0.36535000	-2.12852800	-0.19789000
C	0.72937400	-1.67791500	-0.82046400
H	0.91933400	-2.15466700	-1.78637400
P	3.83706000	1.31234600	0.17695500
C	5.06584700	1.51280000	-1.17646400
H	5.81815800	2.25902400	-0.90510100
H	5.55812300	0.55620900	-1.36800000
H	4.55494700	1.83095600	-2.08856300
C	3.21676300	3.01673700	0.48194900
H	2.66828900	3.36876300	-0.39517700
H	2.53868500	3.01089600	1.33890100
H	4.04848800	3.69782000	0.68468400
C	4.85223600	0.92660300	1.66144700
H	4.20787500	0.88171100	2.54289700
H	5.33487200	-0.04517800	1.53194300
H	5.61827100	1.69274500	1.81313600
Au	2.14688200	-0.27506000	-0.29849500
O	-2.36702100	-1.30556800	0.83939600
C	-2.56515400	-2.74757600	-1.15422100
C	-2.54915200	-1.82067800	-2.30312500
H	-3.22584600	-2.20094900	-3.07910200
H	-2.98615900	-0.86142300	-1.98912200
H	-1.55343400	-1.64473800	-2.70655400
C	-3.88376000	-3.23062700	-0.69633000
H	-3.90971900	-3.49409600	0.35952000
H	-4.68833300	-2.53691100	-0.94657600
H	-4.06467400	-4.15915300	-1.26610300
H	-0.81415000	-3.78117100	-1.54793900
C	-2.66859900	0.00532000	0.58196100
C	-1.81938400	0.90326000	-0.08652700
C	-3.95772600	0.40521500	0.97435400
C	-2.25578700	2.20072400	-0.33575900
H	-0.83551600	0.59362200	-0.41399400
C	-4.39567000	1.69626200	0.71806900
H	-4.59415700	-0.30753800	1.48635700
C	-3.53413000	2.58333000	0.06854400
H	-1.61923100	2.91178400	-0.84682800
H	-5.38201400	2.02481400	1.01917200
N	-3.98641000	3.94727200	-0.19892900
O	-3.20346500	4.71883600	-0.75821900
O	-5.12850900	4.25678200	0.14792300

Table 9: Optimized geometry for **VIa**

Free energy G = -1497.824083 Hartree/particle.

C	1.29637200	3.54189000	0.59010000	H	-5.23701200	-3.81623800	0.22102100
C	0.90781100	2.59181700	-0.57407100	Au	-2.84996300	-0.03044300	-0.25038100
C	-0.20152800	1.85658900	1.43673600	O	2.58773500	1.05553500	0.11940500
C	0.86748200	2.79881200	1.86816200	C	2.08722900	1.71497600	-1.09728500
H	2.35455200	3.80169400	0.60703000	C	1.62598800	0.66168900	-2.10966000
H	0.72922100	4.47311000	0.50155500	H	1.16869800	1.14566300	-2.97782200
H	0.54009200	3.44101400	2.69330200	H	2.47812900	0.07890400	-2.46914600
H	1.68594500	2.18002900	2.26820400	H	0.90342800	-0.03398600	-1.67468100
C	-1.05369900	1.18307900	2.43790900	C	3.17148700	2.59310100	-1.73393800
H	-1.67140800	0.38817200	2.02000000	H	3.56703600	3.33506300	-1.03735500
H	-0.42564900	0.79262700	3.24722600	H	4.00462400	1.98237200	-2.09149800
H	-1.70758200	1.93410100	2.90304400	H	2.75481400	3.12164100	-2.59623100
C	-0.24379600	1.77171100	0.03214300	H	0.54893100	3.15872000	-1.43873800
C	-1.24690800	1.14594900	-0.69917300	C	3.68514400	0.23497200	0.08047000
H	-1.15707500	1.35348900	-1.77007700	C	4.96070000	0.76357300	0.33163300
P	-4.73226900	-1.42753600	0.12027000	C	3.52020500	-1.14696700	-0.10029400
C	-5.54099100	-1.18145700	1.75137300	C	6.06701000	-0.07621400	0.38294200
H	-6.40530800	-1.84400000	1.85294100	H	5.07137000	1.82881800	0.49814000
H	-4.82585100	-1.39575600	2.54925700	C	4.62131100	-1.99394300	-0.05054800
H	-5.86932600	-0.14344000	1.84429200	H	2.52676300	-1.54759700	-0.26597200
C	-6.07540600	-1.19896600	-1.11220400	C	5.88295100	-1.44584400	0.18605000
H	-6.41665400	-0.16112200	-1.09549300	H	7.05911800	0.31105100	0.57639000
H	-5.69626000	-1.42650200	-2.11136800	H	4.51609800	-3.06263700	-0.18667700
H	-6.91680100	-1.86003900	-0.88494600	N	7.04376000	-2.33328800	0.24055700
C	-4.33487200	-3.22027700	0.05616300	O	8.14953200	-1.83034300	0.45391400
H	-3.91274200	-3.46564000	-0.92130700	O	6.85982400	-3.54095800	0.06984300
H	-3.59805400	-3.45928600	0.82671900				

Table 10: Optimized geometry for **TS_{2a}**

Free energy G = -1497.820742 Hartree/particle.

C	1.67317000	0.99020200	-1.58233700	H	3.56054200	1.37746600	3.15722300
C	0.85920300	0.57980700	-2.81038400	H	5.01599900	2.25422700	2.71282100
H	0.91485500	1.36196800	-3.57249600	H	3.53587800	2.48634600	1.76992000
H	1.26748500	-0.34379400	-3.23017500	C	5.17948200	-0.56610800	2.16766900
H	-0.18849300	0.40182300	-2.55734100	H	4.46598700	-0.98647800	2.88981000
O	1.18943100	2.24097900	-1.01121500	H	5.50959800	-1.35983700	1.49328700
C	3.12512400	1.29862300	-1.98328300	H	6.04239300	-0.23312800	2.75717700
H	3.52761600	0.42457200	-2.50645900	C	1.64287100	-0.09279400	-0.51127100
H	3.07976800	2.11651700	-2.70883500	C	2.43071300	-0.53678000	0.37487200
C	4.05840100	1.70673800	-0.83071500	H	2.70424200	-1.21779700	1.15666300
H	4.97586500	2.10929100	-1.28018600	P	-1.90048700	-2.79380400	0.11819700
H	3.60262300	2.52649000	-0.27190300	C	-2.08005700	-4.02235500	-1.23238700
C	4.46405600	0.57146100	0.07311500	H	-2.18156000	-3.50334600	-2.18832300
H	4.89921500	-0.28851300	-0.43757400	H	-1.19247700	-4.65802600	-1.26917400
C	4.57641100	0.59956500	1.43272300	H	-2.96430000	-4.64296600	-1.06060200
C	4.13525500	1.74566500	2.29974400	C	-1.88091800	-3.78002300	1.66595800

H	-0.99533300	-4.41957000	1.68108000	C	-1.66252000	2.40636700	1.28704300
H	-1.84753000	-3.10919400	2.52734800	H	0.42254300	1.89240700	1.46965500
H	-2.77869300	-4.40236600	1.72506600	C	-2.39816700	3.01940900	-0.95883300
C	-3.48873500	-1.87708300	0.14817300	H	-0.87584300	2.97398600	-2.48047500
H	-3.49129500	-1.17332600	0.98366100	C	-2.65801100	2.81239800	0.39686900
H	-3.60770200	-1.31941100	-0.78352300	H	-1.89755600	2.27782000	2.33589100
H	-4.32272200	-2.57586500	0.25961700	H	-3.19231000	3.35384200	-1.61392100
Au	-0.03066800	-1.41670300	-0.13957200	N	-4.01261300	3.03979200	0.90240600
C	-0.10299700	2.36896200	-0.56260900	O	-4.87065900	3.42827200	0.10706800
C	-0.37799300	2.18670900	0.80109800	O	-4.22806000	2.82685800	2.09787300
C	-1.11130700	2.79857700	-1.43738900				

Table 11: Optimized geometry for **IIIa**

Free energy G = -1497.836875 Hartree/particle.

P	3.76020900	-1.96230900	0.21154800	H	-0.43899700	-1.29526800	-1.13472500
C	5.23327900	-1.80982200	-0.87766300	H	-1.68692400	-0.64595000	-2.22528100
H	5.94648500	-2.61167500	-0.66574700	H	0.02750600	-0.39793000	-2.58901900
H	4.92412800	-1.86807800	-1.92397900	O	-1.56820400	0.74961700	0.19188000
H	5.71426800	-0.84342100	-0.70823700	C	0.19008800	3.80509400	0.96768100
C	4.44742300	-1.97656500	1.91589200	C	1.27960500	4.62598300	1.58694800
H	4.90472100	-1.00804000	2.13247300	H	0.80330700	5.54340300	1.96017700
H	3.64218600	-2.15188200	2.63334100	H	1.72681000	4.12616100	2.45020900
H	5.20084700	-2.76286700	2.01792800	H	2.05507100	4.91538900	0.87644400
C	3.15498200	-3.67550300	-0.06327300	C	-0.87152000	3.31755700	1.89872100
H	2.32532400	-3.88344900	0.61680300	H	-0.44582800	3.02290600	2.86059800
H	2.79812300	-3.77586900	-1.09127100	H	-1.53498100	4.17495800	2.08710300
H	3.95697100	-4.39818300	0.11295100	H	-1.46197000	2.50191000	1.49007900
Au	2.11745200	-0.29683700	-0.14938400	C	-2.76227500	0.06848300	0.14343100
C	1.03670900	2.47044900	-0.14283000	C	-2.83352100	-1.18696400	0.76359200
C	-0.70576300	0.85808800	-0.99834000	C	-3.91214700	0.64928000	-0.41205300
C	0.11667700	3.70826800	-0.47528700	C	-4.04203500	-1.87045400	0.81937700
H	2.06710100	2.69713300	0.10121900	H	-1.93659300	-1.61064000	1.20173500
C	-1.15133700	2.02050400	-1.90745200	C	-5.12402300	-0.03156600	-0.36516000
C	-1.20041800	3.36355400	-1.17770500	H	-3.86294000	1.63468100	-0.85948600
H	0.72073500	4.45438000	-0.99462800	C	-5.17242600	-1.28386600	0.24793200
H	-2.12703400	1.79347700	-2.34766300	H	-4.11964500	-2.84069800	1.29288100
H	-0.44250800	2.07338900	-2.74192300	H	-6.02518800	0.39686300	-0.78467700
H	-2.02368000	3.36244400	-0.45986500	N	-6.44772600	-1.99872200	0.30214400
H	-1.41462600	4.16067700	-1.89502500	O	-7.43320700	-1.46670600	-0.21396000
C	0.68150100	1.17398600	-0.41157800	O	-6.47269700	-3.09767200	0.86086600
C	-0.70605800	-0.45482000	-1.78049600				

Table 12: Optimized geometry for **TS_{4a}**

Free energy G = -1497.815575 Hartree/particle.

C	0.04359900	4.56657000	0.07417100	H	0.05861700	5.08416600	1.03777400
C	1.31364100	3.78262000	-0.17055700	H	-0.04187800	5.33893600	-0.69692300
C	-0.49870900	2.28707400	-0.74289400	H	-1.95255600	3.93893900	-0.57515100
C	-1.10161400	3.53020700	-0.02842900	H	-1.45568600	3.23632500	0.96187100

C	-0.69355100	2.28621400	-2.27621200
H	-0.14884800	1.45336200	-2.72803400
H	-1.75175800	2.18381600	-2.52290100
H	-0.33543800	3.22272700	-2.71185400
C	1.01946100	2.45469600	-0.60385100
C	2.04927700	1.49409400	-0.29881200
H	3.01046100	1.76563900	-0.73778400
P	1.85775500	-2.93797900	-0.06716100
C	0.60533200	-3.72866800	-1.15674900
H	0.66317000	-4.81799200	-1.07711200
H	-0.39521000	-3.39751600	-0.86817500
H	0.78441300	-3.43293200	-2.19333400
C	3.45128000	-3.70106400	-0.57411600
H	3.68998100	-3.40380200	-1.59820000
H	4.24920600	-3.35194600	0.08566000
H	3.38698100	-4.79167700	-0.51946300
C	1.52651900	-3.63981700	1.59988100
H	2.28549100	-3.28692000	2.30249400
H	0.54600900	-3.30807900	1.94957400
H	1.54655700	-4.73310500	1.56584600
Au	1.87257100	-0.58505000	-0.15803800
O	-0.88025600	1.03259000	-0.17334800
C	1.89784500	2.57388500	0.92956400
C	3.29293800	3.07625800	1.35101800
H	3.18760500	3.93179400	2.02426000
H	3.79155000	2.26434900	1.88849800
H	3.91474800	3.36513800	0.50377600
C	1.03668100	2.21778500	2.13329300
H	0.11777600	1.69777300	1.86969400
H	1.61771300	1.55498900	2.78159700
H	0.79265900	3.11463000	2.71171100
H	2.20790300	4.31148500	-0.47897500
C	-2.16118600	0.57360900	-0.09987800
C	-3.31338200	1.26590800	-0.50428500
C	-2.27557300	-0.71400700	0.45837200
C	-4.56129200	0.66671500	-0.36077900
H	-3.26111400	2.26104600	-0.92115700
C	-3.51683400	-1.30916900	0.60236100
H	-1.37217400	-1.22248500	0.77535000
C	-4.65501000	-0.61103400	0.18629800
H	-5.46006200	1.18558600	-0.66861200
H	-3.61833300	-2.29819500	1.03030700
N	-5.96550500	-1.23054000	0.33223500
O	-6.95596000	-0.59290700	-0.03656700
O	-6.02068800	-2.36404500	0.81812200

Table 13: Optimized geometry for **Va**

Free energy G = -1497.891967 Hartree/particle.

C	0.41774600	3.85225100	1.95908100
C	-0.54994100	2.49339700	0.15273000
C	-0.85789400	3.07889400	1.55531800
H	0.63865200	3.77769200	3.02947400
H	0.32917100	4.92497800	1.73774000
H	-1.74504900	3.71590500	1.56488200
H	-1.02404500	2.24964100	2.24908600
C	-1.08434500	3.34960300	-1.00381500
H	-0.74393800	2.96707200	-1.97015700
H	-2.17628400	3.37608100	-1.01527200
H	-0.72296200	4.37571300	-0.89414500
C	0.98549800	2.44132100	0.13765700
P	1.50147600	-2.66538300	0.68277900
C	0.13808000	-2.77400000	1.90433900
H	0.05953600	-3.79656200	2.28468200
H	0.33750700	-2.09233600	2.73416400
H	-0.80440900	-2.48930500	1.43162900
C	1.12577800	-3.92920500	-0.59059400
H	0.19715700	-3.66789400	-1.10240000
H	1.93559100	-3.96542500	-1.32284300
H	1.01557200	-4.91066700	-0.12062500
C	2.99282700	-3.27420400	1.55911400
H	3.84037400	-3.29215400	0.87050900
H	3.22610500	-2.60411200	2.38959800
H	2.81566700	-4.28274900	1.94389700
Au	1.79117200	-0.52568400	-0.18690700
O	-0.98376400	1.10753500	-0.01332900
C	1.48739800	3.22969900	1.10746200
H	2.53586400	3.45792400	1.25197000
C	3.01363200	1.37952500	-1.08050600
C	4.08363000	1.70975300	-0.06928700
H	4.45084600	2.72809800	-0.25619200
H	3.72941800	1.66709100	0.96177700
H	4.93602500	1.03430800	-0.17761100
C	3.52637200	0.93976900	-2.43340000
H	2.71868600	0.68996600	-3.12485000
H	4.10764200	1.76362000	-2.86847100
H	4.20352100	0.08492800	-2.34716900
C	1.66742600	1.69315900	-0.92998000
H	1.05287600	1.52765300	-1.81415000
C	-2.27688500	0.70391700	-0.07769300

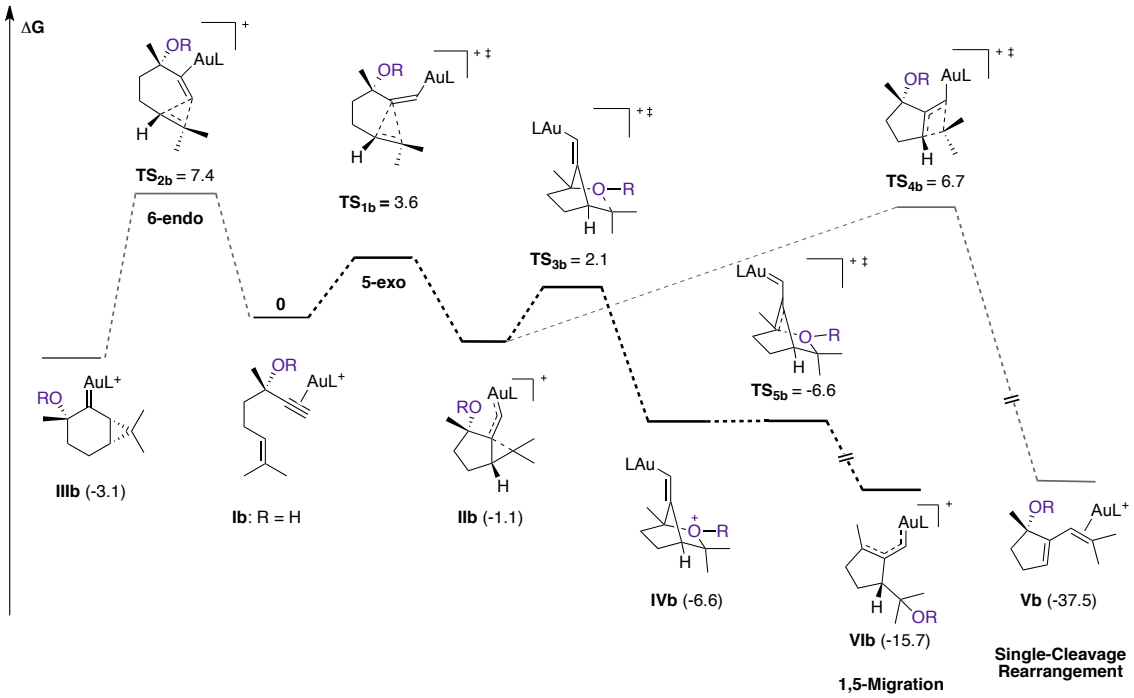

Scheme 16. Reaction pathways and energies for the cyclization of **Ib**, L=PMe_3, ΔG energies are given in kcal·mol^{-1}

Table 14: Optimized geometry for **Ib**

Free energy G = -1062.362318 Hartree/particle.

C	-2.46743700	-1.44743000	0.43923900	H	-0.11965600	3.29749000	-1.41792700
C	-2.93760200	-2.91325900	0.36541100	H	-1.68297100	3.15235100	-2.24796000
H	-3.55757000	-3.12630500	1.24020300	H	-1.34526300	4.53592300	-1.19037500
H	-3.52622900	-3.09315400	-0.53765700	C	-1.58819100	-1.20260300	-0.75257900
H	-2.08277000	-3.59687000	0.36015500	C	-1.02358900	-1.14282100	-1.84493600
O	-1.75056100	-1.20874000	1.64811800	H	-0.73366400	-1.13381700	-2.87673000
H	-1.16378300	-1.96161900	1.81026300	P	2.69374800	0.13592800	0.43357900
C	-3.68691000	-0.49538000	0.43275400	C	3.33352800	1.66487300	-0.34805100
H	-4.17956700	-0.57563700	-0.54279600	H	3.44725000	1.50595400	-1.42262700
H	-4.38227300	-0.90574400	1.17299200	H	2.62693600	2.48149700	-0.18392700
C	-3.42293900	0.98065500	0.78272000	H	4.30268400	1.92755600	0.08552700
H	-4.41267900	1.42888700	0.95525800	C	2.62909900	0.48413700	2.23220700
H	-2.89829300	1.03162300	1.73935200	H	1.89670800	1.27077400	2.42621900
C	-2.71679100	1.77889300	-0.28221100	H	2.33023400	-0.41833800	2.77009100
H	-3.08819200	1.61434300	-1.29534100	H	3.61317900	0.80722100	2.58378600
C	-1.74777600	2.69718600	-0.12531900	C	4.00925100	-1.12118100	0.21599000
C	-1.13728900	3.08772600	1.19868400	H	3.72230000	-2.04301600	0.72683800
H	-1.49430900	2.48556200	2.03589500	H	4.14331800	-1.33226800	-0.84736300
H	-0.04338600	3.00245100	1.15951600	H	4.94957000	-0.75060500	0.63402000
H	-1.35460200	4.13967100	1.42607900	Au	0.63775800	-0.51979000	-0.43361600
C	-1.20195000	3.45428300	-1.31332200				

Table 15: Optimized geometry for **TS_{1b}**

Free energy G = -1062.356538 Hartree/particle.

C	2.23881400	1.56564300	0.12289200
C	1.03408000	2.51920700	-0.04658500
H	1.36509900	3.52525000	0.22399600
H	0.67120300	2.52426400	-1.07672600
H	0.21165200	2.22720200	0.61222000
O	2.72969700	1.61193200	1.46126300
H	2.02031000	1.33413400	2.05888600
C	3.40205700	2.00541000	-0.77906200
H	3.04196100	2.05236800	-1.81189000
H	3.71007500	3.01273700	-0.48396200
C	4.56404500	1.00534300	-0.65891700
H	5.30805100	1.21945400	-1.43457800
H	5.05622000	1.12618200	0.30694000
C	4.03897500	-0.38965000	-0.83888300
H	3.74764500	-0.65306800	-1.85513300
C	4.03047800	-1.39284300	0.08861600
C	4.50998800	-1.24986100	1.50711500
H	4.58750200	-0.21356800	1.83195300
H	3.83641600	-1.77790400	2.19048500
H	5.49301500	-1.72821100	1.60754900
C	3.57410000	-2.76917100	-0.29992800
H	2.73684700	-3.09571500	0.33061300
H	3.27978800	-2.83401900	-1.34986300
H	4.38218700	-3.49078500	-0.12601900
C	1.81084300	0.17649100	-0.22874100
C	0.92908600	-0.72922000	-0.40440700
H	1.09694900	-1.76739700	-0.67071400
P	-3.42372300	0.03589000	0.13418300
C	-3.84502800	1.38570500	1.30527500
H	-3.42532300	1.16123100	2.28858000
H	-3.42014700	2.32643500	0.94744400
H	-4.93080300	1.48822000	1.38985400
C	-4.28361700	0.47280300	-1.42803900
H	-3.86411300	1.39865600	-1.82847900
H	-4.13882500	-0.32438300	-2.16093100
H	-5.35363300	0.60801600	-1.24580200
C	-4.30481800	-1.44307200	0.76987800
H	-4.16181200	-2.27795400	0.08008500
H	-3.89846300	-1.71958100	1.74557400
H	-5.37367000	-1.23248000	0.86814000
Au	-1.12220100	-0.29447600	-0.13666300

Table 16: Optimized geometry for **IIb**

Free energy G = -1062.364012 Hartree/particle.

C	4.38564000	0.90734000	-0.79509400
C	3.57473900	-0.38766800	-0.87174900
C	2.15960500	1.42299200	0.16689800
C	3.65994200	1.82616800	0.20348400
H	5.42577800	0.71536300	-0.51551200
H	4.39619600	1.35115700	-1.79454400
H	3.79481600	2.88053200	-0.05110100
H	4.04336200	1.69319800	1.21633500
C	1.37040400	2.37904000	-0.74239300
H	0.33133900	2.05399900	-0.83979400
H	1.38745900	3.38636600	-0.31108100
H	1.81599500	2.43318000	-1.74063100
C	2.11072000	-0.00319200	-0.42001900
C	0.99199100	-0.74668200	-0.63966400
H	1.17101200	-1.72949200	-1.07414400
P	-3.25844700	0.10804200	0.21023300
C	-3.74565700	1.86982500	0.01419200
H	-4.81026800	2.00102500	0.22859500
H	-3.16006500	2.48828400	0.69890800
H	-3.54157000	2.19271900	-1.00960900
C	-4.41798600	-0.81617000	-0.87596800
H	-4.23111400	-0.55198700	-1.91968300
H	-4.25563400	-1.88968400	-0.75308300
H	-5.45420400	-0.57538300	-0.62145100
C	-3.77810700	-0.33002600	1.91771300
H	-3.60355500	-1.39486700	2.08987200
H	-3.18699600	0.24166500	2.63703400
H	-4.83945800	-0.10906900	2.06329000
Au	-0.97206000	-0.31042700	-0.23740500
O	1.57599800	1.39116800	1.47660200
H	1.56086100	2.29826700	1.81487800
C	3.46232400	-1.28005400	0.26664200
C	3.21950500	-2.73707300	0.01538700
H	4.19998200	-3.21427300	0.16446600
H	2.53614100	-3.18153500	0.74247400
H	2.89912300	-2.96388100	-1.00132600
C	3.85261300	-0.92637300	1.67606100
H	3.23855500	-0.12656200	2.09282800
H	3.76022500	-1.80089300	2.32181900
H	4.89717800	-0.59113000	1.68743000
H	3.61186400	-0.90201200	-1.83023600

Table 17: Optimized geometry for **TS_{3b}**

Free energy G = -1.062.358949 Hartree/particle.

C	4.03443700	-1.15192200	0.18880000	C	0.86246700	-0.70602200	-0.58349400
C	3.42636300	-0.44730000	-0.93448100	H	1.00470700	-1.68703300	-1.04406000
H	3.24269500	-1.16336000	-1.73939700	Au	-1.11918700	-0.28246900	-0.19604700
C	5.18869400	-0.63213300	0.95259600	C	-3.85973900	1.70766800	0.88212400
H	5.22717400	-1.02750100	1.96911500	H	-4.94105500	1.79218500	1.02458100
H	6.07270900	-1.03040400	0.42228400	H	-3.35771400	1.83617800	1.84419400
H	5.26376000	0.45149300	0.95593800	H	-3.52326500	2.49580400	0.20407000
C	3.58142600	-2.52438100	0.51467600	C	-4.19116700	-1.14287200	1.33621000
H	4.42575500	-3.20141000	0.31556900	H	-5.26011900	-0.94151400	1.45226000
H	3.37843400	-2.61843900	1.58696200	H	-4.05426400	-2.15530800	0.94860900
H	2.72118000	-2.85190300	-0.06613000	H	-3.70279200	-1.07284800	2.31119800
O	2.87884600	1.04220500	1.54516000	C	-4.44429800	-0.06090000	-1.34855900
C	2.25587200	1.34636600	0.27629200	H	-4.32164100	-1.05448700	-1.78656300
C	4.06012300	0.87801700	-1.39061700	H	-5.50132800	0.10717600	-1.12288800
H	5.14595500	0.88609100	-1.27234500	H	-4.10613300	0.68378000	-2.07313000
H	3.85983500	0.99261100	-2.45859400	P	-3.42737200	0.06454000	0.17856200
C	3.35730700	2.00487300	-0.58474700	C	1.05081800	2.25720900	0.49191000
H	2.90680800	2.73277500	-1.26366700	H	0.56098400	2.49295200	-0.45610200
H	4.04300000	2.55020600	0.06928700	H	0.31095100	1.79060000	1.14940100
H	2.20555900	0.62579700	2.10459900	H	1.38819600	3.18957200	0.95477200
C	1.97872300	0.00245300	-0.39770900				

Table 18: Optimized geometry for **IVb**

Free energy G = -1062.372835 Hartree/particle.

C	4.07573500	-0.68568300	0.39439800	C	0.76052900	-0.72631000	-0.80494300
C	3.35159500	-0.43051900	-0.95282200	H	0.88070300	-1.58913900	-1.46783800
H	3.46402900	-1.28767500	-1.61853300	Au	-1.17893800	-0.28688800	-0.27973400
C	5.55987700	-0.37815300	0.47337500	C	-4.26716500	1.37067400	-0.82922900
H	5.94275800	-0.58556000	1.47569600	H	-5.31478500	1.50322700	-0.54340500
H	6.08962600	-1.02385100	-0.23386300	H	-3.74471900	2.32639400	-0.73990600
H	5.78155600	0.65982300	0.22510200	H	-4.21578800	1.04196000	-1.87016500
C	3.72912300	-2.02932900	1.01568200	C	-3.75151600	0.73595600	1.95754800
H	4.26562900	-2.81048500	0.46902400	H	-4.82158300	0.88193300	2.13151000
H	4.05694800	-2.07927300	2.05918400	H	-3.36490800	0.01105000	2.67814200
H	2.65975300	-2.24283600	0.95519200	H	-3.23022400	1.68522300	2.10344400
O	3.37833200	0.43335600	1.26087600	C	-4.52307100	-1.36680100	0.11305700
C	2.23134100	1.09355200	0.31460900	H	-4.15908300	-2.14005400	0.79422700
C	3.76301300	0.93019600	-1.56819500	H	-5.55923500	-1.12207600	0.36475600
H	4.84118700	1.06724400	-1.66654000	H	-4.48120900	-1.75458900	-0.90770900
H	3.33104100	1.00893300	-2.56844700	P	-3.45196900	0.12277300	0.24904400
C	3.10360500	1.95991700	-0.59961800	C	1.25364100	1.77096200	1.22992400
H	2.45635700	2.66689400	-1.12565300	H	0.48217400	2.23940700	0.61258700
H	3.82420500	2.54066400	-0.01765700	H	0.75443900	1.06348400	1.89758500
H	2.95469200	0.02809200	2.04082100	H	1.74453000	2.55154300	1.81687800
C	1.92177700	-0.12523800	-0.50847400				

Table 19: Optimized geometry for TS_{5b}

Free energy G = -1062.372866 Hartree/particle.

C	4.03956500	-0.74613200	0.38588300	C	0.76888000	-0.63762900	-0.82519900
C	3.35932200	-0.31776000	-0.95313500	H	0.90905800	-1.48586800	-1.50287500
H	3.45761100	-1.10387800	-1.70385600	Au	-1.17782300	-0.25338300	-0.29753000
C	5.55968600	-0.62184800	0.41830500	C	-4.21444300	1.58546200	-0.48789400
H	5.95282700	-0.99727300	1.36701300	H	-5.26625000	1.66892700	-0.19913700
H	5.99408900	-1.21753400	-0.39045600	H	-3.67629000	2.47297200	-0.14631000
H	5.88704500	0.41235500	0.30155100	H	-4.14216400	1.53168000	-1.57691600
C	3.58978600	-2.13021200	0.84598500	C	-3.78762100	0.24517400	2.05526800
H	2.50348800	-2.23998200	0.80593400	H	-4.85780500	0.37752900	2.23960000
H	4.03594000	-2.89248300	0.20109900	H	-3.44111700	-0.65309600	2.57215500
H	3.92991400	-2.32387100	1.86910900	H	-3.24409100	1.10700500	2.45052600
O	3.50291000	0.28628700	1.34206300	C	-4.55435600	-1.29362800	-0.28520500
C	2.14566000	1.19395900	0.27969900	H	-4.22445300	-2.22600500	0.17936600
C	3.84882900	1.07177200	-1.43094700	H	-5.59092600	-1.09405400	0.00135800
H	4.93393200	1.17998100	-1.43936400	H	-4.49468600	-1.40468100	-1.37055200
H	3.49544200	1.24023900	-2.45115900	P	-3.45856300	0.08130900	0.25314500
C	3.15463300	2.05496000	-0.44542400	C	1.21878800	1.77867900	1.28305300
H	2.60046700	2.84745600	-0.96330200	H	0.49551700	2.39647200	0.73618100
H	3.83501100	2.54745200	0.25336600	H	0.66010600	1.01753900	1.82966000
H	3.06642700	-0.15965500	2.08722900	H	1.75345000	2.43496000	1.97392100
C	1.92637500	-0.00427400	-0.53255500				

Table 20: Optimized geometry for **VIb**

Free energy G = -1062.387406 Hartree/particle.

C	4.10560000	1.31392900	-0.90592400	H	-4.32897700	-0.63894600	-2.03100300
C	3.38579300	-0.05387400	-0.77172300	H	-4.19268200	-2.08728000	-1.01279400
C	1.97041800	1.66715100	0.14331500	H	-5.56579200	-0.97036600	-0.78974200
C	3.33588200	2.25155700	0.04157300	C	-3.99157900	-0.76362800	1.82619100
H	5.16803600	1.27458400	-0.66615800	H	-3.68421500	-1.80972800	1.89551600
H	4.01096000	1.67514600	-1.93469900	H	-3.49305600	-0.19821700	2.61709300
H	3.31478200	3.30668800	-0.25207000	H	-5.07500600	-0.69442100	1.95963000
H	3.76079200	2.21581400	1.05699200	Au	-1.17121400	-0.17797300	-0.22557700
C	0.86065400	2.44829300	0.72723800	O	4.10363400	-0.23391400	1.49695800
H	-0.04571600	1.86413600	0.88850300	H	4.51815600	-0.78358200	2.17644900
H	1.19350700	2.89991000	1.66962400	C	4.03605800	-1.00327500	0.28275800
H	0.63084100	3.28933300	0.05846100	C	3.19136100	-2.26391100	0.52472300
C	1.95674100	0.36371900	-0.38974100	H	3.05819100	-2.84458900	-0.39375700
C	0.81495200	-0.39019600	-0.62945400	H	3.69444300	-2.91000400	1.25259400
H	1.04414000	-1.30623600	-1.18330200	H	2.20682000	-2.01519000	0.93111100
P	-3.50692900	-0.08714100	0.18805500	C	5.44860900	-1.41704900	-0.16068100
C	-4.22045200	1.60532600	0.15228200	H	6.10522800	-0.55260300	-0.28034300
H	-5.29513300	1.56850700	0.35270400	H	5.89629000	-2.07605800	0.59114300
H	-3.73277900	2.22459300	0.90891900	H	5.42055000	-1.96517900	-1.10768200
H	-4.05119300	2.05266800	-0.83003100	H	3.38260900	-0.59435900	-1.72318100
C	-4.50070800	-1.03909800	-1.02887500				

Table 21: Optimized geometry for $\mathbf{TS_{2b}}$

Free energy G = -1062.350514 Hartree/particle.

C	1.65532300	1.87621900	0.04237300
C	0.73069200	2.93127300	-0.57382900
H	1.13180300	3.92943400	-0.37606700
H	0.64152600	2.79531000	-1.65563900
H	-0.27325600	2.86371100	-0.14013000
O	1.75037400	2.05901700	1.45687700
H	0.85263400	2.12597900	1.81309500
C	3.08101200	2.02269200	-0.51281000
H	3.03511100	2.00265500	-1.60740200
H	3.42482200	3.02020600	-0.22163100
C	4.09227300	0.98051600	-0.00588100
H	5.09637000	1.33144000	-0.27909000
H	4.06043300	0.94908900	1.08540200
C	3.91759200	-0.38992100	-0.60873000
H	3.88656600	-0.41121600	-1.69876600
C	4.04405300	-1.59277100	0.02438100
C	4.21396100	-1.75922900	1.50812200
H	4.08118500	-0.83350800	2.06777900
H	3.50891200	-2.50538900	1.89257100
H	5.21947600	-2.14465900	1.72066900
C	4.01628100	-2.87191200	-0.76618800
H	3.19700900	-3.52271300	-0.43013000
H	3.91054000	-2.69706300	-1.83954200
H	4.93957000	-3.43926300	-0.59706900
C	1.13086900	0.46550400	-0.22033100
C	1.62284600	-0.68484800	-0.42689400
H	1.53552300	-1.73092600	-0.64506700
P	-3.25978900	-0.41697500	0.09499300
C	-4.11596400	0.84225700	1.11929000
H	-3.69873700	0.83844800	2.12903400
H	-3.96823900	1.83186500	0.68048500
H	-5.18691000	0.62528200	1.16938500
C	-4.12908500	-0.39711200	-1.52122300
H	-3.98339700	0.57334200	-2.00118800
H	-3.71645400	-1.17488200	-2.16796000
H	-5.19886800	-0.57428700	-1.37797800
C	-3.68412000	-2.03251000	0.85508000
H	-3.26103100	-2.84079700	0.25417000
H	-3.26242300	-2.08423600	1.86151600
H	-4.77008700	-2.15120700	0.90956400
Au	-0.95902100	-0.04221600	-0.08995000

Table 22: Optimized geometry for **IIIb**

Free energy G = -1062.36726 Hartree/particle.

P	3.21481700	0.29810200	0.06298100
C	4.02434100	0.69923800	-1.53805700
H	5.09912500	0.84459600	-1.39553900
H	3.86099700	-0.11669500	-2.24611400
H	3.58734900	1.61244100	-1.94915900
C	3.69514000	1.67596000	1.18067600
H	3.24395100	2.60623300	0.82724300
H	3.32960900	1.47145700	2.18988700
H	4.78297800	1.78835700	1.20526800
C	4.13271100	-1.16207400	0.69708200
H	3.77011700	-1.41438000	1.69657800
H	3.95937800	-2.01525100	0.03670200
H	5.20522500	-0.95273000	0.74359700
Au	0.87552700	-0.03709500	-0.09470500
C	-1.93351000	0.77369200	-0.63730800
C	-1.84338900	-1.62766000	0.15574900
C	-3.47976300	0.65303300	-0.93212900
H	-1.42594800	1.62906600	-1.06564700
C	-3.03811500	-1.85346200	-0.80074300
C	-4.07929600	-0.73725100	-0.71316200
H	-3.68711600	1.09517400	-1.90736200
H	-3.50569700	-2.81663800	-0.56471900
H	-2.65334900	-1.93327600	-1.82415200
H	-4.58037700	-0.78469200	0.25595900
H	-4.84953900	-0.89280600	-1.47415000
C	-1.17535600	-0.28269300	-0.18142400
C	-0.86019100	-2.79721500	0.04293000
H	-0.02845700	-2.66678500	0.74060600
H	-1.37113300	-3.73896300	0.27556300
H	-0.45564900	-2.87705900	-0.97043500
O	-2.28556500	-1.50732500	1.52041900
H	-2.61797000	-2.37285900	1.80119500
C	-3.38739700	1.61313000	0.14775300
C	-3.30606600	3.07705200	-0.18653400
H	-4.29104300	3.50941500	0.03363700
H	-2.57846900	3.59631800	0.44284600
H	-3.08316800	3.26097400	-1.23903200
C	-3.66773000	1.29574700	1.58541200
H	-3.10998500	1.96369600	2.24636100
H	-4.73682300	1.49578500	1.74638000
H	-3.45667400	0.26125500	1.84667000

Table 23: Optimized geometry for **TS_{4b}**

Free energy G = -1062.351564 Hartree/particle.

C	4.54487900	0.24952200	0.23682900
C	3.53339600	-0.56260100	-0.54756100
C	2.40420500	1.48981700	0.07798000
C	3.73434600	1.40807400	0.86646000
H	5.06916700	-0.35793200	0.98070100
H	5.30494600	0.61685700	-0.46095200
H	4.27332500	2.35701700	0.83029200
H	3.50106800	1.20414200	1.91328200
C	2.47144300	2.50165800	-1.09010900
H	1.55143900	2.48077400	-1.68343000
H	2.58935700	3.49984500	-0.65966700
H	3.31789600	2.30601100	-1.75472300
C	2.28921500	0.13415600	-0.63133600
C	1.13686400	-0.71211900	-0.79506600
H	1.17822400	-1.33608100	-1.68847500
P	-3.09650900	0.21254800	0.21845500
C	-3.63010400	1.92745200	-0.16965200
H	-4.68689700	2.06494300	0.07681800
H	-3.03005500	2.63644700	0.40567800
H	-3.47911700	2.12404300	-1.23395000
C	-4.27991300	-0.85697900	-0.69448400
H	-4.14779600	-0.71273400	-1.76951700
H	-4.08513900	-1.90536900	-0.45595500
H	-5.30913000	-0.60865800	-0.41986500
C	-3.52821200	-0.02279800	1.98938500
H	-3.31311300	-1.05322600	2.28275000
H	-2.92554200	0.64884700	2.60571000
H	-4.58869100	0.18657600	2.15675300
Au	-0.83410600	-0.23719300	-0.28416600
O	1.35706700	1.81783700	0.96689300
H	0.51063300	1.75474500	0.49081200
C	2.23614800	-1.41824300	0.21125900
C	2.43523200	-2.88618700	-0.21199600
H	3.29187900	-3.30749500	0.32206100
H	1.53666200	-3.44333900	0.06892900
H	2.59408800	-3.00227200	-1.28413000
C	2.05776500	-1.27261000	1.71592400
H	1.71927700	-0.28008200	2.00861000
H	1.30456400	-1.99607300	2.04279900
H	2.99096300	-1.50843400	2.23768600
H	3.88588500	-1.23609300	-1.32083400

Table 24: Optimized geometry for **Vb**

Free energy G = -1062.42211 Hartree/particle.

C	-4.13359600	-0.76185200	1.46078300
C	-2.65118400	-1.28101200	-0.43929000
C	-3.46611500	-1.93458500	0.70846200
H	-4.19366400	-0.92273200	2.54309300
H	-5.16403800	-0.58997500	1.11866200
H	-4.18157600	-2.67817700	0.34631200
H	-2.75553100	-2.44128200	1.36870400
C	-3.40943500	-1.28867000	-1.77520700
H	-2.86401200	-0.73969700	-2.54877200
H	-3.54721200	-2.31880200	-2.12437000
H	-4.40046300	-0.83832700	-1.66456200
C	-2.42531800	0.14144000	0.08179100
P	2.71132600	-0.77388300	0.22617000
C	2.77614600	-2.46694000	-0.47673600
H	3.74906700	-2.91947100	-0.26421800
H	1.98651300	-3.07973000	-0.03648500
H	2.62656500	-2.41963800	-1.55783100
C	4.13199300	0.11079400	-0.52372500
H	3.97564200	0.20310600	-1.60099100
H	4.21261200	1.11057800	-0.09119800
H	5.05698700	-0.44217500	-0.33675300
C	3.13250300	-0.96662800	2.00045100
H	3.18033500	0.01671700	2.47340800
H	2.36078000	-1.55959700	2.49676100
H	4.09955400	-1.46763200	2.10276400
Au	0.67327700	0.29539400	-0.12451300
O	-1.36401900	-1.89948900	-0.61421100
H	-1.49000400	-2.73509200	-1.08532200
C	-3.26351400	0.41278900	1.09986600
H	-3.36935500	1.37788300	1.58223500
C	-0.86255200	2.18536900	-0.13482400
C	-0.97025100	2.66956000	1.28991900
H	-1.80619700	3.37771000	1.36694300
H	-1.15043300	1.85964500	1.99850000
H	-0.06578600	3.21002500	1.58223800
C	-0.26666000	3.17687500	-1.10839600
H	-0.16269300	2.76178400	-2.11332500
H	-0.93145900	4.04917300	-1.16560000
H	0.70653300	3.54152000	-0.76737600
C	-1.48869600	1.03977300	-0.61201800
H	-1.43867300	0.89071900	-1.69159200

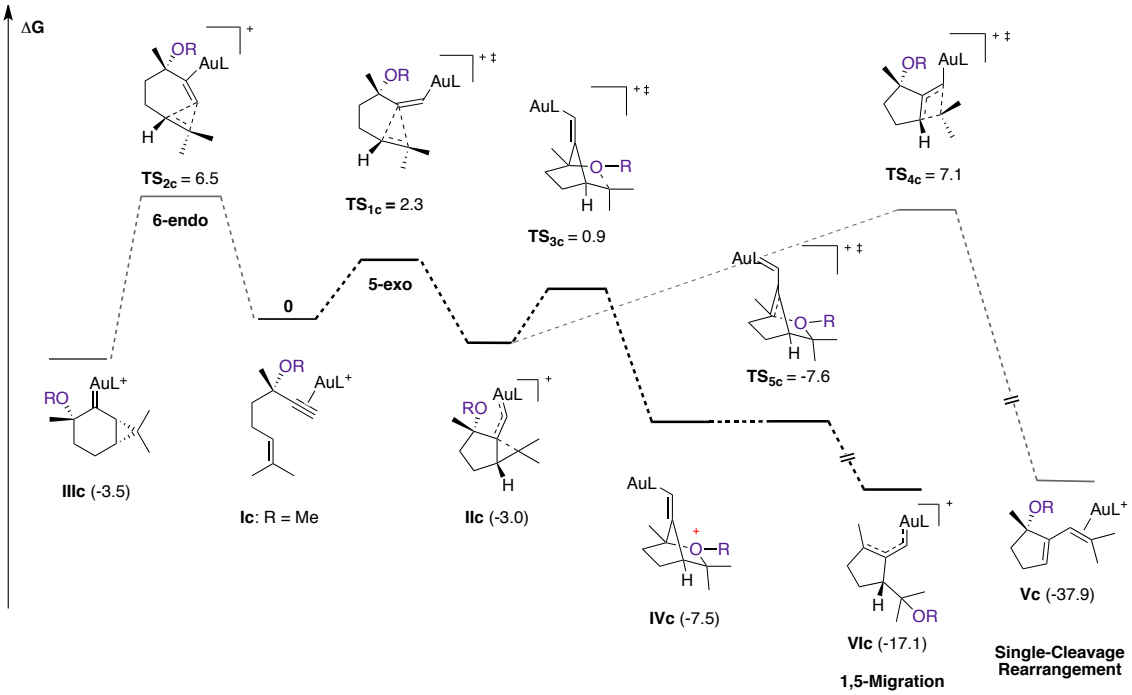

Scheme 17. Reaction pathways and energies for the cyclization of **Ic**, L=PMe_3, ΔG energies are given in kcal·mol^{-1}

Table 25: Optimized geometry for Ic

Free energy G = -1062.016988 Hartree/particle.

C	-2.46743700	-1.44743000	0.43923900	H	-0.11965600	3.29749000	-1.41792700
C	-2.93760200	-2.91325900	0.36541100	H	-1.68297100	3.15235100	-2.24796000
H	-3.55757000	-3.12630500	1.24020300	H	-1.34526300	4.53592300	-1.19037500
H	-3.52622900	-3.09315400	-0.53765700	C	-1.58819100	-1.20260300	-0.75257900
H	-2.08277000	-3.59687000	0.36015500	C	-1.02358900	-1.14282100	-1.84493600
O	-1.75056100	-1.20874000	1.64811800	H	-0.73366400	-1.13381700	-2.87673000
H	-1.16378300	-1.96161900	1.81026300	P	2.69374800	0.13592800	0.43357900
C	-3.68691000	-0.49538000	0.43275400	C	3.33352800	1.66487300	-0.34805100
H	-4.17956700	-0.57563700	-0.54279600	H	3.44725000	1.50595400	-1.42262700
H	-4.38227300	-0.90574400	1.17299200	H	2.62693600	2.48149700	-0.18392700
C	-3.42293900	0.98065500	0.78272000	H	4.30268400	1.92755600	0.08552700
H	-4.41267900	1.42888700	0.95525800	C	2.62909900	0.48413700	2.23220700
H	-2.89829300	1.03162300	1.73935200	H	1.89670800	1.27077400	2.42621900
C	-2.71679100	1.77889300	-0.28221100	H	2.33023400	-0.41833800	2.77009100
H	-3.08819200	1.61434300	-1.29534100	H	3.61317900	0.80722100	2.58378600
C	-1.74777600	2.69718600	-0.12531900	C	4.00925100	-1.12118100	0.21599000
C	-1.13728900	3.08772600	1.19868400	H	3.72230000	-2.04301600	0.72683800
H	-1.49430900	2.48556200	2.03589500	H	4.14331800	-1.33226800	-0.84736300
H	-0.04338600	3.00245100	1.15951600	H	4.94957000	-0.75060500	0.63402000
H	-1.35460200	4.13967100	1.42607900	Au	0.63775800	-0.51979000	-0.43361600
C	-1.20195000	3.45428300	-1.31332200				

Table 26: Optimized geometry for TS_{1c}

Free energy G = -1062.005315 Hartree/particle.

C	2.23881400	1.56564300	0.12289200	H	2.73684700	-3.09571500	0.33061300
C	1.03408000	2.51920700	-0.04658500	H	3.27978800	-2.83401900	-1.34986300
H	1.36509900	3.52525000	0.22399600	H	4.38218700	-3.49078500	-0.12601900
H	0.67120300	2.52426400	-1.07672600	C	1.81084300	0.17649100	-0.22874100
H	0.21165200	2.22720200	0.61222000	C	0.92908600	-0.72922000	-0.40440700
O	2.72969700	1.61193200	1.46126300	H	1.09694900	-1.76739700	-0.67071400
H	2.02031000	1.33413400	2.05888600	P	-3.42372300	0.03589000	0.13418300
C	3.40205700	2.00541000	-0.77906200	C	-3.84502800	1.38570500	1.30527500
H	3.04196100	2.05236800	-1.81189000	H	-3.42532300	1.16123100	2.28858000
H	3.71007500	3.01273700	-0.48396200	H	-3.42014700	2.32643500	0.94744400
C	4.56404500	1.00534300	-0.65891700	H	-4.93080300	1.48822000	1.38985400
H	5.30805100	1.21945400	-1.43457800	C	-4.28361700	0.47280300	-1.42803900
H	5.05622000	1.12618200	0.30694000	H	-3.86411300	1.39865600	-1.82847900
C	4.03897500	-0.38965000	-0.83888300	H	-4.13882500	-0.32438300	-2.16093100
H	3.74764500	-0.65306800	-1.85513300	H	-5.35363300	0.60801600	-1.24580200
C	4.03047800	-1.39284300	0.08861600	C	-4.30481800	-1.44307200	0.76987800
C	4.50998800	-1.24986100	1.50711500	H	-4.16181200	-2.27795400	0.08008500
H	4.58750200	-0.21356800	1.83195300	H	-3.89846300	-1.71958100	1.74557400
H	3.83641600	-1.77790400	2.19048500	H	-5.37367000	-1.23248000	0.86814000
H	5.49301500	-1.72821100	1.60754900	Au	-1.12220100	-0.29447600	-0.13666300
C	3.57410000	-2.76917100	-0.29992800				

Table 27: Optimized geometry for **IIc**

Free energy G = -1062.016335 Hartree/particle.

C	4.38564000	0.90734000	-0.79509400	H	-4.23111400	-0.55198700	-1.91968300
C	3.57473900	-0.38766800	-0.87174900	H	-4.25563400	-1.88968400	-0.75308300
C	2.15960500	1.42299200	0.16689800	H	-5.45420400	-0.57538300	-0.62145100
C	3.65994200	1.82616800	0.20348400	C	-3.77810700	-0.33002600	1.91771300
H	5.42577800	0.71536300	-0.51551200	H	-3.60355500	-1.39486700	2.08987200
H	4.39619600	1.35115700	-1.79454400	H	-3.18699600	0.24166500	2.63703400
H	3.79481600	2.88053200	-0.05110100	H	-4.83945800	-0.10906900	2.06329000
H	4.04336200	1.69319800	1.21633500	Au	-0.97206000	-0.31042700	-0.23740500
C	1.37040400	2.37904000	-0.74239300	O	1.57599800	1.39116800	1.47660200
H	0.33133900	2.05399900	-0.83979400	H	1.56086100	2.29826700	1.81487800
H	1.38745900	3.38636600	-0.31108100	C	3.46232400	-1.28005400	0.26664200
H	1.81599500	2.43318000	-1.74063100	C	3.21950500	-2.73707300	0.01538700
C	2.11072000	-0.00319200	-0.42001900	H	4.19998200	-3.21427300	0.16446600
C	0.99199100	-0.74668200	-0.63966400	H	2.53614100	-3.18153500	0.74247400
H	1.17101200	-1.72949200	-1.07414400	H	2.89912300	-2.96388100	-1.00132600
P	-3.25844700	0.10804200	0.21023300	C	3.85261300	-0.92637300	1.67606100
C	-3.74565700	1.86982500	0.01419200	H	3.23855500	-0.12656200	2.09282800
H	-4.81026800	2.00102500	0.22859500	H	3.76022500	-1.80089300	2.32181900
H	-3.16006500	2.48828400	0.69890800	H	4.89717800	-0.59113000	1.68743000
H	-3.54157000	2.19271900	-1.00960900	H	3.61186400	-0.90201200	-1.83023600
C	-4.41798600	-0.81617000	-0.87596800				

Table 28: Optimized geometry for **TS_{3c}**

Free energy G = -1062.007814 Hartree/particle.

C	4.03443700	-1.15192200	0.18880000	C	0.86246700	-0.70602200	-0.58349400
C	3.42636300	-0.44730000	-0.93448100	H	1.00470700	-1.68703300	-1.04406000
H	3.24269500	-1.16336000	-1.73939700	Au	-1.11918700	-0.28246900	-0.19604700
C	5.18869400	-0.63213300	0.95259600	C	-3.85973900	1.70766800	0.88212400
H	5.22717400	-1.02750100	1.96911500	H	-4.94105500	1.79218500	1.02458100
H	6.07270900	-1.03040400	0.42228400	H	-3.35771400	1.83617800	1.84419400
H	5.26376000	0.45149300	0.95593800	H	-3.52326500	2.49580400	0.20407000
C	3.58142600	-2.52438100	0.51467600	C	-4.19116700	-1.14287200	1.33621000
H	4.42575500	-3.20141000	0.31556900	H	-5.26011900	-0.94151400	1.45226000
H	3.37843400	-2.61843900	1.58696200	H	-4.05426400	-2.15530800	0.94860900
H	2.72118000	-2.85190300	-0.06613000	H	-3.70279200	-1.07284800	2.31119800
O	2.87884600	1.04220500	1.54516000	C	-4.44429800	-0.06090000	-1.34855900
C	2.25587200	1.34636600	0.27629200	H	-4.32164100	-1.05448700	-1.78656300
C	4.06012300	0.87801700	-1.39061700	H	-5.50132800	0.10717600	-1.12288800
H	5.14595500	0.88609100	-1.27234500	H	-4.10613300	0.68378000	-2.07313000
H	3.85983500	0.99261100	-2.45859400	P	-3.42737200	0.06454000	0.17856200
C	3.35730700	2.00487300	-0.58474700	C	1.05081800	2.25720900	0.49191000
H	2.90680800	2.73277500	-1.26366700	H	0.56098400	2.49295200	-0.45610200
H	4.04300000	2.55020600	0.06928700	H	0.31095100	1.79060000	1.14940100
H	2.20555900	0.62579700	2.10459900	H	1.38819600	3.18957200	0.95477200
C	1.97872300	0.00245300	-0.39770900				

Table 29: Optimized geometry for **IVc**

Free energy G = -1062.019293 Hartree/particle.

C	4.07572000	-0.69810800	0.39455100	C	0.75775700	-0.72572000	-0.79323000
C	3.34742100	-0.45006600	-0.94885000	H	0.87430700	-1.58869900	-1.45664600
H	3.44861400	-1.31175900	-1.61043400	Au	-1.18163700	-0.28320300	-0.27217500
C	5.56340900	-0.40080400	0.46535000	C	-4.27535900	1.35612900	-0.84426200
H	5.94393400	-0.56172600	1.47790700	H	-5.32411600	1.48736900	-0.56201800
H	6.08597300	-1.09478000	-0.19965400	H	-3.75650300	2.31445500	-0.76240500
H	5.81273000	0.61309400	0.14647900	H	-4.22047900	1.01839200	-1.88213300
C	3.72354700	-2.02476300	1.04437300	C	-3.76718200	0.74399200	1.94934200
H	4.23525700	-2.82573400	0.50201800	H	-4.83885200	0.88269500	2.11937900
H	4.06067900	-2.04736800	2.08379100	H	-3.37646000	0.02759100	2.67618800
H	2.64916000	-2.21127100	1.01105900	H	-3.25381600	1.69842900	2.08954600
O	3.33948300	0.39237300	1.26461300	C	-4.52059000	-1.37535800	0.11620500
C	2.24014600	1.09187600	0.31696500	H	-4.15591100	-2.14158800	0.80485300
C	3.75319100	0.90572600	-1.58148800	H	-5.55925000	-1.13412900	0.36091100
H	4.83016600	1.04856500	-1.68613900	H	-4.47165700	-1.77048700	-0.90144300
H	3.31970600	0.96836600	-2.58200700	P	-3.45760100	0.12060700	0.24639300
C	3.08766100	1.95047200	-0.63124600	C	1.25736600	1.76086800	1.23290700
H	2.42280900	2.63268000	-1.16810300	H	0.45593500	2.18499600	0.62137900
H	3.80564900	2.57418400	-0.08649800	H	0.81448200	1.04722000	1.92999900
H	3.97163300	1.04541200	1.61891800	H	1.72634200	2.57651600	1.79054700
C	1.92310600	-0.13548700	-0.49503300				

Table 30: Optimized geometry for **TS_{5c}**

Free energy G = -1062.018638 Hartree/particle.

C	4.02798500	-0.75255500	0.39969000	C	0.76774900	-0.64443300	-0.82475900
C	3.35877700	-0.33039300	-0.94693100	H	0.90943000	-1.49942300	-1.49352800
H	3.45419500	-1.12268300	-1.69159400	Au	-1.17809200	-0.25675200	-0.29797600
C	5.54765900	-0.62029200	0.45082400	C	-4.22206500	1.56439600	-0.51697500
H	5.93065400	-0.96634000	1.41528900	H	-5.27284300	1.65138700	-0.22555200
H	5.99383000	-1.24259600	-0.33015200	H	-3.68548200	2.46243300	-0.20142900
H	5.88729900	0.40655500	0.29243700	H	-4.15481500	1.48179900	-1.60441300
C	3.58619700	-2.14005200	0.85553000	C	-3.77204500	0.29769300	2.05863000
H	2.49941900	-2.24042600	0.82906500	H	-4.84122500	0.43102300	2.24809800
H	4.02379000	-2.89852200	0.19948100	H	-3.41668800	-0.58298200	2.59915800
H	3.92912600	-2.32871900	1.87647600	H	-3.22940900	1.17355200	2.42307600
O	3.41983800	0.22189400	1.37091400	C	-4.55196400	-1.30833400	-0.2335710
C	2.13746100	1.19884400	0.26330300	H	-4.21571700	-2.22731000	0.25259400
C	3.85309000	1.05308800	-1.43690100	H	-5.58689900	-1.10416400	0.05573700
H	4.93808300	1.16468900	-1.43535800	H	-4.50035500	-1.44745400	-1.31613900
H	3.51290400	1.20802400	-2.46351600	P	-3.45620900	0.08341800	0.25952000
C	3.14421800	2.05134100	-0.47639300	C	1.20269900	1.78311600	1.25793400
H	2.57882900	2.82064700	-1.01775000	H	0.44528300	2.34802300	0.69952500
H	3.81477500	2.59167300	0.19802200	H	0.69228700	1.01500500	1.83928800
H	4.10572900	0.81313200	1.72325900	H	1.71419800	2.48679100	1.91884300
C	1.92478900	-0.00860000	-0.53552900				

Table 31: Optimized geometry for **VIc**

Free energy G = -1062.03665 Hartree/particle.

C	4.10560000	1.31392900	-0.90592400	H	-4.32897700	-0.63894600	-2.03100300
C	3.38579300	-0.05387400	-0.77172300	H	-4.19268200	-2.08728000	-1.01279400
C	1.97041800	1.66715100	0.14331500	H	-5.56579200	-0.97036600	-0.78974200
C	3.33588200	2.25155700	0.04157300	C	-3.99157900	-0.76362800	1.82619100
H	5.16803600	1.27458400	-0.66615800	H	-3.68421500	-1.80972800	1.89551600
H	4.01096000	1.67514600	-1.93469900	H	-3.49305600	-0.19821700	2.61709300
H	3.31478200	3.30668800	-0.25207000	H	-5.07500600	-0.69442100	1.95963000
H	3.76079200	2.21581400	1.05699200	Au	-1.17121400	-0.17797300	-0.22557700
C	0.86065400	2.44829300	0.72723800	O	4.10363400	-0.23391400	1.49695800
H	-0.04571600	1.86413600	0.88850300	H	4.51815600	-0.78358200	2.17644900
H	1.19350700	2.89991000	1.66962400	C	4.03605800	-1.00327500	0.28275800
H	0.63084100	3.28933300	0.05846100	C	3.19136100	-2.26391100	0.52472300
C	1.95674100	0.36371900	-0.38974100	H	3.05819100	-2.84458900	-0.39375700
C	0.81495200	-0.39019600	-0.62945400	H	3.69444300	-2.91000400	1.25259400
H	1.04414000	-1.30623600	-1.18330200	H	2.20682000	-2.01519000	0.93111100
P	-3.50692900	-0.08714100	0.18805500	C	5.44860900	-1.41704900	-0.16068100
C	-4.22045200	1.60532600	0.15228200	H	6.10522800	-0.55260300	-0.28034300
H	-5.29513300	1.56850700	0.35270400	H	5.89629000	-2.07605800	0.59114300
H	-3.73277900	2.22459300	0.90891900	H	5.42055000	-1.96517900	-1.10768200
H	-4.05119300	2.05266800	-0.83003100	H	3.38260900	-0.59435900	-1.72318100
C	-4.50070800	-1.03909800	-1.02887500				

Table 32: Optimized geometry for **TS_{2c}**

Free energy G = -1062.000076 Hartree/particle.

C	1.65532300	1.87621900	0.04237300	H	3.19700900	-3.52271300	-0.43013000
C	0.73069200	2.93127300	-0.57382900	H	3.91054000	-2.69706300	-1.83954200
H	1.13180300	3.92943400	-0.37606700	H	4.93957000	-3.43926300	-0.59706900
H	0.64152600	2.79531000	-1.65563900	C	1.13086900	0.46550400	-0.22033100
H	-0.27325600	2.86371100	-0.14013000	C	1.62284600	-0.68484800	-0.42689400
O	1.75037400	2.05901700	1.45687700	H	1.53552300	-1.73092600	-0.64506700
H	0.85263400	2.12597900	1.81309500	P	-3.25978900	-0.41697500	0.09499300
C	3.08101200	2.02269200	-0.51281000	C	-4.11596400	0.84225700	1.11929000
H	3.03511100	2.00265500	-1.60740200	H	-3.69873700	0.83844800	2.12903400
H	3.42482200	3.02020600	-0.22163100	H	-3.96823900	1.83186500	0.68048500
C	4.09227300	0.98051600	-0.00588100	H	-5.18691000	0.62528200	1.16938500
H	5.09637000	1.33144000	-0.27909000	C	-4.12908500	-0.39711200	-1.52122300
H	4.06043300	0.94908900	1.08540200	H	-3.98339700	0.57334200	-2.00118800
C	3.91759200	-0.38992100	-0.60873000	H	-3.71645400	-1.17488200	-2.16796000
H	3.88656600	-0.41121600	-1.69876600	H	-5.19886800	-0.57428700	-1.37797800
C	4.04405300	-1.59277100	0.02438100	C	-3.68412000	-2.03251000	0.85508000
C	4.21396100	-1.75922900	1.50812200	H	-3.26103100	-2.84079700	0.25417000
H	4.08118500	-0.83350800	2.06777900	H	-3.26242300	-2.08423600	1.86151600
H	3.50891200	-2.50538900	1.89257100	H	-4.77008700	-2.15120700	0.90956400
H	5.21947600	-2.14465900	1.72066900	Au	-0.95902100	-0.04221600	-0.08995000
C	4.01628100	-2.87191200	-0.76618800				

Table 33: Optimized geometry for **IIIc**

Free energy G = -1062.019139 Hartree/particle.

P	3.21481700	0.29810200	0.06298100	H	-3.50569700	-2.81663800	-0.56471900
C	4.02434100	0.69923800	-1.53805700	H	-2.65334900	-1.93327600	-1.82415200
H	5.09912500	0.84459600	-1.39553900	H	-4.58037700	-0.78469200	0.25595900
H	3.86099700	-0.11669500	-2.24611400	H	-4.84953900	-0.89280600	-1.47415000
H	3.58734900	1.61244100	-1.94915900	C	-1.17535600	-0.28269300	-0.18142400
C	3.69514000	1.67596000	1.18067600	C	-0.86019100	-2.79721500	0.04293000
H	3.24395100	2.60623300	0.82724300	H	-0.02845700	-2.66678500	0.74060600
H	3.32960900	1.47145700	2.18988700	H	-1.37113300	-3.73896300	0.27556300
H	4.78297800	1.78835700	1.20526800	H	-0.45564900	-2.87705900	-0.97043500
C	4.13271100	-1.16207400	0.69708200	O	-2.28556500	-1.50732500	1.52041900
H	3.77011700	-1.41438000	1.69657800	H	-2.61797000	-2.37285900	1.80119500
H	3.95937800	-2.01525100	0.03670200	C	-3.38739700	1.61313000	0.14775300
H	5.20522500	-0.95273000	0.74359700	C	-3.30606600	3.07705200	-0.18653400
Au	0.87552700	-0.03709500	-0.09470500	H	-4.29104300	3.50941500	0.03363700
C	-1.93351000	0.77369200	-0.63730800	H	-2.57846900	3.59631800	0.44284600
C	-1.84338900	-1.62766000	0.15574900	H	-3.08316800	3.26097400	-1.23903200
C	-3.47976300	0.65303300	-0.93212900	C	-3.66773000	1.29574700	1.58541200
H	-1.42594800	1.62906600	-1.06564700	H	-3.10998500	1.96369600	2.24636100
C	-3.03811500	-1.85346200	-0.80074300	H	-4.73682300	1.49578500	1.74638000
C	-4.07929600	-0.73725100	-0.71316200	H	-3.45667400	0.26125500	1.84667000
H	-3.68711600	1.09517400	-1.90736200				

Table 34: Optimized geometry for **TS_{4c}**

Free energy G = -1062.010532 Hartree/particle.

C	4.54487900	0.24952200	0.23682900	H	-4.14779600	-0.71273400	-1.76951700
C	3.53339600	-0.56260100	-0.54756100	H	-4.08513900	-1.90536900	-0.45595500
C	2.40420500	1.48981700	0.07798000	H	-5.30913000	-0.60865800	-0.41986500
C	3.73434600	1.40807400	0.86646000	C	-3.52821200	-0.02279800	1.98938500
H	5.06916700	-0.35793200	0.98070100	H	-3.31311300	-1.05322600	2.28275000
H	5.30494600	0.61685700	-0.46095200	H	-2.92554200	0.64884700	2.60571000
H	4.27332500	2.35701700	0.83029200	H	-4.58869100	0.18657600	2.15675300
H	3.50106800	1.20414200	1.91328200	Au	-0.83410600	-0.23719300	-0.28416600
C	2.47144300	2.50165800	-1.09010900	O	1.35706700	1.81783700	0.96689300
H	1.55143900	2.48077400	-1.68343000	H	0.51063300	1.75474500	0.49081200
H	2.58935700	3.49984500	-0.65966700	C	2.23614800	-1.41824300	0.21125900
H	3.31789600	2.30601100	-1.75472300	C	2.43523200	-2.88618700	-0.21199600
C	2.28921500	0.13415600	-0.63133600	H	3.29187900	-3.30749500	0.32206100
C	1.13686400	-0.71211900	-0.79506600	H	1.53666200	-3.44333900	0.06892900
H	1.17822400	-1.33608100	-1.68847500	H	2.59408800	-3.00227200	-1.28413000
P	-3.09650900	0.21254800	0.21845500	C	2.05776500	-1.27261000	1.71592400
C	-3.63010400	1.92745200	-0.16965200	H	1.71927700	-0.28008200	2.00861000
H	-4.68689700	2.06494300	0.07681800	H	1.30456400	-1.99607300	2.04279900
H	-3.03005500	2.63644700	0.40567800	H	2.99096300	-1.50843400	2.23768600
H	-3.47911700	2.12404300	-1.23395000	H	3.88588500	-1.23609300	-1.32083400
C	-4.27991300	-0.85697900	-0.69448400				

Table 35: Optimized geometry for **Vc**

Free energy G = -1062.074679 Hartree/particle.

C	-4.13359600	-0.76185200	1.46078300	C	3.13250300	-0.96662800	2.00045100
C	-2.65118400	-1.28101200	-0.43929000	H	3.18033500	0.01671700	2.47340800
C	-3.46611500	-1.93458500	0.70846200	H	2.36078000	-1.55959700	2.49676100
H	-4.19366400	-0.92273200	2.54309300	H	4.09955400	-1.46763200	2.10276400
H	-5.16403800	-0.58997500	1.11866200	Au	0.67327700	0.29539400	-0.12451300
H	-4.18157600	-2.67817700	0.34631200	O	-1.36401900	-1.89948900	-0.61421100
H	-2.75553100	-2.44128200	1.36870400	H	-1.49000400	-2.73509200	-1.08532200
C	-3.40943500	-1.28867000	-1.77520700	C	-3.26351400	0.41278900	1.09986600
H	-2.86401200	-0.73969700	-2.54877200	H	-3.36935500	1.37788300	1.58223500
H	-3.54721200	-2.31880200	-2.12437000	C	-0.86255200	2.18536900	-0.13482400
H	-4.40046300	-0.83832700	-1.66456200	C	-0.97025100	2.66956000	1.28991900
C	-2.42531800	0.14144000	0.08179100	H	-1.80619700	3.37771000	1.36694300
P	2.71132600	-0.77388300	0.22617000	H	-1.15043300	1.85964500	1.99850000
C	2.77614600	-2.46694000	-0.47673600	H	-0.06578600	3.21002500	1.58223800
H	3.74906700	-2.91947100	-0.26421800	C	-0.26666000	3.17687500	-1.10839600
H	1.98651300	-3.07973000	-0.03648500	H	-0.16269300	2.76178400	-2.11332500
H	2.62656500	-2.41963800	-1.55783100	H	-0.93145900	4.04917300	-1.16560000
C	4.13199300	0.11079400	-0.52372500	H	0.70653300	3.54152000	-0.76737600
H	3.97564200	0.20310600	-1.60099100	C	-1.48869600	1.03977300	-0.61201800
H	4.21261200	1.11057800	-0.09119800	H	-1.43867300	0.89071900	-1.69159200
H	5.05698700	-0.44217500	-0.33675300				

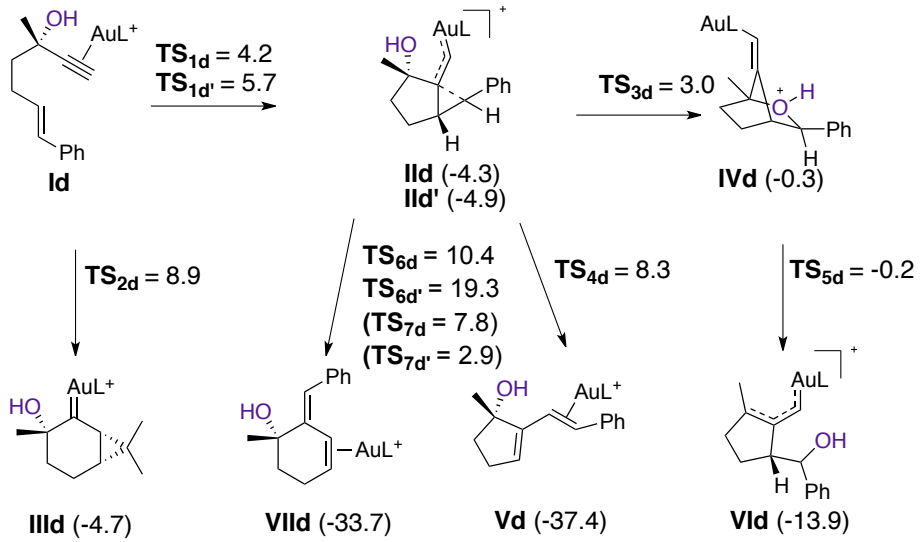

Scheme 18. Reaction pathways and energies for the cyclization of **Id**, L=PMe_3, ΔG energies are given in kcal·mol^{-1}

Table 36: Optimized geometry for **Id**

Free energy G = -1214.764723 Hartree/particle.

C	-3.17810200	0.99257100	0.16754400	C	4.28555300	1.49549700	0.55869700
C	-4.59339200	0.72565300	-0.38139000	H	2.84863300	1.17103000	2.12742000
H	-4.80940500	1.36472000	-1.24122600	C	3.45862200	2.63035900	-1.40408300
H	-4.69988200	-0.31775500	-0.69356200	H	1.39058500	3.19051100	-1.38566400
H	-5.31982000	0.93601400	0.40792100	C	4.51331100	2.02279300	-0.71405400
C	-3.04421200	2.47340600	0.59363200	H	5.09718300	1.02897300	1.10970500
H	-3.92858200	2.68898600	1.20258600	H	3.62676400	3.04781200	-2.39283500
H	-3.11819100	3.09685600	-0.30433600	H	5.50032700	1.96608500	-1.16304400
C	-1.79405300	2.85433200	1.40909800	P	0.96916700	-2.43553700	0.45589800
H	-1.96722600	3.88135900	1.76247700	C	2.67621400	-2.31248200	-0.19779500
H	-1.73031300	2.22467500	2.30153300	H	2.66673300	-2.47656700	-1.27773800
C	-2.20706100	0.65461000	-0.92590600	H	3.07279100	-1.31526900	0.00785700
C	-1.58001900	0.45364000	-1.96575600	H	3.31174900	-3.06481100	0.27832700
H	-1.16838500	0.42850400	-2.95500400	C	1.11762600	-2.24563100	2.27311300
O	-2.92555300	0.19647200	1.32261300	H	1.49416200	-1.24716300	2.50581200
H	-3.23493500	-0.70471700	1.14891600	H	0.13720100	-2.37129000	2.73742900
C	-0.49392900	2.82078900	0.65615600	H	1.80631700	-2.99702400	2.66986100
H	-0.48342300	3.35207700	-0.29551600	C	0.44714500	-4.17087200	0.17918700
C	0.62438100	2.22828000	1.10682400	H	-0.54349000	-4.32770900	0.61195100
H	0.57838700	1.72260100	2.07195400	H	0.40040300	-4.37246500	-0.89337300
C	1.94151600	2.18051300	0.45097800	H	1.16089100	-4.85514000	0.64705200
C	3.01475600	1.57370000	1.13108000	Au	-0.47464700	-0.88114200	-0.49422100
C	2.19090900	2.70970300	-0.83139400				

Table 37: Optimized geometry for TS_{1d}

Free energy G = -1214.75796 Hartree/particle.

C	1.26992500	2.65733300	0.30178700
C	-0.17122800	3.21414700	0.28835200
H	-0.12765700	4.26310000	0.59294900
H	-0.61565700	3.14690300	-0.70720600
H	-0.80512700	2.66802400	0.99243300
O	1.85120400	2.79074700	1.59690700
H	1.30821500	2.29829500	2.22947800
C	2.17350800	3.44582500	-0.65860400
H	1.73023900	3.41464500	-1.65906600
H	2.20675500	4.49072400	-0.33670500
C	3.58140800	2.82322500	-0.66737000
H	4.16690200	3.25186000	-1.48799100
H	4.09109600	3.06290400	0.26897500
C	3.47868000	1.33293300	-0.83012400
H	3.25691200	0.96439500	-1.82939100
C	3.78654500	0.45611900	0.16953100
C	1.24014000	1.22148500	-0.10704800
C	0.68092700	0.09225100	-0.30625500
H	1.19059800	-0.83021600	-0.58217500
P	-3.70017200	-0.57144200	0.06770500
C	-4.59932800	0.65215000	1.10008900
H	-4.18551500	0.65157200	2.11128400
H	-4.47884300	1.64968700	0.67098600
H	-5.66372700	0.40347400	1.14414900
C	-4.56611500	-0.56105200	-1.55107900
H	-4.44490600	0.41672000	-2.02295300
H	-4.13126500	-1.32216700	-2.20308100
H	-5.63125800	-0.76771100	-1.41281400
C	-4.08797300	-2.20482600	0.80927800
H	-3.63968600	-2.99599000	0.20379700
H	-3.67172500	-2.25607300	1.81807000
H	-5.17078100	-2.35255900	0.85552700
Au	-1.40332800	-0.15301500	-0.10984900
H	4.04541500	0.87883100	1.13887300
C	3.79163400	-0.99864300	0.09974400
C	4.02424000	-1.72798400	1.28455100
C	3.56103500	-1.71483000	-1.09535900
C	4.02062500	-3.11953400	1.27982700
H	4.20744800	-1.18885700	2.20990000
C	3.55594300	-3.10817100	-1.09619700
H	3.41006600	-1.18415000	-2.02981800
C	3.78331100	-3.81394500	0.08913300
H	4.20303100	-3.66418900	2.20097600
H	3.38302600	-3.64468100	-2.02398100
H	3.78263800	-4.89961800	0.08348800

Table 38: Optimized geometry for **IId**

Free energy G = -1214.771505 Hartree/particle.

C	0.92070300	2.53487200	0.40744700
C	2.19308600	3.40800000	0.56846900
C	3.11255300	3.01936300	-0.59886900
C	2.87255900	1.51803700	-0.81563500
C	1.39244700	1.27623500	-0.33912300
H	2.65665900	3.17485400	1.53223200
H	1.96058900	4.47608000	0.57497600
H	2.82560500	3.54458400	-1.51458400
H	4.16624700	3.23850900	-0.40775500
H	3.08771800	1.14890400	-1.81518600
C	-0.14724400	3.26216000	-0.42703000
H	-0.99786800	2.60247200	-0.61851900
H	-0.49872400	4.14578900	0.11805600
H	0.25675100	3.59860500	-1.38660200
O	0.38016500	2.13356500	1.66864100
H	-0.00799400	2.91623200	2.08522900
C	3.20623000	0.62600300	0.27395100
H	3.18581900	1.04467700	1.27640000
C	3.63118700	-0.74785000	0.18394400
C	3.91481400	-1.38334800	-1.04766800
C	3.82417000	-1.46672100	1.38716700
C	4.36950300	-2.69602100	-1.06712000
H	3.79282500	-0.84816200	-1.98272200
C	4.28232000	-2.77723200	1.36016000
H	3.61040700	-0.98190200	2.33520100
C	4.55211400	-3.39394600	0.13285200
H	4.58955300	-3.17732800	-2.01424000
H	4.42987800	-3.32058200	2.28752100
H	4.91014200	-4.41855200	0.11091300
C	0.66403400	0.16294800	-0.61858500
H	1.23129600	-0.64647100	-1.08313200
Au	-1.31446300	-0.21519200	-0.24817600
P	-3.58387000	-0.75300300	0.16075500
C	-4.72209800	-0.25428900	-1.19421200
H	-5.75141300	-0.53712700	-0.95521000
H	-4.66865700	0.82777600	-1.33624100
H	-4.41912800	-0.74394200	-2.12283100
C	-3.89128700	-2.55158000	0.38368700
H	-3.30844600	-2.91871600	1.23202100
H	-4.95344200	-2.73982100	0.56603600
H	-3.57753600	-3.08941000	-0.51425100
C	-4.28921900	0.02546800	1.66926200
H	-5.33378400	-0.27067900	1.80199800
H	-3.71213600	-0.28461700	2.54371100
H	-4.23026800	1.11289300	1.58021900

Table 39: Optimized geometry for **TS_{3d}**

Free energy G = -1214.760013 Hartree/particle.

C	1.26451800	2.13028800	0.62344400	C	3.95145300	-2.93928300	-0.57069700
C	1.89839700	3.37650300	-0.03231200	H	2.71588600	-1.44334500	-1.47701600
C	2.75169400	2.85689700	-1.22605100	C	4.98541800	-3.19592300	0.34467300
C	2.68640000	1.31456000	-1.12764900	H	6.38250700	-2.36947700	1.76966100
C	1.26324000	1.08952200	-0.49140100	H	3.50630200	-3.75700200	-1.12685400
H	2.49183300	3.91589600	0.71077200	H	5.32912000	-4.21560800	0.48900200
H	1.11174900	4.05063000	-0.37976800	C	0.34396300	0.22463600	-0.92657300
H	2.31267000	3.16580800	-2.17770300	H	0.66720200	-0.40835000	-1.75849200
H	3.77967700	3.22957300	-1.20587600	Au	-1.59276200	-0.14047900	-0.32197500
H	2.73361400	0.79986900	-2.08994800	P	-3.81797100	-0.64743000	0.30096800
C	-0.04661600	2.40438900	1.34654300	C	-4.95551700	-0.93583400	-1.11607200
H	-0.42691800	1.50136200	1.83355700	H	-5.96641100	-1.15652900	-0.76021000
H	0.11053300	3.17312900	2.10892000	H	-4.98216100	-0.04563600	-1.74916100
H	-0.80699500	2.75504200	0.64446800	H	-4.59069200	-1.77621500	-1.71182900
O	2.26310500	1.66697100	1.58032300	C	-3.98954600	-2.16028500	1.33347200
H	1.91114800	0.86522400	2.00000500	H	-3.41336900	-2.04157100	2.25444700
C	3.70832200	0.77995000	-0.20386100	H	-5.03950000	-2.33704100	1.58458600
H	4.29309100	1.50223300	0.35688500	H	-3.59898700	-3.02211500	0.78684500
C	4.09807200	-0.57113400	-0.04022000	C	-4.64681800	0.66684800	1.28576500
C	5.14550200	-0.85523900	0.88041100	H	-5.66696300	0.36845300	1.54424200
C	3.50864300	-1.64330200	-0.76689800	H	-4.08083200	0.84735800	2.20296100
C	5.58315600	-2.15640100	1.06858200	H	-4.67715200	1.59309100	0.70658900
H	5.59586100	-0.03843000	1.43594300				

Table 40: Optimized geometry for **IVd**

Free energy G = -1214.765179 Hartree/particle.

C	1.33129300	1.83907400	0.69277400	C	3.33849200	-1.58183200	-0.41909000
C	1.79245000	3.22125600	0.21686200	C	5.90138300	-1.99970100	0.62540100
C	2.55980600	2.92336600	-1.11032600	H	5.97815600	0.13527500	0.88543700
C	2.61349100	1.37355100	-1.13595900	C	3.86112800	-2.87188100	-0.34051800
C	1.23671500	1.02522500	-0.56741800	H	2.34539500	-1.42784500	-0.82438300
H	2.40306200	3.71632100	0.97649000	C	5.14005000	-3.08331200	0.18183500
H	0.90650900	3.83982700	0.05006500	H	6.89708700	-2.15868600	1.02707000
H	2.00006500	3.28615700	-1.97506900	H	3.27014700	-3.71270100	-0.69006700
H	3.55240300	3.38132900	-1.13410300	H	5.54281000	-4.08995400	0.23998600
H	2.85591100	0.93529100	-2.10394200	C	0.22793900	0.30639800	-1.08106100
C	0.35434600	1.75397400	1.82942400	H	0.46273000	-0.13074300	-2.05703600
H	0.16245800	0.72037200	2.12895600	Au	-1.66416500	-0.08547000	-0.37436600
H	0.70612700	2.32937400	2.68946800	P	-3.86388200	-0.59938000	0.33845400
H	-0.59458900	2.18169100	1.49452100	C	-5.16777600	0.46147100	-0.40852100
O	2.73567400	1.24117300	1.24282900	H	-6.15660700	0.16969600	-0.04287300
H	2.56401500	0.39796100	1.70665900	H	-4.98217500	1.50716100	-0.15129800
C	3.59796800	0.92453100	-0.03835000	H	-5.14020300	0.36030700	-1.49620200
H	4.42511600	1.62231500	0.08789500	C	-4.39105200	-2.31501800	-0.06258800
C	4.09720700	-0.48513200	0.02502700	H	-3.71965900	-3.02625600	0.42491200
C	5.38240300	-0.70817500	0.54714500	H	-5.41547200	-2.49425700	0.27669500

H	-4.33644200	-2.46906600	-1.14304300	H	-3.46937500	-1.12840300	2.68081000
C	-4.14335100	-0.45093100	2.15067800	H	-3.93238100	0.57248100	2.47064100
H	-5.17815600	-0.70134500	2.40199500				

Table 41: Optimized geometry for **TS_{5d}**

Free energy G = -1214.765017 Hartree/particle.

C	-3.62151800	-0.86291400	0.18458300	H	3.61063300	0.60014600	2.64088500
C	-2.74654400	-1.36449000	-0.99875500	C	4.63489900	1.73594600	-0.91277600
H	-3.01971100	-0.87288700	-1.93237300	H	4.08829200	2.68206700	-0.91758000
O	-2.79331300	-1.25324900	1.36291100	H	5.66422700	1.91450600	-0.58813200
C	-1.29071400	-2.03263300	0.63939900	H	4.64124700	1.33154800	-1.92788000
C	-2.80398500	-2.91218300	-1.03817600	P	3.79715900	0.54925500	0.21466900
H	-3.82355800	-3.29846300	-0.95509900	C	-0.30362700	-2.00729200	1.75383600
H	-2.38494400	-3.27510000	-1.97921300	H	0.62596000	-2.45018000	1.37763700
C	-1.90793100	-3.33501400	0.16474600	H	-0.08667700	-0.99009800	2.08123200
H	-1.08503600	-3.99181700	-0.14111700	H	-0.64098700	-2.61357300	2.59826900
H	-2.44140100	-3.86178100	0.96164700	H	-4.55311100	-1.43162000	0.24151000
H	-3.28883100	-1.83160400	1.96756600	C	-3.90895200	0.61609200	0.21783000
C	-1.32829800	-1.10665700	-0.50873900	C	-5.05558200	1.08157300	-0.44165500
C	-0.37785700	-0.27689700	-0.98256100	C	-3.05810000	1.53513200	0.84447100
H	-0.69546500	0.26410400	-1.87928600	C	-5.33820000	2.44644500	-0.48952900
Au	1.55252300	0.08063900	-0.38106600	H	-5.72875800	0.37426000	-0.91989200
C	4.89824000	-0.92395900	0.22219500	C	-3.34865600	2.90103500	0.80308500
H	5.92001800	-0.63952600	0.49022300	H	-2.18294600	1.18423500	1.37899400
H	4.52642500	-1.65555200	0.94377600	C	-4.48408500	3.36039800	0.13343000
H	4.89970400	-1.38181600	-0.77004200	H	-6.22884400	2.79435000	-1.00406500
C	4.00743800	1.28495700	1.88738900	H	-2.68677000	3.60487800	1.29906100
H	5.06476100	1.47518900	2.09396800	H	-4.70755400	4.42259900	0.10369800
H	3.45394000	2.22555700	1.94445700				

Table 42: Optimized geometry for **VId**

Free energy G = -1214.786797 Hartree/particle.

C	-3.64106700	-2.57046300	-0.75714100	C	-3.35032500	1.23308000	0.21055700
C	-3.11893800	-1.11324900	-0.78608500	C	-2.44360000	1.68885100	1.17778300
C	-1.63508700	-1.25708800	-0.43203800	C	-3.76581800	2.11558900	-0.79752400
C	-1.41127600	-2.50851400	0.16413700	C	-1.95816100	3.00027600	1.13427200
C	-2.66665800	-3.31569500	0.17484500	H	-2.13773800	1.01801800	1.97369600
H	-3.58955200	-3.00017000	-1.76205200	C	-3.27634400	3.42061900	-0.84601500
H	-3.24301200	-0.66151800	-1.77445300	H	-4.48162400	1.78108400	-1.54495600
H	-3.02606400	-3.31643800	1.21516900	C	-2.36847200	3.86719500	0.12072800
H	-2.48290400	-4.36373500	-0.08724600	H	-1.26585700	3.34309700	1.89807900
H	-4.67612900	-2.63990000	-0.41619500	H	-3.61045300	4.09361300	-1.63031200
C	-0.15977600	-3.06605800	0.71945800	H	-1.99538500	4.88653400	0.08847600
H	-0.36648100	-3.53518400	1.68853300	O	-3.73684600	-0.81355400	1.50442000
H	0.18655700	-3.87531600	0.06170000	H	-4.27991500	-0.31852400	2.13309300
H	0.63722700	-2.32828700	0.81913000	C	-0.66841600	-0.29124600	-0.69962700
C	-3.86469000	-0.19898100	0.22522400	H	-1.07778100	0.53892000	-1.28214600
H	-4.92045900	-0.19109500	-0.08569900	Au	1.31299200	-0.08510600	-0.27732200

P	3.61495200	0.29197400	0.16417600
C	4.66340400	-1.21129500	0.03122300
H	5.70876200	-0.96765500	0.24177800
H	4.31681500	-1.96225100	0.74534500
H	4.58489600	-1.62402600	-0.97744900
C	4.39270500	1.51069300	-0.96926800
H	3.87169900	2.46759200	-0.88745600
H	5.44794700	1.64936300	-0.71690400
H	4.31116100	1.15506900	-1.99912800
C	3.94284900	0.94298500	1.85133300
H	3.57232100	0.23408100	2.59566900
H	5.01597600	1.09436700	1.99878000
H	3.42217200	1.89436600	1.98377800

Table 43: Optimized geometry for **TS_{2d}**

Free energy G = -1214.750584 Hartree/particle.

C	-0.05769300	2.78452700	-0.04238800
C	1.22651700	3.29536900	0.61819000
H	1.28552400	4.38216200	0.51022200
H	1.24858800	3.04577800	1.68303900
H	2.10876300	2.84811300	0.14710600
O	-0.07410700	3.11731900	-1.43153300
H	0.76744900	2.83818400	-1.82025800
C	-1.28779600	3.46300500	0.58409400
H	-1.26014200	3.30579200	1.66798900
H	-1.17422100	4.53780800	0.41062900
C	-2.64487400	3.01453300	0.01788300
H	-3.40619800	3.70717100	0.40154300
H	-2.64318600	3.11969400	-1.07149700
C	-3.07308900	1.62111300	0.40153400
H	-3.11283400	1.40920400	1.46949500
C	-3.67021200	0.76598000	-0.47982700
C	-0.18870600	1.26673500	0.08759000
C	-1.14718600	0.43747100	0.15361900
H	-1.54441300	-0.55623400	0.23936000
P	3.40553400	-1.41894500	-0.04082900
C	4.84618100	-0.63736700	0.78432000
H	5.07790000	0.31189900	0.29580200
H	4.60482100	-0.44388500	1.83208700
H	5.71852200	-1.29476800	0.72839900
C	3.19985400	-3.04562200	0.78432100
H	2.92857900	-2.89082200	1.83114500
H	2.40133000	-3.60645900	0.29318000
H	4.13060500	-3.61787100	0.73122400
C	3.97142500	-1.80410900	-1.74368900
H	3.18539700	-2.34414700	-2.27671500
H	4.18340500	-0.87449100	-2.27691300
H	4.87610000	-2.41796400	-1.71272200
Au	1.48319700	-0.08934200	0.03356400
H	-3.67005700	1.05809100	-1.52959600
C	-4.27555200	-0.53053000	-0.19877100
C	-4.73749100	-1.30385100	-1.28412500
C	-4.41363800	-1.05426100	1.10502400
C	-5.31623700	-2.55356000	-1.07788900
H	-4.63900500	-0.91245600	-2.29295500
C	-4.98861900	-2.30499900	1.30744600
H	-4.08364000	-0.47774400	1.96334800
C	-5.44185900	-3.05863800	0.21869600
H	-5.66819200	-3.13286700	-1.92584800
H	-5.09057700	-2.69295100	2.31630800
H	-5.89335400	-4.03234800	0.38258100

Table 44: Optimized geometry for **IIId**

Free energy G = -1214.772281 Hartree/particle.

P	-3.36145500	-1.26451100	-0.01875300
C	-4.40509500	-1.10644100	-1.52373100
H	-5.29699900	-1.73367700	-1.43722200
H	-4.70775200	-0.06410900	-1.65000600
H	-3.83036100	-1.41286400	-2.40105300
C	-3.04993300	-3.06777400	0.14712900
H	-2.45552900	-3.41507200	-0.70137100
H	-2.49163600	-3.25899300	1.06676300
H	-3.99491500	-3.61803700	0.17649300
C	-4.48855000	-0.85451300	1.37316600
H	-3.96533900	-0.99496900	2.32205200
H	-4.79904900	0.19033500	1.29599100
H	-5.37301100	-1.49741000	1.34890600
Au	-1.38786700	0.04692400	-0.08633000
C	1.46050500	0.60160900	-0.78445300
C	0.48051100	2.54834400	0.45697400
C	2.75095800	1.42676400	-1.06707600
H	1.38113500	-0.34474700	-1.30559700
C	1.20681500	3.42181300	-0.59881700
C	2.63835300	2.94509400	-0.86889000
H	3.20579500	1.11146200	-2.00336300
H	1.21992600	4.46267500	-0.25509100
H	0.61866700	3.40512700	-1.52345200
H	3.28693900	3.24309700	-0.04108300

H	3.01917600	3.43929600	-1.76669100
C	0.35865400	1.13530000	-0.13410200
C	-0.87643200	3.15633000	0.81793400
H	-1.39178600	2.53088000	1.55189100
H	-0.73729400	4.15656400	1.24464100
H	-1.51273500	3.25355000	-0.06673800
O	1.27739200	2.41390900	1.65029700
H	1.34598700	3.28893200	2.06000800
C	3.00941700	0.58457800	0.08704000
C	3.67454200	-0.71957900	0.09930900
C	3.87977200	-1.34393200	1.34577600
C	4.13955300	-1.35763800	-1.06778500
C	4.53754900	-2.56832300	1.42527200
H	3.52252300	-0.85837100	2.24947500
C	4.79221700	-2.58343100	-0.98459700
H	3.99899900	-0.89676300	-2.04019000
C	4.99325300	-3.19097900	0.26003800
H	4.69388300	-3.03670500	2.39176800
H	5.15039800	-3.06534900	-1.88872200
H	5.50525300	-4.14647500	0.31971000
H	2.83932900	1.04770400	1.05277900

Table 45: Optimized geometry for **TS_{4d}**

Free energy G = -1214.751493 Hartree/particle.

C	3.47614900	2.62790600	0.22645200
C	2.88869800	1.47469900	-0.55651500
C	1.00533600	2.78719700	0.21962100
C	2.27398400	3.21050100	1.00161500
H	4.29832300	2.31376800	0.87459100
H	3.88937600	3.34865000	-0.48834000
H	2.33206500	4.29442600	1.11753800
H	2.20980400	2.77485300	2.00241400
C	0.55587100	3.83859900	-0.81514700
H	-0.29112000	3.47276700	-1.40428200
H	0.24562400	4.73709300	-0.27522500
H	1.36385600	4.10680900	-1.50224200
C	1.46555200	1.57652500	-0.60653000
C	0.79357100	0.31259700	-0.77953900
H	1.13365700	-0.23725300	-1.65817900
P	-3.40173700	-0.75683200	0.23053200
C	-4.58098000	-0.41501300	-1.13706100
H	-5.59249400	-0.72420300	-0.85839000
H	-4.57896400	0.65420600	-1.36265400
H	-4.26940900	-0.96144100	-2.03060700
C	-3.61462800	-2.54573800	0.59266000
H	-3.29264500	-3.13442800	-0.26967700
H	-2.99982700	-2.82000700	1.45328600
H	-4.66322500	-2.76743800	0.81163800
C	-4.11612100	0.09737600	1.69255800
H	-3.50687300	-0.11810200	2.57370500
H	-4.11744600	1.17678100	1.52338300
H	-5.14076500	-0.24184500	1.87009200
Au	-1.17830300	-0.14991900	-0.26778000
O	-0.01873700	2.50648000	1.15117900
H	-0.79468300	2.16707900	0.67278400
C	2.05521500	0.19101400	0.24928400
H	3.46872400	0.97360400	-1.32455300
H	1.81654900	0.42677800	1.28132000
C	2.86987600	-1.08062100	0.13121900
C	3.27278500	-1.67469200	1.33511900
C	3.22155200	-1.68310700	-1.08266800
C	4.00922200	-2.86095100	1.32311600
H	3.00819800	-1.21380300	2.28218400
C	3.96015000	-2.86665200	-1.08922600
H	2.92948900	-1.24176800	-2.03108000
C	4.35524800	-3.46047500	0.11191800
H	4.31078700	-3.31136100	2.26378100
H	4.22546800	-3.32368400	-2.03746200
H	4.92852000	-4.38219000	0.10197100

Table 46: Optimized geometry for **Vd**

Free energy G = -1214.824362 Hartree/particle.

C	3.97892500	-1.87571600	1.56653500
C	3.14531600	-1.11879600	-0.63245600
C	4.33428200	-0.97904600	0.35742700
H	4.29773400	-1.45179400	2.52557700
H	4.45364300	-2.86481500	1.49670700
H	5.29429300	-1.23408200	-0.09994800
H	4.37753100	0.06790900	0.67313500
C	3.42347800	-2.14139100	-1.74490800
H	2.54063800	-2.29752900	-2.37236500
H	4.23833100	-1.78863200	-2.38788700
H	3.72404700	-3.10543100	-1.32369200
C	2.00878300	-1.57290500	0.28282900
P	-0.54364900	2.92019200	-0.00742100
C	0.70686700	3.81452700	-1.00711500
H	0.48464800	4.88557000	-1.01551600
H	1.69816100	3.65198400	-0.57831400

H	0.69813700	3.43330900	-2.03075600	C	0.62031600	-1.58653400	-0.18847000
C	-2.16802300	3.35701300	-0.73637600	H	0.49234000	-1.70497300	-1.26308500
H	-2.22268800	2.97414300	-1.75799500	H	-0.33383800	-1.62736900	1.70375500
H	-2.96701400	2.90240500	-0.14637800	C	-1.87223600	-2.02071700	0.22748200
H	-2.29595800	4.44303500	-0.74748800	C	-2.86519200	-2.04755900	1.22480300
C	-0.50919700	3.71298500	1.64536300	C	-2.23377600	-2.35083900	-1.09357200
H	-1.27994100	3.27133800	2.28087900	C	-4.18158300	-2.38401000	0.91342800
H	0.46687400	3.54817900	2.10710700	H	-2.59668800	-1.80543200	2.24963900
H	-0.68985600	4.78762700	1.54880800	C	-3.54942300	-2.68354200	-1.40190100
Au	-0.17271900	0.62395000	0.06660700	H	-1.48769700	-2.35695500	-1.88178400
O	2.76537100	0.13822100	-1.21732200	C	-4.52846400	-2.69990900	-0.40165600
H	3.42531600	0.37118300	-1.88558700	H	-4.93326500	-2.40204300	1.69645400
C	2.48366200	-2.00976500	1.46471700	H	-3.81258400	-2.93920300	-2.42371700
H	1.88222900	-2.46368000	2.24672600	H	-5.55236700	-2.96430800	-0.64729800
C	-0.49797700	-1.66898600	0.62736400				

Table 47: Optimized geometry for **TS_{6d}**

Free energy G = -1214.748199 Hartree/particle.

C	-1.03238000	2.37925200	-0.59644700	C	-4.57531700	-2.34807900	-1.17494600
C	-0.31097300	2.67926000	0.75086000	H	-2.93093000	-1.12283600	-1.82953600
C	-1.09386900	1.94207500	1.85304300	C	-5.58388100	-2.52436000	-0.22580700
C	-1.64373100	0.67317600	1.21699300	H	-6.51265900	-1.73364700	1.55467900
C	-1.60458900	0.95749800	-0.41732500	H	-4.46995800	-3.05010500	-1.99636900
H	-0.26370300	3.75905900	0.91569700	H	-6.26248400	-3.36833600	-0.30328800
H	0.71495200	2.30475400	0.70702300	C	-0.74836900	-0.11473500	0.05433700
H	-0.46043600	1.68482600	2.70655300	H	-1.24214500	-1.08351700	0.00553900
H	-1.92286500	2.54848100	2.23037700	Au	1.32769200	-0.32125700	0.04372800
H	-2.05685200	-0.12269200	1.82374800	P	3.65070300	-0.70777900	0.01281900
C	-0.12311300	2.46979000	-1.82591700	C	4.66092100	0.65015100	0.72888000
H	-0.70056800	2.29212400	-2.73711100	H	5.72547400	0.40416100	0.67527500
H	0.30953100	3.47408600	-1.88189000	H	4.47548000	1.57443900	0.17625900
H	0.69428800	1.74644100	-1.77325000	H	4.37836200	0.80379300	1.77313700
O	-2.15949900	3.24208700	-0.75719400	C	4.16108800	-2.20763100	0.94431600
H	-1.82685500	4.14062400	-0.88732200	H	3.66689100	-3.08540000	0.52081500
C	-2.95010700	0.85551300	0.07159500	H	5.24535500	-2.34205200	0.89178000
H	-3.46492700	1.80633400	0.17331000	H	3.85997800	-2.10781500	1.99001400
C	-3.82994200	-0.34547000	-0.02532800	C	4.33280000	-0.95242000	-1.67617800
C	-4.85726100	-0.51968600	0.91533300	H	5.41148100	-1.12866600	-1.63289000
C	-3.70097900	-1.26433000	-1.07721700	H	3.84467300	-1.80958200	-2.14621000
C	-5.72451700	-1.60636900	0.81900800	H	4.13606100	-0.06374700	-2.28074500
H	-4.97502800	0.19670400	1.72392500				

Table 48: Optimized geometry for **TS_{7d}**

Free energy G = -1214.752285 Hartree/particle.

C	-1.26756400	2.50686500	-0.59582300	C	-1.18118000	1.00305000	1.71348500
C	-1.30456200	3.28628100	0.74110100	C	-1.69621000	1.06327200	-0.25851700
C	-0.72773000	2.41897400	1.88487700	H	-2.35671100	3.49744400	0.95309900

H	-0.77065400	4.24009200	0.67490200	H	-6.81364000	-1.65645200	0.38288800
H	0.36748600	2.43003800	1.84487300	H	-3.29022600	-4.02512300	-0.31269300
H	-1.04232700	2.80810300	2.85510500	H	-5.70354700	-3.88111200	0.26885500
H	-1.88434300	0.60725900	2.44953600	C	-0.76653000	0.17300400	0.63419100
C	0.09509700	2.59660000	-1.29766700	H	-1.21707600	-0.81050600	0.74063700
H	0.10259300	1.97463700	-2.19686300	Au	1.28707700	-0.19950700	0.18851900
H	0.28027100	3.63541600	-1.59198200	P	3.51336100	-0.82265500	-0.21692400
H	0.91939000	2.28297200	-0.65227700	C	3.99919700	-2.37079100	0.64359000
O	-2.26346900	3.04099600	-1.47308200	H	5.04208200	-2.61713700	0.42374800
H	-2.02073700	3.95631100	-1.66794000	H	3.87810900	-2.24089100	1.72167300
C	-2.94106900	0.63710000	-0.62326700	H	3.35619900	-3.19048600	0.31445500
H	-3.50030800	1.34933000	-1.22477100	C	3.89210000	-1.12743200	-1.98858200
C	-3.64084200	-0.62851000	-0.36655600	H	3.71648300	-0.21442700	-2.56251400
C	-5.02260800	-0.56764200	-0.09050600	H	4.93525700	-1.43434900	-2.10785000
C	-3.03234900	-1.89611500	-0.45256000	H	3.23769200	-1.91390300	-2.37188000
C	-5.75459100	-1.72618200	0.15386800	C	4.75327200	0.42006700	0.32414500
H	-5.51415800	0.40058500	-0.05377600	H	5.76586400	0.06386200	0.11339000
C	-3.77364200	-3.05649000	-0.22819700	H	4.58441300	1.36124200	-0.20441000
H	-1.99245300	-1.98078700	-0.74922100	H	4.64895300	0.59575400	1.39741000
C	-5.13084500	-2.97620500	0.08993400				

Table 49: Optimized geometry for **VIId**

Free energy G = -1214.818377 Hartree/particle.

C	1.33594700	2.61032400	0.75397500	C	4.22013100	-2.27156000	-1.37039600
C	0.92121300	3.54482200	-0.40511300	H	3.45530500	-0.31500800	-1.81459000
C	-0.20337900	2.98104300	-1.28700500	C	4.53430200	-3.19890300	-0.37465000
C	0.05407900	1.53440200	-1.65239900	H	4.54653800	-3.59244300	1.74741100
C	1.75110000	1.25258000	0.17190700	H	4.43758500	-2.49452100	-2.41077100
H	1.81383900	3.71319400	-1.01781700	H	4.98462900	-4.15117800	-0.63802100
H	0.62341800	4.51542400	0.00672700	C	0.99994800	0.77402500	-0.98857200
H	-1.17840900	3.08678600	-0.79500500	H	1.28875300	-0.18353000	-1.41087700
H	-0.27794700	3.56225800	-2.21255800	Au	-1.23019400	-0.00469700	-0.41330700
H	-0.31915000	1.17595300	-2.61035100	P	-2.97729500	-1.26985800	0.46471800
C	0.21661600	2.45814900	1.80076900	C	-4.62285100	-0.56066900	0.07635200
H	0.57360000	1.84869600	2.63537400	H	-5.40941000	-1.19904900	0.48889900
H	-0.07653500	3.44249800	2.18444800	H	-4.70169400	0.43893900	0.50972900
H	-0.67963300	1.98289500	1.38856300	H	-4.74492400	-0.48772000	-1.00662200
O	2.49579800	3.15276400	1.39349200	C	-3.00978500	-2.98368500	-0.18486000
H	2.21775100	3.94155800	1.87944700	H	-2.08205700	-3.49374600	0.08367800
C	2.77060700	0.55276700	0.72977600	H	-3.85966300	-3.52637600	0.23882200
H	3.20752100	0.98955500	1.62460700	H	-3.09990900	-2.96095500	-1.27324600
C	3.36348000	-0.72623700	0.30806900	C	-2.92759200	-1.43021500	2.29044400
C	3.72382200	-1.65671600	1.30358400	H	-3.77065500	-2.03631300	2.63457400
C	3.64369100	-1.04602300	-1.03480400	H	-1.99180300	-1.90622600	2.59144000
C	4.28850100	-2.88446900	0.96542300	H	-2.98395400	-0.43933500	2.74627100
H	3.54619800	-1.41234700	2.34745100				

Table 50: Optimized geometry for **TS1d'**

Free energy G = -1214.75568 Hartree/particle.

C	-1.01732200	2.69402900	0.18119700	H	5.53404800	-0.85534600	-1.54795700
C	0.01197000	2.95826800	1.29954800	C	4.64989600	0.50689000	1.04783600
H	0.12617100	4.03908700	1.41698900	H	4.53741600	1.52060400	0.65641700
H	-0.31684400	2.52615700	2.24776800	H	4.28271500	0.48320100	2.07653300
H	0.98313500	2.52602200	1.04027400	H	5.70779800	0.22900200	1.03369000
O	-0.59227800	3.28156400	-1.04982000	C	4.05396600	-2.32441400	0.69793900
H	0.26194000	2.89330300	-1.28964400	H	3.67989800	-2.39393500	1.72203300
C	-2.37041500	3.33948900	0.51727900	H	3.56046500	-3.08712900	0.09111500
H	-2.68241200	2.99850800	1.50932700	H	5.13374500	-2.49878300	0.69342600
H	-2.23361700	4.42354700	0.56469000	Au	1.37781900	-0.20781600	-0.03175200
C	-3.41684300	2.94728600	-0.53781700	H	-4.12425800	0.97844200	1.17372500
H	-4.40798800	3.28116700	-0.21159800	C	-3.90523500	-0.87620700	0.09861400
H	-3.19360100	3.45068300	-1.48021100	C	-4.27268200	-1.62026800	1.24026400
C	-3.40105300	1.45110100	-0.74745900	C	-3.61898700	-1.57603000	-1.09518800
H	-3.17621100	1.09046600	-1.74721700	C	-4.35056800	-3.00863000	1.19400900
C	-3.82403000	0.57201800	0.20801200	H	-4.49654400	-1.09507500	2.16472600
C	-1.18523600	1.21864900	-0.01270800	C	-3.69560000	-2.96613600	-1.13690300
C	-0.71573700	0.03927000	-0.12972200	H	-3.35820200	-1.03287800	-1.99760500
H	-1.26250800	-0.87994000	-0.32844000	C	-4.05998900	-3.68595200	0.00523300
P	3.67514500	-0.66126500	0.02081400	H	-4.63690900	-3.56433400	2.08143000
C	4.46894000	-0.62120400	-1.63350500	H	-3.47848800	-3.48899200	-2.06317000
H	3.98880200	-1.35247400	-2.28779200	H	-4.12222400	-4.76917600	-0.03273600
H	4.35058600	0.37286900	-2.07075500				

Table 51: Optimized geometry for **IId'**

Free energy G = -1214.772564 Hartree/particle.

C	-0.85719100	2.45675900	0.42894200	H	5.77672700	0.44622100	-0.16843800
C	-0.36174800	2.24337800	1.86134200	C	4.10071900	-1.11356600	1.84928500
H	-0.02475200	3.19810900	2.27602600	H	3.83244400	-0.27804900	2.50005900
H	-1.15175000	1.84534600	2.50551200	H	3.55507600	-2.00190300	2.17635300
H	0.47673200	1.53965000	1.88055400	H	5.17577400	-1.30047700	1.92547100
O	0.19640700	2.98510000	-0.38954500	C	4.27681300	-2.13096500	-0.87036200
H	0.88487300	2.30209000	-0.44875700	H	3.72919700	-3.03673000	-0.59902900
C	-2.02442000	3.45960800	0.33463800	H	4.12319000	-1.93456100	-1.93407700
H	-2.63505300	3.40981400	1.24175700	H	5.34325800	-2.28278500	-0.68044700
H	-1.63769600	4.47827600	0.26325200	Au	1.33144400	-0.29216200	-0.19651600
C	-2.83848300	3.04756300	-0.90104600	H	-3.33955400	1.26300200	1.11896100
H	-3.87406200	3.39649700	-0.87156900	C	-3.77701700	-0.59856900	0.13542300
H	-2.37651500	3.43661300	-1.81201900	C	-4.11165300	-1.21249900	1.36415500
C	-2.76369100	1.51695700	-0.95032500	C	-3.99450700	-1.30913200	-1.06688000
H	-2.88519600	1.07274600	-1.93436300	C	-4.63911300	-2.49722000	1.39075000
C	-3.26963700	0.75455200	0.16108300	H	-3.95271200	-0.66934500	2.29124900
C	-1.37373200	1.17353800	-0.26581900	C	-4.52047300	-2.59567000	-1.03277200
C	-0.66942300	0.03880100	-0.50577100	H	-3.77217700	-0.85101400	-2.02432500
H	-1.23393400	-0.77682500	-0.96357800	C	-4.84029300	-3.19169800	0.19235500
P	3.64347800	-0.71510200	0.11462200	H	-4.89451300	-2.95970400	2.33841500
C	4.72621500	0.69853900	-0.33912600	H	-4.68996800	-3.13380600	-1.95956200
H	4.58054000	0.94747400	-1.39311800	H	-5.25307600	-4.19553600	0.21231400
H	4.46147300	1.56914100	0.26594200				

Table 52: Optimized geometry for TS_{6d},

Free energy G = -1214.733990 Hartree/particle.

C	1.40128500	1.32618300	0.35624900	H	-5.79722100	-0.81958300	1.46361900
C	2.66986200	2.17435700	0.48501400	C	-4.37417500	1.77391600	0.72980000
H	2.42694700	3.05129600	1.09494300	H	-3.85927000	1.94269300	1.67874200
H	3.48032800	1.64325600	0.98452200	H	-4.03226500	2.52059600	0.00899500
H	3.01902300	2.52308000	-0.48890500	H	-5.45218500	1.88280200	0.87974900
O	0.36821500	2.13328100	-0.21472400	C	-5.01468900	-0.10082300	-1.39816400
H	0.27403300	2.92129500	0.33861600	H	-4.68192300	0.60539100	-2.16273500
C	0.97323000	0.70812600	1.73251600	H	-4.90575300	-1.11521200	-1.78947600
H	1.38850200	1.28243100	2.56461800	H	-6.06708100	0.08632600	-1.16572300
H	-0.11615700	0.77289200	1.78723000	Au	-1.68941600	-0.29298100	-0.27648800
C	1.41050900	-0.76612800	1.77067400	H	2.55323200	-1.44714000	-1.55516700
H	2.40613200	-0.88014200	2.20739900	C	4.08900900	-0.44328900	-0.41738400
H	0.72613900	-1.37440800	2.36943200	C	4.83630300	0.41284000	-1.24190600
C	1.40861200	-1.28706000	0.34027400	C	4.73680600	-1.14338600	0.60895200
H	1.52672400	-2.34817800	0.15398900	C	6.19955200	0.59463100	-1.01460000
C	2.65701500	-0.70685300	-0.76169000	H	4.35022800	0.93595900	-2.06013700
C	1.49106300	0.10842400	-0.59397800	C	6.10196700	-0.95339400	0.83664400
C	0.30288200	-0.73774100	-0.71775100	H	4.18632200	-1.84587400	1.22597900
H	0.39183800	-1.43388600	-1.55330100	C	6.83470300	-0.08224100	0.03003000
P	-3.97618800	0.09071300	0.10628600	H	6.76508700	1.26397500	-1.65548800
C	-4.73414900	-1.04492900	1.33752100	H	6.59021500	-1.49480000	1.64102400
H	-4.62149400	-2.07793900	0.99958600	H	7.89593200	0.06242000	0.20727500
H	-4.22505900	-0.93447200	2.29806800				

Table 53: Optimized geometry for **TS_{7d}**,

Free energy G = -1214.76003199 Hartree/particle.

C	-1.48873500	1.21865700	1.12469800	H	-0.39625500	0.34884200	-2.16475100
C	-2.81125200	1.83405300	1.61672400	P	3.57025400	-0.94233700	0.26520600
H	-2.68783200	2.15163300	2.65768100	C	5.03622400	0.14491400	0.05994800
H	-3.07262800	2.71951600	1.02977100	H	5.13874200	0.42730100	-0.99048000
H	-3.64423700	1.13618200	1.57045900	H	4.90530100	1.05096400	0.65636700
O	-1.11745900	0.09490700	1.93881800	H	5.94233800	-0.37469200	0.38510300
H	-1.05407600	0.40123600	2.85570700	C	3.61024100	-1.45656800	2.02804300
C	-0.39179400	2.31893600	1.17512600	H	3.46049700	-0.58308200	2.66694100
H	-0.52179900	2.95436400	2.05507900	H	2.80700200	-2.17232100	2.21810100
H	0.58372400	1.82936400	1.25846400	H	4.57252000	-1.91912900	2.26666800
C	-0.46085600	3.13619600	-0.11178400	C	3.97274400	-2.46428400	-0.68044300
H	-1.29677900	3.84496900	-0.12071600	H	3.17744700	-3.20001700	-0.53980200
H	0.44136200	3.75200200	-0.25692600	H	4.04461100	-2.22475900	-1.74403000
C	-0.54442800	2.23385100	-1.29317500	H	4.92219400	-2.88696100	-0.33925800
H	-0.85073900	2.68232600	-2.24063200	Au	1.55291200	0.04130300	-0.40633900
C	-2.61217500	0.15496300	-0.98698900	H	-2.51121600	0.11974200	-2.07082800
C	-1.55760500	0.71474000	-0.32272800	C	-3.81189300	-0.53260300	-0.50712900
C	-0.25985400	0.85379200	-1.20720600	C	-3.89575100	-1.17459100	0.74676600

C	-4.90745900	-0.63488400	-1.39016900	C	-6.14381600	-1.92191400	0.23815900
C	-5.05280000	-1.85927600	1.11073900	H	-5.10083800	-2.35487500	2.07580200
H	-3.04366700	-1.14489200	1.41762600	H	-6.90542600	-1.36345200	-1.70272800
C	-6.06689200	-1.30797500	-1.01526400	H	-7.04265000	-2.45789400	0.52775600
H	-4.84518800	-0.17158500	-2.37115200				

Optimization studies for Ib (R= H)

In order to find the optimal conditions to carry out our computational studies, the following conditions were also evaluated using of gold(I) complex **Ib** as model substrate.[38]

Conditions B:

Coordinates and energies for the the cyclization of **Ib** calculated at the B3LYP/6-31G(d,p) (C, H, P, O), SDD(Au) level taking into account solvent effect of CH_2Cl_2 (SMD) and employing PMe_3 as the phosphine.

Conditions C:

Coordinates and energies for the the cyclization of **Ib** calculated at the B3LYP/6-311++G(d,p) (C, H, P, O), SDD(Au) level taking into account solvent effect of CH_2Cl_2 (IEF-PCM) and employing PMe_3 as the phosphine.

Conditions D:

Coordinates and energies for the the cyclization of **Ib** calculated at the M06/6-31G(d,p) (C, H, P, O), SDD(Au) level taking into account solvent effect of CH_2Cl_2 (IEF-PCM) and employing PMe_3 as the phosphine.

Conditions E:

Coordinates and energies for the the cyclization of **Ib** calculated at the M06/6-31G(d,p) (C, H, P, O), SDD(Au) level taking into account solvent effect of CH_2Cl_2 (SMD) and employing PMe_3 as the phosphine.

38 The corresponding coordinates and energies of all the optimized structures found for each scenario are described on the supporting information of Calleja, P.; Pablo, O.; Ranieri, B.; Gaydou, M.; Pitaval, A.; Moreno, M.; Raducan, M.; Echavarren, A. M. *Chem.–Eur. J.* **2016**, *22*, 13613–13618, and are available online. However, these data have not been included in this manuscript due to space constraints.

Conditions F:

Coordinates and energies for the the cyclization of **Ib** calculated at the M06/6-311++G(d,p) (C, H, P, O), SDD(Au) level taking into account solvent effect of CH_2Cl_2 (IEF-PCM) and employing PMe_3 as the phosphine.

Conditions G:

Coordinates and energies for the the cyclization of **Ib** calculated at the wB97XD/6-31G(d,p) (C, H, P, O), SDD(Au) level taking into account solvent effect of CH_2Cl_2 (IEF-PCM) and employing PMe_3 as the phosphine.

Ligand effect

Evaluation on the ligand effect for the computed trends of gold(I) complex **Ib**.

Conditions H:

Coordinates and energies for the the cyclization of **Ib** calculated at the B3LYP/6-31G(d,p) (C, H, P, O), SDD(Au) level taking into account solvent effect of CH_2Cl_2 (IEF-PCM) and employing PPh_3 as the phosphine. ΔG energies are given in $kcal \cdot mol^{-1}$.

Table 54: Optimized geometry for **Ib**

Free energy G = -1637.415168 Hartree/particle.

C	-3.37344100	-1.93342900	0.12781500	H	-4.64014200	4.16917700	-0.82893900
C	-3.27046000	-3.44815800	-0.12992700	C	-2.71486100	-1.22475100	-1.01820700
H	-3.72537700	-3.98031100	0.70974400	C	-2.31026600	-0.74996900	-2.08029900
H	-3.79153800	-3.72662900	-1.04929600	H	-2.19547500	-0.35909400	-3.07187200
H	-2.22417700	-3.75749200	-0.22210400	P	1.60445200	0.08925000	0.07349600
O	-2.74171400	-1.58556000	1.35792900	Au	-0.50420600	-0.45972500	-0.76439200
H	-1.95762700	-2.14228100	1.46829200	C	1.58576200	1.61766100	1.07841700
C	-4.85832800	-1.50697800	0.23695400	C	0.45585500	1.91310600	1.85915500
H	-5.33505400	-1.65882600	-0.73823600	C	2.69203300	2.48117900	1.10280900
H	-5.31448500	-2.22466700	0.92745000	C	0.44009100	3.05316000	2.66243800
C	-5.13669000	-0.08413800	0.75769800	H	-0.41053600	1.25830800	1.83682700
H	-6.20664900	-0.06300400	1.01263300	C	2.66702800	3.62305900	1.90552700
H	-4.59998100	0.06253100	1.69770700	H	3.56713600	2.26884900	0.49747100
C	-4.85925200	1.02587400	-0.22299700	C	1.54441800	3.90904800	2.68517800
H	-5.24104800	0.84664200	-1.22990900	H	-0.43626700	3.27543200	3.26317000
C	-4.26566800	2.20962200	0.00564400	H	3.52469900	4.28832700	1.91832500
C	-3.70782300	2.65342100	1.33625800	H	1.52767700	4.79956500	3.30596500
H	-3.74895700	1.87881700	2.10409300	C	2.27367100	-1.25115300	1.12496800
H	-2.66315100	2.97315800	1.22975400	C	2.97822000	-0.97543100	2.30609100
H	-4.25926900	3.52587300	1.71105600	C	2.08670600	-2.58470800	0.72199600
C	-4.13413600	3.23263100	-1.09846300	C	3.49091600	-2.02467800	3.07203900
H	-3.08114500	3.49218000	-1.27270100	H	3.12664200	0.04899300	2.63026500
H	-4.55974700	2.87613700	-2.04069800	C	2.60684400	-3.62657900	1.48835400

H	1.53821800	-2.80728400	-0.18903500	C	3.31879400	1.39345800	-3.41614700
C	3.30721100	-3.34736200	2.66540900	H	1.41570200	1.56589300	-2.43199800
H	4.03317700	-1.80505100	3.98640400	C	4.99654000	0.07582800	-2.27429200
H	2.46053300	-4.65405900	1.17002800	H	4.41098400	-0.77916100	-0.38861800
H	3.70581100	-4.15991500	3.26498300	C	4.60854000	0.85656200	-3.36410900
C	2.80482900	0.36315200	-1.28158400	H	3.01312600	1.99963300	-4.26323900
C	2.41703000	1.14669500	-2.38231000	H	5.99724200	-0.34258100	-2.23086800
C	4.10001400	-0.17222200	-1.23214800	H	5.30742900	1.04538800	-4.17314900

Table 55: Optimized geometry for **TS_{1b}**

Free energy G = -1637.406000 Hartree/particle.

C	3.75370000	1.49366200	0.08871200	C	-3.48494800	2.31324100	-0.20636600
C	2.55921500	2.45870600	-0.09379200	C	-2.37641200	3.01800700	-2.67679300
H	2.89289600	3.45918300	0.19341100	H	-1.16149500	1.25476800	-2.47091100
H	2.21644900	2.47695000	-1.13058700	C	-3.91600600	3.46668900	-0.86543100
H	1.72189600	2.16697100	0.54610100	H	-3.91875400	2.04917700	0.75243000
O	4.21928200	1.52038700	1.43618000	C	-3.36486800	3.81931200	-2.09866400
H	3.49688700	1.24203100	2.01765300	H	-1.94181600	3.29126500	-3.63340700
C	4.93726100	1.93607700	-0.78658300	H	-4.68199600	4.08832600	-0.41217100
H	4.59886800	1.99008700	-1.82642500	H	-3.70087800	4.71815700	-2.60655900
H	5.23866700	2.94161300	-0.47867800	C	-2.39944400	0.07921500	1.78530100
C	6.09827900	0.93688900	-0.64943800	C	-1.55929500	0.77424600	2.67184400
H	6.86081500	1.16537900	-1.40285000	C	-3.58646900	-0.49422600	2.26491700
H	6.56519400	1.04686200	0.33016600	C	-1.90856700	0.90124000	4.01566000
C	5.58453100	-0.45732200	-0.86181000	H	-0.63310800	1.21366900	2.31191600
H	5.31189500	-0.70425300	-1.88747500	C	-3.92780100	-0.36883400	3.61344500
C	5.55169500	-1.47258900	0.05012100	H	-4.24292400	-1.03785000	1.59367000
C	5.99691700	-1.35219100	1.48209100	C	-3.09230400	0.32791000	4.48829000
H	6.96898800	-1.84760000	1.60383100	H	-1.25389900	1.44019000	4.69361200
H	6.08232200	-0.32094700	1.82090600	H	-4.84679600	-0.81771500	3.97749600
H	5.29703200	-1.87612400	2.14200000	H	-3.35969200	0.42087800	5.53645100
C	5.09934000	-2.84206300	-0.36808200	C	-2.88573200	-1.40379200	-0.70840600
H	4.24867500	-3.17519000	0.24080400	C	-4.12875100	-1.17901200	-1.31964400
H	4.82482200	-2.88965600	-1.42439700	C	-2.37605700	-2.71100200	-0.63591300
H	5.90115200	-3.56966700	-0.19014700	C	-4.85217500	-2.25110800	-1.84595800
C	3.31999700	0.11457500	-0.28729000	H	-4.53141700	-0.17387700	-1.39000300
C	2.45041200	-0.79381300	-0.49499000	C	-3.10545500	-3.77811100	-1.15960900
H	2.62038500	-1.82739600	-0.77622300	H	-1.40968300	-2.89329200	-0.17395100
P	-1.91210800	-0.03498500	0.02209700	C	-4.34327000	-3.54890300	-1.76620100
Au	0.39884800	-0.35945000	-0.24261100	H	-5.81201100	-2.06937100	-2.31954500
C	-2.49344500	1.50501100	-0.78270900	H	-2.70396600	-4.78505600	-1.10068900
C	-1.93751800	1.86822100	-2.02126000	H	-4.90716500	-4.37945900	-2.17970900

Table 56: Optimized geometry for **IIb**

Free energy G = -1637.417530 Hartree/particle.

C	4.88394500	-1.37792300	0.14671200	H	5.23097500	-0.77930500	-1.87274300
C	5.09016800	-0.36437200	-0.87584600	C	5.11219800	-1.16702400	1.61591300

H	4.91809500	-2.08806600	2.16731500	H	-3.64402200	0.89012700	2.19187300
H	6.15942500	-0.87809900	1.77358900	C	-1.77939100	4.01153100	0.83156500
H	4.48375500	-0.37695900	2.02819900	H	-0.75816600	2.65394300	-0.48679400
C	4.68846600	-2.79713800	-0.28156800	C	-2.72479300	4.14702000	1.85187600
H	5.66293100	-3.27663400	-0.09829400	H	-4.12578900	3.12210100	3.13176000
H	3.95621600	-3.32710600	0.33131800	H	-1.25568900	4.88384900	0.45267400
H	4.46448800	-2.91344500	-1.34170700	H	-2.93739800	5.12685100	2.26855200
O	2.90087800	1.35382400	1.40673200	C	-2.42814300	-1.27920000	1.19327400
C	3.58317700	1.37711300	0.15182400	C	-3.70917400	-1.83498400	1.05878200
C	5.89474900	0.90544100	-0.57791300	C	-1.60557000	-1.69034100	2.25604600
H	6.89230400	0.66979200	-0.19601300	C	-4.16039500	-2.78488500	1.97773500
H	6.02944000	1.44006400	-1.52231700	H	-4.35361500	-1.53239700	0.24003200
C	5.06206300	1.74286300	0.41022700	C	-2.06353400	-2.63483600	3.17429200
H	5.23525200	2.81311600	0.27679800	H	-0.60802400	-1.27346500	2.36425800
H	5.31406900	1.50907700	1.44585500	C	-3.34081100	-3.18441700	3.03509300
H	1.99030200	1.06039200	1.23607600	H	-5.15239100	-3.21144100	1.86488100
C	3.59451700	-0.00626800	-0.54503700	H	-1.42125500	-2.94576800	3.99257600
C	2.49494000	-0.74328800	-0.84982800	H	-3.69402500	-3.92457600	3.74665900
H	2.67556700	-1.69758700	-1.34192100	C	-2.82653200	-0.12906000	-1.47900800
Au	0.52375800	-0.33944900	-0.44231400	C	-2.44899700	-1.03147300	-2.48757600
P	-1.78899300	-0.01274600	0.02940700	C	-3.98627600	0.64365000	-1.64395400
C	2.92909000	2.39695100	-0.79805500	C	-3.22628000	-1.16486200	-3.63802500
H	3.49091600	2.48495800	-1.73343300	H	-1.54780800	-1.62750000	-2.37385300
H	1.90397700	2.10448000	-1.04557900	C	-4.75799100	0.50947000	-2.79994400
H	2.91088700	3.37470400	-0.30778700	H	-4.28687100	1.35009000	-0.87703400
C	-2.17109200	1.61601700	0.78309500	C	-4.38058300	-0.39358900	-3.79594700
C	-3.11969700	1.75846600	1.80675500	H	-2.92640600	-1.86436300	-4.41233200
C	-1.49901300	2.75241200	0.30172200	H	-5.65270100	1.11251000	-2.92069000
C	-3.39203000	3.02124400	2.33790200	H	-4.98150700	-0.49336700	-4.69475200

Table 57: Optimized geometry for **TS_{2b}**

Free energy G = -1637.400380 Hartree/particle.

P	-1.80406400	-0.11901700	0.01235900	O	3.14679000	2.04892000	1.42732100
Au	0.51336400	0.17759500	-0.18525200	H	3.34392700	2.96982800	1.65383500
C	3.04392100	-0.61094200	-0.51960500	C	5.38764500	-1.71956000	-0.00472800
C	3.23128000	1.92681600	-0.00090600	C	5.31865900	-2.95878800	-0.85411600
C	5.36495800	-0.48471100	-0.58558600	H	6.19595400	-3.59070200	-0.66984600
H	2.88946900	-1.64065400	-0.77496300	H	4.44565900	-3.56969800	-0.58601900
C	4.70310700	1.97380500	-0.46177100	H	5.27567600	-2.73113000	-1.92181900
C	5.58936200	0.84525800	0.08845700	C	5.47593300	-1.96105300	1.47557400
H	5.38610700	-0.45609200	-1.67585400	H	4.70195300	-2.66878500	1.79476400
H	5.10648500	2.93779000	-0.13090000	H	6.44007200	-2.42884600	1.71302100
H	4.73628500	1.98060600	-1.55777100	H	5.38538300	-1.05250700	2.07064500
H	5.44951900	0.77937300	1.17028700	C	-2.66016000	1.42086400	0.51431400
H	6.63788400	1.12681100	-0.07624200	C	-3.72058500	1.41100800	1.43260900
C	2.63062400	0.56443300	-0.29053100	C	-2.24836500	2.63749800	-0.05538900
C	2.42456800	3.03855800	-0.68392600	C	-4.36119400	2.60467800	1.77240300
H	1.39713300	3.04740600	-0.31033000	H	-4.04601000	0.47966900	1.88398500
H	2.88412800	4.01145000	-0.47745700	C	-2.89543800	3.82498100	0.28408000
H	2.40301100	2.90060800	-1.76866500	H	-1.42346400	2.65645800	-0.76203400

C	-3.95117600	3.80999000	1.19983500	H	-1.85980400	-2.60552700	-4.26144600
H	-5.17950000	2.58953000	2.48567600	H	-4.16760900	-1.91277200	-4.87472500
H	-2.57108300	4.76079000	-0.16059400	C	-2.21611800	-1.38307700	1.27365100
H	-4.44980700	4.73626900	1.46853100	C	-1.45263100	-1.42961300	2.45264900
C	-2.57865600	-0.65943000	-1.55676100	C	-3.27314500	-2.28879600	1.09817600
C	-3.88025000	-0.26898300	-1.90775000	C	-1.75137600	-2.36255100	3.44490600
C	-1.85339200	-1.50230100	-2.41521400	H	-0.62513700	-0.73972200	2.59369100
C	-4.44759900	-0.72252700	-3.10014000	C	-3.56320600	-3.22474900	2.09338700
H	-4.44937300	0.38810100	-1.25832000	H	-3.86720500	-2.26993400	0.19054700
C	-2.42738200	-1.95551600	-3.60270800	C	-2.80575100	-3.26222000	3.26550800
H	-0.84064300	-1.79927400	-2.15740000	H	-1.15682000	-2.39133100	4.35281100
C	-3.72418100	-1.56515100	-3.94663700	H	-4.38109300	-3.92399700	1.94929700
H	-5.45401200	-0.41444200	-3.36625600	H	-3.03294300	-3.99286200	4.03580800

Table 58: Optimized geometry for **IIIb**

Free energy G = -1637.419102 Hartree/particle.

P	1.76817600	-0.06928000	-0.00255000	C	1.68955000	-2.26902100	1.71746200
Au	-0.58853600	0.20016600	0.16645300	C	4.19108600	-1.79946400	2.86825700
C	-3.35809100	-0.73097500	0.69532700	H	4.30005900	-0.07584000	1.58639800
C	-3.37321300	1.66512600	-0.11403800	C	2.18323100	-3.13662500	2.69139100
C	-4.91307000	-0.69242000	0.95306900	H	0.71277300	-2.45123500	1.27775300
H	-2.81827700	-1.56319600	1.12959400	C	3.43375100	-2.90178300	3.26915300
C	-4.59903700	1.83333800	0.81500500	H	5.16193200	-1.61208400	3.31675100
C	-5.57918000	0.66446400	0.71376500	H	1.58897100	-3.98990700	3.00384100
H	-5.11954800	-1.13965600	1.92630300	H	3.81425300	-3.57368400	4.03249200
H	-5.11149600	2.76937100	0.56344000	C	2.25590800	-0.81896800	-1.60398700
H	-4.24090100	1.93839400	1.84570500	C	3.32429300	-1.72206600	-1.71030600
H	-6.06304600	0.68053000	-0.26504800	C	1.53598300	-0.46234800	-2.75699400
H	-6.37133200	0.78421100	1.45842300	C	3.66919200	-2.25517800	-2.95414600
C	-2.64654400	0.35657800	0.24211400	H	3.88415400	-2.01361200	-0.82768700
C	-2.45195900	2.88194100	0.01678600	C	1.88842600	-0.99349000	-3.99756600
H	-1.59925700	2.79130800	-0.66159800	H	0.69912200	0.22675400	-2.68343900
H	-3.00306600	3.79724200	-0.22929000	C	2.95425000	-1.89163700	-4.09714900
H	-2.07468800	2.98274000	1.03870600	H	4.49586400	-2.95524600	-3.02721700
O	-3.77853300	1.51753300	-1.48783100	H	1.32633000	-0.71227500	-4.88288300
H	-4.13934200	2.36658700	-1.78350400	H	3.22347200	-2.31022800	-5.06217700
C	-4.76423400	-1.65366200	-0.12036300	C	2.68394500	1.51500100	0.12415400
C	-4.61237700	-3.10900400	0.22100000	C	2.22922800	2.47852300	1.04052100
H	-5.57055600	-3.59139400	-0.01421900	C	3.82024100	1.78524200	-0.65312700
H	-3.84989500	-3.59249600	-0.39545600	C	2.90721300	3.68900300	1.18176400
H	-4.39883400	-3.27915400	1.27761800	H	1.34543700	2.28257700	1.64149500
C	-5.03023800	-1.35299800	-1.56315900	C	4.49162200	3.00177100	-0.51197600
H	-4.42906900	-1.99473300	-2.21185000	H	4.18040200	1.05350600	-1.36880700
H	-6.08543500	-1.60498100	-1.74326300	C	4.03789300	3.95278400	0.40399600
H	-4.86552900	-0.30972300	-1.82304800	H	2.54856400	4.42741200	1.89235100
C	2.44958100	-1.16142900	1.30489500	H	5.36828300	3.20408400	-1.11969600
C	3.70417000	-0.93069000	1.88918500	H	4.56089200	4.89847600	0.50918500

Table 59: Optimized geometry for **TS_{3b}**

Free energy G = -1637.408203 Hartree/particle.

C	-5.55984700	-1.21346400	-0.13884800	C	1.51054900	0.65646800	-2.69945000
C	-4.96969200	-0.49099500	0.98363000	C	3.84677000	-0.54711400	-3.64305400
H	-4.80671200	-1.19394600	1.80465000	H	4.20749600	-1.11984100	-1.60147400
C	-6.69489700	-0.70337000	-0.93704900	C	1.82664600	0.71657700	-4.05634600
H	-6.69746900	-1.09793200	-1.95476300	H	0.59625700	1.11884500	-2.33818700
H	-7.59042500	-1.11435500	-0.43691800	C	2.99457800	0.11286000	-4.53023900
H	-6.78231600	0.37916100	-0.94211000	H	4.75375600	-1.01995300	-4.00732400
C	-5.11077600	-2.59634500	-0.42330100	H	1.15855800	1.22752300	-4.74304700
H	-5.96080600	-3.26145600	-0.20746400	H	3.23669100	0.15357500	-5.58793300
H	-4.90054900	-2.72512900	-1.49036700	C	2.92541200	-1.34755800	0.74604100
H	-4.25748000	-2.91090700	0.17487600	C	4.18550300	-1.09126100	1.30797800
O	-4.36906100	0.93703400	-1.51360500	C	2.42021400	-2.65863800	0.75693100
C	-3.77088400	1.27209300	-0.24048200	C	4.92859000	-2.13342800	1.86657500
C	-5.60578600	0.84508900	1.40297900	H	4.58692700	-0.08310500	1.31534900
H	-6.68991700	0.85311200	1.27025300	C	3.16877600	-3.69693700	1.31128000
H	-5.41889000	0.98166700	2.47083200	H	1.43990800	-2.86504700	0.33615500
C	-4.88841100	1.95191400	0.58249500	C	4.42327800	-3.43516900	1.86805100
H	-4.45130700	2.69751400	1.25087600	H	5.90153700	-1.92546600	2.30137000
H	-5.56150700	2.47974100	-0.09842100	H	2.76909200	-4.70645900	1.31537400
H	-3.68516900	0.50671400	-2.04923800	H	5.00264400	-4.24239800	2.30589000
C	-3.51064800	-0.05638700	0.46963900	C	2.52779000	1.55543900	0.67849700
C	-2.40092800	-0.76327200	0.69518700	C	1.99255000	2.00274900	1.89856600
H	-2.55374000	-1.73298800	1.17510100	C	3.51971700	2.31652200	0.04202600
Au	-0.41407300	-0.35481400	0.33362300	C	2.45114200	3.18703200	2.47530100
P	1.90953700	-0.02524600	-0.02126300	H	1.21689000	1.42652800	2.39560300
C	-2.56058300	2.17584600	-0.45408300	C	3.97120200	3.50460300	0.62094300
H	-2.08688100	2.43116000	0.49696400	H	3.93827800	1.98751700	-0.90350300
H	-1.81058400	1.69311600	-1.08768900	C	3.43967200	3.94027100	1.83632400
H	-2.88732100	3.09846400	-0.94324500	H	2.03141900	3.52429200	3.41819100
C	2.36761800	0.00017900	-1.79955700	H	4.73759800	4.08822000	0.12000800
C	3.53814000	-0.60389000	-2.28185900	H	3.79105500	4.86563700	2.28271600

Table 60: Optimized geometry for **IVb**

Free energy G = -1637.421966 Hartree/particle.

C	5.61753500	-0.78054800	0.19447700	C	5.28361200	1.18688600	-1.40849600
C	4.90186500	-0.27933800	-1.08684000	H	6.35917500	1.36501200	-1.45143100
H	5.04657000	-0.98097000	-1.90962200	H	4.86789400	1.45333100	-2.38283200
C	7.09367500	-0.46325100	0.35176300	C	4.57796200	1.98662900	-0.26962100
H	7.47356700	-0.85644100	1.29812200	H	3.91315100	2.76174600	-0.66095100
H	7.64346800	-0.94559500	-0.46235000	H	5.27038500	2.46578100	0.42758800
H	7.29492700	0.60777000	0.31621000	H	4.47107600	-0.43707900	1.93358100
C	5.29775300	-2.22696500	0.53610100	C	3.45928100	-0.10478400	-0.61596900
H	5.85971000	-2.87662100	-0.14150600	C	2.31892400	-0.65854800	-1.05173000
H	5.61308400	-2.46893800	1.55626100	H	2.46701100	-1.36836800	-1.87134400
H	4.23447400	-2.44696400	0.41889800	Au	0.36504000	-0.34761700	-0.50048400
O	4.88404400	0.12649600	1.25247900	P	-1.93079900	-0.01839400	0.02880100
C	3.72324300	0.93171100	0.43995400	C	2.71641100	1.38117400	1.45780400

H	1.95856100	1.97871900	0.94379300
H	2.20502500	0.53888500	1.93098000
H	3.18489200	2.00861900	2.22066500
C	-2.49822900	-0.97577100	1.48957700
C	-1.59831700	-1.18147300	2.54868200
C	-3.79881500	-1.49475100	1.58207200
C	-1.99727900	-1.88547100	3.68501300
H	-0.58548200	-0.79392300	2.48152900
C	-4.19194500	-2.20322800	2.71937900
H	-4.50302600	-1.35136100	0.76895300
C	-3.29410400	-2.39833000	3.77099700
H	-1.29420400	-2.03979100	4.49799200
H	-5.19950800	-2.60313200	2.78096000
H	-3.60204800	-2.95239400	4.65259500
C	-2.32383700	1.73854500	0.39331700
C	-3.23441300	2.11440300	1.39207800
C	-1.68817200	2.73428000	-0.36845100
C	-3.50695200	3.46528900	1.62052600
H	-3.72914300	1.35881000	1.99343300
C	-1.96852500	4.08145900	-0.14076600
H	-0.97385200	2.45493900	-1.13829200
C	-2.87724700	4.44871900	0.85544600
H	-4.21155600	3.74635300	2.39737000
H	-1.47337100	4.84269100	-0.73605100
H	-3.09033400	5.49791400	1.03661800
C	-3.04397100	-0.50589800	-1.34839200
C	-2.71638500	-1.64911100	-2.09700400
C	-4.20469800	0.21498400	-1.66615500
C	-3.54341600	-2.06868100	-3.13875200
H	-1.81380300	-2.20851900	-1.86643200
C	-5.02633600	-0.20575600	-2.71437800
H	-4.46816000	1.10346300	-1.10163100
C	-4.69859700	-1.34640200	-3.44982000
H	-3.28146200	-2.95326700	-3.71131200
H	-5.92148700	0.35990000	-2.95462600
H	-5.33818700	-1.66948900	-4.26563300

Table 61: Optimized geometry for **TS_{5b}**

Free energy G = -1637.423236 Hartree/particle.

C	5.59709200	-0.81738000	0.20707900
C	4.90731100	-0.22002200	-1.05887900
H	5.02789700	-0.88732300	-1.91415400
C	7.11346000	-0.66033200	0.26391600
H	7.51371500	-1.15788700	1.15143100
H	7.56458900	-1.12291600	-0.61923700
H	7.41433600	0.38772100	0.29912600
C	5.18442400	-2.26604900	0.45509300
H	4.10086500	-2.39600400	0.40126600
H	5.64506500	-2.91117200	-0.29833600
H	5.53542600	-2.60307700	1.43632400
O	5.03318600	0.04734500	1.30031100
C	3.64599700	1.07240500	0.36462300
C	5.35762300	1.23680100	-1.33371800
H	6.43921400	1.37665600	-1.32544600
H	4.99665800	1.53810100	-2.32027100
C	4.63884800	2.05024300	-0.21967400
H	4.06989400	2.89911800	-0.61898500
H	5.30655200	2.44766600	0.54839000
H	4.60696200	-0.51520700	1.96837100
C	3.46480700	-0.00449900	-0.60918900
C	2.32511600	-0.61126400	-1.00892300
H	2.48925100	-1.35218700	-1.79745500
Au	0.36429300	-0.30990900	-0.49107700
P	-1.94154100	-0.01784600	0.01972700
C	2.70491500	1.47934200	1.43966200
H	1.97319500	2.16389700	0.99257100
H	2.15723800	0.63450900	1.85982700
H	3.22576200	2.03022300	2.22667000
C	-2.27513100	-0.00346900	1.82584200
C	-1.60765200	-0.94098200	2.63307900
C	-3.16718900	0.90248700	2.41755500
C	-1.83962500	-0.97689200	4.00764200
H	-0.90769200	-1.64189300	2.18609900
C	-3.39017600	0.86728600	3.79629600
H	-3.68632900	1.63489800	1.80843400
C	-2.72974500	-0.07085600	4.59133600
H	-1.32171600	-1.70664300	4.62258800
H	-4.08109800	1.57390000	4.24599300
H	-2.90478600	-0.09484700	5.66266200
C	-2.99591500	-1.35088600	-0.67243200
C	-2.65519300	-1.89331200	-1.92306200
C	-4.13208500	-1.82836500	-0.00114000
C	-3.44575400	-2.88940500	-2.49626100
H	-1.77104100	-1.53867700	-2.44565100
C	-4.91700900	-2.82948300	-0.57716600
H	-4.40349900	-1.42542500	0.96922700
C	-4.57653200	-3.35941200	-1.82340600
H	-3.17403500	-3.30297300	-3.46269700
H	-5.79312200	-3.19458100	-0.04991500
H	-5.18739300	-4.13978300	-2.26708800
C	-2.61975200	1.55647200	-0.63728900
C	-1.78069300	2.68269900	-0.67822000
C	-3.94383700	1.66887100	-1.08848300
C	-2.26217200	3.90292200	-1.15262900
H	-0.75032600	2.60224100	-0.34331500
C	-4.41949100	2.89112000	-1.56772600
H	-4.60254100	0.80674400	-1.07221400

C	-3.58174700	4.00793800	-1.59939000	H	-5.44440100	2.96785200	-1.91769400
H	-1.60537900	4.76707200	-1.18112000	H	-3.95414500	4.95585700	-1.97592400

Table 62: Optimized geometry for **VIb**

Free energy G = -1637.437332 Hartree/particle.

C	5.67446300	1.27065600	-0.94997700	C	-3.49060200	0.84599500	2.24554100
C	4.94477400	-0.09298200	-0.82714200	C	-1.99923700	-0.64605800	4.08280800
C	3.54019700	1.63180600	0.09820900	H	-0.83809100	-1.29544300	2.39253900
C	4.91007700	2.20630500	0.00366800	C	-3.80913000	0.88622200	3.60468300
H	6.73626300	1.22205200	-0.70920800	H	-4.07237000	1.43021800	1.54020100
H	5.58361500	1.64026400	-1.97610900	C	-3.06647400	0.14141800	4.52294200
H	4.89711000	3.26409100	-0.28088700	H	-1.41642900	-1.22334900	4.79398000
H	5.33267400	2.15904200	1.01961600	H	-4.63742500	1.50095200	3.94342500
C	2.43610200	2.41578800	0.68853500	H	-3.31555600	0.17701200	5.57914800
H	1.52727000	1.83624700	0.85088600	C	-2.84473900	-1.51903800	-0.64393400
H	2.77382500	2.86292900	1.63124700	C	-3.95592900	-2.08182400	0.00203800
H	2.20874300	3.25999000	0.02273800	C	-2.38761500	-2.08043400	-1.84824700
C	3.51760300	0.33311000	-0.44709100	C	-4.60128000	-3.18843900	-0.55414000
C	2.37197700	-0.40870400	-0.70156600	H	-4.31655600	-1.66338800	0.93598700
H	2.59567900	-1.32292400	-1.26010900	C	-3.03943700	-3.18209400	-2.40164500
P	-1.97018800	-0.05197100	0.02335700	H	-1.52237200	-1.65756800	-2.35141100
Au	0.38476100	-0.17512500	-0.32876200	C	-4.14595300	-3.73809000	-1.75421000
O	5.65125900	-0.29446200	1.44291100	H	-5.45894800	-3.61973800	-0.04707300
H	6.05683700	-0.85251900	2.12094100	H	-2.67920500	-3.60960000	-3.33232900
C	5.58425000	-1.05432400	0.22282300	H	-4.64895600	-4.59997300	-2.18203300
C	4.73017200	-2.31126800	0.45137000	C	-2.72213600	1.40971800	-0.79170200
H	4.59720000	-2.88395300	-0.47217500	C	-3.97140500	1.34519500	-1.42670200
H	5.22599800	-2.96629800	1.17624300	C	-2.02337700	2.62866000	-0.76334500
H	3.74547500	-2.05949800	0.85549200	C	-4.51430600	2.48715000	-2.01979100
C	6.99598400	-1.47407700	-0.21762800	H	-4.51915200	0.40935900	-1.46197500
H	7.65915700	-0.61324700	-0.32680700	C	-2.57329300	3.76708700	-1.35179500
H	7.43551000	-2.14260300	0.53056000	H	-1.05146600	2.68738400	-0.28157600
H	6.96853700	-2.01390800	-1.16940900	C	-3.81857200	3.69702300	-1.98213100
H	4.94057800	-0.62680800	-1.78226900	H	-5.48069200	2.42845100	-2.51105200
C	-2.42064100	0.05674000	1.79771000	H	-2.02721800	4.70505900	-1.32418500
C	-1.67322700	-0.68627100	2.72739400	H	-4.24284100	4.58234100	-2.44590600

Table 63: Optimized geometry for **TS_{4b}**

Free energy G = -1637.404075 Hartree/particle.

C	5.93182300	0.25210900	0.21599400	H	2.92995100	2.45806900	-1.71330200
C	4.96619800	-0.56600100	-0.61997100	H	3.90051800	3.47180600	-0.62112900
C	3.75897000	1.43288000	0.04105800	H	4.70245800	2.34211400	-1.73231200
C	5.06917300	1.36203800	0.86315600	C	3.70339700	0.09974800	-0.71687200
H	6.45849300	-0.36234000	0.95228800	C	2.58432500	-0.77391800	-0.93942500
H	6.69478900	0.66740700	-0.45082200	H	2.66637000	-1.37016700	-1.84842700
H	5.57915300	2.32746000	0.87591500	P	-1.69203200	0.01905400	0.02629200
H	4.81448300	1.11335200	1.89506300	Au	0.59393300	-0.37316000	-0.45491600
C	3.82920900	2.48645400	-1.08963300	O	2.67932900	1.69991000	0.91111900

H	1.84676800	1.62741600	0.41236000	C	-2.18746100	-0.63367600	1.66827600
C	3.68827200	-1.48087400	0.07415400	C	-3.43887900	-1.22996900	1.88481300
C	3.93202900	-2.92865400	-0.39387800	C	-1.28320700	-0.51944900	2.73822000
H	4.78459900	-3.34581200	0.15001700	C	-3.78025000	-1.70075600	3.15455300
H	3.04086500	-3.51699300	-0.15693100	H	-4.14531500	-1.33118500	1.06761500
H	4.12452700	-3.00374300	-1.46433300	C	-1.63209000	-0.98549400	4.00559900
C	3.46481000	-1.39335800	1.57728800	H	-0.30760900	-0.06775000	2.58135400
H	3.09648400	-0.41975800	1.89570500	C	-2.88006500	-1.57858200	4.21467100
H	2.71948600	-2.14390900	1.85740600	H	-4.74979100	-2.16321700	3.31228200
H	4.38886800	-1.62750300	2.11582700	H	-0.92750900	-0.89177300	4.82632700
H	5.36021100	-1.19640500	-1.40910100	H	-3.14774000	-1.94749200	5.20017600
C	-2.80895900	-0.76306000	-1.20061900	C	-2.12015700	1.80384400	0.03144800
C	-2.42295500	-1.98220900	-1.78259500	C	-1.56534300	2.62757400	-0.96336000
C	-4.03676000	-0.18585100	-1.55976400	C	-2.98548600	2.36180900	0.98367200
C	-3.25829300	-2.61811300	-2.70112400	C	-1.88005100	3.98534600	-1.00754100
H	-1.46921500	-2.43162400	-1.51978700	H	-0.88919400	2.20811500	-1.70357600
C	-4.86715100	-0.82458600	-2.48283400	C	-3.29192800	3.72400300	0.93861800
H	-4.34402300	0.75987000	-1.12520700	H	-3.41874300	1.74020800	1.76014600
C	-4.48048200	-2.03955200	-3.05261300	C	-2.74216000	4.53575000	-0.05493000
H	-2.95131500	-3.55943400	-3.14661600	H	-1.44779900	4.61337200	-1.78057000
H	-5.81456300	-0.37051800	-2.75665200	H	-3.96071100	4.14780000	1.68151800
H	-5.12731600	-2.53190300	-3.77241900	H	-2.98118400	5.59440900	-0.08599500

Table 64: Optimized geometry for **Vb**

Free energy G = -1637.471641 Hartree/particle.

C	5.33513900	0.90238000	1.40840400	H	2.68530900	-4.18547300	-1.28426000
C	3.77518800	1.30719300	-0.45650700	H	0.99537800	-3.85232700	-0.91975200
C	4.51356800	2.01102800	0.71289600	C	2.91052800	-1.13400200	-0.71510400
H	5.38987600	1.02500600	2.49593100	H	2.86998800	-0.98596400	-1.79538500
H	6.37392600	0.87743400	1.04970600	C	-2.71792900	-0.68095400	-1.03847600
H	5.12317100	2.85483600	0.37772300	C	-2.52074700	-2.02795000	-1.38355700
H	3.75247000	2.39412400	1.39957600	C	-3.85311000	-0.00420300	-1.51192400
C	4.50993600	1.47012700	-1.79566200	C	-3.45173500	-2.69011800	-2.18349400
H	4.02840900	0.89265900	-2.59059300	H	-1.63922600	-2.55535200	-1.03070000
H	4.51495000	2.52413600	-2.09692200	C	-4.77904600	-0.67155600	-2.31589300
H	5.55056800	1.14281100	-1.71145800	H	-4.01425900	1.03883600	-1.25991900
C	3.73766700	-0.15203100	0.00550000	C	-4.58061500	-2.01248900	-2.65120500
P	-1.50461600	0.14856100	0.05382400	H	-3.29130400	-3.73098700	-2.44694600
Au	0.67604000	-0.62473200	-0.28034200	H	-5.65316200	-0.14105200	-2.68054500
O	2.41557100	1.75520200	-0.59363800	H	-5.30103300	-2.52713900	-3.27958600
H	2.41476300	2.62585900	-1.01575100	C	-2.05395100	-0.13665700	1.77732800
C	4.61486100	-0.35727400	1.00509700	C	-3.38454000	-0.46424700	2.07887500
H	4.84465700	-1.32110300	1.44549800	C	-1.11883900	-0.00523600	2.81766200
C	2.40009900	-2.34260500	-0.25376000	C	-3.77191800	-0.65588000	3.40662700
C	2.52743000	-2.81840700	1.17193400	H	-4.11571000	-0.57454500	1.28489100
H	3.41378400	-3.46112800	1.25829900	C	-1.51384100	-0.19175100	4.14201200
H	2.63720600	-1.99856800	1.88295800	H	-0.08474100	0.23978500	2.59140100
H	1.66306400	-3.42715000	1.45122900	C	-2.83985500	-0.51968300	4.43725800
C	1.93200000	-3.38751400	-1.24066500	H	-4.80206700	-0.91331800	3.63256900
H	1.80686600	-2.98313200	-2.24751000	H	-0.78563700	-0.08854200	4.94049500

H	-3.14434400	-0.67265800	5.46809900	C	-2.46538700	4.15578700	0.32458700
C	-1.66838800	1.94484900	-0.26882300	H	-2.79236000	2.39952900	1.52296100
C	-1.10071800	2.47378900	-1.44096600	C	-1.90482500	4.67552700	-0.84282000
C	-2.35101700	2.79372600	0.61393400	H	-0.78534600	4.23338700	-2.63499500
C	-1.22447000	3.83237400	-1.72666000	H	-2.99376700	4.80712400	1.01387900
H	-0.56244600	1.82665500	-2.12803700	H	-1.99440400	5.73474400	-1.06371300

Conditions I:

Coordinates and energies for the the cyclization of **Ib** calculated at the B3LYP/6-31G(d,p) (C, H, P, O), SDD(Au) level taking into account solvent effect of CH_2Cl_2 (IEF-PCM) and employing (1,3-diphenyl)imidazol-2-ylidene (NHC) as the ligand. ΔG energies are given in kcal·mol^{-1}.

Table 65: Optimized geometry for **Ib**

Free energy G = -1289.458116 Hartree/particle.

Au	0.66577500	-0.34224200	-0.69647500	H	2.52465400	-1.13633000	1.89368100
C	3.25914900	2.45068000	1.18351700	C	-0.18682400	-1.83559600	-2.10534700
C	2.17274400	3.24500700	1.00469300	H	0.11353400	-1.75580100	-3.13168300
H	4.21690100	2.65018100	1.63564300	C	-0.69643400	-2.17341800	-1.03343900
H	2.00209900	4.28036100	1.25063900	C	-1.39954600	-2.79760600	0.13079200
C	1.66789200	1.20599000	0.17086900	C	-2.44714300	-1.83406600	0.72960200
N	1.20749400	2.46903300	0.37867200	H	-2.85493700	-2.33541000	1.61371400
N	2.93332400	1.20320300	0.66947400	H	-1.91389300	-0.94497100	1.08509200
C	-0.09530400	2.95488600	0.00667500	C	-2.01666400	-4.12564400	-0.34514000
C	-2.20872100	3.91454500	0.64318600	H	-1.23712100	-4.81142200	-0.69060900
C	-1.73885700	3.43972200	-1.68396400	H	-2.54318900	-4.58442400	0.49610300
C	-2.60560300	3.91515000	-0.69656000	H	-2.72188900	-3.97284300	-1.16503900
H	-2.87889700	4.28533700	1.41200700	O	-0.45878100	-3.02764700	1.18068000
H	-2.04013500	3.44997300	-2.72656500	H	0.15121900	-3.72556900	0.89922200
H	-3.58625300	4.29063600	-0.97118900	C	-3.59264500	-1.41599700	-0.21121100
C	3.82686900	0.07482700	0.67730000	H	-4.19718700	-2.28882700	-0.47140900
C	5.92781900	-0.90749700	0.03341100	H	-3.16467100	-1.04098300	-1.15187600
C	4.35251900	-2.16928800	1.37003400	C	-4.44124000	-0.33130000	0.40148000
C	5.57904300	-2.08075700	0.70688300	H	-3.92367400	0.61947400	0.54079000
H	6.88006600	-0.83546300	-0.48211700	C	-5.72289500	-0.39938100	0.79610200
H	4.08438700	-3.07511800	1.90441400	C	-6.40823900	0.80618500	1.39537400
H	6.26400000	-2.92269100	0.71907900	H	-7.29146900	1.08922200	0.80755800
C	-0.47398100	2.96156700	-1.33778000	H	-6.76932000	0.58937200	2.40934900
H	0.21646100	2.61001400	-2.09685500	H	-5.74198000	1.67176600	1.44790300
C	-0.94932800	3.43147700	1.00271600	C	-6.59606800	-1.62607000	0.69297500
H	-0.63583700	3.41396900	2.04146900	H	-6.98562900	-1.90199400	1.68127900
C	5.05087000	0.17814100	0.01349700	H	-7.47152800	-1.42439400	0.06209400
H	5.30665400	1.08994500	-0.51671700	H	-6.07907700	-2.49526400	0.28244300
C	3.47008700	-1.08756900	1.36444100				

Table 66: Optimized geometry for $\mathbf{TS_{Ib}}$

Free energy G = -1289.443049 Hartree/particle.

C	-3.28129400	0.66881300	0.93818700	N	2.59093500	1.78101200	-0.20726300
C	-2.21041200	1.55018300	1.62040100	N	3.37113700	-0.22294900	-0.03239900
H	-2.70668500	2.43349300	2.03582300	C	4.46577400	0.63485100	-0.03046500
H	-1.71529900	1.01655100	2.43465300	H	5.47848400	0.26970500	0.01977900
H	-1.46222000	1.87178200	0.89370400	C	3.97580800	1.89377700	-0.14019000
O	-3.86603300	1.36325600	-0.17126100	H	4.47563900	2.84625600	-0.20573600
H	-4.32102700	2.14371100	0.17860100	C	1.70614000	2.90667800	-0.32366900
C	-4.36014700	0.24449200	1.95478000	C	0.78037400	2.95959900	-1.36865700
H	-3.87133300	-0.25558100	2.79790800	C	1.80737200	3.94669300	0.60311700
H	-4.85857800	1.13610100	2.35092600	C	-0.06483600	4.06569500	-1.47300700
C	-5.35788700	-0.70599400	1.27447800	H	0.73449500	2.15351300	-2.09253900
H	-6.01199300	-1.15483300	2.03020600	C	0.96423600	5.05225600	0.48230500
H	-5.99255900	-0.14808900	0.58421100	H	2.52829000	3.88400000	1.41192000
C	-4.59231500	-1.78594000	0.56450000	C	0.02623000	5.11167200	-0.55132300
H	-4.13253400	-2.53523400	1.20757200	H	-0.78478300	4.11303300	-2.28387600
C	-4.56526300	-2.02007100	-0.78345800	H	1.03788700	5.86212800	1.20106300
C	-5.26298000	-1.16804500	-1.80762400	H	-0.62878000	5.97260800	-0.64097200
H	-4.67183400	-1.11483600	-2.72711500	C	3.47735900	-1.65207800	0.07238900
H	-6.22009800	-1.63566000	-2.07412700	C	4.16012500	-2.20498000	1.15795000
H	-5.44963700	-0.15395000	-1.45832200	C	2.92266300	-2.46409800	-0.92004100
C	-3.85839700	-3.22876900	-1.32167300	C	4.28083400	-3.59231200	1.25224300
H	-3.07105600	-2.93601900	-2.02824900	H	4.57935800	-1.55803900	1.92187900
H	-3.42500900	-3.85039300	-0.53516900	C	3.04094900	-3.85059900	-0.80958900
H	-4.56480400	-3.84343700	-1.89371100	H	2.42005600	-2.01387000	-1.76912000
C	-2.62706400	-0.54301800	0.37072400	C	3.71896000	-4.41557800	0.27340700
C	-1.58983900	-1.18571100	-0.01394500	H	4.80835000	-4.02714300	2.09516700
H	-1.57879300	-2.20562400	-0.38540800	H	2.61385700	-4.48643100	-1.57866000
Au	0.29867200	-0.28186300	-0.05249400	H	3.81336600	-5.49406400	0.35179000
C	2.20625800	0.47665900	-0.12874700				

Table 67: Optimized geometry for **IIb**

Free energy G = -1289.455487 Hartree/particle.

C	-5.03369100	-1.55793500	1.09568700	Au	0.24735000	-0.36377400	-0.01398300
C	-3.93366200	-2.22731300	0.26870600	O	-2.87422900	1.21580300	0.22294900
C	-3.16525000	0.05567600	1.00208900	H	-1.90927800	1.27530000	0.12923400
C	-4.69983100	-0.05603100	1.14967100	C	-3.77529600	-1.93940500	-1.14849700
H	-6.02564600	-1.75518600	0.67858800	C	-3.18514100	-3.00254000	-2.02790600
H	-5.01183400	-1.99808900	2.09666500	H	-4.04977400	-3.46074300	-2.53121900
H	-5.04221100	0.39999000	2.08149600	H	-2.53976000	-2.59503800	-2.80901700
H	-5.17945000	0.49064500	0.33646100	H	-2.67203400	-3.79337600	-1.48089300
C	-2.49588700	0.15501000	2.38541600	C	-4.44664300	-0.80492500	-1.87793100
H	-1.40524900	0.16246300	2.29666600	H	-4.13061300	0.17435300	-1.51771900
H	-2.82007600	1.08108900	2.86939300	H	-4.22718700	-0.86437400	-2.94527500
H	-2.77719100	-0.68857300	3.02390900	H	-5.53261100	-0.88234400	-1.74113400
C	-2.69986100	-1.26004500	0.32858300	H	-3.70990100	-3.25894200	0.53464100
C	-1.42045700	-1.53900300	-0.05542700	C	2.00123400	0.74770700	-0.04728400
H	-1.27218000	-2.52817300	-0.48743100	N	2.15550800	2.09934600	-0.12406100

N	3.27423800	0.26146700	-0.01339700
C	4.20510300	1.29278600	-0.06405900
H	5.26678000	1.10737700	-0.05641800
C	3.50113500	2.44902200	-0.13923700
H	3.82498300	3.47578900	-0.18869700
C	3.63034300	-1.12999900	0.05587300
C	4.41480300	-1.57773100	1.12079600
C	3.21102400	-2.00534400	-0.94902400
C	4.77639500	-2.92459200	1.18207100
H	4.72704500	-0.88267000	1.89359300
C	3.57053100	-3.35197200	-0.87214600
H	2.62230800	-1.63197900	-1.77987000
C	4.35225400	-3.81234200	0.19033600
H	5.38406800	-3.27841900	2.00877800
H	3.24924000	-4.03672400	-1.65065000
H	4.63425500	-4.85923600	0.24266900
C	1.08685400	3.05889100	-0.18792500
C	0.99626100	3.89856600	-1.29983700
C	0.17744300	3.15845000	0.86772200
C	-0.02692500	4.84648200	-1.35625700
H	1.71227200	3.80393100	-2.10996300
C	-0.84791700	4.10354200	0.79582900
H	0.28401900	2.51489500	1.73423000
C	-0.95061300	4.94712700	-0.31318000
H	-0.10337600	5.50076100	-2.21881100
H	-1.55872300	4.18488600	1.61167600
H	-1.74614700	5.68392100	-0.36206700

Table 68: Optimized geometry for **TS_{2b}**

Free energy G = -1289.440073 Hartree/particle.

C	-1.74435700	-2.67513500	0.09512900
C	-0.65765800	-3.44698200	-0.66060600
H	-0.73377700	-4.51156000	-0.42034300
H	-0.76656900	-3.32313400	-1.74230300
H	0.33878900	-3.09280100	-0.37870000
O	-1.57989600	-2.83367000	1.50802100
H	-0.66809500	-2.59652100	1.73212300
C	-3.13170700	-3.24147100	-0.24630100
H	-3.22944700	-3.29872700	-1.33634600
H	-3.14767900	-4.26791900	0.13304800
C	-4.31989100	-2.46738500	0.34615600
H	-5.21568100	-3.09389500	0.24179900
H	-4.16173200	-2.32665700	1.41797700
C	-4.59794800	-1.16126400	-0.35370000
H	-4.66148600	-1.22762000	-1.44057300
C	-5.03595800	0.00135200	0.21467000
C	-5.13861500	0.23749000	1.69432200
H	-4.71162100	-0.56568800	2.29449000
H	-4.64755400	1.17928600	1.96630300
H	-6.19437000	0.34728100	1.97366300
C	-5.44120500	1.16224100	-0.65008800
H	-4.82240100	2.04442700	-0.43411500
H	-5.37134600	0.93421700	-1.71616300
H	-6.47343600	1.45656300	-0.42500400
C	-1.67650000	-1.18297000	-0.22202400
C	-2.50888200	-0.23842000	-0.40197900
H	-2.72933500	0.78290200	-0.64277200
Au	0.14512100	-0.06504500	-0.18866800
C	1.94104100	0.91374900	-0.02850400
N	2.13791800	2.25721700	0.07908400
N	3.18083500	0.36855000	0.10524900
C	3.48135300	2.54408800	0.29581800
C	4.13645600	1.35756700	0.31257300
H	3.84180700	3.55553300	0.38828800
H	5.18300500	1.12550100	0.42348000
C	1.11055300	3.25866500	0.00108200
C	0.30126700	3.33608600	-1.13520100
C	0.95744300	4.15790000	1.05853200
C	-0.68643700	4.32036900	-1.20094500
H	0.45515000	2.64539900	-1.95715700
C	-0.02706500	5.14397000	0.97700400
H	1.59280100	4.07841000	1.93483200
C	-0.85127900	5.22398200	-0.14815300
H	-1.31566000	4.38837300	-2.08280500
H	-0.15177800	5.84416700	1.79675500
H	-1.61598100	5.99211500	-0.20679600
C	3.48505900	-1.03524700	0.05798900
C	3.16142600	-1.77656500	-1.08079400
C	4.12952500	-1.62734200	1.14637000
C	3.47587700	-3.13628200	-1.11865100
H	2.68435200	-1.29054500	-1.92483700
C	4.44609100	-2.98567600	1.09352900
H	4.37057500	-1.03429600	2.02283000
C	4.11730500	-3.74109100	-0.03483200
H	3.22974300	-3.71774200	-2.00142500
H	4.94500000	-3.45201200	1.93700900
H	4.36467200	-4.79731200	-0.07137000

Table 69: Optimized geometry for **IIIb**

Free energy G = -1289.457997 Hartree/particle.

Au	-0.04840700	-0.07831900	-0.07741500	N	-2.78863900	1.34173300	0.27885900
C	2.70340500	-0.93679700	0.64820500	N	-3.04720700	-0.79755600	0.24541500
C	2.65250400	0.08406100	-1.68119900	C	-4.15752000	1.10318600	0.34618200
C	4.21055300	-1.34844000	0.46720300	H	-4.87469500	1.90323600	0.42991900
H	2.13652500	-1.45025400	1.41527300	C	-4.32005500	-0.24233000	0.32445300
C	3.79567300	-0.89194000	-2.00767700	H	-5.20727700	-0.85121400	0.38420400
C	4.83203000	-1.01358000	-0.88709900	C	-2.20618000	2.65439800	0.26522100
H	4.36657400	-2.36834500	0.81758200	C	-1.23397100	2.99412600	1.20967100
H	4.28040200	-0.55720300	-2.93040100	C	-2.64089000	3.58052200	-0.68570100
H	3.35132800	-1.87236700	-2.21294200	C	-0.67887700	4.27485700	1.18487400
H	5.40905900	-0.08840000	-0.82012600	H	-0.93096100	2.27015900	1.95815200
H	5.54167800	-1.80718100	-1.13848000	C	-2.08620700	4.86121100	-0.69406800
C	1.96490000	-0.31948300	-0.36316800	H	-3.39281700	3.29679100	-1.41501600
C	1.66673900	0.13663800	-2.85137500	C	-1.10310400	5.20830200	0.23586100
H	0.87860400	0.87431300	-2.66649100	H	0.07447900	4.54520200	1.91806800
H	2.19916000	0.41294200	-3.76676200	H	-2.41890300	5.58330900	-1.43284500
H	1.18554200	-0.83405700	-3.00520000	H	-0.67316100	6.20490400	0.22462800
O	3.24375000	1.38525500	-1.49952000	C	-2.79430700	-2.21043800	0.18089400
H	2.52564200	2.02948100	-1.41137700	C	-1.96267100	-2.81187100	1.12884200
C	4.08801600	-0.34879800	1.51780800	C	-3.40705900	-2.96484400	-0.82208100
C	4.00933000	-0.81740300	2.95301700	C	-1.72990000	-4.18634400	1.05572700
H	5.00592700	-0.70097900	3.39622000	H	-1.51849600	-2.21272300	1.91619400
H	3.31650200	-0.20520500	3.53712500	C	-3.17458300	-4.33991300	-0.87937900
H	3.72303000	-1.86781400	3.03827000	H	-4.04664200	-2.47899100	-1.55202300
C	4.47969400	1.09687200	1.35917800	C	-2.33395600	-4.95070100	0.05443900
H	3.91393700	1.72244600	2.05510000	H	-1.08683300	-4.65976700	1.79094800
H	5.54006600	1.17920200	1.63260000	H	-3.64607800	-4.93014000	-1.65861900
H	4.34121800	1.47135600	0.34786400	H	-2.15434300	-6.02004900	0.00511800
C	-2.09263500	0.17324900	0.20435400				

Table 70: Optimized geometry for **TS_{3b}**

Free energy G = -1289.44547 Hartree/particle.

C	-4.97121500	0.05242200	0.80334100	H	-3.39029900	2.60732000	-2.24619500
C	-4.19689000	1.27325000	0.61018900	H	-4.65559200	1.42206100	-2.54925800
H	-4.01658300	1.73384100	1.58472200	H	-3.14057500	-1.32513400	-1.40083600
C	-6.13808300	-0.31593900	-0.02749900	C	-2.76807300	0.76328900	0.08152600
H	-6.31433200	-1.39295100	-0.04402600	C	-1.70842800	0.55948300	0.87054400
H	-7.00037600	0.14118800	0.49081100	H	-1.91033700	0.66537500	1.94039200
H	-6.10692200	0.08584500	-1.03627600	Au	0.24770100	0.10342300	0.43962300
C	-4.68335200	-0.81902500	1.96728400	C	-1.72363000	0.61895700	-2.29217400
H	-5.59150600	-0.86192800	2.58611700	H	-1.13789400	1.53063200	-2.15048400
H	-4.51169100	-1.84772200	1.62970400	H	-1.08390800	-0.23510300	-2.05077700
H	-3.84733500	-0.47899100	2.57562100	H	-2.01772700	0.54907300	-3.34397100
O	-3.72931100	-0.58892100	-1.62708600	C	2.23126100	-0.36562400	0.04754600
C	-2.98055800	0.63373400	-1.42685600	N	3.27180300	0.49711300	-0.13232500
C	-4.64428700	2.24930500	-0.48922400	N	2.76800000	-1.59678400	-0.19074500
H	-5.73096600	2.31139500	-0.58358000	C	4.11390400	-1.49961900	-0.53144700
H	-4.29451600	3.24603800	-0.20911700	C	4.43049300	-0.18293700	-0.49507200
C	-3.94835600	1.78241400	-1.79707200	H	4.71712800	-2.36881900	-0.73636700

H	5.36480000	0.32730000	-0.66289800
C	3.19984600	1.92484700	0.00321800
C	3.61648800	2.72964800	-1.05972200
C	2.74089500	2.48984200	1.19589300
C	3.56438900	4.11806400	-0.92687700
H	3.96445500	2.27343900	-1.98101800
C	2.68371200	3.87952900	1.31369300
H	2.44446400	1.84860200	2.01857700
C	3.09474300	4.69426900	0.25586100
H	3.88450600	4.74671500	-1.75173900
H	2.32873200	4.32321000	2.23858300
H	3.05342300	5.77449600	0.35448800
C	2.05393000	-2.84036000	-0.12768700
C	1.36100100	-3.18840500	1.03469900
C	2.08642200	-3.69903200	-1.22911300
C	0.67922000	-4.40546200	1.08331800
H	1.36848100	-2.51965900	1.88817200
C	1.40995500	-4.91827300	-1.16519300
H	2.62406400	-3.40984600	-2.12651800
C	0.70290900	-5.27102500	-0.01313400
H	0.14177400	-4.68112900	1.98526000
H	1.43153200	-5.58720600	-2.01968000
H	0.17690900	-6.21952400	0.03201900

Table 71: Optimized geometry for **IVb**

Free energy G = -1289.458878 Hartree/particle.

C	4.84880300	-1.34769600	0.22832300
C	4.16421600	-0.83910900	-1.06830600
H	4.15180800	-1.62080200	-1.82962500
C	6.36372100	-1.27208900	0.30502900
H	6.72168800	-1.66923400	1.25829200
H	6.78818700	-1.88131700	-0.49890200
H	6.73331800	-0.25223200	0.19554500
C	4.31372900	-2.68947500	0.70453300
H	3.22520100	-2.74233800	0.63333300
H	4.73811100	-3.47738300	0.07548000
H	4.62406600	-2.89278500	1.73482300
O	4.33003700	-0.25206900	1.22810000
C	3.27258600	0.67530200	0.37729100
C	4.76910500	0.50907300	-1.53189400
H	5.85623500	0.50034900	-1.62765900
H	4.35627100	0.76203900	-2.51111500
C	4.26163400	1.50627600	-0.44495400
H	3.72167200	2.35206900	-0.87969400
H	5.05634900	1.91101400	0.18725500
H	3.84903300	-0.68456200	1.95799700
C	2.79412700	-0.38784000	-0.56504100
C	1.55752500	-0.79249200	-0.89598100
H	1.56874400	-1.58656500	-1.65111700
Au	-0.31561900	-0.20457000	-0.31016600
C	2.40960600	1.36946400	1.38781900
H	1.72806000	2.03453900	0.85072000
H	1.79864100	0.66594200	1.95938100
H	3.01472000	1.97562900	2.06720500
C	-2.28358000	0.29070200	0.14210000
N	-3.33864900	-0.56842200	0.25514600
N	-2.84746200	1.52814300	0.24679700
C	-4.22750400	1.44207500	0.40217900
H	-4.84615800	2.31687000	0.51825400
C	-4.53629900	0.12311400	0.40799200
H	-5.47865100	-0.38437600	0.53324100
C	-3.25500400	-2.00043500	0.19621700
C	-2.39560700	-2.68587700	1.05881300
C	-4.05962000	-2.69109100	-0.71321500
C	-2.33179100	-4.07867300	0.99335800
H	-1.79592600	-2.13436400	1.77427500
C	-3.99521800	-4.08449600	-0.76249900
H	-4.71669900	-2.14336800	-1.38130300
C	-3.12981700	-4.77940000	0.08562600
H	-1.66620500	-4.61497900	1.66247500
H	-4.61686700	-4.62358500	-1.47028500
H	-3.08066300	-5.86291400	0.04245000
C	-2.13708300	2.77502600	0.18732300
C	-2.46792700	3.69956700	-0.80557700
C	-1.15604900	3.06129900	1.13929900
C	-1.79918300	4.92415900	-0.84853200
H	-3.23137400	3.45689500	-1.53775900
C	-0.48860400	4.28611600	1.08307100
H	-0.93298600	2.33829000	1.91616900
C	-0.80835900	5.21725500	0.09150100
H	-2.05097000	5.64486600	-1.61999600
H	0.27110900	4.51655800	1.82340600
H	-0.29074900	6.17072000	0.05499500

Table 72: Optimized geometry for **TS_{5b}**

Free energy G = -1289.459186 Hartree/particle.

C	4.82805600	-1.36268300	0.26601200
C	4.16626500	-0.82945200	-1.04278400

H	4.14151400	-1.60771600	-1.80769000
C	6.35194900	-1.41076400	0.26826200
H	6.71746300	-1.84684200	1.20181700
H	6.70001600	-2.03574600	-0.55987600
H	6.79209000	-0.41836400	0.16206400
C	4.23126800	-2.69264200	0.71742600
H	3.13875200	-2.67125800	0.70984500
H	4.56329600	-3.48801400	0.04410800
H	4.57789400	-2.94890100	1.72452000
O	4.43433500	-0.29089500	1.25793500
C	3.21215000	0.78528800	0.27389000
C	4.81281100	0.49644400	-1.51551500
H	5.90169700	0.46580400	-1.57320400
H	4.43918600	0.73479500	-2.51441600
C	4.29402100	1.53343400	-0.47739800
H	3.82785300	2.40487000	-0.95228300
H	5.06340600	1.91044200	0.20074400
H	3.94687700	-0.69729400	1.99468800
C	2.79981000	-0.34271200	-0.56833200
C	1.55983400	-0.80338900	-0.84535600
H	1.58049900	-1.64287700	-1.54929100
A	-0.31609400	-0.20840700	-0.29115700
C	2.39643100	1.46377000	1.31600100
H	1.75005900	2.18895900	0.80784800
H	1.75169800	0.76890500	1.85674100
H	3.03196700	2.01851600	2.01073200
C	-2.28701100	0.29201000	0.13892500
N	-3.34454800	-0.56451600	0.24389600
N	-2.84727700	1.53095700	0.24008600
C	-4.22824800	1.44864700	0.38606000
H	-4.84524100	2.32517600	0.49763400
C	-4.54086000	0.13033900	0.38921900
H	-5.48548800	-0.37448900	0.50783200
C	-3.26388000	-1.99682300	0.18386500
C	-2.41015100	-2.68501900	1.04987900
C	-4.06521700	-2.68427800	-0.73085400
C	-2.34845300	-4.07785200	0.98230900
H	-1.81365700	-2.13599800	1.76995000
C	-4.00305800	-4.07768000	-0.78200500
H	-4.71781100	-2.13427400	-1.40145000
C	-3.14313000	-4.77550900	0.06933300
H	-1.68738700	-4.61647900	1.65400000
H	-4.62209100	-4.61449400	-1.49377800
H	-3.09574600	-5.85902100	0.02459900
C	-2.13224500	2.77577600	0.18487200
C	-2.44265900	3.69419900	-0.82019200
C	-1.16746200	3.06542900	1.15229700
C	-1.76937500	4.91644800	-0.85983800
H	-3.19412300	3.44878800	-1.56376900
C	-0.49544000	4.28806200	1.09939500
H	-0.96077100	2.34768500	1.93864900
C	-0.79451800	5.21306500	0.09563300
H	-2.00537400	5.63258600	-1.64046300
H	0.25113100	4.52207300	1.85192500
H	-0.27353700	6.16477700	0.06196100

Table 73: Optimized geometry for VIb

Free energy G = -1289.477097 Hartree/particle.

C	5.07131200	0.87075900	-0.95329700
C	4.25238200	-0.43145900	-0.75133300
C	2.97920500	1.42719300	0.09570900
C	4.38313300	1.90733000	-0.04671400
H	6.13034900	0.76306100	-0.71905100
H	4.99380700	1.18932500	-1.99757600
H	4.42875400	2.94328300	-0.40074600
H	4.82089200	1.90097900	0.96313300
C	1.93977200	2.30906000	0.66730600
H	1.00252400	1.79548800	0.88062200
H	2.32871600	2.78326100	1.57639400
H	1.73950900	3.12876500	-0.03604100
C	2.86243800	0.11076500	-0.38136700
C	1.66198600	-0.56377300	-0.59134400
H	1.82760000	-1.52109500	-1.09671000
Au	-0.28927000	-0.16538700	-0.24258800
O	4.99408100	-0.56312600	1.51415400
H	5.35876600	-1.11811100	2.21747400
C	4.84311300	-1.37904700	0.33851100
C	3.90634200	-2.55591400	0.65357400
H	3.71226100	-3.16826800	-0.23289500
H	4.37113000	-3.20360500	1.40531500
H	2.95174200	-2.21019000	1.06029400
C	6.21003900	-1.92618900	-0.10412200
H	6.93004500	-1.12414400	-0.28092400
H	6.61933400	-2.57847600	0.67503700
H	6.11945100	-2.51973800	-1.01944800
H	4.19886300	-1.01237300	-1.67732700
C	-2.31802200	0.14077500	0.06953100
N	-2.97718800	1.32739600	0.19008100
N	-3.29120200	-0.80494500	0.19583000
C	-4.53517600	-0.21725000	0.39046000
H	-5.43035100	-0.80253900	0.52327500
C	-4.33726500	1.12464000	0.39011400
H	-5.02863400	1.94445300	0.49763100
C	-3.08305100	-2.22591400	0.13184500
C	-2.20175000	-2.84302100	1.02298600
C	-3.79051400	-2.97034900	-0.81465400

C	-2.01603000	-4.22462300	0.94849300	C	-1.70560800	3.00630600	-1.06587300
H	-1.68195400	-2.25054800	1.76796600	C	-1.91557500	4.77559600	1.09388800
C	-3.60384800	-4.35228000	-0.87315700	H	-3.00347600	3.19005700	2.08439700
H	-4.46767600	-2.47206600	-1.50107000	C	-1.13274700	4.27734700	-1.14159600
C	-2.71509200	-4.97947500	0.00334500	H	-1.65214800	2.31971600	-1.90379300
H	-1.33370000	-4.71016100	1.63898100	C	-1.23730000	5.16177000	-0.06487500
H	-4.14878500	-4.93497200	-1.60893600	H	-1.99963200	5.46023700	1.93181500
H	-2.57120000	-6.05417500	-0.04684000	H	-0.61810700	4.57904700	-2.04843200
C	-2.37045200	2.62781600	0.10293000	H	-0.79645600	6.15151400	-0.13088300
C	-2.48448900	3.50405000	1.18433600				

Table 74: Optimized geometry for **TS_{4b}**

Free energy G = -1289.440554 Hartree/particle.

C	-5.04338700	-1.78981200	0.36578600	N	3.14219900	0.51933300	0.01697800
C	-3.67538800	-2.42854300	0.24096400	N	1.87418500	2.25410000	-0.14573200
C	-3.30063200	-0.22341600	1.16614800	C	3.18091900	2.72073100	-0.04409000
C	-4.76398500	-0.29787400	0.66419900	C	3.97825600	1.62968200	0.05832400
H	-5.65132200	-1.94105900	-0.53130600	H	3.41756400	3.77142100	-0.08224300
H	-5.57362400	-2.27853600	1.19055900	H	5.04990900	1.53777400	0.12710100
H	-5.45762700	0.11490200	1.39973600	C	0.73423300	3.11921500	-0.27078100
H	-4.84712100	0.30639400	-0.24113500	C	0.52448800	4.10765300	0.69368900
C	-3.20396300	-0.31719600	2.70733500	C	-0.12439600	2.98633500	-1.36469900
H	-2.16040300	-0.35434400	3.03535900	C	-0.56461700	4.97014600	0.56119200
H	-3.67078000	0.57913300	3.12478400	H	1.20010600	4.19236800	1.53889600
H	-3.72453700	-1.19621900	3.09903400	C	-1.21578700	3.84872000	-1.48161800
C	-2.66025100	-1.53240300	0.68361600	H	0.07019600	2.22805200	-2.11529600
C	-1.35873100	-1.74608100	0.09894800	C	-1.43642800	4.84025900	-0.52258800
H	-0.97355700	-2.75114500	0.27707100	H	-0.73281600	5.73842600	1.30912500
Au	0.19420000	-0.36659900	-0.03151100	H	-1.88553000	3.75106100	-2.33016500
O	-2.70651400	0.96800000	0.69763100	H	-2.28334800	5.51195100	-0.62141800
H	-1.74283600	0.91554800	0.83437300	C	3.61249500	-0.83531600	0.10249300
C	-2.53815600	-1.98936500	-1.01510900	C	3.31101100	-1.74128000	-0.91762500
C	-2.27748800	-3.31067200	-1.76205600	C	4.38768000	-1.21779000	1.19940600
H	-3.15349600	-3.57576900	-2.36102000	C	3.78033100	-3.05265900	-0.82430800
H	-1.42787200	-3.15273600	-2.43312700	H	2.72976800	-1.41690800	-1.77392900
H	-2.04045200	-4.13878500	-1.09408700	C	4.85951100	-2.52910500	1.27729700
C	-2.91400700	-0.85839100	-1.96096800	H	4.60738500	-0.50108500	1.98426900
H	-2.90805800	0.11603300	-1.47591900	C	4.55373100	-3.44765800	0.27014800
H	-2.18210200	-0.83593300	-2.77465300	H	3.55117900	-3.76019900	-1.61494400
H	-3.89740700	-1.03889300	-2.40739400	H	5.46023800	-2.83183100	2.12902700
H	-3.58486900	-3.50661400	0.30810300	H	4.92124400	-4.46694100	0.33537300
C	1.83552200	0.89269500	-0.09679500				

Table 75: Optimized geometry for **Vb**

Free energy G = -1289.510806 Hartree/particle.

C	4.26397900	-2.23468600	-1.35784900	H	5.06953800	-1.50242500	-1.48260100
C	1.83244900	-2.43989400	-1.68335300	H	4.74038100	-3.22486300	-1.39469500
C	3.14951100	-2.09462500	-2.41589500	H	3.30683500	-2.71593900	-3.30123400

H	3.07903000	-1.05273900	-2.74316500
C	1.41032900	-3.90206100	-1.88676300
H	0.51227800	-4.14746700	-1.30719900
H	1.19160400	-4.08100100	-2.94394800
H	2.20540500	-4.58593800	-1.57538700
C	2.18785100	-2.14751800	-0.21361600
Au	-0.07233000	-0.17969000	0.57913400
O	0.80721200	-1.56705600	-2.19066800
H	-0.05688300	-1.94296100	-1.97235100
C	3.52223400	-2.06199800	-0.05853200
H	4.03855200	-1.94485000	0.88773800
C	1.15925800	-1.54581900	2.08461900
C	2.30199600	-0.70767600	2.60529300
H	3.00755800	-1.35624700	3.14171400
H	2.84875400	-0.19791800	1.81101600
H	1.93773400	0.03211700	3.32345200
C	0.17559200	-2.00670900	3.13844800
H	-0.65281700	-2.57834400	2.71387600
H	0.70673900	-2.65288900	3.85004300
H	-0.22506200	-1.16478400	3.71061600
C	1.13836000	-2.12765100	0.81942000
H	0.33038800	-2.84212400	0.65183300
C	-1.18357600	1.37050700	-0.15446200
N	-0.74910100	2.61558500	-0.48729100
N	-2.49256100	1.34207800	-0.52522000
C	-1.77010800	3.35044200	-1.07661400
H	-1.62787600	4.37004200	-1.39559800
C	-2.86546000	2.55027300	-1.10122900
H	-3.86998100	2.73276500	-1.44633900
C	-3.37496400	0.21601200	-0.37996100
C	-3.60593200	-0.32509500	0.88700100
C	-4.00189800	-0.30485700	-1.51389500
C	-4.46575900	-1.41768900	1.01260700
H	-3.12968300	0.11256700	1.75751400
C	-4.86637400	-1.39186000	-1.37428600
H	-3.80705800	0.12828000	-2.48969800
C	-5.09486300	-1.95173800	-0.11485700
H	-4.65241300	-1.84122300	1.99434000
H	-5.35492000	-1.80267800	-2.25197100
H	-5.76649200	-2.79809700	-0.01135000
C	0.58453100	3.11595500	-0.28858800
C	1.31530700	3.55251200	-1.39530900
C	1.11549300	3.18041200	1.00152900
C	2.60367700	4.05392100	-1.20390900
H	0.88453600	3.48899100	-2.38941100
C	2.40832500	3.67594500	1.17911000
H	0.51906500	2.86090300	1.84927500
C	3.15206400	4.11207300	0.07975900
H	3.17866300	4.39221000	-2.05987100
H	2.82706000	3.73242800	2.17884200
H	4.15493800	4.50143600	0.22387000

General Conclusions

The research developed in this Doctoral Thesis has led to the following results:

– A novel approach for the synthesis of C_{3h}-symmetric aryltrindenes by a threefold Pd-catalyzed cross-coupling of four C_{15} trindene fragments and its application for the synthesis of a new trindane-based crushed fullerene C_{60} has been developed. The central motif's trindene C_{15} skeleton was constructed through a triple gold(I)-catalyzed oxidative cyclization, highlighting the ability of gold catalysis towards the construction of molecular complexity (see Chapter I). In a parallel study, a new crushed fullerene $C_{60}H_{24}$, which proved to form C_{60} upon laser irradiation, could be prepared through a Pd-catalyzed sixfold arylation (see the corresponding publication in the appendix).

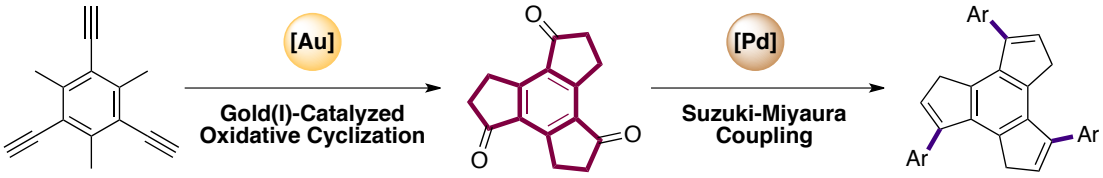

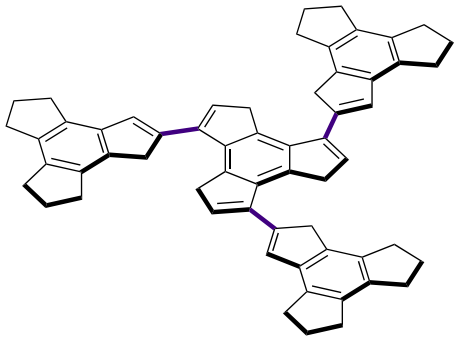

– We have extended the scope of the intramolecular gold(I)-catalyzed [2+2+2] cycloaddition reaction to *O*-protected homopropargylic and allylic oxo-1,5-enynes. Although the preliminary results obtained for oxo-1,5-enynes demonstrated that the control of the diastereoselectivity would be more challenging with these substrates, under the optimized reaction conditions, the cyclization of (Z)- and (*E*)- isomers takes place with moderate to excellent yields and increased selectivity in most of the cases, providing access to octahydro-1*H*-indenes skeletons. Furthermore, a mechanistic picture for this transformation has been proposed, which was supported by DFT calculations (see Chapter II).

– The mastery of gold(I) complexes for the construction of complex polycyclic scaffolds has been applied in the context of the total synthesis of natural products. Thus, two different methodologies have been used in the construction of the core skeleton of two families of natural products, the pycnanthuquinones and the carexanes. Furthermore, the first total synthesis of racemic carexane I was completed from the resulting dihydronaphthalene derivative in 4 steps and 18% overall yield (see Chapter III).

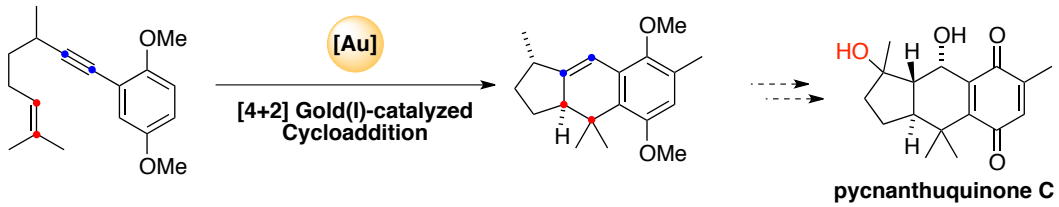

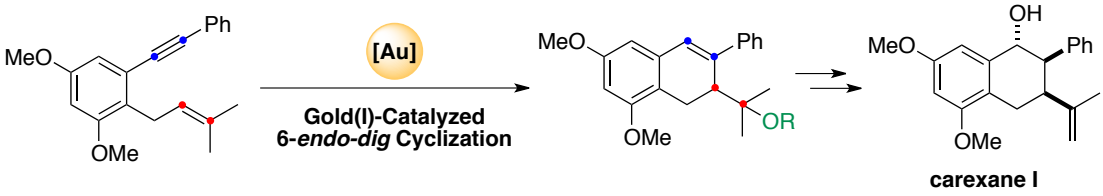

– We have performed a computational examination of gold(I)-catalyzed skeletal rearrangements of model 1,6-enynes bearing OR groups at the propargyl position. DFT calculations suggest that after the initial cyclization, the 1,5-OR migration proceeds stepwise through a cyclic intermediate although the cleavage occurs though a very low barrier. The nature of the propargylic alkoxy group and the substitution pattern at the alkene moiety play a crucial role for the formation of the 1,5-migration product *vs.* other possible competitive processes (see Chapter IV).

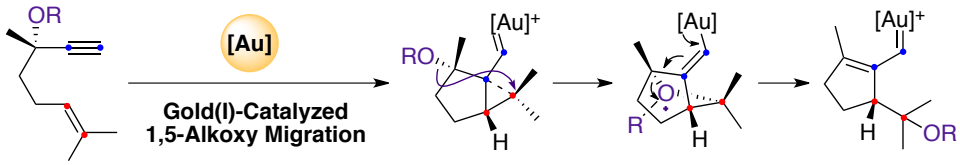

Appendix

ChemPubSoc Europe
DOI: 10.1002/ejoc.201600311
EurJOC European Journal of Organic Chemistry
Full Paper

Fullerenes

Synthesis of a Crushed Fullerene $C_{60}H_{24}$ through Sixfold Palladium-Catalyzed Arylation

Ruth Dorel,[a] Paula de Mendoza,[a] Pilar Calleja,[a] Sergio Pascual,[a] Esther González-Cantalapiedra,[a][‡] Noemí Cabello,[a] and Antonio M. Echavarren*[a,b]

Dedicated to Professor Achille Umani-Ronchi in the occasion of his 80th birthday

Abstract: The synthesis of a new C_{3v}-symmetric crushed fullerene $C_{60}H_{24}$ (**5**) has been accomplished in three steps from truxene through sixfold palladium-catalyzed intramolecular arylation of a *syn*-trialkylated truxene precursor. Laser irradiation of **5** induces cyclodehydrogenation processes that result in the formation of C_{60}, as detected by LDI-MS.

Introduction

Truxene (10,15-dihydro-5*H*-diindeno[1,2-*a*:1′,2′-*c*]fluorene) (**1**) is a useful platform for the threefold synthesis of crushed fullerene $C_{60}H_{30}$ (**2**) and other C_{3v}-symmetric molecules (Scheme 1),[1–3] as well as being an attractive building block for the preparation of new materials to be used in molecular electronics.[4] The laser-induced cyclodehydrogenation in the gas phase to form closed-shell C_{60} fullerene has been previously demonstrated for **2** ("crushed fullerene")[5] and other related functionalized compounds,[6] whereas flash-vacuum pyrolysis was used in the synthesis of fullerene C_{60} from $C_{60}H_{27}Cl_3$ as the precursor.[7]

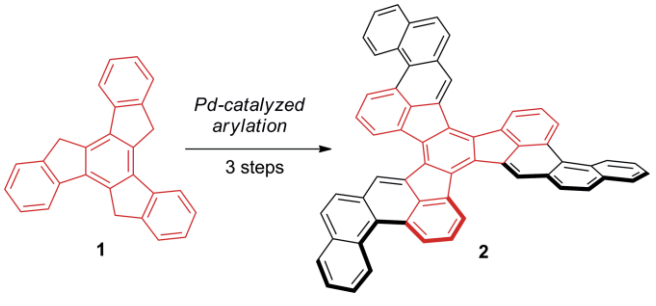

Scheme 1. Synthesis of crushed fullerene $C_{60}H_{30}$ (**2**).

Fullerene C_{60} and triazafullererene $C_{57}N_3$ were also formed from **2** and $C_{57}H_{33}N_3$[8] precursors, respectively, by cyclodehydrogenation on a platinum surface.[9] STM images were obtained for deposited triangular fullerene precursors that, after annealing at 750 K, formed round-shaped C_{60}, indistinguishable from those images of authentic C_{60} fullerene, and ball-shaped heterofullerene $C_{57}N_3$, which was previously unknown.

We now report our efforts towards the synthesis of new crushed fullerenes already containing 78 of the 90 C–C bonds present in C_{60} fullerene. We envisioned two possible truxene-

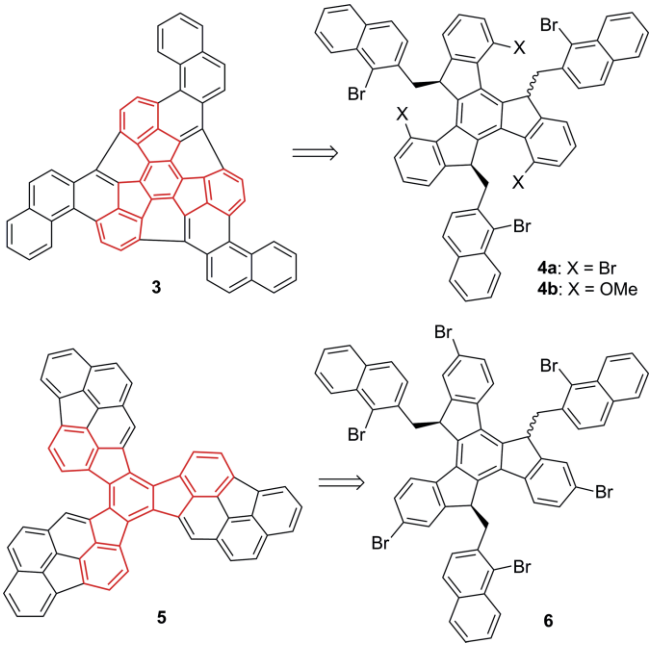

Scheme 2. Retrosynthetic strategy for crushed fullerenes $C_{60}H_{24}$ **3** and **5**.

[a] *Institute of Chemical Research of Catalonia (ICIQ), Barcelona Institute of Science and Technology,*
Av. Països Catalans 16, 43007 Tarragona, Spain
E-mail: aechavarren@iciq.es
http://www.iciq.org/research/research_group/prof-antonio-m-echavarren/
[b] *Departament de Química Orgànica i Analítica, Universitat Rovira i Virgili, C/ Marcel·lí Domingo s/n, 43007 Tarragona, Spain*
[‡] Current address: Medicinal Chemistry Department, Spanish National Cancer Research Centre (CNIO)
C/ Melchor Fernández Almagro 3, 28029 Madrid, Spain
Supporting information and ORCID(s) from the author(s) for this article are available on the WWW under http://dx.doi.org/10.1002/ejoc.201600311.

based $C_{60}H_{24}$ isomers **3** and **5**, which are more advanced crushed fullerenes than **2** and could be respectively accessed from the suitably functionalized trialkylated truxene precursors **4** and **6** by means of multiple Pd-catalyzed direct arylations (Scheme 2).[10] These π-expanded truxenes could also give rise to C_{60} by laser-promoted cyclodehydrogenation (Scheme 3). Interestingly, **5** was proposed to be a plausible intermediate in the formation of C_{60} fullerene,[11] although its synthesis and characterization have never been reported.

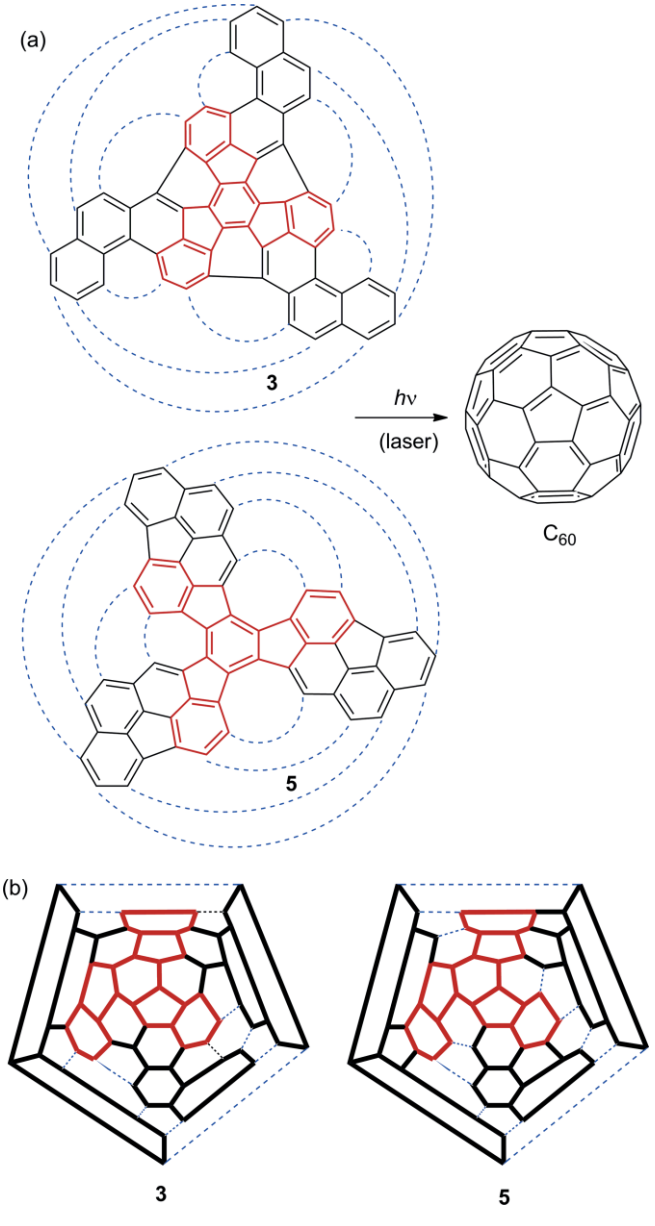

Scheme 3. (a) Laser-induced formation of C_{60} fullerene from **3** and **5**. (b) Schlegel projections of **3** and **5** onto C_{60}.

Although remarkable multiple intermolecular palladium-catalyzed arylations have been reported,[12] for the intramolecular palladium-catalyzed arylation reaction of bromoarenes, the formation of **5** from **6** would involve the highest order (sixfold) arylation of this type to date.[12a]

Results and Discussion

4,9,14-Trisubstituted truxenes **7** were prepared by acid-catalyzed trimerization of the corresponding 7-substituted 1-indanones.[1b] Triple alkylation of their lithium or sodium trianions afforded the expected products **4** as crude mixtures of *syn* and *anti* isomers, as determined from ^{1}H NMR spectra of the crude materials, which surprisingly could not be isomerized in the presence of base to form exclusively the *syn* isomer, as we had previously observed in the vast majority of cases.[1a] Thus, **4a** was obtained as a 1.3:1 mixture of *syn* and *anti* isomers after chromatographic purification, whereas in the case of **4b**, pure *anti* isomer was isolated after column chromatography and precipitation from mixtures of CH_2Cl_2 and pentane (Scheme 4). The structure of *anti*-**4b** was confirmed by X-ray diffraction analysis.[13]

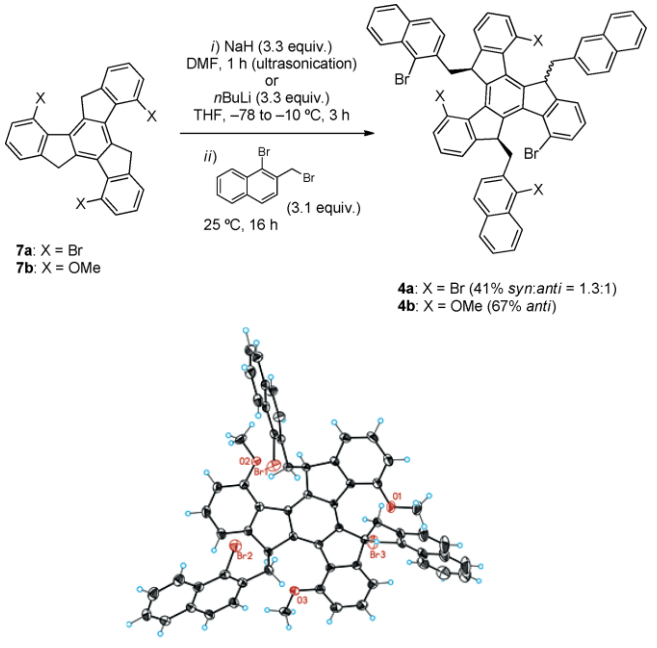

Scheme 4. Synthesis of trialkylated precursors **4** and X-ray crystal structure of *anti*-**4b**.

Given that all attempts to convert **4a** directly into crushed fullerene **3** by Pd-catalyzed intramolecular direct arylation afforded complex mixtures from which **3** could not be identified, we turned our attention to the cyclization of **4b**. It seemed clear to us that this cyclization could be sequentially carried out by initial triple Pd-catalyzed cyclization of **4b** to form **8** after dehydrogenation, followed by triple demethylation, formation of the corresponding tristriflate, and subsequent triple Pd-catalyzed intramolecular arylation (Scheme 5). After screening a range of reaction conditions, we found that the triple Pd-catalyzed cyclization of *anti*-**4b** proceeded in moderate yield in the presence of $Pd(OAc)_2$ and PhDavePhos. Treatment of the resulting mixture with 2,3-dichloro-5,6-dicyano-1,4-benzoquinone (DDQ) forced the triple dehydrogenation to afford **8** in 31 % yield over the two steps, the structure of which was confirmed by X-ray diffraction.[13] Demethylation of **8** was carried out with BBr_3 to form **9** as a poorly soluble solid in excellent yield. However, conversion of **9** into tristriflate **10** could only be achieved

ChemPubSoc Europe
EurJOC European Journal of Organic Chemistry
Full Paper

at low temperatures and in low yield. Furthermore, **10** turned out to be unstable under ambient conditions, and attempts to cyclize this tristriflate to form **3** in the presence of different Pd catalysts failed, providing complex mixtures, presumably due to its low stability.

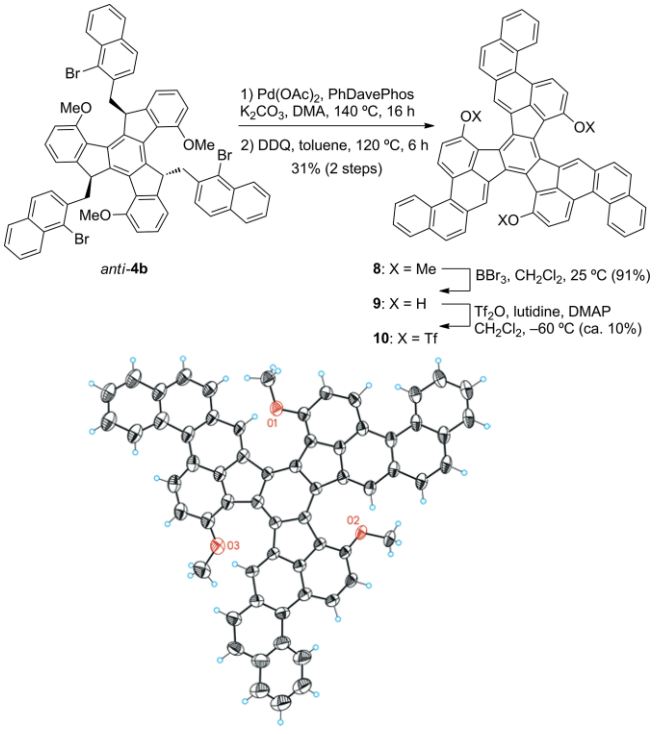

Scheme 5. Synthesis tristriflate **10** from *anti*-**4b** and X-ray crystal structure of **8**.

Not discouraged by these results, we decided to focus our efforts on the synthesis of crushed fullerene **5**. Thus, tribromotruxene **11** was prepared by direct bromination of truxene,[1b] which can be readily obtained in a multigram scale from 1-indanone.[14] Triple alkylation of the corresponding sodium trianion with 1-bromo-2-(bromomethyl)naphthalene furnished the desired hexabrominated precursor **6**. The triple alkylation of **11** afforded mixtures of *anti* and *syn* isomers that, as happened in the case of **4**, could not be isomerized in the presence of base to form exclusively the *syn* isomer.[1a] Nevertheless, pure *syn* isomer could be obtained upon precipitation from mixtures of CH_2Cl_2 and pentane (Scheme 6). A conceivable alternative synthesis of **5** by the direct acid-catalyzed triannulation strategy[15] would require the development of a synthesis of unknown ketone indeno[4,3,2,1-*lmno*]acephenanthrylen-1(2*H*)-one or its regioisomer.[16]

Hexabromotruxene *syn*-**6** was next subjected to different palladium-catalyzed direct arylation reaction conditions. Due to the high insolubility of both *syn*-**6** and the product of this transformation, LDI-MS experiments were used as a tool to find the optimal conditions for the intramolecular arylation. When $Pd(OAc)_2$, $BnMe_3NBr$, and K_2CO_3[1g] were used under different reaction conditions, only complex mixtures were detected, and no clear formation of **5** was observed. The use of phosphine ligands such as Xantphos, 1,3-bis(diphenylphosphanyl)propane (dppp) or PhDavePhos did not result in any improvement. Fortunately, when ethylenebis(diphenylphosphine) (dppe) was used as the ligand, we were able to observe clear evidence for the formation of **5**. After extensive optimization of the reaction conditions, LDI experiments of the isolated solid in positive and negative modes showed a single peak at *m*/*z* 744 with an experimental isotopic pattern that was consistent with the theoretical distribution calculated for **5** (Figure 1). This peak corresponds to the target crushed fullerene, which could be isolated in 44 % yield as a highly insoluble orange solid. Formation of **5** from *syn*-**6** involves a remarkable sequence of nine reactions catalyzed by palladium: sixfold intramolecular arylation and a triple dehydrogenation process.

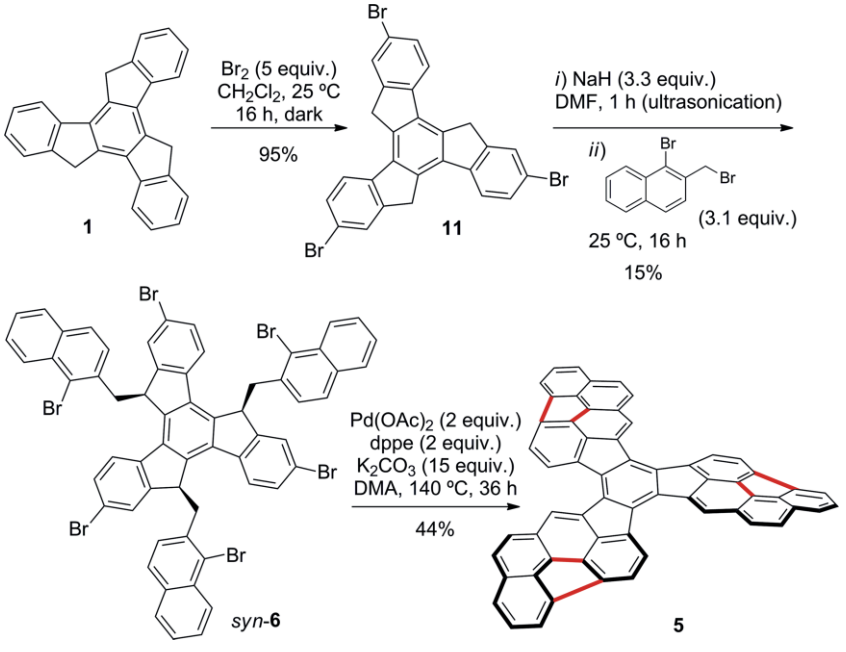

Scheme 6. Synthesis of crushed fullerene $C_{60}H_{24}$ (**5**).

ChemPubSoc Europe
EurJOC European Journal of Organic Chemistry
Full Paper

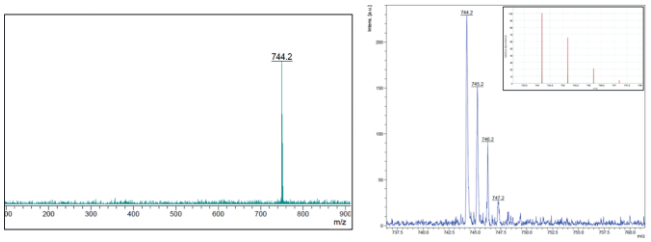

Figure 1. (left) LDI$^-$ mass spectrum of crushed fullerene $C_{60}H_{24}$ (**5**). (right) Theoretical and experimental isotopic pattern for $C_{60}H_{24}$ (**5**).

To verify that **5** is a direct precursor of C_{60} fullerene, a sample of pure $C_{60}H_{24}$ was analyzed by MALDI and LDI-MS in positive and negative modes by using increasing laser powers, and the results in positive mode were compared to those arising from the analogous experiments on a sample of pure C_{60}. MALDI-MS analysis at the threshold of ion formation in negative mode using 2,5-dihydroxybenzoic acid (DHB) as the matrix showed exclusively the molecular ion of **3**, whereas at a higher laser power in the range of 129 μJ, this precursor ion underwent threefold H_2 loss giving $[C_{60}H_{22}]^{\bullet-}$, $[C_{60}H_{20}]^{\bullet-}$, and $[C_{60}H_{18}]^{\bullet-}$ (*m/z* 742, 740, and 738, respectively, Figure 2, a). On the other hand, when the sample was analyzed in positive mode by LDI-MS to avoid interferences derived from the matrix at a laser power in the range of 126 μJ, a peak at *m/z* 721 corresponding to the formation of $[C_{60} + H]^{\bullet+}$ could be identified, which underwent further C_2 fragmentations to give a series similar to that resulting from pure C_{60} fullerene (Figure 2, b).[5b]

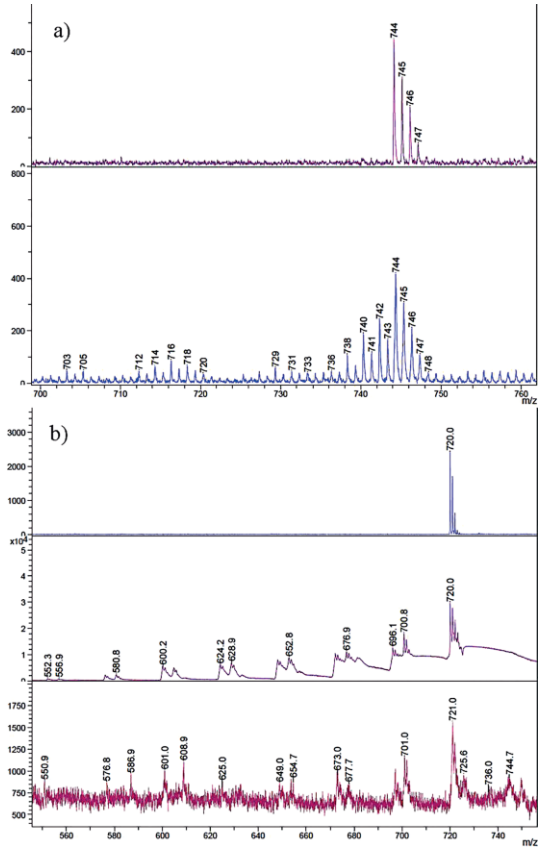

Figure 2. (a) (top) MALDI$^-$ mass spectrum of **5** at the threshold of ion formation using DHB as the matrix. (bottom) MALDI$^-$ mass spectrum of **5** at 129 μJ using DHB as the matrix. (b) (top) LDI$^+$ mass spectrum of C_{60} fullerene at a laser power of 106 μJ. (center) LDI$^+$ mass spectrum of C_{60} fullerene at a laser power of 115 μJ. (bottom) LDI$^+$ mass spectrum of **5** at a laser power of 126 μJ.

Conclusions

A new, advanced crushed fullerene $C_{60}H_{24}$ has been synthesized by a sixfold palladium-catalyzed intramolecular arylation, which takes place in a remarkable 44 % yield, equivalent to an average 87 % yield per C–C bond formation, and subsequent in situ dehydrogenation. Open-shell C_{60} derivative **5** gives rise to C_{60} fullerene by applying high-power laser irradiation in LDI-MS experiments. On-surface cyclodehydrogenation experiments to form C_{60} are underway.

Experimental Section

General Procedures: Reactions were performed under argon atmosphere in solvents dried by passing through an activated alumina column on a PureSolvTM solvent purification system (Innovative Technologies, Inc., MA). Thin-layer chromatography was carried out using TLC aluminum sheets coated with 0.2 mm of silica gel (Merck Gf234). Chromatographic purifications were carried out using flash grade silica gel (SDS Chromatogel 60 ACC, 40–60 μm). NMR spectra were recorded at 25 °C with a Bruker Avance 300, 400 Ultrashield and Bruker Avance 500 Ultrashield apparatus, or at 120 °C with a Bruker Avance 500 Ultrashield apparatus. Mass spectra were recorded with a MicroTOF Focus Bruker Daltonics mass spectrometer (ESI) or with an Autoflex Bruker Daltonics (MALDI and LDI) equipped with a nitrogen laser (337 nm) with a mean energy of 165.6 μJ per pulse and a beam dimension of 4 × 2.5 mm. Samples were measured at least four times under the same conditions and a minimum of 200 shots were accumulated per full spectrum. Melting points were determined with a Büchi melting point apparatus. Crystal structure determinations were carried out with a Bruker-Nonius diffractometer equipped with an APPEX 2 4K CCD area detector, a FR591 rotating anode with Mo-Kα radiation, Montel mirrors as monochromator and a Kryoflex low-temperature device (*T* = –173 °C). Full-sphere data collection was used with w and j scans. Programs used: Data collection APEX-2, data reduction Bruker Saint V/.60A and absorption correction SADABS. Structure Solution and Refinement: Crystal structure solution was achieved by using direct methods as implement in SHELXTL and visualized by using the program XP. Missing atoms were subsequently located from difference Fourier synthesis and added to the atom list. Least-squares refinement on F^2 using all measured intensities was carried out using the program SHELXTL. All non-hydrogen atoms were refined including anisotropic displacement parameters.

5,10,15-Tris[(1-bromonaphthalen-2-yl)methyl]-4,9,14-tribromo-10,15-dihydro-5*H*-diindeno[1,2-*a*:1′,2′-*c*]fluorine (4a): A suspension of 4,9,14-tribromo-10,15-dihydro-5*H*-diindeno[1,2-*a*:1′,2′-*c*]-fluorene (360 mg, 0.62 mmol) in anhydrous DMF (5 mL) was added over a suspension of NaH (60 % in mineral oil, 82 mg, 2.04 mmol) in anhydrous DMF (5 mL) at 0 °C under Ar atmosphere. After ultrasonicating the resulting mixture for 50 min, a solution of 1-bromo-2-(bromomethyl)naphthalene (577 mg, 1.92 mmol) in anhydrous DMF (10 mL) was added and the mixture was stirred at room temperature for 16 h. H_2O (20 mL) was added and the precipitate formed was filtered off and dissolved in CH_2Cl_2 (50 mL). The result-

ChemPubSoc Europe
EurJOC European Journal of Organic Chemistry
Full Paper

ing green solution was dried with $MgSO_4$, filtered and concentrated under reduced pressure. Purification by silica gel column chromatography (cyclohexane/CH_2Cl_2 8:2) gave a major fraction containing **4a** as a mixture of *syn* and *anti* isomers together with unidentified impurities. This fraction was partially dissolved in CH_2Cl_2 (10 mL) and precipitated with pentane (30 mL). The supernatant was removed and the solid was washed again with pentane (3 × 20 mL) and dried under reduced pressure giving the title compound, yield 331 mg (0.268 mmol, 41 %); pale-yellow solid; *syn*/*anti* = 1.3:1; m.p. 298–300 °C. ^{1}H NMR (500 MHz, $CDCl_3$): δ = 8.22–8.16 (m, 4.9 H, *syn*, *anti*), 8.13 (d, *J* = 8.5 Hz, 2 H, *anti*), 7.80 (d, *J* = 9.6 Hz, 1 H, *anti*), 7.74–7.69 (m, 5.9 H, *syn*, *anti*), 7.68–7.63 (m, 5.9 H, *syn*, *anti*), 7.62–7.58 (m, 4.9 H, *syn*, *anti*), 7.57–7.47 (m, 10 H), 7.46–7.43 (m, 3.9 H, *syn*), 7.43–7.39 (m, 4.9 H, *syn*, *anti*), 7.36–7.33 (m, 3 H, *anti*), 7.26 (d, *J* = 8.4 Hz, 3.9 H, *syn*), 7.09 (t, *J* = 8.4 Hz, 1 H, *anti*), 6.96 (t, *J* = 7.6 Hz, 3.9 H, *syn*), 6.89 (dt, *J* = 7.4, 0.9 Hz, 3.9 H, *syn*), 6.87–6.84 (m, 1 H, *anti*), 6.81 (d, *J* = 7.6 Hz, 1 H, *anti*), 6.79–6.76 (m, 1 H, *anti*), 6.63 (t, *J* = 7.6 Hz, 1 H, *anti*), 6.44 (t, *J* = 7.5 Hz, 1 H, *anti*), 6.41–6.36 (m, 2 H, *anti*), 6.12 (dd, *J* = 8.5, 6.1 Hz, 3.9 H, *syn*), 5.99 (dd, *J* = 9.7, 5.9 Hz, 1 H, *anti*), 3.77–3.71 (m, 3.9 H, *syn*), 3.70–3.67 (m, 1 H, *anti*), 3.59 (dd, *J* = 13.8, 7.0 Hz, 1 H, *anti*), 3.49 (dd, *J* = 13.8, 6.6 Hz, 1 H, *anti*), 3.22 (dd, *J* = 13.8, 8.0 Hz, 1 H, *anti*), 3.16 (dd, *J* = 14.1, 8.6 Hz, 3.9 H, *syn*), 2.76 (dd, *J* = 13.9, 9.8 Hz, 1 H, *anti*) ppm. ^{13}C NMR (126 MHz, $CDCl_3$): δ = 150.66, 150.31, 149.54, 149.16, 144.95, 144.43, 142.51, 142.41, 141.14, 140.64, 139.30, 138.95, 137.65, 137.26, 137.23, 137.01, 136.87, 136.68, 136.30, 135.92, 133.31, 133.28, 133.24, 133.20, 133.15, 132.91, 132.85, 132.37, 132.24, 132.21, 132.20, 128.27, 128.18, 128.08, 128.02, 127.97, 127.94, 127.88, 127.86, 127.84, 127.79, 127.74, 127.68, 127.60, 127.40, 127.37, 127.24, 127.17, 127.14, 126.99, 126.87, 126.84, 126.25, 126.02, 125.99, 125.85, 125.80, 125.64, 125.52, 123.88, 123.79, 123.32, 123.30, 116.11, 115.99, 115.19, 52.49 (*anti*), 52.14 (*syn*), 50.45 (*anti*), 49.98 (*anti*), 42.12 (*anti*), 41.53 (*anti*), 39.95 (*anti*), 39.31 (*syn*) (aromatic peaks missing due to overlapping) ppm. HRMS (MALDI$^+$): *m*/*z* calcd. for $C_{60}H_{35}{}^{79}Br_3{}^{81}Br_3$ [M – H]$^+$ 1234.7772; found 1234.7785.

(5*R,10*S**,15*S**)-5,10,15-Tris[(1-bromonaphthalen-2-yl)methyl]-4,9,14-trimethoxy-10,15-dihydro-5*H*-diindeno[1,2-*a*:1′,2′-*c*]fluorine (*anti*-4b):** To a mixture of 4,9,14-trimethoxy-10,15-dihydro-5*H*-diindeno[1,2-*a*:1′,2′-*c*]fluorine (600 mg, 1.39 mmol) in anhydrous THF (55 mL) at –78 °C was added *n*BuLi (2.5 M in hexanes, 1.94 mL, 4.86 mmol) and the mixture was slowly warmed to –10 °C for 3 h. Then, 1-bromo-2-bromomethylnaphthalene (1.67 g, 5.56 mmol) in anhydrous THF (20 mL) was added and the mixture was warmed to room temperature. After 30 min at that temperature, the mixture was diluted with EtOAc and washed with saturated aqueous NaCl, dried with $MgSO_4$, and the volatiles evaporated. The residue was purified by chromatography (cyclohexane/CH_2Cl_2, 8:2 to 1:1) to give **4b** as a 3:1 mixture of *anti*/*syn* isomers together with unidentified impurities. After precipitation from CH_2Cl_2/pentane mixtures, pure *anti*-**4b** was obtained, yield 1.01 g (0.93 mmol, 67 %); m.p. 193–195 °C. ^{1}H NMR (400 MHz, $CDCl_3$): δ = 8.25 (dt, *J* = 8.6, 1.0 Hz, 1 H), 8.22 (d, *J* = 8.6 Hz, 1 H), 8.18 (dd, *J* = 8.6, 1.0 Hz, 1 H), 7.78 (d, *J* = 7.0 Hz, 1 H), 7.73 (d, *J* = 7.0 Hz, 1 H), 7.65 (d, *J* = 8.4 Hz, 1 H), 7.61 (d, *J* = 5.5 Hz, 1 H), 7.59 (d, *J* = 6.2 Hz, 1 H), 7.55 (dt, *J* = 8.7, 1.6 Hz, 1 H), 7.51 (dd, *J* = 6.2, 1.4 Hz, 1 H), 7.49–7.41 (m, 5 H), 7.38 (d, *J* = 8.4 Hz, 1 H), 7.32 (ddd, *J* = 8.0, 6.8, 1.2 Hz, 1 H), 7.14–7.09 (m, 1 H), 7.06 (d, *J* = 7.6 Hz, 1 H), 7.02 (d, *J* = 7.6 Hz, 1 H), 6.94 (dd, *J* = 8.1, 7.4 Hz, 1 H), 6.86–6.76 (m, 4 H), 6.68 (dt, *J* = 7.4, 0.9 Hz, 1 H), 6.40 (dt, *J* = 7.4, 0.9 Hz, 1 H), 5.74 (dd, *J* = 8.3, 5.8 Hz, 1 H), 5.64 (t, *J* = 6.2 Hz, 1 H), 5.47 (dd, *J* = 9.5, 5.3 Hz, 1 H), 4.13 (s, 3 H), 4.08 (s, 3 H), 4.06 (s, 3 H), 4.04–4.00 (m, 1 H), 3.79 (dd, *J* = 14.0, 5.9 Hz, 1 H), 3.64 (dd, *J* = 13.8, 6.3 Hz, 1 H), 3.50 (dd, *J* = 14.2, 5.3 Hz, 1 H), 3.21 (dd, *J* = 14.0, 8.3 Hz, 1 H), 2.85 (dd, *J* = 14.1, 9.5 Hz, 1 H) ppm. ^{13}C NMR (101 MHz, $CDCl_3$): δ = 154.45, 154.30, 154.14, 150.07, 148.98, 142.91, 141.24, 141.09, 138.18, 137.74, 137.15, 136.21, 136.15, 135.88, 133.17, 133.11, 132.34, 132.29, 129.73, 128.55, 128.42, 128.21, 128.13, 128.02, 127.96, 127.87, 127.78, 127.76, 127.73, 127.57, 127.47, 126.99, 126.88, 126.77, 126.53, 126.50, 125.79, 125.72, 125.69, 125.61, 125.51, 125.28, 118.22, 117.73, 117.67, 110.04, 109.92, 109.84, 56.07, 55.96, 55.61, 50.97, 50.04, 49.56, 42.78, 41.68, 41.57 (peaks missing due to overlapping) ppm. HRMS (ESI$^+$): *m*/*z* calcd. for $C_{63}H_{45}Br_3NaO_3$ [M + Na]$^+$ 1109.0811; found 1109.0779.

3,13,23-Trimethoxybenzo[1,2-*e*:3,4-*e*′:5,6-*e*′′]tribenzo[*l*]-acephenanthrylene (8): Compound *anti*-**4b** (400 mg, 0.37 mmol), $Pd(OAc)_2$ (82.4 mg, 0.37 mmol), PhDavePhos (70.6 mg, 0.19 mmol) and K_2CO_3 (102.3 mg, 0.74 mmol) were suspended in anhydrous DMA (1.9 mL, 0.2 M) in a sealed tube under Ar atmosphere, and the mixture was heated at 140 °C for 16 h. After cooling to room temperature, $CHCl_3$ (20 mL) was added and the mixture was washed with saturated aqueous NaCl (3 × 15 mL), dried with $MgSO_4$, and concentrated to dryness. The resulting crude material was dissolved in toluene (10 mL), then DDQ (840 mg, 3.7 mmol) was added and the reaction was stirred at 120 °C for 6 h. After cooling to room temperature, the solution was washed with 2 M solution of KOH (3 × 10 mL), dried with $MgSO_4$, and concentrated to a volume of ca. 2 mL (higher yields were obtained when the crude material was not taken to dryness). Purification by flash chromatography (cyclohexane/$CHCl_3$, 7:3 to 0:1) afforded the product as a brownish solid that became insoluble after drying, yield 96.5 mg (0.11 mmol, 31 % over two steps); m.p. >300 °C. ^{1}H NMR (400 MHz, $C_2D_2Cl_4$): δ = 9.24 (d, *J* = 8.4 Hz, 3 H), 9.10 (d, *J* = 9.1 Hz, 3 H), 8.42 (s, 3 H), 8.12 (dd, *J* = 8.0, 1.4 Hz, 3 H), 8.06 (d, *J* = 8.6 Hz, 3 H), 7.94 (d, *J* = 8.6 Hz, 3 H), 7.85 (ddd, *J* = 8.4, 6.8, 1.5 Hz, 3 H), 7.74 (ddd, *J* = 7.9, 6.8, 1.0 Hz, 3 H), 7.61 (d, *J* = 9.2 Hz, 3 H), 4.12 (s, 9 H) ppm. ^{13}C NMR (101 MHz, $C_2D_2Cl_4$): δ = 153.16, 136.34, 134.69, 133.49, 133.17, 131.87, 131.04, 130.06, 129.66, 128.72, 128.29, 128.15, 128.02, 126.57, 126.13, 126.08, 125.52, 121.55, 121.54, 113.70, 54.79 ppm. HRMS (MALDI$^+$): *m*/*z* calcd. for $C_{63}H_{36}O_3$ [M]$^+$ 840.2664; found 840.2673.

3,13,23-Trihydroxybenzo[1,2-*e*:3,4-*e*′:5,6-*e*′′]tribenzo[*l*]acephenanthrylene (9): To a mixture of **8** (70 mg, 0.08 mmol) in anhydrous CH_2Cl_2 (10 mL) was added BBr_3 (1.0 M in CH_2Cl_2, 2.12 mL, 2.12 mmol) and the mixture was stirred at room temperature for 5 d. After cooling to 0 °C, H_2O (10 mL) was slowly added, the aqueous phase was extracted with CH_2Cl_2 (10 mL), the combined organic layers were dried with $MgSO_4$ and the volatiles evaporated. The solid was triturated with hexanes and EtOAc to obtain **9** as a brown solid with low solubility in organic solvents, yield 57.4 mg (0.07 mmol, 91 %); m.p. >300 °C. ^{1}H NMR (400 MHz, [D_6]acetone): δ = 10.00 (s, 3 H), 9.32 (d, *J* = 8.5 Hz, 3 H), 9.15 (d, *J* = 9.0 Hz, 3 H), 9.01 (s, 3 H), 8.24 (d, *J* = 8.6 Hz, 3 H), 8.16 (d, *J* = 7.9 Hz, 4 H), 8.02 (d, *J* = 8.6 Hz, 3 H), 7.88–7.83 (m, 3 H), 7.75–7.71 (m, 6 H) ppm. Full ^{13}C NMR spectroscopic data could not be recorded due to the low solubility of the product. HRMS (FAB$^+$): *m*/*z* calcd. for $C_{60}H_{30}O_3$ [M]$^+$ 798.2195; found 798.2194.

(5*S,10*S**,15*S**)-2,7,12-Tribromo-5,10,15-tris[(1-bromonaphthalen-2-yl)methyl]-10,15-dihydro-5*H*-diindeno[1,2-*a*:1′,2′-*c*]fluorene (*syn*-6):** A suspension of **11** (360 mg, 0.62 mmol) in anhydrous DMF (5 mL) was added over a suspension of NaH (60 % in mineral oil, 82 mg, 2.04 mmol) in anhydrous DMF (5 mL) at 0 °C under Ar atmosphere. After ultrasonicating the resulting mixture for 50 min, a solution of 1-bromo-2-(bromomethyl)-naphthalene (577 mg, 1.92 mmol) in anhydrous DMF (10 mL) was added and the mixture was stirred at room temperature for 16 h.

H_2O (20 mL) was added and the precipitate formed was filtered off and redissolved in CH_2Cl_2 (50 mL). The resulting green solution was dried with $MgSO_4$, filtered, and concentrated under reduced pressure. Purification by silica gel column chromatography (cyclohexane/CH_2Cl_2, 8:2) gave a major fraction containing the desired *syn*-compound together with variable amounts of the *anti*-isomer and unidentified impurities. This fraction was partially dissolved in CH_2Cl_2 (10 mL) and precipitated with pentane (30 mL). The supernatant was removed and the solid was washed again with pentane (3 × 20 mL) and dried under reduced pressure to give the title compound, yield 121 mg (0.098 mmol, 15 %); pale-yellow solid; m.p. > 300 °C. ^{1}H NMR (500 MHz, $CDCl_2CDCl_2$, 120 °C): δ = 8.37 (d, J = 9.3 Hz, 3 H), 7.77 (d, J = 2.9 Hz, 3 H), 7.76 (d, J = 3.0 Hz, 3 H), 7.63 (ddd, J = 8.5, 6.9, 1.4 Hz, 3 H), 7.56–7.49 (m, 6 H), 7.37 (dd, J = 8.1, 1.9 Hz, 3 H), 7.05 (d, J = 1.9 Hz, 3 H), 6.86 (d, J = 8.3 Hz, 3 H), 4.72 (dd, J = 7.1, 7.1 Hz, 3 H), 3.79 (dd, J = 13.7, 6.4 Hz, 3 H), 3.34 (dd, J = 13.9, 8.2 Hz, 3 H) ppm. ^{13}C NMR (126 MHz, $CDCl_2CDCl_2$, 120 °C): δ = 148.2, 140.1, 138.2, 135.6, 133.1, 132.1, 129.6, 128.1, 128.1, 127.4, 126.9, 126.9, 126.4, 125.7, 124.6, 122.8, 119.8, 46.1, 40.6 (one aromatic carbon missing due to overlapping) ppm. HRMS (MALDI$^+$): m/z calcd. for $C_{60}H_{35}{}^{79}Br_3{}^{81}Br_3$ $[M - H]^+$ 1234.7772; found 1234.7809.

Triindeno[4,3,2,1-*lmno*]acephenanthrylene (5): A mixture of *syn*-**6** (62.8 mg, 0.051 mmol), $Pd(OAc)_2$ (22.9 mg, 0.102 mmol), dppe (40.5 mg, 0.102 mmol), and K_2CO_3 (105.7 mg, 0.765 mmol) in anhydrous DMA (0.5 mL) under Ar atmosphere was heated at 140 °C in a sealed tube for 36 h. After cooling to room temperature, H_2O (5 mL) was added and the precipitated solid was filtered off and washed by centrifugation with H_2O (6 × 15 mL), acetone (6 × 15 mL), satd. aq. NaCN (3 × 15 mL), acetone (6 × 15 mL) and finally CH_2Cl_2 (5 × 15 mL) until the liquid phase remained colorless. After drying the remaining solid under reduced pressure, crushed fullerene $C_{60}H_{24}$ was obtained, yield 16.8 mg (0.023 mmol, 44 %); dark-orange highly insoluble solid; m.p. > 300 °C. NMR spectroscopic data could not be acquired due to the low solubility of the compound. HRMS (LDI$^-$): m/z calcd. for $C_{60}H_{24}$ $[M]^-$ 744.1883; found 744.1848.

Acknowledgments

The authors thank the Ministerio de Economía y Competitividad (MINECO) (Severo Ochoa Excellence Accreditation 2014–2018, SEV-2013-0319, project number CTQ2013-42106-P), the European Research Council (ERC) (Advanced Grant 321066), the Agència de Gestió d'Ajuts Universitaris (AGAUR) (2014 SGR 818), and the ICIQ Foundation.

Keywords: Fullerenes · Truxene · Palladium · Arylation · Mass spectrometry

[1] a) Ó. de Frutos, B. Gómez-Lor, T. Granier, M. Á. Monge, E. Gutiérrez-Puebla, A. M. Echavarren, *Angew. Chem. Int. Ed.* **1999**, *38*, 204–207; *Angew. Chem.* **1999**, *111*, 186; b) B. Gómez-Lor, Ó. de Frutos, P. A. Ceballos, T. Granier, A. M. Echavarren, *Eur. J. Org. Chem.* **2001**, 2107–2114; c) Ó. de Frutos, T. Granier, B. Gómez-Lor, J. Jiménez-Barbero, A. Monge, E. Gutiérrez-Puebla, A. M. Echavarren, *Chem. Eur. J.* **2002**, *8*, 2879–2890; d) M. Ruiz, B. Gómez-Lor, A. Santos, A. M. Echavarren, *Eur. J. Org. Chem.* **2004**, 858–866; e) B. Gómez-Lor, E. González-Cantalapiedra, M. Ruiz, Ó. de Frutos, D. J. Cárdenas, A. Santos, A. M. Echavarren, *Chem. Eur. J.* **2004**, *10*, 2601–2608; f) E. González-Cantalapiedra, M. Ruiz, B. Gómez-Lor, B. Alonso, D. García-Cuadrado, D. J. Cárdenas, A. M. Echavarren, *Eur. J. Org. Chem.* **2005**, 4127–4140; g) B. Gómez-Lor, Ó. de Frutos, A. M. Echavarren, *Chem. Commun.* **1999**, 2431–2432.

[2] a) W. Y. Lai, R. D. Xia, D. C. C. Bradley, W. Huang, *Chem. Eur. J.* **2010**, *16*, 8471–8479; b) H. J. Xia, J. T. He, B. Xu, S. P. Wen, Y. W. Li, W. J. Tian, *Tetrahedron* **2008**, *64*, 5736–5742; c) M. S. Yuan, Z. Q. Liu, Q. Fang, *J. Org. Chem.* **2007**, *72*, 7915–7922; d) X.-Y. Cao, H. Zi, W. Zhang, H. Lu, J. Pei, *J. Org. Chem.* **2005**, *70*, 3645–3653; e) M.-T. Kao, J.-H. Chen, Y.-Y. Chu, K.-P. Tseng, C.-H. Hsu, K.-T. Wong, C.-W. Chang, C.-P. Hsu, Y.-Y. Liu, *Org. Lett.* **2011**, *13*, 1714–1717; f) Y. Xie, X. Zhang, Y. Xiao, Y. Zhang, F. Zhou, J. Qi, J. Qu, *Chem. Commun.* **2012**, *48*, 4338–4340; g) G. Zhang, F. Rominger, M. Mastalerz, *Chem. Eur. J.* **2016**, *22*, 3084–3093.

[3] a) A. Mueller, K. Y. Amsharov, M. Jansen, *Tetrahedron Lett.* **2010**, *51*, 3221–3225; b) M. A. Kabdulov, K. Y. Amsharov, M. Jansen, *Tetrahedron* **2010**, *66*, 8587–8593.

[4] F. Goubard, F. Dumur, *RSC Adv.* **2015**, *5*, 3521–3551.

[5] a) B. Gómez-Lor, C. Koper, R. H. Fokkens, E. J. Vlietstra, T. J. Cleij, L. W. Jenneskens, N. M. M. Nibbering, A. M. Echavarren, *Chem. Commun.* **2002**, 370–371; b) M. M. Boorum, Y. V. Vasil'ev, T. Drewello, L. T. Scott, *Science* **2001**, *294*, 828–831.

[6] M. Kabdulov, M. Jansen, K. Y. Amsharov, *Chem. Eur. J.* **2013**, *19*, 17262–17266.

[7] L. T. Scott, M. M. Boorum, B. J. McMahon, S. Hagen, J. Mack, J. Blank, H. Wegner, A. de Meijere, *Science* **2002**, *295*, 1500–1503.

[8] B. Gómez-Lor, A. M. Echavarren, *Org. Lett.* **2004**, *6*, 2993–2996.

[9] a) G. Otero, G. Biddau, C. Sánchez-Sánchez, R. Caillard, M. F. López, C. Rogero, F. J. Palomares, N. Cabello, M. A. Basanta, J. Ortega, J. Méndez, A. M. Echavarren, R. Pérez, B. Gómez-Lor, J. A. Martín-Gago, *Nature* **2008**, *454*, 865–868; b) K. Amsharov, N. Abdurakhmanova, S. Stepanow, S. Rauschenbach, M. Jansen, K. Kern, *Angew. Chem. Int. Ed.* **2010**, *49*, 9392–9396; *Angew. Chem.* **2010**, *122*, 9582.

[10] a) A. M. Echavarren, B. Gómez-Lor, J. J. González, Ó. de Frutos, *Synlett* **2003**, 585–597; b) S. Pascual, P. de Mendoza, A. M. Echavarren, *Org. Biomol. Chem.* **2007**, *5*, 2727–2734.

[11] T.-C. Chang, A. Naim, S. N. Ahmed, G. Goodloe, P. B. Shevlin, *J. Am. Chem. Soc.* **1992**, *114*, 7603–7604.

[12] See: a) E. A. Jackson, B. D. Steinberg, M. Bancu, A. Wakamiya, L. T. Scott, *J. Am. Chem. Soc.* **2007**, *129*, 484–485; b) K. Mochida, K. Kawasumi, Y. Segawa, K. Itami, *J. Am. Chem. Soc.* **2011**, *133*, 10716–10719; c) Q. Zhang, K. Kawasumi, Y. Segawa, K. Itami, L. T. Scott, *J. Am. Chem. Soc.* **2012**, *134*, 15664–15667; d) K. Kawasumi, Q. Zhang, Y. Segawa, L. T. Scott, K. Itami, *Nat. Chem.* **2013**, *5*, 739–744.

[13] CCDC 1467307 (for *anti*-**4b**), and 1467308 (for **8**) contain the supplementary crystallographic data for this paper. These data can be obtained free of charge from The Cambridge Crystallographic Data Centre.

[14] E. V. Dehmlow, T. Kelle, *Synth. Commun.* **1997**, *27*, 2021–2031.

[15] A. W. Amick, L. T. Scott, *J. Org. Chem.* **2007**, *72*, 3412–3418.

[16] The parent hydrocarbon 1,2-dihydroindeno[4,3,2,1-*lmno*]acephenanthrylene is also an unknown compound. Indeno[4,3,2,1-*lmno*]acephenanthrylene is also unknown but has been proposed as an intermediate in the formation of cyclopenta[*cd*]pyrene by flash vacuum pyrolysis: M. Sarobe, H. C. Kwint, T. Fleer, R. W. A. Havenith, L. W. Jenneskens, E. J. Vlietstra, J. H. V. Lenthe, J. Wesseling, *Eur. J. Org. Chem.* **1999**, 1191–1200.

Received: March 14, 2016
Published Online: May 2, 2016

JACS
JOURNAL OF THE AMERICAN CHEMICAL SOCIETY
Article
pubs.acs.org/JACS

Aerobic Linear Allylic C–H Amination: Overcoming Benzoquinone Inhibition

Christopher C. Pattillo, Iulia I. Strambeanu, Pilar Calleja,[▽] Nicolaas A. Vermeulen,[⊥] Tomokazu Mizuno,[§] and M. Christina White*

Roger Adams Laboratory, Department of Chemistry, University of Illinois, Urbana, Illinois 61801, United States

Supporting Information

ABSTRACT: An efficient aerobic linear allylic C–H amination reaction is reported under palladium(II)/bis-sulfoxide/Brønsted base catalysis. The reaction operates under preparative, operationally simple conditions (1 equiv of olefin, 1 atm O_2 or air) with reduced Pd(II)/bis-sulfoxide catalyst loadings while providing higher turnovers and product yields than systems employing stoichiometric benzoquinone (BQ) as the terminal oxidant. Pd(II)/BQ π-acidic interactions have been invoked in various catalytic processes and are often considered beneficial in promoting reductive functionalizations. When such electrophilic activation for functionalization is not needed, however, BQ at high concentrations may compete with crucial ligand (bis-sulfoxide) binding and inhibit catalysis. Kinetic studies reveal an inverse relationship between the reaction rate and the concentration of BQ, suggesting that BQ is acting as a ligand for Pd(II) which results in an inhibitory effect on catalysis.

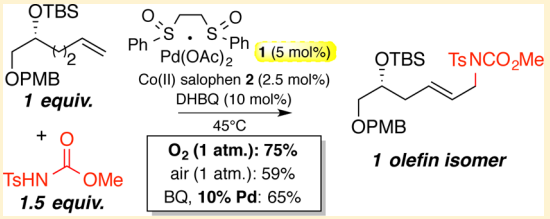

INTRODUCTION

Nature routinely uses molecular oxygen (O_2) as a stoichiometric oxidant for metalloenzyme catalyzed C–H bond oxidations.[1] In the context of chemical synthesis, the economic and environmental advantages of using O_2 for these purposes are clear: O_2 is an abundant, highly atom-efficient oxidant per weight that generates no toxic byproducts.[2] Less evident, however, is the potential for employing this oxidant in a manner that would *increase* the catalytic efficiency of oxidation reactions.

Since an early report that benzoquinone (BQ) is capable of acting as an effective stoichiometric oxidant for Pd-catalyzed olefin oxidations, BQ has become the most common terminal oxidant for palladium-catalyzed oxidations proceeding via Pd(II)/Pd(0) redox cycles.[3,4] We and others have demonstrated that at BQ may fill a dual role in Pd-catalyzed C–H oxidation reactions by acting as both an oxidant and a π-acidic ligand to promote reductive eliminations at the metal.[5] Allylic C–H oxidations that benefit from this effect operate under the principle of *serial ligand catalysis*, wherein distinct ligands promote specific steps along a catalytic cycle (Scheme 1A).[5c] Under these conditions, the reversibly coordinating bis-sulfoxide ligand coordinates to Pd(II) to promote a C–H cleavage step and generate a reactive π-allylPd(II) intermediate. BQ may then coordinate to this electrophilic intermediate via an η^2-π complex and act as a π-acidic ligand to promote reductive eliminations at the metal center.[5] We hypothesized that when activation of the electrophilic metal center is not required for functionalization, these BQ-Pd(II)L_n interactions may prove detrimental in systems using weakly coordinating ligands. By competing with the essential bis-sulfoxide binding event at the metal, BQ binding at high concentrations may lead to an inhibitory effect on catalysis.

Scheme 1. Benzoquinone (BQ) Ligand Effects

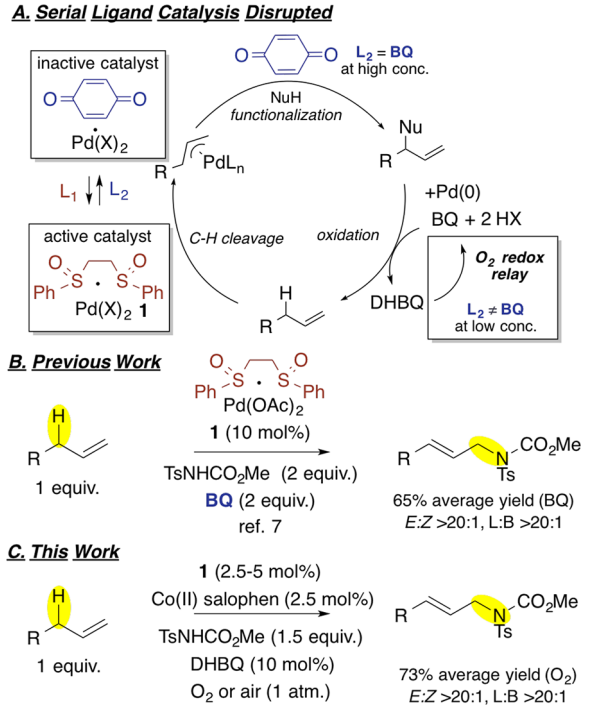

Received: October 28, 2015
Published: January 5, 2016

DOI: 10.1021/jacs.5b11294
J. Am. Chem. Soc. 2016, 138, 1265–1272

Herein, we describe the development of an efficient intermolecular linear allylic C−H amination (LAA) reaction employing a cobalt-mediated redox-relay catalytic cycle that uses molecular oxygen as the terminal oxidant under mild (1 atm, 45 °C) and preparatively useful conditions (1 equiv of olefin, 1.5 equiv of nitrogen nucleophile). This improved system enables the reaction to proceed with catalytic quantities of BQ, thus reducing the potential for inhibitory binding of BQ to the Pd(II) catalyst. As a result, this system affords higher or comparable yields while operating at *lower* catalyst loadings than those previously developed using superstoichiometric BQ as the terminal oxidant. The aerobic LAA reaction even remains operational at reduced oxygen concentrations found in air. Kinetic experiments substantiate the hypothesis of an inhibitory BQ effect at high concentrations and indicate that the improved efficiency of the aerobic system results from the low concentration of BQ present in the reaction mixture.

DESIGN PRINCIPLES

Palladium(II)/bis-sulfoxide catalysis has emerged as a general platform for allylic C−H oxidations, aminations, dehydrogenations, halogenations, and alkylations of α-olefins.[6,7] Common to all of these C−H functionalization reactions is the use of 10 mol% Pd/bis-sulfoxide catalyst and stoichiometric quinone oxidants such as BQ. Additionally, the majority of these reactions exploit BQ as a π-acidic ligand, often in combination with Lewis or Brønsted acid cocatalysts, to activate the electrophilic π-allylPd intermediate toward functionalization.[5,6h,7a]

Given the ubiquity of nitrogen functionality in bioactive compounds, its selective and general introduction represents a particularly powerful synthetic strategy.[8] We disclosed a catalytic Brønsted base activation mode for the intermolecular LAA reaction that proceeds via activation of the nitrogen nucleophile.[7b] Importantly, this reaction is no longer dependent on the π-acidic effect of BQ for functionalization. Under these conditions, we noted a slight increase in reaction yield when a bulky quinone—having diminished ability to coordinate to Pd—was employed as a terminal oxidant.[7b] With these considerations in mind, we chose the LAA reaction as a platform to evaluate the hypothesis that replacing BQ with O_2 as a stoichiometric oxidant can improve the catalytic efficiency of Pd(II)-catalyzed oxidations with catalysts employing weakly coordinating ligands.

Scheme 2. Proposed Mechanism for Aerobic Linear Allylic Amination (LAA) with Redox-Relay Catalysis

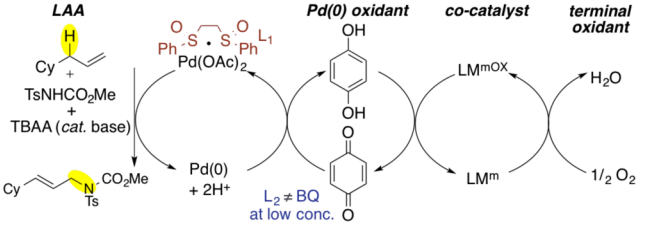

While a variety of important Pd-catalyzed oxidations of alcohols and olefins have been developed using O_2 as a stoichiometric oxidant, analogous C−H oxidation processes are scarce.[4,9−14] Pd(II)-catalyzed C−H oxidation reactions often proceed with no formal ligands [e.g., $Pd(OAc)_2$] or weakly coordinating, oxidatively stable ligands such as bis-sulfoxide.[10]

Table 1. Reaction Optimization

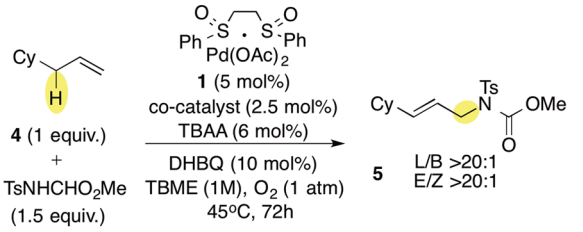

Entry[a]	catalyst/co-catalyst	Oxidant	Yield of 5[b]
1[c]	10 mol% **1**/--	BQ (2 equiv.)	84%
2[c]	5 mol% **1**/--	BQ (2 equiv.)	20%
3[d]	**1**/Co(II)(salophen) **2**	O_2 (1atm)	68%
4	**1**/Co(II)(salophen) **2**	O_2 (1atm)	79%(78%)[e]
5	**1**/Co(II)(TPP)	O_2 (1atm)	60%
6	**1**/Co(II)(salen)	O_2 (1atm)	74%
7	**1**/Mn(III)(salen)	O_2 (1atm)	8%
8	**1**/Fe(II)Pc	O_2 (1atm)	39%
9	**1**/$VO(acac)_2$ **3**	O_2 (1atm)	48%
10[f]	**1**/$VO(acac)_2$ **3**	O_2 (1atm)	75% (80%)[g]
11[f]	**1**/VO(TPP)	O_2 (1atm)	53%
12[f]	**1**/VO(Salophen)	O_2 (1atm)	54%
13[f,h]	**1**/$VOSO_4$	O_2 (1atm)	65%
14	**1**/--	O_2 (1atm)	17%
15[i]	$Pd(OAc)_2$/DAF	O_2 (1 atm)	*trace*
16[c]	**1**/--	2,5-DMBQ (1 equiv.)	72%

[a] Conditions are as listed above unless noted. Co(II)(salophen) = N,N'-bis(salicylidene)-1,2-phenylenediaminocobalt(II); Co(II)(TPP) = cobalt(II) meso-tetraphenylporphine; Co(II)(salen) = (1R,2R)-(-)-1,2-cyclohexanediamino-N,N'-bis(3,5-di-t-butylsalicylidene)cobalt(II); Mn(III)(salen) = (1R,2R)-(-)-1,2-cyclohexanediamino-N,N'-bis(3,5-di-t-butylsalicylidene)manganese(III) chloride; Fe(II)Pc = iron(II) phthalocyanine; $VO(acac)_2$ = vanadyl acetylacetonate; VO(TPP) = vanadyl meso-tetraphenylporphine; VO(salophen) = N,N'-bis(salicylidene)-1,2-phenylenediaminovanadium(IV) oxide. [b] Isolated yield; average of at least 2 runs at 0.4 mmol scale. [c] Conditions from ref. 7b. [d] 1M TBME, 2 equiv. $TsNHCO_2Me$. [e] Number in parenthesis is yield at 24h. [f] 2 equiv. $TsNHCO_2Me$, 1M THF. [g] Number in parentheses is yield with 1 mol% co-catalyst on a 0.8 mmol scale for accurate co-catalyst weight. [h] 1 mmol scale used for accurate co-catalyst weights. [i] 5 mol% $Pd(OAc)_2$, 5 mol% 4,5-diazafluoren-9-one (DAF), with identical conditions to entries 4-9.

For allylic C−H acetoxylations and aminations under such conditions, the slow electron transfer directly between Pd(0) and O_2 relative to the rapid formation of palladium black via precipitation of palladium metal is thought to result in deleterious olefin isomerization processes and contribute to the requirement for high catalyst loadings.[11−14] While aerobic Pd(II)-catalyzed LAA reactions have been reported, their utility is limited by requirements such as excess alkene (e.g., 3−7 equiv relative to nucleophile), high Pd catalyst loadings (e.g., 10−20 mol%), and elevated pressures (e.g., 6−10 atm O_2 or air).[12,13] Significant amounts of double bond isomerization in both the starting materials and products (up to 50%) necessitate the use of large excesses of olefin and limit applications in fine chemical synthesis.[12−14]

We considered two possible strategies for engaging molecular oxygen as the terminal oxidant for the LAA reaction under preparatively useful conditions. While oxidatively stable ligands which promote direct oxidation of Pd(0) with molecular oxygen have been developed, these ligands have not yet demonstrated the same generality in C−H oxidation processes as compared to the bis-sulfoxide ligand class.[2a,4,15] A more general approach, compatible with the continued use of bis-sulfoxides, would be through the use of redox-active cocatalysts that act as electron transfer reagents to relay electrons from

DOI: 10.1021/jacs.5b11294
J. Am. Chem. Soc. 2016, 138, 1265−1272

Pd(0) to O_2 at rates that compete with Pd(0) precipitation (Scheme 2). An early example of this is seen in the Pd(II)-catalyzed Wacker oxidation of ethylene to acetaldehyde that uses catalytic $Cu(II)Cl_2$ to shuttle electrons from Pd(0) to O_2.[16] Unfortunately, unligated metal salts generally have a deleterious effect on Pd(II)/bis-sulfoxide catalysis, possibly by sequestering the bis-sulfoxide ligand that binds weakly and reversibly to Pd(II). Alternatively, a variety of base metal complexes with covalent, nonexchangeable ligands are known to catalyze the oxidation of dihydroquinones to the corresponding quinones with O_2.[17,18] In a notable series of seminal publications, Bäckvall and co-workers demonstrated that this form of redox-relay catalysis enabled catalytic quantities of BQ to be effective at regenerating $Pd(II)(OAc)_2$ catalysts for the 1,4-diacetoxylation of dienes, acetoxylation of cyclohexene, and oxidation of terminal olefins to methyl ketones.[19] Mechanistic studies of processes proceeding via serial ligand catalysis have demonstrated that high concentrations of BQ are required to effectively interact with the Pd(II) species to promote π-allyl Pd(II) functionalizations.[5c,f,g] Collectively, this led us to hypothesize that in the context of an aerobic redox-relay catalytic cycle, the low concentration of BQ present would diminish its ability to effectively compete with the bis-sulfoxide ligand for Pd(II) but would remain an efficient electron carrier for Pd(0)/ Pd(II) reoxidation.

REACTION DEVELOPMENT

An efficient aerobic LAA process (1 equiv of olefin, reduced Pd catalyst loadings, 1 atm O_2) was first evaluated with a series of established redox-active cocatalysts. At reduced catalyst loading (5 mol%), a substantial diminishment in yield is observed under standard LAA conditions using stoichiometric BQ as the oxidant (Table 1, entry 1 versus 2). In contrast, the combination of Co(salophen) (2.5 mol%)/dihydroquinone (10 mol%) under a balloon of O_2 (1 atm) allowed for the Pd/bis-sulfoxide catalyst **1** loading to be cut in half (10 mol% to 5 mol%) and the nitrogen nucleophile loadings reduced (2 equiv to 1.5 equiv) with no diminishment in selectivity while maintaining a good yield (entries 3 and 4 versus 1). We were also encouraged by the observation that, under these optimized conditions, no significant decrease in yield was observed after reducing the reaction time to 24 h (79% versus 78% yield, entry 4). A series of other base metal cocatalysts were evaluated; however, none was found to be more efficient than Co(salophen) **2** (entries 5–8). Interestingly, $VO(acac)_2$ **3**/DHBQ in THF solvent appeared to be equally effective as a redox cocatalyst system to Co(salophen) **2**/DHBQ, albeit at higher loadings of nitrogen nucleophile (1.5 equiv versus 2 equiv, entries 9 and 10). Although never explored in aerobic Pd(II)-catalyzed reactions, $VO(acac)_2$ **3** had been reported to catalyze the aerobic oxidation of hydroquinones to quinones at ambient temperatures and pressures of O_2.[18] We were initially encouraged by the observation that the vanadium cocatalyst loading could be reduced to 1 mol% with no diminishment in yield, suggesting it is an efficient electron-transfer agent (entry 10). Additional vanadium catalysts were also evaluated (entries 11–13), and under these conditions only $VOSO_4$ was comparable to $VO(acac)_2$ **3**, affording a 65% yield of the desired product (entry 13). Omission of the redox cocatalyst under these aerobic conditions resulted in significantly diminished yields, confirming its central role in Pd(II)/bis-sulfoxide **1** catalyst regeneration (entry 14). The $Pd(OAc)_2$/4,5-diazafluoren-9-one (DAF) system known to enable linear allylic acetoxylations using O_2 as the terminal oxidant provided only trace quantities of aminated product under these conditions (entry 15).[15] Notably, when using stoichiometric amounts of bulky 2,5-dimethylbenzoquinone (2,5-DMBQ) as a terminal oxidant, where methyl groups shield both olefin faces from binding to Pd, we observed comparable yields to the aerobic conditions (Table 1, entry 4 vs 16).

REACTION SCOPE

We began our investigations into the scope and reproducibility of the aerobic LAA reaction with a variety of unactivated α-olefins, the most challenging substrates for amination (Table 2). Both the Co(salophen) **2** and $VO(acac)_2$ **3** redox cocatalyst systems were evaluated under fragment-coupling stoichiometries of olefin (1 equiv of terminal olefin and 1.5 or 2 equiv of nitrogen nucleophile). It is significant to note that these preparative conditions contrast those of previously reported aerobic allylic C–H amination methods (*vida supra*).[12,13]

Table 2. Aliphatic Substrates

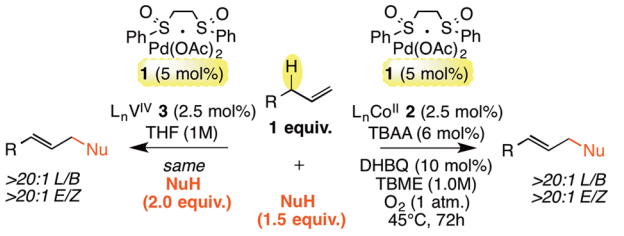

Entry	Product	This Work Co[a,b]	This Work V[a,c]	Previously BQ or O_2
1	TBDPSO, CO_2Me, N, Ts, **6**	77%[d]	46%	-
2	BnO, CO_2Me, N, Ts, **7**	54%[e] (30%)[f] [±2%]	44% [±14%]	-
3	BzO, CO_2Me, N, Ts, **8**	75%[g] (70%)[f]	81%	78%[h] 92:8[i]
4	CO_2Me, N, Ts, **9**	67%	58%	53%[j]
5	CO_2Me, N, Ts, **(-)-10**	55%	23%[k]	54%[l]
6	NHCbz, CO_2Me, N, Ts, **(+)-11**	86%	15%[k]	55%[l]
7	PMBO, OTBS, CO_2Me, N, Ts, **(+)-12**	75% (64%)[f]	69%	65%[l]
8	TBDPSO, CO_2Me, N, Ts, **(+)-13**	77%	67%	57%[l]

[a] Isolated yield, average of at least 2 runs at 0.4 mmol scale. [b] 5 mol% **1**, 2.5 mol% **2**, 6 mol% TBAA, 10 mol% DHBQ, 1.5 equiv. $TsNHCO_2Me$, 1M TBME, O_2 balloon. [c] 5 mol% **1**, 2.5 mol% **3**, 6 mol% TBAA, 10 mol% DHBQ, 2 equiv. $TsNHCO_2Me$, 1M THF, O_2 balloon. [d] 20:1 L:B. [e] 11:1 E:Z, 14:1 L:B. [f] Number in parenthesis is yield after 24 hours. [g] 15:1 L:B. [h] Yield reported in ref. 12; conditions employing 3 equiv. of olefin substrate, 10 mol% Pd, and 6 atm. O_2. [i] Ratio of allylic to non-allylic isomers (see ref. 12). [j] Yield reported in ref. 12; conditions employing 1 equiv. of olefin substrate, 20 mol% Pd, and 6 atm. O_2. [k] Reported yield of one run . [l] Yield reported in ref. 7a.

DOI: 10.1021/jacs.5b11294
J. Am. Chem. Soc. 2016, 138, 1265–1272

When comparing the Co(salophen) **2** and $VO(acac)_2$ **3** redox cocatalysts over a range of substrates at reduced Pd/bis-sulfoxide **1** catalyst loadings (5 mol%), we found both furnished products generally in excellent regio- and stereoselectivities (>20:1 linear:branched and >20:1 *E*:*Z*). The system employing Co uniformly furnished allylic amination products with higher turnover numbers (TON) and product yields comparable to or exceeding those using BQ.[7] For example, substrates with branching oxygen, carbon, or nitrogen functionality in the homoallylic or bis-homoallylic positions (Table 2, entries 5−8) proceed on average with 16% higher isolated yields and average TON of 14.6 versus average TON of 5.7 when compared to the Pd/bis-sulfoxide **1**/Cr(salen) catalyzed system using BQ as a stoichiometric oxidant.[7a] Additionally, for substrates where a direct comparison can be made with previously reported aerobic LAA reactions, the same trend in yields and TONs is observed (entries 3 and 4).[12] We also note that higher yielding substrates can be run for 24 h without a significant decrease in yield (entries 3 and 7). The mass balance for these reactions is generally high, with unbranched substrates (e.g., entries 1−3) furnishing predominantly linear *E*-allylic amine (L:B = 20:1, 14:1, and 15:1, respectively) and small quantities of isomerized recovered starting material (entries 1 and 3, 11% and 4%, respectively). Branched substrates (e.g., entry 7) give isomerically pure products and small amounts of recovered starting material as a mixture of isomerized (ca. 10%) and terminal olefin (ca. 9%) (see Supporting Information; Table 2, entry 7).

Unfortunately, the $VO(acac)_2$ **3** system proved to be less robust, generally providing linear allylic amine products in diminished yields and with significantly lower reproducibility between experiments than the Co system (see Table 2 entry 2 standard deviation, and Supporting Information). Although in several cases yields for the vanadium system were comparable (entries 4, 7, and 8; see also Scheme 4, below) or even exceeded (entry 3) those of the Co system, no clear trend emerged for predicting these observed differences in reaction efficiency (see Supporting Information).

We next investigated the reactivity of the new aerobic LAA system for a variety of activated allylarene substrates (Table 3). Under these conditions, both electron poor and electron rich aromatic rings are well tolerated, furnishing products as one olefin isomer in good to excellent yields (entries 1−3). Additionally, efficient reactivity is observed for highly functionalized, electron rich aromatic systems (entries 4 and 5). Tolerance for medicinally relevant heterocyclic aromatic functionality is demonstrated in the aerobic LAA of an indole heterocycle (entry 6). In some cases, reactions may be run for 24 h without a significant decrease in yield (entries 4 and 5). We were also pleased to find that often the Pd catalyst loading could be further reduced to 2.5 mol% while still maintaining useful yields of aminated product (entries 1−5). In general, under these aerobic conditions, the yields and TONs are significantly higher than those of the BQ system (entries 4 and 5). When comparing these results with a previous aerobic system, we again observe higher catalyst TONs and product yields (entry 1).[12]

It was previously demonstrated that substrates containing sensitive terminal epoxides and unprotected alcohols may be aminated with the base-promoted LAA reaction in useful yields.[7b] A potential limitation of this aerobic LAA system, which employs a Lewis-acidic redox cocatalyst, is poor tolerance of highly Lewis basic functionality. Under our optimized aerobic LAA conditions employing the Co-

Table 3. Aromatic Substrates

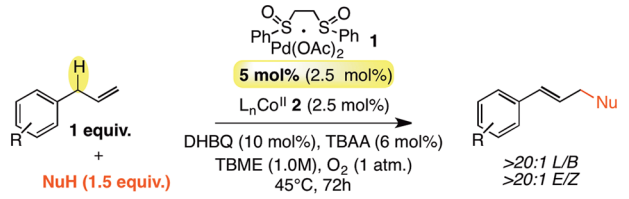

Entry		Product	Co[a]	BQ or O_2
1	R=*o*-OMe	**14**	96% (69%)[b]	75%[c]
2	R=*o*-OTBS	**15**	91% (47%)[b]	-
3	R=*p*-CF_3	**16**	79% (60%)[b]	-
4		**17**	94%[d] (63%)[b,e]	81%[f]
5		**18**	91% (70%)[b] [69%][g]	72%[h]
6		**19**	56%	-
7		**(+)-20**	68%[i]	54%[f]

[a] Isolated yield, average of at least 2 runs at 0.4 mmol scale. [b] 2.5 mol% **1** was used. [c] Yield reported in ref. 12; conditions employing 3 equiv. of olefin substrate, 10 mol% Pd, and 6 atm. O_2. [d] Reaction complete at ca. 12 h. [e] Reaction complete after 24 hours. [f] Yield reported in ref. 7b; conditions employing 10 mol% **1**, 2 equiv BQ. [g] Number in brackets is yield after 24 hours with 2.5 mol% of catalyst **1**. [h] Yield reported in ref. 7a; conditions employing 10 mol% **1**, 2 equiv BQ. [i] 5 mol% **1**, 6 mol% DIPEA, 1 equiv. 2,5-DMBQ, 0.66M TBME, 2 equiv. $TsNHCO_2Me$, 45°C, 24h.

(salophen) **2** cocatalyst, we obtained a lower (ca. 30%) yield for a terminal epoxide substrate (Table 3, entry 7). We attribute this diminished reactivity to deleterious side reactions of the terminal epoxide in the presence of the Lewis acidic Co cocatalyst. Analogous Co(salen) complexes are known to catalyze ring opening reactions of terminal epoxides with water.[20] Additional attempts to use the $VO(acac)_2$ system with a similar terminal epoxide substrate led to no significant improvement in yield. We next looked to conditions employing the sterically hindered quinone oxidant 2,5-DMBQ, which had shown equal efficiency to the aerobic conditions at reduced Pd loadings (Table 1, entry 16), and found that C−H amination proceeded in 68% yield after 24 h (Table 3, entry 7). This constitutes a nearly 15% increase in yield relative to stoichiometric BQ conditions run with twice the Pd loading and longer reaction times (72h).[7b] This result illustrates the complementarity of a bulky, readily available quinone to our aerobic conditions, allowing for efficient amination of substrates containing Lewis-acid-sensitive functionality.

Reactivity with Reduced O_2 Concentrations. We next sought to assess the efficiency of the aerobic LAA conditions under reduced concentrations of O_2 considered beneficial for application of such aerobic chemistry in the synthesis of fine chemicals (Table 4).[21] The aerobic LAA reaction was evaluated under identical conditions of temperature, pressure and catalyst loadings (45 °C, 1 atm, 5−2.5 mol%), now at the significantly reduced O_2 concentrations found in air.

DOI: 10.1021/jacs.5b11294
J. Am. Chem. Soc. 2016, 138, 1265−1272

The aerobic LAA reaction run with air furnished aliphatic and aromatic aminated products with the same isomeric purities while maintaining synthetically useful yields at 1 equiv of substrate and low catalyst loadings. Yields of aminated products were generally diminished relative to those of the analogous system using O_2. Decreasing the catalyst loadings from 5 mol% to 2.5 mol% with aromatic substrates in some cases still allowed for a useful reaction to proceed (Table 4, entries 5–7). These findings demonstrate that the DHBQ/Co(salophen)/O_2 redox-relay is able to remain operative even under reduced concentrations of molecular oxygen. Whereas focused reaction optimization to develop an aerobic LAA reaction using air is an important future goal, it is significant to note that for the majority of substrates run under air, aminated products were generated in comparable yields with higher TONs relative to the LAA reaction using stoichiometric BQ oxidant.[7]

Table 4. Allylic C–H Amination Using Air

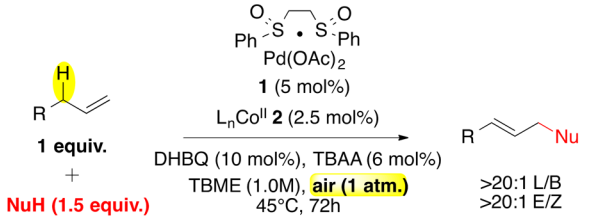

Entry	Product	Yield[a]
1	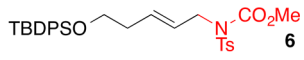 **6**	66%
2	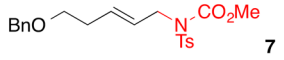 **7**	52%[b]
3	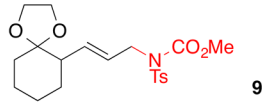 **9**	57%
4	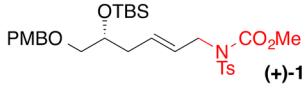 **(+)-12**	59%
5	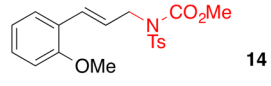 **14**	62%[c]
6	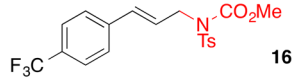 **16**	71% (45%)[c]
7	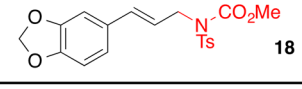 **18**	90% (75%)[c]

[a] Isolated yield, average of at least 2 runs at 0.4 mmol scale. [b] 11:1 E/Z [c] 2.5 mol% **1** was used.

Late-Stage C–H Amination and Streamlining. Late-stage C–H oxidation is a powerful approach for the streamlining and diversification of complex natural products and compounds of medicinal interest.[22] With optimal conditions in hand, we sought to evaluate the performance of functionally and topologically complex substrates under our aerobic LAA reaction (Scheme 3). A glucose-derived substrate **21**, bearing an abundance of oxygenated functionality, furnished the corresponding allylic amine **22** in 76% yield as a single diastereomer, after only 24 h.

Scheme 3. Reactivity of Functionally Diverse Substrates

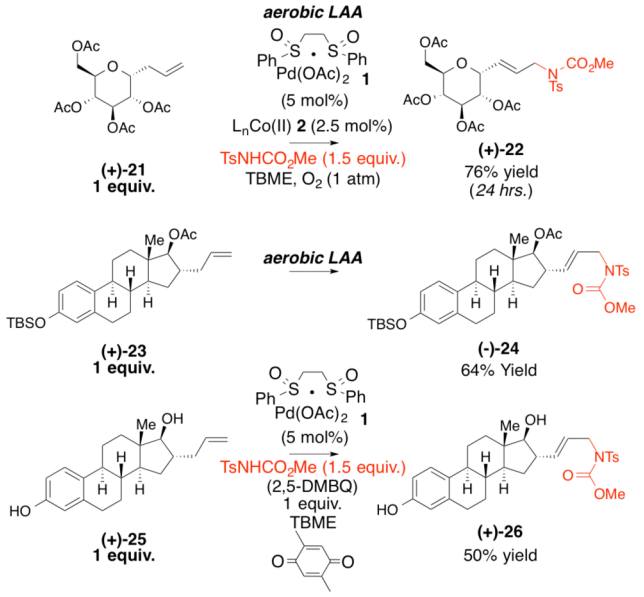

Estrone derivatives were evaluated in both their protected **23** and unprotected forms **25**. When the aerobic LAA reaction was applied to protected estrone derivative **23**, the LAA product **24** was furnished in good yield (64%).[7b] Based on previous results demonstrating the limited compatibility of Lewis basic functionality under our aerobic LAA conditions, we evaluated **25** under conditions employing 2,5-DMBQ (1 equiv) as the stoichiometric oxidant. Gratifyingly, these conditions afforded the allylic amine product **26** in 50% yield using only 5 mol% of Pd catalyst.[7b] These results demonstrate the applicability of these aerobic LAA conditions to afford useful yields of functionalized complex molecules, as well as the increase in reaction efficiency possible under conditions that limit detrimental Pd–quinone interactions.

Scheme 4. Streamlined Synthesis of a Deoxynegamycin Analogue

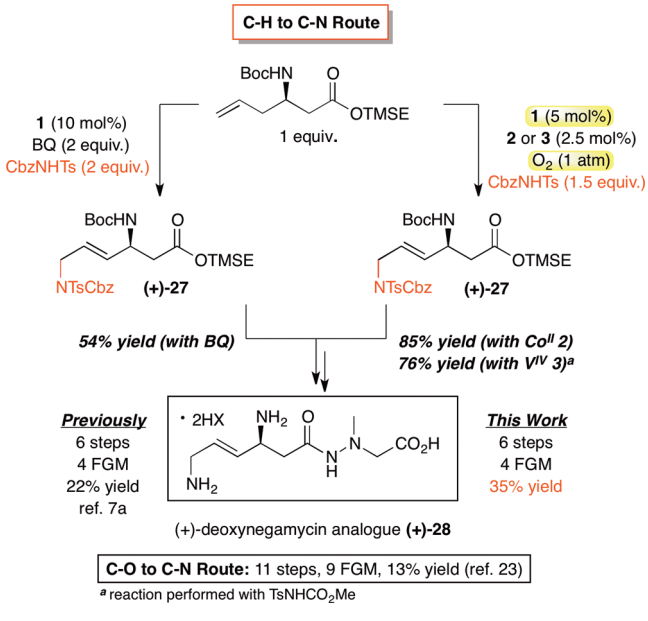

DOI: 10.1021/jacs.5b11294
J. Am. Chem. Soc. 2016, 138, 1265–1272

Given the improved synthetic efficiency of the aerobic LAA reaction with respect to both catalyst loadings and product yields, we sought to re-evaluate the LAA reaction in the context of synthetic streamlining. The LAA reaction has been previously used in the context of a streamlined synthesis of **28**, a rigidified analogue of the antibiotic deoxynegamycin (Scheme 4).[7a] This C−H to C−N bond-forming route eliminated five steps, all of which were functional group manipulations, and proceeded with higher overall yield as compared to the previous route based on allylic C−O substitution.[7a,23] When applying the new aerobic amination conditions to the key C−H amination step of the previous synthesis, we were delighted to find that these optimized conditions afforded a nearly 30% increase in yield of aminated intermediate under Co **2** cocatalysis with 5 mol% of Pd/bis-sulfoxide catalyst **1** (Scheme 4). The increased efficiency of this key C−N bond-forming step now affords a 35% overall yield of deoxynegamycin analogue **28**, a nearly 3-fold increase in yield as compared to the C−O to C−N route.[23]

THE BENZOQUINONE EFFECT

We have demonstrated that the linear allylic amination (LAA) reaction run under aerobic conditions and conditions using bulky quinone terminal oxidants (2,5-DMBQ) lead to both improved product yields and catalyst turnover relative to the previous system relying on stoichiometric BQ as the terminal oxidant. We hypothesized that the mechanistic basis for these differences is that at high concentrations, BQ acts as an inhibitory ligand for this Pd(II)/bis-sulfoxide catalysis (Table 5A). As a preliminary evaluation of this, we increased the concentration of BQ under the aerobic reaction conditions and measured the effect on overall yields. Strikingly, under both Co(salophen) **2** and $VO(acac)_2$ **3** cocatalysis, a significant diminishment in yield was observed (Table 5B, entries 1−3 and 4−6, respectively).

Although stable Pd(0)/BQ complexes are known, Pd(II)/BQ complexes are fleeting and have been proposed as intermediates within catalytic cycles largely based on kinetic studies.[24] In the $Pd(OAc)_2$-catalyzed diacetoxylation of 1,3-dienes using MnO_2 as the stoichiometric oxidant, a linear dependence of reaction rate on BQ concentration supported the hypothesis that BQ acts as a π-acidic ligand for Pd(II) to promote functionalization.[5a] In order to more definitively demonstrate the inhibitory effect of BQ, we measured the rate of reaction under the aerobic LAA conditions—a scenario where an appreciable accumulation of dihydroquinone is unlikely—in the presence of increasing amounts of BQ. Reaction rates were measured at 5 mol% Pd(II)/bis-sulfoxide **1** while varying the BQ concentration between 0.066 and 0.66 M (10−100 mol% relative to substrate). These experiments were performed in triplicate between 1 and 150 min after initiating the reaction (Figures S3−S8, Supporting Information). A plot of the inverse of the reaction rate at various concentrations of BQ is shown in Figure 1. The LAA reaction rate shows a clear inverse dependence on BQ: a 10-fold increase in [BQ] results in a nearly 9-fold decrease in reaction rate.

Table 5. Effect of Elevated BQ on Reaction Yields

A. Proposed Catalyst Inhibition by Benzoquinone

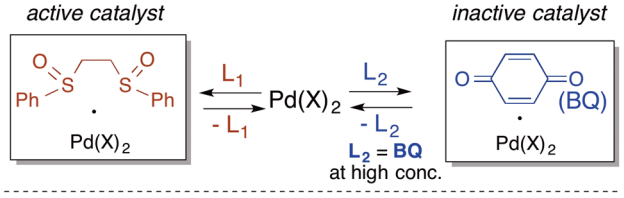

B. Preliminary Investigation of BQ Inhibition

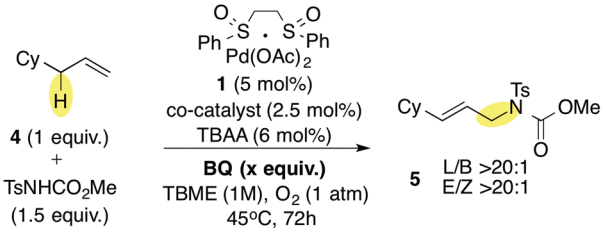

Entry[a]	co-catalyst	BQ equivalents	Yield of 5[b]
1	Co(II)(salophen) **2**	0.1 equiv.	81%
2	Co(II)(salophen) **2**	0.5 equiv.	56%
3	Co(II)(salophen) **2**	1 equiv.	50%
4	$VO(acac)_2$ **3**	0.1 equiv.	70%
5	$VO(acac)_2$ **3**	0.5 equiv.	40%
6	$VO(acac)_2$ **3**	1 equiv.	25%

[a] Conditions are as listed above unless otherwise noted.
[b] Isolated yield; average of two runs at a 0.4 mmol scale.

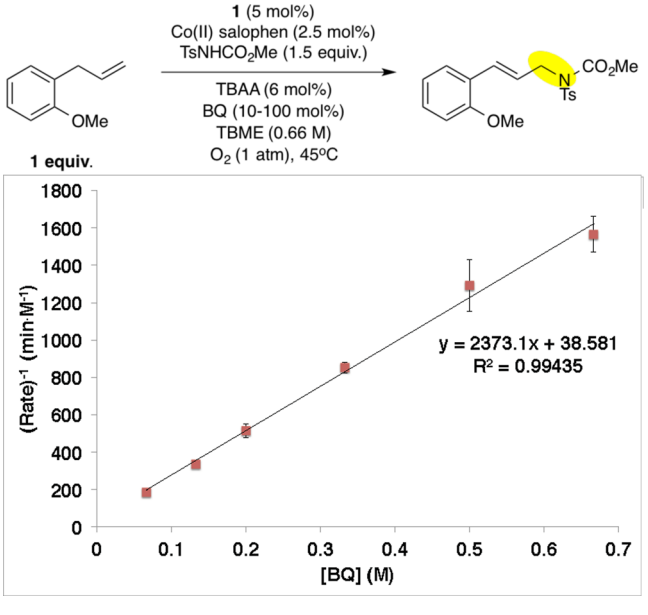

Figure 1. Inverse relationship between rate and BQ concentration.

Collectively, these data indicate that BQ has an inhibitory effect on the LAA reaction at high concentrations. While this is consistent with the hypothesis that interactions of BQ with the Pd(II)/bis-sulfoxide catalyst are detrimental to reaction efficiency, future mechanistic studies will be directed at elucidating the precise mechanism for BQ inhibition.

CONCLUSIONS

We have demonstrated that using an O_2/Co/catalytic dihydroquinone redox relay in combination with our Pd/bis-sulfoxide catalysis enables aerobic linear allylic amination reactions of terminal olefins to proceed at reduced Pd catalyst

DOI: 10.1021/jacs.5b11294
J. Am. Chem. Soc. 2016, 138, 1265−1272

loadings and higher reaction efficiency than the previous system relying on stoichiometric BQ. Kinetic experiments show for the first time an inhibitory effect of BQ on Pd(II) oxidative catalysis. Collectively this data implies that for reactions relying on Pd(II) catalysts with weakly coordinating ligands (e.g., bis-sulfoxide) to promote key steps in the catalytic cycle (e.g., C−H cleavage), interactions of BQ when present in high concentrations with the Pd(II) catalyst may be detrimental to reaction efficiency. For such systems, adopting a system which uses molecular oxygen as a stoichiometric oxidant offers not only practical environmental benefits but may also lead to enhanced catalytic efficiency.

EXPERIMENTAL PROCEDURE

General Procedure for the Linear Allylic Amination (LAA) Reaction. To an oven-dried 10 mL round-bottom flask containing a PTFE-covered stir bar was added tetra-*n*-butylammonium acetate in the glovebox, followed by carbamate nucleophile, dihydroquinone, metal cocatalyst, and catalyst **1** on the benchtop. Due to the hygroscopic nature of TBAA, the reaction flask was not opened until all solids were ready to be transferred into the flask. The terminal olefin (preweighed in a 0.5 dram vial) was transferred to the reaction flask using the corresponding solvent (1 M). The flask was then attached to a cold-water condenser, previously purged briefly with oxygen, and equipped with an O_2 balloon. The flask was secured with a Teflon adaptor, sealed with Teflon tape, and the reaction was allowed to stir at 400 rpm in a 45 °C oil bath for 24−72 h or until completed by TLC. Upon completion, a workup with an aqueous solution of 5% K_2CO_3 may be used to remove remaining nucleophile and water-soluble impurities. (*Generally this workup leads to higher purity of isolated products.*) Alternatively, the reaction may diluted with dichloromethane and flushed through a 3−5 cm silica gel plug with an 80% ethyl acetate/20% hexanes mixture to separate the product from metal catalysts. If no workup is necessary, the reaction mixture may also be directly loaded onto a silica gel column using dichloromethane or toluene. Purification of the products is done using flash column chromatography, in general, with a gradient of 10−30% EtOAc/hexanes. We have also found that 10−30% acetone/hexanes or 10−50% ether/pentane gradients are effective solvent systems for purification.

For reactions run under air, the same general procedure outlined above was employed, the only change being a balloon of air was used. While the reaction condenser may be left opened to air, we have noted rapid and continual loss of the very volatile TBME solvent under this scenario and recommend the use of an air balloon.

ASSOCIATED CONTENT

Supporting Information

The Supporting Information is available free of charge on the ACS Publications website at DOI: 10.1021/jacs.5b11294.

Experimental procedures and characterization data, including Tables S1 and S2, Schemes S1−S3, and Figures S1−S8 (PDF)

^1H and ^{13}C NMR spectra for all new compounds (PDF)

AUTHOR INFORMATION

Corresponding Author

*mcwhite7@illinois.edu

Present Addresses

[∇]P.C.: Institute of Chemical Research of Catalonia (ICIQ), Av. Països Catalans 16, 43007 Tarragona, Spain

[⊥]N.A.V.: Department of Chemistry, Northwestern University, 2145 Sheridan Rd., Evanston, IL 60208, USA

[§]T.M.: Graduate School of Engineering, Nagoya University, Furo-cho, Chikusa, Nagoya 464-8603, Japan

Notes

The authors declare no competing financial interest.

ACKNOWLEDGMENTS

Financial support was provided by the NIH/NIGMS (2R01 GM 076153B) and ARRA supplemental funding. We thank Sigma-Aldrich for a generous gift of Pd/bis-sulfoxide catalyst (**1**) (product no. 684821), Johnson Matthey for a generous gift of $Pd(OAc)_2$, Anitox for a generous gift to explore α-olefin oxidations, Mr. Jeffrey D. Sayler for help with substrate synthesis and initial studies for Table 3, and Ms. Jennifer R. Griffin and Mr. Stephen E. Ammann for checking the experimental procedure in Table 2, entry 2.

REFERENCES

(1) (a) Berkessel, A. In *Diversity-Based Approaches to Selective Biomimetic Oxidation Catalysis*; van Eldik, R., Reedijk, J., Eds.; Advances in Inorganic Chemistry *58*; Elsevier: Amsterdam, 2006; pp 1−28. (b) Ortiz de Montellano, P. R. *Chem. Rev.* **2010**, *110*, 932.

(2) (a) Stahl, S. S. *Angew. Chem., Int. Ed.* **2004**, *43*, 3400. (b) Piera, J.; Bäckvall, J. E. *Angew. Chem., Int. Ed.* **2008**, *47*, 3506. (c) Cavani, F.; Teles, J. H. *ChemSusChem* **2009**, *2*, 508.

(3) Moiseev, I. I.; Vargaftik, M. N.; Syrkin, Y. K. *Dokl. Akad. Nauk SSSR* **1960**, *133*, 377.

(4) Popp, B. V.; Stahl, S. S. In *Palladium-Catalyzed Oxidation Reactions: Comparison of Benzoquinone and Molecular Oxygen as Stoichiometric Oxidants*; Meyer, F., Limberg, C., Eds.; Topics in Organometallic Chemistry *22*; Springer: New York, 2007; pp 149−189.

(5) (a) Bäckvall, J. E.; Byström, S. E.; Nordberg, R. E. *J. Org. Chem.* **1984**, *49*, 4619. (b) Castaño, A. M.; Bäckvall, J. E. *J. Am. Chem. Soc.* **1995**, *117*, 560. (c) Chen, M. S.; Prabagaran, N.; Labenz, N. A.; White, M. C. *J. Am. Chem. Soc.* **2005**, *127*, 6970. (d) Bar, G. L. J.; Lloyd-Jones, G. C.; Booker-Milburn, K. I. *J. Am. Chem. Soc.* **2005**, *127*, 7308. (e) Chen, X.; Li, J. J.; Hao, X. S.; Goodhue, C. E.; Yu, J. Q. *J. Am. Chem. Soc.* **2006**, *128*, 78. (f) Fraunhoffer, K. J.; Prabagaran, N.; Sirois, L. E.; White, M. C. *J. Am. Chem. Soc.* **2006**, *128*, 9032. (g) Covell, D. J.; White, M. C. *Angew. Chem., Int. Ed.* **2008**, *47*, 6448. (h) Hull, K. L.; Sanford, S. S. *J. Am. Chem. Soc.* **2009**, *131*, 9651. (i) Osberger, T. J.; White, M. C. *J. Am. Chem. Soc.* **2014**, *136*, 11176.

(6) (a) Chen, M. S.; White, M. C. *J. Am. Chem. Soc.* **2004**, *126*, 1346. (b) Fraunhoffer, K. J.; White, M. C. *J. Am. Chem. Soc.* **2007**, *129*, 7274. (c) Young, A. J.; White, M. C. *J. Am. Chem. Soc.* **2008**, *130*, 14090. (d) Lin, S.; Song, C. X.; Cai, G. X.; Wang, W. H.; Shi, Z. J. *J. Am. Chem. Soc.* **2008**, *130*, 12901. (e) Rice, G. T.; White, M. C. *J. Am. Chem. Soc.* **2009**, *131*, 11707. (f) Nahra, F.; Liron, F.; Prestat, G.; Mealli, C.; Messaoudi, A.; Poli, G. *Chem. - Eur. J.* **2009**, *15*, 11078. (g) Stang, E. M.; White, M. C. *J. Am. Chem. Soc.* **2011**, *133*, 14892. (h) Braun, M. G.; Doyle, A. G. *J. Am. Chem. Soc.* **2013**, *135*, 12990.

(7) (a) Reed, S. A.; White, M. C. *J. Am. Chem. Soc.* **2008**, *130*, 3316. (b) Reed, S. A.; Mazzotti, A. R.; White, M. C. *J. Am. Chem. Soc.* **2009**, *131*, 11701.

(8) (a) Collet, F.; Dodd, R. H.; Dauban, P. *Chem. Commun.* **2009**, 5061. and references therein (b) Jeffrey, J. L.; Sarpong, R. *Chem. Sci.* **2013**, *4*, 4092. and references therein (c) Paradine, S. M.; Griffin, J. R.; Zhao, J.; Petronico, A. L.; Miller, S. M.; White, M. C. *Nat. Chem.* **2015**, *7*, 987.

(9) For examples of aerobic olefin oxidation, see: (a) Larock, R. C.; Hightower, T. R.; Hasvold, L. A.; Peterson, K. P. *J. Org. Chem.* **1996**, *61*, 3584. (b) Brice, J. L.; Harang, J. E.; Timokhin, V. I.; Anastasi, N. R.; Stahl, S. S. *J. Am. Chem. Soc.* **2005**, *127*, 2868. For examples of aerobic alcohol oxidation, see: (c) Jensen, D. R.; Pugsley, J. S.; Sigman, M. S. *J. Am. Chem. Soc.* **2001**, *123*, 7475. (d) Ferreira, E. M.; Stoltz, B. M. *J. Am. Chem. Soc.* **2001**, *123*, 7725. For examples of aerobic C−H oxidation, see: (e) Zhang, Y. H.; Yu, J. Q. *J. Am. Chem. Soc.* **2009**, *131*, 14654 and ref s8−10 and 15..

DOI: 10.1021/jacs.5b11294
J. Am. Chem. Soc. 2016, 138, 1265−1272

(10) (a) Sigman, M. S.; Schultz, M. J. *Org. Biomol. Chem.* **2004**, *2*, 2551. (b) Gladysz, J. A.; Bedford, R. B.; Fujita, M.; Gabbaï, F. P.; Goldberg, K. I.; Holland, P. L.; Kiplinger, J. L.; Krische, M. J.; Louie, J.; Lu, C. C.; Norton, J. R.; Petrukhina, M. A.; Ren, T.; Stahl, S. S.; Tilley, D. T.; Webster, C. E.; White, M. C.; Whiteker, G. T. *Organometallics* **2014**, *33*, 1505.
(11) Mitsudome, T.; Umetani, T.; Nosaka, N.; Mori, K.; Mizugaki, T.; Ebitani, K.; Kaneda, K. *Angew. Chem., Int. Ed.* **2006**, *45*, 481.
(12) Liu, G.; Yin, G.; Wu, L. *Angew. Chem., Int. Ed.* **2008**, *47*, 4733.
(13) Shimizu, Y.; Obora, Y.; Ishii, Y. *Org. Lett.* **2010**, *12*, 1372.
(14) Yin, G.; Wu, Y.; Liu, G. *J. Am. Chem. Soc.* **2010**, *132*, 11978.
(15) Campbell, A. N.; White, P. B.; Guzei, I. A.; Stahl, S. S. *J. Am. Chem. Soc.* **2010**, *132*, 15116.
(16) (a) Smidt, J.; Hafner, W.; Jira, R.; Sedlmeier, J.; Sieber, R.; Ruttinger, R.; Kojer, H. *Angew. Chem.* **1959**, *71*, 176. (b) Henry, P. M.; Keith, J. A. *Angew. Chem., Int. Ed.* **2009**, *48*, 9038.
(17) (a) Németh, S.; Szeverény, Z.; Simándi, L. I. *Inorg. Chim. Acta* **1980**, *44*, 107. (b) Rio, M. F.; Pujol, D.; Charreton, C. B.; Fauvet, M. P.; Gaudemer, A. *J. Chem. Soc., Perkin Trans. 1* **1984**, 1971.
(18) (a) Tatsuno, Y.; Tatsuda, M.; Otsuka, S. *J. Chem. Soc., Chem. Commun.* **1982**, 1100. (b) Hwang, D. R.; Chu, C. Y.; Wang, S. K.; Uang, B. J. *Synlett* **1999**, *1*, 77.
(19) (a) Bäckvall, J. E.; Awasthi, A. K.; Renko, Z. D. *J. Am. Chem. Soc.* **1987**, *109*, 4750. (b) Bäckvall, J. E.; Hopkins, R. B.; Grennberg, H.; Mader, M. M.; Awasthi, A. K. *J. Am. Chem. Soc.* **1990**, *112*, 5160.
(20) Schaus, S. E.; Brandes, B. D.; Larrow, J. F.; Tokunaga, M.; Hansen, K. B.; Gould, A. E.; Furrow, M. E.; Jacobsen, E. N. *J. Am. Chem. Soc.* **2002**, *124*, 1307.
(21) (a) Witt, A.; Teodorovic, P.; Linderberg, M.; Johansson, P.; Minidis, A. *Org. Process Res. Dev.* **2013**, *17*, 672. (b) Osterberg, P. M.; Niemeier, J. K.; Welch, C. J.; Hawkins, J. M.; Martinelli, J. R.; Johnson, T. E.; Root, T. W.; Stahl, S. S. *Org. Process Res. Dev.* **2015**, *19*, 1537.
(22) (a) Fraunhoffer, K. J.; Bachovchin, D. A.; White, M. C. *Org. Lett.* **2005**, *7*, 223. (b) Chen, M. S.; White, M. C. *Science* **2007**, *318*, 783. (c) Stang, E. M.; White, M. C. *Nat. Chem.* **2009**, *1*, 547. (d) Kim, J.; Ashenhurst, J. A.; Movassaghi, M. *Science* **2009**, *324*, 238. (e) Chen, K.; Baran, P. S. *Nature* **2009**, *459*, 824. (f) Chen, M. S.; White, M. C. *Science* **2010**, *327*, 566. (g) Malik, H. A.; Taylor, B. L.; Kerrigan, J. R.; Grob, J. E.; Houk, K. N.; Dubois, J. N.; Hammann, L. G.; Patterson, A. W. *Chem. Sci.* **2014**, *5*, 2352. (h) He, J.; Hamann, L. G.; Davies, H. M. L.; Beckwith, R. E. J. *Nat. Commun.* **2015**, *6*, 5943.
(23) Raju, B.; Anandan, S.; Gu, S.; Herradura, P.; O'Dowd, H.; Kim, B.; Gomez, M.; Hackbarth, C.; Wu, C.; Wang, W.; Yuan, Z.; White, R.; Trias, J.; Patel, D. V. *Bioorg. Med. Chem. Lett.* **2004**, *14*, 3103.
(24) For spectroscopic evidence of π-allylPd(II)/BQ complexes, see: Bäckvall, J. E.; Gogoll, A. *Tetrahedron Lett.* **1988**, *29*, 2243.

DOI: 10.1021/jacs.5b11294
J. Am. Chem. Soc. 2016, 138, 1265−1272

UNIVERSITAT ROVIRA I VIRGILI
Gold-Catalyzed Synthesis of 5 and 6-Membered Rings for the Construction of Molecular Diversity
Pilar Calleja Ramos